

# REMOVAL OF FLUORIDE FROM INDUSTRIAL WASTE WATER

Ph.D. THESIS

by

TEJ PRATAP SINGH



DEPARTMENT OF CHEMICAL ENGINEERING  
INDIAN INSTITUTE OF TECHNOLOGY ROORKEE  
ROORKEE – 247 667 (INDIA)  
APRIL , 2017

# REMOVAL OF FLUORIDE FROM INDUSTRIAL WASTE WATER

A THESIS

*Submitted in partial fulfilment of the requirements for the award of the degree*

*of*

DOCTOR OF PHILOSOPHY

*in*

CHEMICAL ENGINEERING

*by*

TEJ PRATAP SINGH



DEPARTMENT OF CHEMICAL ENGINEERING  
INDIAN INSTITUTE OF TECHNOLOGY ROORKEE  
ROORKEE – 247 667 (INDIA)  
APRIL , 2017



**©INDIAN INSTITUTE OF TECHNOLOGY ROORKEE, ROORKEE-2017  
ALL RIGHTS RESERVED**



# INDIAN INSTITUTE OF TECHNOLOGY ROORKEE ROORKEE

## CANDIDATE'S DECLARATION

I hereby certify that the work which is being presented in the thesis entitled "**REMOVAL OF FLUORIDE FROM INDUSTRIAL WASTE WATER**" in partial fulfilment of the requirement for the award of the Degree of Doctor of Philosophy and submitted in the Department of Chemical Engineering , Indian Institute of Technology Roorkee, Roorkee India is an authentic record of my own work carried out during a period from August, 2012 to April , 2017 under supervision of Dr. Chandrajit Balomajumder, Professor, Department of Chemical Engineering, Indian Institute of Technology Roorkee, Roorkee India.

The matter presented in this thesis has not been submitted by me for the award of any other degree of this or any other Institute.

(TEJ PRATAP SINGH)

This is to certify that the above statement made by the candidate is correct to the best of my knowledge.

(CHANDRAJIT BALOMAJUMDER)  
Supervisor

The Ph.D. viva-voce examination of **MR TEJ PRATAP SINGH**, Research Scholar, has been held on .....

Chairman, SRC

Signature of External Examiner

This is to certify that the student has made all the corrections in the thesis.

Signature of Supervisor

Head of the Department

Dated:

## **ACKNOWLEDGEMENT**

I take this opportunity to express my deep sense of gratitude to all those, who have made it possible for the successful completion of this work and submit it in the hands of learned elites.

I wish to express my sincere indebtedness to my supervisors Dr. Chandrajit Balomajumder, Department of Chemical Engineering, Indian Institute of Technology Roorkee, for providing his valuable guidance, encouragement, help and kind support in all respects during the completion of this work. I also thank him for providing facilities for my research work in Chemical Engineering Department. The kind-heartedness, love and affection extended by him to me a source of inspiration during the completion of this work and have made my stay here memorable.

I would also like to thank to all staff and management of the Fluid Particle Research Laboratory, Chemical Engineering Department and the Institute Computer Centre for cooperating with me and helping me in every possible ways.

Last, but not the least, it is all due to the blessings of God and with the support my family that I have come up with this work within the time frame.

**TEJ PRATAP SINGH**

## **ABSTRACT**

Water is an essential natural resource for sustaining existence of humans and their surroundings that are perceived to be free and unlimited gift given to us. As regards the chemical composition of surface or subsurface, it can easily be seen as one of the most significant factors having a great effect on the usefulness of water for all kinds of life as well as industrial or agricultural purposes. Freshwater is found as surface as well as groundwater. On one hand groundwater constitutes barely 0.6% from the overall water available on this planet; on the other hand it is the most reliable and the most recommended source of water for domestic purposes everywhere. This is more so especially in countries with sufficient potential to achieve the status of developed nations, such as India, as processing of this groundwater, with disinfection, is generally not needed. Groundwater covers 80% of the total requirement of water for domestic use and 50% of in rural India for agrarian purposes. In the present age of economic and industrial development, groundwater is becoming more and more polluted because of industrialization and urbanization. During the last few decades, the continually-increasing population, urbanization and industrialization, as well as exploitation of available resources have yielded a kind of decline in the quality level of water and also decrease in the amount of water available per capital in various developing countries.

When it comes to considering health detriments due to fluoride, it can be seen as a grave concern related to our environment everywhere in the world. These detriments can happen owing to changes in nature as well as due to human activities. Drinking water containing fluoride may be beneficial or detrimental depending upon its concentration and total amount consumed. Fluoride concentrations between 0.5-1.5 mg/L are beneficial, especially to infants for the prevention of dental caries or tooth decay, but concentrations above 1.5 mg/L cause mottling of teeth in mild cases but fluorosis (dental or skeletal) and several neurological disorders in severe cases. Defluoridation is usually done through absorption, chemical as well as electrochemical processes, and dialysis or the ion-exchange process. When it comes to choosing the most effective, eco-friendly and cost-effective process, absorption can be found as the best one.

Among various treatment procedure used for defluoridation, batch adsorption process gives satisfactory results to an extent. In this study, we have studied fluoride removal using *citrus*

limetta peel, Java Plum Seed (*Syzygium cumini*), banana peel, groundnut shell, Neem leaves (*Azadirachta indica*) as it serves as a low cost, easily available and a highly effective adsorbent. These adsorbents were collected from local market of Roorkee, Haridwar, Uttarakhand, India. It was washed with distilled water several times, crushed and sieved to get a particle size range of 0.5 – 2.0 mm. The adsorbents so developed were used for removal of fluoride and further the batch process is optimized by varying the adsorbent dose, pH, fluoride concentration and time of contact. The detailed characterization pertaining to physio-chemical, structural and morphological properties of agricultural waste were also carried out. The adsorption capacity of all adsorbents was compared to that of GAC. GAC was chosen as the control since a considerable work has been reported in the literature. On the basis of result obtained, we can conclude that java plum (*Syzygium cumini*) seed is the best adsorbent in the present list of adsorbents for defluoridation process for same biological conditions.

Equilibrium and kinetics and modeling of adsorption and SAB process were also done. To study the mechanism of adsorbate transfer from the solution to the surface of the adsorption particles Weber-Morris's equation was applied. It was observed that macropore diffusion rate is greater than micropore diffusion rate. The kinetic of the process has been studied using pseudo first order, pseudo second order and Elovich model. The isotherm equation including the conventional Freundlich, Langmuir and Temkin isotherm have been fitted with the equilibrium adsorption and SAB data. The fitness of the isotherm towards the prediction of specific uptake was analyzed by computing standard deviation to calculate squared sum of errors (SSE) function.

Column and continuous studies are done so as to study the defluoridation capacity of the adsorbent in continuous mode. The effect of flow rate, fluoride concentration and bed height is studied. The Empty Bed Residence Time, Thomas model and bed Depth Service Time design model were used to inspect the effect of the different operating variables such as bed depth; flow rate and initial concentration. The performances of the column were tested on these simple fixed bed design models. To evaluate the possibilities of regeneration and reuse of the adsorbents, desorption experiments were conducted. We also examined the effects of co-existing ions on the adsorption capacity in batch mode.

Bioaccumulation studies have been carried out for studying the effectiveness of single microorganisms. The single cultures of nitrogen fixing bacteria *Acinetobacter baumannii*

(MTCC No.-11451) were used for fluoride bioaccumulation from water and soil. Initially the microorganism acclimatized to grow at higher fluoride concentration and their ability to accumulate fluoride was measured. The effect of initial fluoride concentration and sucrose (as second carbon source) concentration on the removal efficiency was studied for single microorganism. It was found to have maximum efficiency at about 20 mg/L of fluoride concentration. *Acinetobacter baumannii* (MTCC No.-11451) was found to be most efficient bacterial strain on the basis of fluoride removal capacity.

Simultaneous adsorption and bioaccumulation studies were conducted in SBB reactor using *Acinetobacter baumannii* (MTCC No.-11451) immobilized on java plum seed (*Syzygium cumini*). Optimum condition, estimated by adsorption and bioaccumulation studies was maintained in SAB process. SAB process was used for removal of fluoride at higher concentration than 20 mg/l from synthetic simulated waste water and real industrial effluent, both in batch and continuous reactor. To overcome the drawbacks and adsorption and bioaccumulation integration of adsorption in the form of immobilized cell technology and bioremediation is carried out in the present study. The recent development, commonly known as, simultaneously adsorption and bioaccumulation (SAB) has been used by a few researchers and results was found to be better than individual adsorption or bioaccumulation. Due to the biolayer formation on the adsorbent bed simultaneous adsorption and bioaccumulation occurs simultaneously. Adsorption and bioaccumulation have successfully supplemented to each other here microbial mass bio accumulate toxic substance into simpler product as well as biosorbes some of them on the other hand. Adsorption of toxic substances on to a adsorbent reduces the inhibitory effect of the substance on the microbial growth. Accordingly, simultaneous adsorption and bioaccumulation (SAB) is expected to be more efficient as compared to adsorption and bioaccumulation alone.

Granular/powdered activated carbon is most widely used adsorbent for fluoride removal. The surface chemistry of activated carbon on the chemical characteristic of adsorbate such as functional group, ionic nature, polarity and solubility determine the nature of binding mechanism as well as the extent and strength of adsorption. GAC has good adsorption capacity and biolayer formation capacity. In the search of more effective and economical adsorbents agriculture byproducts e.g. *citrus lematta* peel, banana peel, groundnut shell, neem leaves, turmeric, GAC and java plum seed, etc. were used in present work for the removal of fluoride compounds. These adsorbents have been successfully used for the adsorptive



removal of many other toxic substances. However SAB process along with this agriculture waste based adsorbent for fluoride removal has not been reported yet.

Continuous studies were carried out using packed column along with *Acinetobacter baumannii* (MTCC No.-11451). The effect of bed height and flow rate on fluoride removal capacity of the column was studied. The continuous processes were found to be feasible and effective for removal of higher concentrations of fluoride pointing towards development of new and efficient technology for fluoride removal.

We had taken two aquatic plant species which were selected for the studies were *Ipomoea aquatica* [Water spinach] and *Eichhornia crassipes* [Water Hyacinth] in the phytoremediation of fluoride study. These were very common aquatic plants which can easily found in water bodies like pond, lake, river etc. They were grown in plant growth chamber and studied for 10 days exposure period to fluoride of different concentrations and pH. The removal efficiency of *Ipomoea aquatica* [Water spinach] was found 40.988 % and for *Eichhornia crassipes* [Water Hyacinth] it was found 58.894 %. Results show that water hyacinth had better removal efficiency to remediate fluoride. In pH study for both the plants shows negative results, as we increase or decrease the pH of the solution the removal efficiency was decreased for both the plants. Accumulation of fluoride was found mainly in the roots for both plants. It was found 872.866  $\mu\text{g/g D}_w$  for *Ipomoea aquatica* and 1148.479  $\mu\text{g/g D}_w$  for *Eichhornia crassipes*. Both the plants show the biomass degradation due to the fluoride exposure.

# CONTENTS

<b>Chapter</b>	<b>Title</b>	<b>Page No.</b>
	Candidate Declaration	i
	Acknowledgement	ii
	Abstract	iii
	Contents	vii
	List of Tables	xix
	List of Figures	xxiii
	Nomenclature	xxix
<b>1</b>	<b>Introduction</b>	<b>1-6</b>
	1.0 General	1
	1.1 Objectives of the present study	3
	1.2 Organization of Thesis	3
<b>2</b>	<b>Literature Review</b>	<b>7-60</b>
	2.0 Sources of Fluoride	7
	2.1 Indian Scenario	8
	2.1.1 Fluorspar	8
	2.1.2 Apatite and Rock Phosphate	8
	2.1.3 Phosphorites	8
	2.2 Physicochemical Properties of Fluoride Compounds	9
	2.3 Various Health Impacts of Fluoride	9
	2.3.1 Dental Fluorosis	12
	2.3.2 Skeletal Fluorosis	13
	2.4 Defluoridation of Water	13
	2.4.1 Flocculation	14
	2.4.2 Ion Exchange Methods	14
	2.4.3 Coagulation Process	15
	2.4.4 Adsorption	15
	2.5 Adsorption Isotherms	17
	2.5.1 Isotherm Model by Langmuir	17
	2.5.2 Isotherm Model by Freundlich	18
	2.5.3 Isotherm Model by Temkin	19
	2.6 Adsorption Kinetics and Equilibrium Capacity	19
	2.6.1 Pseudo First Order Model	20
	2.6.2 Pseudo Second Order Model	20
	2.7 Use of Bio Adsorbents and Advantages	21

2.8	SAB Process	21
2.9	Estimation of Fluoride	22
2.9.1	Titrimetry	22
2.9.2	Methods based on Potentiometric	22
2.9.3	Methods based on Spectrophotometric	23
2.10	Review of Previous Work Done by Various Authors on Different Methodologies for Removal of Fluoride	24
2.11	Phytoremediation Review	39
2.11.1	Techniques/Strategies of Phytoremediation	40
2.11.2	Phytodegradation	41
2.11.3	Phytoaccumulation / Phytoextraction	41
2.11.4	Phytostabilization	41
2.11.5	Rhizofiltration	41
2.11.6	Phytovolatilization	41
2.11.7	Constructed Wetland	43
2.11.8	Floating Platform	43
2.11.9	The advantages and disadvantages of phytoremediation are discussed in the Table (Belz., 1997, Tangahu., 2011)	44
2.10	Work Done by Different Authors on Phytoremediation of Heavy Metals	45
2.11	Error function	57
2.12	Objective	58
2.12.1	Research Needs	58
2.12.2	Objective of Present Work	58
<b>3</b>	<b>Experimental Setup and Instrumentation</b>	<b>61-72</b>
3.0	Motivation	61
3.1	Apparatus and Reagents	61
3.1.1	Standard Fluoride Solution	61
3.1.2	Reagent A	61
3.1.3	Reagent B	61
3.1.4	Reagent S	61
3.1.5	Reference Solution	62
3.2	Preparation of Calibration Curve	62
3.3	Details of Experimental Setup	63
3.3.1	Analytical Instrumentals used for the Present Investigation	63
3.3.2	Removal of fluoride in column reactor	64
3.3.3	Instrumentation and Control	66
3.3.4	Limitation of the Set-up	66

3.4 Analytical and Auxiliary Instruments Used in the Present Study	66
3.4.1 Analytical Instruments	66
3.4.2 Auxiliary Equipments	66
3.5 Calibration of Measuring Instruments	66
3.5.1 Calibration of pH Meter	66
3.5.2 Calibration of D.O. Meter	67
3.5.3 Calibration of Experimental Setup	67
3.6 Artificial Photosynthesis Chamber	71
3.6.1 Instrumentation and Control	71
3.6.2 Limitation of the Set up	71
3.7 Concluding Remarks	72
<b>4 Experimental Procedure</b>	<b>73-98</b>
4.0 General	73
4.1 Design of experiments	73
4.2 Batch Adsorption Studies	75
4.2.1 Adsorbents and their preparation method	75
4.2.1.1 Granular activated carbon (GAC)	76
4.2.1.2 Citrus limetta peel	76
4.2.1.3 Groundnut shell	76
4.2.1.4 Neem leaves	76
4.2.1.5 Java plum seed (Syzgiumcumini)	76
4.2.1.6 Turmeric and MnO <sub>2</sub> coated turmeric	77
4.2.1.7 Banana Peel	77
4.2.2 Characterization of adsorbents	77
4.2.2.1 FTIR Analysis of Adsorbents	77
4.2.2.2 X-ray diffraction (XRD) and Scanning Electron Microscope (SEM) Analysis of Adsorbent	78
4.2.2.3 Physical and chemical property of Adsorbent	78
4.2.2.3.1 BET (Brunauer- Emmet-Teller) surface area	78
4.2.2.3.2 Proximate analysis	78
4.2.2.3.3 Volatile material	79
4.2.2.3.4 Ultimate analysis	79
4.2.3 Experimental program for batch adsorption study	80
4.2.4 Batch Experiments	81
4.2.4.1 Batch adsorption studies onto the removal of fluoride at various pH for simulated synthetic waste water	81

4.2.4.2	Batch adsorption studies onto the removal of fluoride at various temperatures ( $^{\circ}\text{C}$ ) for simulated synthetic waste water	81
4.2.4.3	Batch adsorption studies onto the removal of fluoride at various adsorbent doses (mg/g) for simulated synthetic waste water	81
4.2.4.4	Batch adsorption studies onto the removal of fluoride at various initial concentrations (mg/L) for simulated synthetic waste water	82
4.2.4.5	Batch adsorption studies onto the removal of fluoride at various contact time for simulated synthetic waste water	82
4.3	SAB Process	86
4.3.1	Materials	86
4.3.2	Growth of Bacteria (Actinobacter)	86
4.4	Procedure for Growth of Bacteria	87
4.4.1	Preparation of Agar Media	87
4.4.2	Preparation of Petri Dishes	87
4.4.3	Inoculation of Bacteria	88
4.4.4	Sterilization	88
4.5	Methods of Microbial Work	88
4.6	Batch Experiments	88
4.7	Growth Curve of Bacteria	88
4.7.1	Experimental program	89
4.8	Fixed-Bed Design Models	90
4.9	Bed Depth Service Time (BDST) Design Model	93
4.10	Empty Bed Residence Time Design Model	94
4.11	Thomas Model	96
4.12	Fixed-Bed Column/Bio-column Experiments	97
<b>5</b>	<b>Result &amp; Discussion</b>	<b>99-252</b>
5.0	Introduction	99
5.0.1	Batch adsorption studies	99
5.0.2	Bio removal	99
5.0.3	In this section simultaneous adsorption and bio accumulation	99
5.0.4	In this section continuous simultaneous removal of fluoride was carried out in packed Bed column	100
5.0.5	In this section the uptake of fluoride by aquatic macrophyte water hyacinth (Eichhornia crassipes) from phytoremediation	100
5.1	Batch adsorption studies	100
5.1.1	Characterization of adsorbent	100

5.1.2 FTIR spectrum before and after adsorption of fluoride from simulated synthetic waste water	102
5.1.2.1 FTIR spectrum of GAC before and after adsorption	102
5.1.2.2 FTIR spectrum of Citrus limetta peel before and after adsorption	103
5.1.2.3 FTIR spectrum of Ground nut shell before and after adsorption	104
5.1.2.4 The FTIR spectrum of Neem leaves pre and post absorption	105
5.1.2.5 FTIR spectrum of virgin turmeric and MnO <sub>2</sub> coated Turmeric before and after adsorption	106
5.1.2.6 FTIR spectrum of Java plum seed (Syzgiumcumini) before and after adsorption	107
5.1.2.7 FTIR spectrum of Banana peel before and after adsorption	108
5.1.3.8 Concluding Remark of the Section 5.1.2	109
5.1.3 FE SEM (Field Emission Scanning electron microscopy) and EDX (Energy Dispersive X-ray) analysis	118
5.1.3.1 Analysis of Granular activated carbon (GAC)	118
5.1.3.1.1 SEM analysis of Granular activated carbon (GAC)	118
5.1.3.1.2 EDX analysis of Granular activated carbon (GAC)	118
5.1.3.2 Analysis of Citrus limetta peel	119
5.1.3.2.1 SEM analysis of Citrus limetta peel	119
5.1.3.2.2 EDX analysis of Citrus limetta peel	119
5.1.3.3 Analysis of Ground nut shell	120
5.1.3.3.1 SEM analysis of Ground nut shell	120
5.1.3.3.2 EDX analysis of Ground nut shell	120
5.1.3.4 Analysis of Neem leaves	121
5.1.3.4.1 SEM analysis of Neem leaves	121
5.1.3.4.2 EDX analysis of Neem leaves	121
5.1.3.5 Analysis of virgin Turmeric and MnO <sub>2</sub> coated turmeric	121
5.1.3.5.1 SEM analysis of virgin Turmeric and MnO <sub>2</sub> coated turmeric	121
5.1.3.5.2 EDX analysis of virgin Turmeric and MnO <sub>2</sub> coated turmeric	122
5.1.3.6 Analysis of Java plum seed (Syzgiumcumini)	122
5.1.3.6.1 SEM analysis of Java plum seed (Syzgiumcumini)	122

5.1.3.6.2 EDX analysis of Java plum seed (Syzgiumcumini)	123
5.1.3.7 Analysis of Banana peel	123
5.1.3.7.1 SEM analysis of Banana peel	123
5.1.3.7.2 EDX analysis of Banana peel	124
5.1.3.8 Concluding remark	132
5.1.4 Effect of batch adsorption process parameters	132
5.1.4.1 Effect of pH for removal of fluoride	132
5.1.4.1.1 Effect of pH for removal of fluoride by GAC	132
5.1.4.1.2 Effect of pH for removal of fluoride by Citrus limetta peel	133
5.1.4.1.3 Effect of pH for removal of fluoride by Ground nut shell	133
5.1.4.1.4 Effect of pH for removal of fluoride by Neem leaves	134
5.1.4.1.5 Effect of pH for removal of fluoride by Virgin turmeric and MnO <sub>2</sub> coated turmeric	134
5.1.4.1.6 Effect of pH for removal of fluoride by Java plum seed (Syzgiumcumini)	135
5.1.4.1.7 Effect of pH for removal of fluoride by Banana peel	136
5.1.4.2 Effect of Dose for removal of fluoride	141
5.1.4.2.1 Effect of Dose for removal of fluoride by GAC	141
5.1.4.2.2 Effect of Dose for removal of fluoride by Citrus limetta peel	141
5.1.4.2.3 Effect of Dose for removal of fluoride by Ground nut shell	141
5.1.4.2.4 Effect of Dose for removal of fluoride by Neem leaves	142
5.1.4.2.5 Effect of Dose for removal of fluoride by Virgin turmeric and MnO <sub>2</sub> coated turmeric	142
5.1.4.2.6 Effect of Dose for removal of fluoride by Java plum seed (Syzgiumcumini)	142
5.1.4.2.7 Effect of Dose for removal of fluoride by Banana peel	143
5.1.4.3 Reaction time impact on fluoride elimination	147
5.1.4.3.1 Effect of Contact time for removal of fluoride by GAC	147
5.1.4.3.2 Effect of Contact time for removal of fluoride by Citrus limetta peel	147
5.1.4.3.3 Effect of Contact time for removal of fluoride by Ground nut shell	147

5.1.4.3.4	Effect of Contact time for removal of fluoride by Neem leaves	148
5.1.4.3.5	Effect of Contact time for removal of fluoride by Virgin turmeric and MnO <sub>2</sub> coated turmeric	148
5.1.4.3.6	Effect of Contact time for removal of fluoride by Java plum seed (Syzgiumcumini)	149
5.1.4.3.7	Effect of Contact time for removal of fluoride by Banana peel	149
5.1.4.4	Effect of initial concentration	153
5.1.4.4.1	Effect of initial concentration for removal of fluoride by GAC	153
5.1.4.4.2	Effect of initial concentration for removal of fluoride by Citrus limetta peel	153
5.1.4.4.3	Effect of initial concentration for removal of fluoride by Ground nut shell	154
5.1.4.4.4	Effect of initial concentration for removal of fluoride by Neem leaves	154
5.1.4.4.5	Effect of initial concentration for removal of fluoride by Virgin turmeric and MnO <sub>2</sub> coated turmeric	154
5.1.4.4.6	Effect of initial concentration for removal of fluoride by Java plum seed (Syzgiumcumini)	155
5.1.4.4.7	Effect of initial concentration for removal of fluoride by Banana peel	155
5.1.4.4.7	Concluding remark	159
5.1.6	Adsorption kinetics	159
5.1.6.1	Adsorption Kinetics of fluoride removal by GAC	160
5.1.6.1.1	Concluding Remarks	160
5.1.6.2	Adsorption Kinetics of fluoride removal by Citrus limetta peel	160
5.1.6.2.1	Concluding Remarks	161
5.1.6.3	Adsorption Kinetics of fluoride removal by Ground nut shell	161
5.1.6.3.1	Concluding Remarks	162
5.1.6.4	Adsorption Kinetics of fluoride removal by Neem leaves	162
5.1.6.4.1	Concluding Remarks	163
5.1.6.5	Adsorption Kinetics of fluoride removal by Virgin turmeric and MnO <sub>2</sub> coated turmeric	163
5.1.6.5.1	Concluding Remarks	164
5.1.6.6	Adsorption Kinetics of fluoride removal by Java plum seed (Syzgiumcumini)	164
5.1.6.6.1	Concluding Remarks	164



5.1.6.7 Adsorption Kinetics of fluoride removal by Banana peel	165
5.1.6.7.1 Concluding Remark	165
5.1.7 Isotherms study	173
5.1.7.1 Isotherms study of fluoride removal by GAC	173
5.1.7.1.1 Concluding Remarks	174
5.1.7.2 Isotherms study of fluoride removal by Citrus limetta peel	174
5.1.7.2.1 Concluding Remarks	175
5.1.7.3 Isotherms study of fluoride removal by Ground nut shell	175
5.1.7.3.1 Concluding Remarks	175
5.1.7.4 Isotherms study of fluoride removal by Neem leaves	175
5.1.7.4.1 Concluding Remarks	176
5.1.7.5 Isotherms study of fluoride removal by Virgin turmeric and MnO <sub>2</sub> coated turmeric	176
5.1.7.5.1 Concluding Remarks	176
5.1.7.6 Isotherms study of fluoride removal by Java plum seed (Syzygiumcumini)	177
5.1.7.6.1 Concluding Remarks	177
5.1.7.7 Isotherms study of fluoride removal by Banana peel	178
5.1.7.7.1 Concluding Remarks	178
5.1.8 Comparative Study of Batch and Column Performance of Fluoride Adsorption by Java Plum Seed (Syzygiumcumini)	187
5.1.8.1 The Column Adsorption Experiment	187
5.1.8.2 Batch Adsorption Experiment	188
5.1.8.3 Mathematical Modeling	189
5.1.8.3.1 Thomas Model	189
5.1.8.3.2 The Empty Bed Residence Time Model (EBRT)	190
5.1.8.3.4 Continuous Column Study Using Java Plum Seeds (Syzygiumcumini)	191
5.1.8.3.4.1 Fixed-Bed Design Models	191
5.1.8.3.4.2 Bed Depth Service Time Model	191
5.1.8.3.5 Effect of Bed Depth	194
5.1.8.3.6 Effect of Flow Rate	196
5.1.8.3.7 Effect of Empty Bed Contact Time	197
5.1.8.3.8 Thomas Model	197
5.1.8.4 Batch Study	198

5.1.8.4.1 Effect of Adsorption Kinetics and Contact Time	198
5.1.8.4.2 Effect of pH	200
5.1.8.4.3 Adsorption Isotherm Models	200
5.1.8.5 Characterization of the Java plum seed (Syzgiumcumini)	202
5.1.8.5.1 SEM	202
5.1.8.5.2 EDX	203
5.1.8.5.3 Concluding Remarks on Continuous Adsorption Column Study Using Java Plum Seed (Syzgiumcumini)	205
5.1.9 Continuous Study on Citrus Limetta Peel (Bioremoval Process)	205
5.1.9.1 General	205
5.1.9.2 Optimization of Parameter	205
5.1.9.2.1 pH Optimization	205
5.1.9.2.2 Dose Optimization	206
5.1.9.2.3 Initial Concentration	207
5.1.9.2.4 Contact Time	208
5.2.0 SAB Adsorption Kinetics	209
5.2.0.1 Pseudo-first Order Model	209
5.2.0.2 Pseudo-Second-Order Model	210
5.2.0.3 Concluding Remarks	210
5.2.1 SAB Adsorption Isotherms	211
5.2.1.1 Langmuir Model	211
5.2.1.2 Freundlich Isotherm	212
5.2.1.3 Temkin Model	212
5.2.2 SAB Continuous Reactor Study Treatment of Fluoride Bearing Contaminated Water Using SAB in a Laboratory Scaled up – Flow Bio – Column Reactor by Java plum seed (Syzgiumcumini)	215
5.2.2.1 Materials and Methods	215
5.2.2.1.1 Chemicals	215
5.2.2.1.2 Strains and Medium	215
5.2.2.1.3 Acclimatization	216
5.2.2.1.4 Batch Bioaccumulation Experiments	216
5.2.2.1.5 Experimental Setup	216
5.2.2.1.5.1 The Empty Bed Residence Time Model (EBRT)	217
5.2.2.1.5.2 Fixed-Bed Design Models	218
5.2.2.1.5.3 Bed Depth Service Time Model	218

5.2.2.1.5.4 Effect of Flow Rate	221
5.2.2.1.5.5 Effect of Bed Height	222
5.2.2.1.5.6 Effect of Empty Bed Contact Time	224
5.2.2.1.5.7 Variation of pH and DO (Dissolved Oxygen) of Treated Waste Water with Time	225
5.2.2.1.5.8 Concluding Remarks	226
5.2.3 Distribution of Residence Time for Packed Bed Column Reactor Using a Packing of Bio-Adsorbent (Java plum seed ( <i>Syzgiumcumini</i> ))	227
5.2.3.1 Experimental Setup	227
5.2.3.2 Materials	227
5.2.3.3 Procedures	228
5.2.3.4 Reactions Involved	228
5.2.3.5 Results and Discussion	228
5.2.3.5.1 Calculation of Dispersion Number	229
5.2.3.5.2 Calculation of Pellet Number	230
5.2.3.5.3 Concluding Remarks	230
5.2.4 Implementation of the present work for treatment of fluoride contaminated AIS auto glass effluent	231
5.2.4.1 Concluding remarks	233
5.2.5 Experimental Setup	234
5.2.6 Prepreation of Hoagland's Solution	234
5.2.7 Result and Discussion	235
5.2.8 Effect of Initial Fluoride Concentration	236
5.2.9 Effect of pH	237
5.2.10 Effect of Initial Concentration on Percentage Removal	238
5.2.11 Accumulation of Fluoride	238
5.2.11.1 Concluding Remarks	239
5.3 Comparative Study of <i>Ipomoea Aquatica</i> and <i>Eichhornia Crassipes</i>	239
5.3.1 Results and Discussions	239
5.3.1.1 Removal of Fluoride with Time	239
5.3.2 Chlorophyll Study for <i>Ipomoea aquatica</i> and <i>Eichhornia crassipes</i>	242
5.3.3 Accumulation of Fluoride in Different Parts of Plants	244
5.3.4 Bio Mass Degradation	245
5.3.5 Effect of Contact Time on Concentration	246
5.3.7 Effect of Contact Time on Percentage Removal	248
5.3.8 Effect of pH	249
5.3.8 .1 Concluding Remarks	250

<b>6</b>	<b>Summary of the Work, Conclusion and Scope for Future</b>	<b>253-260</b>
	6.1 Introduction	253
	6.2 Summary of the Present Work	253
	6.2.1 Adsorptive	255
	6.2.2 Adsorptive and Bio removal (batch)	255
	6.2.3 Bio Column Reactor	255
	6.2.4 Fixed Bed Column Reactor	256
	6.2.5 Phytoremediation	257
	6.2.6 Conclusion of the Present Work	257
	6.3 Scope of Future Investigation	259
	List of Publications	261
	References	263
Appendix	A Derivation of BDST Equation	273
Appendix	B Effect of initial Fluoride Concentration	275





## LIST OF TABLE

<b>Table No.</b>	<b>Particulars</b>	<b>Page No.</b>
2.0	Industries using Fluoride with Major Examples of Such Companies	7
2.1	Concentration of Fluorides in different Minerals. (Shrikant et al., 2012)	8
2.2 (a)	Properties of fluoride (SinghTP. Majumder, C.B.2017)	9
2.2 (b)	Physiochemical Property of Various Fluoride Compounds	9
2.3 (a)	Fluoride Affected Areas in India (SinghTP. Majumder, C.B.2015)	10
2.3 (b)	Effects of Different Concentration of Fluoride (Jacks et al., 2005)	11
2.3 (c)	Effect of Various Type of Fluorosis (Jacks et al., 2005)	12
2.3 (d)	Maximum Permissible Limit of Fluoride in Drinking Water as Per the Standards of Various Organizations (Malay et al., 2011)	13
2.3 (e)	Information summary on the Excessive Fluoride in Ground Water in India (Malay et al., 2011)	13
2.5.3	Mathamatical Corealation of Isotherms	19
2.10	List of Different Adsorbents Used by Different Researchers	37
2.11 (a)	Phytoremediation: Plant Utilized and their Roles (Prasad and Freitas., 2003)	39
2.11(b)	Application of Phytoremediation (Nagendran et al., 2006)	42
2.11.9	Advantages and disadvantages of Phytoremediation	44
2.10 (a)	Summary of Work Done on Phytoremediation by Authors	51
2.10 (b)	Represents the Values of Various Parameters Obtained by Different Scholars for Wastewater of Industries	54
3.3.1	Analysis Techniques/Instrument Used for the Analysis for Various Parameters	63
3.3.2	Salient feature of Fixed Bed Column/Bio-column Reactor	64
4.1	Summary of various experiments conducted in the present study	75
4.2.4	Range of Operating Parameter for adsorption studies of Fluoride from Simulated Synthetic Waste Water	82
4.2.4.1	Run number of experiments conducted to study the effect of varying pH onto the removal of fluoride from simulated synthetic waste water by various adsorbents	84
4.2.4.2	Run number of experiments conducted to study the effect of varying temperature onto the removing of fluoride from simulated synthetic waste water through various absorbents	84
4.2.4.3	Run number of experiments conducted to study the effect of varying dose onto the removing of fluoride from simulated synthetic waste water through various absorbents	85
4.2.4.4	Run number of experiments conducted to study the effect of varying fluoride concentration onto the removal of fluoride from simulated synthetic waste water by various adsorbents	85

4.2.4.5	Run number of experiments conducted to study the effect of varying contact time onto the removal of fluoride from simulated synthetic waste water by various adsorbents	86
4.3.1	Composition of Media for Microorganisms	86
4.12	Salient feature of Fixed Bed Column/Bio-Column Reactor	97
5.1.1	BET Surface Area and Ultimate and Proximate Analysis of all the Adsorbents	101
5.1.2.1	FTIR Analysis for GAC in Tabular Form	103
5.1.2.2	FTIR Analysis for Citrus Limetta in Tabular Form	104
5.1.2.3	FTIR analysis of Groundnut shells before and after adsorption	105
5.1.2.4	FTIR analysis of Neem leaves before and after adsorption	105
5.1.2.5 (a)	FTIR analysis of Turmeric before and after adsorption	106
5.1.2.5(b)	FTIR analysis of MnO <sub>2</sub> coated Turmeric before and after adsorption	107
5.1.2.6	FTIR analysis Java plum seed (Syzgiumcumini) before and after adsorption	108
5.1.2.7	FTIR analysis Banana peel before and after adsorption	109
5.1.3.1.2	EDX analysis of Granular activated carbon before and after adsorption of fluoride in tabular form	119
5.1.3.2.2	EDX Analysis of Citrus Limetta peel before and after adsorption of fluoride	119
5.1.3.3.2	EDX analysis of Ground nut shells before and after adsorption of fluoride	120
5.1.3.4.2	EDX analysis of Neem leaves before and after adsorption of fluoride	121
5.1.3.5.2	EDX analysis of virgin turmeric and MnO <sub>2</sub> coated turmeric before and after adsorption of fluoride	122
5.1.3.6.2	EDX analysis of Java plum seed (Syzgiumcumini) before and after adsorption of fluoride	123
5.1.3.7.2	EDX analysis of Banana peel	124
5.1.6.1	Various kinetic parameters for studied models for GAC	160
5.1.6.2	Various kinetic parameters for studied models for Citrus limetta peel	161
5.1.6.3	Various kinetic parameters for studied models for Ground nut shell	162
5.1.6.4	Various kinetic parameters for studied models for Neem leaves	162
5.1.6.5	Various kinetic parameters for studied models for Virgin turmeric and MnO <sub>2</sub> coated turmeric	163
5.1.6.6	Various kinetic parameters for studied models for Java plum seed (Syzgiumcumini)	164
5.1.6.7	Various kinetic parameters for studied models for Banana peel	165
5.1.6.9	Summary of Kinetics model parameters for removal of Fluoride from Simulated Synthetic Waste Water	172

5.1.7.1	Isotherm parameters obtained by fitting experimental data for the studied models	174
5.1.7.2	Isotherm parameters obtained by fitting experimental data for the studied models	174
5.1.7.3	Isotherm parameters obtained by fitting experimental data for the studied models	175
5.1.7.4	Isotherm parameters obtained by fitting experimental data for the studied models	176
5.1.7.5	Isotherm parameters obtained by fitting experimental data for the studied models	176
5.1.7.6	Isotherm parameters obtained by fitting experimental data for the studied models	177
5.1.7.7	Isotherm parameters obtained by fitting experimental data for the studied models	178
5.1.7.8	Summary of isotherm model parameters for removal of Fluoride from Simulated Synthetic Waste Water	187
5.1.8.3.4.2(a)	Data of Variable Bed depth at a fixed flow rate in a fixed bed column for the removal of 20mg/L of Fluoride by Java Plum Seed (Syzgiumcumini)	193
5.1.8.3.4.2(b)	Constant of BDST Curve	194
5.1.8.3.8	Liberalized Thomas Model Parameter at 7.5% Breakthrough	198
5.1.8.4.3	Langmuir and Freundlich Isotherm Parameters for the Adsorption of Fluoride on Java plum seed (Syzgiumcumini)	202
5.1.8.5.2	EDX analysis of Java plum seed (Syzgiumcumini) before and after adsorption of fluoride in tabular form	203
5.1.9.2.3	Cooperative Data for Different Optimization Parameters for Bioremoval and Adsorption	207
5.2.0.2	Comparison Table for Kinetic Study in Bio-Removal and Adsorption Process	210
5.2.1	Comparative Data for Adsorption Isotherm for Adsorptive and Bio Removal	215
5.2.2.1.2	Composition of Media for Microorganisms	216
5.2.2.1.5 (a)	Data of Variable Bed Depth at a Fixed Flow Rate in a Fixed-bed Bio Column Reactor for the Removal of 20mg/l of Fluoride by Java plum seed (Syzgiumcumini)	220
5.2.2.1.5 (b)	Constant of BDST curve	221
5.2.3.1	Feature of Bio-column Reactor	228
5.2.3.5	Experimental Residence Time Distributions for Packed Bed Reactor	231
5.2.4(a)	Characteristics of AIS auto glass industrial waste water (Mangalore, Near Roorkee, India)	231
5.2.4 (b)	Removal of fluoride from AIS glass industry effluent in the column reactor by Acinetobacter baumannii with time (h)	232



5.2.5	Atmospheric Conditions for Plant Growth Chamber	234
5.2.6	Constituents of Hoagland Solution	235
5.2.7	Variation of Contact Time on Removal of Fluoride	235
5.2.11	Accumulation of Fluoride in Root, Stem and Leaves for <i>Eichhornia crassipes</i>	238
5.3.1.1 (a)	Data Showing Effect of Contact Time on Fluoride Concentration	240
5.3.1.1 (b)	Percentage Removal of Fluoride	241
5.3.2 (a)	Chlorophyll Results of <i>Ipomoea aquatica</i> before and after Exposure to 20 ppm Fluoride Solution for 10 Days	244
5.3.2 (b)	Chlorophyll Results for <i>Eichhornia crassipes</i> before and after Exposure to 20 ppm Fluoride Solution for 10 Days	244
5.3.3 (a)	Accumulation of fluoride in Root, Stem and Leaves for <i>Ipomoea aquatica</i>	244
5.3.3 (b)	Accumulation of fluoride in Root, Stem and Leaves for <i>Eichhornia crassipes</i>	245
5.3.4 (a)	Summary of Bio Mass Degradation for <i>Ipomoea aquatica</i>	246
5.3.4 (b)	Summary of Bio mass Degradation for <i>Eichhornia crassipes</i>	246
5.3.5	Initial and Final concentration of Fluoride	246
5.3.8	Percentage Removal of Fluoride	248
5.3.8	Summary of Percentage Removal with pH Variation	249
6.2.1	Summary of optimized parameters and results obtained of various selected adsorbents for Fluoride removal	254

## LIST OF FIGURE

<b>Figure No.</b>	<b>Particulars</b>	<b>Page No.</b>
2.9.3 (a)	Formation of the SPADNS – ZrOCl <sub>2</sub> complex	23
2.9.3 (b)	Reaction of the Complex with Fluoride Ions	23
2.11.1	Mechanisms of Phytoremediation [source- Google Image]	41
2.11.7	Constructed wetland [source- Google Image]	43
2.11.8	Floating Platform [source-Google Image]	44
3.2	Calibration Curve	62
3.3.2 (a)	Photograph of Continuous Column Reactor	65
3.3.2 (b)	Line Diagram of Continuous Column Reactor	65
3.4.1	Photographic Images of Analytical Instruments Used in the Present Investigation	67
3.4.2	Photographic Images of Some Auxiliary Instruments used during the Present Investigation	68
3.4.2	Photographic Images of Some Auxiliary Instruments used during the Present Investigation	69
3.4.2	Photographic Images of Some Auxiliary Instruments used during the Present Investigation	70
3.6 (a)	Artificial Photosynthesis Chamber	71
3.6	Growth of (b) Ipomoea Aquatics plant and (c) water hyacinth Roots and Leaves	72
4.1	Experimental program for removal of Fluoride from Simulated synthetic waste water from glass industries using different treatment methods	74
4.2.3	Systematic block diagram of batch experiments for fluoride removal by adsorption using various adsorbents	80
4.3.2	Growth Curve Model	87
4.7	Calibration curve between Optical Density versus time (h)	89
4.7.1	Schematic block diagram of batch experimentation on removal of fluoride in SAB system	90
4.8	Mass Balance in a Fixed-Bed Column Element	92
4.12	Experimental Setup for Fixed Bed Column/Bio-column Reactor	97
5.1.2.1 (a)	FTIR spectra of GAC before adsorption of Fluoride	110
5.1.2.1 (b)	FTIR spectra of GAC after adsorption of Fluoride	110
5.1.2.2 (a)	FTIR spectra of <i>Citrus Limetta Peel</i> before Adsorption	111
5.1.2.2 (b)	FTIR spectra of <i>Citrus Limetta Peel</i> after Adsorption	111
5.1.2.3 (a)	FTIR spectra of ground nut shell before Adsorption	112
5.1.2.3 (b)	FTIR spectra of ground nut shell after Adsorption	112
5.1.2.4 (a)	FTIR spectra of Neem Leaves before Adsorption	113

5.1.2.4 (b)	FTIR spectra of Neem Leaves after Adsorption	113
5.1.2.5 (a)	FTIR spectra of Turmeric before Adsorption	114
5.1.2.5 (b)	FTIR spectra of turmeric after adsorption	114
5.1.2.5 (a)	FTIR spectra of MnO <sub>2</sub> coated turmeric before adsorption	115
5.1.2.5 (b)	FTIR spectra of MnO <sub>2</sub> coated turmeric after Adsorption	115
5.1.2.6 (a)	FTIR spectra of <i>Java plum seed</i> ( <i>Syzygiumcumini</i> ) before Adsorption	116
5.1.2.6 (b)	FTIR spectra of <i>Java plum seed</i> ( <i>Syzygiumcumini</i> ) after Adsorption	116
5.1.2.7 (a)	FTIR spectra of Banana peel before Adsorption	117
5.1.3.7 (b)	FTIR spectra of Banana peel after Adsorption	117
5.1.3.1.1	SEM of GAC (a) before adsorption (b) after fluoride adsorption	125
5.1.3.1.2	EDX of GAC (a) before adsorption (b) after fluoride adsorption	125
5.1.3.2.1	SEM of <i>Citrus limetta peel</i> (a) before adsorption (b) after fluoride adsorption	125
5.1.3.2.2	EDX of <i>Citrus limetta peel</i> (a) before adsorption (b) after fluoride adsorption	126
5.1.3.3.1	SEM of Ground nut shell (a) before adsorption (b) after fluoride adsorption	127
5.1.3.3.2	EDX of Ground nut shell (a) before adsorption (b) after fluoride adsorption	127
5.1.3.4.1	SEM of Neem leaves (a) before adsorption (b) after fluoride adsorption	128
5.1.3.4.2	EDX of Neem leaves (a) before adsorption (b) after fluoride adsorption	128
5.1.3.5.1	SEM of Turmeric (a) before adsorption (b) after fluoride adsorption	129
5.1.3.5.2	EDX of Turmeric (a) before adsorption (b) after fluoride adsorption	129
5.1.3.5.1	SEM of MnO <sub>2</sub> coated Turmeric (c) before adsorption (d) after fluoride adsorption	130
5.1.3.5.2	EDX of MnO <sub>2</sub> coated Turmeric (c) before adsorption (d) after fluoride adsorption	130
5.1.3.6.1	SEM of <i>Java plum seed</i> ( <i>Syzygiumcumini</i> ) (a) before adsorption (b) After fluoride adsorption	131
5.1.3.6.2	EDX of <i>Java plum seed</i> ( <i>Syzygiumcumini</i> ) (a) before adsorption (b) After fluoride adsorption	131
5.1.3.7.1	SEM of Banana peel (a) before adsorption (b) after fluoride adsorption	132
5.1.3.7.2	EDX of Banana peel (a) before adsorption (b) after fluoride adsorption	132
5.1.4.1.1	Effect of pH for removal of fluoride by GAC	137
5.1.4.1.2	Effect of pH for removal of fluoride by <i>Citrus limetta peel</i>	137
5.1.4.1.3	Effect of pH for removal of fluoride by Ground nut shell	138
5.1.4.1.4	Effect of pH for removal of fluoride by Neem leaves	138

5.1.4.1.5	Effect of pH for removal of fluoride by (a)Virgin turmeric (b) MnO <sub>2</sub> coated turmeric	139
5.1.4.1.6	Effect of pH for removal of fluoride by <i>Java plum seed</i> ( <i>Syzygiumcumini</i> )	140
5.1.4.1.7	Effect of pH for removal of fluoride by Banana peel	140
5.1.4.2.1	Effect of Dose for removal of fluoride by GAC	144
5.1.4.2.2	Effect of Dose for removal of fluoride by <i>Citrus limetta peel</i>	144
5.1.4.2.3	Effect of Dose for removal of fluoride by Ground nut shell	145
5.1.4.2.4	Effect of Dose for removal of fluoride by Neem leaves	145
5.1.4.2.5	Effect of Dose for removal of fluoride by (a)Virgin turmeric (b) MnO <sub>2</sub> coated turmeric	146
5.1.4.2.6	Effect of Dose for removal of fluoride by <i>Java plum seed</i> ( <i>Syzygiumcumini</i> )	146
5.1.4.2.7	Effect of Dose for removal of fluoride by Banana peel	147
5.1.4.3.1	Effect of Contact time for removal of fluoride by GAC	150
5.1.4.3.2	Effect of Contact time for removal of fluoride by <i>Citrus limetta peel</i>	150
5.1.4.3.3	Effect of Contact time for removal of fluoride by Ground nut shell	151
5.1.4.3.4	Effect of Contact time for removal of fluoride by Neem leaves	151
5.1.4.3.5	Effect of Dose for removal of fluoride by (a)Virgin turmeric (b) MnO <sub>2</sub> coated turmeric	152
5.1.4.3.6	Effect of Contact time for removal of fluoride by <i>Java plum seed</i> ( <i>Syzygiumcumini</i> )	152
5.1.4.3.7	Effect of Contact time for removal of fluoride by Banana peel	153
5.1.4.4.1	Effect of initial concentration for removal of fluoride by GAC	156
5.1.4.4.2	Effect of initial concentration for removal of fluoride by Citrus limetta	156
5.1.4.4.3	Effect of initial concentration for removal of fluoride by Ground nut shell	157
5.1.4.4.4	Effect of initial concentration for removal of fluoride by Neem leaves	157
5.1.4.4.5	Effect of initial concentration for removal of fluoride by (a)Virgin turmeric (b) MnO <sub>2</sub> coated turmeric	158
5.1.4.4.6	Effect of initial concentration for removal of fluoride by <i>Java plum seed</i> ( <i>Syzygiumcumini</i> )	158
5.1.4.4.7	Effect of initial concentration for removal of fluoride by Banana peel	159
5.1.6.1	Kinetic models for GAC (a) Pseudo-first order model (b) Pseudo-second order model and (c) Intra-particle Diffusion model	166
5.1.6.2	Kinetic models for Citrus Limetta Peel (a) Pseudo-first order model (b) Pseudo-second order model and (c) Intra-particle Diffusion model	167
5.1.6.3	Kinetic models for Ground nut shell (a) Pseudo-first order model (b)	168

	Pseudo-second order model and (c) Intra-particle Diffusion model	
5.1.6.4	Kinetic models for Neem leaves (a) Pseudo-first order model (b) Pseudo-second order model and (c) Intra-particle Diffusion model	169
5.1.6.5	Kinetic models for Virgin turmeric and (ii) MnO <sub>2</sub> coated turmeric (a) Pseudo-first order model (b) Pseudo-second order model and (c) Intra-particle Diffusion model	170
5.1.6.6	Kinetic models for <i>Java plum seed (Syzygiumcumini)</i> (a) Pseudo-first order model (b) Pseudo-second order model and (c) Intra-particle Diffusion model	171
5.1.6.7	Kinetic models for Banana peel (a) Pseudo-first order model (b) Pseudo-second order model and (c) Intra-particle Diffusion model	172
5.1.7.1	Isotherm models for GAC (a) Langmuir isotherm model (b) Freundlich isotherm model and (c) Temkin isotherm model	179
5.1.7.2	Isotherm models for Citrus Limetta peel (a) Langmuir isotherm model (b) Freundlich isotherm model and (c) Temkin isotherm model	180
5.1.7.3	Isotherm models for Ground nut shell (a) Langmuir isotherm model (b) Freundlich isotherm model and (c) Temkin isotherm model	181
5.1.7.4	Isotherm models for Neem leaves (a) Langmuir isotherm model (b) Freundlich isotherm model and (c) Temkin isotherm model	182
5.1.7.5	Isotherm models for MnO <sub>2</sub> coated turmeric (a) Langmuir isotherm model (b) Freundlich isotherm model and (c) Temkin isotherm model	183
5.1.7.5.	Isotherm models for Turmeric (d) Langmuir isotherm model (e) Freundlich isotherm model and (f) Temkin isotherm model	184
5.1.7.6	Isotherm models for <i>Java plum seed (Syzygiumcumini)</i> (a) Langmuir isotherm model (b) Freundlich isotherm model and (c) Temkin isotherm model	185
5.1.7.7.	Isotherm models for Banana peel (a) Langmuir isotherm model (b) Freundlich isotherm model and (c) Temkin isotherm model	186
5.1.8.3.4.2	BDST Plot at 7.5% Breakthrough in a Fixed-bed Column at Different Flow Rates	193
5.1.8.3.5. (a)	Effect of Bed Depth on breakthrough time at a constant flow rate of 23 ml min <sup>-1</sup> (Co=20 mgL <sup>-1</sup> )	195
5.1.8.3.5. (b)	Effect of Bed Depth on breakthrough time at a constant flow rate of 12 ml min <sup>-1</sup> (Co=20 mgL <sup>-1</sup> )	195
5.1.8.3.5. (c)	Effect of Bed Depth on breakthrough time at a constant flow rate of 40 ml min <sup>-1</sup> (Co=20 mgL <sup>-1</sup> )	196
5.1.8.3.5. (d)	Effect of Bed Depth on breakthrough time at a 100 cm fixed Bed Column (a) 40 (b) 23, (c) 12 ml min <sup>-1</sup> (Co=20 mgL <sup>-1</sup> )	196
5.1.8.3.7	Adsorbent Exhaustion Rate versus EBRT	197
5.1.8.3.8	Liberalized Thomas Model plot at 7.5% Breakthrough for Adsorption of 20 mg L <sup>-1</sup> Fluoride Solution with 23 mL min <sup>-1</sup> Flow	198

	Rate at Different Bed Depths	
5.1.8.4.1 (a)	Pseudo-Second Order Model	199
5.1.8.4.1 (b)	Percentage Removal versus Time	199
5.1.8.4.2	Effect of pH on Fluoride Adsorption on <i>Java plum seed</i> ( <i>Syzygiumcumini</i> ) (Initial Fluoride Concentration 20 mg/L Equilibrium Contact Time 1 hr, Adsorbent Dose 20g/L, Shaken Speed 120 rpm and Temp 30± 1 °C)	200
5.1.8.4.3 (a)	Freundlich Isotherm Plot for Fluoride Adsorption on <i>Java plum seed</i> ( <i>Syzygiumcumini</i> ) (Initial Fluoride Concentration 20 mg L <sup>-1</sup> , Initial pH 6.9±0.1, Equilibrium Contact Time 1 hour, Adsorbent Dosage 20 g/L, Shaken Speed 120 rpm and Temperature 30±1°C).	201
5.1.8.4.3 (b)	Langmuir Isotherm Plot for Fluoride Adsorption on <i>Java plum seed</i> ( <i>Syzygiumcumini</i> ) (Initial Fluoride Concentration 20 mg L <sup>-1</sup> , Initial pH 6.9±0.1, Equilibrium Contact Time 1 hour, Adsorbent Dosage 20 g/L, Shaken Speed 120 rpm and Temperature 30±1°C)	202
5.1.8.5.1	SEM image of <i>Java plum seed</i> ( <i>Syzygiumcumini</i> ) before adsorption and after adsorption	204
5.1.8.5.2	EDX of <i>Java plum seed</i> ( <i>Syzygiumcumini</i> ) before and after adsorption	204
5.1.9.2.1	Graph Plotted between the Percentage Removal of Fluoride and pH and Effect of pH on the (ii) <i>Bio Removal of Fluoride</i> and (i) <i>Citrus Limetta peel</i>	206
5.1.9.2.2	Graph Plotted Between the Percentage Removal of Fluoride and Dose and Effect of Adsorbent Dose on the (ii) <i>Bio Removal of Fluoride</i> and (i) <i>Citrus Limetta peel</i>	207
5.1.9.2.3	Graph Plotted Between (i) Percentage Removal versus Initial Concentration (mg/l), (ii) Adsorption Capacity q <sub>e</sub> (mg/g) and (iii) Residual Concentration c <sub>e</sub> (mg/l)	208
5.1.9.2.4	Graph Plotted Between the Percentage Removal of Fluoride and Contact Time (h) on the Bio Removal of Fluoride	209
5.2.0.1	Pseudo First Order Kinetics Plotted between Log (q <sub>e</sub> -q <sub>t</sub> ) versus Time (h)	209
5.2.0.2	Pseudo Second Order Kinetics Plotted between t/q <sub>t</sub> versus Time (h)	210
5.2.1.1 (a)	Graph for Langmuir Isotherm Model Plotted between 1/q <sub>e</sub> vs. 1/c <sub>e</sub> for Bio Removal	213
5.2.1.1 (b)	Graph for Langmuir Isotherm Model Plotted between 1/q <sub>e</sub> vs. 1/c <sub>e</sub> for Adsorption	213
5.2.1.2 (a)	Graph for Freundlich Isotherm Model Plotted between log (q <sub>e</sub> ) vs. log(c <sub>e</sub> ) for Bio Removal	213
5.2.1.2 (b)	Graph for Freundlich Isotherm Model Plotted between Log (q <sub>e</sub> ) vs. log(c <sub>e</sub> ) for Adsorption	214
5.2.1.3 (a)	Graph for Temkin Isotherm Model Plotted between q <sub>e</sub> vs. ln(c <sub>e</sub> ) for Bio Removal	214
5.2.1.3 (b)	Graph for Temkin Isotherm Model Plotted Between q <sub>e</sub> vs. ln(c <sub>e</sub> ) for Adsorption	214

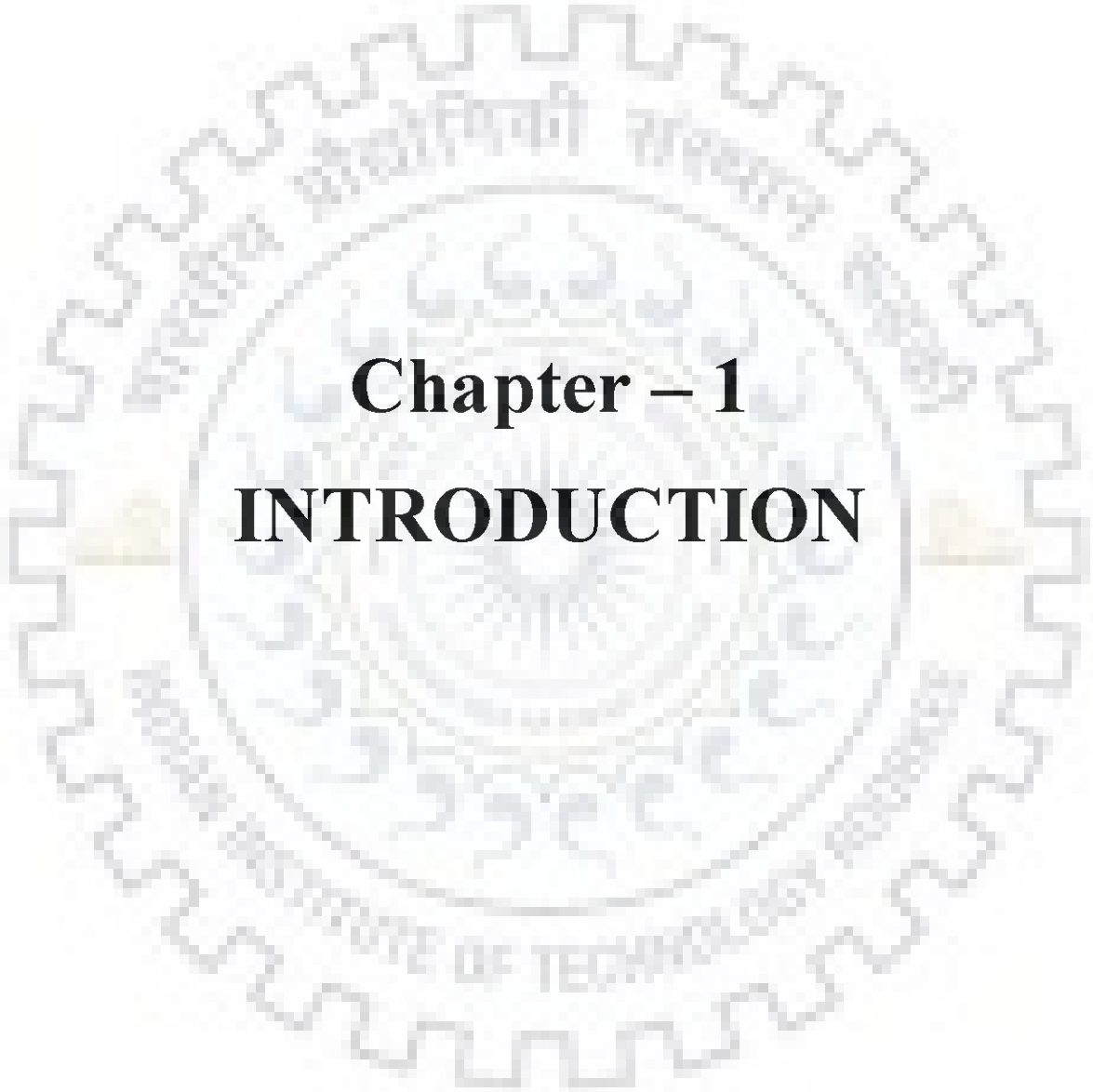
5.2.2.1.5.3	BDST Plot at 7.5% Breakthrough in a Fixed-Bed Column at Different Flow Rates	220
5.2.2.1.5.4	Effect of Flow Rate on the Fluoride Removal in the Biocolumn Reactor (Height=100cm, Initial Fluoride Concentration= 20mg/L)	222
5.2.2.1.5.5(a)	Effect of Bed Height on Fluoride Removal in the Bio-Column Reactor (Flow rate: 12 ml/min, Initial Fluoride Concentration= 20mg/L)	223
5.2.2.1.5.5(b)	Effect of Bed Height on Fluoride Removal in the Bio-Column Reactor (Flow Rate: 23 ml/min, Initial Fluoride Concentration = 20mg/L)	223
5.2.2.1.5.5(c)	Effect of Bed Height on Fluoride Removal in the Bio-Column Reactor (Flow Rate: 40 ml/min, Initial Fluoride Concentration= 20mg/L)	224
5.2.2.1.5.6	Adsorbent Exhaustion Rate versus EBRT	224
5.2.2.1.5.7(a)	Change of pH with Time of Operation in Bio-Column Reactor	225
5.2.2.1.5.7(b)	Variation of DO with Time	226
5.2.3.5	Graph Showing Variation of Exit Age Distribution with Reduced Time for Packed Bed Reactor	230
5.2.4	Removal of fluoride from AIS glass industry effluent in the column reactor by <i>Acinetobacter baumannii</i>	233
5.2.7	Effect of Contact Time on Percentage Removal	236
5.2.8	Concentration versus Time for Fluoride Having Constant pH for <i>Water Hyacinth</i>	237
5.2.9	Percentage Removal versus Concentration Study with varying pH for <i>Water Hyacinth</i>	237
5.3.10	Percentage Removal Vs Time for <i>Water Hyacinth</i>	238
5.2.11	Accumulation for 20 ppm for <i>Water Hyacinth</i>	239
5.3.1.1 (a)	Effect of Time on Concentration of Fluoride	241
5.3.1.1 (b)	Shows Percentage Removal of Fluoride from Water in Touch with Plants (ii) <i>Eichhornia crassipes</i> and (i) <i>Ipomoea aquatica</i> for Concentration of 20 mg/L	242
5.3.2 (a)	Chlorophyll Study for <i>Ipomoea aquatic</i>	243
5.3.2 (b)	Chlorophyll Study for <i>Eichhornia crassipes</i>	243
5.3.3	Pictorial Representation of Fluoride Accumulated by Different Parts of Plant	245
5.3.6 (a)	Effect of Contact Time on Concentration of Fluoride for <i>Ipomoea aquatica</i>	247
5.3.6 (b)	Effect of Contact Time on Concentration of Fluoride for <i>Eichhornia crassipes</i>	247
5.3.7 (a)	Percentage Removal versus Time for Fluoride Having Constant pH for <i>Ipomoea aquatic</i>	248
5.3.7 (b)	Percentage Removal versus Time for Fluoride Having Constant pH	249

**NOMENCLATURE****SYMBOLS**

a	Slope of BDST plot ( $\text{h cm}^{-1}$ )
b	Intercept on the ordinate of BDST plot (h)
B	Langmuir constant ( $\text{mg g}^{-1}$ )
$C_b$	Breakthrough fluoride concentration ( $\text{mg L}^{-1}$ )
$C_e$	Equilibrium solute concentration ( $\text{mg L}^{-1}$ )
$C_o$	Column influent or initial fluoride concentration ( $\text{mg L}^{-1}$ )
$C_t$	Column effluent fluoride concentration at time t ( $\text{mg L}^{-1}$ )
D	Packed-bed column depth (cm)
$D_{\min}$	Minimum bed depth sufficient to prevent the effluent concentration to exceed the desired breakthrough concentration at zero time (cm)
$D_e$	Effective diffusion coefficient ( $\text{cm}^2 \text{s}^{-1}$ )
DW	Dry weight
$\epsilon$	Bed porosity (dimensionless)
K	Adsorption rate constant ( $\text{L mg}^{-1} \text{h}^{-1}$ )
$K_d$	The linear distribution coefficient ( $\text{cm s}^{-1}$ )
$K_F$	Adsorption capacity ( $\text{mg g}^{-1}$ ) based on Freundlich isotherm
$k_T$	Thomas rate constant ( $\text{L min mg}$ )
m	Mass of adsorbent in column (g)
n	Freundlich adsorption equilibrium constant (dimensionless)
$N_o$	Average adsorption capacity per volume of bed ( $\text{mg cm}^{-3}$ )
$q_o$	Maximum solid phase concentration of the solute ( $\text{mg g}^{-1}$ )
q	Amount of solute adsorbed per unit weight of material ( $\text{mg g}^{-1}$ )
$q_m$	Maximum adsorption capacity ( $\text{mg g}^{-1}$ )
$Q_v$	Volumetric flow rate ( $\text{mL min}^{-1}$ )
$T_b$	The service time at breakthrough point (h)
V	Throughput volume (mL)
v	Linear flow rate through the bed ( $\text{cm h}^{-1}$ )



$V_a$	Bulk volume (L)
$V_b$	Volume of water treated at breakthrough (L)
$V_p$	Porous volume (L)
$x$	Liquid retention time (min)
$y$	Adsorbent exhaustion rate ( $\text{g L}^{-1}$ )
$\alpha$	Minimum liquid retention time (min)
$\beta$	Minimum adsorbent exhaustion rate ( $\text{g L}^{-1}$ )
$\gamma$	EBRT constant ( $\text{min g L}^{-1}$ )
$\rho_s$	Density of the solid phase ( $\text{g cm}^{-3}$ )
$\alpha$	is Initial sorption rate ( $\text{mg/g.min}$ ).
$\beta$	is related to extent of surface coverage and activation energy for chemisorptions.
$k_1$	is the rate constant of pseudo first-order kinetics.
$k_2$	is the rate constant for the pseudo second-order kinetics.
$q_e$	is the amount of fluoride adsorbed on adsorbent ( $\text{mg/g}$ ).
$q_t$	is the amounts of fluoride adsorbed on adsorbent at equilibrium and at time $t$ (min).
$K_{ip}$	is the intra-particle diffusion rate constant
$R^2$	is the correlation coefficient
SSE	is sum of squared error



**Chapter – 1**  
**INTRODUCTION**

## INTRODUCTION

---

### 1.0 General

Water is generally regarded as a universal solvent as it has the power to mix almost all minerals which comes in its touch due to its polar and non-polar nature. Some elements like fluoride are necessary for human beings in trace amount, but if taken in higher concentration can cause toxic effects. Concentration of fluoride is increasing in water bodies due to the various reasons. This increase can be due to rapid growth in population of cities and increase in the number of modern industries (anthropogenic source of fluoride) as well as geo-chemical dissolution of fluoride bearing minerals (natural source of fluoride).

In India, along with major parts across the globe, where drinking water contains more fluoride (F) than maximum permissible limit have serious health problems for human beings as endemic skeletal fluorosis (WHO, 1984, Anasuya et al., 1996). Presence of fluoride with concentration much higher than permissible limit has caused severe health related hazards for humans, major of which is skeletal and dental fluorosis.

High amount of fluoride in consumable water often results in demolition of enamel of teeth and cause much more problems which are altogether termed fluorosis (WHO, 2006, D. Ortiz et al., 2003). In India, problem of high level of contaminants in water (both consumable and waste water) appears in toxicological and geo-environmental issues to be focused upon. Since thirty years, many diseases have been stressed upon among which “fluorosis” is one of them. It is caused by excessive amount of fluoride in water resources.

Fluorosis has achieved an alarming dimension all over the globe. It is wide spread even in developing countries like China, Kenya, Algeria, Turkey, Morocco, Senegal, Thailand and Argentina and in the developed countries like USA and Japan. In India, prevalence of fluorosis is one of the serious health problems.

Presently, 17 states of India which are endemic to fluorosis are Karnataka, Delhi, Tamil Nadu, J&K, Haryana, U.P, Andhra Pradesh, Maharashtra, Gujarat, Kerala, Rajasthan, Punjab and Himachal Pradesh.

In India the water fluoride level varies between 2-29 ppm, as against the maximum allowed limit in drinking water according to Indian Standard (IS 10500, 2005) and guideline of World Health Organization (WHO) is 1.0 - 1.5 ppm. In tropical countries like Mexico, Costa Rica etc. people suffer from skeletal fluorosis, although the concentration of fluoride detected is lower than permissible limit in consumable water. Epidemiological inspection tells us that chronic fluoride toxicity might be influenced by nutritional status. Generally fluoride is dissolved in contaminated water and is easily absorbed by the human body. After which it is distributed all over the body crossing membranes and going into tissues very quickly.

In recent decades, human dependency on groundwater increases as we exploit groundwater to meet our need of water. This dependency can be attributed to the scarceness, bacteriological pollution and non-handiness of surface waters in under-developed as well as developing countries. In order to provide right facilities for safe drinking water for rural areas in India, a large number of tube well, hand pumps etc. are being provided since 1970 because there is hardly any bacteriological contamination in ground water. As a result the number of patients with diseases due to water problem has reduced a lot, but still it leads to appearance of other hazards for health as in major areas of India there is a problem of excess chemical compounds like fluoride and arsenic in groundwater. These issues arise as major among the geo-environmental issues which our country is presently facing (Oliverj et al., (1986), Muhammad F and Anita Ramli, (2011)).

Many strategies were proposed and examined all over the world for removal of fluoride from water. They are mostly based upon the principles of absorption, ion exchange and precipitation. However, these have several disadvantages limited efficiency, high cost technology, taboo limitations and unnoticeable breakthrough (Nawlakhe et al., 1979). Use of lime, gypsum-fluorite filters, dolomite, granulated bone media, activated carbon, superphosphate, tri-calcium phosphate bone charcoal, magnesite, alum, poly aluminium chloride, activated alumina and aluminium sulphate is needed for carrying out these methods (Phantumvanit et al., (1988), NVR et al., (1988)). Some methods were used to remove high amount of fluoride from water bodies such as adsorption (Liao and Shi, (2005),

Lvl, (2007)), (Pommerenk and Schafran, (2005), precipitation (Reardon and Wang, (2000)), ion-exchange (Castelc et al., (2000)), electrodialysis (Amor et al.,(2001)) and electrochemical methods (Fengshen et al., (2003)). Among these, precipitation and adsorption are two most important techniques used for water defluoridation.

A very little attention is given and no concrete work is done in the preliminary stages to the presence of these chemical compounds, as symptoms of diseases are seen after a long time of consumption of contaminated water.

### **1.1 Objectives of the present study**

Due to rapid industrialization there is a negative consequence on the environment, which affects human beings and even flora and fauna. Effluents discharged from the various industries contaminate ground water, surface water and other sources of drinking water. Therefore the treatment of toxic pollutants is essential. In the present work simultaneous removal of fluoride from industrial waste water using synthetic simulated waste water containing fluoride based on industrial waste water composition was carried out. Based on extensive literature review following objectives have been laid down:

- Estimation of the best adsorbent for the maximum individual and simultaneous removal of fluoride from single synthetic simulated waste water in batch process.
- Simultaneous adsorption and bio-accumulation of fluoride with using consortium culture of *Acinetobacter baumannii* (MTCC No. 11451) in SBB (Simultaneous Bioaccumulation) batch reactor.
- Continuous study for simultaneous removal of fluoride from synthetic simulated waste water in continuous flow packed bed reactor (PBCFR).
- Extension of present study for the treatment of real industrial waste water.
- Phytoremediation of fluoride from single solution in artificial photosynthesis chamber using *Aquatic* macrophyte water hyacinth (*Eichhornia crassipes*).

### **1.2 Organization of Thesis**

The present thesis has been divided into the following chapters for the easy understanding of the subject matter. The present thesis is organized as follows:

## **Chapter 1: Introduction**

This chapter deals with the importance of topic, health effect, treatment technologies available, problem identification and objectives of the work.

## **Chapter 2: Literature Review**

This chapter deals with the review of all possible literature, published regarding fluoride remediation from synthetic as well as industrial water, using various methods such as adsorption, bio removal, SAB (Simultaneous adsorption and bioaccumulation of fluoride), continuous reactor study and phytoremediation.

## **Chapter 3: Experiment setup and Instrumentation**

In this chapter deals with the experimental set up, equipment/ instrument used for the present study.

## **Chapter 4: Experimental Program**

This chapter deals with the details of experimental conducted the present work in the sequential order.

## **Chapter 5: Results and Discussions**

This chapter describes the results and discussion of the present work as follows:

- 1. Batch adsorption study:** Batch adsorption studies for the removal of fluoride from single solution were carried out. Characterization of biosorbent such as BET surface area, Ultimate and Proximate analysis, FTIR, SEM and EDX were conducted for the confirmation of adsorption of fluoride. The effects of process parameters like pH, temperature, adsorbent dose (mg/g), contact time (h) and initial concentration of fluoride (mg/L) were investigated. Kinetic adsorption equilibrium isotherm modelling was also carried out.
- 2. Bio-removal of fluoride:** Bio removal of fluoride from single substrate solution of fluoride was conducted. The bacterial strain *Acinetobacter baumannii* MTCC 11451 is used to complete this study. This bacterium was supplied by Microbial Type Culture Collection, Chandigarh, India. The strains were revived according to the instructions given by MTCC (MTCC guidelines). Cultures were stored on agar plates till further use and were sub-cultured after every 15-30 days. All inoculations were performed in aseptic conditions in laminar air flow unit (Rescholar

equipment, India). Various kinetics models such as Bed Depth Service Time Model, Empty Bed Contact Time and Fixed-Bed Design Models, were applied for the experimental data.

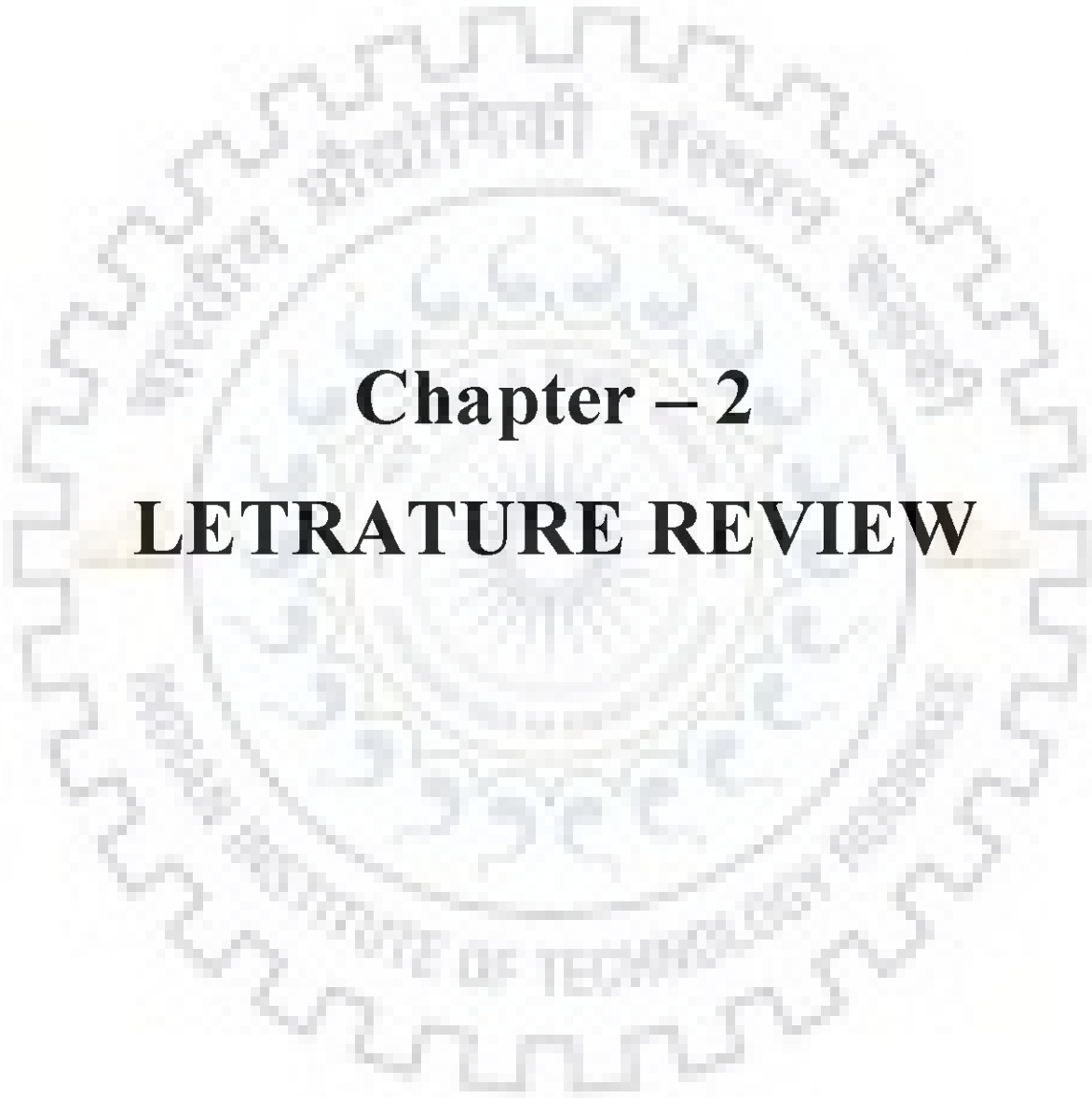
3. **SAB (Simultaneous adsorption and bioaccumulation of fluoride)** : In this section simultaneous adsorption and bio-accumulation of fluoride were carried out immobilizing the bacterium *Acinetobacter baumannii* onto the surface various adsorbent such as *Citrus limetta peel*, *Java plum seed (Syzygiumcumini)*, selected based on the batch adsorption studies. Characterization of adsorbent before and after SAB process such as BET surface area, Ultimate and proximate analysis, FTIR, SEM and EDX were also carried out. Kinetics and equilibrium adsorption isotherm modelling were also carried out for SAB study.
4. **Continuous Study:** In this section continuous simultaneous removal of fluoride was carried out in packed bed column. The *Java plum seed (Syzygiumcumini)* waste was packed in the continuous column reactor in synthetic simulated waste water was used for the experiment. *Acinetobacter baumannii* was immobilized on to the surface of packed bed for the simultaneous adsorption and bioaccumulation of fluoride. The effect of process parameters such as bed height (cm), flow rate (mL/min), pH and dissolved oxygen (DO) were also investigated. Kinetic modeling of the experimental data was also performed.
5. **Phytoremediation:** In this section the uptake of fluoride by *Aquatic* macrophyte water hyacinth (*Eichhornia crassipes*) from single simulated synthetic waste water in the artificial photosynthesis chamber was conducted. The chlorophyll content of the plant was also measured before and after uptake of fluoride to understand the effect of fluoride on to the plants and environment.

## **Chapter 6: Conclusion and Recommendation**

This chapter deals with the detailed conclusion of the present study as described above.







## **Chapter – 2**

# **LITERATURE REVIEW**

## LITERATURE REVIEW

---

### 2.0 Sources of Fluoride

Fluorine is highly reactive and is found naturally as  $\text{CaF}_2$ . It is an essential constituent in minerals like topaz, fluorite, fluorapatite, cryolite, phosphorite, fluorapatite, etc.

Many industries use fluoride containing salts such as hydrofluoric acid. Table 2.0 lists out the various industries which use fluoride as one of its initial products. Fluoride dust and fumes pollute the air of our surroundings, inhaling this dust or fumes are as dangerous as consuming fluoride containing food or water.

In the developed countries which rely too much on industries, industrial fluorosis emerged as one of the serious threat. In India, industrialization is going on done at a very rate, thus increasing the hazardous effects of industrial fluorosis which reached its threshold state and is causing problems of water and food borne fluorochosis and endemic.

**Table 2.0: Industries using Fluoride with Major Examples of Such Companies**

S.No	Industry	Major Examples	Country Name
1.	Aluminium	Bharat Aluminium Co. Ltd., Hindalco Industries Ltd	India
2.	Steel	SAIL, Bajaj Steel Industry	India
3.	Chemical Industries I	Tata Chemicals, UPL Limited	India
4.	Automobile Industry	Hero, Honda, Suzuki, Yamaha	India
5.	Glass	Asahi India Glass Limited, Hindustan National Glass and Industries Ltd	India
6.	Bricks	-----	
7.	Phosphate Fertilizer	Coromandel International Ltd., Gujarat State Fertilizers & Chemicals Ltd.	India
8.	Welding	Ador, ESAB	India
9.	Refrigeration	Sea Bird Refrigeration Pvt. Ltd., Rama refrigeration	India
10.	Rust Removal	-----	
11.	Oil Refinery	Essar Refinery (Essar Oil), Haldia Refinery (IOC),	India
12.	Plastic	Supreme Industries, Nilkamal	India
13.	Pharmaceutical	Ranbaxy Laboratories Ltd., Cipla Ltd.	India
14.	Toothpaste.	Unilever, ITC	India

## 2.1 Indian Scenario

In India, fluorided commonly occurs in earth's crust as Fluorspar ( $\text{CaF}_2$ ), Appetite and Rock Phosphate and Phosphoresces Table 2.1. (Shrikant et al.2012).Contains information about concentration of fluoride in various minerals.

### 2.1.1 Fluorspar

Fluorspar occurs in sandstone, quartz, barite, granite, calcite and limestone. The major deposits of the above are found in nine states of India viz. Gujarat, Andhra Pradesh, Himachal Pradesh, Madhya Pradesh, Tamil Nadu, Bihar, West Bengal, Rajasthan, and Jammu & Kashmir.

### 2.1.2 Apatite and Rock Phosphate

In India, the two states which are rich in apatite and rock phosphate are Andhra Pradesh and Bihar. Minor occurrences have also been reported from other states, viz. Tamil Nadu, West Bengal, Rajasthan, Gujarat, and Odisha.

### 2.1.3 Phosphorites

Phosphorites (sedimentary phosphate deposits) are the third major source of fluoride. Regions in India where there is excess of phosphorites are North-West of India, comprising the States of Jammu & Kashmir, Uttar Pradesh, Tamil Nadu, and Rajasthan. There are few minor occurrences in other state also. Fluoride occurs significantly in rocks, soils, plants and crops, drugs, industrial processes etc.

**Table 2.1: Concentration of Fluorides in different Minerals.** (Shrikant et al., 2012).

S.No.	Minerals	Fluoride (mg/L)
1.	Meteorites	28-30
2.	Dunite	12
3.	Basalt	100
4.	High Calcium	520
5.	Granite	---
6.	Alkali rocks	1200-8500
7.	Shale	740
8.	Sand stone	270
9.	Deep sea clays	1300
10.	Deep sea carbonates	540

## 2.2 Physicochemical Properties of Fluoride Compounds

Different properties of fluoride are given in Table 2.2(a) (SinghTP. Majumder, C.B.2017)

**Table 2.2 (a): Properties of fluoride** (SinghTP. Majumder, C.B.2017)

Property	Value
Physical State	Pale Yellow Green Coloured Gas
Melting Point	-219°C
Boiling Point	-188°C
Density	$1.8 \times 10^{-3}$ g/cm <sup>3</sup> at 20°C
Water Solubility	42 g/L at 10°C
Atomic Mass	18.998403 g/mol

The physicochemical properties of fluorides available in the form of Sodium Fluoride (NaF), Hydrogen Fluoride (HF) and Fluorsilicic acid are given in Table. 2.2(b). (Singh TP. Majumder, C.B.2017)

**Table 2.2(b): Physiochemical Property of Various Fluoride Compounds**  
(SinghTP. Majumder, C.B.2017)

S.No	Property	Sodium fluoride (NaF)	Hydrogen Fluoride (HF)	Fluorsilicic acid
1.	Physical State	White Crystalline Solid	Colourless liquid or gas with pungent smell	colourless solid with pungent smell
2.	Density(g/cm <sup>3</sup> )	2.5600	----	1.220
3.	Solubility in water	42g/L at 10°C	Readily soluble below 20°C	Miscible
4.	Acidity	-----	Strong Acid in Liquid form, Weak as an aqueous phase	Strong Acid

## 2.3 Various Health Impacts of Fluoride

Ministry of Rural Development, Government of India conducted a survey recently of which reveals that in more than 8700 villages a population of not less than 30 million people are infected by fluoride related diseases which is a cause of great concern for the developing countries like India. Table 2.3 (a) (SinghTP. Majumder, C.B.2015). Incorporates the fluoride affected area statewise in India. Till today there is no permanent cure for this ailment so prevention measures should be

implemented properly. To get rid of this ailment it is necessary to derive a method by means of which we could remove fluoride from the contaminants water. We must also consider economic status, local conditions, literacy of community, availability of media, reuse of exhausted media, and viability of the treatment method before taking it into use. The major fluoride affected areas across the country are as follows:

**Table 2.3 (a): Fluoride Affected Areas in India** (SinghTP. Majumder, C.B.2015)

S.No.	Name of State	Affected districts	Range of F <sup>-</sup> (mg/L.)
1.	Assam	Goalpara, Kamrup, Karbi Anglong, and Nagaon	1.45 - 7.8
2.	Andhra Pradesh	Adilabad, Anantpur, Chittoor, Guntur, Hyderabad, Karimnagar, Khammam, Krishna, Kurnool, Mahbubnagar, Medak, and Nalgonda	1.8 - 8.4
3.	Bihar	Aurangabad, Banka, Buxar, Jamui, Kaimur (Bhabua), Munger, Nawada, Rohtas, and Supaul	1.7 - 2.85
4.	Chhattisgarh	Bastar, Bilaspur, Dantewada, Janjgir-Champa, Jasper, Canker, Korba, Koriya, Mahasamund, Raipur, Rajnandgaon, and Surguja	1.5 - 2.7
5.	Delhi	East Delhi, North West Delhi, South Delhi, South West Delhi, West Delhi, Kanjhawala, Najafgarh, and Alipur	1.57 - 6.10
6.	Gujarat	Ahmadabad, Amreli, Anand, Banaskantha, Bharuch, Bhavnagar, Dohad, Junagadh, Kachchh, Mehsana, Narmada, Panchmahals, Patan, Rajkot, Sabarkantha, Surat, Surendranagar, and Vadodara	1.6 - 6.8
7.	Haryana	Bhiwani, Faridabad, Gurgaon, Hissar, Jhajjar, Jind, Kaithal, Kurushetra, Mahendragarh, Panipat, Rewari, Rohtak, Sirsa, and Sonapat	1.5 - 17
8.	Jammu, Kashmir	Doda, Rajauri, and Udhampur	2.0 - 4. 21
9.	Karnataka	Bagalkot, Bangalore, Belgaun, Bellary, Bidar, Bijapur, Chamarajanagar, Chikmagalur, Chitradurga, Davangere, Dharwad, Gadag, Gulburga, Haveri, Kolar, Koppal, Mandya, Mysore, Raichur, and Tumkur	1.5 - 4.4
10.	Kerala	Palakkad, Palghat, Allepy, Vamanapuram, and Alappuzha	2.5 - 5.7
11.	Maharashtra	Amravati, Chandrapur, Dhule, Gadchiroli, Gondia, Jalna, Nagpur, and Nanded	1.51 - 4.01
12.	Madhya Pradesh	Bhind, Chhatarpur, Chhindwara, Datia, Dewas, Dhar, Guna, Gwalior, Harda, Jabalpur, Jhabua, Khargaon, Mandsaur, Rajgarh, Satna, Seoni, Shajapur, Sheopur, and Sidhi	1.5 - 10.7

S.No.	Name of State	Affected districts	Range of F <sup>-</sup> (mg/L.)
13.	Orissa	Angul, Balasore, Bargarh, Bhadrak, Bandh, Cuttack, Deogarh, Dhenkanal, Jajpur, Keonjhar, and Sonapur	1.52 - 5.2
14.	Punjab	Amritsar, Bhatinda, Faridkot, Fatehgarh Sahib, Firozpur, Gurdaspur, Mansa, Moga, Muktsar, Patiala, and Sangrur	0.44 - 6.0
15.	Rajasthan	Ajmer, Alwar, Banaswara, Barmer, Bharatpur, Bhilwara, Bikaner, Bundi, Chittaurgarh, Churu, Dausa, Dhaulpur, Dungarpur, Ganganagar, Hanumangarh, Jaipur, Jaisalmer, Jalor, Jhunjhunun, Jodhpur, Karauli, Kota, Nagaur, Pali, Rajsamand, Sirohi, Sikar, SawaiMadhopur, Tonk, and Udaipur	1.54 - 11.3
16.	Tamilnadu	Coimbatore, Dharmapuri, Dindigul, Erode, Karur, Krishnagiri, Namakkal, Perambalur, Puddukotai, Ramanathapuram, Salem, Sivaganga, Theni, Thiruvannamalai, Tiruchirapally, Vellore, and Virudhunagar	1.5 - 3.8
17.	Uttar Pradesh	Agra, Aligarh, Etah, Firozabad, Jaunpur, Kannauj, Mahamaya Nagar, Mainpuri, Mathura, and Mau	1.5 - 3.11
18.	West Bengal	Bankura, Bardhaman, Birbhum, Dakshindinajpur, Malda, Nadia, Purulia, and Uttardinajpur	1.5 - 9.1

Fluoride hinders the path of enzymes that produce acid-breeding oral bacteria whose acid chunk away our tooth enamel. Some researchers believe that harmful effects caused by fluoride are more than its helpful effects. Table 2.3 (b) provides the effect of amount of fluoride on our body. (Jacks et al., 2005)

**Table 2.3 (b): Effects of Different Concentration of Fluoride (Jacks et al., 2005)**

Concentration of fluoride	Medium	Effects
1 ppm	Water	Dental caries reduction
2 ppm or < 2 ppm	Water	Mottled enamel (dental fluorosis)
8 ppm	Water	10% osteosclerosis
20-80mg/day	Water or food	Crippling skeletal fluorosis
50 ppm	Water or food	Thyroid changes
100 ppm	Water or food	Growth retardation
125 ppm	Water or food	Kidney changes
2.5-5.0g	Acute dose	Death

Presently there is no doubt all over the world that fluoride if taken in excessive amount results in loss of calcium from tooth matrix, causing cavity formation instead of remedying it throughout life thus causing dental fluorosis. Incurable crippling of skeletal fluorosis can be caused by chronic, cumulative and severe over exposure. Table 2.3 (c) (Jacks et al., 2005) shows various form of diseases occurred due to fluoride.

**Table 2.3 (c): Effect of Various Type of Fluorosis (Jacks et al., 2005)**

Type	Effect
Skeletal Fluorosis	Effects Bone and Skeleton Major areas are neck, hip, shoulder and knee Joint Not easily Detectable In severe cases complete rigidity of joints.
Non-Skeletal Fluorosis	Effected part is Soft tissue Cardiac problem Still Birth Male Infertility
Dental Fluorosis	Teeth becomes yellow No treatment Cosmetic implication Common in Children

Fluoride is an electronegative element and thus having a (-) ve charge which is attracted by positively charged ions like calcium ( $Ca^{+}$ ). In our body, bones and tooth have highest amount of calcium thus attracting maximum amount of fluoride and thus deposited as calcium fluor apatite crystals. Intake of fluoride with concentration above 1.5 mg/L may cause several serious deformations. Maximum allowed extent of fluoride defined by different organizations in drinking water which a human can intake is given in Table 2.3(d) (Malay et al., 2011). Table 2.3(e) shows the number of habitations in different states where fluoride concentration in water is more than those of prescribed level which is 1.5 mg/L.

### 2.3.1 Dental Fluorosis

Even when the concentration of fluoride is in the range 0.7-1.5 mg/L in consumable water it has been observed that there are cases of mottled teeth. The minimal intake that can cause very mild or mild fluorosis is estimated around 0.1mg/kg body weight, which means for a person weighting 70 kg fluorosis may be caused, if he takes 7 mg of fluoride in a day.

### 2.3.2 Skeletal Fluorosis

This occurs when a large amount of fluoride gets deposited inside our skeleton which is more in cancellous bone than cortical bone. Fluoride poisoning leads to pain associated with rigidity and restrictive movements of knee and pelvic joints, shoulder joints along with cervical and lumbar spine.

**Table 2.3 (d): Maximum Permissible Limit of Fluoride in Drinking Water as Per the Standards of Various Organizations (Malay et al., 2011)**

S.No	Organization	Max. permissible limit of fluoride ions
1.	U.S. Public Health Standard	0.8
2.	International standard for drinking water	0.5
3.	Recommendation by Indian Council of Medical Research	1.0
4.	The Public health, Engineering manual and Code of Practice Committee, Govt. of India	1.0
5.	Guidelines issued by WHO	1.5
6.	Indian Standard Bureau	1.2
7.	ISI recommendation	1.5

**Table 2.3 (e): Information summary on the Excessive Fluoride in Ground Water in India (Malay et al., 2011)**

State	Number of Habitation with excess fluoride	State	Number of Habitation with excess of fluoride
Gujarat	2378	Orissa	1138
Andhra Pradesh	7548	Madhya Pradesh	201
Kerala	287	Rajasthan	16560
Karnataka	860	Punjab	700
Himachal Pradesh	488	West Bengal	21
Haryana	334	Uttar Pradesh	1072
Meghalaya	33	Tamil Nadu	527

### 2.4 Defluoridation of Water

Solvent extraction, ion exchange, chemical oxidation, electrochemical methods, adsorption and biological methods are treatment technologies used to remove fluoride from wastewater. Selection of an effective and adequate treatment technique depends on various factors like economy and



wastewater characteristics. Scientist are working hard to find new alternatives that have low losses and are cheap, economic, eco-friendly, and competent.

There are basically three approaches for treating water supplies to remove fluoride: Flocculation, Ion exchange methods, and Adsorption.

### 2.4.1 Flocculation

The Nalgonda technique uses the principle of flocculation. To flocculate fluoride ions in the water a coagulant known as Alum (hydrate aluminium salts) is generally utilized for water treatment. Lime is added to the solution as operation performs better in basic medium. To disinfect water from other harmful bacteria bleaching powder can be used. After stirring continuously for some time, elements coagulate into flocs that weights more than water and settle down at the bottom of the container. This process can be proceeded at any scale either big or small thus making this technique suitable for both household use and community use. The household versions use a pair of 20-litres buckets, with a settling time between 1-2 hours. After the process of coagulation, settling is completed. Treated water is then withdrawn from a tap which is located 5 cm above the bottom of the first bucket, safely above the gangue level and then stored in the second bucket for drinking.

### 2.4.2 Ion Exchange Methods

Ion-exchange resins have also been evaluated for fluoride removal from drinking water. Fluoride can be removed from water with a strongly basic anion-exchange resin containing quaternary ammonium functional groups. The fluoride ions replace the chloride ions of the resin. The exchange reaction is as follows:



The process of exchange of ions continues until all the sites on the resin are occupied. The resin is then backwashed with water that is supersaturated with dissolved sodium chloride salt. New chloride ions then replace the fluoride ions, leading to the recharge of resin and starting the process again. The driving force for the replacement of chloride ions from the resin is the stronger electronegativity of the fluoride ions.

**Advantages:**

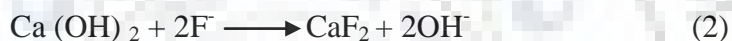
- Fluoride is removed up to 90-95 %.
- Taste and colour of water are retained.

**Limitations:**

- Other anions reduce the efficiency.
- Expensive technique because of resin cost.
- Regeneration of waste disposal.
- To maintain the pH, pre-treatment is required.

**2.4.3 Coagulation Process**

Most commonly used coagulant for precipitation is lime and alum. Lime reacts with fluoride and forms insoluble precipitate  $\text{CaF}_2$ . After precipitation,  $\text{OH}^-$  ions released and pH of the water is increased up to 11-12.



Minimum solubility of fluoride to precipitate  $\text{CaF}_2$ , is 8.0 mg/L. Removal of fluoride in this case is not possible upto WHO limit (1.5 mg/L) because of its solubility.

**Advantages:**

- It can be used upto very high concentration (3000 mg/L) in industries, before the discharge of waste water.

**Disadvantages:**

- It increases the pH of waste water.
- For drying of sludge, large space is required.
- The taste of treated water is not good.

**2.4.4 Adsorption**

Another technique, which can be used to clean water, is passing it through a packed column with strong adsorbent kept inside which can adsorb contaminants of water. Commonly used adsorbents are ion exchange resins, activated charcoal and activated alumina ( $\text{Al}_2\text{O}_3$ ). Like the previous method, this method is also valid for both household and community level purposes. In this case, if adsorbent adsorbs maximum amount of fluoride ions and becomes saturated, thus no more fluoride is adsorbed,

then instead of changing it with new adsorbent we can backwash it with an alkali solution or mild acid so that it cleans down and restarts adsorbing fluoride ions from water. The waste obtained by backwashing is rich in fluoride concentration as it does have accumulated fluoride so we must be extra careful while dumping this waste as it can cause recontamination of nearby groundwater. Theoretically it is economical to have defluoridation equipment connected to a community hand pump rather in household, reasons for which are attributed to economics of sales; but we must also consider that proper maintenance of a community owned facility is an issue which comes up often, to tackle this is a pre-requisite of a good and responsible organisation.

In the techniques of water treatment, there is a unique standing of adsorption process. The adsorption process makes use of power of certain solids to accumulate specific substances from solution onto their surfaces (Kumar et al., 2004). McBain first introduced the term sorption (Seader and Henley, 2011), this does includes selective transfer of some of the minerals to the surface and force into the bulk of liquid. In a general adsorption process, the adsorbed solutes are referred to as adsorbate and the adsorbing agent is the adsorbent.

Theoretically, the adsorption of solute on to solid particles normally takes four essential steps:

- Solutes diffuses through the fluid to an area near the solid particle surface,
- Solute diffuses into the external surface of the particle,
- Solute diffuses into the pore wall,
- Solute adsorbs to the internal surfaces of the pore wall.

Adsorption operation is divided into two major parts namely, bulk separation and purification depending on the concentration in the fluid which is fed to the adsorbed component. Previously when adsorption is applied in daily life it only uses the mechanism of purification, for example from last five centuries it is known to improve taste of water adsorption with the use of charred wood.

Adsorption methods can be implemented for the removal of fluoride due to physical, chemical, or ion exchange interactions with the adsorbents. Two types of contacting systems of adsorption are usually encountered namely, the batch and fixed-bed processes. Batch type processes are usually limited to the treatment of small volumes of effluents whereas the bed column systems have the advantage of continuous operation up to the point of saturation. Fixed-bed processes can be set up

with relative ease and provides continuous treatment with a long breakthrough time, and they are widely used for small and large scale application.

The criteria for selection of suitable sorbent are; cost of the media and running costs, ease of operation, adsorption capacity, potential for reuse, number of useful cycles, and the possibility of regeneration. Some of the most frequently encountered adsorbents are reviewed in this section.

## **2.5 Adsorption Isotherms**

Generally, there is a priceless curve in the form of a surface assimilation isotherm, which depicts the process that moderates releasing or retention/ movability of a material through the aqueous environments of media with aqueous porous or it may do so for a solid-phase with a constant pH including temperature. The propotion of the absorbed quality and the quantity left over in the solution, called surface assimilation equilibrium is finalized as an absorbate having a phase with the adsorbent through a proper amount of period, and its absorbate concentration in the solution mass has been in a competent equilibrium through the concentration of surface. Normally, the correlation, implying significant part for functional pattern, study for modelling, as well as related systems activites towards surface assimilation, has been represented through graphs depicting the solid-phase against its left-over concentration.

### **2.5.1 Isotherm Model by Langmuir**

Adsorption isotherm propounded by Langmuir, basically derived to explain gas–solid phase surface assimilation on sufficiently activated carbon, has usually been brought into use to measure and differentiate from the functioning of various bio-sorbents. Conceptually, this practical model considers surface assimilation of one molecule thickness, which happens at a definite count of certain sites which are localized and are not different and just equivalent, with no steric hindrance with lateral contact of the absorbed molecules, and it can happen on neighboring sites. While deriving the isotherm of Langmuir, we relate it to surface assimilation which is homogeneous, where every molecule has sorption activation energy with constant enthalpies (every shite shows the same chemical affinities for the absorbate) and there is no transmigration of the absorbate for the surface plane of the adsorbent. If it is depicted graphically, it is shown as a plateau with an equilibrium saturation point in which when a molecule is engaged with a location, no further assimilation of surface can continue. Furthermore, the theory by Langmuir has established a relation between quick

reductions of the intermolecular attractive forces with the detachment increase. Here, a constant with no dimension, generally referred to factor of separation ( $R_L$ ) as by Webber and Chakkravorti can be represented as:

$$R_L = \frac{1}{1+C_0K_L} \quad (3)$$

Where,

$K_L$  Langmuir constant (L/mg),

$C_0$  Absorbate starting concentration (mg/L),

In the present condition, lower  $R_L$  value shows that the surface assimilation is favoured. So theoretically,  $R_L$  value signifies the surface assimilation character as either favourable ( $0 < R_L < 1$ ), linear ( $R_L = 1$ ), unfavourable ( $R_L > 1$ ) or irreversible ( $R_L = 0$ ).

### 2.5.2 Isotherm Model by Freundlich

The Freundlich isotherm has been the original verified correlation relating the imperfect with reversible surface assimilation, irrespective of the monolayer creation. This practical model is utilised for surface assimilation multilayer, with unequal distribution of surface assimilation affinities and heat over the plane of diverse nature. In the past, it helped as the surface assimilation of charcoal from animal and it significantly depicted that the absorbate onto a specified quantity of absorbent to the solute ratio was not a constant at unequal solution concentrations. Regarding this, the total adsorbed sum is the abridgement of absorption on all sites (all with bonding energy) engaging the strongest binding sites first, until surface assimilation energy is reduced to a great extent upon the surface assimilation procedure completion.

In the scenario, isotherm propounded by Freundlich is widely used in systems which are heterogeneous especially for extremely interactive species or for organic compounds on properly activated carbon and molecular sieves. The curve slope varying from 0 to 1 is a quantified representation of the strength of surface assimilation or heterogeneity of surface, with becoming much heterogeneous as it approaches towards zero.

A number less than unity directs towards procedure of chemisorptions whereas higher than 1 suggests of supportive surface assimilation. Its non-linearized equations and linearized are depicted in Table 2.5.3 recently, isotherm by Freundlich has been under criticism for its limitation of deficient

for a fundamental thermodynamic basis, as it does not approach the Henry's law at diminishing concentrations.

### 2.5.3 Isotherm Model by Temkin

The isotherm propounded by Temkin is one of the earlier models describing the surface assimilation of hydrogen atoms on electrodes of platinum placed in solutions which are acidic. This isotherm has a term which clearly takes into account the correlation of adsorbent-adsorbate interactions. By not considering the extremely minimal and high values of concentrations, the model takes that the surface assimilation heat (which is a function of temperature) for the number of molecules in the layer would decrease linearly instead of logarithmically with coverage. As can be seen by the equation, its formulation considers a homogeneous separation of combining energies (to a limiting maximum binding energy).

**Table 2.5.3: Mathematical Corelation of Isotherms.**

S.No	Isotherm	Non-Linear Form	Linear Form	Plot
1.	Langmuir	$q_e = \frac{Q_0 b C_e}{1 + b C_e}$	$\frac{C_e}{q_e} = \frac{1}{b Q_0} + \frac{C_e}{Q_0}$ $\frac{1}{q_e} = \frac{1}{Q_0} + \frac{C_e}{b Q_0 Q_0}$ $q_e = Q_0 - \frac{q_e}{b C_e}$ $\frac{q_e}{C_e} = b Q_0 - b q_e$	$\frac{C_e}{q_e}$ vs $C_e$ $\frac{1}{q_e}$ vs $\frac{1}{C_e}$ $q_e$ vs $\frac{q_e}{C_e}$ $\frac{q_e}{C_e}$ vs $q_e$
2.	Freundlich	$q_e = K_f C_e^{1/n}$	$\log q_e = \log k_f + \frac{1}{n} \log c_e$	$\log q_e$ vs $\log C_e$
3.	Temkin	$q_e = \frac{RT}{bt} \ln A T C_e$	$q_e = \frac{RT}{bt} \ln A T + \frac{RT}{bt} \ln C_e$	$q_e$ vs $\ln C_e$

### 2.6 Adsorption Kinetics and Equilibrium Capacity

The most important study of adsorption is kinetic study; it determines the rate of adsorption of the process. Various types of models are used to describe the kinetic study. Pseudo first order and pseudo second order models are well familiar to explain the rate of adsorption with respect to the contact time. After a long time of adsorption, a relation is found between the equilibrium concentration of fluoride (final concentration) and optimum time. Optimum time is the contact time of adsorption after which negligible change occurs in the final concentration. Equilibrium capacity of adsorbent is amount of adsorbate adsorbed per unit adsorbent. It is calculated at the optimum time of adsorption process. Adsorption capacity can be defined by:

$$q_e = \frac{(C_0 - C_e) V}{m} \quad (4)$$

Where

$q_e$  Adsorption capacity,

$C_0$  Initial concentration,

$C_e$  Equilibrium concentration,

$V$  Volume of sample,

$m$  Mass of adsorbent.

### 2.6.1 Pseudo First Order Model

The pseudo first order (Lagergren's) rate equation is one of the most widely used rate equation to describe the adsorption of adsorbate from the liquid phase (Meenakshi and Vishwanathan 2007, Ho et al., 2000). The linear form of pseudo first-order rate expression of Lagergren is given as:

$$\log(q_e - q_t) = \log(q_e) - \left(\frac{K_1}{2.303}\right) t \quad (5)$$

Where,

$q_e$  Adsorption capacity at equilibrium (mg/g),

$q_t$  Adsorption capacity at time  $t$  (mg/g),

$K_1$  the rate constant of pseudo first-order kinetics model ( $\text{min}^{-1}$ ).

### 2.6.2 Pseudo Second Order Model

The adsorption kinetics was also described as pseudo-second order process by using following equation,

$$\frac{t}{q_t} = \frac{t}{q_e} + \frac{1}{K_2 q_e^2} \quad (6)$$

Where,

$q_e$  Adsorption capacity at equilibrium (mg/g)

$q_t$  Adsorption capacity at time  $t$  (mg/g)

$K_2$  The rate constant for the pseudo second-order kinetics (mg/g.min)

Intra Particle Diffusion kinetics non linear model:

$$q_t = k_{id} * t^{0.5}$$

Intra Particle Diffusion kinetics linear model:

$$q_t = k_{id} * t^{0.5} + I.$$

## 2.7 Use of Bio Adsorbents and Advantages

A large number of bio adsorbents have been reported in the literature for the removal of pollutants. These are activated bagasse, wheat straw raw activated carbon etc. The use of bio adsorbent is more beneficial for water quality because it does not degrade the quality of waste water. It is a good source of vitamin C. There is no complex formation with water as like conventional adsorbent. Conventional adsorbents form a complex in water because of which an additional treatment is required. But in case of bio adsorbent no need of further treatment of water is required. Mostly conventional adsorbents are used for the removal of fluoride. The use of non-conventional adsorbent (bio adsorbent) would be beneficial for the water quality as well as economical for the treatment of fluoride. We are using three bio adsorbents Banana peel, *Citrus Limetta Peels* and Ground nut shell for the removal of fluoride because of their advantages.

## 2.8 SAB Process

Biological and adsorption processes are common phenomenon in our natural ecosystem. In the environment, organic pollutants are generally degraded by simultaneous adsorption and bioaccumulation (SAB). Fluoride waste water industries are Glass, Electroplating, Aluminium, Steel, Chemical industries and Oil Refinery. Concentration of fluoride in industrial waste water varies generally from 15 mg/L to 20 mg/L. Fluoride is essential, but is also dangerous for human health in excess. In potable water fluoride concentration should not be less than 0.5 mg/L and cannot be exceed 1.5 mg/L. The ever increasing demand for water has caused considerable attention focused towards recovery and the re-use of waste water (Annadurai et al., 2000).

For purification of waste water based on simultaneous adsorption and bioaccumulation basically two types of mechanisms are involved. The availability of adsorbents increases the surface of liquid-solid phase. Microbial cells, pollutants, enzymes and oxygen are adsorbed. Physicochemical reaction is also possible due to surface catalysis on the surface of adsorbent (Kalinske, 1972). Microbial enzymes (*Actinobacter*) are immobilized on the surface of adsorbent. Bio-regeneration depends on adsorbent adsorption capacity. It has highly increased and the adsorbent adsorption system is continuing for a long time compared to simple adsorption process. As a result, when simultaneous



adsorption and bioaccumulation occurred, the removal efficiency of fluoride and waste water quality becomes considerably much better (Perrotti and Rodman, 1974).

## **2.9 Estimation of Fluoride**

Some of the commonly used methods for estimating the fluoride concentration are as follows:

### **2.9.1 Titrimetry**

A typical titration contains an unusual metal found in the earth, for example thorium, in addition to fluoride-containing solution. The ions of fluoride are expected to do reaction with the titration, as a result of which, an indicator dye is used to treat the solution, such as Alizarin Red S or SPADNS. A colour change that indicates abnormal presence of thorium reacting to the indication dye can be observed clearly as well as detected through the use of various techniques based on instrumentation. The composition as well as pH of the solution has to be carefully moderated, and then its interaction with foreign substances has to be averted with the help of a partition done earlier. It can be seen as a precisely regulated method, and time-taking process. Besides, the observations rely mostly on the experience as well as the skills possessed by the experimenter.

### **2.9.2 Methods based on Potentiometric**

Concentration of Fluoride within potable water is easily estimated with the help of direct investigation based on potentiometric through use of selective electrodes of fluoride ion (Jacobson et al. 1977). The only crystals lanthanum electrode had been first brought into use by Frant and Ross (1968), and it has given a reliable method for making analysis of the fluoride concentration. A single crystal of lanthanum fluoride with 0.5–1.0 % europium (II) is used as the sensor, and is fixed at the lower floor of a cylindrical tube of glass, and it functions as the source electrode as well as the solution of reference. The solution for reference is normally 0.1M potassium chloride mixed with 0.001M sodium fluoride, and is sufficient for the electrode of fluoride. The electrode of Chloride Silver – silver is used as electrode of reference and goes into this solution to make contact. The electrode is brought into use to finalize the concentration as well as the action of the element of fluoride contained in water with the help of a suitable curve of calibration. There is no action from the electrode to complex or bound fluoride. In order to rectify it, a solution called buffer solution with a potency which is highly ionic, is introduced in this, such that ions of the fluoride with complex molecules get free. In case when the fluoride concentration is under 15 mg/L, methods of

straight potentiometric may be applied. This method is not as much affected by disturbances from other metals when compared to Spectrophotometry.

### 2.9.3 Methods based on Spectrophotometric

As regards this method, a metal compound, such as from Iron, Aluminium, Cerium, Lanthanum, Thorium, or Zirconium react does reaction with dye meant as indicator to prepare a complex with small constant of dissociation. This complex makes reaction further with fluoride producing a complex which is new. Due to the change in the the complex configuration, the surface assimilation spectrum takes a shift in respect to the spectrum for the reagent solutions which are free from fluoride. This change can be seen by means of a Calorimeter. One of the dyes which are highly necessary, used in this technique is Trisodium 2-(parasulfophenylazo)-1, 8-dihydroxy-3, and 6-naphthalene disulfonate, commonly called SPADNS. A more commonly applied dye is Erichrome Cyanine R. The dye does reaction with ions of metal to produce a hued complex. When the SPADNS dye is utilised, Zirconium does reaction with SPADNS to prepare a complex which is red in colour. Fluoride takes away the red colour from the complex, thus the change in absorption can be worked out by using a Calorimeter.

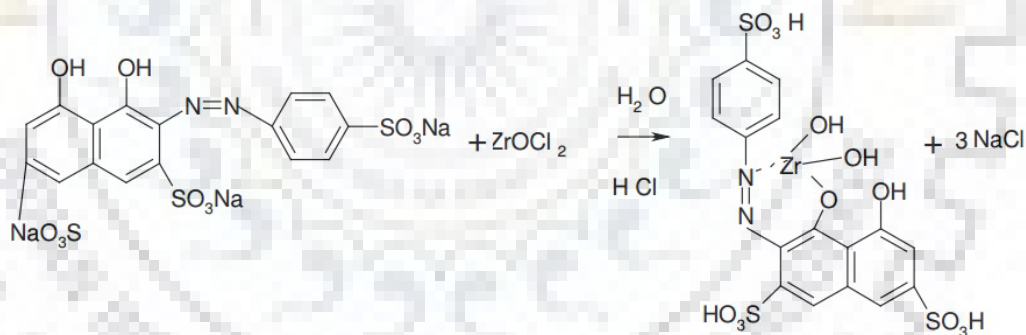


Fig. 2.9.3 (a) Formation of the SPADNS – ZrOCl<sub>2</sub> complex

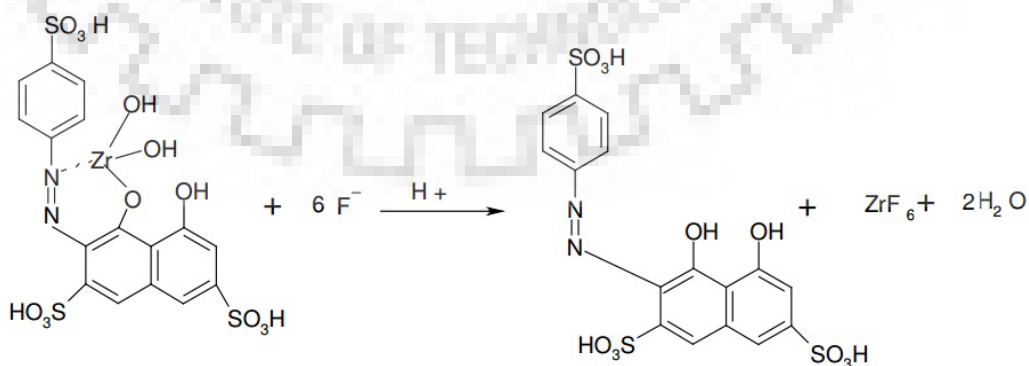


Fig. 2.9.3 (b) Reaction of the Complex with Fluoride Ions

## 2.10 Review of Previous Work Done by Various Authors on Different Methodologies for Removal of Fluoride

An extensive literature review has been performed on defluoridation. The review is discussed as follows:

**Xiaolin Yu et al., (2013)** this report shows that composites uses the consolidated advantage of HA and cellulose which have strong affinity and very high specific surface area towards fluoride. Composites are characterized using techniques of SEM, TG, XRD, XPS and FTIR. Observations were done for fluoride adsorption. It was found that when Freundlich and Langmuir isotherm models were applied to experimental data they were in good agreement. When initial concentration of fluoride is 10 mg/L, the residual concentration using more than 3 g/L of adsorbent dose could meet the norms laid by WHO on standards of drinking water. Cellulose hydroxyapatite (HA) nano composites were a good option to be used as adsorbent for the cause of fluoride removal. Adsorption kinetics indicates that the adsorption rate is rapid. The composite materials show a high adsorption capacity of fluoride compared with the nano-size Cellulose HA. It was also found that on fluoride removal no significant effect was laid by coexisting anions. Thus, Cellulose HA nano composites have a great potential as a novel adsorbent for the fluoride removal from drinking water.

**S.K. Swaina et al., (2013)** this study remarks on the decontamination of fluoride from water bodies using a newly developed hybrid material of (Fe/Zr)-alginate (FZCA) micro particles. In batch adsorption experiments various physical and chemical parameters such as pH, initial fluoride concentration, equilibrium, contact time and adsorbent dose were studied. Maximum removal of fluoride was observed at pH 6.0 in 210 min. The sorption follows pseudo-second order kinetics. The result indicated that the maximum sorption capacity ( $q_m$ , mg/g), 0.981, is related to the Langmuir adsorption model for which both experimental and calculated values are quite close to each other. Thermodynamic parameters such as, negative value of  $\Delta G^0$ , indicated the spontaneity of adsorption process. Fluoride could be rinsed (89% washed at pH 12.0) and can be regenerated and reuse for sustainable operation for a number of cycles.

**V. Sivasankar et al., (2012)** in this report, author activates Tamarindus indica Fruit Shells (TIFSs) by the means of ammonium carbonate. The material used have a BET surface area of 473 m<sup>2</sup>/g, which is used for the studies undergo removal of fluoride by stirring dynamics and shaking experiments. The highlighting feature of ACA-TIFSC is that CaCO<sub>3</sub> compounds are also present in

the carbon matrix which is easily verified from the results obtained after the defluoridation studies. It is to be noted that by the means of ACA-TICSF groundwater sample with fluoride concentration more than 1.5 mg/L were treated efficiently. In Shaking and Stirring sorption methods fluoride removing capacity of ACA-TIFSC was increased to a maximum of 8% and 11% respectively. Whatever the concentration of fluoride anions from 2 to 8 mg/L, the agitation method exhibited a significant influence on the kinetic behaviour. From the results of co-ion interference studies, bicarbonate ion was found to be the best competitor against fluoride.

**Pankaj Garg et al., (2012)** reported removal of fluoride by using an absorbent which is Mg-Hap and also which is a calcium-magnesium based. The result of various factors such as contact time, beginning concentration of fluoride, pH, as well as coexisting ions (Sulphate, Bicarbonate, Nitrate, and Chloride) had been investigated to assess the conduct of absorbent in numerous situations. It was observed that extracting Calcium and Magnesium (Ca-Mg) was insignificant because the hard-state in all samples which had been treated was observed to go up by 12.13 mg/L as  $\text{CaCO}_3$ . The uptake capacity was reduced by 41% with equilibrium pH going up from 6.5 to 8.7 and an almost equal conduct has been seen for extracting of Ca-Mg. It was also observed that taking away of fluoride from a matter that is aqueous highly relies on contact time, pH, initial stage concentration, and  $\text{CO}_3^{2-}$  existing anions. The levels of pH of the solution at the initial stage made considerable impact upon the absorption power of MgHAp. Hence, Mg-HAp, which is a calcium-magnesium based absorbent, has come up as having very good power of defluoridation.

**Prasanta Kumar Raul et al., (2012)** have reported the use of iron oxide-hydroxide nano particles, which gives very good result in terms of removal of fluoride over a good range of pH. In this study effect of stirring speed, adsorbent dose, contact time, pH and temperature were reported. The iron oxide-hydroxide nano particles have been reported as a good adsorbent for fluoride removal from wastewater. At room temperature the maximum fluoride which can be absorbed by sorbents is found to be 16.70 mg/g. The adsorption on iron oxide hydroxide nano-particles of fluoride ions is under the influence of pH of the medium used. Data of equilibrium sorption reveals that best model for this process is Freundlich isotherm which is followed by Langmuir model. Temkin and Dubinin-Radushkevich models also fit the data but not as well as the above mentioned two models. In presence of hydroxide ion the nano-particles has comparatively low adsorption of fluoride. From this paper it is expected that new approaches were provided in the field of developing iron oxide-

hydroxide nano-particles which can be further explored and sealed up in order to have a reliable adsorbent media to remove fluoride from drinking water.

**Xiaomin Dou et al., (2012)** studied that mechanism of adsorption and defluoridation of a high capacity hydrous zirconium oxide adsorbent. Maximum capacities of adsorption were obtained as 124 and 68 mg of fluoride per gram of adsorbent in batch studies when pH of the medium was 4 and 7 respectively. Analysis from XPS shows that a seven-coordinate polyhedral zirconium oxyfluoride species,  $ZrO_2F_5$  and possibly some of  $ZrO_3F_4$  is formed on the adsorbent's surface by exchange reactions between surface hydroxyl groups with fluoride. This material is described as one of the best bio-adsorbent ever demonstrated with maximum adsorption capacity for fluoride. Kinetic studies of the data revealed that the fluoride adsorption follows the mechanism of pseudo-second-order rate law zeta potential analyses, FTIR spectroscopy, Surface titration, XPS measurements and Raman spectroscopy verifies that removal of fluoride happened by this adsorbent is due to exchange of fluoride with surface hydroxyl groups and electrostatic interaction between fluoride and charging surface. The good performance of hydrous zirconium oxide makes it a potentially attractive adsorbent for defluoridation of water.

**Bina Rani et al., (2012)** investigated the aspects related to kinetics in batch method to understand the effectiveness as well as practicability of brick powder of adsorbents and had been used on aqueous sample prepared in laboratory and groundwater samples with high fluoride concentration obtained from two villages, viz Reenu and Mardatoo located in Rajasthan, India. Different factors were taken into account for observation, for example, dose effect, pH effect and adsorbent reaction time to carry out observations and results. It was found out that there could be an ideal situation i.e. pH (6-8) with dose of adsorbents (0.6-10 gm/100ml.) defluoridation percentage from aqueous (simulated synthetic) sample, may be amplified from 29.8% to 54.4% for brick powder and 47.6% to 80.4% for chemically activated carbon (CAC) and a rise in reaction time of 15 to 120 min. Removal of Fluoride had been found to be 48.73% and 56.4% from groundwater samples with 3.14 mg/L and 1.21 mg/L fluoride, in the same manner under the most ideal situations. Brick powder's Defluoridation efficiency can be made evident on the chemical interface of fluoride with the metal oxides in proper pH situations. It was further found that presence of other ions in groundwater had not significantly influenced the defluoridation method, and thus indicating signifying that brick powder can be an ideal adsorbent for fluoride.

**Eric Togarepi et al., (2012)** studied the adsorbent capacities of chemically and heat treated sand for defluoridation of water. In this study effect of various parameters like pH, initial fluoride concentration, dosage and contact time were investigated using batch system. The results obtained highlight that activated sand can be used as one of the adsorbents for removal of fluoride from water. To make this possible, the sand was coated with 10% of  $\text{Fe}_2\text{O}_3$ , pH within the range of 5.7-6.3, and for removal of fluoride from water. It was also observed that with increase in initial fluoride concentration and adsorbent dosage, the adsorption increases. From this study, it was revealed that 12 g of adsorbent is needed to adsorb first 90% of the fluoride in 50 ml of 10 mg/L fluoride solution. The best model describing this sorption process is Freundlich isotherm as it fits data obtained. In this study, the maximum sorption found was 10.3 mg/g. In accordance with these results, physicochemically treated sand is a significant candidate as an adsorbent for the removal of ions of fluoride. The isotherms by Langmuir and Freundlich were employed in order to prepare the equilibrium based on sorption data obtained. The findings proved that by making use of an ideal dose of 0.24 g/ml, upto 90% fluoride elimination could be obtained.

**Das Kumar Malay et al., (2011)** reported that fluoride can be a naturally occurring part of normal water sample. Using water containing excess fluoride in big periods of time results in a serious disease called Fluorosis. It is a disease that has harmful effects; it upsets teeth, soft tissues and bones in the body. Fluoride enters the body through water, drugs, food, industrial wastes etc. Main producer of fluoride for humans is normal water, constituting 75-90% of daily intake. The main sources that lead to ground water contamination with fluorides are fluoride with rocks like cryolite, hydroxyl apatite, fluor spar, and fluor apatite. The concentrations of ground water fluoride is affected by numerous factors such as velocity of flowing water, availability and solubility of fluoride minerals, temperature, pH, and calcium concentration and bicarbonate ions found in water. The fluoride elimination percentage had been found to be a function of adsorbent dose and only give a rise to defluoridation effectiveness up to a dose of 5 g/100 ml for a definite initial fluoride concentration. Basic test was carried out by using natural adsorbents such as much activated bauxite, much activated alumina and activated rice husk. Equilibrium of surface adsorption analysis was carried out and using Freundlich isotherm, it was found out that activated alumina came up as an ideal option as it gave an insignificant equilibrium constant (0.601) along with slope (0.152). The next adsorbent used, activated bauxite, gave a equilibrium constant of 0.593 and slope of 0.965. It

was followed by much activated rice husk having equilibrium constant 0.155 with slope of 0.659. So, much activated alumina can be considered as the most appropriate absorbent among the ones studied and much activated rice husk is not a good absorbent for this function.

**Wei Ma et al., (2011)** to remove fluoride ions from aqueous solution calcination product of Mg–Al–Fe hydrotalcite compound at 500 °C (HTlc500) was used as the adsorbent, while on the other hand by co-precipitation method Mg–Al–Fe hydrotalcite compound was synthesized. Batch adsorption studies were conducted under various equilibration conditions, such as different calcined temperature, co-existing anions, initial fluoride ions concentrations, adsorbent dose, pH and contact time. It was reported that HTlc500 had maximum capacity of adsorption of 14 mg/g at pH 6 when the adsorbent dose was 0.2g/L. Adsorption data were well described by the pseudo-first order kinetic model and Langmuir isotherm model. This process is well described by both of the models. The calculation of the thermodynamic parameters shows that the adsorption process is an endothermic and spontaneous process.

**Madhumita Bhaumik et al., (2011)** report that adsorption is a quick process and some adsorbent have a high affinity for fluoride which depends upon pH of the solution, adsorbent dose and temperature. From equilibrium modelling, data is in good agreement with Langmuir–Freundlich isotherms and Freundlich isotherms. On the other hand pseudo second-order model describes well adsorption kinetics. Material was effective in water defluoridation. The fluoride uptake was very rapid and depends on the initial concentration, temperature, adsorbent dose and pH. Thermodynamic parameters verify the endothermic nature and spontaneity of adsorption of fluoride. Fluoride adsorption proceeds by ion exchange mechanism. Adsorption of fluoride in the presence of other anions such as chloride, nitrate, sulphate and phosphate was not affected remarkably. More than 97% of the adsorbed fluoride on the nanocomposites of PPy/Fe<sub>3</sub>O<sub>4</sub> was at pH 12. The adsorbent retained the original adsorption capacity after one complete adsorption–desorption cycle, confirming the reusability of the nanocomposite for fluoride removal.

**C.M.Vivek Vardhan et al., (2011)** investigated defluoridation of water by the means of physico-chemical process of coagulation and adsorption by using easily available and cheap materials like seed extracts of Moringa Oleifera (Drum stick), chemicals like Manganese Chloride and Manganese Sulphate and Rice Husk. A solution with rice husk concentration of 6 g/L is successful in removing

83% of fluoride from fluoride solution of concentration 5 mg/L which is attained after achieving equilibrium in a time span of 3 hours. Data obtained was fitted with the Absorption model of Langmuir which must be rearranged linearised. Studies involving Fixed Bed down flow show the empirical use of Rice Husk, Manganese Sulphate, rice husk, Manganese Chloride and Moringa oleifera seed extracts (MOE) were used to conduct standard jar test and they accomplished fluoride removal of 92, 92, 94, 91, percent from a 5 mg/L test solution at a dosage of 1000 mg/L. If the pH of medium is slightly acidic (6.0) process of defluoridation is favoured. The experimental investigations clearly suggested that these adsorbents are effective enough in removing fluoride from water upto permissible levels. It is to be noted that pH doesn't have a role when range is between 3 and 10 but if we increase pH beyond 10 there is a steep decrease in removal of fluoride.

**Shihabudheen et al., (2011)** in this paper talks about Nanomagnesia (NM), its preparation, its application in purification of water. The result obtained by the author indicates towards the point that adsorption of fluoride by NM is highly favourable and the capacity does not vary in the pH range which is usually encountered in groundwater. The equilibrium data is well fitted with Freundlich equation while adsorption kinetics follows pseudo second-order equation. Experimental evidence verifies that fluoride removal happened through isomorphic substitution of fluoride in brucite. Using precipitation–sedimentation filtration techniques a batch household defluoridation unit was developed which addresses the problems of high fluoride concentration as well as the problem of alkaline pH of the magnesia treated water. Ultra fine MgO nanoparticles (3–7 nm) were synthesized through a novel self-sustained combustion route. The flying off of the combustion product from the reaction vessel was completely arrested and thereby 100% recovery of the product, without additional product recovery mechanism, was achieved.

**Muhammad Farooq et al., (2011)** showed that combined oxides display varied properties of surface as against single oxide systems. It was also found out that the point zero charge of Al<sub>2</sub>O<sub>3</sub> to the MgO loading went up and moved between the PZCs of pure oxides of Al<sub>2</sub>O<sub>3</sub> and MgO. The surface area, pore diameter and pore volume came down as the MgO contents went up, as few of the Al<sub>2</sub>O<sub>3</sub> channels had been intercepted by MgO. Low amounts of MgO did not vary the total structure of Al<sub>2</sub>O<sub>3</sub> however; high presence of MgO varied the structural as well as other textural properties of alumina. In addition to this, it was seen that the activation strength of thermal decomposition of Mg



$(\text{NO}_3)_2 \cdot 6\text{H}_2\text{O}$  worked out by Friedman approach, went up as the  $\text{Mg}(\text{NO}_3)_2 \cdot 6\text{H}_2\text{O}$  loading was raised onto alumina.

**M. G. Sujana et al., (2010)** in the present, reports of iron oxide hydroxide of nano scale which were synthesized by water in oil micro emulsion method. As starting materials, we choose  $\text{FeCl}_3$ , hexanol and a non-ionic surfactant span 80. The data obtained by batch adsorption tell us that defluoridation efficiency is highly affected by the parameters studied. Indication of fast kinetics was collected by establishment of equilibrium in less than 1 hour of contact time. It is observed that second order kinetic model is followed by adsorption data. The isothermal data is fitted to both Freundlich and Langmuir models and maximum removal of fluoride by Langmuir model estimated is 62.89 mg/g for the concentration range of 10-30 mg/L.

**Sujana and Anand (2010)** conducted adsorption and desorption experiments in order to get more information about mechanism of adsorption on the surfaces of ferrous and aluminium hydroxide. XRD results points towards new complexes formation involving fluoride on the adsorbent surface. The concentration of other anions like arsenate had a negative effect on the defluoridation efficiency of the adsorbent. The maximum removal observed when 0.5 M NaOH was used was 80.5 %.

**Sujana et al., (2010)** investigated removal of fluoride by amorphous iron and aluminium hydroxides having various molar ratios. The composition (ratio of Al:Fe) of the mixed compound are 1:0, 0:1, 1:1, 1:2 and 1:3. Optimum pH for adsorption of fluoride was noted to be 4-5 for sorbent having ratio 0:1, 1:2, 1:3, while for the rest it was found to be in the domain of 4.0-7.5 due to both specific and non-specific adsorption which take place on the surface of sorbent. All collected samples shows high Langmuir adsorption capacity and the maximum adsorption capacity is shown by oxide adsorbent with molar ratio of 1:1 of 91.7 mg/g.

**Liu et al., (2010)** studied fluoride elimination by using what is known as synthetic siderite. Synthetic siderite has come up as a powerful sorbent for the arsenic absorption. The synthetic siderite displayed high absorption capacity for fluoride elimination, up to 1.775 mg/g in the batch experiments with an absorbent dosage to 5 g/L and a beginning fluoride concentration of 20 mg/L at the temperature of 25°C. The contents of  $\text{Cl}^-$  and  $(\text{NO}_3)^-$  anions put a little impact on fluoride absorption, while  $(\text{PO}_4)^{3-}$  considerably changed fluoride elimination from aqueous solution. The

method of fluoride elimination by synthetic siderite was explained using XRD and SEM results. The high elimination efficiency of synthetic siderite was due to the absorption of fluoride on the fresh goethite over large specific surface area. So precipitation of ferric hydroxide with fluoride, caused by dissolution of specifically clean synthetic siderite with resulting oxidization of, was also a contributor to the determination of fluoride on the absorbent.

**Ch. Chakrapani et al., (2010)** reported absorption of fluoride onto these activated carbons. Effect of contact time in the removal of fluoride from aqueous solution at neutral pH was studied. Five kinetic models; the pseudo first-order and second-order equations, intra particle diffusion, pore diffusion and the Elovich equation, were selected to follow adsorption process. The fitting of the kinetic data demonstrate that the dynamics of sorption could be better described by pseudo second-order model indicating a chemisorptive rate-limiting for all the three adsorbents, NCDC, NCMC and NCAC. Though the plots of intra particle diffusion render straight lines with good correlation coefficient, they fail to pass through origin in each case. This suggests that the process is 'complex' with more than one mechanism limiting the rate of sorption. The good fitting of the kinetic data, to Bingham's and Elovich equations indicates that pore diffusion plays a vital role in controlling the rate of reaction.

**Liu et al., (2010)** fabricated Al–Ce varied absorbent using the co-precipitation method and studied its functioning in elimination of fluoride. The XRD and SEM outcomes show that the varied absorbent has an undefined structure having some nanoparticles which are aggregated. The highest sorption competence of the Al–Ce absorbent for fluoride was found to be 91.4 mg /g at 25°C. The absorption process of fluoride onto the absorbent was quick, and the highest absorption competence was gained at about 6 pH level. The higher sorption capacity at lower solution pH was attributed to the surface charge of Al–Ce adsorbent. The adsorbent was effective in fluoride removal from aqueous solution via electrostatic interaction due to its high zero point of potential. Zeta potential measurement and FTIR analysis confirmed that the protonated hydroxyl groups and the hydroxyl groups on the adsorbent surface were involved in the fluoride adsorption at low and high solution pH, respectively.

**R. N. Yadav et al., (2010)** used Aluminum Ammonium Sulphate for defluoridating constituent within potable water earthenware, aluminium fluoride is less toxic than other fluorides and observed

that this earthenware reduce the fluoride concentration in potable water. Freundlich and Langmuir experiments were conducted using these earthenwares. They came up with the finding that the fluoride ions isotherm takes the varied model of the Freundlich and Langmuir isotherm. The absorption occurred on some fixed sites within the soil pot. Findings demonstrated that Aluminum Ammonium Sulphate are fit to be used in earthenware (soil pots) to bring down the fluoride concentration within the water used for domestic puposes.

**Jayaram et al., (2009)** studied the use of AILS known as aluminium hydroxide impregnated limestone for perfect elimination of fluoride from poor potable water. The absorption in respect of treated lime stone was highly diminished at level 2 of pH, which was due to the dissolution of aluminium hydroxide within an environment with acidic presence. The highest sorption efficiencies of the AILS and limestone absorbents had been observed as 84.03 mg / g and 43.10 mg / g,. FTIR experiments showed that the fluoride absorption onto AILS had physisorption nature.

**Karthikeyan and Elango (2009)** studied bismuth aluminate (BA) and aluminium titanate (AT) as adsorbents for removal of fluoride based on the fact that AT exhibits low thermal expansion coefficient, low thermal conductivity, high refractivity, and is insoluble in water whereas BA is water insoluble material, nontoxic, and antacid, which make them better suited for defluoridation applications. The amounts of fluoride adsorbed from 4 mg/L initial fluoride concentration by BA and AT were 1.55 and 0.85 mg/g, respectively at 30°C. The results demonstrated the comparatively greater fluoride elimination competence of absorbents in an acidic extent and it has been detailed using  $pH_{pzc}$  of the absorbents (7.1 in BA, 7.4 in AT). There was no significant impact from the present vying ions on the fluoride elimination strength of AT. XRD, also FTIR study of the absorbent pre and post absorption showed that fluoride ions had been absorbed chemically by these absorbents.

**Camacho et al., (2009)** fabricated a highlyactivated alumina with the help of a specific technique called the sol gel. Covering of manganese oxide ( $MnO_2$ ) or calcium oxide (CaO) had been conducted to better the alumina surface functioning. The outcomes of the absorption experiments indicated that the activated alumina treated with calcium oxide (CaO-AA) absorbent demonstrated highest strength for adsorption in the case of fluoride. CaO-AA had been observed to take up 10 and 5 times more fluoride than sol – gel  $MnO_2$ -AA and AA with the equal concentration level at the beginning stage.

It was observed that the alkalinity of the adsorbent affected the adsorption capacity. The Langmuir monolayer adsorption capacity of MnO<sub>2</sub>-AA and CaO-AA were 10.18 and 101.01 mg/g, respectively. It was concluded that chemisorption was responsible for the adsorption of fluoride onto the unmodified and modified adsorbent.

**Srimurali et al., (2008)** observed that highly activated alumina can be highly functional in the fluoride elimination. The impact of increase in alkalinity, pH, calcium as well as carbonates had been observed to reduce the strength of absorption. The effects of sulphates, chlorides, magnesium, sodium, potassium present were observed as minimal as far as the efficiency of absorption. The studies based on revival, which were also carried out, proved that the revived AA is also applied potentially for the fluoride elimination and minimizes the length of the method besides being highly practical particularly for semiurban/village areas.

**Maliyekkal et al., (2008)** observed that the alumina treated with magnesia has a higher rapid and higher fluoride elimination activity. The experiments demonstrated that pH came up as the most powerful aspect, and the perfect value for pH was in the range of 5-7.5. Nothing was observed of the ions common interfering onto the fluoride elimination process. Absorption had been observed extremely rapid during the initial one hour, later reaching the semi-equilibrium value within 3 hours. Kinetics had been found to take after the semi second-order model indicating fluoride elimination is likely to be a result of absorption through chemical process. The data for equilibrium had been found to be perfectly presented through the isotherm models of Sips and Toth. The rate of absorption of magnesia-treated alumina was observed to be very high than that of alumina which is activated. The revival of adsorbent had been found as relatively simple using 2 percent NaOH solution.

**S. Ayoob et al., (2008)** observed that the absorption mechanics is demonstrated by semi second-order model. XRD studies indicated the contents of multiple oxide layers and this further pointed towards the sorption happening on sites with heterogeneous binding. The analysis of FTIR statistics have shown that the method of an eminent ligand exchange mechanism in elimination of fluoride process leads to increase in pH levels. Elovich and Intra particle models based on diffusion had been seen to be most suitable and it further disclosed that diffusion is critical as regards absorption. Characteristics of desorption had been studied as poor thus clearing prospects of irreversibility of absorption of the fluoride. It also indicates that the sorption process does not along consist of ion

exchange. The rate limit is likely to be the surface site binding energy heterogeneity or the other reactions which control the fluoride elimination.

**Vivek et al., (2007)** observed that the highly activated alumina had high uptake strength of 2045 mg/L. It was further observed that the activated alumina already used up can be revived and again put through process for fluoride elimination cycles and there is not much loss to its strength. As regards DDU, production of proper water was found to go up with the increase in the contents of AA provided the depth of absorbate was going down. The production of proper water also went down for the same content of AA by changing the DDU diameter. It had been observed that the change of SSY and AA depth / DDU cross-sectional area displayed linear relationship.

**Maliyekkal et al., (2006)** basically applied alumina and manganese oxide to make manganese-oxide covered alumina (MOCA) and investigated prospects of sorbent for fluoride removal of potable water by batch as well as experiments based on continuous process. Fluoride Absorption to MOCA had been found to be higher and more rapid than AA in the initial time and had been observed to be almost constant over 3 h. The contained degree of absorption beyond 3 h had been attributed to the AA surface action which changed  $\text{pH}_{\text{zpc}}$  to a below level. It was observed that the perfect reduction of the ions of fluoride occurred within a 4-7 pH limit. The Langmuir maximum absorption strength for fluoride of MOCA came around 2.65 times higher than AA (2.851 mg/ g). The MOCA had been found to be perfectly revived by making use of 2.5% NaOH as eluent. The absorption strength of fluoride at the level of outcome for both the absorbents (AA and MOCA) had been very much changed because of bed depth.

**Sushree Swarupa Tripathy et al., (2006)** demonstrated that alumina treated with alum possesses a better competence for fluoride elimination. SEM, XRD, and Electrophoretic studies revealed a uniform impregnation of alum on to alumina. With the help of the kinetic experiments, it had been observed that the elimination of fluoride was highly rapid during the beginning, i.e. Initial 10 to 60 minutes, and then achieved the highest level of 92 % during the next 3 hours. The best pH level of fluoride elimination had been 6.5 and increasing pH further lead to reduction in the fluoride removal. EDAX studies were also performed and it was seen that there is a superficial presence of the fluoride on the alum-treated activated alumina. The experiments based on revival indicated that the AIAA can be revived at pH 12 with 0.1 M NaOH and then neutralizing using 0.1 M HCl. The absorbent

can again be brought into use further after the treating of alum. Fluoride elimination strength of the AIAA had been up to 0.2 mg/ L.

**Shimelis et al., (2006)** compared the capacities of absorption of thermally processed hydrated alumina (THA), with untreated hydrated alumina (UHA) obtained using locally fabricated aluminium sulphate hydrolysis for removal of fluoride from a solution which is aqueous. The removal strength of fluoride increased as absorbent dosage rose. Fluoride absorption efficiency showed an increase and growth in the thermal treatment temperature to 200 °C, but this extra increase in temperature brought to low reduction efficiency. In continual full bed column, process at 300 °C was conducted using it as the most conducive parameter. Great fluoride elimination efficiency was achieved by making use of both THA and UHA in 4.0–9.0 pH range. The absorption observations fitted well with the model of Freundlich isotherm having a very little competence of 7.0 mg F<sup>-</sup>/g , 23.7 mg F<sup>-</sup>/g for UHA then THA, respectively. The outcomes of continual full bed column studies achieved by means of THA indicated that 4.5 g of THA is likely to impregnate 6 L of normal water possessing 20 mg/L fluoride before breakthrough.

**Shihabudheen M. Maliyekkal et al., (2006)** observed that MOCA absorption rate in comparison to AA had been very fast. The fluoride absorption on to the MOCA took after the Langmuir Isotherm Model. The loading strength of the MOCA had been 2.65 times of AA. pH Level of the solution impacted the fluoride removal and was found to be optimum between 4-7 pH ranges. There was no marked effect of competing ions on the elimination of fluoride. The absorption had been observed to take after the second order dynamics through a correlation coefficient higher than 0.98. The constant of saturation of MOCA had been observed 2.5 times more than AA that had been 1.25 g/L. Desorption studies were also conducted and it had been observed that MOCA is normally regenerated by 2.5 percent of NaOH.

**Sushree Swarupa Tripathy et al., (2005)** studied about process of defluoridation through the means of alum-impregnated activated alumina (AIAA) adsorption. All the experiments were carried out in a batch-mode. The impact of using different factors like effect of pH (pH 2–8), absorbent content (0.5–16 g/L), reaction time, and beginning level of fluoride concentration (1–35 mg/L) had been studied for finding out adsorption competence of AIAA. Bradley equation was correlated with both isotherm data as well as adsorbant data. It was observed that when pH of solution is 6.5, AIAA

is able to remove around 99% of fluoride from water after 3 hours; 20 mg of fluoride is present in 1 litre of water solution and dose of 8 g/L. The desorptions studies showed that this adsorbant can be reused once it follows a simple base-acid rinsing procedure; 0.1M NaOH with pH level of 12 and then cancelling out with 0.1M HCl. From the study, the conclusion can be derived that the alum treated activated alumina possesses greater efficiency for elimination of fluoride from proper water.

**Pietrelli (2005)** also investigated prospects of MGA that stands for metallurgical grade alumina to study surface assimilation of fluoride in various test situations. The maximum rate of absorption had been found as pH 5–6 which was attributed to the fact that for these pH levels, the fluoride ions are below  $F^-$  ionic forms which give the maximum solidarity for the fluoro-alumina interface. At higher pH values, the fluoride adsorption onto MGA sites decreased drastically, and it was due to the adverse conduct with hydroxide ions towards the binding on the MGA surface.

**R. K. Gangal., (2005)** studied samples from a number of twenty-five villages and observed that the NF membranes can take away around 95% fluoride from the ground water in a solitary step and also remain unchanged by the composition of source water. It was deduced that NF is used worldwide to bring down to a minimum the use of aluminium which itself is highly detrimental for the human health.

**Ghorai and Pant (2004)** studied the removal of fluoride through activated alumina (AA) (Grade OA-25) in batch and continual method processes. Absorption strength of 1450 mg/kg had been achieved at the level seven (7) of pH. Percentage fluoride removal increased in the pH arrangement of 4 to 7 then decreased later. Hydroxyl ions as well as silicates had been observed to vie much powerfully with fluoride ions to alumina replace sites at pH level greater than 7, whereas, at pH level lower than 7, the soluble alumino-fluoro complexes had been produced as a result of the presence of aluminium ions in the treated water. Lower fluoride deduction as well as premature saturation had been observed at greater concentration and for a greater flow rate. A negligible reduction had been observed in the taking-up strength following every revival cycle. Revival process yielded 85% strength with the level of AA taken into account. A reduction of 5% in taking-up capability of AA had been observed following 5 cycles.

**Subhashini Ghorai et al., (2004)** observed that at a pH level of seven, the AA (Grade OA-25) can take away a considerable quantity of 1450 mg/kg. The successful studies observed that a kind of

interacting impact of the absorption capability and absorption rate on the absorption exists. The absorption strength had been observed relying on the rate of the flow, incoming fluoride concentration, and also bed height. The competence is much greater when there is a high reaction time and there is a low fluoride concentration. When there is a high fluoride concentration, it yields greater success curves.

**Subhashini Ghorai et al., (2004)** observed that fluoride elimination is dependent upon adsorbent dosage, level of pH, as well as contact time. It was also observed that the absorption took after the first order dynamics and Freundlich & Langmuir isotherms. This had been found through the observations that the method of fluoride elimination is complicated resulting in the surface absorption with intra particle diffusion contributing as a step towards the determination of the rate. Sharp breakthrough curves were received with a higher initial fluoride concentration.

**J. L. Reyes Bahena et al. (2002)** observed that absorption of fluoride onto the alpha-Al<sub>2</sub>O<sub>3</sub> is quick over the first 60 minutes during the reaction. The highest capacity had been found from 5 to 6 pH levels and for initial fluoride ion concentration level of 3 and 10 mg/L. It was also seen that increasing pH above 6 lead to a sharp decrease in the uptake, while it is less at the pH<sub>pzc</sub> of the adsorbent which is 9.2. Synopsis of work done by the researcher's alongwith the adsorbents used by them for removal of fluoride is shown below in the tabular form:

**Table 2.10: List of Different Adsorbents Used by Different Researchers**

S. No.	Author	Adsorbent	Initial F Conc. (ppm)	pH	Removal Efficiency (%)	Adsorbing Capacity (mg/g)
1.	Alemayehu Mekonen et. al. 2001	Alum PAC slurry	6 to 20	5.8 to 6.5	83 to 90	---
2.	Nigamananda das et. al. 2005	Activated titanium rich bauxite	10	5.5 to 6.5	94.5	3.8
3.	S. Venkatamohan et. al. 2006	Spirogyra	5	2	64	1.272
4.	S. V. Raminaiah et. al., 2007	Pleurotus Ostreatus	5	7	52	---
5.	M. Islam et al. 2007	quick lime	50	5.0 to 6.5	80.6	---
6.	Ali Tor et. al., 2008	Granular red mud	5	4.7	---	0.851
7.	Srimanth kagne et.	Bleaching powder	5	6.7	75	12.78



S. No.	Author	Adsorbent	Initial F Conc. (ppm)	pH	Removal Efficiency (%)	Adsorbing Capacity (mg/g)
	al. 2008					
8.	M. Karthikeyan et. al. 2008	Various grades of graphite	10	7	94 to 99	3.13
9.	R. S. Sathish et. al. 2008	Zr ion impragnated coconut fiber carbon	20	4	98	40.076
10.	Imam Bakhsh Solangi et. al. 2009	Modified Amberlite	5	9	93	90
11.	Baris Kemer et. al. 2009	Activated waste mud	92.5	5	82	7.33
12.	A. R. Tembulkar et. al. 2009	Neem, Peepal	5	2	84.9	1.482
13.	Yulin Tang et. al. 2009	Activated alumina	51	5 to 10.5	76	10
14.	S. Ayoob et. al. 2009	Alumina cement granules	20	3 to 11.5	95	4.75
15.	S. Jagtap et. al. 2009	Magnetic chitosan	140	7	89.2	22.49
16.	E. Kumar et. al. 2009	Granular ferric hydroxide	100	7	95	7
17.	Sairam Sundaram et. al. 2009	Nano-hydroxy appetite	10	< 5.9	96	2.84
18.	E. Tchomgui Kamaga et. al. 2010	Charcoal	10	7	93.3	19.05
19.	Sivasankar et. al. 2010	MnO <sub>2</sub> <sup>-</sup> coated tamarind shell	2 to 5	6.5	98	1.99
20.	Kalyan das et. al. 2010	AlOH coated rice husk	10 to 60	7	97	10
21.	N. Vishwanathan et. al. 2010	Alumina/ Chitosan Composite	10	7	97	---
22.	X. Dou et. al. 2011	Zirconium iron oxide	10	7	92	9.8
23.	M. Islam et al. 2011	Basic oxygen furnace slag	50	7	70 to 88	8.07
24.	Wei Ma et. al. 2011	Mg-Al-Fe hydrotalcite compound	10	6	85	14
25.	Lin Chen et. al. 2012	Iron-Doped Titanium Oxide Nanoadsorbent	50	5	---	53.22
26.	Prasanta Kumar Raul et. al. 2012	Iron Oxide-Hydroxide Nanoparticles	10	7.28	95	16.7
27.	M. Mohapatra et.	Mg-doped	10 to	1 to 10	98	64

S. No.	Author	Adsorbent	Initial F Conc. (ppm)	pH	Removal Efficiency (%)	Adsorbing Capacity (mg/g)
	al. 2012	nanoferrihydrate	150			
28.	Hui Deng et. al. 2012	metal ion-loaded (Sir(IV), Al(III), Fe(III)) fibrous protein (MFP)	38	4.0 to 9.0	---	58.41
29.	T. Poursaberi et. al. 2012	zirconium (IV)-metalloporphyrin grafted Fe <sub>3</sub> O <sub>4</sub> nanoparticles	10	5.5	92±1.7	---
30.	Liyuan Chai et. al. 2013	Sulfate-doped Fe <sub>3</sub> O <sub>4</sub> /Al <sub>2</sub> O <sub>3</sub> nanoparticles	50	7	90	70

### 2.11 Phytoremediation Review

In recent years, researchers concentrated their attention to fluoride removal from water. Till date, the focus was on the consequences arising due to fluoride on human health but consequences of high dose of fluoride on plant is a bit ignored. So this study, basically concentrates on effects of fluoride on plants using phytoremediation technique for the removal of fluoride.

Phytoremediation is formed with two words “phyto” a Greek word which refers to plant and second word “remediation” which refers to restoring balance. The concept of phytoremediation was first introduced by Rufus Chaney in 1983. Thus, phytoremediation is the technique in which plants are used for the purpose of cleaning the environment from the pollutants in air, water and soil (Cunningham et al., 1997). Some plants used for the phytoremediation are listed below in Table 2.11(a) (Prasad and Freitas, 2003).

**Table 2.11(a): Phytoremediation: Plant Utilized and their Roles** (Prasad and Freitas., 2003).

S.No	Plant name	Role in phytoremediation
1	Alyssum	Nickel accumulator
2	Amaranthus retroflexus	Accumulator of <sup>137</sup> Cs
3	Armoracia rustica	Hairy-root cultures remove heavy metals
4	Armeria maritime	Lead accumulator
5	Atriplex prostrate	Removes salt from soil

6	<i>Azolla pinnata</i>	Accumulator of lead, copper, cadmium, and iron
7	<i>Brassica canola</i>	Remediates <sup>137</sup> Cs-contaminated soil
8	<i>B. juncea</i>	Hyperaccumulator of metals
9	<i>Cannabis sativa</i>	Hyperaccumulator of metals
10	<i>Cardamonopsis hallerii</i>	Hyperaccumulator of metals
11	<i>Ceratophyllum demersum</i>	Metal accumulator
12	<i>Datura innoxia</i>	Barium accumulator
13	<i>Eucalyptus sp.</i>	Removes sodium and arsenic
14	<i>Eichhornia crassipes</i>	Accumulator of lead, copper, cadmium, and iron
15	<i>Helianthus annuus</i>	Accumulator of lead and uranium. Removes <sup>137</sup> Cs and <sup>90</sup> Sr in hydroponic reactors
16	<i>Hydrocotyle umbellata</i>	Accumulator of lead, copper, cadmium, and iron
17	<i>Kochia scoparia</i>	Removes <sup>137</sup> Cs and other radionuclides
18	<i>Lemna minor</i>	Accumulator of lead, copper, cadmium, and iron
19	<i>Phaseolus acutifolius</i>	Accumulator of <sup>137</sup> Cs
20	<i>Pteris vittata</i>	Arsenic hyperaccumulator
21	<i>Salix sp.</i>	Phytoextraction of heavy metals, waste water, and leachate

### 2.11.1 Techniques/Strategies of Phytoremediation

Phytoremediation is done through mainly five mechanisms they are as follows:

- 1- Phytodegradation,
- 2- Phytoaccumulation/Phytoextraction,
- 3- Phytostabilization,
- 4- Phytofiltration/Rhizofiltration,
- 5- Phytovolatilization.

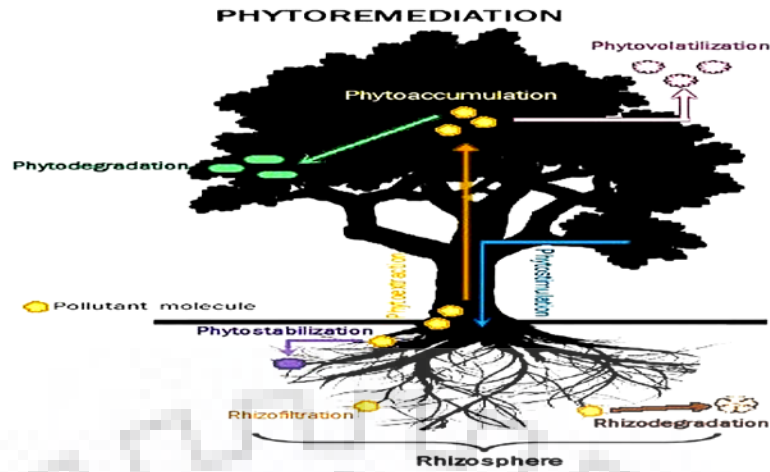


**Fig 2.11.1: Mechanisms of Phytoremediation [source- Google Image]**

### **2.11.2 Phytodegradation**

Phytodegradation is the process of decomposition of organic pollutants by the action of enzymes produced by plants such as oxygenase, dehalogenase etc. Green plants act as “Green Liver” for the biosphere. Phytodegradation mechanism is limited for the organic pollutants; heavy metals are not degraded by this mechanism (susarla et al., 2002).

### **2.11.3 Phytoaccumulation / Phytoextraction**

Phytoaccumulation is the process in which heavy metals are taken from the soil by roots and transferred to parts of the plant above the ground like stem leaves etc. (Kumar et al., 1995).

### **2.11.4 Phytostablization**

In Phytostablization the heavy metals in the soil or water are stabilized. By this mechanism pollutants are stabilized near the roots through sorption, complexation, precipitation etc. Pollutants having high toxicity are converted in to less toxic substances and get accumulated in plants by which they are immobilized and out of the food chain.

### **2.11.5 Rhizofiltration**

This mechanism involves the removal of the pollutants floating on the surface of the water. Certain plants have very dense roots which act as the filtration media for the water and the pollutant floating on the surface get trapped in it (Dushenkov et al., 1995).

### **2.11.6 Phytovolatilization**

Phytovolatilization is the process in which the pollutants are taken from soil and water through roots

and via tree released in the atmosphere. In this mechanism, the pollutants are only transferred from one place to another. Liberation of contaminants through phytovolatilization converts a ground problem to an air problem (Salt et al., 1995).

The explanations of methods involved in phytoremediation are listed in the Table 2.11 (b) (Nagendran et al., 2006).

**Table 2.11 (b): Application of Phytoremediation** (Nagendran et al., 2006).

Medium	S. No	Application	Types of plants	Description	Contaminants
Water/ Waste Water	1	Phytotrans-formation	Trees and grasses	Sorption, uptake, and transformation of contaminants.	Organics, including nitro aromatics and chlorinated aliphatics.
	2	Rhizosphere biodegradation	Grasses, alfalfa, many other species including trees	Microbial biodegradation in the rhizosphere stimulated by plants.	Organics; e.g., PAHs, petroleum hydrocarbons, TNT, pesticides.
	3	Phyto-stabilization	Various plants with deep or fibrous root systems	Stabilization of contaminants by binding, holding soils, and/or decreased leaching.	Metals, organics.
	4	Phytoextraction	Variety of natural and selected hyperaccumulators, e.g. Thalasspi, Alyssum, Brassica	Uptake of contaminants from soil into roots or harvestable shoots.	Metals, inorganic, radionuclides.
Soil	1	Rhizofiltration	Aquatic plants [e.g., duckweed, pennywort], also Brassica, sunflower	Sorption of contaminants from aqueous solutions onto or into roots.	Aquatic plants [e.g., duckweed, pennywort], also Brassica, sunflower.
	2	Phyto-volatilization	Trees for VOCs in ground water; Brassica, grasses, wetlands plants for Se, Hg in soil/sediments.	Uptake and volatilization from soil water and groundwater; conversion of Se and Hg to volatile chemical species.	Trees for VOCs in ground water; Brassica, grasses, wetlands plants for Se, Hg in soil/sediments.
	3	Vegetative	Trees such as	Use of plants to	Trees such as poplar,

Medium	S. No	Application	Types of plants	Description	Contaminants
		Caps	poplar, plants and grasses.	retard leaching of hazardous compounds from landfills.	plants and grasses.
	4	Constructed wetlands	Free-floating, emergent, or submergent vegetation; reeds, cattails, bamboo.	Use of plants as part of a constructed ecosystem to remediate contaminants from aqueous waste streams.	Free-floating, emergent, or submergent vegetation; reeds, cattails, bamboo.

The techniques described in the above Table 2.11 (b) are applied in two different ways, they are as follows:

### 2.11.7 Constructed Wetland

In order to treat waste water generated by the industries like glass, aluminium, refineries, electroplating, semiconductor, fertilizers etc, this type of system is generally used. Wetlands are the manmade/artificial water bodies which resemble naturally occurring water bodies [example- ponds, lakes etc] as shown in Fig. 2.11.8. Wetlands are gaining popularity among industries day by day as they are economical than the water treatment plants. Wetland system can also be more efficient if it is integrated with mechanisms like Phytofiltration, phytoextraction.

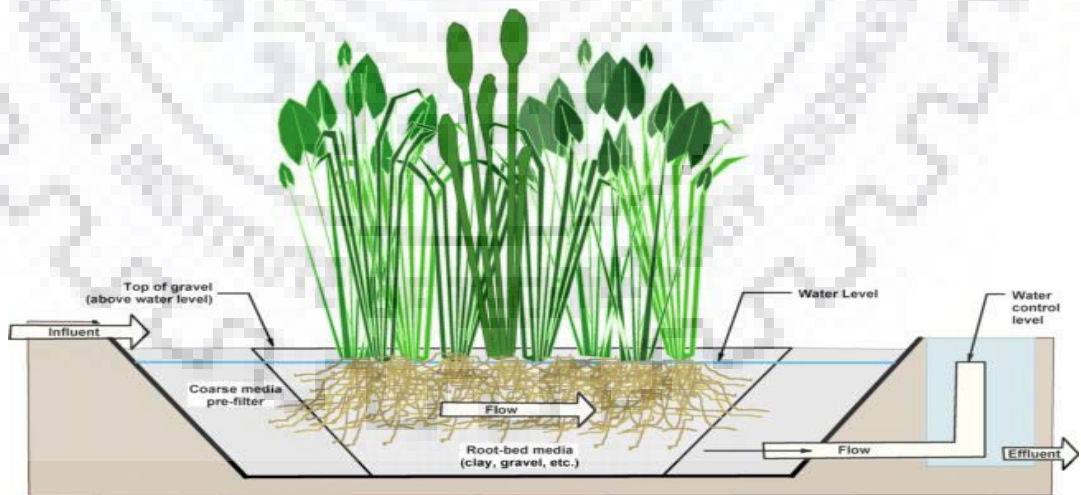


**Fig. 2.11.7: Constructed wetland [source- Google Image]**

### 2.11.8 Floating Platform

Floating platform is a large structure floating on the surface of water. These types of platforms are

very popular in Europe and America. Such types of platforms are constructed by the materials which can float on water easily, and the plants are grown on that. The terrestrial plants are used for this type of platforms because they have very dense roots which help in Phytofiltration; as a result they are very efficient in the treatment of waste water.



**Fig 2.11.8 Floating Platform [source-Google Image]**

**2.11.9 The advantages and disadvantages of phytoremediation are discussed in the Table (Belz., 1997, Tangahu., 2011).**

**Table 2.11.9: Advantages and disadvantages of Phytoremediation**

<b>S.No</b>	<b>Advantages</b>	<b>Disadvantages</b>
1	Aesthetically pleasing	It is a time taking process [dependent on seasons] for the cleaning of the site
2	Environmental friendly technique	Limited to regions having low pollutant levels within root zone of plants
3	Wide range of applicability for different types of contaminants, including organic pollutants	Used for remediating medium levels of contamination
4	Use solar energy	Cannot Remediate dense non aqueous liquids
5	Can be used to stimulate microorganisms by the release of nutrients and oxygen transport from roots	Poses the danger of contaminates entering the food chain
6	Low cost	Liberation of contaminants through phytovolatilization, converts a ground problem into an air problem.
7	Helps to reduce soil erosion	Less effective on extremely hydrophobic pollutants

S.No	Advantages	Disadvantages
8	Less disruptive than current techniques	Dependence on the climate conditions for growth
9	Dual possibility of in-situ and ex-situ treatment	Plantation of a foreign species may affect biosphere
10	In-situ treatment decreases the extent of spreading of contaminants	Proper disposal for the harvested plant biomass is a requisite

## 2.10 Work Done by Different Authors on Phytoremediation of Heavy Metals

**Sinha et al, (2000)** used *Hydrilla verticillata* for the remediation of fluoride. The experiment was carried out in triplets; plant was grown in 10% of Hoagland nutrient solution containing different concentration of fluoride. The intensity of light that was provided was  $114 \mu \text{mole m}^{-2} \text{s}^{-1}$  at  $26^\circ \text{C}$  for a photoperiod of 14/10 hr. The experiment was conducted for 3, 5 and 7 days. One set of plant was harvested on 3<sup>rd</sup> day, second on 5<sup>th</sup> day and third on 7<sup>th</sup> day. The effect of fluoride on the chlorophyll content, protein and carotenoid was determined. Result shows that, as the concentration of fluoride increases in solution the chlorophyll and protein content of the plant decreases. Accumulation of fluoride in the plant also increases with concentration, in 20 ppm solution maximum accumulation of  $1892 \mu\text{g/g}$  was found on 7<sup>th</sup> day, if we increase concentration leaching of fluoride takes place. Maximum fluoride removed from 2.5 ppm solution was 24.4%.

**Sirish and Gandhi et al., (2013)** Performed lab scale experiment on *Lpomoea Aquatica*, which is commonly known as water spinach. They studied the effect of chromium and fluoride on the plant. Experiment was carried out for 10 days. After which removal efficiency and accumulation of both the pollutants in plant was determined by UV spectrophotometer. The removal of fluoride was 37% and chromium was 86%. Chromium was mostly accumulated in leaves and fluoride was accumulated in roots. For removal of chromium, phytoextraction mechanism was followed by the plant while for fluoride phytovolatilization was used.

**Bunthiyal and Sharma et al., (2012)** investigated the eight species of tree [*A. Nilotica*, *A. Tortilis*, *A. Senegal*, *P. Juliflora*, *P. Cineraria*, *C. Fistula*, *A. Lebbeck* and *A. Indica*] for the remediation of fluoride from soil and water. These eight species of plant were grown in different concentration of fluoride by hydroponic cultures under  $1000 \text{lm/m}^2$  light intensity having 14/10 hr light period with 70% relative humidity and  $30^\circ\text{C}$  operating temperature. After that three species with maximum removal efficiency were selected for the study of soil. Maximum removal found was  $1322 \mu\text{g/g}$  at 50



mg/L after 10 days by *P. Juliflora*. Then *A. Tortilis*, *P. Juliflora* and *C. Fistula* were grown in soilrite having different concentration of fluoride. As the experiment completed it was found that the accumulation of fluoride was greater in water grown plant than in soil grown.

**Mondal et al., (2014)** performed their study on six species of macrophytes. [*Pistia Stratiotes*, *Eichhornia crassipes*, *Nymphaeoides indica*, *Ceratophyllum demersum*, *Lemna major*, *Azolla pinnata*] and estimated the growth parameter, chlorophyll content and isothermal study for each plant. Among all the plants *Nymphaeoides indica* shows the best result. All the plants show best removal efficiency up to 72 hours after which it was decreased significantly. After 72 hours of contact time *Eichhornia crassipes* gave best removal efficiency of 57.8%.

**Diaz and Pedraza (2010)** reported tolerance of 17 plant species to Hydrogen Fluoride [HF], among which eight species were selected for growing in hydroponic culture for 21 days. Among these eight species only three plants [*S. Officinarum*, *P. Torbira* and *C. Japonica*] were capable of removing fluoride after the exposure of 21 days. *S. Officinarum* accumulates maximum fluoride 1.6 mg/L in 21 days. The removal efficiency of *P. Tobira* was 15%, *C. Japonica* was 7.5% and *S. Officinarum* was 40%.

**Singh and Verma (2013)** studied the physiological effects on the popular seedlings when irrigated with water containing fluoride of 100-500 ppm. After the exposure to 500 ppm fluoride containing water for six weeks seedlings shows considerable changes in leaf expansion, stomatal conductance, and growth. Plant biomass, photosynthesis  $\text{CO}_2$  assimilation, chlorophyll fluorescence yield and harvest index.

**Sekome et al., (2012)** performed two lab scale experiments: both the systems consisted of three ponds connected in series seeded with algae and duckweed. In this research paper ability of algae and duckweed ponds to be used as a post treatment option for textile wastewaters has been studied. The effect of pH, redox potential and dissolved oxygen on heavy metal removal has also been studied. The experiments were performed under two light regimes (photoperiod of 16/8 hr and 24 hr) and two different metal loadings. The hydraulic retention time was seven days. The heavy metals studies were Cd (0.05 mg/L), Cr (1.5 mg/L), Cu (0.1 mg/L), Pb (0.25 mg/L) and Zn (1.25 mg/L), the experiments were performed continuously for 3 weeks. The experiments showed good results for

both Cr (94 % and 98%) and Zn (70% and 80%), although it showed similar removal efficiencies for Pb, Cd and Cu ranging from 20 to 30% but it was not up to the mark.

**Pandey (2012)** examined the heavy metal removal ability of *Azollacaraliniana*. The study area was a Fly ash pond of NTPC Unchahar located in Umran village. Random samples of plants and FA effluent was collected and analyzed for the presence of heavy metals. The presence of Pb, Fe, Mn, Zn, Cd, Ni, Cr, and Cu was detected. Presence of a large amount of *Azollacaroliniana* on the metal rich fly ash pond exposed its toxicity tolerant capability. The ability of *A. Coraliniana* to remove the heavy metals from the fly ash pond is due to its high bio-concentration factor.

**Lin et al., (2011)** examined the Cr uptake capability of *Leersiahexandra Swartz* for Cr (III). They collected the plant seedlings from the riverside: the seedlings were properly washed and placed in pots filled with 1.5 L of 20% Hoagland's solution. The uptake of Cr under different conditions such as introduction of metabolic inhibitor, at low temperatures (2 °C), introduction of ion channel blockers and effect of Fe on Cr uptake was studied. The result showed presence of DNP and low temperature limited the chromium uptake (verifying the fact that Cr uptake is dependent on metabolic activities), whereas there was no effect observed on the uptake of Cr due to the addition of ion channel blockers.

**Chen et al. (2011)** performed both hydroponic and pot experiments using the plant species *Vetiverzizanioides*. They tested the plant species on its uptake capacity of lead, copper and zinc. The effect of additions of different chelators such as EDTA, EDDS, and citric acid has also been examined on the heavy metal removal. The hydroponic experiments were performed in 2 L experimental tanks filled with 1.5 L of nutrient solution (Hoagland), the concentration of heavy metals was kept constant at 5 mg/L and concentration of the three chelators was kept at 5 mM. For the pot experiments the soil was also spiked with Cu, Zn and Pb respectively. It was well mixed and air dried for 5 days in order to mimic local contaminated soils. In the hydroponic experiments, EDTA caused the most significant toxic signs on vetiver as compared to EDDS and citric acid. In the pot experiment, the major finding was that vetiver perceived to act as a hyperaccumulator during treatment for Cu with EDDS, Zn with all the three chelators and for Pb with EDTA and EDDS.

**Hoang Ha et al. (2011)** reported that the metal accumulating ability of *eleocharisacicularis*; they exposed the plant to In, Ag, Pb, Cu, Cd and Zn under laboratory conditions. The experiments were performed in a hydroponic setup with the plants being allowed to grow directly in 2 L beakers. The experiments were conducted for fifteen days. After the experimental run on the analysis of the results it was found out that the plant is a good species for both remediation and phytomining.

**Khan et al. (2009)** investigated the effective metal removing ability of constructed wetlands. The area of study chosen was the Swabi district of Pakistan, a free flow surface wetland having 7 cells was constructed in the Gadoonam Azai Industrial Estate (GAIE). Variety of native plant seedlings (such as *Typhylatifolia*, *Phragmitesaustralis*, *Juncus articulates*, *Lemnagibba* etc) were transported and cultivated on the CW; plants were chosen on the bases of their growing ability and heavy metal tolerance. The experimental study was conducted for about one year in which samples of wastewater from the inlet, outlet and all the cells of CW was collected along with the samples of sediments and plants.

**Mishra and Tripathi (2009)** studied the metal (Cr and Zn) uptake capability of *Eichhornia crassipes*. The plants were grown in 15 L tanks filled with water up to 10 L. The metal concentration used was 5, 10, 15, 20 mg/L. The solution was added in each tank consisting of single metal ions. The experiments were performed for 11 days. The plants performed extremely well in removal of both Zn and Cr; it safely removed Zn for all concentrations without showing any toxicity, but in case of chromium plants showed some morphological toxicity for 15, 20 mg/L of concentration. During the 11 days a total of 95% of Zn and 84% of chromium were removed.

**Natarajan et al. (2008)** investigated the effect of plant density and nutrient concentration on the uptake of arsenic. The plant species used was Chinese brake fern. The experiment done was a hydroponic field experiment where the contaminated ground water was brought from the site and the plants were made to grow in 30 L of contaminated water. The remediation treatment comprised of different number of plant species per chamber, two types of nitrogen dilutions and two phosphorous dilutions. Low levels of phosphorus showed good result for the removal whereas change in nitrogen levels showed no affect.

**Rai (2008)** reported the phytoremediation ability of a small free floating plant *Azollapinnata*, This plant species was used to remove concentration of 0.5, 1 and 3 mg/L for both Cd and Hg the fern

was grown in twenty four aquariums having capacity of forty litres. The experiment study was carried out for 13 days. At the end the experiment, metal contents in the solution were reduced up to a range of 70% to 94%.

**Meyers et al. (2008)** examined the effect of Pb on *Brassica juncea*. The species was grown in a hydroponic setup. It was given a growth time of 14 days after plant growth it was exposed to Pb for 3 days at concentrations of 3.2, 32 and 217  $\mu\text{m}$ . It was found out that the lead ions were restricted to the root tissues by performing Atomic Absorption Spectroscopy (AAS) on the plant samples. Other different kinds of testing such as STEM and EDS were done to discern the effect of Pb on the plant and also to find more about its uptake mechanism.

**Zhang et al. (2007)** utilized various ornamental hydrophytes such as *R. Carnea*, *A. Gramineus*, *A. Orientale*, *A. Calamus*, *I. Pseudacorus*, and *L. Salicaria* in a constructed wetland experiment to observe the treatment capacity of each ornamental hydrophyte for domestic or rural wastewater. All the hydrophytes used in the study adapted well to the wastewater; the initial concentration of heavy metals (Cr, Cu, Mn, Pb, Cd, and Fe) was 0.201, 2.031, 2.024, 0.211, 0.021 and 2.015 respectively. The experiment was performed for more than 15 days. Most of the hydrophytes were fairly efficient in reducing the amount of BOD, COD, TN, TP and heavy metals from the wastewater. Out of all the hydrophytes *A. Gramineus* was the best in removing all the pollutants from the wastewater. The heavy metal removal ranged from 76.9% to 99.1%. The highest removal for heavy metals was by *I. Pseudacorus*, the heavy metal removal followed the trend  $\text{Cr} > \text{Pb} > \text{Cd} > \text{Fe} > \text{Cu} > \text{Mn}$ .

**January et al. (2007)** exposed the Sundance Sunflowers to different kinds of heavy metals. The metals were introduced at a constant concentration of 30mg/L. There were three sets of experiments performed. The experimental setup consisted of two chambers being utilised simultaneously, 7 Sundance sunflowers were used per compartment. The first run examined the influence of EDTA on Cd, Cr, and Ni. The run examined the influence of As. The third run examined the effect of fifth metal addition and chelators on the Sundance sunflowers.

**Bragato et al. (2006)** studied the effective metal removing ability of constructed wetland. The study area was a pre-existing wetland named Ca di Mezzo which was constructed in 2000. This study was carried out to examine growth structure and heavy metal accumulating ability of the two plants:

*Phragmites australis* and *Bolboschoenus maritimus* present in the region. The sampling was done from three sites of the basin, over a period of six months. The presence of Cu, Cr, Zn, and Ni, were detected in the wetland.

**Ali et al. (2004)** conducted two experimental runs under hydroponic conditions. The effect of Cd and the combined effect of Cd, Cu and Zn were also examined on the growth, tolerance and mineral composition of the plant species *Phragmites australis*. In the first run, the plant was exposed to the individual metal ion cadmium, the concentration was kept at 0.5, 1, 2 mg/L neither the root nor shoot were affected by the concentration of 0.5 and 1 but the concentration of 2 mg/L significantly decreased the root number and the shoot length. In the second run the plant was exposed to a combined mixture of metal ions having different ratios, in each case at least one ion was present in high concentration (0.5:2; 2:2:2; 0.5:5:2 mg/L for Cd, Cu and Zn). The combined metal exposure significantly decreased the root and shoot length and the plant fresh weight.

**Maine et al. (2004)** reported that the Cr (III) uptake ability of two free floating plants *Salvinia herzogii* and *Pistia stratiotes*. They were grown outdoors in plastic aquariums containing water taken from the lake: the plants needed about 30 to 35 days to reach full maturity. In this study three types of experiments were performed. First, the cleansing capacities of both the plants were determined at different Cr concentrations (1, 2, 4 and 6 mg/L). Second, the Cr distribution in the various parts of the plants was evaluated with time. Third, the season of increase of Cr in the aerial parts was examined whether it was due to the translocation from roots or direct contact between leaves and the solution containing metals. Both macrophytes effectively eliminated Cr from water at all the concentrations. Larger the initial concentration, larger the accumulation was observed.

**Kamal et al. (2004)** examined the metal removal ability of free floating plants (parrot feather, creeping primrose, and water hyacinth) from contaminated water. The plants were grown hydroponically and were given 2 weeks to acclimatize before the addition of the contaminants. The experiment was performed in 55 L tanks with a photoperiod of 16/8 hr. All the three plants were able to remove metals from the contaminated water. The average removal efficiency for the three plant species was 99.8% of Hg, 76.7% of Fe, 41.62% of Cu and 33.9% of Zn.

**Axtell et al. (2003)** examined the uptake ability of aqueous Pb and Ni of Lemna Minor (an aquatic plant) and the Pb uptake ability of Microspora (Micro-algae). In batch experiments. In the batch study the biomass was exposed to a single addition of metal, whereas Semi-Batch study consisted of adding similar amount of metal but in small additions over the course of the study. The experiments were conducted for 10 days. The initial concentration of Pb added was 0,5,10 mg/L and of Ni was 0, 2.5, 5.0 mg/L. The removal of lead for microspore was 97% (Batch study) and 95% (Semi-Batch study). The removal of Pb and Ni for L. Minor was 76% and 82% respectively. Summary of work done on phytoremediation by authors is given in Table 2.10

**Table 2.10 (a) Summary of Work Done on Phytoremediation by Authors**

Reference	Type of water	Metals	Plant species	Techniques used	Remarks
Sinha et al. [2000]	Simulated water	Fluoride	Hydrilla verticillata	Hydrophonic study	Maximum removal of 24.4% at 2.5 ppm and maximum accumulation of 1892 µg/g fluoride at 20 ppm, if we increase concentration leaching takes place.
Sirish and Gandhi et al. [2013]	Simulated water	Fluoride and Chromium	Ipomoea Aquatica	Pot-culture experiment	Chromium is removed By 86% and Fluoride is removed by 37% Ipomoea Aquatica follows phytovoltization mechanism in case of fluoride and phytoextraction mechanism in chromium
Mondal et al. [2014]	Simulated water	Fluoride	Six Floating macrophytes [pistia Stratiotes, Eichhornia crassipes, Nymphaea indica, Ceratophyllum demersum, Lemna major, Azolla pinnata]	Floating Platform	Nymphaea indica shows the best removal efficiency rather than other macrophytes, most of the macrophytes show highest fluoride removal during 24h to 48h, but after 72h their efficiency reduces drastically Macrophytes are better for the removal of F for higher concentration
Bunthiyal and Sharma et al.	Simulated water and Soilrite	Fluoride	A. tortilis, A. nilotica, A. senegal, P. cineraria, P.	Floating Platform and Plastic	Removal of F increased with respect to concentration in the nutrient medium as well as number of days. P.

Reference	Type of water	Metals	Plant species	Techniques used	Remarks
[2012]			juliflora, C. fistula, A. indica and A. lebbeck	trays	juliflora accumulated maximum F [ 1322 µg/g at 50 ppm after 10 days]
Diaz and Pedraza [2010]	Simulated water	Fluoride	Cemellia japonica, Pittosporum tobira, and Saccharum officinarum	Floating platform	At 4 mg F/L, Sugar cane [Saccharum officinarum] removed 40% of F compared to the 7.5% and 15% removed by C. Japonica and P. Tobira, respectively.
Singh and Verma [2013]	Simulated water	Fluoride	Populus deltoids L. clone-S7C15	Constructed Wetland	Seedlings showed decreases in the following physiological characteristics: growth leaf expansion photosynthetic CO <sub>2</sub> assimilation, stomatal conductance, chlorophyll fluorescence yield, plant biomass, and harvested index.
Pandey. [2012]	Fly ash pond	Fe, Mn, Zn, Cd, Ni, Cu, Pb, Cr	Azolla Aroliniana	Constructed wetland	Maximum accumulation of Fe and Zn might be the reasons responsible for lowest accumulation of Cd, in both parts of the fern.
Sekom o et al., [2012]	Textile wastewater	Cd, Cr, Cu, Pb, Zn	Duckweed and algae	Free Floating	Both plants are suitable for heavy metal removal, especially Cr and Zn at lower concentration.
Liu et al., [2011]	Water containing CrCl <sub>3</sub>	Cr	Leersia Hexandra	Pot-culture experiment	Uptake of Cr by roots of L. Hexandra was significantly decreased by metabolic inhibitors and low temperature.
Chen et al., [2011]	Water	Cr, Zn, Pb	Vetiveria Zizanioides	Floating platform	Chelator-assisted Phytoremediation with vetiver can be a green alternate to the conventional, physio-chemical techniques
Hoang Ha el al., [2010]	Water	In, Ag, Pb, Cu, Cd, Zn	Eleocharis Acicularis	Floating platform	Eleocharis acicularis is a good option for phytoremediation and phytomining
Khan et	Wastewater	Cd, Cr,	Typha latifolia,	Construct	Cd>Cr>Fe>Pb>Cu>Ni trend

Reference	Type of water	Metals	Plant species	Techniques used	Remarks
al., [2009]	er	Cu, Ni, Fe, Pb	Juncus articulates, Lemna Gibba	ed wetlands	of removal was observed
Natarajan et al., [2008]	Groundwater collected from south Floride	As	Pterisvittata	Floating platform	Low levels of phosphorus showed good As removal
Rai, [2008]	Water	Hg, Cd	Azolla Pinnata	Floating platform	Azollapinnata growth was inhibited
Mishra and Tripathi, [2008]	Water	Cr, Zn	Eichhornia crassipes	Free Floating	E. crassipes is a good accumulator of Cr and Zn,
January et al., [2007]	Water	Cd, Cr, Ni, As, Fe	Sundance Sunflowers	Hydroponic greenhouse experiment	EDTA caused a reduction in metal uptake
Meyers et al., [2007]	Water	Pb	Brassica Juncea	Floating platform	B. Juncea has significant potential for use in removing toxic ions from water
Zhang et al., [2007]	Wastewater	Cr, Pb, Cd	R. Carnea, A. Gramineus	Constructed wetlands	Iris pseudacorus and Acorusgramineus are outstanding in adapting on cleaning urban sewage compared to other plants.
Bragato et al., [2006]	Lagoon watershed	Cr, Ni, Cu, Zn	Phragmitesaustralis	Constructed Wetland	The heavy metal content in plants is highest in late autumn after senescence (field study)
Maine et al., [2004]	Water	Cr	Salviniaherzogii, pistiastratiotes	Floating platform	Cr uptake occurred mainly during the first 24 h
Kamal et al., [2004]	Water	Fe, Zn, Cu, Hg	Parrot feather, creeping primrose, water mint	Floating platform	Creeping primrose has the least tolerance to heavy metal toxicity
Ali et al., [2004]	Water	Cd, Cu, Zn	Phragmitesaustralis	Hydroponic study	Combined metal conc. Decreased root, shoot length



Reference	Type of water	Metals	Plant species	Techniques used	Remarks
Axtell et al., [2003]	Water	Pb, Ni	L. Minor, Microspora	Free Floating	Both showed good removal

**Table 2.10(b): Represents the Values of Various Parameters Obtained by Different Scholars for Wastewater of Industries**

S.No	Name of Industry	Year	Author's name/ Handbook Data	Parameters	Unit	Avg Conc.
1	Semicouductor	--	John L. McDonough & James C. O'Shaughnessy	pH		1.1-1.5
				Fluoride	mg/L	340
				Total Acidity	mg/L	10,000 CaCO <sub>3</sub> pH @8.3
				Total Calcium	mg/L	5.6
				Antimony	mg/L	<0.05
				Arsenic		<0.025
				Beryllium		<0.1
				Cadmium		<0.05
				Chromium		<0.1
				Copper		<0.1
				Lead		<0.01
				Mercury		<0.001
				Nickel		< 0.050
				Selenium		< 0.050
				Silver		< 0.050
Thallium		< 0.050				
Zinc		0.034				
2	Automotive	2004	Jan Gruwez & Michel Schauwvliege	pH	-	3,6
				Conductivity	µS/cm	19150
				Zinc	mg Zn/L	1450
				Nickel	mg Ni/L	640
				Manganese	mg Mn/L	705
Total phosphate	mg P/L	5920				

S.No	Name of Industry	Year	Author's name/ Handbook Data	Parameters	Unit	Avg Conc.
				Nitrate	mg N/L	1510
				Ammonium	mg N/L	218
				Free fluoride	mg F/L	200
				Total fluoride	mg F/L	1784
				Sodium	mg Na/L	4750
3	Smelting Unit	2014	Vo Anh Khue & Li Tian Guo	pH		5.00
				Cu	(mg/L)	4.680
				F	(mg/L)	22.177
				Pb	(mg/L)	3.046
				As	(mg/L)	1.302
4	Electroplating	1997	Sohair I. Abouelega	pH		7.1-7.8
				COD	mg O <sub>2</sub> /L	570- 1930
				Suspended Solids	mg/L	122-844
				Oil & Grease	mg/L	48-647
				Total Iron	mg/L	0.7-44
				Total Chromium	mg/L	0.02-4.5
				Nickel	mg/L	0.8-5
				Copper	mg/L	0.9-3.4
				Zinc	mg/L	0.2-1.7
				Total Cyanide	mg/L	0.04-6.5
				Lead	mg/L	2.5-89
				Fluoride	mg/L	0.1-56
5	Desalination	2004	P.I. Ndiaye	Fluoride	mg/L	460
				Sulphate	mg/L	60
				Chloride	mg/L	20
6	Glass		Pollution prevention and abatement	pH		6-9
				TSS	mg/L	50
				COD	mg/L	150

S.No	Name of Industry	Year	Author's name/ Handbook Data	Parameters	Unit	Avg Conc.
			Handbook	Oil & Grease	mg/L	10
				Lead	mg/L	0.1
				Arsenic	mg/L	0.1
				Antimony	mg/L	0.5
				Fluoride	mg/L	20
				Total Metal	mg/L	10
7	Electroplating	2007	Sorg et al;	TSS	mg/L	20
				Arsenic	mg/L	0.1
				Cadmium	mg/L	0.1
				Chromium (Hexavalent)	mg/L	0.1
				Chromium(Total)	mg/L	0.5
				Copper	mg/L	3-10
				Lead	mg/L	0.2
				Nickel	mg/L	0.5
				Silver	mg/L	0.5
				Total metals	mg/L	10
				Cyanide	mg/L	0.2
				Fluorides	mg/L	15-20
				Trichloroethylene	mg/L	0.05
				Trichloroethane	mg/L	.05
				Phosphorous	mg/L	5
8	Steel industrial	2010	Vahid Khatibikamal et al;	F <sup>-</sup>	mg/L	5
				Cl <sup>-</sup>	mg/L	219.6
				So <sub>4</sub> <sup>-2</sup>	mg/L	180
				Na <sup>+</sup>	mg/L	135.4
				K <sup>+</sup>	mg/L	4.9
				Mg <sup>2+</sup>	mg/L	16.6
				Ca <sup>2+</sup>	mg/L	56.1
				BOD	mg/L	8.5
				COD	mg/L	35
9	Fertilizer	2006	Barbara Grzmil et	F <sup>-</sup>	mg/L	0.168

S.No	Name of Industry	Year	Author's name/ Handbook Data	Parameters	Unit	Avg Conc.
			al;	Al <sup>3+</sup>	mg/L	0
				Fe <sup>3+</sup>	mg/L	0
				Na <sup>+</sup>	mg/L	0.055
				K <sup>+</sup>	mg/L	0.013
				Mg <sup>2+</sup>	mg/L	0.023
				Ca <sup>2+</sup>	mg/L	.097
				PH		2.8
				Po4 <sup>3-</sup>	mg/L	.096
				Si <sup>4+</sup>	mg/L	0.011
				Ti <sup>4+</sup>	mg/L	0

### 2.11 Error function

The error function MPSD (Marquardt's percent standard deviation) and RMSE were used to estimate the fit between experimental and predicted value for both kinetic models. The equation for MPSD and RMSE error function is given below (ESI for RSC advances, Royal Society of Chemistry 2015; Foo et al., 2010):

$$\text{MPSD} = 100 * \sqrt{\sum_{i=1}^N \frac{1}{N-P} \left( \frac{(q_{e \text{ expt}} - q_{e \text{ cal}})}{q_{e \text{ expt}}} \right)^2}$$

$$\text{RMSE} = 100 * \sqrt{\sum_{i=1}^N \frac{1}{N-2} (q_{e \text{ expt}} - q_{e \text{ cal}})^2}$$

Where,

$q_e$  Specific uptake of adsorbent at equilibrium (mg/g) of adsorbent

MPSD Marquardt's percent standard deviation

RMSE Residual root mean square error

$q_{e \text{ expt}}$  Experimental pecific uptake (mg/g)

$q_{e \text{ cal}}$  Calculated pecific uptake (mg/g)

N no of observation in the experiment

P no of parameters in the regression model

## **2.12 Objective**

### **2.12.1 Research Needs**

In order to overcome environmental and health hazards fluoride must be removed from water and waste waters. For the removal of fluoride several techniques have been investigated. A greater share of studies on defluoridation by adsorbents was carried out in batch experiments and very few numbers of studies were done in the field of fixed bed column systems are in bio-column reactor. Moreover, most of the past reports on adsorptive removal of these inorganic anion have not considered desorption after the adsorbent is saturated with anions. Easy desorption is important for reutilising of the adsorbent again and again as this reduces operational costs. It is important to explore highly efficient, low cost adsorbents (bio-adsorbent) that can be easily regenerated for reutilization purpose over several operational cycles without significant loss of adsorptive capacity. The adsorbents selected should have good hydraulic conductivity to prevent filters clogging during a fixed bed treatment process. The mathematical modelling of column data is important for designing treatment plants for the removal of fluoride from water and wastewaters. A fitting numerical solution will be crucial to scale-up back with new operating conditions and a well-researched and novel model can be used as a reliable solution to optimise, predict and design the breakthrough curves of fixed bed columns in real water treatment processes.

### **2.12.2 Objective of Present Work**

A survey of past literature reveals that many adsorption media have been used successfully to remove pollutants from potable and wastewater. Based on extensive review of literature, objective of present work has been formulated as to evaluate the adsorption efficiency/adsorption capacity of low cost adsorbent for fluoride removal from industrial waste water using adsorption and bioaccumulation techniques. Hence, an attempt has been made in the present study to prepare few adsorption media for removal of fluoride from water.

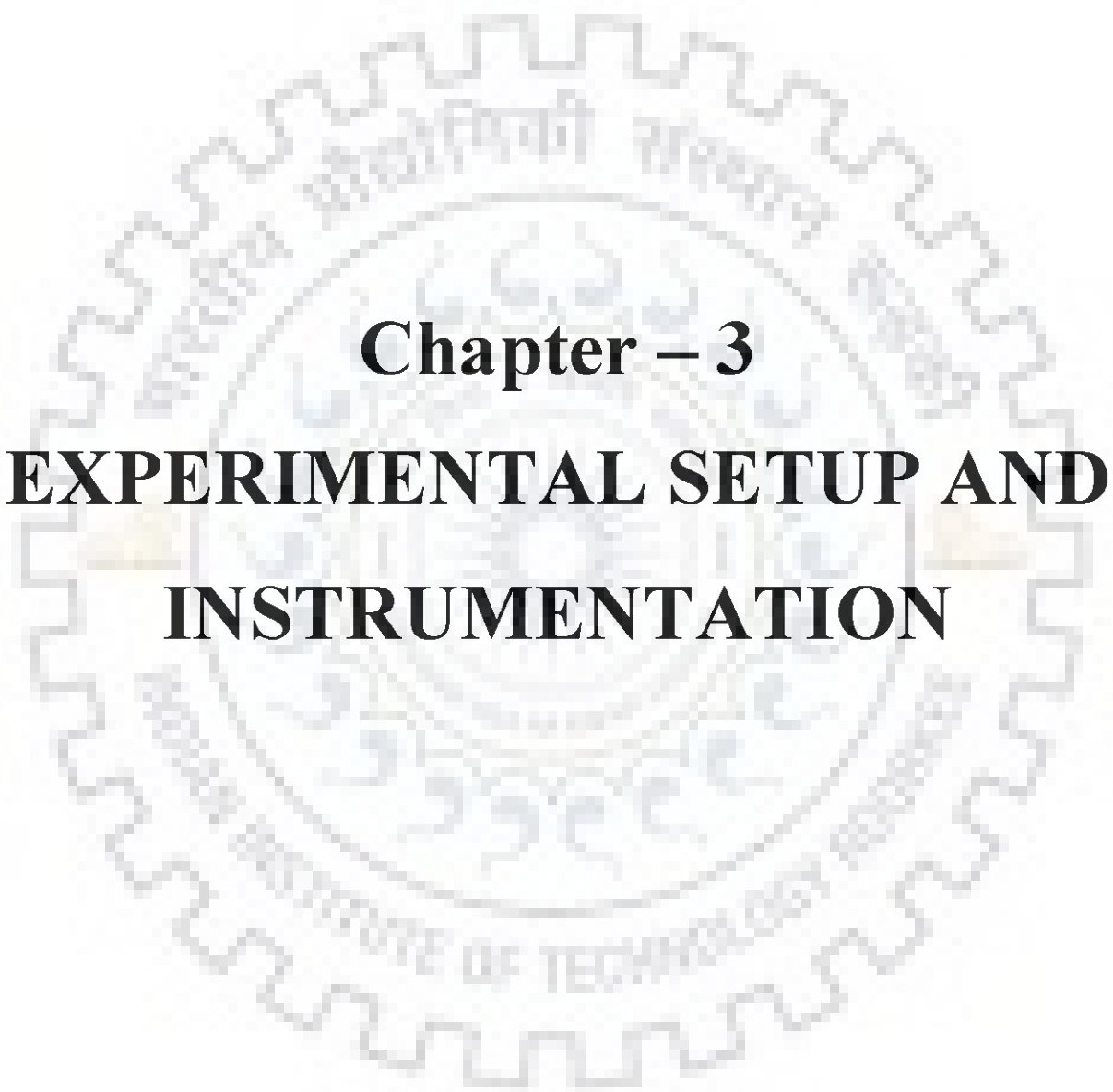
Studies will have been performed in the following sequences:

- Preparation and activation of adsorbent.
- Experimental comparison of adsorbents.
- Study of adsorption isotherms.
- Study of kinetic models.
- Column Study and Breakthrough analysis.

- Bio-Column Study and Breakthrough analysis.
- Selection of adsorbent on the basis of fluoride removal efficiency/adsorption capacity.
- Characterization of adsorbent like SEM, EDX and FTIR etc.
- Optimization process parameters like time, temperature, pH, fluoride concentration and adsorbent dose.
- Comparison between adsorptive and bio removal process.
- Study on biological removal of fluoride.
- Treatment of synthetic waste water in batch SAB reactor.
- Treatment of synthetic waste water in continuous SAB reactor.
- Treatment of real industrial waste water.







**Chapter – 3**  
**EXPERIMENTAL SETUP AND**  
**INSTRUMENTATION**



# EXPERIMENTAL SETUP AND INSTRUMENTATION

---

### 3.0 Motivation

This chapter deals with the experimental setup and instrumentation used for the removal of fluoride from synthetic simulated waste water by bioaccumulation, adsorption of fluoride using *Acinetobacter baumannii* (MTCC 11451), continuous column reactor and phytoremediation. Further, the experimental design, range of experimental parameters, details of setups and analytical instruments used in the present study are described later in this chapter.

### 3.1 Apparatus and Reagents

In our laboratory, spectrophotometer was used to measure the all assembled amounts. As the sample holder we used reagent bottles. The reagents were prepared as follows (Bellack and Schouboe 1958).

#### 3.1.1 Standard Fluoride Solution

A solution of concentration 100 mg/L was prepared by dissolving reagent grade sodium fluoride in distilled water. This was diluted further in order to obtain solutions with concentration ( $C_F$ ) in the range 1-6 mg/L.

#### 3.1.2 Reagent A

In 100 mL of distilled water 0.958 g of SPADNS was dissolved and it was diluted to 500 mL. If protected from direct sunlight this solution is indefinitely stable.

#### 3.1.3 Reagent B

In 25 mL of distilled water 0.133 g of Zirconyl chloride octahydrate was dissolved. After which 350 mL of concentrated hydrochloric acid (LR grade) was added to it. The mixture was then diluted with water to make up the final volume to 500 mL.

#### 3.1.4 Reagent S

To make a single reagent, equal volumes of reagent A and B were mixed henceforth referred to as reagent S. When kept away from light this reagent is stable for more than 2 years (APHA, 1975).

### 3.1.5 Reference Solution

Reagent S (5 mL) was mixed with 20 mL of distilled water to obtain the reference solution.

### 3.2 Preparation of Calibration Curve

The concentration of fluoride in the aqueous solution was determined by using UV-Spectrophotometer. A standard solution of fluoride was scanned and it was found that maximum absorbance occur at a wavelength of 570 nm. At this fixed wavelength absorbance corresponding to different concentration of fluoride solution was measured and a calibration curve was prepared between absorbance and fluoride concentration. The calibration curve between absorbance versus concentration was found to be linear for the fluoride concentration range of 0.0 to 1.4 mg/L with correlation coefficient ( $R^2$ ) =0.99. Then calibration curve was plotted between absorbance and concentration of standard fluoride solution for further use (Fig.3.2).

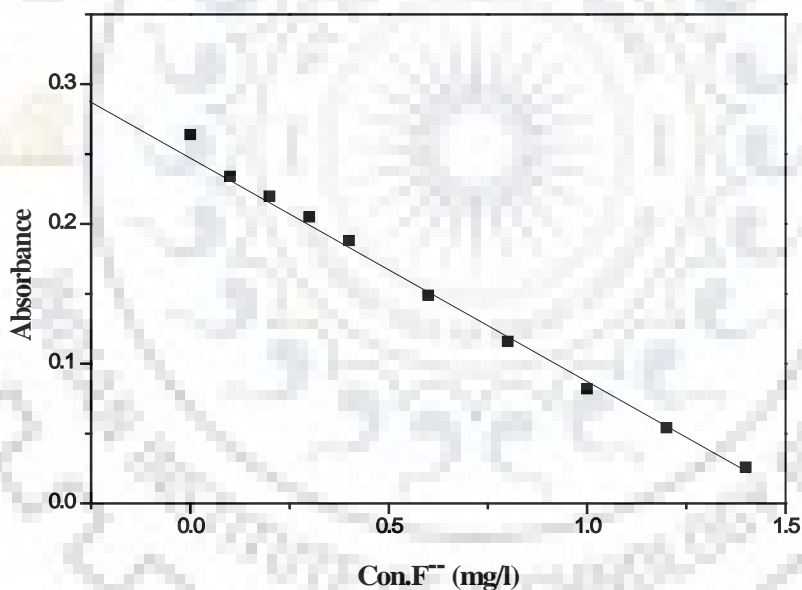


**Fig 3.2: Calibration Curve**

### 3.3 Details of Experimental Setup

#### 3.3.1 Analytical Instrumentals used for the Present Investigation

Analytical instrument are used in the present study where atomic adsorption spectroscopy (AAS), UV-Visible spectroscopy (FTIR), elemental analyzer, surface analyzer, X-Ray diffractometer, scanning electron microscope (SEM) etc. The photographs of the experimental setup have been given in Fig 3.3.2 (a) and (b). The techniques adopted for the analysis of various parameters and the instrument used for the analysis have been enlisted in Table.3.3.1.

**Table 3.3.1: Analysis Techniques/Instrument Used for the Analysis for Various Parameters**

Parameters	Methods	Model/ manufacture/ Specification
Cyanide concentration	Picric acid Colorimetric Method (510 nm) Iamarino (1989), A distillation method was also tried	Cyanide distillation apparatus are per APHA standards (Patil and Paknikar (2000a), Dash et al. (2008))
		Model DR-3000 UV-Spectrophotometer Hach©, USA and Model Lambda 35 Spectrometer Parkin- Elmer, USA.
pH	Digital pH meter with Electrode Mondal And Majumder, (2007)	NAINA NIG- 333, India and Model pH 720, WTW®, Germany
Shaking and Incubation	Orbital incubator Shaker Durdum et al. (1991)	Metrex Scientific Instrument Pvt. Ltd. New Delhi, India.
Straining and analysis of Microorganisms	Microscopic method mondal and Majumder,(2007)	Leica, Labindia Instruments Pvt. Ltd. India
Biomass Concentration (Optical Density)	U.V. Spectrophotometric Method Akcil et al.(2003)	Model DR – 3000 UV- VIS Spectrophotometer Hach. USA and Model Lambda 35 Spectrophotometer, Parkin - elmer
Centrifugation	Centrifugation method Mondal and Majumder (2007)	BiofuseStratos, Germany
Microbial examination	Scanning electron Microscopic(SEM) Analysis Mathur and Majumder, (2006)	Model LEO 335VP, LEO Electron Microscopy Ltd UK.
Surface Area pore	Surface Area Analyzing method	ASAp 2010 V2. 00C

Parameters	Methods	Model/ manufacture/ Specification
Area, Pore volume	et al.(2006)	Micrometrics.
CHNS	CHNS Analyzing Method mondal et al.(2006)	Elemental Analyser system , GmbH , Model Vario- EL V 3.00
FTIR	KBR Plate method	Thermo FTIR, model AVATAR 370
Ash Content	Ignition at 1100 <sup>0</sup> C	Muffle Furnace, NSW, India
Bulk density of GAC	Pycnometer	Pycnometer

### 3.3.2 Removal of fluoride in column reactor

This test was conducted in a SS pipe reactor column. The schematics diagram of the experimental setup is shown in Fig. 3.3.2 (a) & (b). SS columns pipe of different lengths viz  $Z_1 = 20$ ,  $Z_2 = 40$ ,  $Z_3 = 60$ ,  $Z_4 = 80$  and  $Z_5 = 100$  cm and 9 cm inside diameter had been brought in use, and the top of reactor was at 100 cm with net volume of 6.36 lit. Four equidistant ports of diameter 1.25 cm were introduced in the reactor for the collection of samples along the height of reactor (excluding inlet and outlet). The top portion and the bottom portion of the reactor were connected to the main column with the help of two joints, based on a SS screen (Mesh no: 16 BSS, aperture breadth: 1.00 mm).

**Table: 3.3.2 Salient feature of Fixed Bed Column/Bio-column Reactor**

Sr. No.	Description	Value
1	Reactor with Diameter (cm)	9.0
2	Reactor with height (cm)	100
3	Reactor with volume (liters)	5.03
4	Total numbers of sample points	5.0
5	Sampling point height (cm)	20,40,60,80 and 100 cm
6	Sample point diameter (cm)	1.25
7	Complete Absorbent Weight (gm)	2420
8	Density of Bed (gm/cc)	0.7166
9	Reactor Net volume (liters)	6.36



**Fig 3.3.2 (a) Photograph of Continuous Column Reactor**

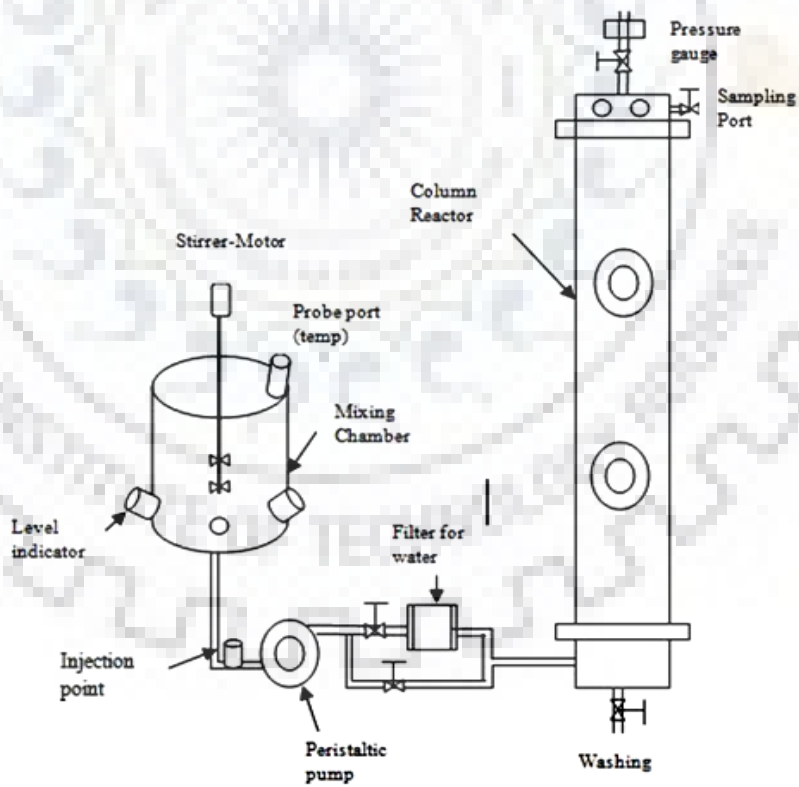


**Fig. 3.3.2 (b) Line Diagram of Continuous Column Reactor**

### **3.3.3 Instrumentation and Control**

Liquid flow rate was controlled and calibrated by peristaltic pump procured from Miclins India, Chennai. pH meter and D.O meter were used to measure the pH and D.O of the effluent samples respectively in mixing tanks as well as at the outlet of reactor.

### **3.3.4 Limitation of the Set-up**

Measuring instruments like pH meter, D.O meter were table top type. Therefore, the cross checking of the data collected from these instruments was essential. To insert the probes of the pH and D.O meter at the outlet of the reactor, a dead volume of around 300 mL had to be created.

## **3.4 Analytical and Auxiliary Instruments Used in the Present Study**

### **3.4.1 Analytical Instruments**

A number of analytical instruments used in the present study are UV-V is Spectrophotometer, Fourier Transform Infrared spectrophotometer (FT-IR), BET Surface area analyser, Fe-SEM Analysis. The photograph of analytical instrument used in the present study is given in Fig. 3.4.1(a-d).

### **3.4.2 Auxiliary Equipments**

Auxiliary equipment used in the present study were orbital cum incubator shaker, hot air oven, laminar airflow unit, pH meter, dissolved oxygen meter, muffle furnace, centrifuge, autoclave, water bath, Milli-Q water unit and weighing balance etc. The photographic image of Auxiliary Equipment's used in the present study is shown in Fig. 3.4.2.

## **3.5 Calibration of Measuring Instruments**

Calibration of instruments is very essential to get reliable data in the experiments. The procedure for the calibration of pH meter, D.O. meter and instruments used for the experimentation is given below:

### **3.5.1 Calibration of pH Meter**

Calibration of pH meter was done using pH buffers as per the instruction manual provided by the manufacturer.

### 3.5.2 Calibration of D.O. Meter

Calibration of D.O meter was done using sodium thiosulphite solution as per the instruction manual provided by the manufacturer.

### 3.5.3 Calibration of Experimental Setup

For batch experiments the temperature of incubator cum shaker was calibrated with the help of a pre-calibrated thermometer. For column study, variable speed peristaltic pump and rotameters required calibration before the start-up of experiments in column reactor. The rotameters were purchased with calibration certificate. Calibration of the peristaltic pump (Model PP-20) was done according to the instruction manual provided by Miclins India Ltd.



(a) Fe-SEM QUANTA 200 FEG (FEI Netherlands) (b) Spectrophotometer (HACH DR 5000)



BET Surface Area Analyzer

(d) FTIR Spectrometer (Thermo Model AVATR 370)

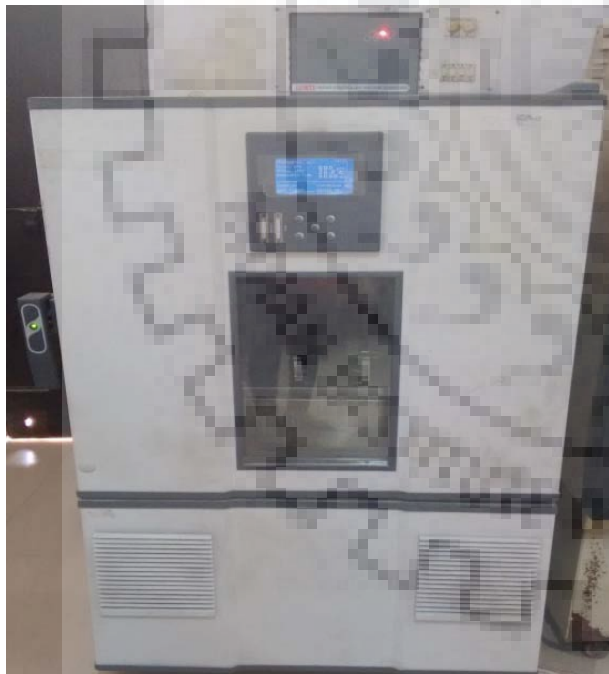
**Fig.3.4.1: Photographic Images of Analytical Instruments Used in the Present Investigation**



(a) Research Centrifuge REMI



(b) Muffle Furnace



(c) Orbital Shaker Cum Incubator



(d) Hot Air Oven

**Fig. 3.4.2 Photographic Images of Some Auxiliary Instruments used during the Present Investigation**





(e) Autoclave, Rivotek



(f) Laminar Air Flow Unit, Researcher Equipment



(g) DO meter



(h) Millipore water

**Fig. 3.4.2 Photographic Images of Some Auxiliary Instruments used during the Present Investigation**



(i) Weighing Balance, SHIMADZU, Japan



(j) REM Cyclone, Mixer



(k) pH meter (Toschon Pvt. Ltd., India)



(l) Peristaltic pump

**Fig.3.4.2 Photographic Images of Some Auxiliary Instruments used during the Present Investigation**

### **3.6 Artificial Photosynthesis Chamber**

The artificial photosynthesis chamber was used for the growth of aquatic macrophyte water hyacinth collected from solani river Roorkee, India. The plant was exposed to the toxic pollutant fluoride solution. The temperature, relative humidity and light intensity can be controlled in chamber. The Photographic image of plant growth chamber and water hyacinth is shown in Fig. 3.6. The plants were grown in 500 mL container made of polypropylene in nutrient Hoagland solution.

#### **3.6.1 Instrumentation and Control**

The maintenance of 24 h light and dark cycle, temperature, pressure and relative humidity is required.

#### **3.6.2 Limitation of the Set up**

Maintain of oxygen and Carbon-dioxide contain in the chamber for the photosynthesis is required.

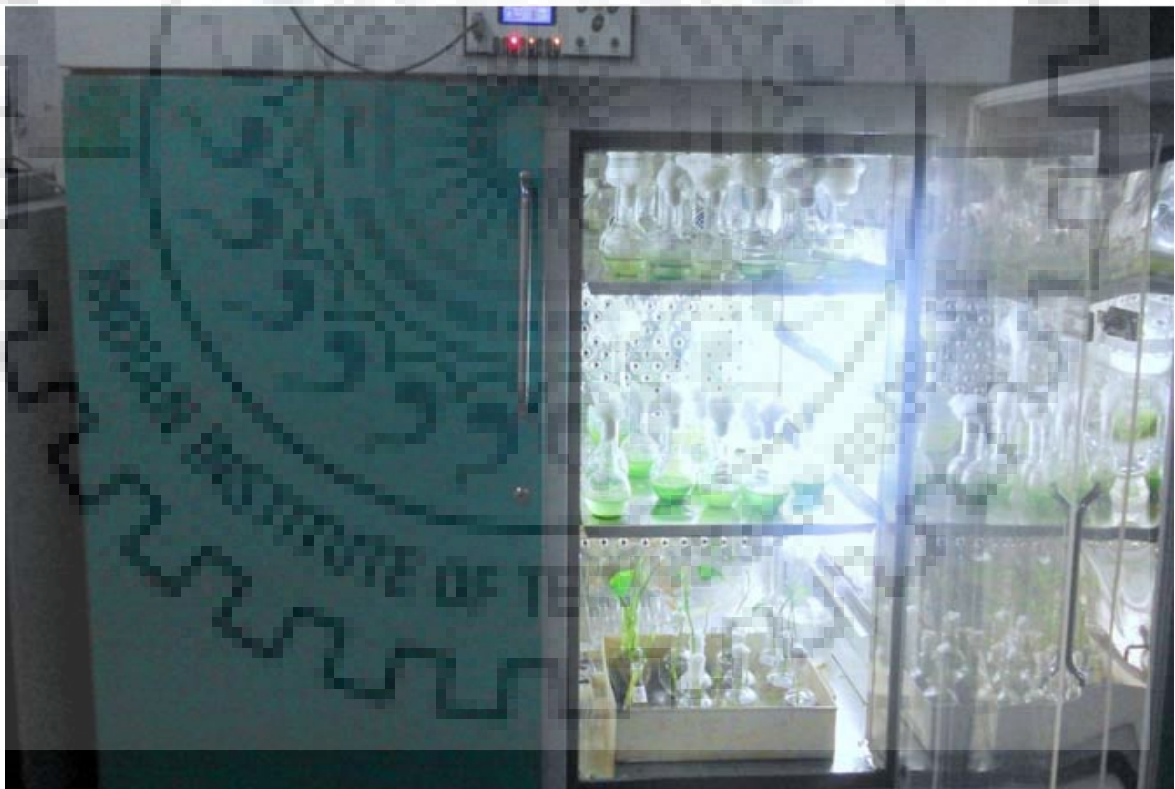


**Fig. 3.6 (a) Artificial Photosynthesis Chamber**



(b)



(c)



(b)

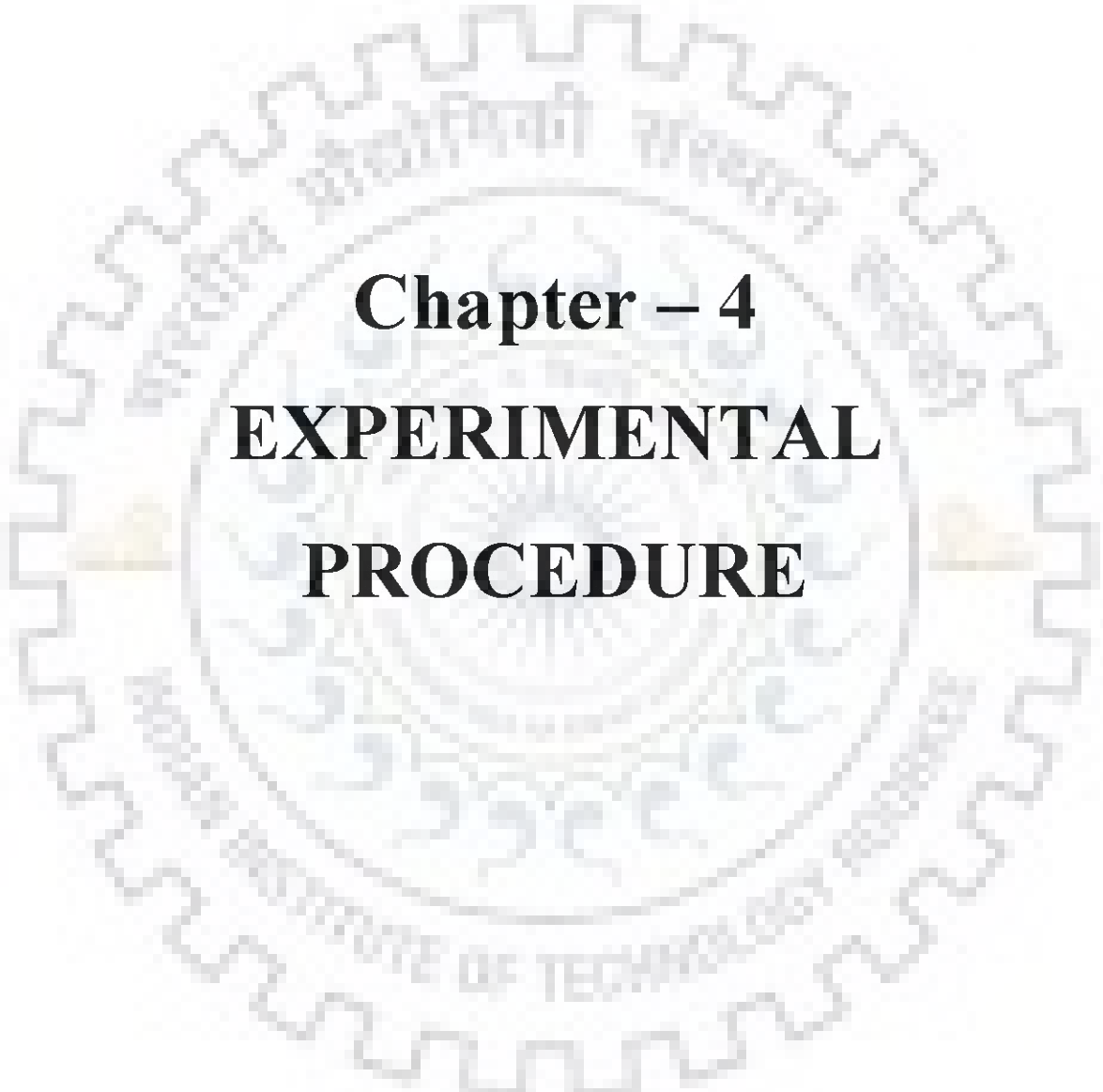


(c)

**Fig 3.6 Growth of (b) Ipomoea Aquatics plant and (c) water hyacinth Roots and Leaves**

### **3.7 Concluding Remarks**

This chapter is concerned with the understanding of the experimental set up formulated and the calibration of various instruments used for the experimentation.



**Chapter – 4**  
**EXPERIMENTAL**  
**PROCEDURE**

## EXPERIMENTAL PROCEDURE

---

### 4.0 General

On the base of the extensive literature review, objectives and aims an extensive program for removal of fluoride from simulated synthetic waste water by using different methods like Adsorption, Biological study, Simultaneous Adsorption Bioaccumulation (SAB) system, Continuous bioreactor system, Continuous system for phytoremediation has been made. In this chapter the experimental procedure for removal of fluoride from simulated synthetic waste water by using granular activated carbon (GAC), Peel, Groundnut Shell, Neem Leaves, Turmeric and MnO<sub>2</sub> coated turmeric, *Java plum seed (Syzgiumcumini)* and Banana peel is explained.

### 4.1 Design of experiments

Experimental programme is necessary to achieve the objectives of every research work. For the present study, it is given in figure 4.1. A total of 215 number of experiments as detailed in annexure A1-A43 were carried out for the removal of fluoride from synthetic simulated waste water by adsorption, bioaccumulation of fluoride, simultaneous adsorption and bioaccumulation, continuous reactor and phytoremediation. Adsorptive removal of fluoride from synthetic simulated waste water has been performed with pre treated agriculture waste adsorbent like Granular activated carbon (GAC), *Citrus Limetta Peel*, Groundnut Shell, Neem Leaves, *Java plum seed (Syzgiumcumini)* and Banana peel (Annexure A1 to A9). According to the experimental results of fluoride from synthetic simulated waste water, the adsorbent *Citrus Limetta Peel*, *Java plum seed (Syzgiumcumini)* were selected for adsorption of fluoride (Annexure A19 to A23). Biological removal of fluoride was carried out using bacterium *Acinetobacter baumannii* (MTCC 11451). Single substrate solution of fluoride is given in Annexure A24 to A29. The bio sorbent *Citrus limetta peel* and *Java plum seed (Syzgiumcumini)* were used as support for the immobilization of bacterium *Acinetobacter baumannii* (MTCC 11451) in single substrate solution and *Citrus Limetta Peel* for simultaneous adsorption and bioaccumulation of fluoride. Experimental data for adsorption and bioaccumulation of fluoride from single substrate solution is given in Annexure A32 to A35 respectively. *Java plum seed (Syzgiumcumini)* biomass as adsorbent were selected as packed bed in continuous reactor for the adsorption of fluoride (Annexure A32). Consortium culture of *Acinetobacter baumannii* (MTCC

11451) was immobilized onto the surface of packed bed for the adsorption and bioaccumulation of fluoride (Annexure A41). Phytoremediation studies has been performed in artificial phyto synthetic chamber using *Ipomoea aquatics Plant* (Roots and Leaves) and Roots of *Eichhornia Crassipes* for single solution is given in Annexure A42 to Annexure A43, respectively. The fluoride analysis, preparation of single waste water of fluoride and preparation and characterization of adsorbent, calibration of measuring instrument and set up . Design of experiments, experimental procedure and data recording for adsorbity removal, bioaccumulation of fluoride from simulated synthetic waste water have been discussed in this chapter. The summary of experiment carried out is given in Table 4.1.

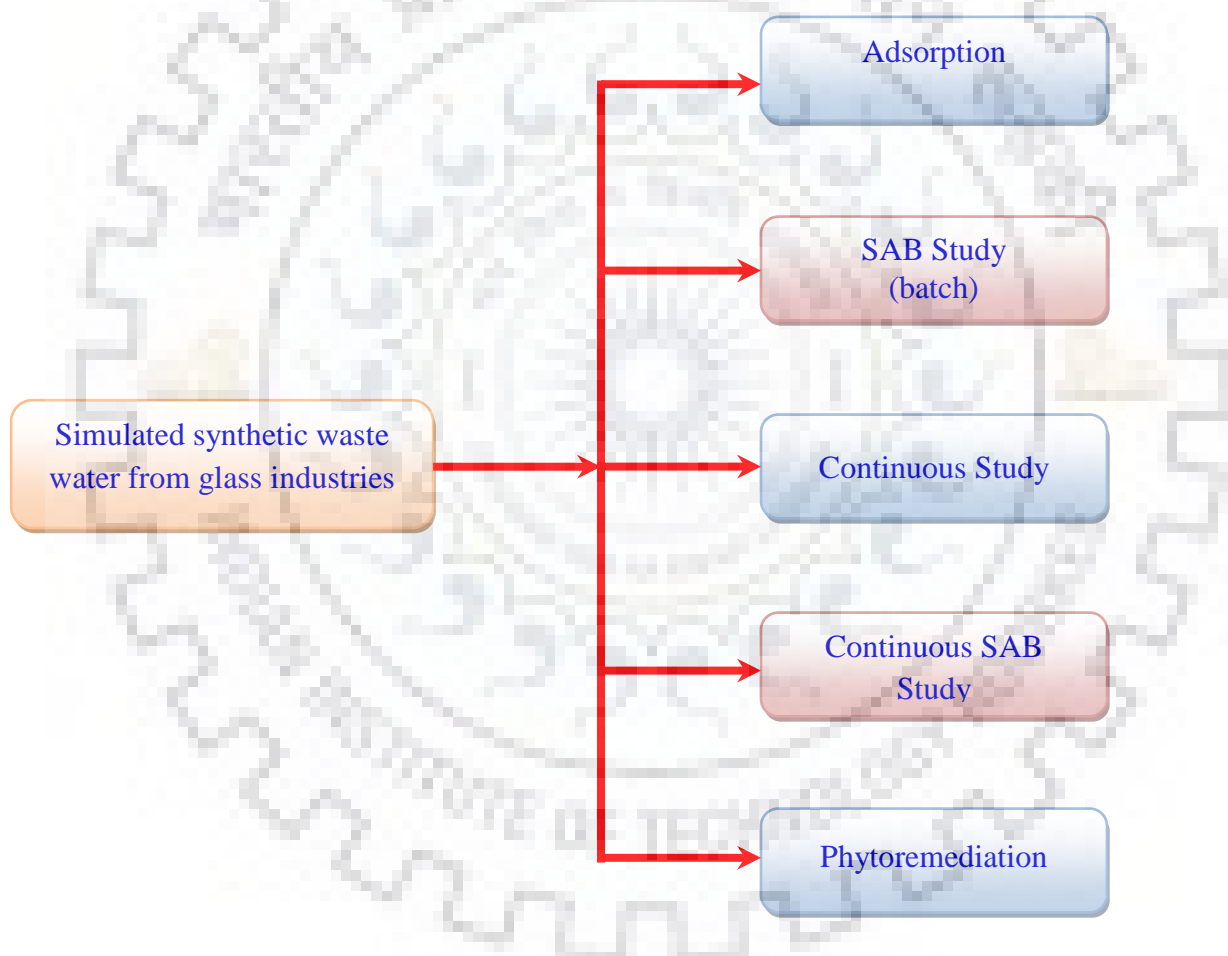


**Figure 4.1: Experimental program for removal of Fluoride from Simulated synthetic waste water from glass industries using different treatment methods**

**Table 4.1: Summary of various experiments conducted in the present study**

Process	Raw material	Batch study	Column study	Phyto remediation study using Ipomoea Aquatics Plant and Eichhornia Crassipes
Adsorption study for removal of fluoride from synthetic simulated waste water	Granular activated carbon (GAC)	1		
	<i>Citrus limetta peel</i>	2		
	Groundnut shell	3		
	Neem leaves	4		
	Turmeric and MnO <sub>2</sub> coated turmeric	5		
	<i>Java plum seed (Syzgiumcumini)</i>	6		
	Banana peel	7		
Bio removal of fluoride from synthetic simulated waste water	<i>Citrus limetta peel</i>	8		
	Neem leaves	9		
	<i>Java plum seed( Syzgiumcumini)</i>	10		
SAB study for removal of fluoride from synthetic simulated waste water (batch)	<i>Citrus limetta peel</i>	11		
	<i>Java plum seed(Syzgiumcumini)</i>	12		
Continuous SAB Study for removal of fluoride from synthetic simulated waste water	Consortium culture of <i>Acinetobacter baumannii</i> (MTCC 11451) immobilized on <i>Java plum seed (Syzgiumcumini)</i> waste biomass		13	
Phytoremediation	<i>Ipomoea aquatica</i> and <i>Eichhornia crassipes</i>			14

## 4.2 Batch Adsorption Studies

### 4.2.1 Adsorbents and their preparation method

The adsorbent used in the present study for the removal of fluoride from *Citrus limetta peel*, Groundnut shell, Neem leaves, Turmeric and MnO<sub>2</sub> coated turmeric, *Java plum seed (Syzgiumcumini)* and Banana peel. These adsorbents are easily available and cheaper in cost across the country. In the present study, they were collected from local place.



#### **4.2.1.1 Granular activated carbon (GAC)**

Granular activated carbon was purchased from HIMEDIA. It was crushed in rotary crusher to the desired particle size and after crushing; it was washed with Millipore water in triplicates and then dried in the hot air oven at 50 °C.

#### **4.2.1.2 *Citrus limetta peel***

*Citrus limetta peel* was collected from the fruits and juice centre outside of IIT Roorkee, India, washed several times in clean water after which it was left for four days in sun light for drying purpose. Following which, the sample-portion has been dried up with hot-air oven temperature 120 °C over a period of 2 days. Jaw crusher was used to crush dried material. Once crushed, this material is sieved using a mesh ASTM of 510 µm. For further use fined (retained) matter has been taken.

#### **4.2.1.3 Groundnut shell**

Groundnut shells were collected and simply washed with lukewarm water after which they were dried in sunlight for 2 days. The dried sample was further kept in a hot-air oven with temperature 100 °C for a period of 24 hours so that no moisture is left. Jaw crusher is used to crush out material after which it is screened using 510 µm mesh ASTM, for further use. The screened (retained) material is then placed in a container.

#### **4.2.1.4 Neem leaves**

Neem leaves were obtained from the IIT Roorkee campus, Roorkee, India. It was cleaned with water several times to remove the dirt adhering on the surface in triplicate. After washing it was dried in sun light for 6-7 hours. Following which this sample-portion has been dried up in the hot-air oven with temperature 40 °C over a period of 2 days. Jaw crusher was used to crush dried material. Once crushed, this material is sieved using mesh of 510 µm ASTM. For further use fined (retained) matter has been taken. The material is consequently stored within a vacuum box to use it further.

#### **4.2.1.5 *Java plum seed (Syzygiumcumini)***

*Java plum seed (Syzygiumcumini)* were collected from the local market in Roorkee, India. After the collection, the seeds are washed 3-4 times using regular tap water to remove all dust from the seeds. *Java plum seed (Syzygiumcumini)* are initially dried in the sunlight for 2 days, following which they are dried up in a hot-air oven within temperature 80 °C – 100 °C over 36 h. This material is

pulverized with a crusher, then screened through a mesh ASTM of 510  $\mu\text{m}$ , fined (retained) material is then stored in a container for further use. The material is consequently stored in an airtight container for later use.

#### **4.2.1.6 Turmeric and $\text{MnO}_2$ coated turmeric**

Turmeric was purchased from the local market in Roorkee, India. After collection, it was washed 3-4 times using regular tap water to remove all dust. Turmeric initially dried in the sunlight for 2-3 days, following which it was dried-up in a hot-air oven within temperature of 80  $^{\circ}\text{C}$  – 100  $^{\circ}\text{C}$  over a period of 36 h. This matter has been is pulverized with a crusher and fined using a mesh ASTM of 510  $\mu\text{m}$ ; Retained product is stored within a box to use it further.

We treated the screened material for 24 hours in  $\text{MnO}_2$ . Following the treatment, to make material neutral, it is washed with distilled water many times. Washed material is then left for 24 hours in hot-air oven with temperature of 90 $^{\circ}\text{C}$  with drying purpose. The product is consequently stored in vacuum box to use it further.

#### **4.2.1.7 Banana Peel**

Banana peels gathered from local market were used as low cost natural bio-adsorbent. It is washed four to five times by tap water to remove dust and finally washed with Millipore water. Banana peels are initially dried in sunlight for 3-4 days and then shrivelled in hot air oven at 50  $^{\circ}\text{C}$  – 80  $^{\circ}\text{C}$  for a period of 36 hrs. Banana peels are then puin jaw-crusher, followed by screening in 510  $\mu\text{m}$  ASTM mesh. For further use, the product is put in a vacuum box.

### **4.2.2 Characterization of adsorbents**

#### **4.2.2.1 FTIR Analysis of Adsorbents**

The functional groups existing in the bio-adsorbents after and before the adsorption of bio-adsorbents were estimated by utilizing Fourier Transform Infrared Spectroscopy (FTIR Spectroscopy) (Thermo Nicolet, Magna with 7600). These samplings had been analysed by the method of pellet by preparing sample pallets and KBr (1:10 w/w) for each sample. The spectra were collected in the range between 4000 - 400  $\text{cm}^{-1}$ .

#### 4.2.2.2 X-ray diffraction (XRD) and Scanning Electron Microscope (SEM) Analysis of Adsorbent

In order to study structure of bio adsorbents, X-ray diffraction of these adsorbent was carried out using X-ray diffractometer (Bruker AXS, Diffractometer D8, and Germany). To cover all the possible peaks the scanning angle ( $2\theta$ ) range was varied from  $10$  to  $90^\circ$ . Copper was used as a source to emit characteristic X-ray and only K- $\alpha$  ray were emitted from the shell to emit electron having sufficient energy. Nickel was used to filter the X-rays and allow only monochromatic X-rays to pass through it to fulfil necessary condition of diffraction. K radiation was maintained at  $1.542 \text{ \AA}$  whereas rotational speed of goniometer was fixed at  $1^\circ/\text{min}$ . When incident X-ray on sample satisfies the Bragg's equation ( $n\lambda=2d\sin\theta$ ) constructive interference takes place and at this condition Intensity peaks occurs. Identification of compound was done by using international centre for diffraction data (ICDD) library.

#### 4.2.2.3 Physical and chemical property of Adsorbent

##### 4.2.2.3.1 BET (Brunauer- Emmet-Teller) surface area

The (BET) surface area ( $\text{m}^2/\text{g}$ ) and bulk density ( $\text{g/L}$ ) of various adsorbents were calculated using surface area analyser ASAP 2010 Micrometrics, USA) (Chattopadhyaya et al., 2006).

##### 4.2.2.3.2 Proximate analysis

The moisture present in adsorbents (Granular activated carbon (GAC), *Citrus Limetta Peel*, Groundnut Shell, Neem Leaves, Turmeric and  $\text{MnO}_2$  coated turmeric, *Java plum seed* (*Syzygiumcumini*) and Banana peel was calculated using 3-4 g of adsorbent. The adsorbents were kept in oven at high temperature of  $105^\circ\text{C}$  for 1 hour. Later on heating it was well ventilated and weighted (Branzini et al., 2012). Result was obtained in the form of difference in weight of adsorbent, shown following formula was used to calculate the moisture content in the adsorbent.

$$X = \frac{W_i - W_f}{W_i}$$

Where;

$W_i$  initial wt of adsorbent,

$W_f$  final wt of adsorbent,

X moisture content wt %.

#### 4.2.2.3.3 Volatile material

The volatile material present in adsorbents (Granular activated carbon (GAC), *Citrus limetta Peel*, Groundnut Shell, Neem Leaves, Turmeric and MnO<sub>2</sub> coated turmeric, *Java plum seed* (*Syzygiumcumini*) and Banana peel) was calculated by taking 1 g of raw material. The adsorbent were kept in oven at high temperature of 750°C for 7 minute. After heating it was well ventilated and weighted (Babu et al., 2008). Result was obtained in the form of difference in wieght of adsorbents.

$$X = \frac{W_i - W_f}{W_i}$$

Where;

W<sub>i</sub> initial wt of adsorbent

W<sub>f</sub> final wt of adsorbent

X volatile content wt %

#### 4.2.2.3.4 Ultimate analysis

The C(%), H(%) and N(%) content present in adsorbent (Granular activated carbon (GAC), *Citrus Limetta Peel*, Groundnut Shell, Neem Leaves, Turmeric and MnO<sub>2</sub> coated turmeric, *Java plum seed* (*Syzygiumcumini*) and Banana peel were calculated by ultimate analysis table 5.1.1. Ultimate analysis is carried out by taking 1 g of adsorbent and kept it in hot air oven at a high temperature of 450°C for 1 hour (Acar et al., 2004). Fixed carbon was calculated by deducting from sum of the moisture content volatile matter and ash expressed as percent.

#### 4.2.3 Experimental program for batch adsorption study

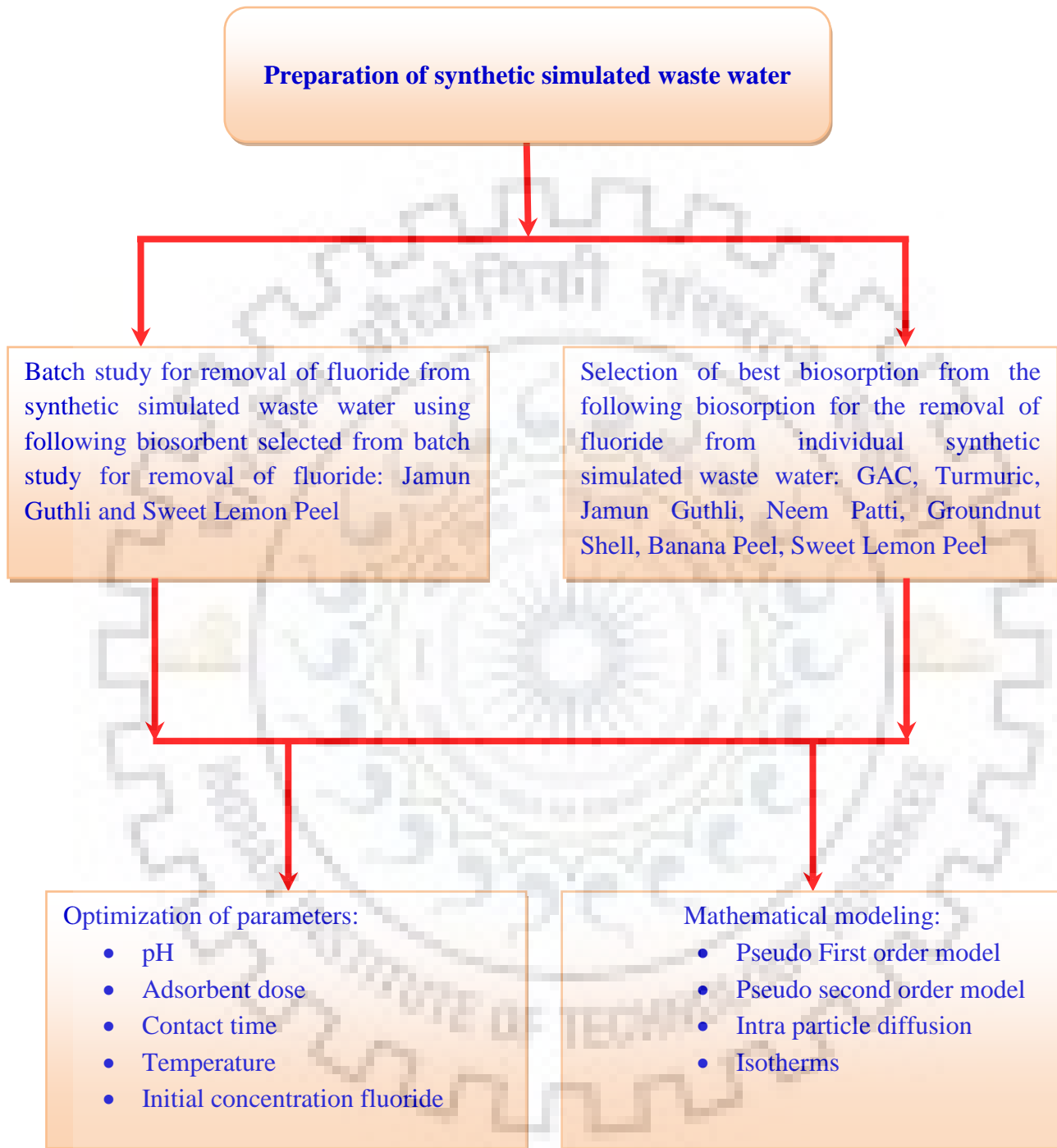


**Fig.4.2.3 Systematic block diagram of batch experiments for fluoride removal by adsorption using various adsorbents.**

#### **4.2.4 Batch Experiments**

Batch experiments were carried out in 250 ml round bottom flask with working volume of sample 100 ml at 30<sup>0</sup>C and 120 rpm in an incubator- shaker (Metrex, MO-250, India). All batch experiments were conducted for the optimization of parameters like contact time, initial concentration, pH and dose of adsorbents. Microbial culture was cultivated in batch mode. A preliminary test shown that the equilibrium adsorption and bio-degradation contact time was obtained after 86 hour. At the end of this period, the solutions were centrifuged and residual concentrations of fluoride at the equilibrium were determined. The effect of various parameters like adsorbent dose, pH and initial concentration of fluoride and contact time were studied as shown in Table 4.2.4.

##### **4.2.4.1 Batch adsorption studies onto the removal of fluoride at various pH for simulated synthetic waste water**

The pH impact on the fluoride absorption within 2-11 was studied using simulated synthetic waste water. These experiments had been conducted in thrice and average values were reported in Annexure (A1 to A7). The run number of various adsorbent like (Granular activated carbon (GAC), *Citrus Limetta Peel*, Groundnut Shell, Neem Leaves, Turmeric and MnO<sub>2</sub> coated turmeric, *Java plum seed (Syzgiumcumini)*) and Banana peel for the adsorption of fluoride is given in Table 4.2.4.1.

##### **4.2.4.2 Batch adsorption studies onto the removal of fluoride at various temperatures (°C) for simulated synthetic waste water**

The effect of various temperatures (°C) from 20-40<sup>0</sup>C was carried out for single component solution of fluoride as shown in Table.4.2.4.2.

##### **4.2.4.3 Batch adsorption studies onto the removal of fluoride at various adsorbent doses (mg/g) for simulated synthetic waste water**

The batch experiments were carried out to study the effect of adsorbent dose (mg/g) for the adsorption of fluoride from simulated synthetic waste water onto the surface of various adsorbents. The experimental data associated with the effect of adsorbent dose for the simulated synthetic waste water is shown in Table.4.2.4.3.

#### 4.2.4.4 Batch adsorption studies onto the removal of fluoride at various initial concentrations (mg/L) for simulated synthetic waste water

In the present work, batch adsorption studies for various adsorbents to evaluate the effect of initial concentration of 10 -30 mg/L for simulated synthetic waste water of fluoride was carried out. All the experimental data generated for the investigation of the effect of initial concentration were used for equilibrium isotherm modelling, given in Table.4.2.4.4.

#### 4.2.4.5 Batch adsorption studies onto the removal of fluoride at various contact time for simulated synthetic waste water

The effect of contact time was carried out for equilibrium condition when driving force becomes zero. The concentration gradient between adsorbent surface and synthetic solution of fluoride becomes zero. All the experiments were carried out thrice and average values were reported in Table.4.2.4.5. The results of these experimental run were also used for the kinetics modelling of the adsorption process with each adsorbent using intra particle diffusion, pseudo second order and pseudo first order.

**Table 4.2.4: Range of Operating Parameter for adsorption studies of Fluoride from Simulated Synthetic Waste Water**

Experiment	Operating Parameters				
	pH	Temp ( <sup>0</sup> C)	Dose (g/L)	Initial conc of Fluoride (mg/L)	Contact time (min)
<b>GAC</b>					
Effect of pH	<b>2-11</b>	30	4	20	60
Effect of Temp	4	<b>20-40</b>	4	20	60
Effect of adsorbent dose	4	30	<b>4-40</b>	20	60
Effect of Contact Time	4	30	32	20	<b>20-180</b>
Effect of Initial Conc.	4	30	32	<b>10-30</b>	160
<b>Citrus Limetta Peel</b>					
Effect of pH	<b>3-11</b>	30	2	20	60
Effect of Temp	5	<b>20-40</b>	2	20	60
Effect of adsorbent dose	5	30	<b>2-20</b>	20	60

Experiment	Operating Parameters				
	pH	Temp ( <sup>0</sup> C)	Dose (g/L)	Initial conc of Fluoride (mg/L)	Contact time (min)
Effect of Contact Time	5	30	10	20	<b>5-60</b>
Effect of Initial Conc.	5	30	10	<b>10-30</b>	40
<b><i>Java Plum Seed (Syzygiumcumini)</i></b>					
Effect of pH	<b>2-9</b>	30	2	20	60
Effect of Temp	6	<b>20-40</b>	2	20	60
Effect of adsorbent dose	6	30	<b>2-20</b>	20	60
Effect of Contact Time	6	30	12	20	<b>5-60</b>
Effect of Initial Conc.	6	30	12	<b>10-30</b>	40
Experiment	Operating parameters				
	pH	Temp ( <sup>0</sup> C)	Dose (g/L)	Initial conc of Fluoride (mg/L)	Contact time (min)
<b>Ground nut Shell</b>					
Effect of pH	<b>2-12</b>	30	4	20	60
Effect of Temp	7	<b>20-40</b>	4	20	60
Effect of adsorbent dose	7	30	<b>4-20</b>	20	60
Effect of Contact Time	7	30	18	20	<b>10-90</b>
Effect of Initial Conc.	7	30	18	<b>10-30</b>	90
<b>Banana Peel</b>					
Effect of pH	<b>2-12</b>	30	4	20	60
Effect of Temp	6	<b>20-40</b>	4	20	60
Effect of adsorbent dose	6	30	<b>4-20</b>	20	60
Effect of Contact Time	6	30	20	20	<b>10-90</b>
Effect of Initial Conc.	6	30	20	<b>10-30</b>	75



Experiment	Operating Parameters				
	pH	Temp ( <sup>0</sup> C)	Dose (g/L)	Initial conc of Fluoride (mg/L)	Contact time (min)
<b>Neem Patti</b>					
Effect of pH	<b>2-10</b>	30	2	20	60
Effect of Temp	4	<b>20-40</b>	2	20	60
Effect of adsorbent dose	4	30	<b>2-20</b>	20	60
Effect of Contact Time	4	30	12	20	<b>5-60</b>
Effect of Initial Conc.	4	30	12	<b>10-30</b>	40

**Table.4.2.4.1 Run number of experiments conducted to study the effect of varying pH onto the removal of fluoride from simulated synthetic waste water by various adsorbents**

Adsorbents	Table no.	Run no.
Granular activated carbon	A.1	1-10
<i>Citrus Limetta Peel</i>	A.2	39-47
Groundnut Shell	A.3	77-87
Neem Leaves	A.4	115-122
Turmeric	A.5	151-162
MnO <sub>2</sub> coated turmeric	A.6	190-200
<i>Java plum seed</i> (Syzgiumcumini)	A.7	228-235
Banana peel	A.8	262-273

**Table.4.2.4.2 Run number of experiments conducted to study the effect of varying temperature onto the removing of fluoride from simulated synthetic waste water through various adsorbents**

Adsorbents	Table no.	Run no.
Granular activated carbon	A.1	11-15
<i>Citrus Limetta Peel</i>	A.2	48-52
Groundnut Shell	A.3	88-92
Neem Leaves	A.4	123-127
Turmeric	A.5	163-157
MnO <sub>2</sub> coated turmeric	A.6	201-205

<b>Adsorbents</b>	<b>Table no.</b>	<b>Run no.</b>
<i>Java plum seed</i> ( <i>Syzygiumcumini</i> )	A.7	236-240
Banana peel	A.8	274-278

**Table.4.2.4.3 Run number of experiments conducted to study the effect of varying dose onto the removing of fluoride from simulated synthetic waste water through various adsorbents**

<b>Adsorbents</b>	<b>Table no.</b>	<b>Run no.</b>
Granular activated carbon	A.1	16-25
<i>Citrus Limetta Peel</i>	A.2	53-61
Groundnut Shell	A.3	93-101
Neem Leaves	A.4	128-136
Turmeric	A.5	168-176
MnO <sub>2</sub> coated turmeric	A.6	206-214
<i>Java plum seed</i> ( <i>Syzygiumcumini</i> )	A.7	241-247
Banana peel	A.8	279-287

**Table.4.2.4.4 Run number of experiments conducted to study the effect of varying fluoride concentration onto the removal of fluoride from simulated synthetic waste water by various adsorbents**

<b>Adsorbents</b>	<b>Table no.</b>	<b>Run no.</b>
Granular activated carbon	A.1	26-30
<i>Citrus Limetta Peel</i>	A.2	62-66
Groundnut Shell	A.3	102-106
Neem Leaves	A.4	137-140
Turmeric	A.5	177-181
MnO <sub>2</sub> coated turmeric	A.6	215-219
<i>Java plum seed</i> ( <i>Syzygiumcumini</i> )	A.7	248-251
Banana peel	A.8	288-292

**Table.4.2.4.5 Run number of experiments conducted to study the effect of varying contact time onto the removal of fluoride from simulated synthetic waste water by various adsorbents**

Adsorbents	Table no.	Run no.
Granular activated carbon	A.1	31-38
<i>Citrus Limetta Peel</i>	A.2	67-76
Groundnut Shell	A.3	107-114
Neem Leaves	A.4	141-150
Turmeric	A.5	182-189
MnO <sub>2</sub> coated turmeric	A.6	220-227
<i>Java plum seed (Syzgiumcumini)</i>	A.7	252-261
Banana peel	A.8	293-300

### 4.3 SAB Process

#### 4.3.1 Materials

The following chemical were used in this research work: sodium Chloride, Agar, Tryptone, Yeast Extract, Millipore water, *CitrusLimetta Peel* adsorbents, Bacteria (*Actinobacter baumannii*).

**Table 4.3.1: Composition of Media for Microorganisms**

Micro-organisms	Media compositions (g/l)
<i>Acinetobacter baumannii</i> (MTCC 11451)	Sodium Chloride, NaCl (10) Tryptone (10) Yeast Extract (5)

#### 4.3.2 Growth of Bacteria *Acinetobacter baumannii* (MTCC 11451)

Growth is orderly increase in quantity of the cellular constituents. It depends on the ability of the cell to form new protoplasm from nutrients available in the environment. Growth of bacteria corresponds to increase in cell mass and ribosomes, synthesis of new cell wall, duplication of chromosomes and plasma membrane, septum formation and division of cell.

Bacterial population growth studies require inoculation of viable cell into a sterile broth medium and inoculation of the culture under optimum pH, temperature and shaking speed. Under these conditions, the cell will reproduce rapidly and dynamic of the microbial growth can be charted by means of a

population growth curve which is plotted between increase in number of cell and time. The stage of typical growth curve:

- Lag phase
- Growth phase
- Stationary phase
- Death phase

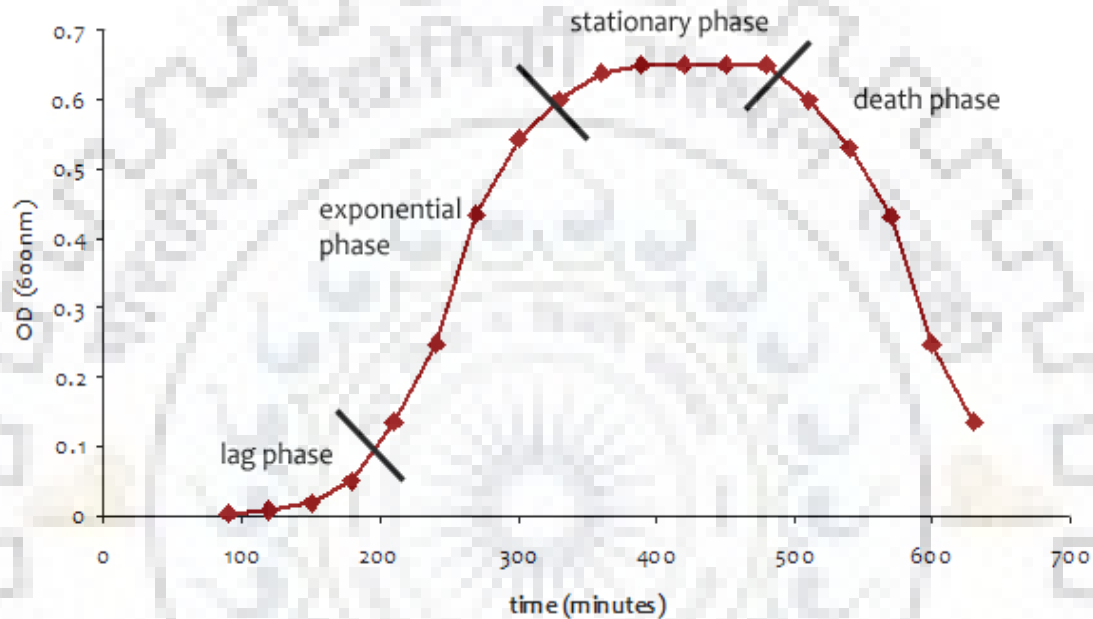


**Fig. 4.3.2: Growth Curve Model**

#### **4.4 Procedure for Growth of Bacteria**

##### **4.4.1 Preparation of Agar Media**

Sodium chloride (10gm/L), Tryptone (10gm/l), Yeast extract (5gm/L) and agar (20gm/L) are dissolved in 1 liter of millipore water and sterilized at 121°C. Prepared sample used to provide as nutrients for microbial culture.

##### **4.4.2 Preparation of Petri Dishes**

Petri dishes are small flat bottomed container made from clear glass. They have two halves—a top and bottom which slot into one another, this protect from unwanted contaminants. Petri dish must be completely sterilized before they are used for growing bacteria. In laminar chamber, very carefully pour the warm agar solution (obtained from sterilization) into the bottom part of the petri dish and quickly replace the top half of the petri dish to avoid any air born bacteria.

#### **4.4.3 Inoculation of Bacteria**

Once the agar solution hardened and the petri dishes are at room temperature. It is inoculated with the designed strain.

#### **4.4.4 Sterilization**

A widely used method for heat sterilization is autoclave. In this process water is heated to a temperature of 121-134°C. To achieve sterility, a holding time of at least 45 minutes at 121°C, (250°F) at 100 kPa or 15 psi is required. Proper autoclave treatments will kill all active fungi, bacteria, viruses and also bacterial spores, which are quite resistant. For effective sterilization steam needs to penetrate the autoclave uniformly.

#### **4.5 Methods of Microbial Work**

All the chemicals used in this study were obtained from Himedia Laboratories Pvt. Ltd. Mumbai India. Stock solution containing 20 mg/l fluoride was prepared by diluting 1 ml of 2000 mg/l fluoride in 100 ml Millipore water (Q - H<sub>2</sub>O, Millipore Corp. Having resistance of 18.2 MX-cm). A complete solution of 2000 mg/l is prepared by dissolving 0.442 mg of extra pure sodium fluoride in 100 ml of millipore water. Microbial culture obtained from MTCC centre Chandigarh India.

#### **4.6 Batch Experiments**

Batch experiments were carried out in 250 ml round bottom flask with working volume of sample 100 ml at 30<sup>0</sup>C and 120 rpm by an incubator-cum- shaker (Metrex, MO-250, India). All these batch experiments were conducted for the optimization of parameters like contact time, initial concentration, pH and dose of adsorbents. Microbial culture are cultivated a preliminary test showed that the equilibrium adsorption and bio-accumulation contact time was obtained after 86 hour. At the end of this period, the solutions were centrifuged and residual concentrations of fluoride at the equilibrium were determined.

#### **4.7 Growth Curve of Bacteria**

The freeze-dried culture bacteria strain *Acinetobacter baumannii* (MTCC 11451) was purchased from MTCC Chandigarh. The *Acinetobacter baumannii* (MTCC 11451) was grown in both L.B media and N.B media to examine the growth and % removal of fluoride. A L.B medium is shown in Table 4.3.1. The culture was inoculated in 100 ml media in 250 ml of conical flask and then

incubated in an incubated shaker with agitation speed of 120 rpm at 30<sup>0</sup>C. The conical flask containing growth media was steam sterilized in autoclave at 120<sup>0</sup>C for 30 minutes at pressure of 15 psi.

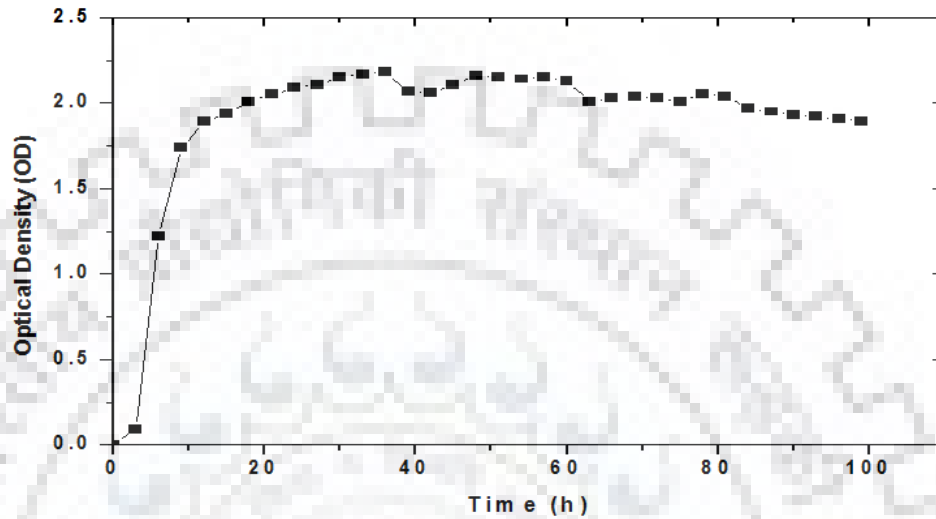


**Fig. 4.7: Calibration curve between Optical Density versus time (h)**

#### **4.7.1 Experimental program**

Experiments were carried out for biological removal of fluoride from simulated synthetic waste water of fluoride (Figure. 4.7.1). This illustrates the complete sequence of the experiment performed for fluoride removal by SAB process in the batch studies.

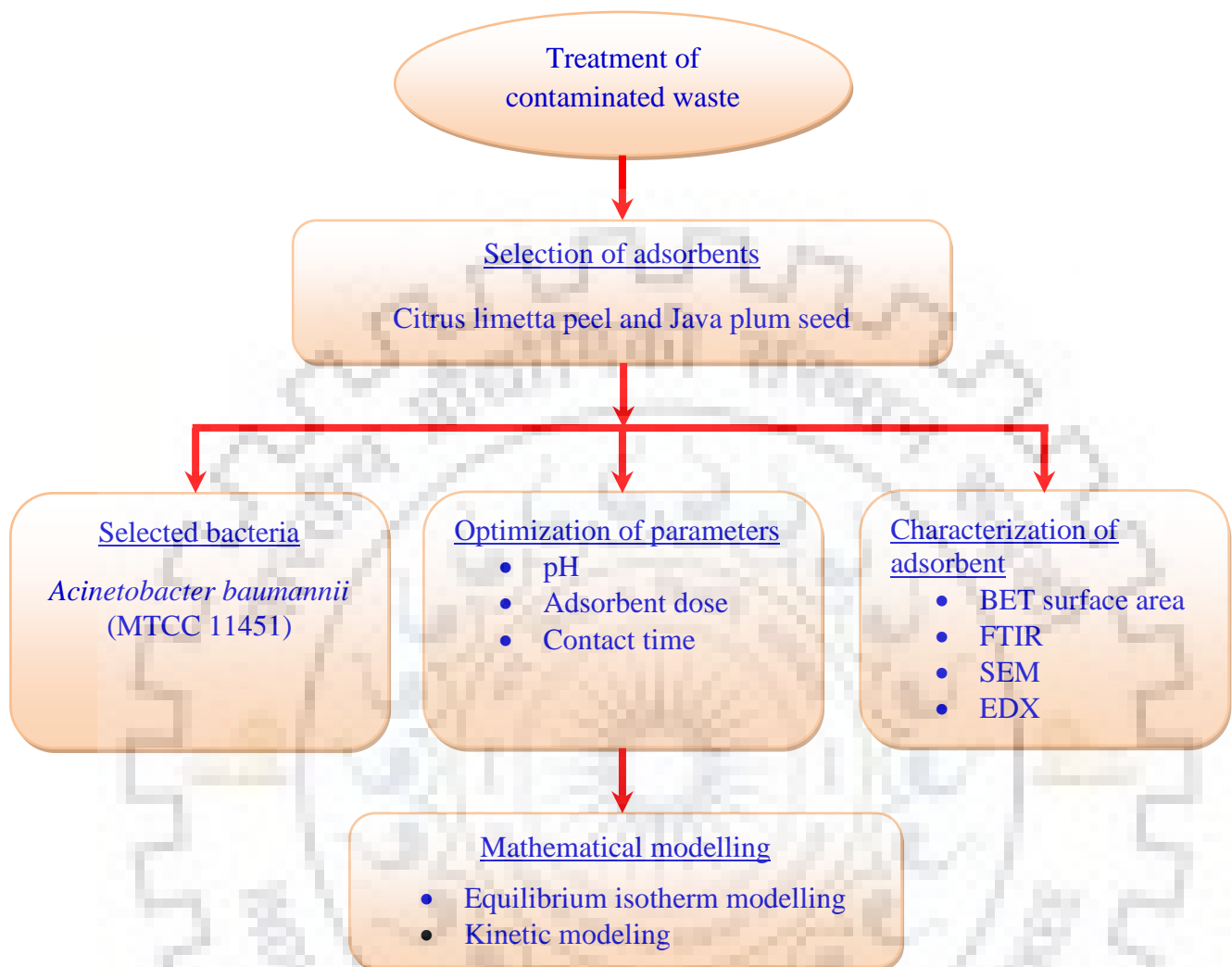


**Figure 4.7.1: Schematic block diagram of batch experimentation on removal of fluoride in SAB system**

#### 4.8 Fixed-Bed Design Models

To design batch treatment units, batch adsorption models are simple and useful, while their application to design continuous treatment units is more complicated. One dimensional advection dispersion equation that assumes linear sorption isotherm of the solute on to the solid surface is a commonly used fixed-bed mathematical model for flow and reaction in porous materials (Zewge F, (2001)).

$$\frac{\partial C}{\partial t} = D_e \frac{\partial^2 C}{\partial x^2} - Vx \frac{\partial C}{\partial x} - \rho_s \frac{1-\varepsilon}{\varepsilon} K_d \frac{\partial C}{\partial t} \quad (7)$$

Where,

- C Concentration of the solute;
- $D_e$  Effective diffusion coefficient;
- $\rho_s$  Density of the solid phase;
- $\varepsilon$  Porosity of the bed;
- q Mass of solute sorbed per unit of sorbent;
- $v_x$  Average linear velocity of pore fluid in the x direction;
- $K_d$  Linear distribution coefficient.

To predict the breakthrough curve in more accurate manner is the main objective of the above mentioned model. But in order to apply this model, we need to have physical and kinetic parameter which can be obtained either from batch adsorption studies or from estimated literature values. In addition to that, the models also require the solution of a number of non-linear partial differential equations which include physical as well as kinetic parameters. These equations can be solved only by numerical methods that are time consuming and tedious (Singh and Mazumder, 2015). Therefore, we need to seek other simplified models to design a fixed-bed adsorption column.

For this system, the balance can be expressed according to the following equation:

$$QvC_0 = QvC_t + Vp \frac{\partial C}{\partial t} + m \frac{\partial q}{\partial t} \quad (8)$$

Where;

$Qv$  is the volumetric flow of the solution in the column ( $L \text{ min}^{-1}$ ),  $C_0$  and  $C_t$ , respectively, the influent and effluent solute concentrations ( $mg \text{ L}^{-1}$ ),  $QvC_0$  the influent flow of solute in the column ( $mg \text{ min}^{-1}$ ),  $QvC_t$  the effluent flow of solute leaving the column ( $mg/\text{min}$ ),  $Vp$  the pore volume (L);  $Vp = \frac{1}{1-\varepsilon} (Va)$  where  $V_a$  is the bulk Volume and  $\varepsilon$  the porosity,  $Vp \frac{\partial C}{\partial t}$  the flow rate through the bed depth column ( $mg \text{ min}^{-1}$ ) and  $m \frac{\partial q}{\partial t}$  the amount of solute adsorbed onto adsorbent ( $mg \text{ min}^{-1}$ ) where  $m$  is the mass of adsorbent and  $\frac{\partial q}{\partial t}$  the adsorption rate.

The operation of fixed-bed adsorption column is commonly expressed in terms of mass balance as shown below.



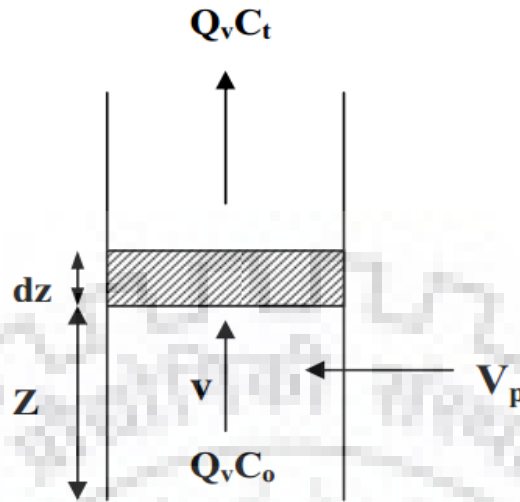


**Fig. 4.8 Mass Balance in a Fixed-Bed Column Element**

For this system, the balance can be expressed according to the following equation:

$$QvCo = QvCt + Vp \frac{\partial c}{\partial t} + m \frac{\partial q}{\partial t} \quad (8)$$

Where  $Q_v$  is the volumetric flow of the solution in the column ( $L \text{ min}^{-1}$ ),  $C_0$  and  $C_t$ , respectively, the influent and effluent solute concentrations ( $\text{mg L}^{-1}$ ),  $QvC_0$  the influent flow of solute in the column ( $\text{mg min}^{-1}$ ),  $QvC_t$  the effluent flow of solute leaving the column ( $\text{mg min}^{-1}$ ),  $V_p$  the pore volume ( $L$ );  $V_p = \frac{1}{1-\varepsilon} (V_a)$  where  $V_a$  is the bulk Volume and  $\varepsilon$  the porosity,  $V_p \frac{\partial c}{\partial t}$  the flow rate through the bed depth column ( $\text{mg min}^{-1}$ ) and  $m \frac{\partial q}{\partial t}$  the amount of solute adsorbed onto adsorbent ( $\text{mg min}^{-1}$ ) where  $m$  is the mass of adsorbent and  $\frac{\partial q}{\partial t}$  the adsorption rate.

From mass balance of a fixed-bed reactor, the determining factors of the balance for a given bed depth of the column are the linear flow rate  $v$ , the initial solute concentration, the adsorption potential and the pore volume even if the later parameter may be neglected. Therefore, in order to optimize the adsorption process in a packed-bed column it is necessary to examine these parameters and to estimate their influence (Bayari et al., 1995).

By varying the above process parameters, the optimum conditions for the column operation can be predicted through different design methods. There are a number of simple design models available which are based upon general assumption. These include BDST, EBRT, and Thomas model.

The applicability of simplified models is extensively studied for the removal of organic solutes by activated carbon. And their applicability to model fluoride adsorption is now emerging. Ghorai (Viswanathan et al., 2009) indicated that bed depth service time (BDST) model was applied successfully for fluoride adsorption on to activated alumina.

#### 4.9 Bed Depth Service Time (BDST) Design Model

In a fixed-bed system, the main design criterion is to predict how long the adsorbent material will be able to sustain removing a specified amount of solute from solution before regeneration is needed. This period of time is called the service time of the bed (Singh and Mazumder, 2015). The BDST model describes a relation between the service time of the column and the depth of packed bed column. The original work on the BDST model was carried out by Bohart and Adams (Meenakshi and Vishwanathan, (2007)) on the adsorption, in dynamic system, of the chlorine onto activated charcoal and those of Thomas (Lagergren, 1898) on the adsorption of the ions by zeolites. The authors demonstrated that the system agrees with Eq. (9) (The derivation of Eq. 9 is indicated in appendix A).

$$\ln \left[ \frac{C_o}{C_b} - 1 \right] = \ln \left( e^{(KN_o/v)D} - 1 \right) - KC_o T_b \quad (9)$$

In the relation  $e^{(KN_o/v)D} \gg 1$  thus  $\ln(e^{(KN_o/v)D}) - 1$  approximately equal to  $\frac{KN_o}{v} D$ , that is the reason why Hutchins (Weber and Morris, (1963)) proposed the following linear equation between the column bed depth (D) and the service time ( $T_b$ ):

$$T_b = \frac{N_o}{C_o v} D - \frac{1}{KC_o} \ln \left( \frac{C_o}{C_b} - 1 \right) \quad (10)$$

Here

- $T_b$  Service time at breakthrough point (h),
- $N_o$  Absorption capacity of the bed ( $\text{mg cm}^{-3}$ ),
- D Depth of the packed-bed column (cm),
- v Linear flow rate through the bed ( $\text{cm h}^{-1}$ ),

- $C_0$  Initial concentration of fluoride ( $\text{mg L}^{-1}$ )  
 $C_b$  Concentration of fluoride at breakthrough point ( $\text{mg L}^{-1}$ )  
 $K$  Adsorption rate constant ( $\text{L mg}^{-1} \text{ h}^{-1}$ ).

Equation 10 can be written in the form of a straight line (i.e.,  $y = m \cdot x + c$ ). The quantified value of the slope ( $m$ ) =  $N_0/C_0V$  and the intercept ( $c$ ) =  $- \{1/KC_0 [\ln (C_0/C_b-1)]\}$ . Total absorption capacity of the system ( $N_0$ ) and the rate constant ( $K$ ) can be found out with help of the slope and intercept of the straight line plotted as the service time against the bed depth. The value of lowest bed depth ( $D_{\min}$ ) that represents the theoretical depth of adsorbent required to stop the adsorbent concentration from going beyond  $C_b$ , can be achieved by putting  $T_b = 0$ . Thus, Eq.10 can be written as:

$$D_{\min} = \frac{v}{KN_0} \ln\left(\frac{C_0}{C_b} - 1\right) \quad (11)$$

The slope of straight line obtained from Eq. 10, can also apply to indicate the functioning of bed. In case, there is any variation for the beginning fluoride concentration (from  $C_{01}$  to  $C_{02}$ ), Hutchins (Weber and Morris, (1963)) propounded that new slope  $a_2$  and new intercept  $b_2$  can be assessed as follows with the help of Eq. (12) and Eq. (13), respectively:

$$a_2 = a_1 \frac{C_{01}}{C_{02}} \quad (12)$$

$$b_2 = b_1 \frac{C_{01}}{C_{02}} \frac{\ln\left[\left(\frac{C_{02}}{C_b}\right)-1\right]}{\ln\left[\left(\frac{C_{01}}{C_b}\right)-1\right]} \quad (13)$$

Further, if there is any variation in volume-related rate of flow of fluoride solution to the same absorption functioning, new slope and intercept remains unaltered and can be denoted as (McKay et al. 1984):

$$a_2 = a_1 \frac{Q_1}{Q_2} = a_1 \frac{v_1}{v_2} \quad (14)$$

#### 4.10 Empty Bed Residence Time Design Model

The Empty Bed Residence Time (EBRT) Model, or sometimes referred to as empty bed contact time (EBCT), is a design procedure used to determine the optimum adsorbent usage in the fixed-bed adsorption column. McKay and Bino (Liao and Shi, 2005) proposed that the capital and operation costs of the adsorption system for a fixed liquid flow rate, feed concentration and adsorbent characteristics were almost entirely dependent on EBRT and adsorbent exhaustion rate only. The

EBRT is the time required for the liquid to fill the column, on the basis that the column contains no adsorbent packing, and is a direct function of liquid flow rate and column bed volume.

$$EBRT = \frac{\text{Bed volume}}{\text{Volumetric flow rate of the liquid}} \quad (15)$$

The adsorbent exhaustion rate is the weight of adsorbent used in the column per volume of liquid treated at the time breakthrough occurs. That is

$$\text{Adsorbent exhaustion rate} = \frac{\text{Mass of adsorbent used}}{\text{Volume of liquid treated at breakthrough}} \quad (16)$$

Data used for the EBRT model can be obtained from the BDST analysis. Once a breakthrough percentage is specified, the service time for the column before breakthrough can be found, thus obtaining the adsorbent exhaustion rate and the EBRT at various adsorbent bed heights. Then the adsorbent exhaustion rates are plotted against the EBRT values, and a single line relating these two variables is called the operating line, can be sketched.

It can be predicted that the lower the adsorbent exhaustion rate, the longer the EBRT, the smaller the amount of adsorbent is needed per unit volume of feed treated which implies a lower operating cost; however, a larger column will have to be used. In contrast, if the adsorbent exhaustion rate is large, the EBRT will be smaller and a small column is needed which means a lower capital investment; nevertheless, the amount of adsorbent used will increase which requires a higher operation cost. This economic tread-off between the capital investment on a larger column and the saving on the adsorbent cost may be used to determine the size of the adsorption column (Kumar et al., 2009).

It is important to establish the operating line in order to select the optimum combination of adsorbent exhaustion rate and the liquid retention time. Based on the fact that the operating line will approach a minimum at both axes, and the relationship between the adsorbent exhaustion rate  $Y$  and the liquid retention time  $X$  is inversely proportional, the following mathematical form of equation for the operating line is assumed (Aharoni et al., 1979):

$$(x-\alpha)(Y-\beta) = \gamma \quad (17)$$

Where

- $x$  Liquid retention time or EBRT (min)
- $y$  Adsorbent exhaustion rate (g/ L)
- $\alpha$  Minimum liquid retention time (min)

- $\beta$  Minimum adsorbent exhaustion rate (g/ L)
- $\gamma$  Constant (min g/ L)

#### 4.11 Thomas Model

For the continuous flow adsorption system, the Thomas model can be used to describe the adsorption kinetics, maximum solid phase concentration ( $q_o$ ) and Thomas rate constant ( $k_T$ ) and can be written as (Gupta et al., 2007):

$$\frac{C_t}{C_o} = \frac{1}{\left(1 + \exp\left[\frac{k_T q_o m - C_o V}{Q_v}\right]\right)} \quad (18)$$

Where,

- $C_o$  Initial fluoride concentration (mg/l)
- $C_t$  Concentration of fluoride at time t, (mg/l)
- $Q_v$  Volumetric flow rate of the fluoride solution (ml/min)
- $q_o$  Maximum solid phase concentration of fluoride (maximum column adsorption capacity) (mg/g)
- $k_T$  Thomas rate constant (L min mg);
- $V$  Throughput volume (L)
- $M$  Mass of adsorbent (g)

And the linearized form can be expressed as:

$$C_o \ln \left( \frac{C_o}{C_t} - 1 \right) = k_T q_o \frac{m}{Q_v} - k_T C_o \frac{V}{Q_v} \quad (19)$$

From the plot of  $\ln \left( \frac{C_o}{C_t} - 1 \right)$  against throughput volume (V), we can determine the Thomas rate constant and the maximum adsorption capacity.

#### 4.12 Fixed-Bed Column/Bio-column Experiments

For Continuous study a column/Bio-Column reactor was used and the optimised values of pH, temperature were taken from batch experimental study. *Java plum seed (Syzgiumcumini)* was used as adsorbent. The particle size used was 2-4 mm.

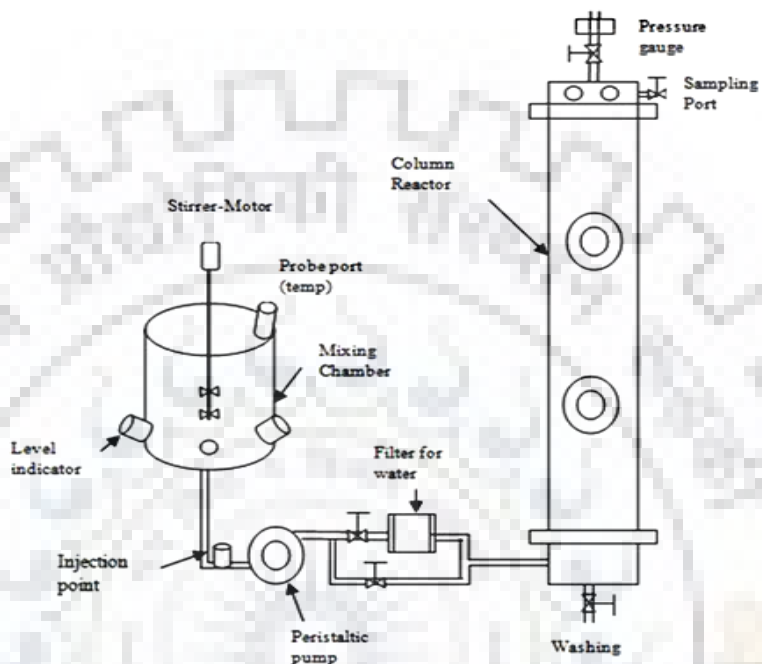


**Fig. 4.12 Experimental Setup for Fixed Bed Column/Bio-column Reactor**

**Table: 4.12 Salient feature of Fixed Bed Column/Bio-Column Reactor**

Sl. No.	Description	Value
1	Reactor Diameter (cm)	9.0
2	Reactor Height (cm)	100
3	Reactor Volume (liters)	6.36
4	Numbers of sample point	5
5	Height of sampling points (cm)	20, 40, 60, 80 and 100 cm
6	Diameter Sample Point (cm)	1.25
7	Complete weight of Absorbent (gm)	2420
8	Bed- Density (gm /cc)	0.7166
9	Reactor's Actual Volume (Liters)	2.9

The test had been conducted in a reactor column of SS pipe. The systematic diagram for the test-setup is presented in Fig. 4.12. SS pipe columns of different lengths ( $Z_1 = 20$ ,  $Z_2 = 40$ ,  $Z_3 = 60$ ,  $Z_4 = 80$  and  $Z_5 = 100$  cm) and 9 cm inside diameter had been brought in use, and the top of reactor was at 100 cm with net volume of 6.36 liters. Four equidistant ports of diameter 1.25 cm were introduced in the reactor for the collection of samples along the height of reactor (excluding inlet and outlet). The top portion and the bottom portion of the reactor were connected to the main column with the help of two joints, based on SS screen (mesh no: 16 BSS, breadth aperture: 1.00 mm). Reactor had been filled with a certain quantity of *Java plum seeds* (*Syzgium cumini*) (Bio adsorbent) possessing a particle size 2-4 mm as a fixed-bed adsorber. Bed had been sealed with the help of rubber gasket and cotton pads to prevent the leakage of effluent and loss of adsorbent. Afterwards, bed had been made wet using pure water, and then left overnight to make certain a compact arrangement of particle with no voids or channels. Fluoride solution of the concentration (20 mg/l) was used in this bed of *Java plum seed* (*Syzgiumcumini*) for an up-movement way. This was done to avert the flowing of fluid because of the influence of the gravitational force. It also ensures an equal spread of effluent throughout column. The tests had been conducted with room temperature. A peristaltic pump had been brought in use to regulate and maintain constant rates of flow (12, 23 and 40 ml/min) in each experiment. The rate of flow of the peristaltic pump was checked regularly by collecting sample of the effluent at intermediate times and calculated by making use of a Measuring Cylinder. Samples of effluent had been taken with an intermission of 1 h, and then were assessed through spectrophotometric (SPADNS) process for residual fluoride ion concentration through UV spectrophotometer (Hach, DR 5000). Desired breakthrough concentration ( $C_b$ ) was taken as 7.5 % of the starting concentrations (20 mg/L).



**Chapter – 5**  
**RESULTS AND DISCUSSIONS**



## Chapter – 5

### RESULTS AND DISCUSSIONS

---

#### 5.0 Introduction

This Chapter deals with the brief discussion on the result of the experiment conducted for the removing of fluoride from single simulated synthetic waste water by using various treatment technologies. For the systematic discussion on the work it has been divided into several sections such as Batch adsorption studies, Bioaccumulation study of simultaneous adsorption and bioaccumulation of fluoride in batch mode, Continuous reactor study for simultaneous removal of fluoride and Phytoremediation in SAB reactor.

**5.0.1 Batch adsorption studies** were carried out for the removal of fluoride from single simulated synthetic waste water using various adsorbent like granular activated carbon (GAC), *citrus limetta* (sweet lemon peel), turmeric, MnO<sub>2</sub> coated turmeric, banana peel, ground nut shell (GNS) and neem leaves. Characterization of adsorbents such as BET surface area, Ultimate and Proximate analysis, FTIR, SEM and EDX were conducted for the confirmation of adsorption of fluoride. The effects of process parameters like pH, temperature, adsorbent dose (mg/g), contact time (h) and initial concentration of fluoride (mg/L) were investigated. Kinetic modelling, adsorption equilibrium isotherm modelling was carried out.

**5.0.2 Bio removal** of fluoride from single substrate solution of fluoride was conducted. The bacterial strain *Acinetobacter baumannii* MTCC 11451 was used in this study. This bacterium was procured from Microbial type culture collection, Chandigarh, India. The strains were revived according to the instructions given by MTCC (MTCC guidelines). Cultures were stored on agar plates till further use and were sub cultured after every 15-30 days. All inoculations were performed in aseptic conditions in laminar air flow unit (rescholar equipment, India). Various kinetics models such as Fixed-Bed Design Models, Bed Depth Service Time Model and Empty Bed Contact Time were also applied to the experimental data.

**5.0.3** In this section **simultaneous adsorption and bio accumulation** of fluoride were carried out by immobilizing the bacterium *Acinetobacter baumannii* onto the surface of various adsorbent such as *Citrus limetta peel*, *Java plum seed (Syzygiumcumini)*, selected based on the batch adsorption studies. Characterizations of adsorbent before and after SAB process such as BET surface area,

Ultimate and proximate analysis, FTIR, SEM and EDX were also carried out. Kinetics and equilibrium adsorption isotherm modelling were also done for SAB study.

**5.0.4** In this section **continuous simultaneous removal** of fluoride was carried out in **packed Bed column**. The *Java plum seed (Syzgiumcumini)* waste was packed in column in synthetic simulated waste water used for the experiment as per batch study. *Acinetobacter baumannii* was immobilized on to the surface of packed Bed for the simultaneous adsorption and bioaccumulation of fluoride. The effect of process parameters such as bed height (cm), flow rate (mL/min), pH and DO were also investigated. Kinetic modeling of the experimental data was also performed.

**5.0.5:** In this section the uptake of fluoride by aquatic macrophyte water hyacinth (*Eichhornia crassipes*) from **phytoremediation** ie simulated synthetic waste water in the artificial photosynthesis chamber was conducted. The chlorophyll content of the plant was also measured before and after uptake of fluoride.

Due to page limitation, microbial growth studies and the batch SAB studies have not been included here. However, these sections have been published in the referred journals “*Asian Journal of Pharmaceutical and Research, Vol 9 Suppl December 3 2016*”.

## **5.1 Batch adsorption studies**

### **5.1.1 Characterization of adsorbent**

In this section the results of the studies on removing of fluoride from simulated synthetic waste water by using various adsorbents like granular activated carbon (GAC), *citrus limetta*, turmeric, MnO<sub>2</sub> coated turmeric, banana peel, ground nut shell (GNS) and neem leaves were used for the removal of fluoride from simulated synthetic waste water. The maximum percentage removal of fluoride obtained for the adsorbent using single component solution were applied for simultaneous adsorption for fluoride from simulated synthetic waste water using granular activated carbon (GAC), *citrus limetta* (sweet lemon peel), turmeric, MnO<sub>2</sub> coated turmeric, banana peel, ground nut shell (GNS) and neem leaves.

The physiochemical property of all the seven adsorbent for the adsorption of fluoride from single simulated synthetic waste water is provided in table 5.1.1. Besides, ultimate and proximate analysis SEM, FTIR, EDX and BET surface area analysis of all the adsorbent before and after adsorption have been presented below.

### 5.1.1 BET surface area and ultimate and proximate analysis of all the adsorbents

The Physico chemical properties of all the seven bio-adsorbents before and after the adsorption have been provided in Table 5.1.1.

Name of Adsorbent	Particle size (mm)	Element analysis before and after adsorption (%)		Proximate analysis (%)	BET Surface area before and after adsorption (m <sup>2</sup> /g)		Pore Volume (m <sup>3</sup> /g)		Bulk Density (g/L)	
		Element	Before		After	Before	After	Before		After
GAC	0.5-2.0	C	75	76	Ash: 9.4 Moisture: 8.54 Volatile Content: 82.06	246.11	583.23	0.245	0.345	605.02
		H	1.9	1.09						
		N	0	11.9						
<i>Citrus Limeira Peel</i>	0.5-2.0	S	0	0	Ash: 8.93 Moisture: 8.86 Volatile Content: 82.21	29.61	58.098	0.0074	0.011	227.1
		C	33.8	34.2						
		H	3.94	4						
		N	2.38	2.6						
		S	0.06	0.06						
		C	40.9	41						
Banana peel	0.5-2.0	H	4.2	4	Ash: 8.768 Moisture: 7.9 Volatile Content: 83.252	28.33	42.067	0.0106	0.023	700.3
		N	8.4	8.5						
		S	0.06	0.06						
		C	37	76						
		H	4	4						
		N	4	14						
Groundnut	0.5-2.0	S	6	6	Ash: 2.58 Moisture: 9.71 Volatile Content: 87.71	41.901	67.43	0.0211	0.045	388.9
		C	54	56						
		H	6.22	6.22						
		N	0.65	12.6						
		S	0.07	0.069						
		C	36	38						
Neem patti	0.5-2.0	H	6.4	6.4	Ash: 8.55 Moisture: 8.15 Volatile Content: 83.3	22.67	56.536	0.0211	0.034	350.6
		N	0.7	12.6						
		S	0.08	0.06						
		C	44	45						
		H	3.4	3.4						
		N	0	9						
<i>Jawa plum</i>	0.5-2.0	S	0	0	Ash: 4.98 Moisture: 6.94 Volatile Content: 88.08	29.61	60.412	0.0047	56	92.1
		C	44	45						
		H	3.4	3.4						
		N	0	9						
		S	0	0						
		C	44	45						

## 5.1.2 FTIR spectrum before and after adsorption of fluoride form simulated synthetic waste water

FTIR is an important tool for the identification and characterization of functional groups present into the adsorbents that may be helpful for fluoride ion adsorption from synthetic waste water. FTIR spectroscopy analysis was done in solid phase, in the range of wavelength from 400-4000  $\text{cm}^{-1}$  (Gupta et al., 2007). The graph between absorbance (% transmittance) vs wave number ( $\text{cm}^{-1}$ ) was plotted from data obtained using double beam spectrophotometer has been shown from the Fig. 5.1.2.1 (a) to Fig.5.1.2.7 (b).

### 5.1.2.1 FTIR spectrum of GAC before and after adsorption

Major functional groups present in GAC were worked out with the use of Fourier Transform Infrared spectroscopy (Thermo Nicolet, Magna 7600) both before and after adsorption of fluoride. The samples were prepared by pellet (pressed disk) method by mixing equal amounts of KBr in each sample. The FTIR spectra of GAC before adsorption of fluoride and after adsorption of fluoride in the selected spectral range of 4000-400  $\text{cm}^{-1}$  are shown in Fig. 5.1.2.1 (a) and Fig. 5.1.2.1 (b) respectively which gives evident about the presence of many functional groups on the surface of the GAC.

A broad band between 3100 and 3734  $\text{cm}^{-1}$  in FTIR graph is indicative of the presence of both free and hydrogen bonded OH groups on the adsorbent surface. This stretching is due to both the silanol groups (Si-OH) and adsorbed water (peak at 3434  $\text{cm}^{-1}$ ) on the surface. C-O group stretching from aldehydes and ketones can also be inferred from peaks in the region of 1600  $\text{cm}^{-1}$  (Wasewar, 2009). The peak at 1582 indicated N-H bending and it's shifted to 1575  $\text{cm}^{-1}$  due to adsorption of fluoride and the next peak was at 1582 which indicate. C=C, C=N Stretching of Quinoid ring. Fluoride adsorption was confirmed in range between 1350 and 1100  $\text{cm}^{-1}$ , which indicate the C-F stretching. Also the wave number 800-400  $\text{cm}^{-1}$  indicates the stretching of C-X (X = F, Cl, Br or I) which confirm fluoride adsorption. Wave number shifted from 1393  $\text{cm}^{-1}$  to 1398  $\text{cm}^{-1}$  assigned the reactivity of carboxylate anion C=O stretching for the adsorption process. A large number of peaks corresponding to various groups disappear after the fluoride adsorption, which indicates utilization of these groups during the adsorption process (Wasewar et al., 2009).

**Table 5.1.2.1 FTIR Analysis for GAC in Tabular Form**

Wave number (cm <sup>-1</sup> ) Before adsorption	Wave number (cm <sup>-1</sup> ) After adsorption	Groups
3100	3734	Free and hydrogen bonded OH group
3434	3434	Stretching due to silanol (Si-OH) group and adsorbed water
1600	-	CO group stretching due to both aldehydes and ketones
1582	1575	N-H bending
1582	-	C=C, C=N Stretching of Quinoid ring
1350	1100	C-F stretching
800	400	stretching of C-X (X = F, Cl, Br or I)
1393	1398	carboxylate anion C=O stretching

### 5.1.2.2 FTIR spectrum of *Citrus limetta peel* before and after adsorption

The functional groups in biosorbents pre and post absorption of fluoride were worked out using Fourier transform infrared spectroscopy (Thermo Nicolet, Magna 7600). These samples had been analysed by pellet (pressed disk) method by making pallets of sample and KBr (1:10 w/w) for each sample. The spectrum was collected in the range between 4000 - 400 cm<sup>-1</sup>. Fig. 5.1.2.2 (a) and Fig. 5.1.2.2 (b) show FTIR spectra on *citrus limetta* biosorbent in the selected spectral range of 4000-400 cm<sup>-1</sup>, which gives evident about the presence of many functional groups on the surface of the biosorbent.

The range of different wave numbers is assigned to different functional groups present in the adsorbent (Karthikeyan, 2016). The main active functional group responsible for fluoride biosorption surface is N-H groups as the wave number shifted from 3402.99 cm<sup>-1</sup> to 3427.75 cm<sup>-1</sup>. The next biosorption peak was at 1640.36 cm<sup>-1</sup> which shifted to 1634.57 cm<sup>-1</sup>, perhaps because of the complexation of amide group( N-H stretching and C=O stretching vibration) with fluoride ion. The next peak was at 1514.06 which vanished after adsorption due to formation of C=C, C=N Stretching of Quinoid ring. Wave number shifted from 1436.51 cm<sup>-1</sup> to 1386.09 cm<sup>-1</sup> assigned the reactivity of carboxylate anion C=O stretching for the biosorption process. The band

Of 622.46 could be attributed to the presence of Fe-O bond; however it shifted to 595.85  $\text{cm}^{-1}$  after adsorption of fluoride as shown below in the Table 5.1.2.2.

**Table 5.1.2.2 FTIR Analysis for *Citrus Limetta* in Tabular Form**

Wave number ( $\text{cm}^{-1}$ ) Before adsorption	Wave number ( $\text{cm}^{-1}$ ) After adsorption	Groups
3402.99	3427.7	N-H Stretching vibration
2924.99	2922.8	Aliphatic C-H Stretching
1741.4	–	Aliphatic acid C=O Stretching
1640.4	1634.6	Amide groups( N-H stretching and C=O stretching vibration)
1514.0	–	C=C, C=N Stretching of Quinoid ring
1436.5	1386.1	C=C, C=N Stretching of Benzenoid ring
1062.5	1050.5	C=O Stretching in chitosan
622.5	595.8	Fe-O bond

### 5.1.2.3 FTIR spectrum of Ground nut shell before and after adsorption

The functional groups in biosorbents pre and post absorption of fluoride had been worked out using Fourier transform infrared spectroscopy (Thermo Nicolet, Magna 7600). These samples had been analysed by pellet (pressed disk) method by making pallets of sample and KBr (1:10 w/w) for each sample. The spectrum was collected in the range between 4000 - 400  $\text{cm}^{-1}$ .

In FTIR analysis of groundnut shell before and after adsorption of fluoride, were analysed according to Karthikeyan, 2016. The spectra of groundnut shell before and after adsorption are shown in Fig.5.1.2.3 (a) and Fig.5.1.2.3 (b). As indicated in these Figures, there is shifting of some peaks whereas other peaks disappear after the adsorption process as shown through Table 5.1.2.3. This confirms that there is adsorption of fluoride which is responsible for changes in spectrum.

**Table 5.1.2.3 FTIR analysis of Groundnut shells before and after adsorption**

Wave No. (cm <sup>-1</sup> ) Before analysis	Wave No. (cm <sup>-1</sup> ) After analysis	Groups
3401.0	3418.6	N-H stretching vibrations
2925.2	2924.5	Aliphatic C-H stretching
1741.1	-	Aliphatic acid C=O stretching
1615.2	1609.4	N-H bending
1510.4	-	C=C, C=N stretching of quinoid ring
1430.7	1439.3	C=C, C=N stretching of benzenoid ring
1383.1	1384.5	N-O stretching

**5.1.2.4 The FTIR spectrum of Neem leaves pre and post absorption**

The functional groups in biosorbents pre and post adsorption of fluoride had been worked out using Fourier transform infrared spectroscopy (Thermo Nicolet, Magna 7600). These samples had been analysed by pellet (pressed disk) method by making pallets of sample and KBr (1:10 w/w) for each sample. The spectrum was collected in the range between 4000 - 400 cm<sup>-1</sup>. Fig.5.1.2.4 (a) and Fig.5.1.2.4 (b) show FTIR spectra on neem leaves biosorbent in the selected spectral range, which also indicates about the presence of many functional groups in the biosorbent (Singha and Das 2011, Gupta et al; 2007) (Table 5.1.2.4).

**Table 5.1.2.4 FTIR analysis of Neem leaves before and after adsorption**

Wave No. (cm <sup>-1</sup> ) Before analysis	Wave No. (cm <sup>-1</sup> ) After analysis	Groups
3418.4	3386.9	Surface O-H stretching
2924.6	2925.0	Aliphatic C-H stretching
1622.2	1642.9	Unsaturated groups like alkene C=C
1034.8	1031.2	Sulphonic acid S=O stretching
598.6	580.2	Metal-Halogen stretching

### 5.1.2.5 FTIR spectrum of virgin turmeric and MnO<sub>2</sub> coated Turmeric before and after adsorption

FTIR study on MnO<sub>2</sub>-coated turmeric and turmeric bio sorbent are used to know the adsorption capacity of fluoride on the surface of bio sorbent by analyzing the active functional groups. To identify the functional groups, Fourier transform infrared spectroscopy (FTIR) analysis was done for turmeric based adsorbent and MnO<sub>2</sub>-coated turmeric adsorbent. Table 5.1.2.5 shows the wave numbers of various functional groups present before and after bio sorption process for turmeric based adsorbent and MnO<sub>2</sub>-coated turmeric adsorbent (Singh and Majumder 2016).

The table given below shows different functional groups found in turmeric before and after adsorption process and MnO<sub>2</sub>-coated bio sorption. Shift in wave number from 3389.1 cm<sup>-1</sup> to 3392.1 cm<sup>-1</sup> and from 3420.8 cm<sup>-1</sup> to 3416.8 cm<sup>-1</sup> in case of MnO<sub>2</sub>-coated turmeric are caused by adsorption on surfaces of active functional groups of O-H and NH which are the main functional groups responsible for bio sorption of fluoride (Singha and Das, 2011). Change in wave number from 2922.6 cm<sup>-1</sup> to 2927.3 cm<sup>-1</sup> in Aliphatic C-H stretching groups which may be responsible for bio sorption of fluorides. Shift of peaks from 1506.7 cm<sup>-1</sup> to 1515.0 cm<sup>-1</sup> are mainly associated to reaction of unsaturated alkene groups which is more probably responsible for bio sorption of fluorides for MnO<sub>2</sub> coated turmeric adsorbent( Zhang et al., 2007). The wave number at 558.5 cm<sup>-1</sup> could be given to Mn-O bond (Parida et al., 2004) and it showed variability for adsorption of fluoride from 558.5 cm<sup>-1</sup> to 595.2 cm<sup>-1</sup> in MnO<sub>2</sub> coated turmeric bio sorption process and from 530.2 cm<sup>-1</sup> to 587.9 cm<sup>-1</sup> in virgin turmeric bio sorption. Fluorides occurrences on the surface of MnO<sub>2</sub> coated turmeric and virgin turmeric bio sorbent can be seen from the peaks appeared at 538.5 cm<sup>-1</sup> and 508.8 cm<sup>-1</sup> as shown below in the Table 5.1.2.5 (a) and Table 5.1.2.5 (b).

**Table 5.1.2.5 (a) FTIR analysis of Turmeric before and after adsorption**

Wave No. (cm <sup>-1</sup> ) Before analysis	Wave No. (cm <sup>-1</sup> ) After analysis	Groups
3389.1	3392.1	O-H and N- H Stretching
2922.6	2927.3	Aliphatic C-H stretching
1628.1	1632.9	Unsaturated group, alkene
1513.8	1512.3	Aromatic C-NO <sub>2</sub> stretching
1031.5	1036.1	C-O ether stretching



Wave No. (cm <sup>-1</sup> ) Before analysis	Wave No. (cm <sup>-1</sup> ) After analysis	Groups
530.2	587.9	Metal-Halogen stretching
518.2	508.8	Metal-Halogen stretching

**Table 5.1.2.5 (b) FTIR analysis of MnO<sub>2</sub> coated Turmeric before and after adsorption**

Wave No. (cm <sup>-1</sup> ) Before analysis	Wave No. (cm <sup>-1</sup> ) After analysis	Groups
3420.8	3416.8	O-H and N- H Stretching
-	-	Aliphatic C-H stretching
-	-	Unsaturated group, alkene
1506.7	1515.0	Aromatic C-NO <sub>2</sub> stretching
-	-	C-O ether stretching
558.5	595.2	Metal-Halogen stretching
-	538.5	Metal-Halogen stretching

#### 5.1.2.6 FTIR spectrum of *Java plum seed* (*Syzygiumcumini*) before and after adsorption

Fourier Transform Infrared Spectroscopy (FTIR) analysis (Thermo Nicolet, Magna 7600) was performed to determine the functional groups present in the bio-adsorbents before and after the fluoride adsorption experiment. Pellet was prepared by mixing equal amounts of Potassium bromide (KBr) and the sample for the analysis. 4000 – 400 cm was selected as the spectral range. The resulting spectra obtained for samples taken before and after fluoride adsorption are shown in Fig. 5.1.2.6 (a) and Fig. 5.1.2.6 (b) respectively.

A broad band between 3100 and 3734 cm<sup>-1</sup> in FTIR graph is indicative of the presence of both free and hydrogen bonded OH groups on the adsorbent surface. Peak at 3403.27 to 3372.43 cm<sup>-1</sup> shows hydrogen-bonded OH group of alcohols and phenols (Yang and Lua. 2003). This stretching is due to both the silanol groups (Si-OH) and adsorbed water (peak at 3434 cm<sup>-1</sup>) on the surface. C-O group and stretching from aldehydes and ketones can also be inferred from peaks in the region of 1600 cm<sup>-1</sup> (Wasewar, 2009.). Fluoride adsorption was confirmed in range between 1350 and 1100 cm<sup>-1</sup>, which indicate the C-F stretching. Also the wave number 800–400 cm<sup>-1</sup> indicate the stretching C-X

stretching (X = F, Cl, Br or I) which confirm fluoride adsorption as shown below in the Table 5.1.2.6.

**Table 5.1.2.6 FTIR analysis *Java plum seed (Syzgiumcumini)* before and after adsorption**

Wave No. (cm <sup>-1</sup> ) Before analysis	Wave No. (cm <sup>-1</sup> ) After analysis	Groups
574.4	608.5	Metal halogen stretching
1026.6	1050.1	Silicon stretching Si-O-Si
1157.7	1261.9	Organic sulphate Stretching C-SO <sub>4</sub> <sup>-1</sup>
1371.7	1372.4	Carboxilate anion C=O stretching
1625.9	1641.6	Unsaturated groups like alkene C=C
2925.0	2923.6	Aliphatic C-H stretching
3403.3	3372.4	hydrogen-bonded OH group of alcohols and phenols
3100	3734	Free and hydrogen bonded OH group

### 5.1.2.7 FTIR spectrum of Banana peel before and after adsorption

The functional groups in biosorbents pre and post absorption of fluoride were worked out using Fourier transform infrared spectroscopy (Thermo Nicolet, Magna 7600). These samples had been analysed by pellet (pressed disk) method by making pellets of sample and KBr (1:10 w/w) for each sample. The spectrum was collected in the range between 4000 - 400 cm<sup>-1</sup>.

The range of different wave numbers assigned the functional group present in the adsorbent is shown in the Fig.5.1.2.7 (a) and Fig.5.1.2.7 (b). The aromatic bond stretching lie in the range 606-700 cm<sup>-1</sup> similarly for the silicon stretching Si-O-Si (1045-1382 cm<sup>-1</sup>), organic sulphate stretching (1383-1450 cm<sup>-1</sup>), Secondary amine (1500-1605 cm<sup>-1</sup>), cyanide ion stretching (2000-2554 cm<sup>-1</sup>), Thiol stretch (2556-2918 cm<sup>-1</sup>), Methyl ester stretch (2919-3217 cm<sup>-1</sup>), OH Stretching (3217-3909 cm<sup>-1</sup>).

Table 5.1.2.7 is taken from Gupta et al., 2007 for functional group detection.

**Table 5.1.2.7 FTIR analysis Banana peel before and after adsorption**

Wave No. (cm <sup>-1</sup> ) Before analysis	Wave No. (cm <sup>-1</sup> ) After analysis	Groups
3217	3909	OH Stretching
2919	3217	Methyl ester stretch
2556	2918	Thiol stretching
2000	2554	Cyanide ion stretching
1500	1605	Secondary amine
1383	1450	Organic sulphate stretching
1045	1382	Silicon stretching Of Si-O-Si
606	700	Aromatic bond stretching

#### 5.1.3.8 Concluding Remark of the Section 5.1.2

The various functional group peaks for the different biosorbent (GAC, citrus limetta, ground nut shell, banana peel, neem leaves, turmeric and MnO<sub>2</sub> coated turmeric) is the displacement of this functional group with the fluoride ion during the adsorption process. FTIR analysis described the presence of various functional groups on the adsorbent's surface.

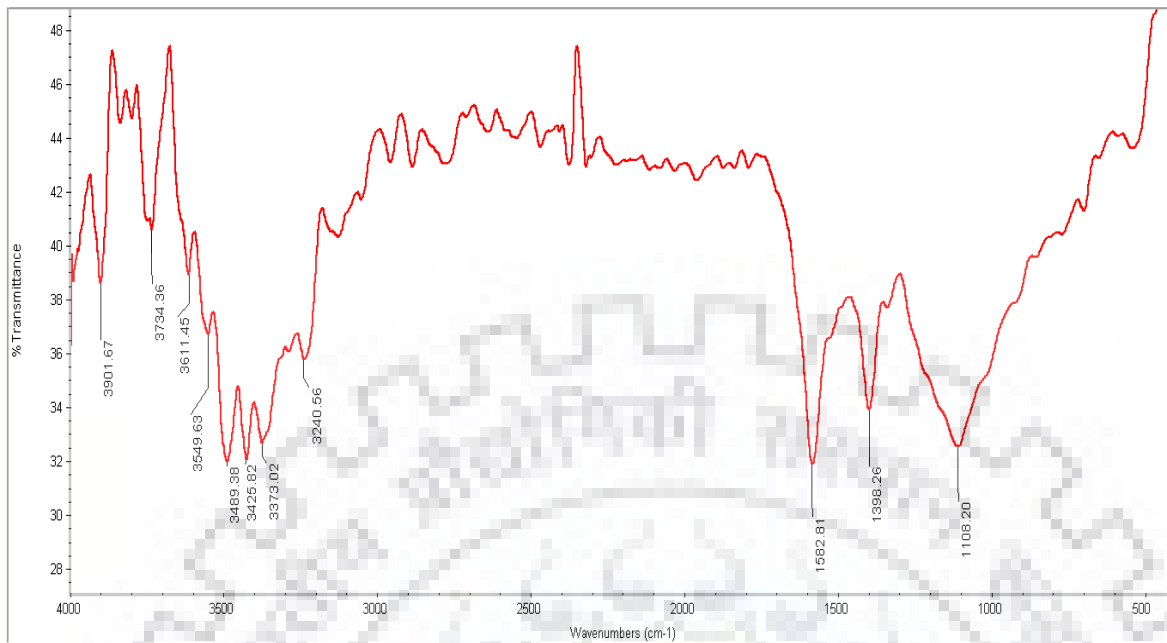


**Fig. 5.1.2.1 (a) FTIR spectra of GAC before adsorption of Fluoride**

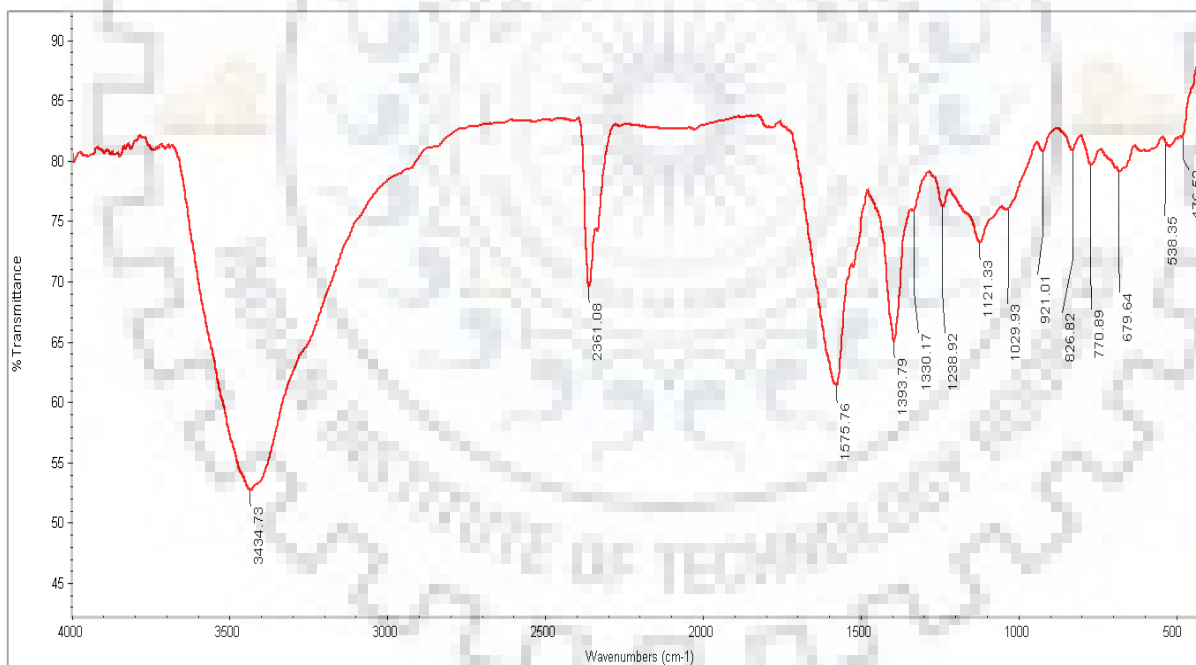


**Fig. 5.1.2.1 (b) FTIR spectra of GAC after adsorption of Fluoride**

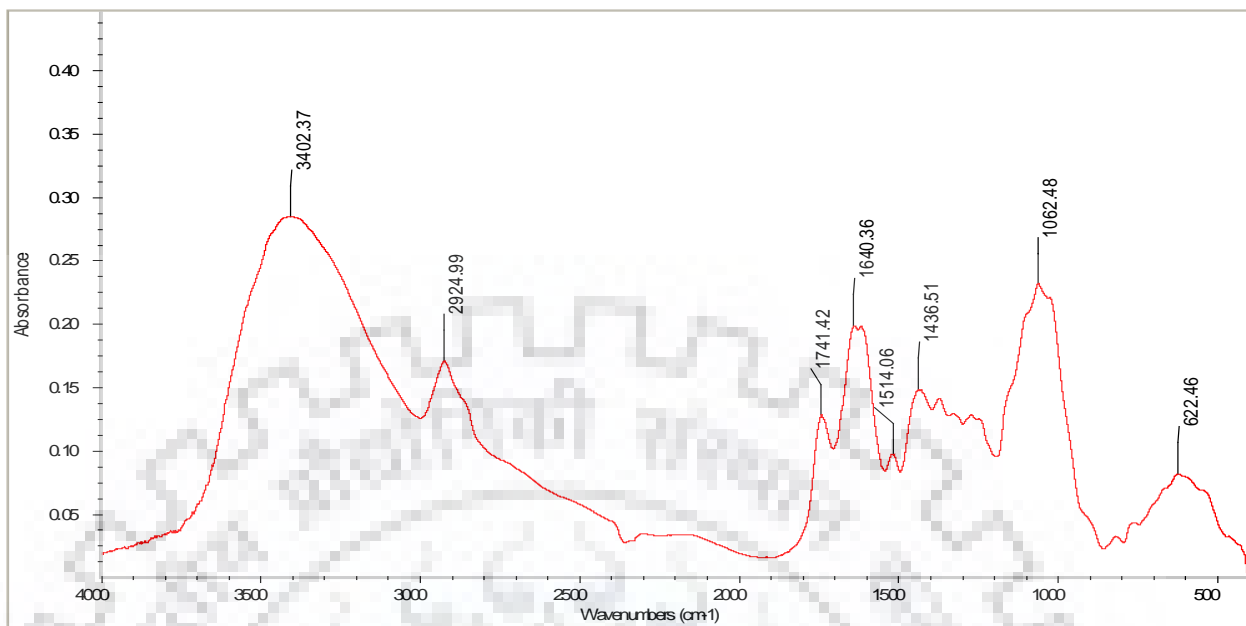


**Fig. 5.1.2.2 (a) FTIR spectra of *Citrus Limetta Peel* before Adsorption**

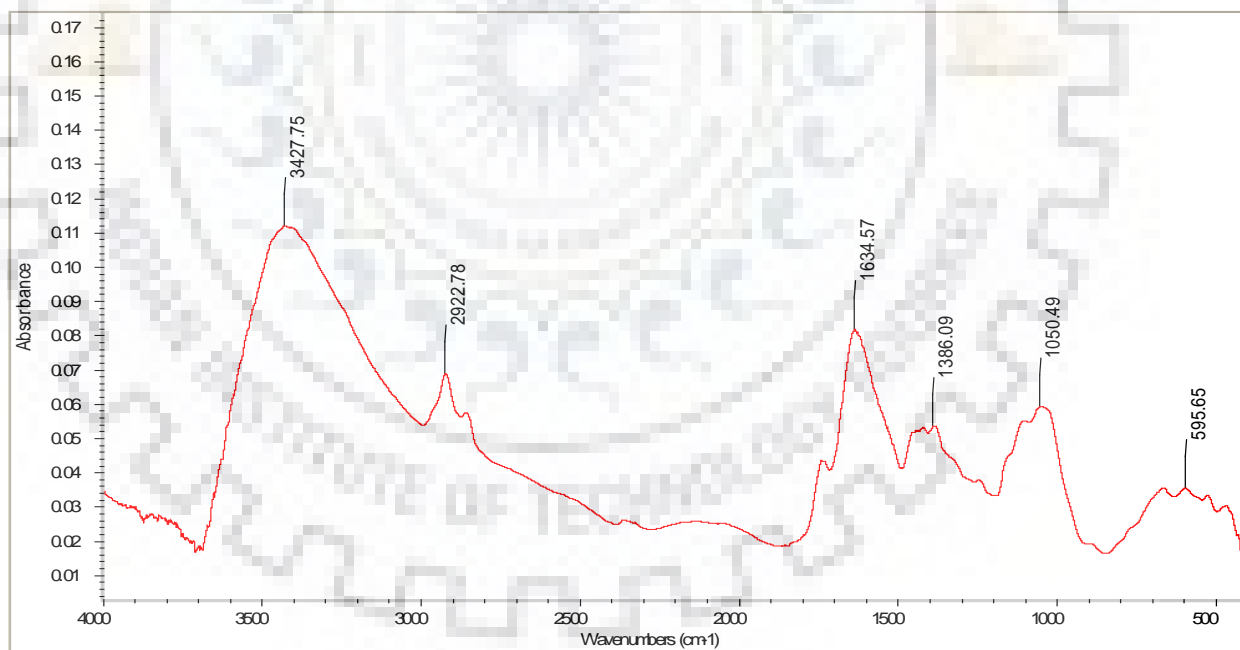


**Fig. 5.1.2.2 (b) FTIR spectra of *Citrus Limetta Peel* after Adsorption**

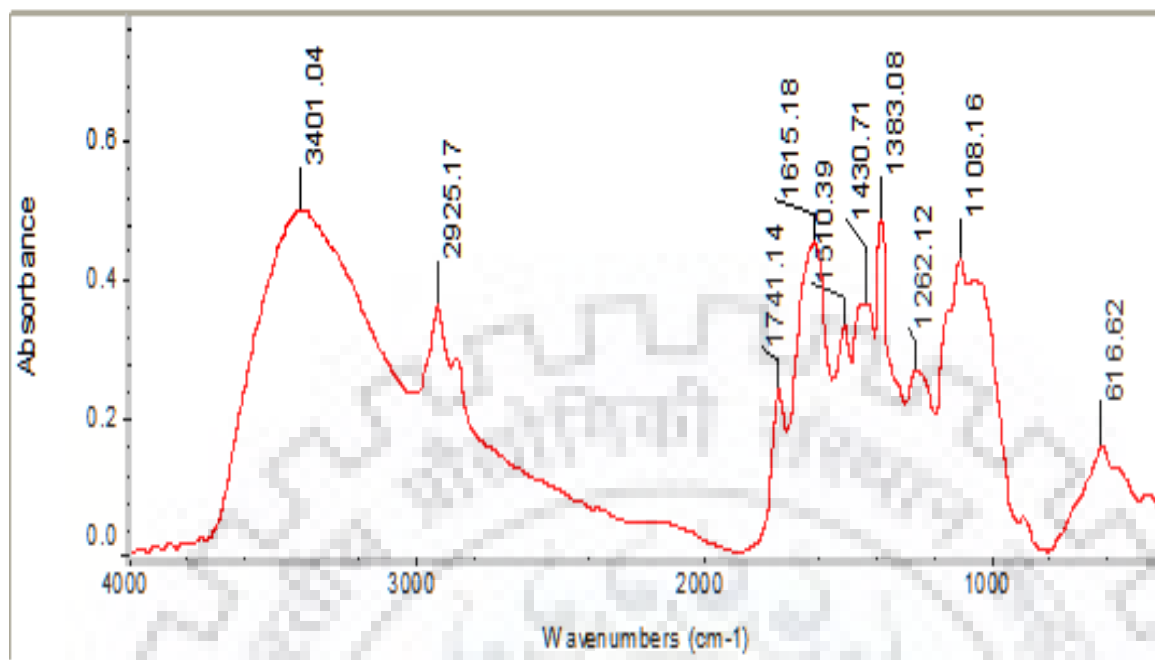


**Fig. 5.1.2.3 (a) FTIR spectra of ground nut shell before Adsorption**

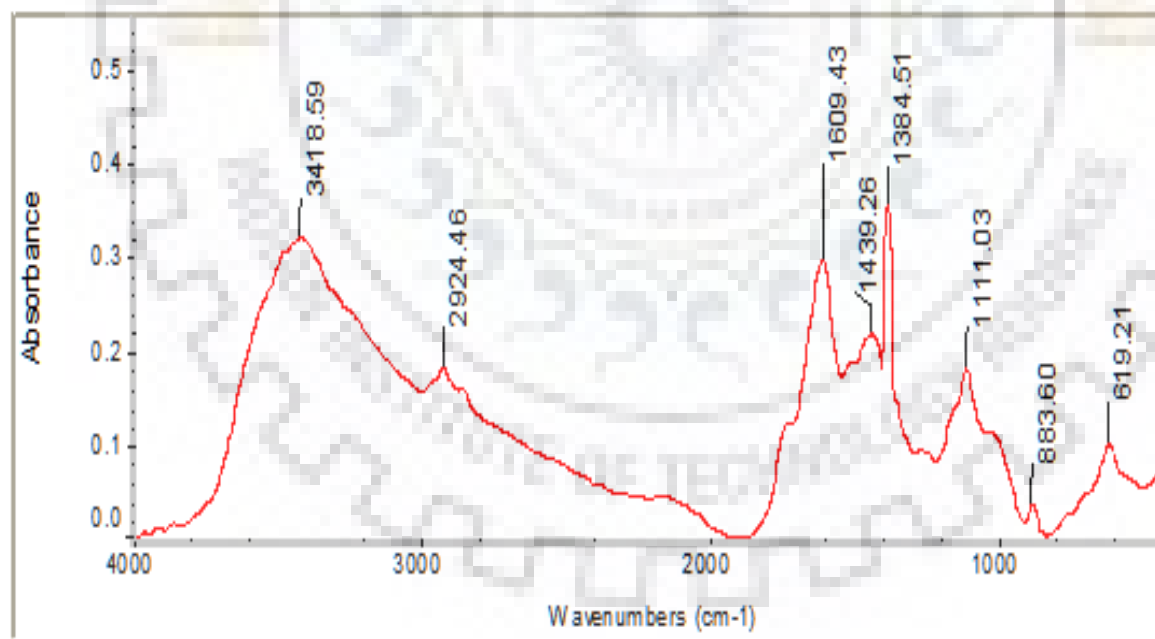


**Fig. 5.1.2.3 (b) FTIR spectra of ground nut shell after Adsorption**

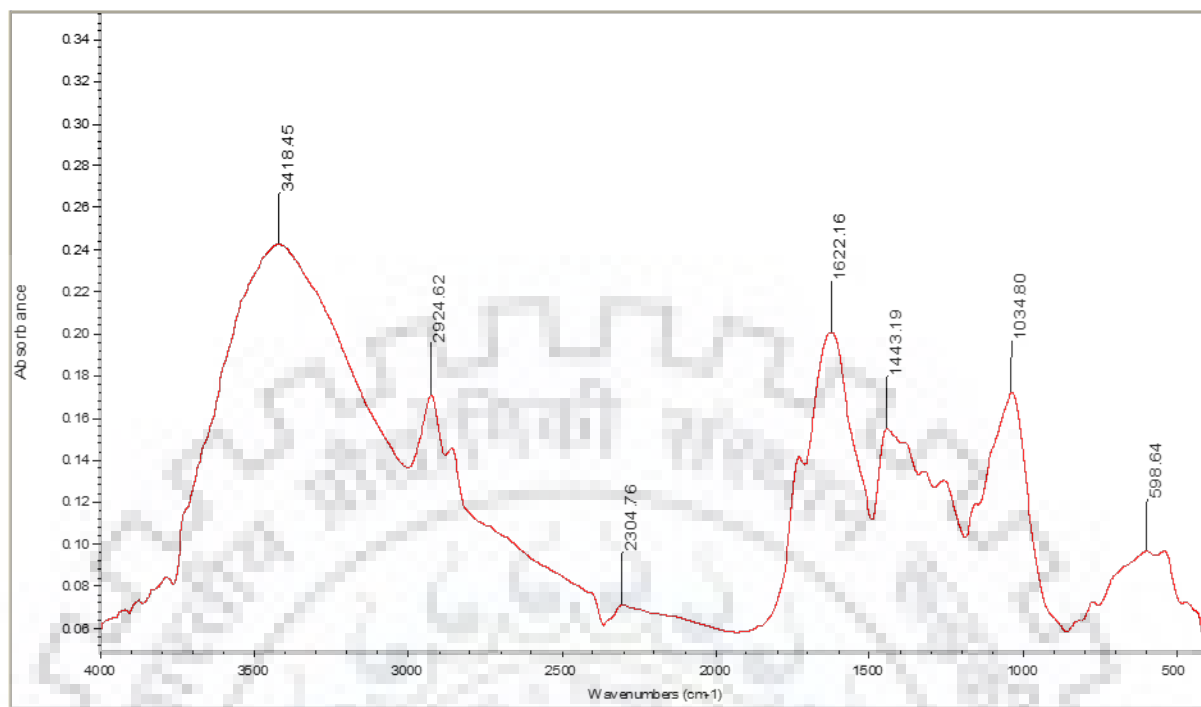


**Fig. 5.1.2.4 (a) FTIR spectra of Neem Leaves before Adsorption**

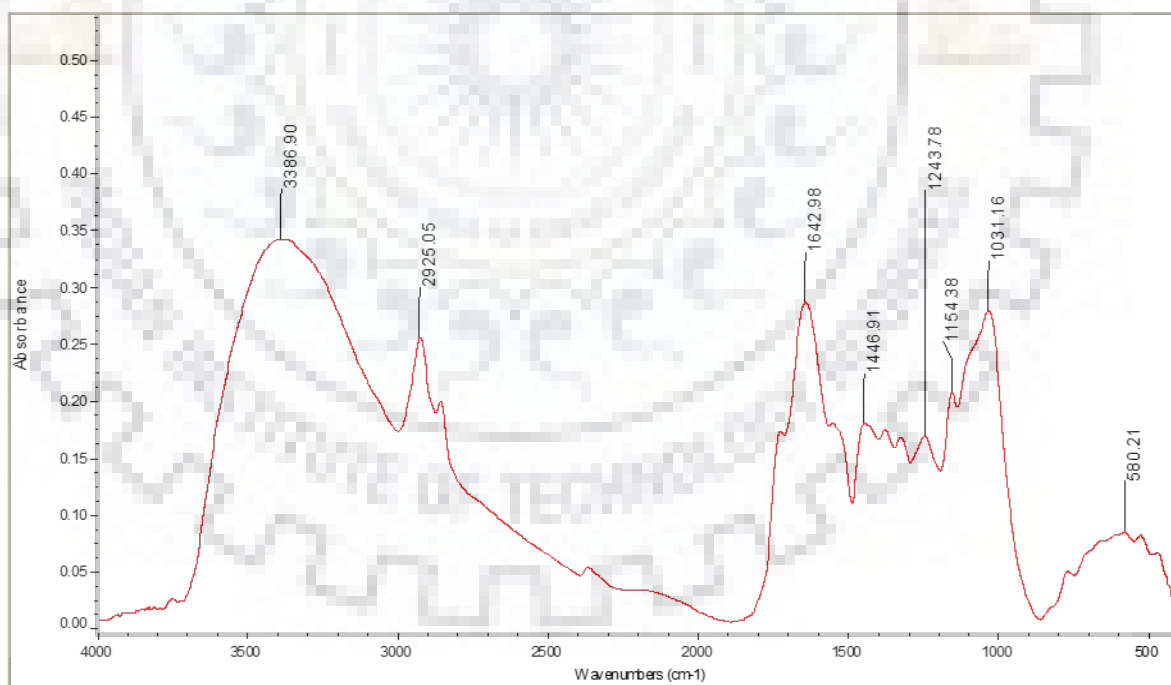


**Fig. 5.1.2.4 (b) FTIR spectra of Neem Leaves after Adsorption**

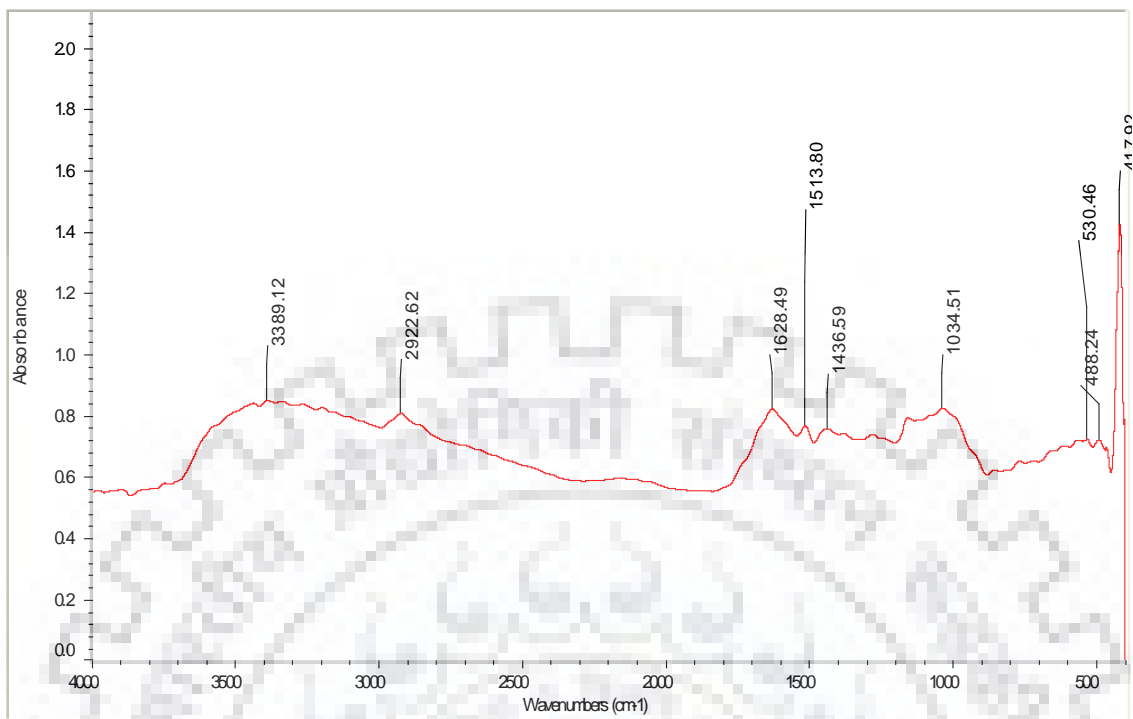


**Fig. 5.1.2.5(a) FTIR spectra of Turmeric before Adsorption**

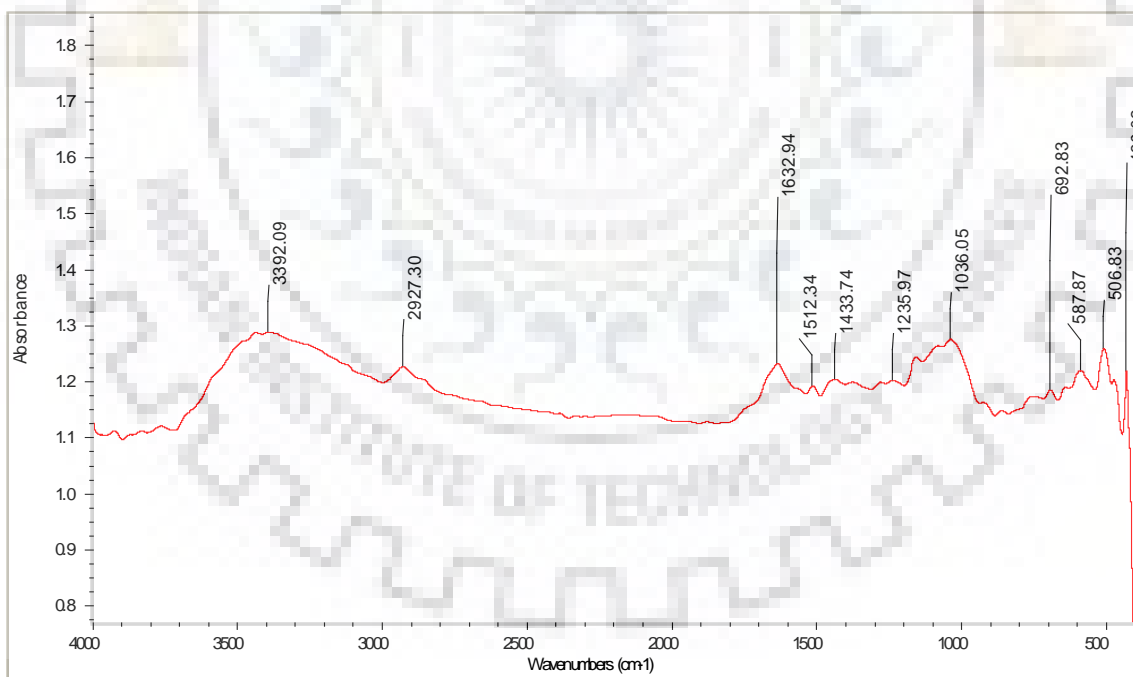


**Fig. 5.1.2.5 (b) FTIR spectra of turmeric after adsorption**



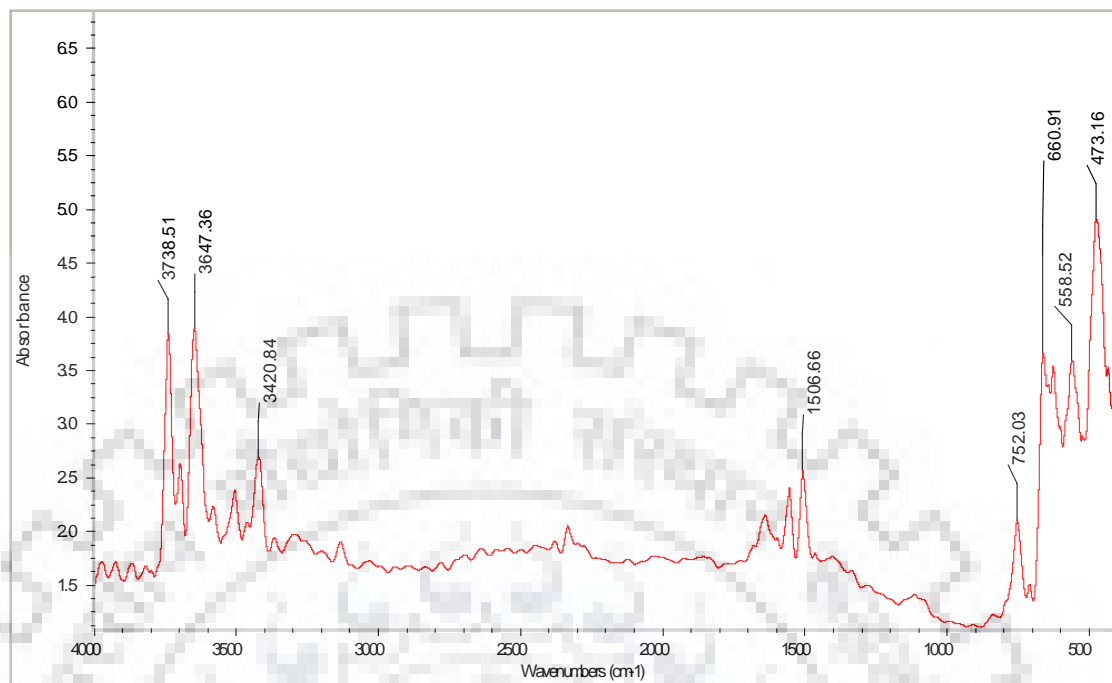


**Fig. 5.1.2.5 (a) FTIR spectra of MnO<sub>2</sub> coated turmeric before adsorption**

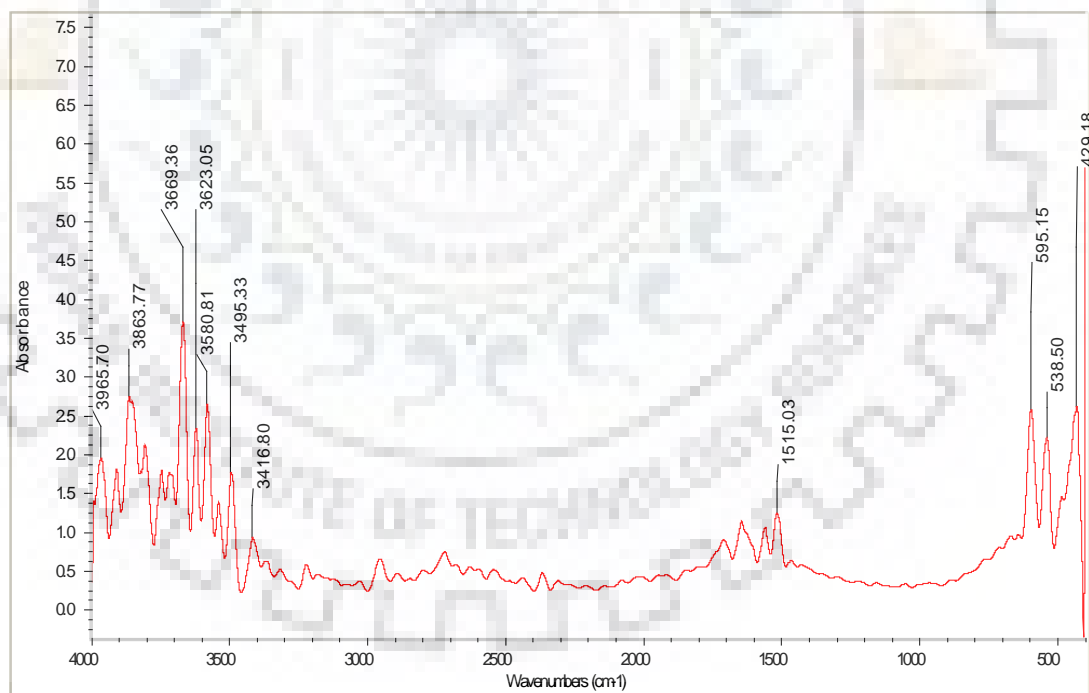


**Fig. 5.1.2.5 (b) FTIR spectra of MnO<sub>2</sub> coated turmeric after Adsorption**

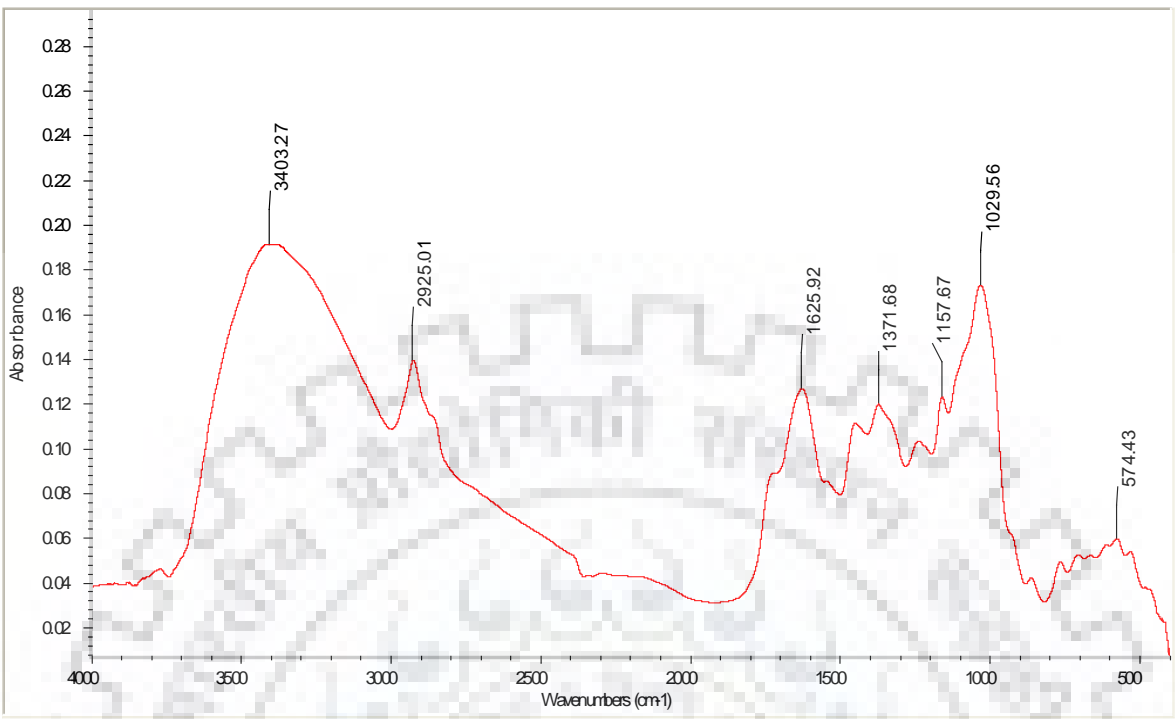


**Fig. 5.1.2.6 (a) FTIR spectra of *Java plum seed* (*Syzgiumcumini*) before Adsorption**

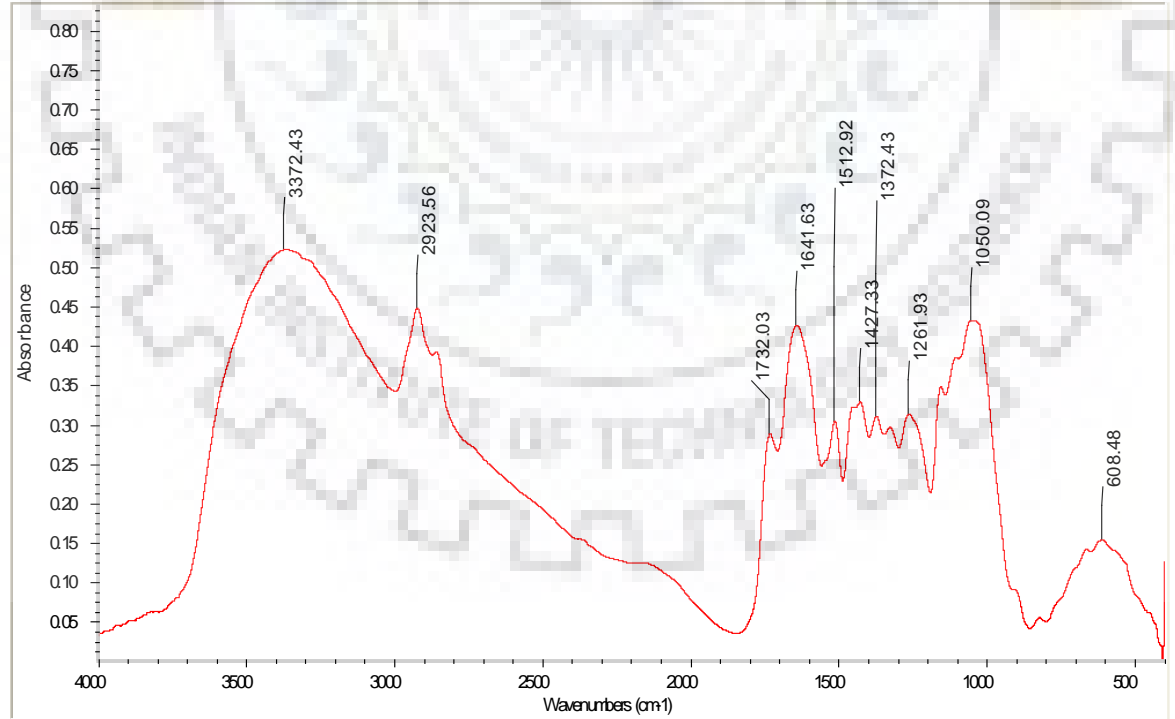


**Fig. 5.1.2.6 (b) FTIR spectra of *Java plum seed* (*Syzgiumcumini*) after Adsorption**

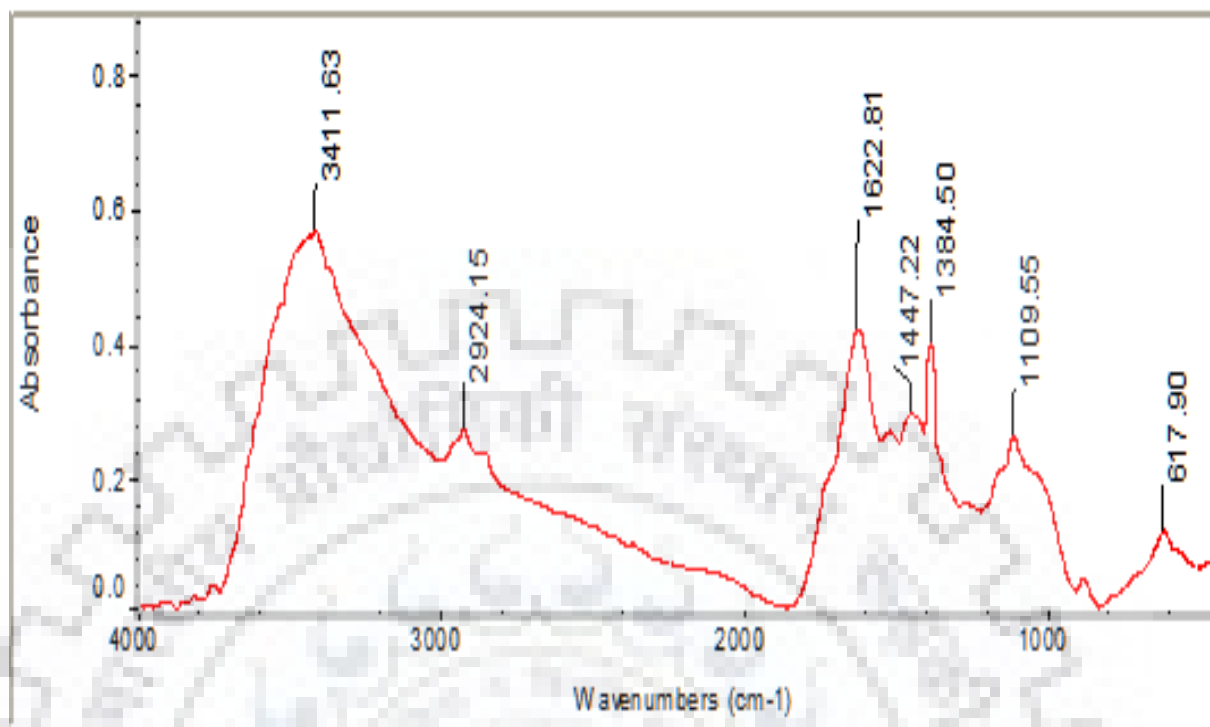


**Fig. 5.1.2.7 (a) FTIR spectra of Banana peel before Adsorption**

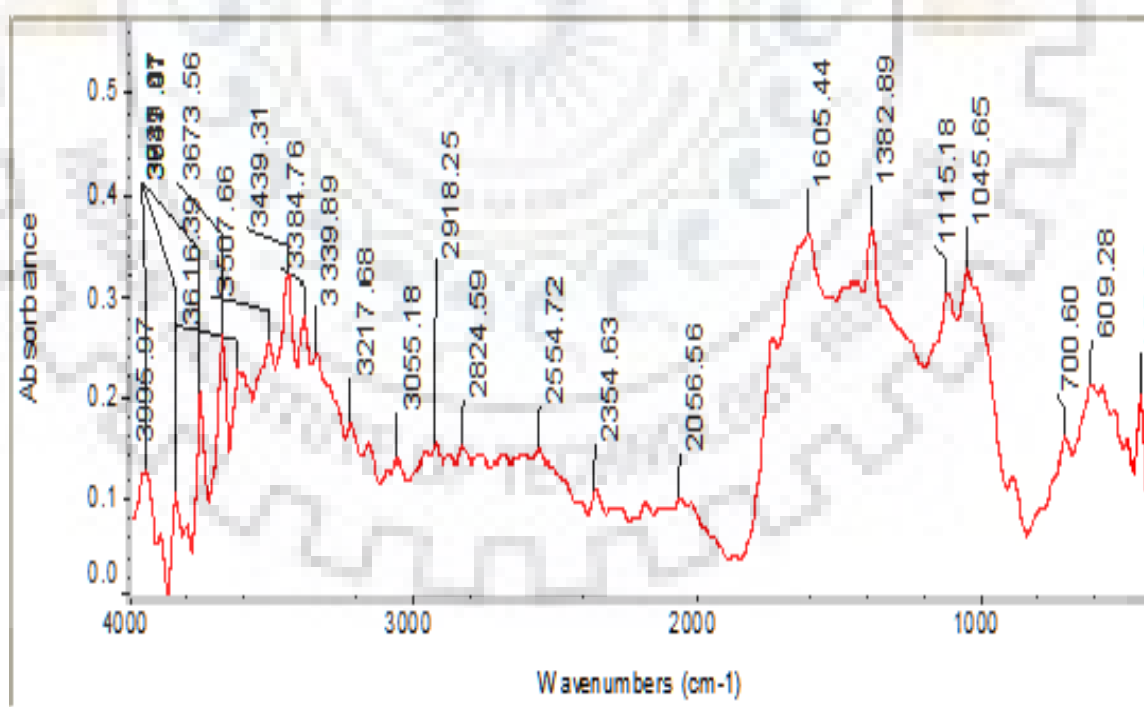


**Fig. 5.1.3.7 (b) FTIR spectra of Banana peel after Adsorption**

### **5.1.3 FE SEM (Field Emission Scanning electron microscopy) and EDX (Energy Dispersive X-ray) analysis**

The surface morphology of pre-treated adsorbents like Granular activated carbon (GAC), *citrus limetta*, Ground nut shell, Neem leaves, *Java plum seed* (*Syzygiumcumini*) and Banana peel were captured using FESEM (Field Emission Scanning electron microscopy). The EDX and FESEM (Field Emission Scanning electron microscopy) photographs of pre treated biomass with and without load of fluoride from simulated synthetic waste water solution is shown in Fig.5.1.3.1.1 (a) to Fig.5.1.3.7.2 (b). The change in the surface morphology of all seven biosorbents after the adsorption of fluoride is confirmed by the EDX spectrum which shows the change in the peak after adsorption. As the sample was non-conducting, it was coated with gold in presence of argon, an inert gas. After the completion of coating processes the sample were analysed in FESEM.

#### **5.1.3.1 Analysis of Granular activated carbon (GAC)**

##### **5.1.3.1.1 SEM analysis of Granular activated carbon (GAC)**

The morphological study of GAC was carried out with scanning electron microscope (SEM). First the sample of GAC was coated with gold in the presence of argon, an inert gas then sample was analyzed with SEM. The Fig.5.1.3.1.1 (a) indicates that SEM images of GAC before adsorption of fluoride and Fig.5.1.3.1.1 (b) indicated that SEM images of GAC after adsorption of fluoride. Fig.5.1.3.1.1 (a) clearly show that at 1000X magnifications GAC has highly porous structured and both small and large pore are present. After adsorption of fluoride on the surface GAC and fluoride ions are deposited in inside the pores of GAC and morphological structure of GAC was drastically changed (Wasewar et al., 2009) which clearly shown in Fig.5.1.3.1.1 (b).

##### **5.1.3.1.2 EDX analysis of Granular activated carbon (GAC)**

The EDX analysis of GAC before and after adsorption of fluoride is shown in Fig.5.1.3.1.2 (a) and Fig.5.1.3.1.2 (b) respectively. It is evident that various elements compositions of GAC sample before and after adsorption of fluoride are shown in Table 5.1.3.1.2. When the EDX analysis was carried out after the fluoride adsorption, it was found that 0.6 % by wt. of the fluoride was present which confirmed the adsorption of fluoride.

**Table 5.1.3.1.2 EDX analysis of Granular activated carbon before and after adsorption of fluoride in tabular form**

Element	Weight % before Biosorption	Weight % after Biosorption
C K	85.3	86.96
O K	11.96	9.5
FK	--	0.6
AlK	0.3	0.77
CaK	2.08	2.14

### 5.1.3.2 Analysis of *Citrus limetta peel*

#### 5.1.3.2.1 SEM analysis of *Citrus limetta peel*

The surface morphology of the *citrus limetta peel* was demonstrated by scanning electron micrograph (SEM) of *citrus limetta peel* before and after adsorption studies respectively as shown in Fig. 5.1.3.2.1 (a) and Fig. 5.1.3.2.1 (b). SEM analysis shows that adsorbent had porous and irregular surface. This analysis revealed that the surface porosity is mainly responsible for the adsorption (Singh, T. P., Majumder, C. B. 2016). The surface morphology was found to change from smooth to rough and fluoride biosorption was observed by the occupation of pores on *Citrus limetta* surface which exhibited a rough texture.

#### 5.1.3.2.2 EDX analysis of *Citrus limetta peel*

The EDX analysis of *citrus limetta peel* before and after adsorption of fluoride is shown in Fig 5.1.3.2.2 (a) and Fig 5.1.3.2.2 (b) respectively. It is evident that various elements such as oxygen, carbon and very small amount of calcium were present initially but the fluoride was not present before adsorption. When the EDAX analysis was carried out after the fluoride adsorption, it was found that fluoride present was 0.89 wt% which confirmed the biosorption of fluoride (Singh, T. P., Majumder, C. B. 2016).

**Table 5.1.3.2.2: EDX Analysis of *Citrus Limetta peel* before and after adsorption of fluoride**

Element	Weight % Before Biosorption	Weight % After Biosorption
C K	45.9	44.5
O K	51.1	53.6

Element	Weight % Before Biosorption	Weight % After Biosorption
AlK	2.4	0.69
KK	0.58	0.29
FK	-	0.89

### 5.1.3.3 Analysis of Ground nut shell

#### 5.1.3.3.1 SEM analysis of Ground nut shell

Characterization of adsorbents groundnut shell was studied by using SEM micrograph. The morphology of the adsorbents before adsorption is shown in Fig.5.1.3.3.1 (a). It has been shown that adsorbents are heterogeneous, amorphous in nature, micro porous and irregular structure. Irregular structure will support the adherence of the fluoride. After the adsorption of fluoride it has been observed from SEM that the vacant pores on the surface of groundnut shells were occupied by fluoride and surface becomes rough as shown in figure Fig.5.1.3.3.1 (b).

#### 5.1.3.3.2 EDX analysis of Ground nut shell

EDX analysis of adsorbents shows the chemical constituents and composition of compounds present on the surface of adsorbents. Through this method, it has been shown the percentage weight of components available in adsorbents (Gupta et al., 2007) as shown (Fig.5.1.3.3.2 (a)).

From the analysis of chemical constituents it has been found that proteins and polysaccharides are inside the biomass cell. Metals like Al, Ca are also present in the adsorbents. Moneomes fluoride is present after the adsorption process (Fig.5.1.3.3.2 (b)).

**Table 5.1.3.3.2: EDX analysis of Ground nut shells before and after adsorption of fluoride**

Element	Weight % Before Biosorption	Weight % after Biosorption
CK	54.3	50.9
OK	39.7	44.5
FK	-	1.3
AlK	4.7	1.5
CaK	1.3	1.8

### 5.1.3.4 Analysis of Neem leaves

#### 5.1.3.4.1 SEM analysis of Neem leaves

SEM Analysis has been used for investigating the surface morphology of Neem leaves. As shown in Fig.5.1.3.4.1 (a) and Fig.5.1.3.4.1 (b) respectively before and after adsorption of fluoride which shows that this adsorbent possessed irregular as well as porous surface. The change in the adsorbent strength of biosorbent had been primarily because of the variation in their surface porosity (Singh T. P., Majumder, C. B. 2016).

#### 5.1.3.4.2 EDX analysis of Neem leaves

EDX of Neem leaves before and after adsorption of fluoride ions is shown in Fig.5.1.3.4.2 (a) and Fig.5.1.3.4.2 (b). From the analysis, this had been obvious that different elements like Carbon, Oxygen and a little quantity of Potassium etc. had been found in the fresh adsorbent. Whereas, EDX of the adsorbent taken after adsorption shows the presence of fluorides ion on the surface of adsorbent which confirmed the adsorption of fluoride (Singh T. P., Majumder, C. B. 2016).

**Table 5.1.3.4.2 EDX analysis of Neem leaves before and after adsorption of fluoride**

Element	Weight % Before Biosorption	Weight % after Biosorption
C K	62.4	55.7
O K	36.0	38.8
FK	--	0.18
AlK	0.69	1.1
KK	0.00	0.35
CaK	0.81	2.3

### 5.1.3.5 Analysis of virgin Turmeric and MnO<sub>2</sub> coated turmeric

#### 5.1.3.5.1 SEM analysis of virgin Turmeric and MnO<sub>2</sub> coated turmeric

Fig.5.1.3.5.1 (a) and 5.1.3.5.1 (c) shows the SEM (scanning electron micrograph) of turmeric before and after biosorption studies respectively. From Fig.5.1.3.5.1 (b) and Fig.5.1.3.5.1 (d), we observe that, surface morphology was changed from more porous and smooth to rough and being filled of the porous portion after adsorption process. The surface of turmeric after adsorption was filled by various aggregates of fluorides particles in between the pores, which gives good adsorption capability of turmeric for fluoride removal. Fig.5.1.3.5.1 (b) and Fig.5.1.3.5.1 (d), show the change

in surface morphology of virgin Turmeric and MnO<sub>2</sub>-Coated. After coating with MnO<sub>2</sub> the surface morphology is changed and become rougher relative to uncoated. This confirms that fluoride has been absorbed in to the voids of MnO<sub>2</sub> coated turmeric. The difference in surface porosity of the bio sorbent determines the capacity of adsorbent (Singh and Majumder, 2016).

### 5.1.3.5.2 EDX analysis of virgin Turmeric and MnO<sub>2</sub> coated turmeric

EDX analysis of virgin turmeric before and after adsorption of fluoride ions are shown in Fig.5.1.3.5.2 (a) and Fig.5.1.3.5.2 (b). As shown in these Figures, various elements such as carbon, oxygen and trace amount of potassium was present before adsorption but fluoride was not present. After adsorption, we obtained about 9.26 wt % of fluorides on the surface of adsorbent which confirmed the adsorption of fluoride by turmeric as shown in Fig.5.1.3.5.2 (b), (Singh and Majumder 2016). Also we observe appearance of fluoride on the surfaces of MnO<sub>2</sub>-Coated turmeric as shown in Fig.5.1.3.5.2 (d) and the adsorbent before adsorption of fluoride is shown in Fig.5.1.3.5.2 (c).

**Table 5.1.3.5.2: EDX analysis of virgin turmeric and MnO<sub>2</sub> coated turmeric before and after adsorption of fluoride**

Element	Turmeric Before biosorption		Turmeric After biosorption		Biosorption before MnO <sub>2</sub> -Coating		Biosorption after MnO <sub>2</sub> -Coating	
	Weight %	Atomic %	Weight %	Atomic %	Weight %	Atomic %	Weight %	Atomic %
C K	20.3	26.9	25.7	32.0	-	-	-	-
OK	69.2	68.9	65.01	60.7	22.3	49.7	20.4	42.7
K K	10.6	4.3	-	-	-	-	-	-
Mn K	-	-	-	-	77.7	50.3	72.2	44.1
F K	-	-	9.3	7.3	-	-	7.5	13.2

### 5.1.3.6 Analysis of *Java plum seed* (*Syzygiumcumini*)

#### 5.1.3.6.1 SEM analysis of *Java plum seed* (*Syzygiumcumini*)

SEM analysis was performed to study the surface morphology of *Java plum*. Fig.5.1.3.6.1 (a) and Fig.5.1.3.6.1 (b) show the SEM scanning images obtained for before and after the fluoride adsorption process. These images revealed that the adsorbent has irregular and porous surface. The SEM scanning of the adsorbent after fluoride adsorption show fluoride deposits on the pores and



surfaces of Java plums. It was observed that the difference in the adsorption capacities of *java plum seed* (*Syzygiumcumini*)s of different sizes was mainly due to the differences in their surface porosity.

#### 5.1.3.6.2 EDX analysis of *Java plum seed* (*Syzygiumcumini*)

EDX analysis is an analytical technique to determine the elemental composition of a sample, and can be used to determine the presence and the amount of all elements on in the adsorbents. Table 5.5 tabulates all the information obtained from EDX analysis. It is clear from the data that Carbon, Oxygen, Silicon and a small amount of Aluminium are present on the adsorbent prior to adsorption; no Fluoride was present before adsorption. Fig.5.1.3.6.2 (a) and Fig.5.1.3.6.2 (b) shows the EDX before and after adsorption of fluoride. Analysis for the adsorbent after the adsorption process show a clear presence of Fluorine in the sample, along with some amounts of magnesium and calcium, which can be explained by the presence of these elements in the synthetic simulated industrial wastewater.

**Table 5.1.3.6.2: EDX analysis of *Java plum seed* (*Syzygiumcumini*) before and after adsorption of fluoride**

Element	Weight % Before Biosorption	Weight % after Biosorption
CK	48.97	49.5
OK	48.3	47.1
SiK	2.1	0.7
AlK	0.61	0.63
MgK	–	0.23
CaK	–	1.3
FK	–	0.59

#### 5.1.3.7 Analysis of Banana peel

##### 5.1.3.7.1 SEM analysis of Banana peel

Characterization of adsorbent banana peel was studied by using SEM micrograph. The morphology of banana peel before adsorption is shown in Fig.5.1.3.7.1 (a). As shown in Fig.5.1.3.7.1 (a), adsorbent is heterogeneous, amorphous in nature, micro porous and irregular structure. Irregular structure will support the adherence of the fluoride. After the adsorption of fluoride it has been

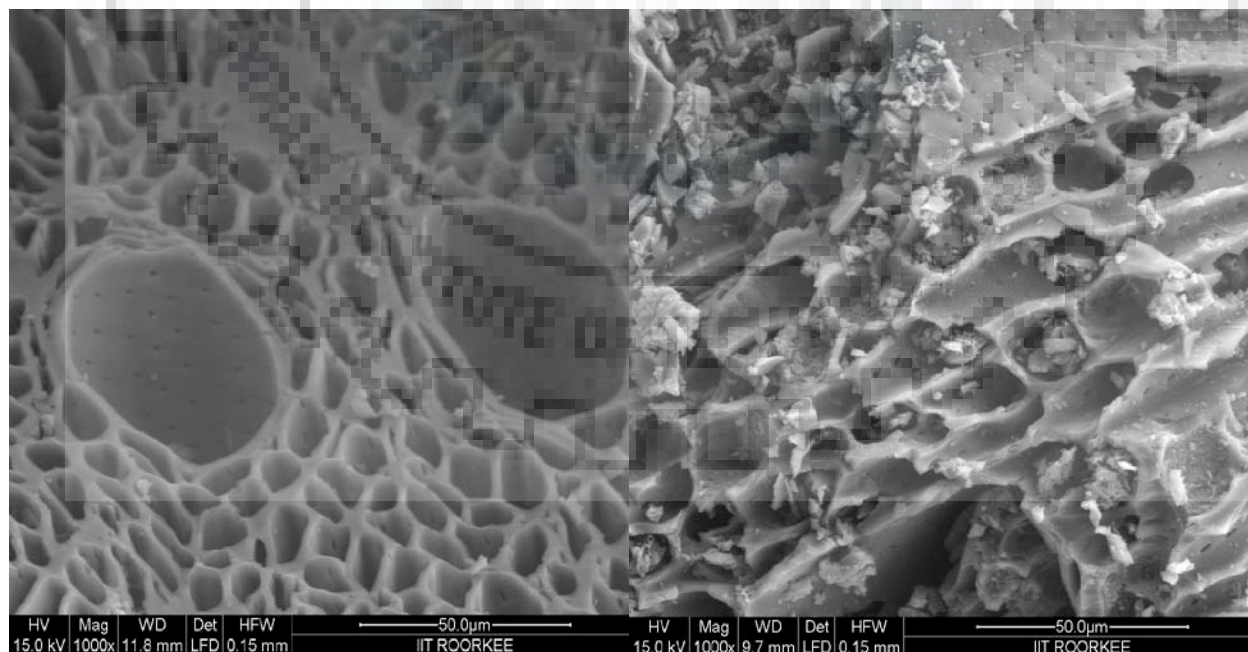
observed from the SEM micrograph (Fig.5.1.3.7.1 (b)), that the micro porosity, irregularity, cracks like pores are decreased. (Gupta et al., 2007).

### 5.1.3.7.2 EDX analysis of Banana peel

EDX analysis of adsorbents show the chemical constituents and composition of compounds present on the surface of adsorbents. Fig.5.1.3.7.2 (a) and Fig.5.1.3.7.2 (b) show the EDX before and after adsorption of fluoride. Chemical Composition of compounds is given in the Tables 5.1.3.7.2. (Gupta et al., 2007)

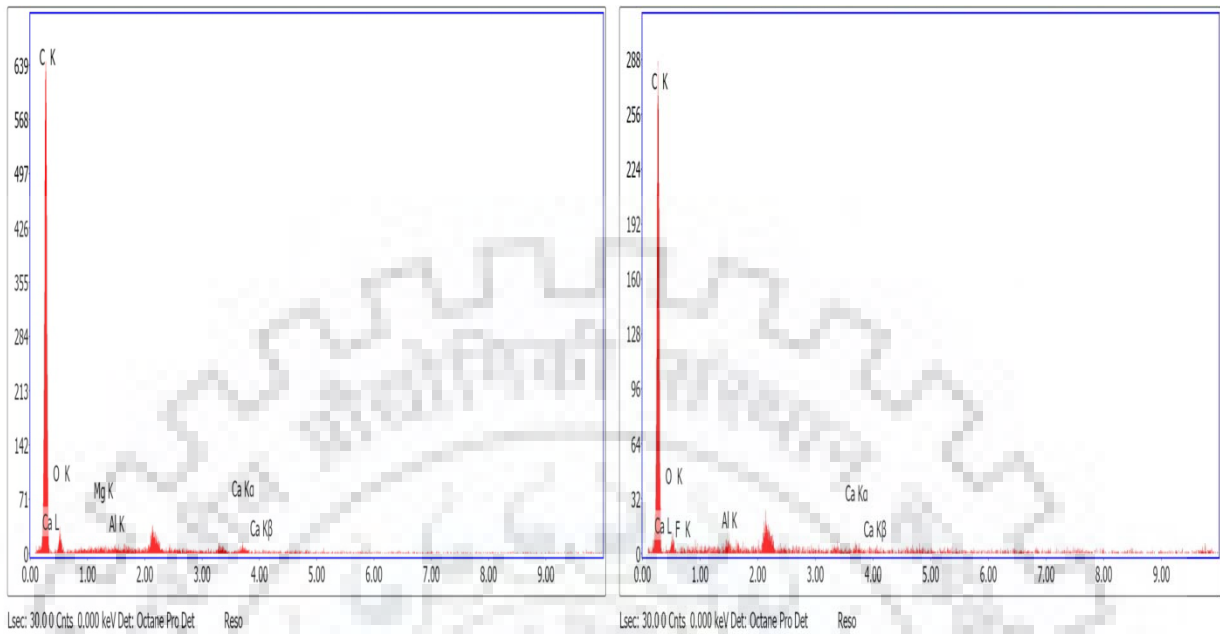
**Table 5.1.3.7.2 EDX analysis of Banana peel**

Element	Weight % Before Biosorption	Weight % after Biosorption
CK	58.2	57.7
OK	41.1	41.0
AlK	0.71	1.2
SiK	-	0.11
FK	-	0.03



**Fig.5.1.3.1.1 (a) SEM before adsorption**

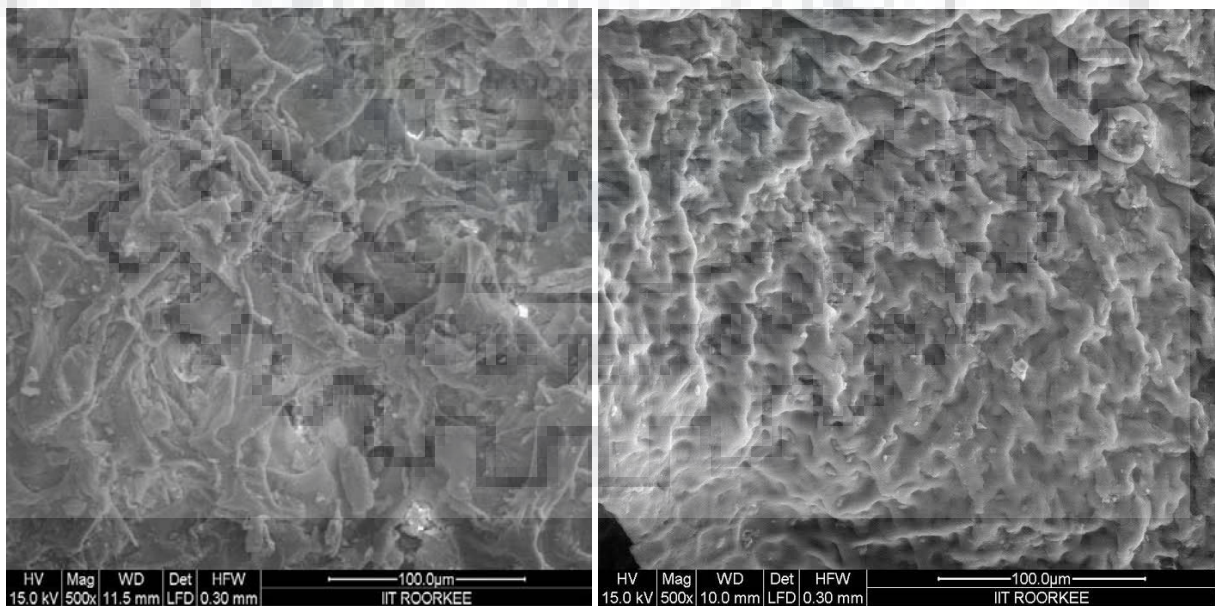
**Fig.5.1.3.1.1 (b) SEM after fluoride adsorption**



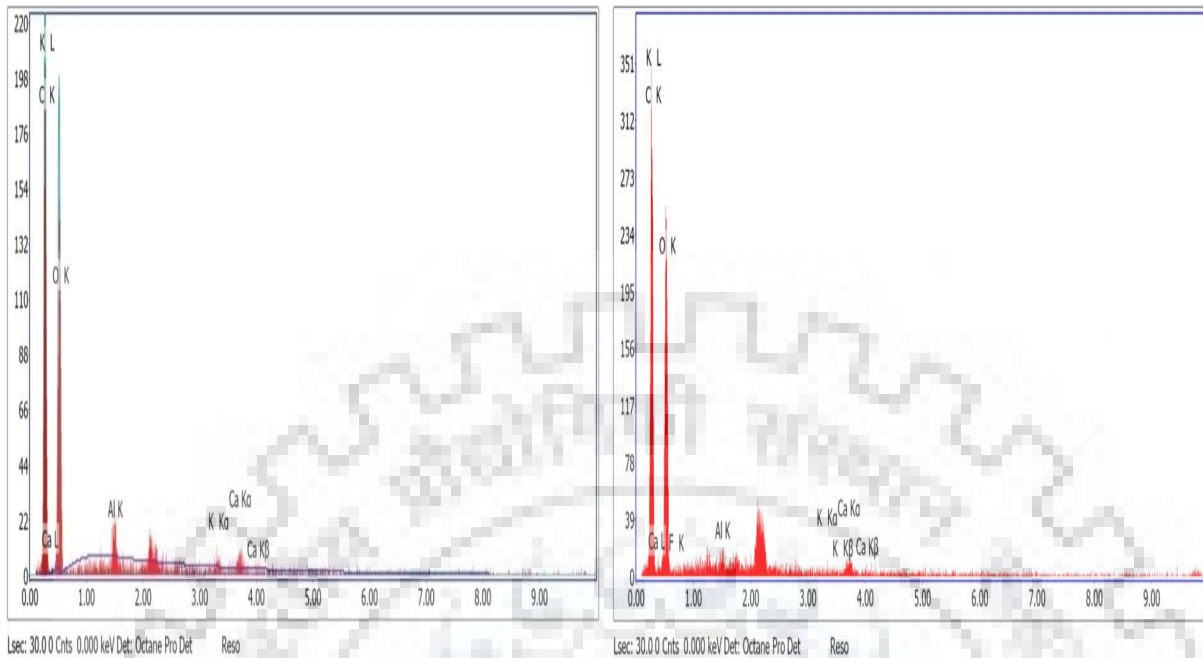
**Fig.5.1.3.1.2 (a) EDX before adsorption      Fig.5.1.3.1.2 (b) EDX after fluoride adsorption**

Fig. 5.1.3.1.1 SEM of GAC (a) before adsorption (b) after fluoride adsorption

Fig. 5.1.3.1.2 EDX of GAC (a) before adsorption (b) after fluoride adsorption



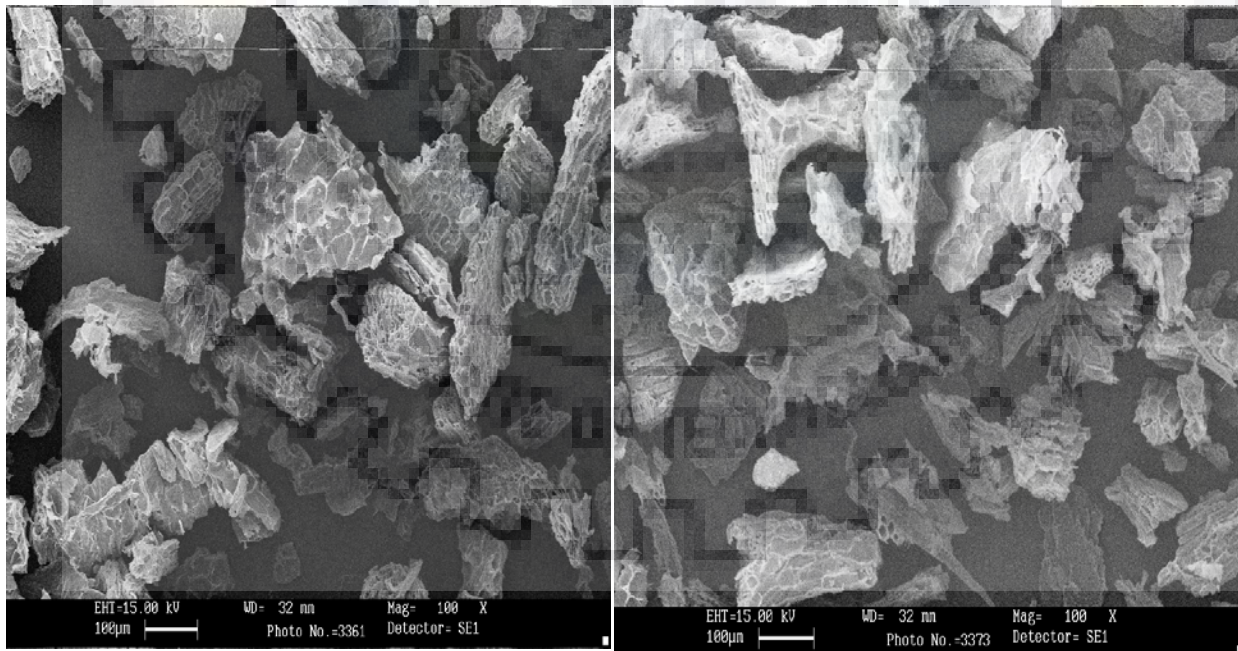
**Fig. 5.1.3.2.1 (a) SEM before adsorption      Fig 5.1.3.2.1 (b) SEM after fluoride adsorption**



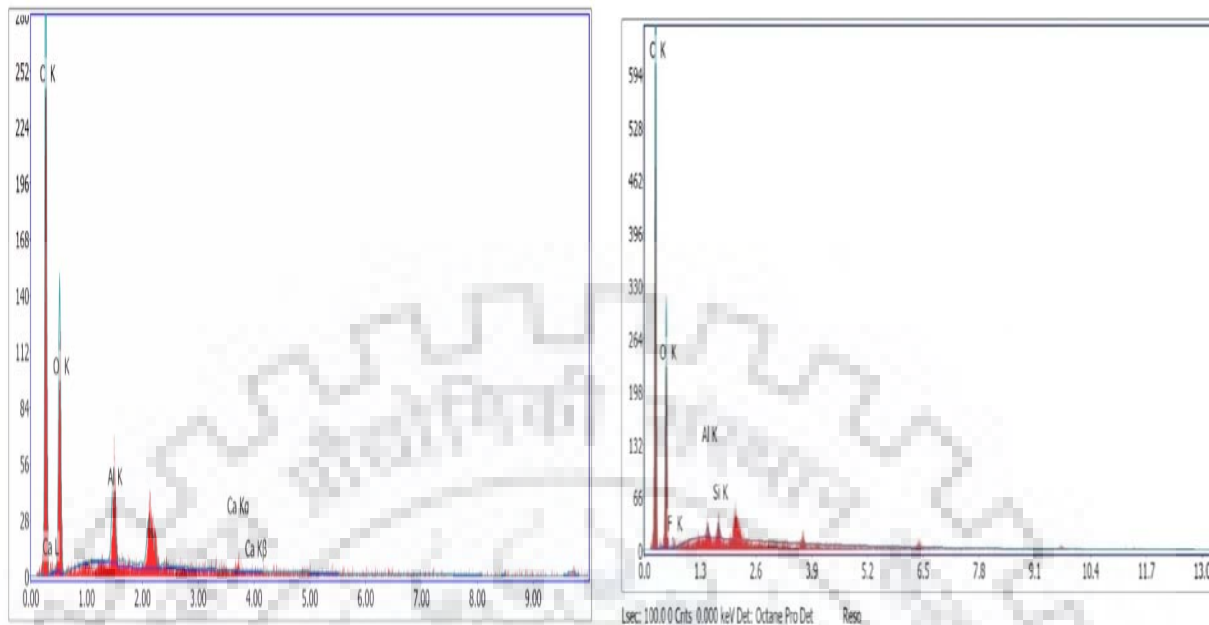
**Fig.5.1.3.2.2 (a) EDX before adsorption      Fig.5.1.3.2.2 (b) EDX after fluoride adsorption**

Fig. 5.1.3.2.1 SEM of *Citrus limetta peel* (a) before adsorption (b) after fluoride adsorption

Fig. 5.1.3.2.2 EDX of *Citrus limetta peel* (a) before adsorption (b) after fluoride adsorption



**Fig.5.1.3.3.1 (a) SEM before adsorption      Fig 5.1.3.3.1 (b) SEM after fluoride adsorption**

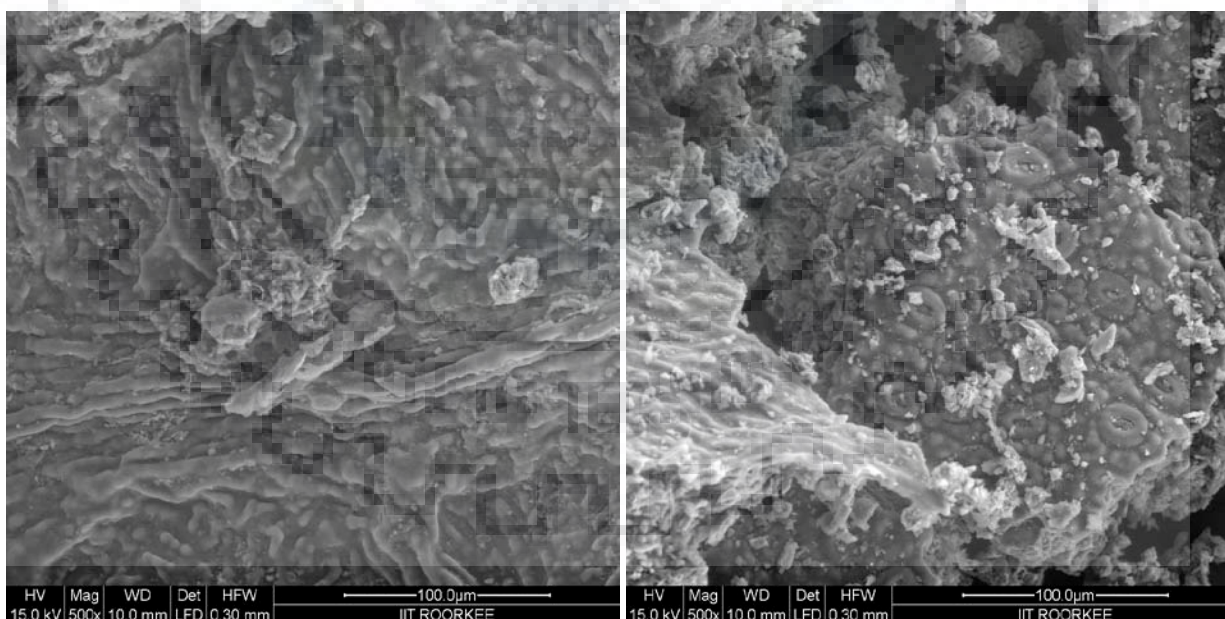


**Fig.5.1.3.3.2 (a) EDX before adsorption**

**Fig.5.1.3.3.2 (b) EDX after fluoride adsorption**

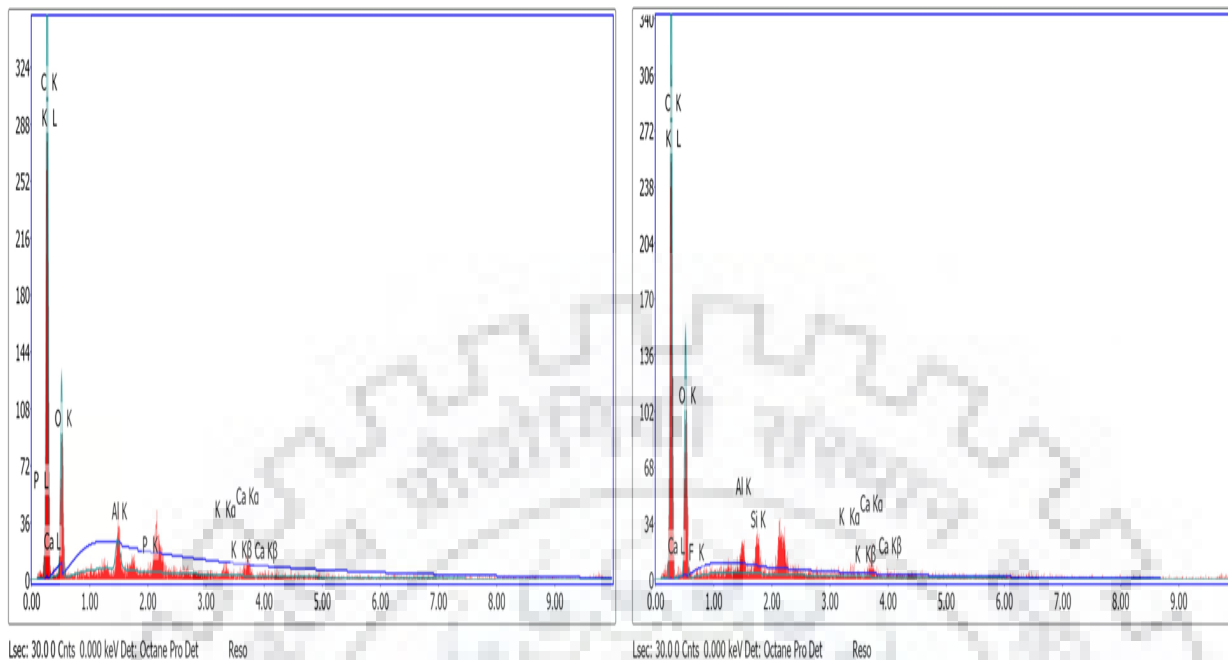
Fig. 5.1.3.3.1 SEM of Ground nut shell (a) before adsorption (b) after fluoride adsorption

Fig. 5.1.3.3.2 EDX of Ground nut shell (a) before adsorption (b) after fluoride adsorption



**Fig. 5.1.3.4.1 (a) SEM before adsorption**

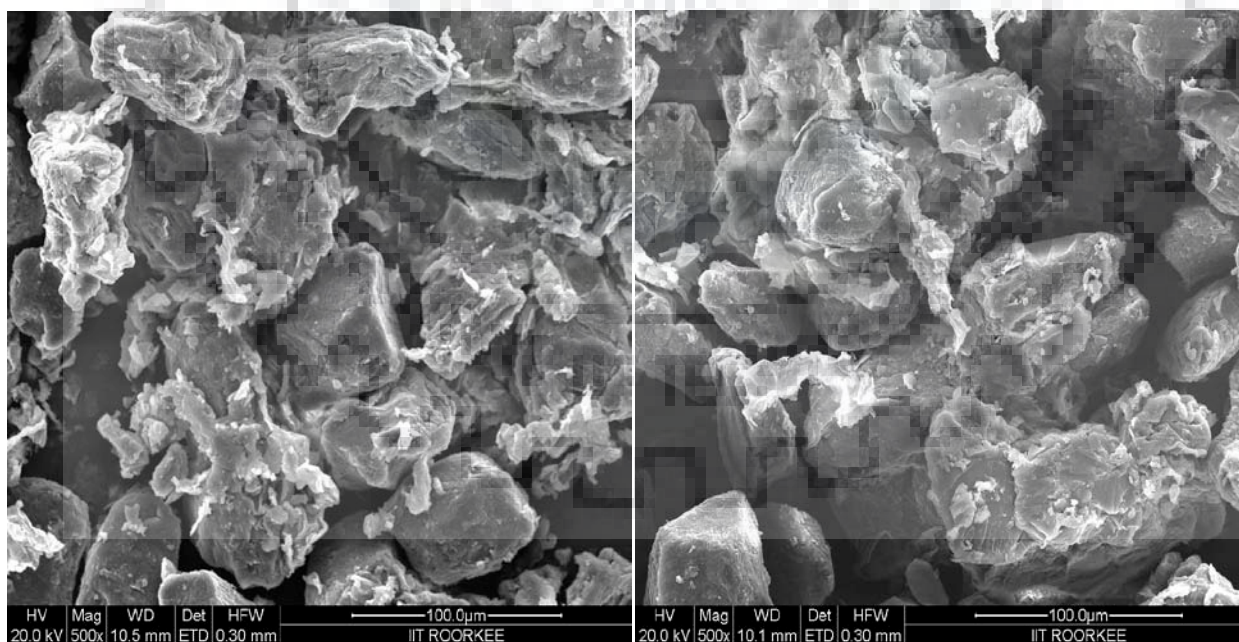
**Fig 5.1.3.4.1 (b) SEM after fluoride adsorption**



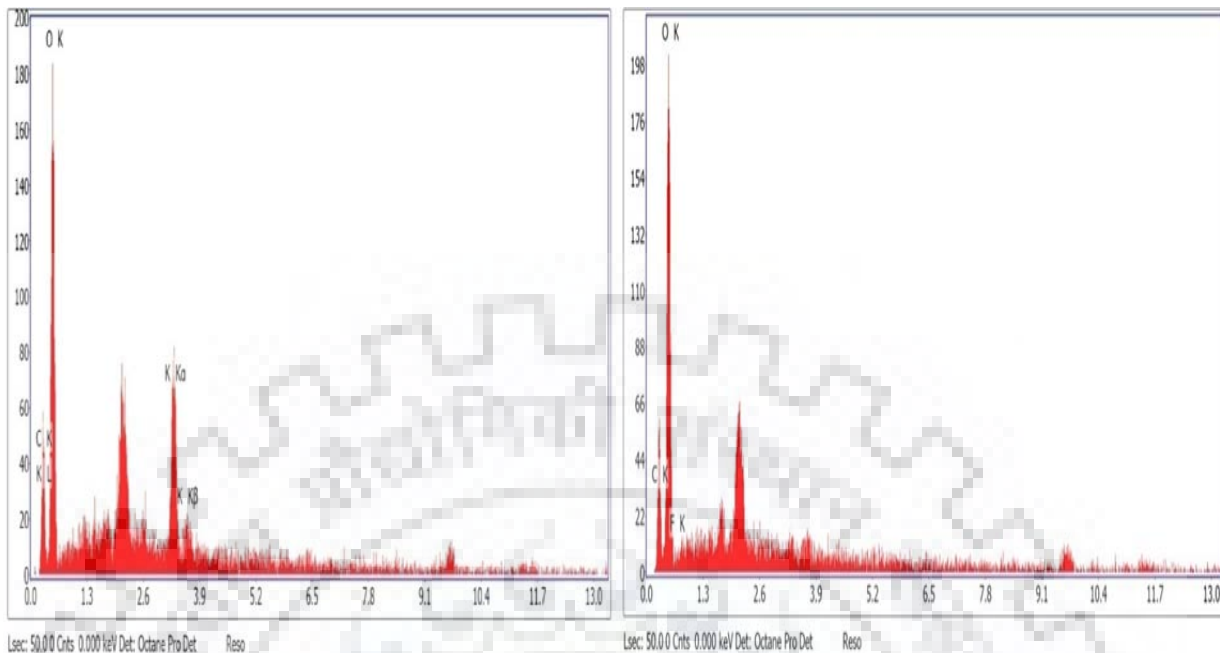
**Fig.5.1.4.4.2 (a) EDX before adsorption      Fig.5.1.4.4.2 (b) EDX after fluoride adsorption**

Fig. 5.1.3.4.1 SEM of Neem leaves (a) before adsorption (b) after fluoride adsorption

Fig. 5.1.3.4.2 EDX of Neem leaves (a) before adsorption (b) after fluoride adsorption



**Fig. 5.1.3.5.1 (a) SEM before adsorption      Fig 5.1.3.5.1 (b) SEM after fluoride adsorption**

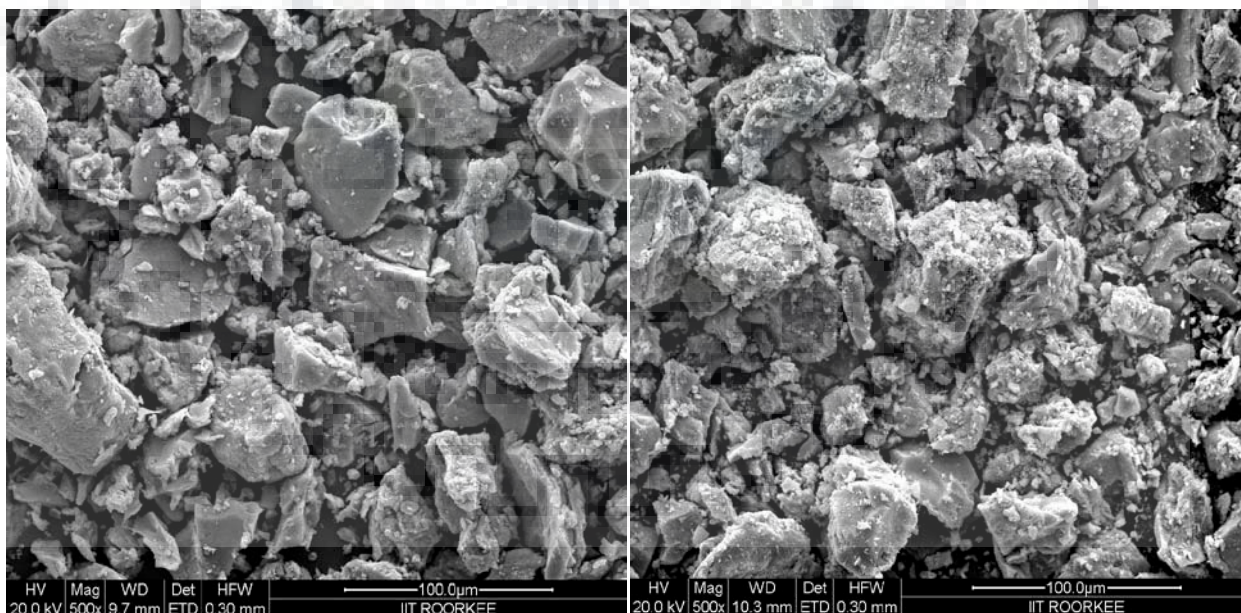


**Fig.5.1.3.5.2 (a) EDX before adsorption**

**Fig.5.1.3.5.2 (b) EDX after fluoride adsorption**

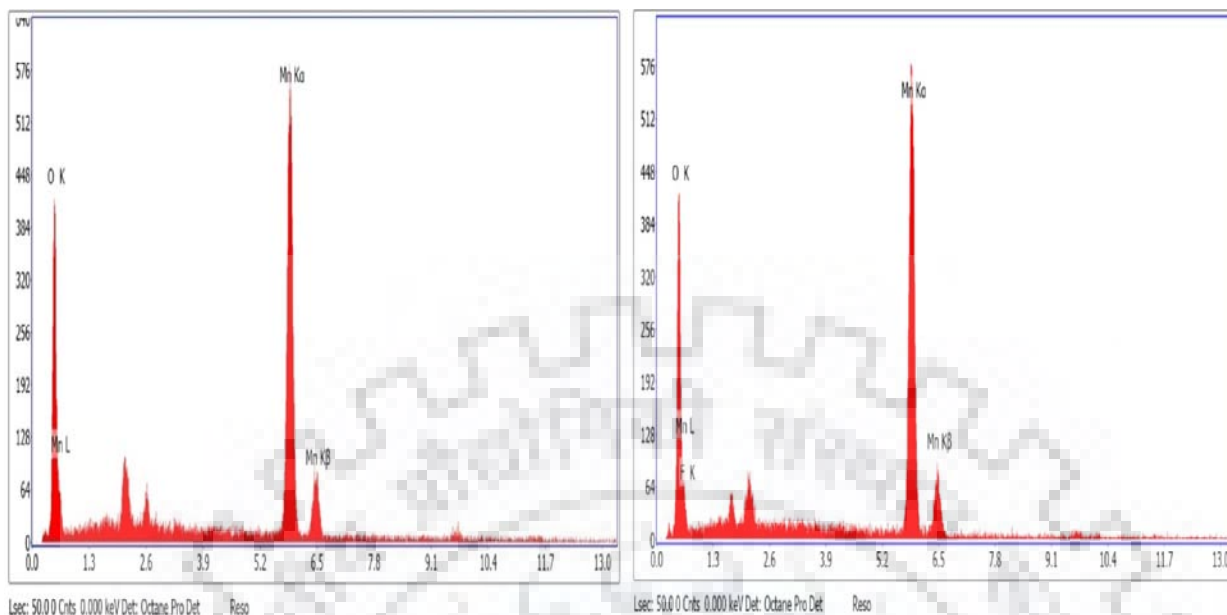
Fig. 5.1.3.5.1 SEM of Turmeric (a) before adsorption (b) after fluoride adsorption

Fig. 5.1.3.5.2 EDX of Turmeric (a) before adsorption (b) after fluoride adsorption



**Fig. 5.1.3.5.1 (c) SEM before adsorption**

**Fig 5.1.3.5.1 (d) SEM after fluoride adsorption**



**Fig.5.1.4.5.2 (c) EDX before adsorption**

**Fig.5.1.4.5.2 (d) EDX after fluoride adsorption**

Fig. 5.1.3.5.1 SEM of MnO<sub>2</sub> coated Turmeric (c) before adsorption (d) after fluoride adsorption

Fig. 5.1.3.5.2 EDX of MnO<sub>2</sub> coated Turmeric (c) before adsorption (d) after fluoride adsorption

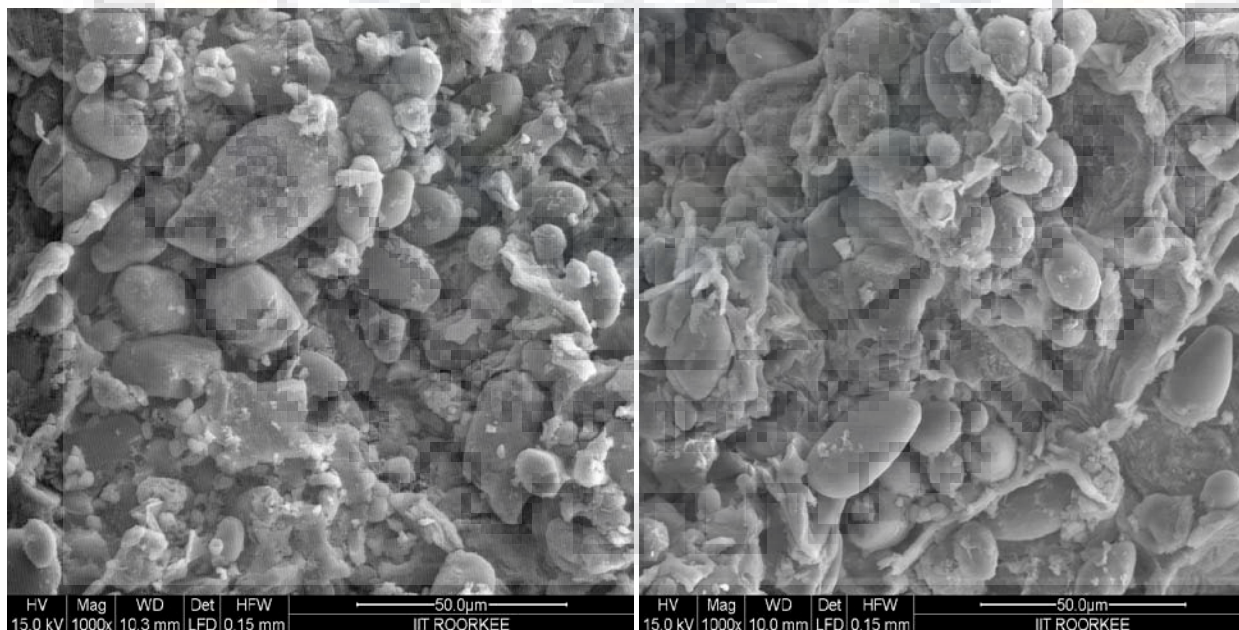


**Fig. 5.1.3.6.1 (a) SEM before adsorption**

**Fig 5.1.3.6.1 (b) SEM after fluoride adsorption**



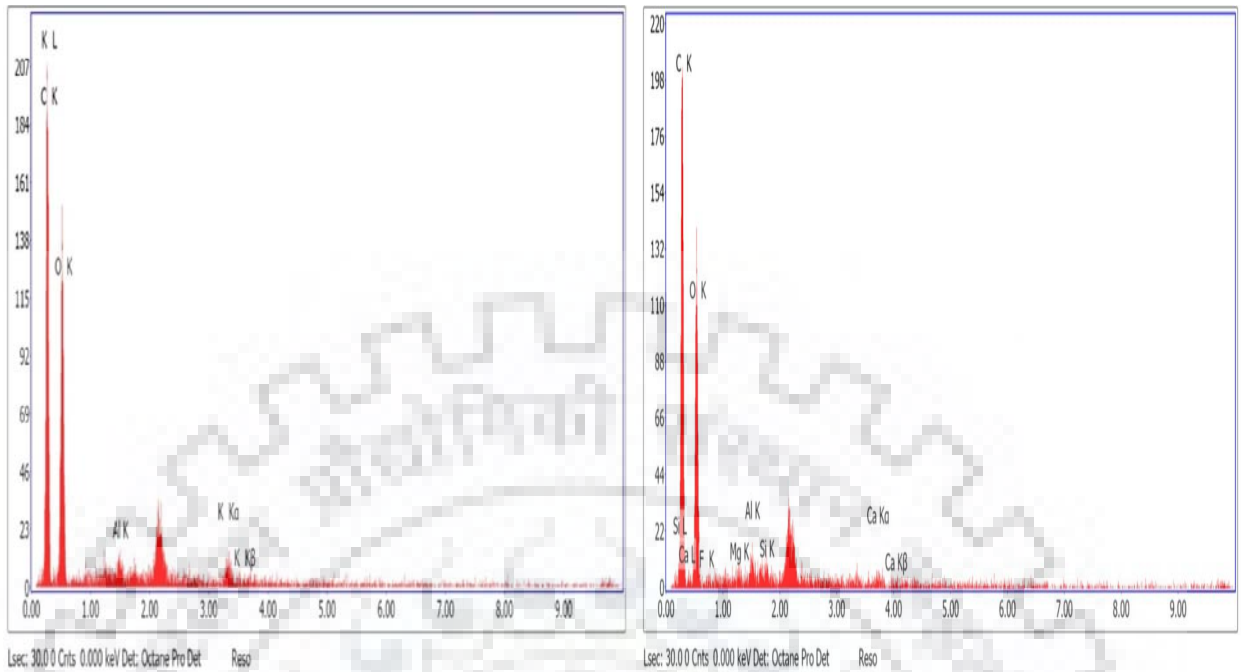


**Fig.5.1.3.6.2 (a) EDX before adsorption**

**Fig.5.1.3.6.2 (b) EDX after fluoride adsorption**

**Fig. 5.1.3.6.1 SEM of *Java plum seed (Syzgiumcumini)* (a) before adsorption**

**(b) After fluoride adsorption**

**Fig. 5.1.3.6.2 EDX of *Java plum seed (Syzgiumcumini)* (a) before adsorption**

**(b) After fluoride adsorption**

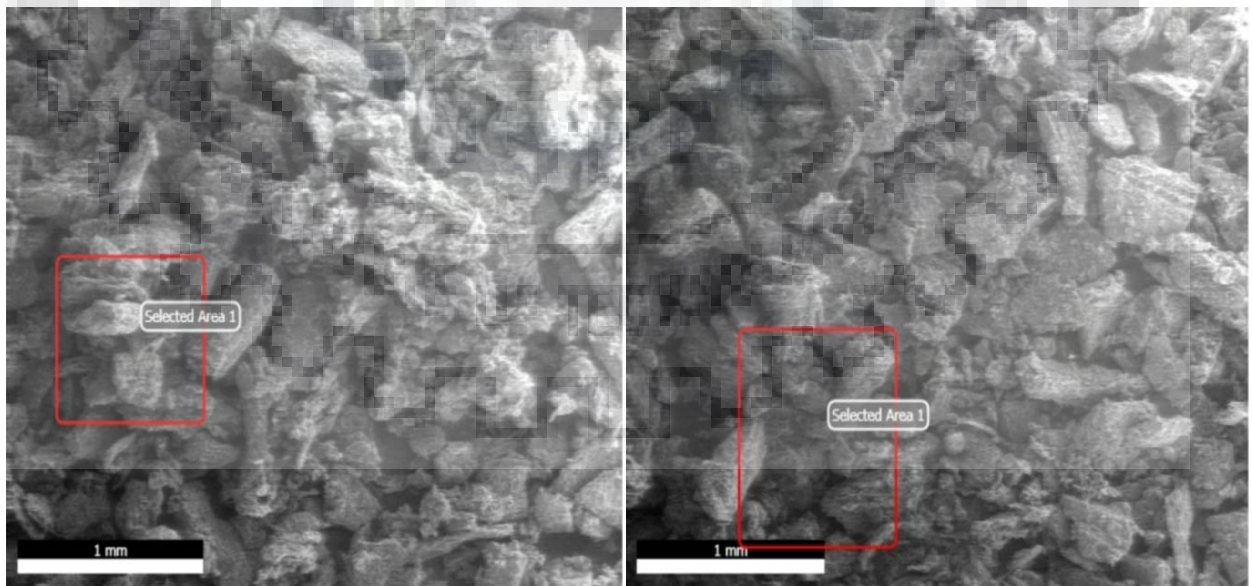


**Fig. 5.1.3.7.1 (a) SEM before adsorption**

**Fig. 5.1.3.7.1 (b) SEM after fluoride adsorption**

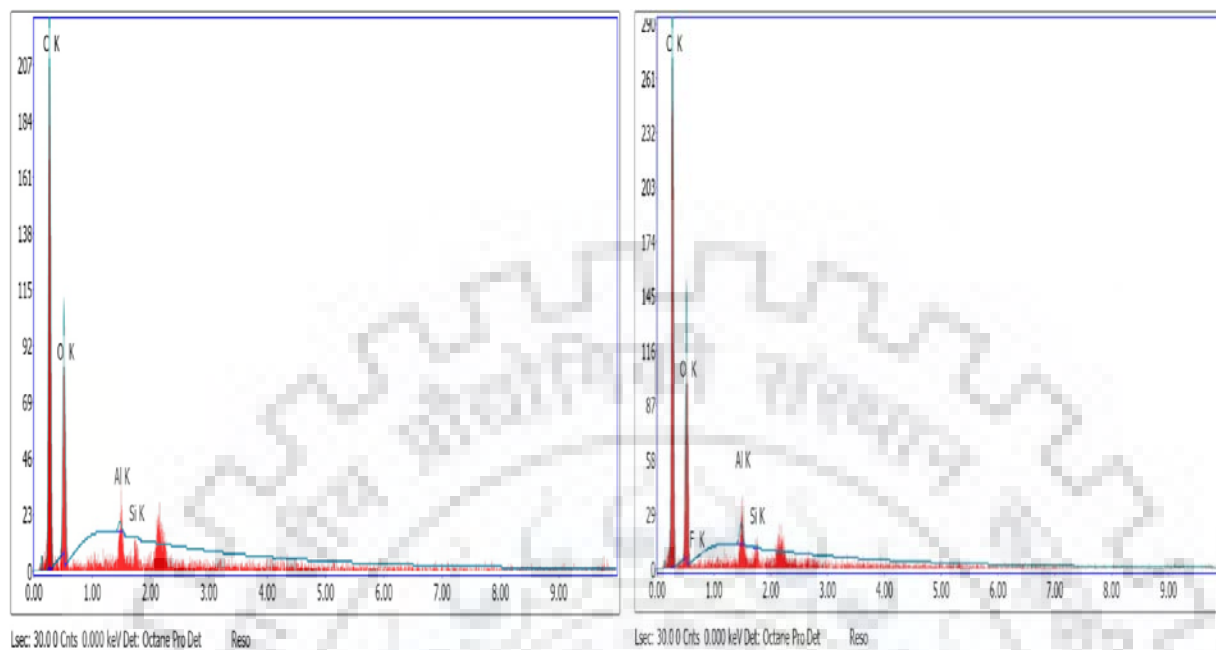


**Fig. 5.1.3.7.2 (a) EDX before adsorption      Fig. 5.1.3.7.2 (b) EDX after fluoride adsorption**

Fig. 5.1.3.7.1 SEM of Banana peel (a) before adsorption (b) after fluoride adsorption

Fig. 5.1.3.7.2 EDX of Banana peel (a) before adsorption (b) after fluoride adsorption

### 5.1.3.8 Concluding remark

EDX spectrum and SEM of various bio sorbent like GAC, *Citrus limetta peel*, Ground nut shell, Turmeric and MnO<sub>2</sub> coated turmeric, Neem leaves, *Java plum seed (Syzygiumcumini)* and Banana peel confirm the adsorption of fluoride from simulated synthetic waste water.

### 5.1.4 Effect of batch adsorption process parameters

Batch adsorption experiments were carried out to 50 ml flat bottom flask in an incubator cum shaker at 120 rpm, Size of adsorbent 2-4mm, dose, pH and temperature (30°C). The residual concentration of fluoride was measured in UV spectrophotometer DR 5000 HACH.

#### 5.1.4.1 Effect of pH for removal of fluoride

##### 5.1.4.1.1 Effect of pH for removal of fluoride by GAC

The pH of solution significantly affects the adsorption of fluoride. Adsorption of fluoride was carried out with various initial pH ranges in between 2 and 11. The more effective removal of fluoride onto the GAC was found at pH of 4–6. Fig.5.1.4.1.1 shows the effect of pH on fluoride

adsorption on GAC. Maximum percentage removal of fluoride was 97.96% found at pH 4. It is observed that removal of fluoride at pH 3 is lower compared to at pH 4–6. As per the speciation of fluoride, it is present generally as HF instead of anionic fluoride ion (F<sup>-</sup>) (Deng et al. 2011), which could be the reason for less adsorption. At pH 6 and above, the surface of adsorbent came to be deprotonated, which is unfavourable for the fluoride adsorption. The fluoride present as anionic ion. However, as increasing pH of solution increase, the hydroxide concentration increases which would compete with the fluoride for the adsorption sites (Thakre et al. 2011).

#### **5.1.4.1.2 Effect of pH for removal of fluoride by *Citrus limetta peel***

The pH effect on removing of fluoride had been studied within 2-12 and the findings have been reported in the Fig.5.1.4.1.2. In process of adsorption on bio adsorbents, pH plays a major role. The effect of pH on the % removal of fluoride ions by biosorption on the surface of *Citrus limetta* is shown in Fig. 5.1.4.1.2. The initially adsorption increases with the pH. After pH 5, it started decreasing with the increasing pH as per the speciation of fluoride, it is present generally as HF instead of anionic fluoride ion (F<sup>-</sup>) (Deng et al. 2011), which could be the reason for less adsorption. At pH 5 above, the surface of adsorbent came to be deprotonated, which is unfavourable for the fluoride adsorption. The fluoride present as anionic ion. The optimum pH for biosorption of *Citrus limetta* was found to be 5 which gave 91.00 % removal. After that it was found to be decreased with the increase in pH.

#### **5.1.4.1.3 Effect of pH for removal of fluoride by Ground nut shell**

The relationship between pH and fluoride removal was studied in the domain of 2-12 and the results obtained are shown in Fig.5.1.4.1.3. The pH of the solution plays major role in adsorption process. Fig.5.1.4.1.3 shows the relationship between percentage removal and pH. It is observed that in the range of pH 1-7 the percentage removal increases because of more adsorption of fluoride on bio adsorbent. The maximum removal of 88.5% was observed at pH 7 in 1.5 hr. On increasing pH above from pH 7, the removal efficiency decreases. As per the speciation of fluoride, it is present generally as HF instead of anionic fluoride ion (F<sup>-</sup>) (Deng et al. 2011), This could be the reason for less adsorption. At pH 7 and above, the surface of adsorbent came to be deprotonated, which is unfavourable for the fluoride adsorption. In this ranges fluoride is present as anionic ion. So the optimum value for maximum removal comes out to be at pH 7.

#### **5.1.4.1.4 Effect of pH for removal of fluoride by Neem leaves**

The pH of solution significantly affects the adsorption of fluoride. Adsorption of fluoride was carried out with the various initial pH in between 2 and 10. The more effective removal of fluoride onto the neem leaves was found at pH 4. Fig.5.1.4.1.4 indicates the effect of pH on fluoride adsorption by using neem Leaves. Maximum percentage removal of fluoride was 83.5% at pH 4. It was observed that removal of fluoride at pH 3 is lower compared to the pH 4–6. As per the speciation of fluoride, it is present generally as HF instead of anionic fluoride ion (F<sup>-</sup>) (Deng et al. 2011), which could be the reason for less adsorption. At pH 6 and above, the surface of adsorbent came to be deprotonated, which is unfavourable for the fluoride adsorption. The fluoride is present as anionic ion. However, with the increase in pH of the hydroxide concentration increases which would compete with the fluoride for the adsorption sites (Thakre et al. 2011).

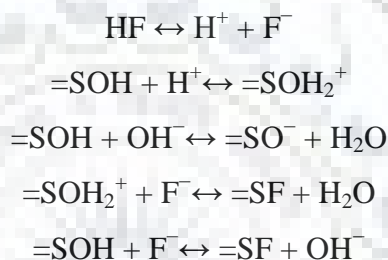
#### **5.1.4.1.5 Effect of pH for removal of fluoride by Virgin turmeric and MnO<sub>2</sub> coated turmeric**

The effect of pH on removal of fluoride ion from waste water was carried out in batch reactor. pH range from 2-12 were considered in the present study. Other parameters are kept constant. The effect of pH on percentage fluoride removal for turmeric based bio sorbent is given in Fig.5.1.4.1.5. Charges of the bio sorbents and fluoride ion distribution in natural water depend on the condition of its pH (Basha et al., 2009). So, pH is the most important parameter for maximum fluoride removal. Effects of pH on fluoride removal by turmeric are shown in Fig.5.1.4.1.5. It is observed that increase in percentage of fluoride removal increases from pH 2.0 to 6.0 and start to decrease from pH 7.0 to 12.0 for both turmeric based bio sorbent and MnO<sub>2</sub> coated turmeric bio sorbent. Maximum percentage of fluoride removal (92.52 %) was achieved at pH 6 for turmeric based bio sorbent and 87.54 % removal for MnO<sub>2</sub> coated turmeric bio sorbent at pH 6 ( Fig.5.1.4.1.5).

Micro-molecules in most of bio sorbents have groups such as alcohol, carboxyl, phosphate, phenol, thiol, and amino groups. The process reaches forward when the process of protonation and that of deprotonation of the functioning groups happens across the surface of bio adsorbent (Mohan and Karthikeyan, 1997). The ionic form of fluoride in the solution and the electric charge on the bio adsorbent is governed by pH of solution where it is observed that net charge at the outside of bio adsorbent has been negative. The positive charge is present on the surface of bio-adsorbent form bonds with fluoride ions having negative charge. In the case of Turmeric based bio sorbent,

maximum adsorption was observed at pH (pH = 7). This indicates that the outside of Turmeric is cationic type (H<sup>+</sup>) in nature (Gulay et al., 2005). When value of pH is lower (<7), the surface of the absorbent has positive charge and, probably anionic exchange sorption process occurs. The related sorption inhibition that happened at the basic level of pH (>7) due to hydroxyl ion increasing, resulting in the forming of aqua-complexes; thus, desorption happened (Killedar and Bhargava, 1993).

According to various study of optimization of pH, adsorption on bio-adsorbent is mostly noted in the acidic range. In present case, we noted that fluoride removal was obtained in less acidic range thus making it beneficial and economically. To understand the fluoride sorption behaviour under different pH values, the following reactions are considered (Onyango et al., 2004)



Where =SOH, =SOH<sub>2</sub><sup>+</sup> and =SO<sup>-</sup> represent the neutral, protonated and deprotonated sites on turmeric and MnO<sub>2</sub> Coated Turmeric and =SF is the active site-fluoride complex (S = Turmeric /MnO<sub>2</sub>-coated turmeric).

#### 5.1.4.1.6 Effect of pH for removal of fluoride by *Java plum seed* (*Syzgiumcumini*)

The pH of the synthetic simulated waste-water solution plays a vital role in determining the efficiency of fluoride removal by adsorption. As the pH change, the reactivity of the functional groups responsible for the adsorption will change as well. To determine the optimal range of pH for fluoride adsorption by *Java plum seed* (*Syzgiumcumini*) adsorbent, the process was carried out at various pH values ranging from pH 2 to pH 10. Fig.5.1.4.1.6 shows the % removal of fluoride obtained at all the pH values used. All other parameters were maintained constant. As can be seen from the graph, the rate of fluoride removal was maximum obtained at the pH 6. For *Java plum* adsorbent; more than 93.2 % of fluoride present was removed between this pH ranges. The amount of fluoride removed approached a constant value for pH > 7 which decreases later. Solution pH of less than 4 was found to be unsuitable for this process, with diminishing fluoride removal as the pH

decreased further as per the speciation of fluoride, it present generally as HF instead of anionic fluoride ion (F<sup>-</sup>) (Deng et al. 2011), which could be the reason for less adsorption. At pH 6 above, the surface of adsorbent came to be deprotonated, which is unfavourable for the fluoride adsorption. The fluoride is present as anionic ion. However, as increasing pH of solution, the hydroxide concentration increases which would compete with the fluoride for the adsorption sites which signifies the requirement of a slightly acidic environment for efficient fluoride removal using java plum adsorbents.

#### **5.1.4.1.7 Effect of pH for removal of fluoride by Banana peel**

The pH effect on removing of fluoride had been studied within 2-12; the findings have been represented in illustration. 5.1.4.1.7. In process of adsorption on bio adsorbents, pH plays a major role. The dependency of removal efficiency of the adsorbents with pH of the test sample of fluoride has been represented in 5.1.4.1.7. The findings conclude a powerful relation in the absorption of fluoride with the sample's pH level, due to which absorption-process appears to increase with rising level of pH, in the range of pH 1–7. Maximum adsorption was 93.1 % observed at a pH 6, within an hour. Several scholars found out that biosorption depends upon the aqueous phase pH level, as well as functioning groups upon bio sorbent, and relative ionic states (at particular pH) (Aharoni and Ungarish, 1977, Pavlatou and Polyzopolous, 1988). When it comes to the biosorption process micro molecules, mostly these have groups such as amino, carboxyl, alcohol, thiol, phosphate and phenol. This process is conducted through the protonation and deprotonation of functioning groups across the outside of bio adsorbent (Rudzinski et al., 1998). The pH level controlled the ionic structure of fluoride in it, and the electrical charge, or it can be said that the functioning groups with polysaccharides and proteins across biosorbent, so that it is observed the complege charge across the outside of bio-adsorbent remains positive. This charge closely binds the fluoride ions with negative charge. When there is the lower value of pH, the outside of the adsorbent becomes positively charged, and then fluoride sorption happened, perhaps by anionic exchange sorption process. In a medium that is acidic, due to the protonation, action across the outside of the functioning groups like amino, carboxyl, etc. makes it positively charged.

As per the findings related to pH optimization, absorption related to bio adsorbent is mainly seen when there is acidic range pH level. Removing of fluoride, on the other hand, related to this study has found in a lower acidic range that is better and less-consuming for this purpose.

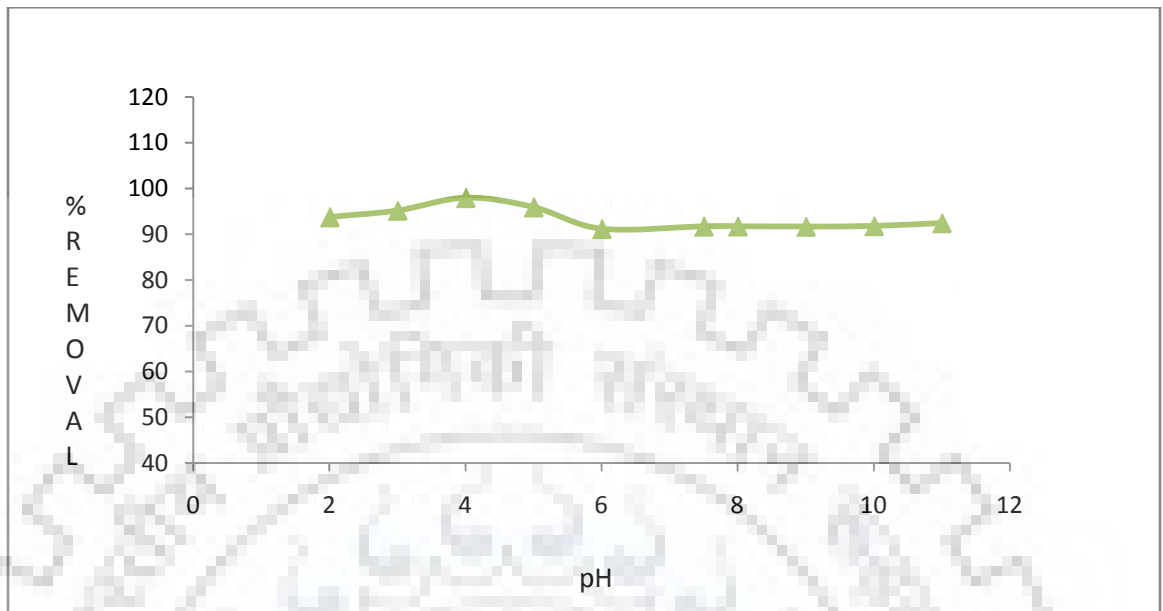


**Fig. 5.1.4.1.1** Effect of pH for removal of fluoride by GAC

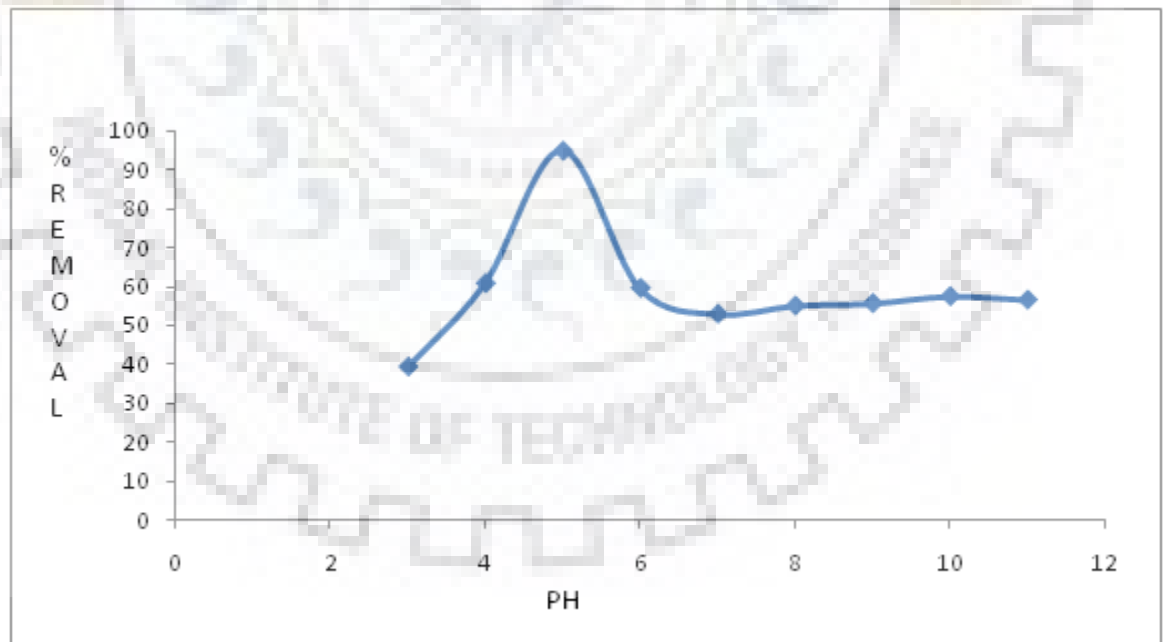


**Fig. 5.1.4.1.2** Effect of pH for removal of fluoride by *Citrus limetta peel*

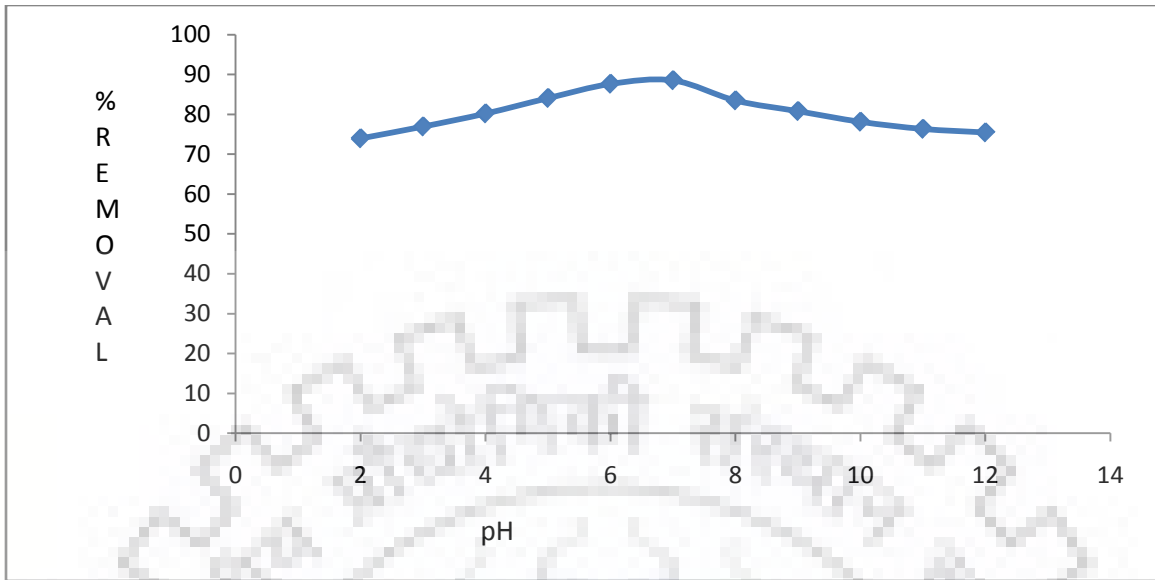


**Fig. 5.1.4.1.3 Effect of pH for removal of fluoride by Ground nut shell**

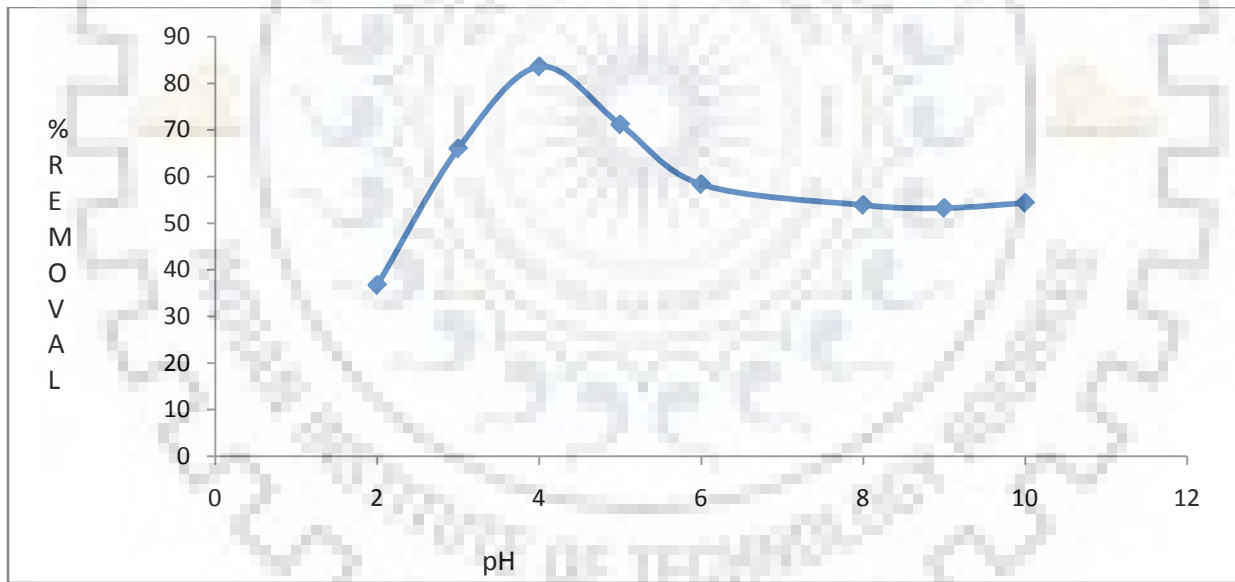


**Fig. 5.1.4.1.4 Effect of pH for removal of fluoride by Neem leaves**



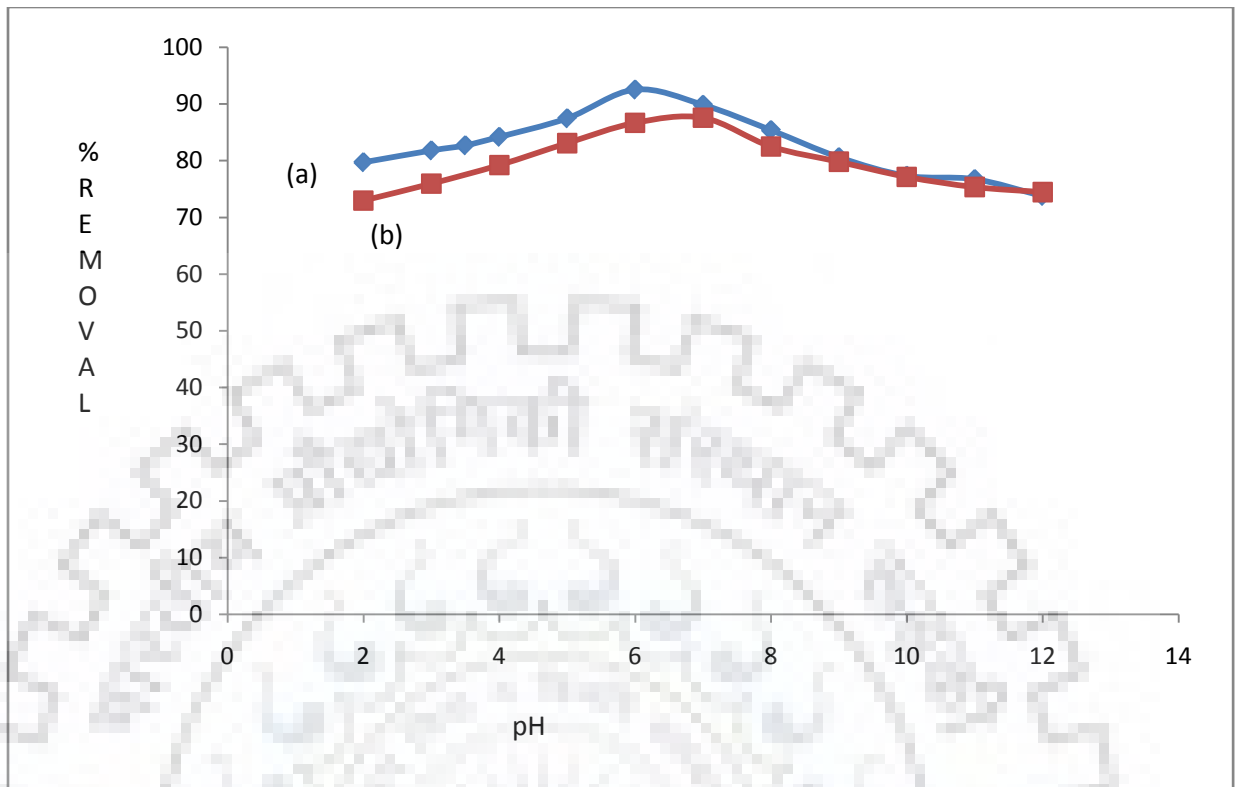


**Fig. 5.1.4.1.5 Effect of pH for removal of fluoride by (a) Virgin turmeric (b) MnO<sub>2</sub> coated turmeric**

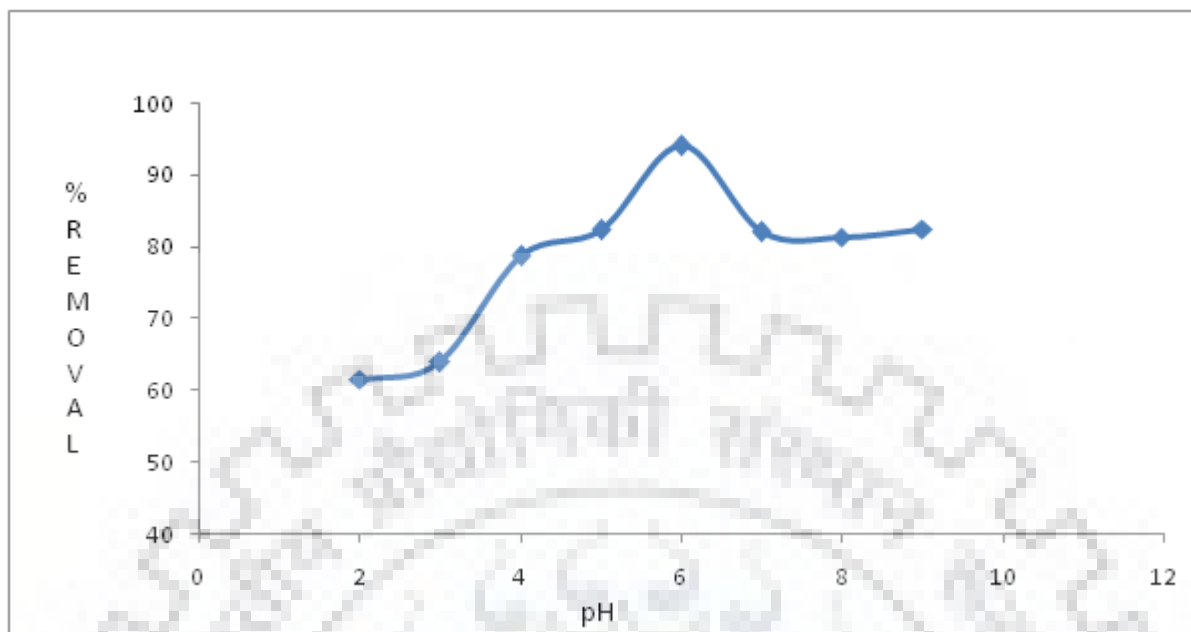


**Fig. 5.1.4.1.6 Effect of pH for removal of fluoride by *Java plum seed (Syzgiumcumini)***

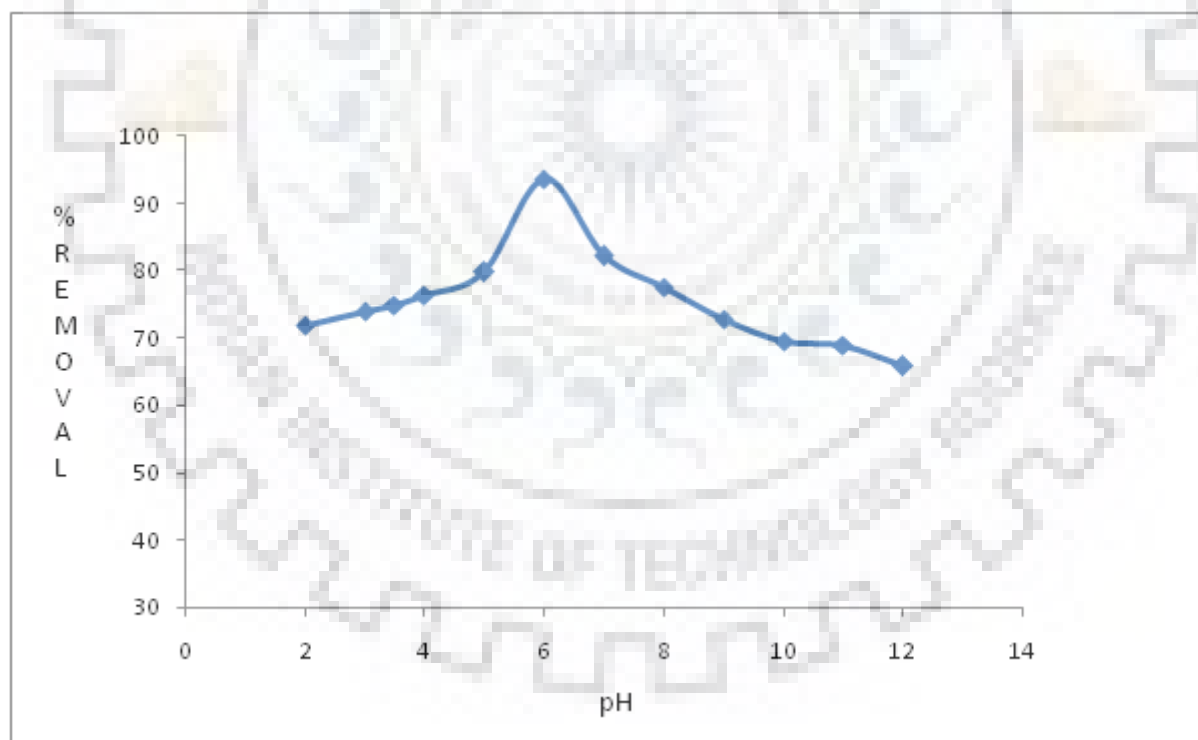


**Fig. 5.1.4.1.7 Effect of pH for removal of fluoride by *Banana peel***

#### **5.1.4.2 Effect of Dose for removal of fluoride**

##### **5.1.4.2.1 Effect of Dose for removal of fluoride by GAC**

Experiment of fluoride removal was carried out with GAC as adsorbent to study the effect of dose on fluoride removal by GAC. Fluoride removal efficiency is dependent on dose concentration of adsorbent. Fig.5.1.4.2.1 show that removal of fluoride enhanced with increasing dose of adsorbent. Higher availability of surface and the pore volume are responsible for enhancing adsorption of solute (Mohammad and Majumder, 2014). Upto some extent removal was increased with increasing concentration of dose, after that removal was constant even on increasing adsorbent / concentration. Maximum removal of fluoride was 97.4 % at 32 g/L dose. It occurred due to the covering of working sites with greater dosage, thereby reduction in the net surface area (Prakasam et al., 1998).

##### **5.1.4.2.2 Effect of Dose for removal of fluoride by *Citrus limetta peel***

The removing strength of fluoride has been very much dependent on adsorbent dose in a sample examination. Dose effect of citrus limetta over percentage removing of fluoride can be observed in Illustration No. 5.1.4.2.2. The percentage removal increased till 10 gm/L after that there was slight change thus optimum dose is 10 g/L which gave 94.3 % removal. Upto some extent removal was increased with increasing concentration of dose after the removal was constant on increasing dose concentration. This can be attributed to the covering of active sites at higher dosage, thus leading to a reduction in the net surface area (Prakasam et al., 1998).

##### **5.1.4.2.3 Effect of Dose for removal of fluoride by Ground nut shell**

Fluoride removal efficiency is strongly related to concentration of adsorbent dose in the test sample. With increasing dose of adsorbent in the sample removal of fluoride increases as shown in Fig.5.1.5.2.3. At the start, removal of fluoride increases with the increase in dose up to an extent after which slight variation in removing of fluoride is observed indicating the curve becomes flat showing no change in fluoride removal even after increasing the dose. Removal efficiency for groundnut increases from 62.8 % to 89.9 % respectively when dose varies from 2-20 g/L. Without any major change in fluoride removing efficiency when dose is varied from 12-20 g/L for groundnut shell. So the optimum value for dose is 16 g/L. Upto some extent removal was increased with increasing concentration of dose after that removal was constant on increasing dose concentration. This occurred due to the covering of functioning sites with greater dose amounts, thereby bringing down the net surface area (Prakasam et al., 1998).

#### **5.1.4.2.4 Effect of Dose for removal of fluoride by Neem leaves**

Fluoride removal efficiency is dependent on dose concentration of adsorbent. Fig.5.1.4.2.4 indicates that removal of fluoride enhanced with the increase in dose of adsorbent. Higher availability of surface and the pore volume are responsible for enhancing adsorption of solute (Mohammad and Majumder, 2014). Upto some extent, removal was increased with increasing concentration of dose and after that removal was constant on increasing dose concentration. Removal of fluoride was 85.5 % at 16 g/L dose .It occurred due to the covering of functioning sites with greater dose amounts, thereby bringing down net surface area (Prakasam et al., 1998).

#### **5.1.4.2.5 Effect of Dose for removal of fluoride by Virgin turmeric and MnO<sub>2</sub> coated turmeric**

The effect of turmeric dose on fluoride removal was studied in batch reactor. Various doses of bio sorbents were considered in present study (2, 4, 6, 8, 10, 12, 14, 16, 18 and 20 g/ L) and all other parameters kept constant. Removing efficiency of fluoride is highly related to concentration of bio sorbent dosage. With increasing doses of bio sorbent in the sample removal of fluoride increases as shown in Fig.5.1.4.2.5.

The percentage of fluoride removal increased with increasing bio sorbent dose. The rate of fluoride removal increases with increasing bio sorbent dose for turmeric based bio sorbent and increase up to 77.67 % at 12 g/L dose for MnO<sub>2</sub> coated turmeric bio sorbent. Increasing adsorbent dose after 12 g/L has no significant effect on fluoride removal for MnO<sub>2</sub> coated turmeric bio sorbent. This may be due to increase in number of active site per unit volume of solution which may lead to increase in fluoride removal (Mondal et al., 2007b). Increasing bio sorbent dose above the optimum can cause partial aggregation and overlapping of active site of bio sorbent which protects the binding site and causes reduction in efficiency of fluoride removal (Giri et al., 2013).

#### **5.1.4.2.6 Effect of Dose for removal of fluoride by Java plum seed (*Syzygiumcumini*)**

A study to evaluate the effect of adsorbent dose on fluoride removal from the synthetic solution was conducted. The dose values of adsorbent used for this study are 2, 4, 8, 10, 12, 16, and 20 g/L. The results obtained for percentage fluoride removed corresponding to the dose used are displayed in Fig.5.1.4.2.6. All other parameters were maintained constant for the purpose of this study. The results obtained show that increase in adsorbent dose from 8 g/L to 10 g/L rapidly increases the

amount of fluoride removed, reaching a maximum fluoride removal (99.41%) at an adsorbent dose of 10 g / L. As the dose increases beyond 12 g / L, it is observed that the fluoride removal approaches a steady value, thus indicating no further impact of dose increase on the fluoride removal. For an adsorbent dose of less than 8 g/L, the fluoride removal degrades further as we reduce the dose amount. Upto some extent removal was increased with increasing concentration of dose after that removal was constant on increasing dose concentration. It occurred due to covering of functioning sites with greater dose amounts, thereby bringing down the net surface area. (Prakasam et al., 1998).

#### **5.1.4.2.7 Effect of Dose for removal of fluoride by Banana peel**

Removing strength of fluoride mainly depends upon concentration of adsorbent dose amount in sampling for examination. The removing of fluoride rises when we increase dose amount of adsorbent through the sample, as demonstrated Illustration No.5.1.4.2.7. In the beginning, removing of fluoride rises with the rising dose amount till a degree, but later that in a slow manner changes in the removing of fluoride indicating, the curve gets a lapse as flat showing the greater fluoride absorption happens with highest dose amount and the removing becomes the same. Adsorbents possess a greater surface with pore volume due to which adsorption rises, and afterwards absorption of fluoride remains the same with greater dose amount caused by the saturation of pore volume and adsorbent surface. Competence of removal for banana peel increases from 70.23 to 94.95% within dosage of 2-20 g/L. It happens without any significant variations in removing strength for fluoride with the dosage of 16-20 g/L for banana peel respectively. This can be attributed to the overlapping of active sites at higher dosage, thus leading to a reduction in the net surface area (Prakasam et al., 1998).

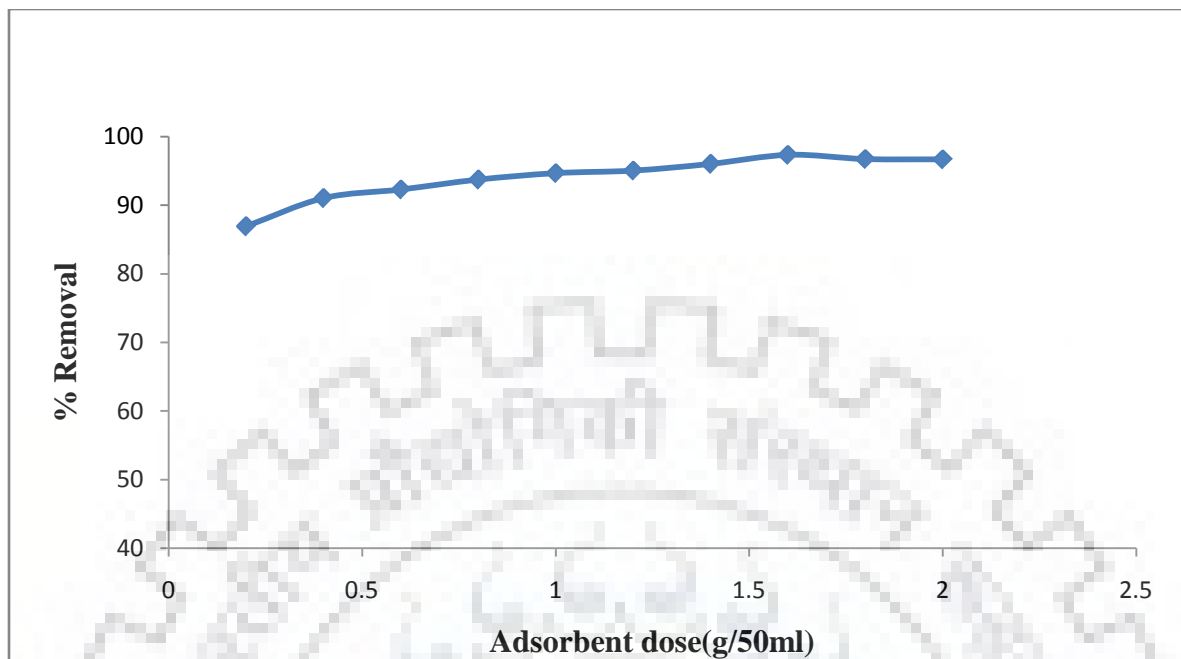


**Fig. 5.1.4.2.1** Effect of Dose for removal of fluoride by GAC

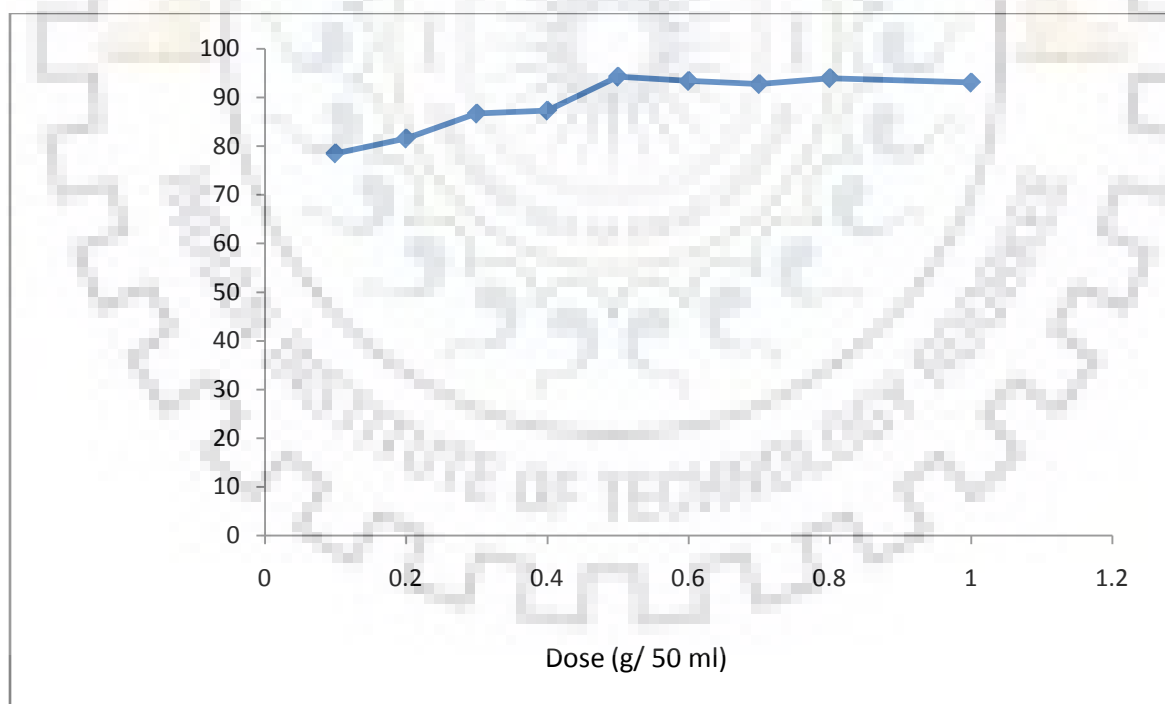


**Fig. 5.1.4.2.2** Effect of Dose for removal of fluoride by *Citrus limetta peel*

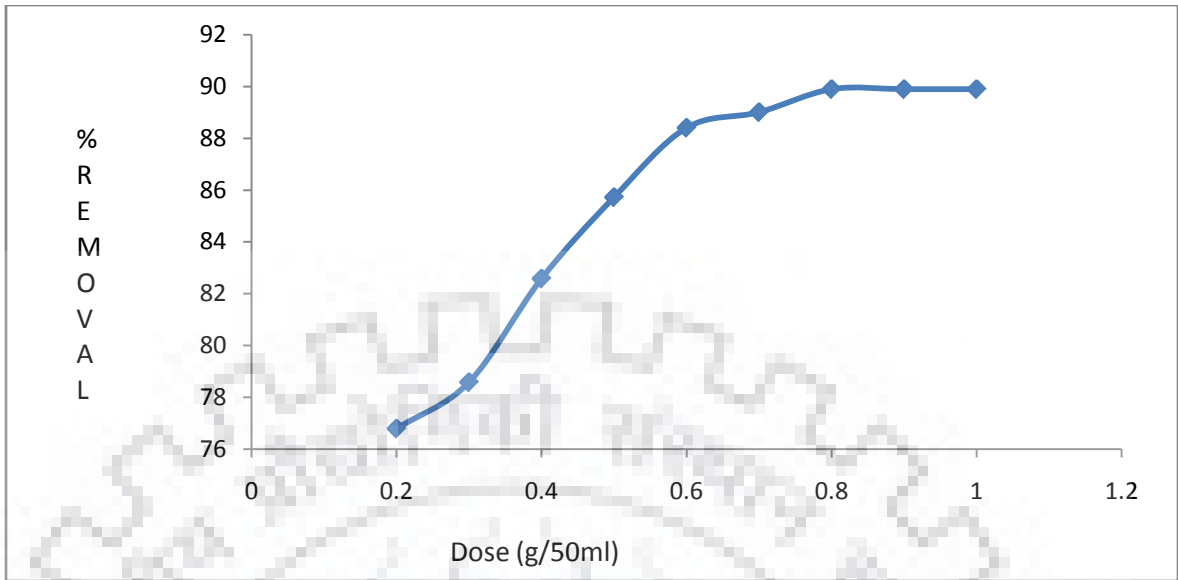


**Fig 5.1.4.2.3 Effect of Dose for removal of fluoride by Ground nut shell**

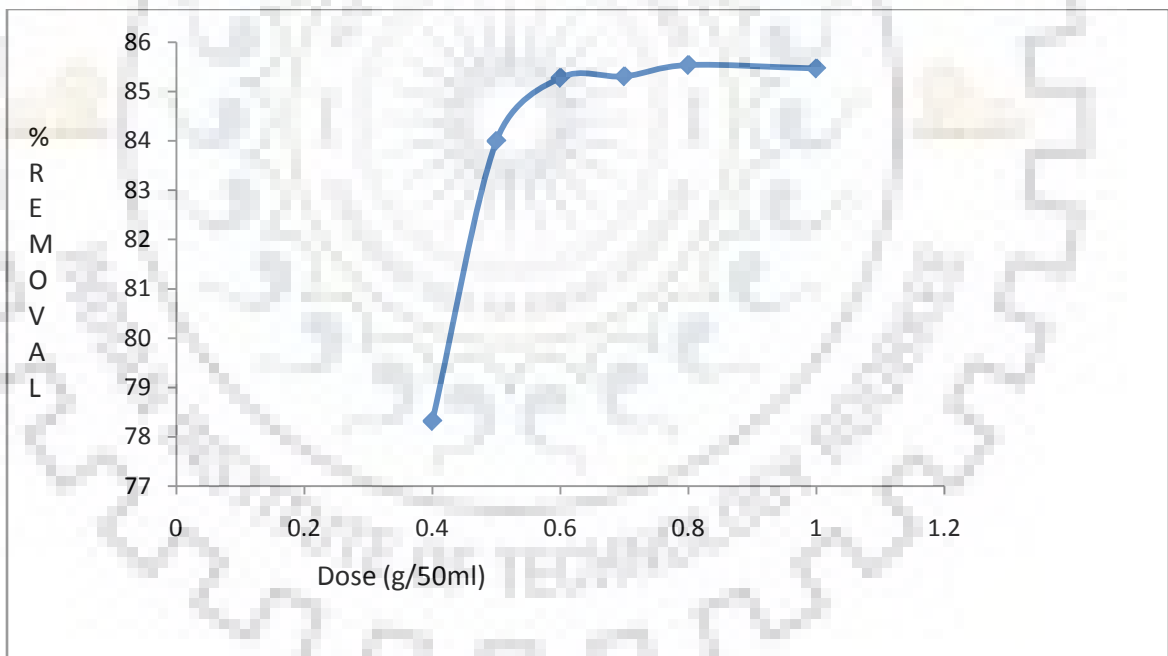


**Fig.5.1.4.2.4 Effect of Dose for removal of fluoride by Neem leaves**

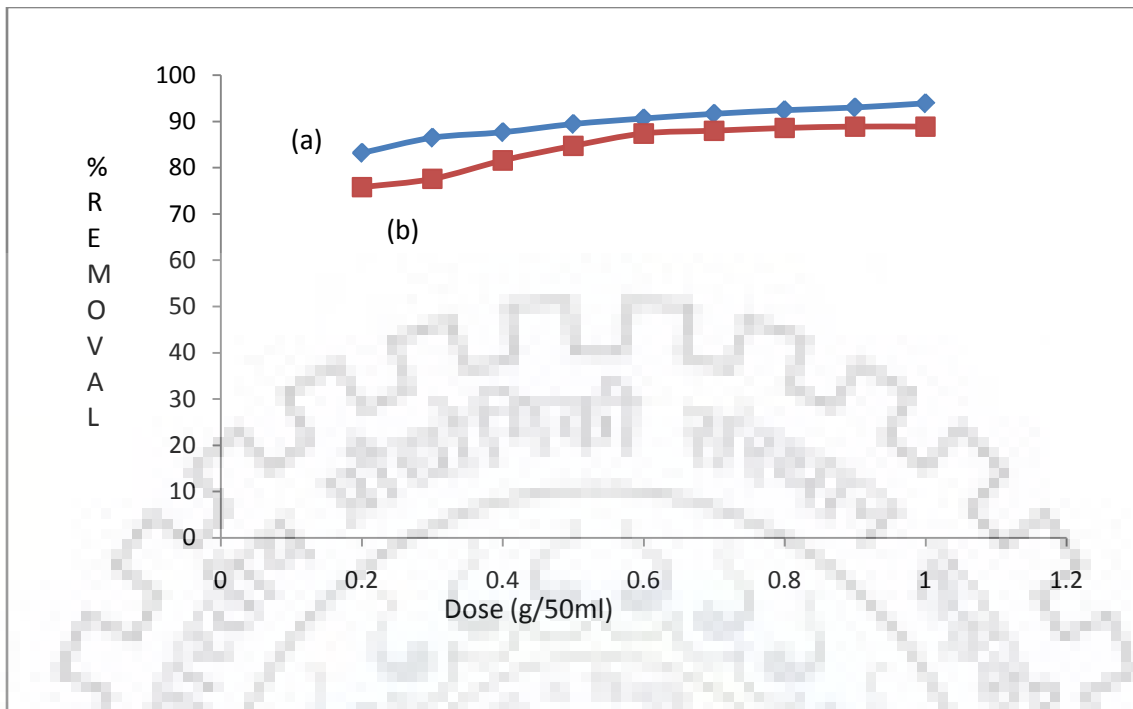


**Fig.5.1.4.2.5 Effect of Dose for removal of fluoride by (a) Virgin turmeric (b) MnO<sub>2</sub> coated turmeric**

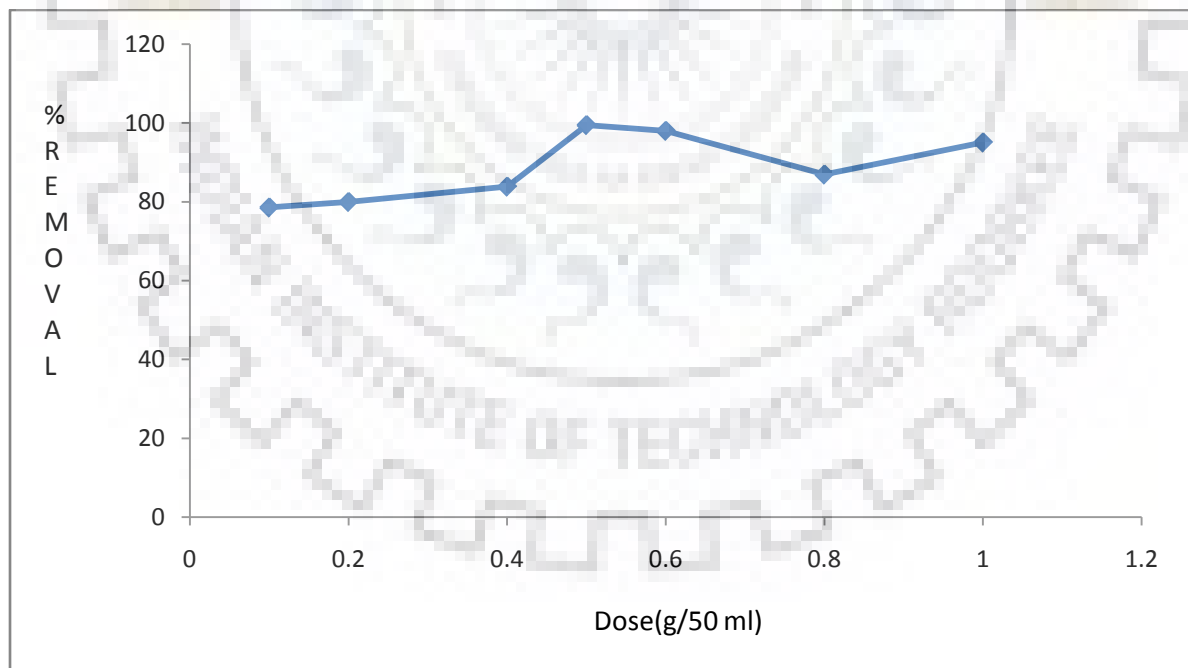


**Fig. 5.1.4.2.6 Effect of Dose for removal of fluoride by Java plum seed (Syzgiumcumini)**



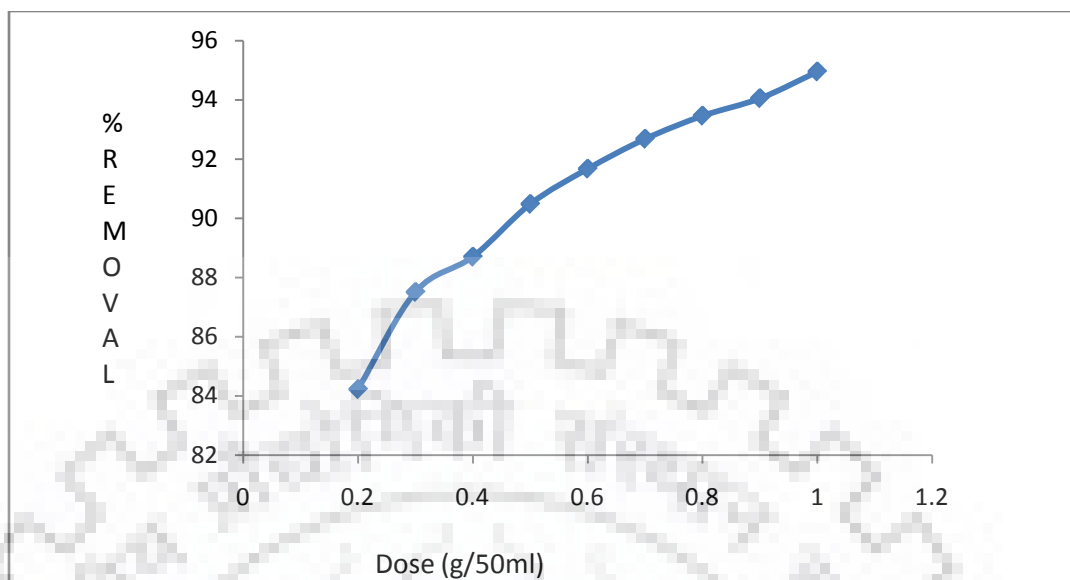


**Fig. 5.1.4.2.7 Effect of Dose for removal of fluoride by Banana peel**

### **5.1.4.3 Reaction time impact on fluoride elimination**

#### **5.1.4.3.1 Effect of Contact time for removal of fluoride by GAC**

From Fig. 5.1.4.3.1, it was found that the fluoride uptake capacity increases with the increase in contact time to some level at optimum pH and dose. Further uptake of fluoride was found constant trend due to adsorption of fluoride on surface and in to the pore of adsorbent thus less availability of active sites and surface area for further uptake of fluoride and equilibrium stage occurs (Mohammad and Majumder, 2014; Mohan et al., 2003).

#### **5.1.4.3.2 Effect of Contact time for removal of fluoride by *Citrus limetta peel***

The effect of contact time on the removal efficiency of the citrus limetta was explained by a plot between time  $t$  (min) and amount of fluoride adsorbed  $q_t$  (mg/g) as shown in Fig.5.1.4.3.2. It is observed that the exclusion of fluoride ions increases with increase in contact time to some level at optimum pH and dose. Further increase in contact time does not increase the uptake due to deposition of fluoride ions on the available adsorbent. The optimum contact time for maximum percentage removal was 40 min at which absorption capacity is 1.915.

#### **5.1.4.3.3 Effect of Contact time for removal of fluoride by Ground nut shell**

It is observed that the exclusion of fluoride ions increases with the increase in contact time to some level at optimum pH (=7) and dose (12 g/L). Further increase in contact time does not increase the

uptake due to deposition of fluoride ions on the available adsorption pore volume and surface area on bio adsorbent materials as shown in Fig.5.1.4.3.3. However, equilibrium is attained after some time of adsorption. In the current case, the equilibrium time was recorded as 75 min for groundnut shell and the equilibrium adsorption capacity was observed as 1.137. Fig.5.1.4.3.3 explains the adsorption capacity of groundnut shells at different contact times.

#### **5.1.4.3.4 Effect of Contact time for removal of fluoride by Neem leaves**

From Fig.5.1.4.3.4, it was found that the fluoride percentage removal increases with the increase in contact time to some level at optimum pH and dose. Further uptake of fluoride was found constant trend due to adsorption of fluoride on surface and in to the pore of adsorbent thus less availability of active sites and surface area for further uptake of fluoride and equilibrium stage occurs (Mohammad and Majumder, 2014; Mohan et al., 2003).

#### **5.1.4.3.5 Effect of Contact time for removal of fluoride by Virgin turmeric and MnO<sub>2</sub> coated turmeric**

The effect of contact time on fluoride removal was studied in batch reactor. In present study different contact times were considered (10, 20, 30, 40, 50, 60, 70, 80, 90 and 100 minutes) and all other parameters kept constant. Removal efficiency of fluoride is strongly related to with contact time. With increasing contact time, percentage of fluoride removal increases as shown in Fig. 5.1.4.3.5.

Fig. 5.1.4.3.5 explains the efficiency of removal of fluoride by two considered bio adsorbents (Turmeric and MnO<sub>2</sub> Coated Turmeric) at different contact times. In in this study, the equilibrium times were recorded at 60 and 75 min for MnO<sub>2</sub> coated turmeric and turmeric respectively. The initial peak portion revealed a high sorption uptake of the fluoride ions on to the adsorbent. The second stage indicated a sluggish uptake of fluoride ions that showed the usage of all active sites over the adsorbents surface and fulfilment of equilibrium saturation. The third stage indicated the saturation stage in which, the sorption uptake was comparatively less (Ramanaih et al., 2007). This is because of that, at initial stage there is a lot of bio sorbent active site accessible and gradually become saturated with fluoride ion. In this study, 93.97% fluoride ion removal at 60 min and 90% removal at 75 min were obtained for MnO<sub>2</sub> coated turmeric and turmeric respectively. Optimum contact time of 75 minutes and removal efficiency of 90.00% for arsenic by using orange peel were reported by (Kamsonlian et al., 2012a).

#### **5.1.4.3.6 Effect of Contact time for removal of fluoride by *Java plum seed (Syzgiumcumini)***

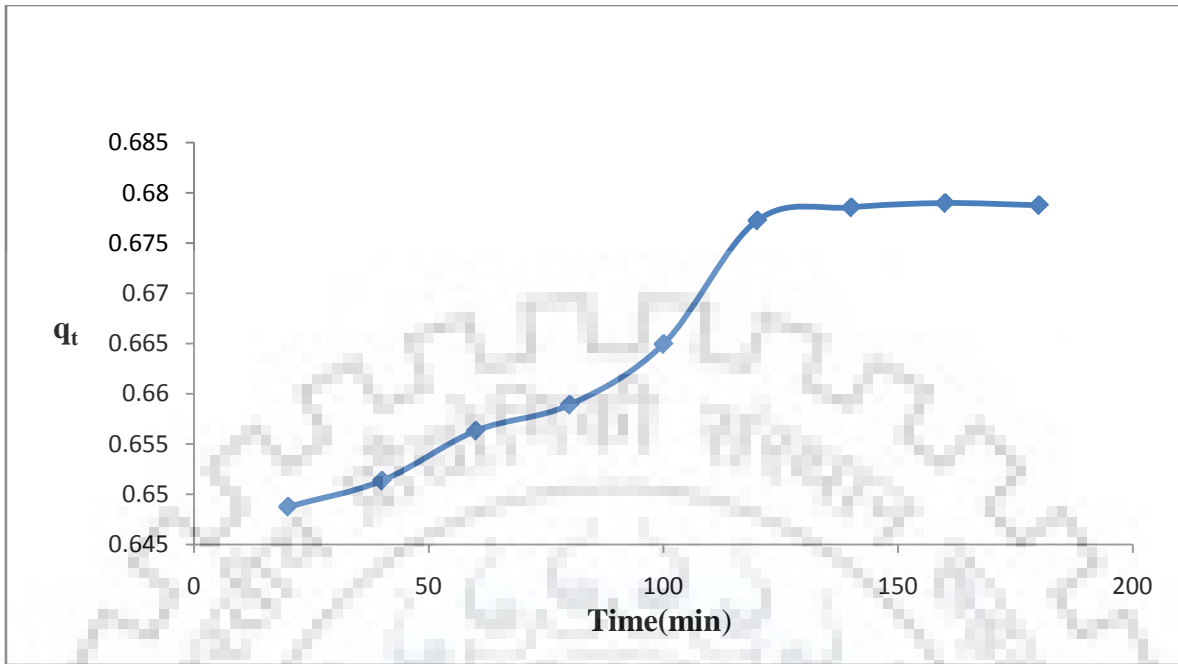
A study to evaluate the effect of contact time of adsorbent with the synthetic simulated solution on fluoride removal was conducted in a batch reactor. For this study, the time interval selected for evaluation were 5, 10, 15, 20, 25, 30, 35, 40, 50, and 60 minutes, where percentage of fluoride removal was checked. All other parameters were maintained constant for this study.

Fig.5.1.4.3.6 shows the percentage fluoride removal obtained for different contact time period. Initially, for a period of 5 minutes, a rapid rise in fluoride removal was obtained. This was followed by a period where the removal of fluoride increased in an almost linear fashion, till an equilibrium fluoride removal percentage was obtained at the 40 minutes mark, when 95.89 % of fluoride was removed. After this, the increase in contact time lead to no further significant removal of fluoride from synthetic solution because further uptake of fluoride was found constant trend due to adsorption of fluoride on surface and in to the pore of adsorbent thus less availability of active sites and surface area for further uptake of fluoride and equilibrium stage occurs (Mohammad and Majumder, 2014; Mohan et al., 2003).

#### **5.1.4.3.7 Effect of Contact time for removal of fluoride by Banana peel**

In this experiment, it was observed that the exclusion of fluoride ions increases with increase in contact time to some level at the optimum pH and dose levels. Further increase in contact time does not lead to an increase in the uptake due to deposition of fluoride ions on the available adsorption pore volume and surface area on bio adsorbent materials, as shown in Fig.5.1.4.3.7.

However, the uptake progressively approached an almost steady value, denoting establishment of equilibrium. In the current case, the equilibrium was established after 60 min for banana peel. The initial peak portion revealed the high sorption uptake of the fluoride ions on to adsorbents. The second stage revealed the sluggish uptake of fluoride ions that showed the utilization of all active sites over the adsorbents surface and establishment of saturation or equilibrium stage. The third stage indicated the equilibrium stage in which, the sorption uptake was relatively small (Mohan et al., 2003).



**Fig. 5.1.4.3.1 Effect of Contact time for removal of fluoride by GAC**

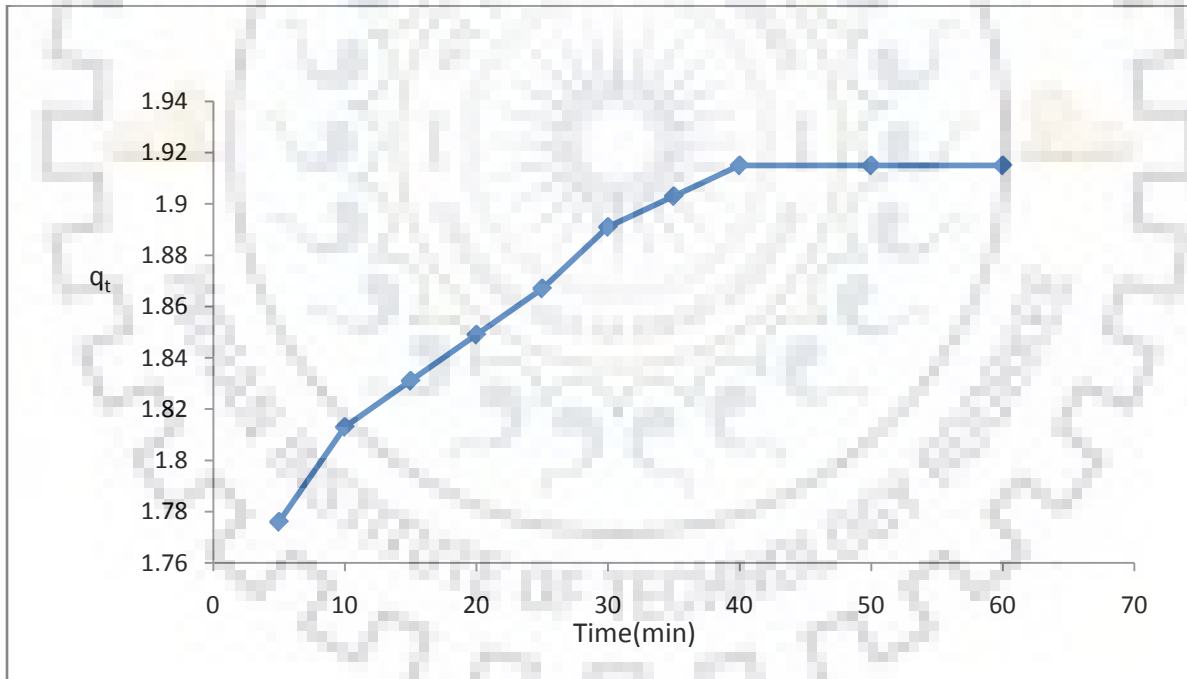


**Fig. 5.1.4.3.2 Effect of Contact time for removal of fluoride by *Citrus limetta* peel**

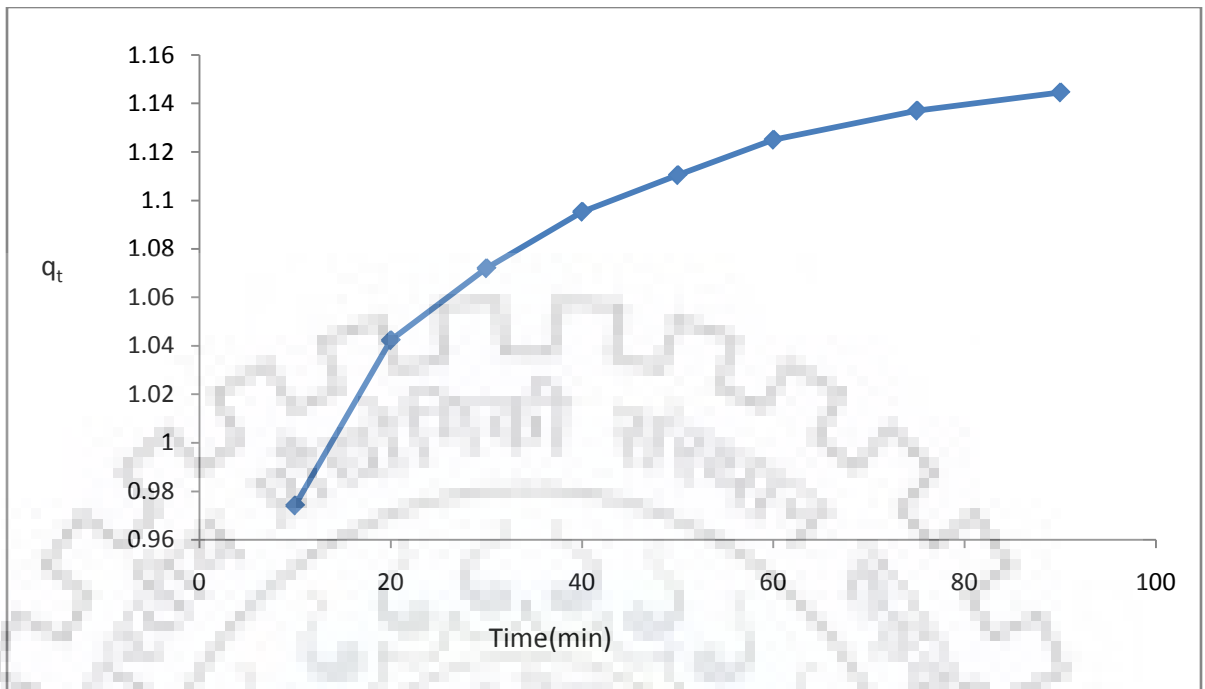


**Fig. 5.1.4.3.3 Effect of Contact time for removal of fluoride by Ground nut shell**

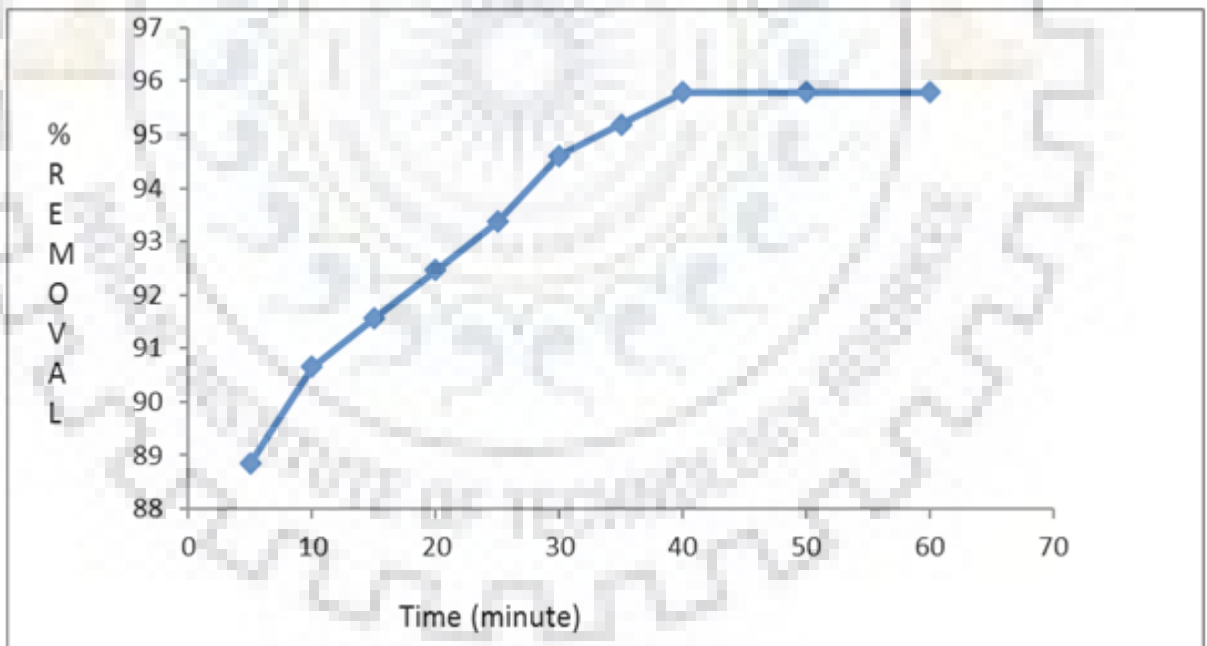


**Fig. 5.1.4.3.4 Effect of Contact time for removal of fluoride by Neem leaves**

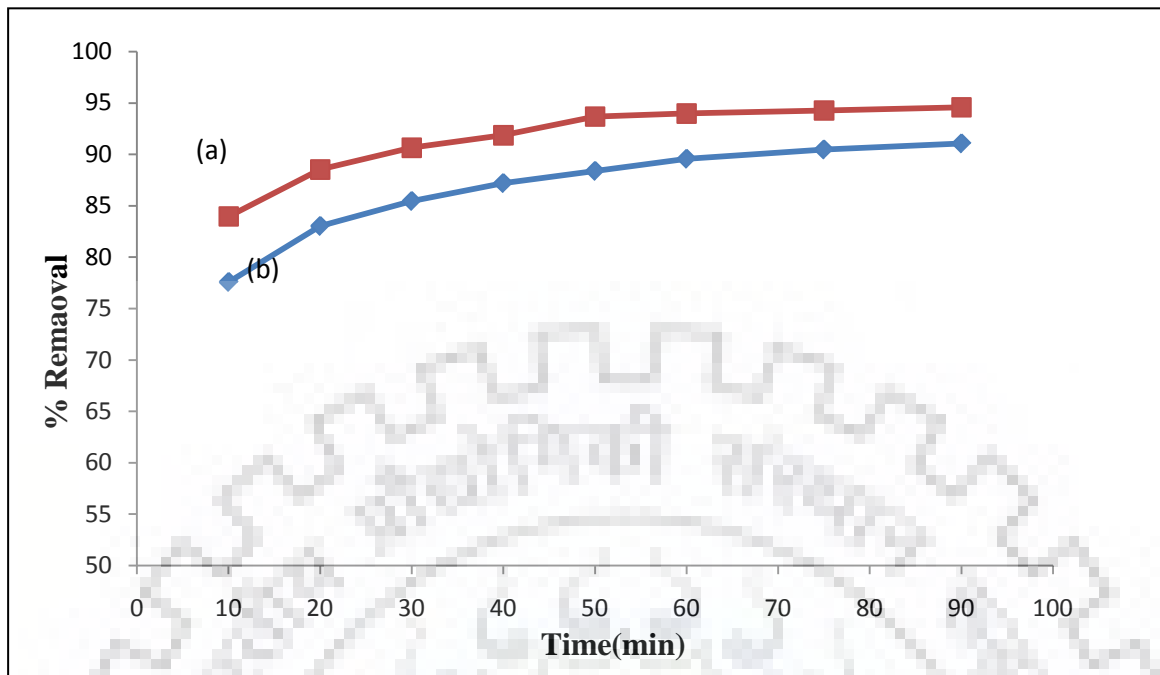


**Fig.5.1.4.3.5 Effect of Dose for removal of fluoride by  
(a)Virgin turmeric (b) MnO<sub>2</sub> coated turmeric**

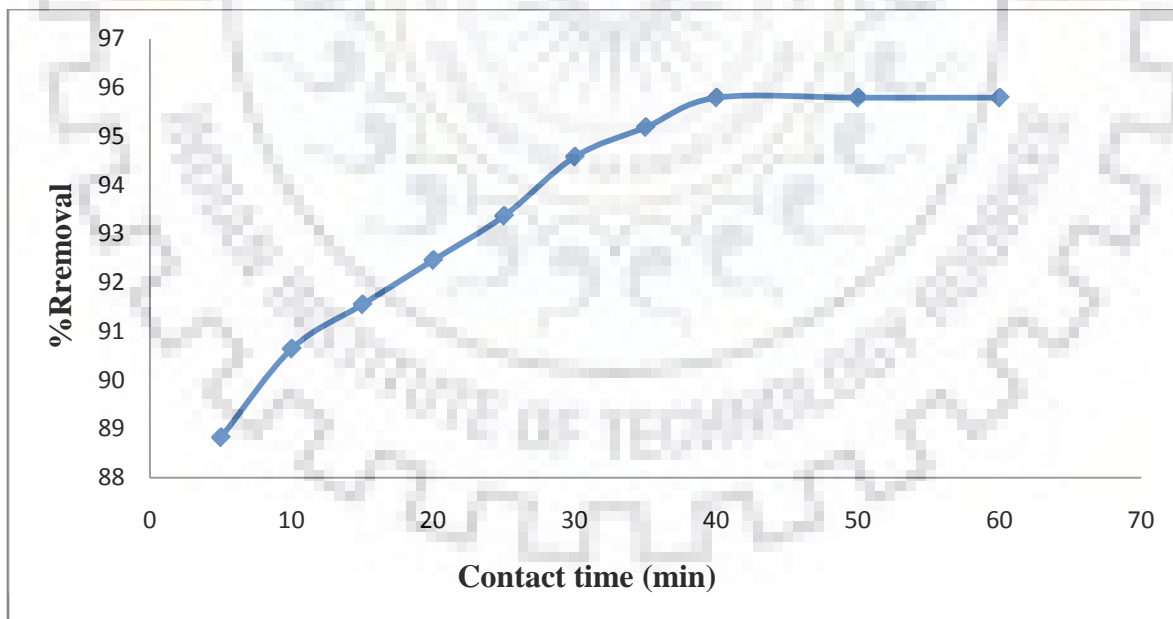


**Fig. 5.1.4.3.6 Effect of Contact time for removal of fluoride by *Java plum seed* (*Syzgiumcumini*)**

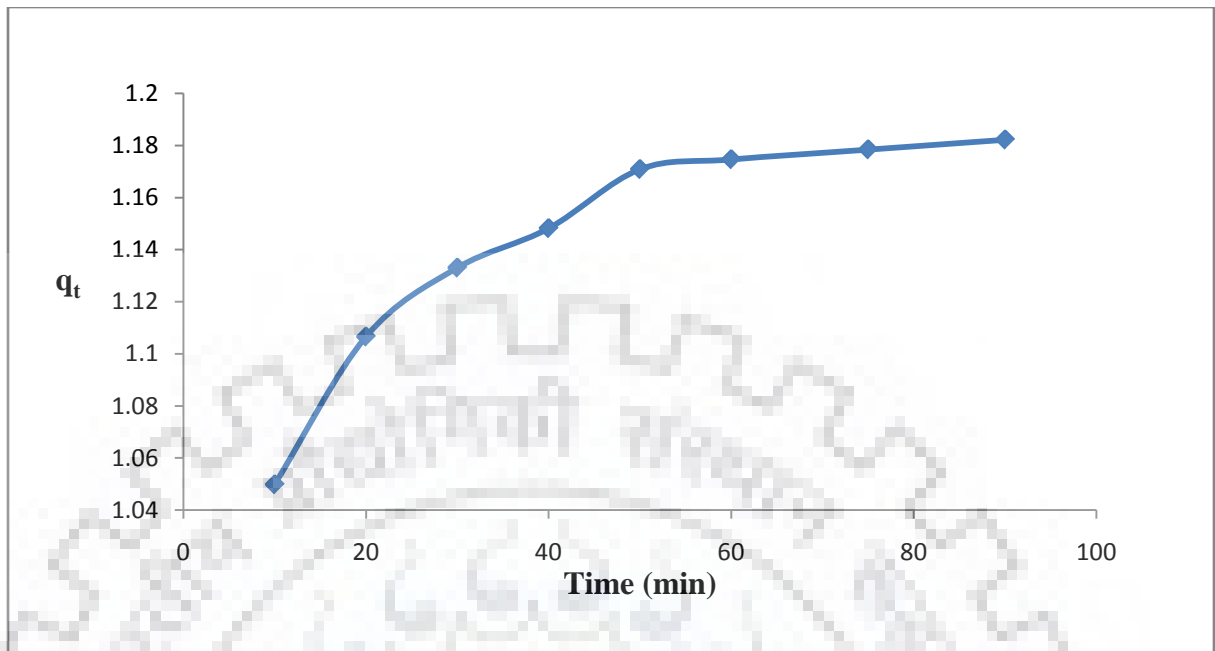


**Fig. 5.1.4.3.7 Effect of Contact time for removal of fluoride by Banana peel**

#### **5.1.4.4 Effect of initial concentration**

##### **5.1.4.4.1 Effect of initial concentration for removal of fluoride by GAC**

Effect of initial concentration feed solution of Fluoride on removal percentage is shown in Fig.5.1.4.4.1. Initial concentration was varied from 10 mg/L to 30 mg/L. Fig.5.1.4.4.1 indicated that removal percentage of fluoride was decreased on increasing initial concentration due to fixed dose of adsorbent capacity, adsorbents gets saturated at high concentration (Mohammad and Majumder, 2014; Mohan et al., 2003). Active sites and pore volume occupied with fluoride thus decreased adsorption of fluoride. Similar kind of trends previously reported in literature (Chakrabarty and Sarma, 2012; Mohan and Karthikeyan, 1997).

##### **5.1.4.4.2 Effect of initial concentration for removal of fluoride by *Citrus limetta peel***

The outcome of initial fluoride concentration was studied at their pH, contact time, and optimum dose on adsorbents on various concentrations of fluoride solutions (10, 15, 20, 25, 30 mg/L). Fig.5.1.4.4.2 shows the effect of initial fluoride concentration on the efficiency of fluoride removal. It was observed that even after increasing fluoride initial concentration there was negligible change in percentage removal, thus we can even use citrus limetta adsorbent for high fluoride concentration. Fig.5.1.4.4.1 indicates that removal percentage of fluoride was decreased on increasing initial concentration due to fixed dose of adsorbent capacity, adsorbents gets saturated at high

concentration (Mohammad and Majumder, 2014; Mohan et al., 2003). Active sites and pore volume occupied with fluoride thus decreased adsorption of fluoride. Similar kind of trends previously reported in literature (Chakrabarty and Sarma, 2012; Mohan and Karthikeyan, 1997).

#### **5.1.4.4.3 Effect of initial concentration for removal of fluoride by Ground nut shell**

The outcome of initial fluoride concentration was studied at their pH, contact time, and optimum dose on adsorbents on different concentrations of fluoride solutions (10, 15, 20, 25, 30 mg/L). Fig.5.1.4.4.3 describes the impact of initial fluoride concentration on the efficiency of fluoride removal. Removal efficiency decreases when there is increase in fluoride conc.

After the conc. of 20 g /L, removal efficiency decreases rapidly because removal percentage of fluoride was decreased on increasing initial concentration due to fixed dose of adsorbent capacity. Adsorbents gets saturated at high concentration (Mohammad and Majumder, 2014; Mohan et al., 2003). Active sites and pore volume occupied with fluoride thus decreased adsorption of fluoride. Similar kind of trends previously reported in literature (Chakrabarty and Sarma, 2012; Mohan and Karthikeyan, 1997).

#### **5.1.4.4.4 Effect of initial concentration for removal of fluoride by Neem leaves**

Effect of initial concentration of feed solution of Fluoride on removal percentage was shown in fig.5.1.4.4.4. Initial concentration varies from 5 mg/L to 25 mg/L. Fig.5.1.4.4.4 indicates that removal percentage of fluoride decreases on increasing initial concentration due to fixed dose of adsorbent capacity adsorbents gets saturated at high concentration (Mohammad and Majumder, 2014; Mohan et al., 2003). Active sites and pore volume occupied with fluoride thus decreased adsorption of fluoride. Similar kind of trends previously reported in literature (Chakrabarty and Sarma, 2012; Mohan and Karthikeyan, 1997).

#### **5.1.4.4.5 Effect of initial concentration for removal of fluoride by Virgin turmeric and MnO<sub>2</sub> coated turmeric**

The outcome of initial fluoride concentration was studied at their pH, contact time, and optimum dose on adsorbents on various concentrations of fluoride solutions (10, 15, 20, 25, 30 mg/L). Fig.5.1.4.4.5 describes the impact of initial fluoride concentration on the efficiency of fluoride removal. The results illustrated that fluoride removal potency decreased by increasing the initial fluoride concentration attributed to fixed dose of biosorbent.



Pore volume and active sites of the adsorbents are stuffed by fluoride and its removal comes down. Similar trend has been reported for removal of fluoride by using neem charcoal (Chakrabarty and Sharma, 2012).

#### **5.1.4.4.6 Effect of initial concentration for removal of fluoride by *Java plum seed (Syzgiumcumini)***

A study to evaluate the effect of initial concentration of fluoride in the synthetic solution on fluoride removal was conducted; the results obtained are shown in Fig.5.1.4.4.6. The study was conducted for initial fluoride concentrations of 10, 15, 20, 25, and 30 mg/L. It is clear that the amount of fluoride removed decreases as the fluoride concentration in the synthetic solution increases. As it can be seen from Fig.5.1.4.4.6 that the initial removal obtained was 94.9% for an initial fluoride concentration of 10 g/L, which steadily decreased as the initial concentration was increased because removal percentage of fluoride was decreased on increasing initial concentration due to fixed dose of adsorbent capacity. Adsorbents gets saturated at high concentration (Mohammad and Majumder, 2014; Mohan et al., 2003). Active sites and pore volume occupied with fluoride thus decreased adsorption of fluoride. Similar kind of trends previously reported in literature (Chakrabarty and Sarma, 2012; Mohan and Karthikeyan, 1997).

#### **5.1.4.4.7 Effect of initial concentration for removal of fluoride by Banana peel**

The outcome of initial fluoride concentration on the adsorption was studied at their optimum dose, contact time, and pH on adsorbents using different concentration of fluoride solutions (10, 15, 20, 25, 30 mg / L). Fig.5.1.4.4.7 describes the effect of initial fluoride concentration on the efficiency of fluoride removal. The results illustrated that efficiency of fluoride removal was decreased by increasing the initial fluoride concentration, as the fixed dose of adsorbent means that the capacity of adsorbents gets saturated at high concentration.

Pore volume and active sites of the adsorbents filled with fluoride finally decreased. Similar trend has been reported for fluoride removal by using Neem charcoal (Chakrabarty and Sarma, 2012), (Mohan and Karthikeyan, 1997).

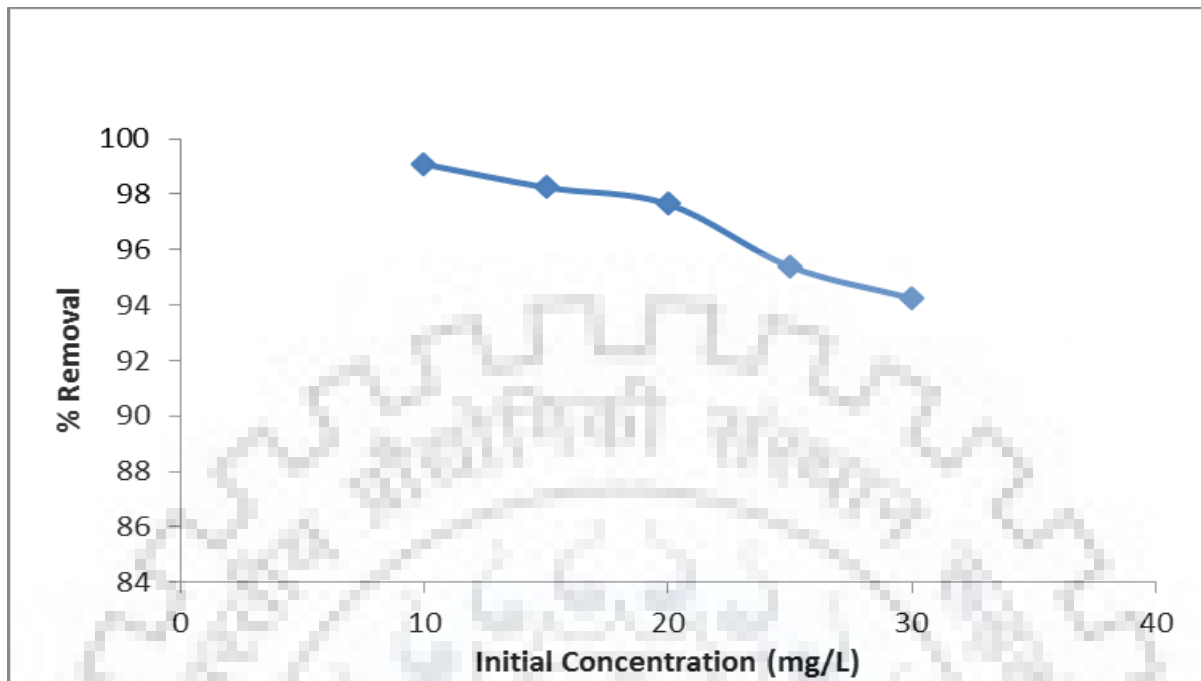


**Fig. 5.1.4.4.1 Effect of initial concentration for removal of fluoride by GAC**

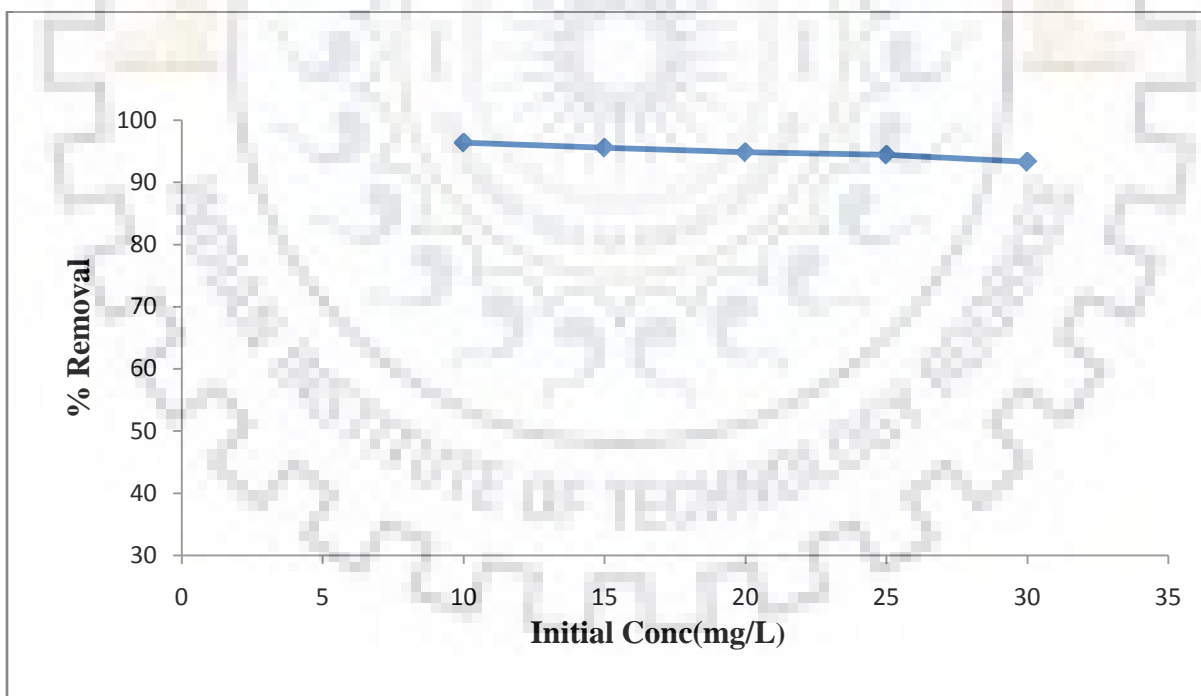


**Fig. 5.1.4.4.2 Effect of initial concentration for removal of fluoride by Citrus limetta**

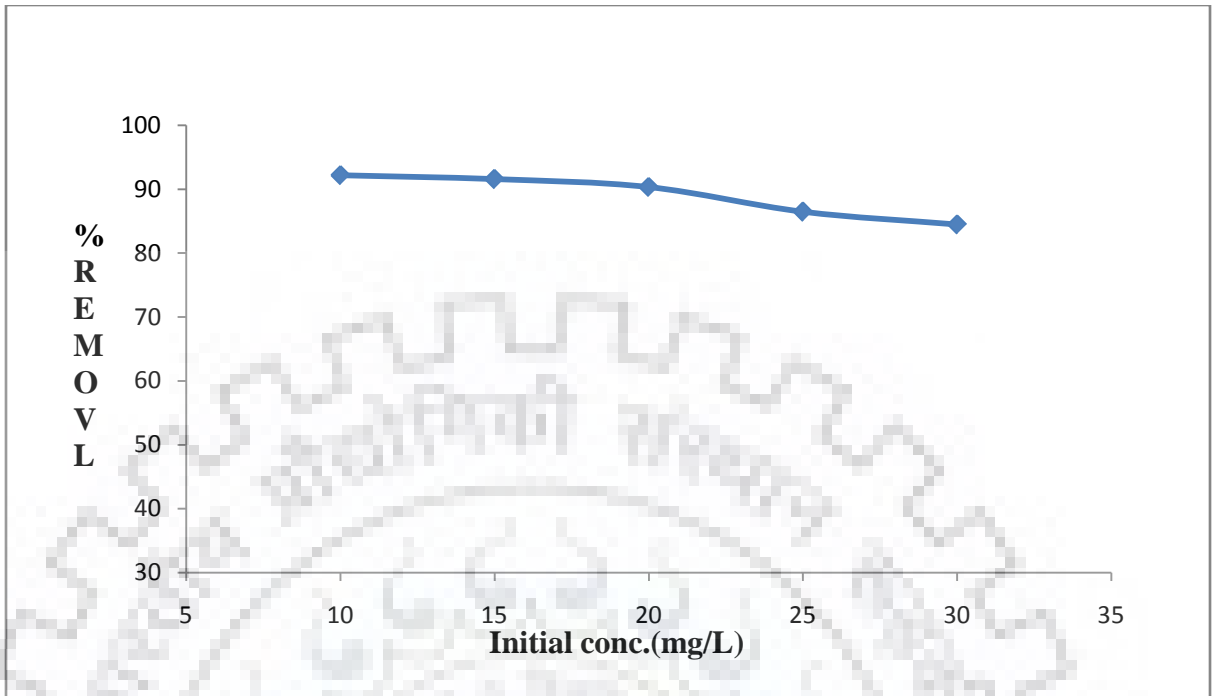


**Fig. 5.1.4.4.3 Effect of initial concentration for removal of fluoride by Ground nut shell**

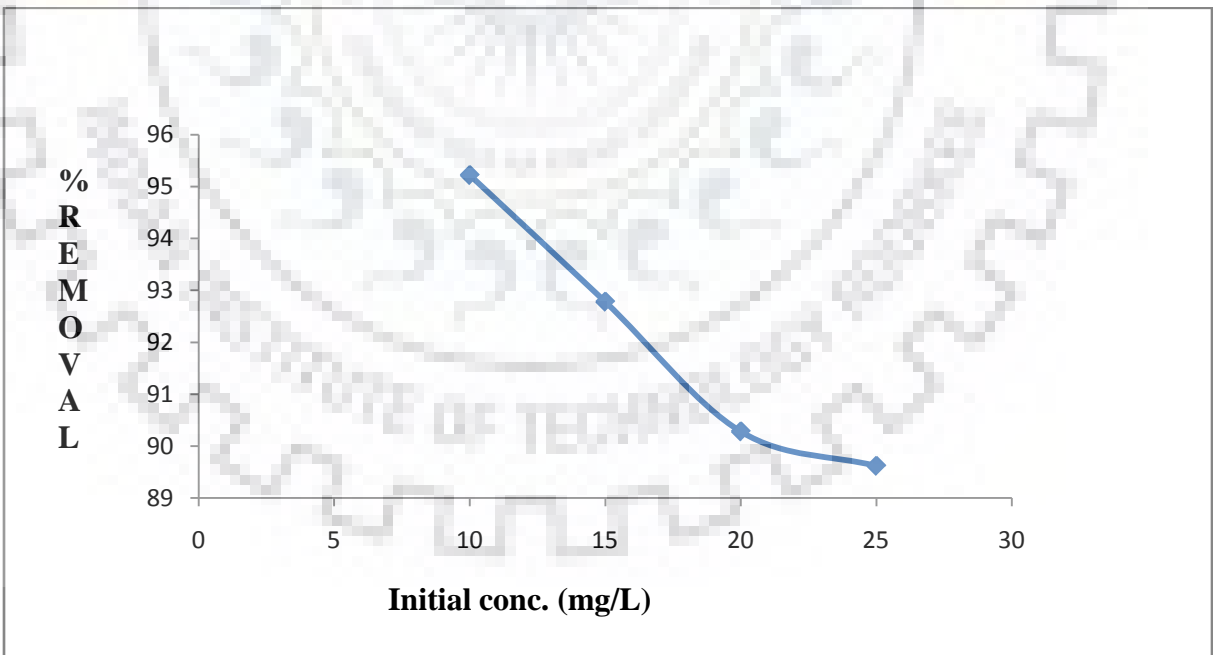


**Fig. 5.1.4.4.4 Effect of initial concentration for removal of fluoride by Neem leaves**

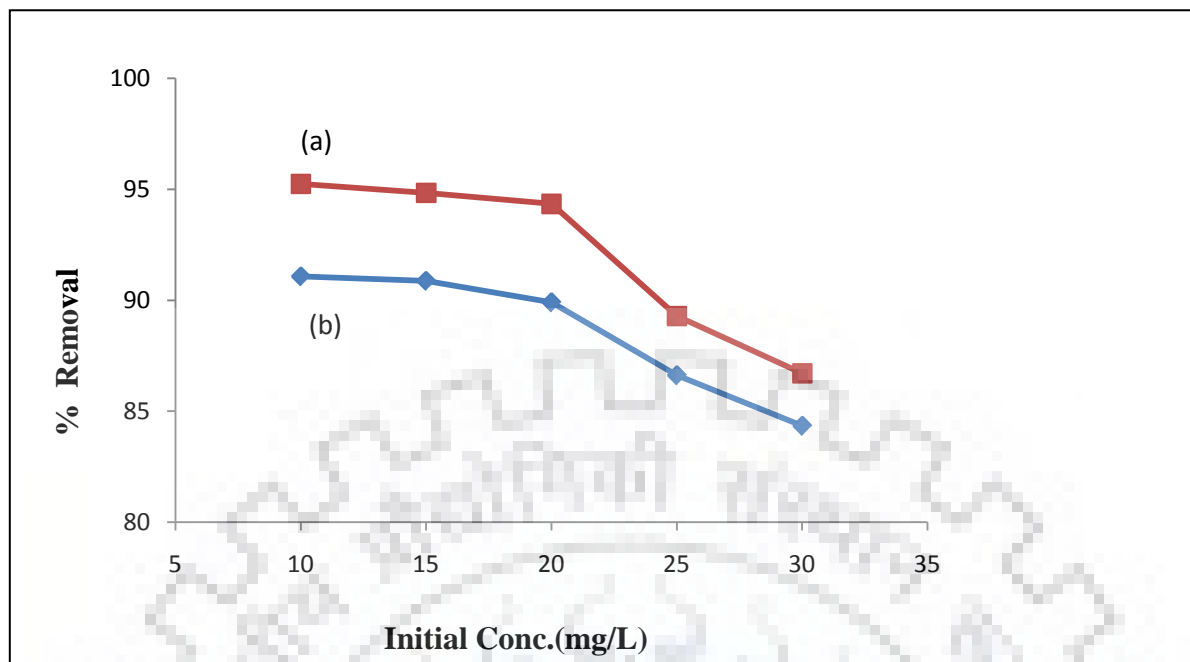


**Fig.5.1.4.4.5** Effect of initial concentration for removal of fluoride by (a) Virgin turmeric (b) MnO<sub>2</sub> coated turmeric

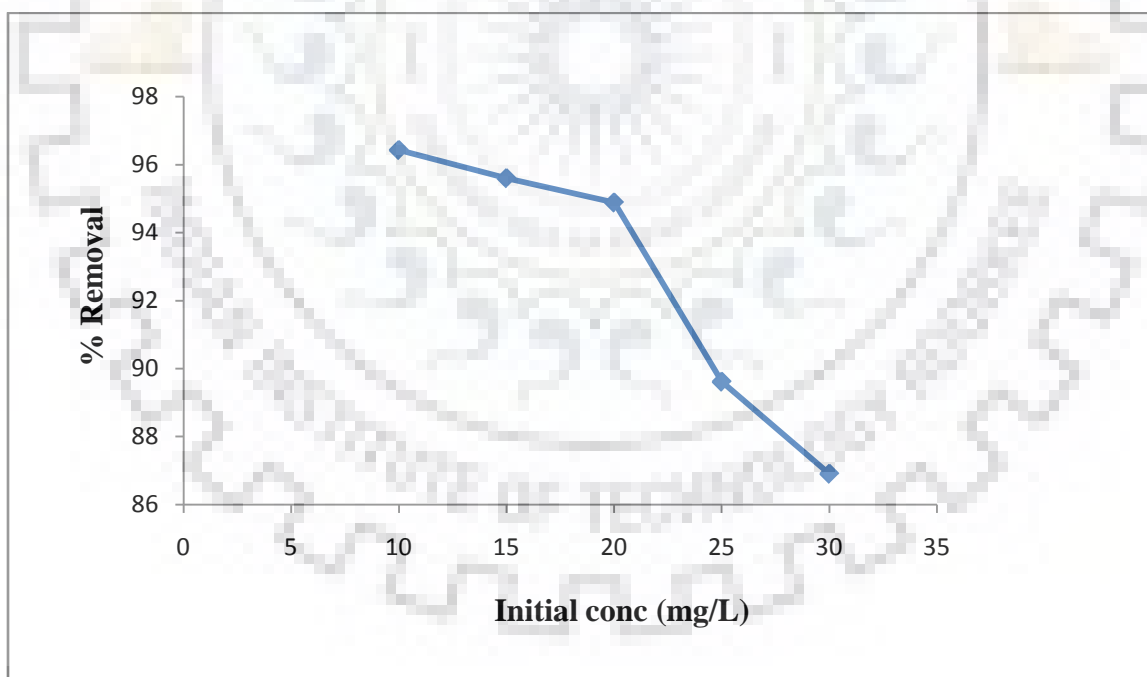


**Fig.5.1.4.4.6** Effect of initial concentration for removal of fluoride by *Java plum seed (Syzgiumcumini)*

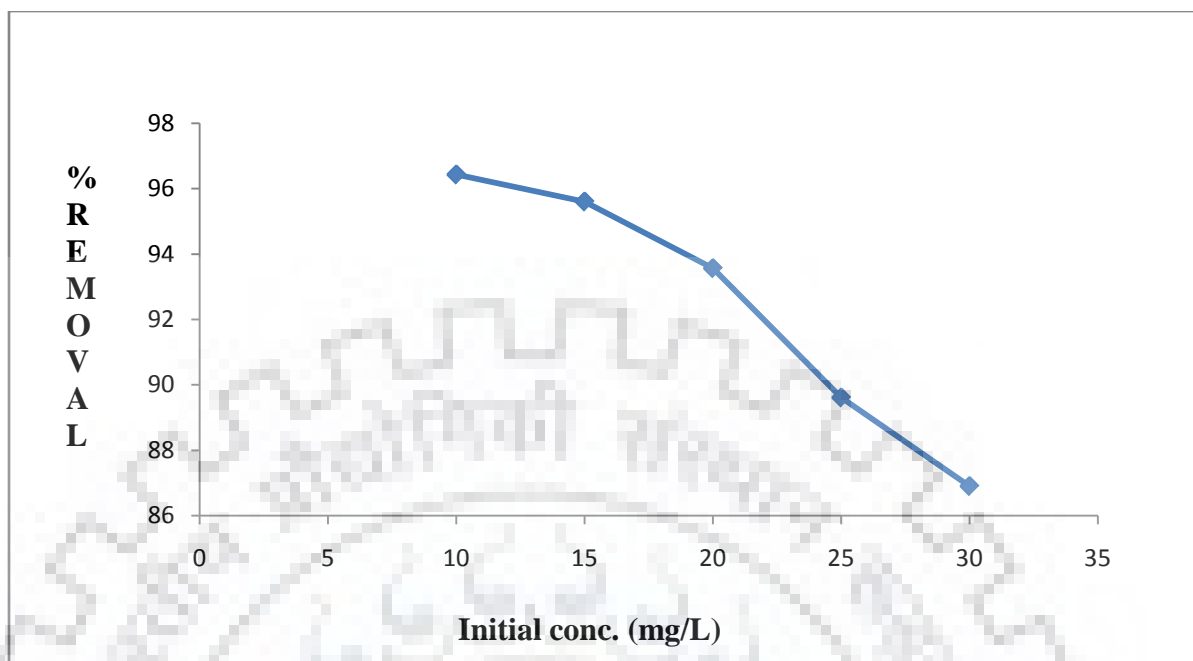


**Fig. 5.1.4.4.7 Effect of initial concentration for removal of fluoride by Banana peel**

#### **5.1.4.4.7 Concluding remark**

The effect of different parameters on removal of fluoride by adsorbents was carried out. Upto some extent fluoride removal was increased with increasing dose of adsorbents after that removal was found constant on increasing dose concentration. In contact time effect study it was found that the fluoride uptake of capacity increases with increase in contact time up to its equilibrium. The more effective removal of fluoride onto the adsorbent was found at optimum pH. Removal percentage of fluoride was decreased on increasing initial concentration due to fixed dose of adsorbent capacity adsorbents get saturated at high concentration.

#### **5.1.6 Adsorption kinetics**

The kinetic parameters for the adsorption of fluoride from a synthetic simulated waste on to the surface of various adsorbent like GAC, *Citrus limetta peel*, Ground nut shell, Neem leaves, Virgin turmeric and MnO<sub>2</sub> coated turmeric, *java plum* and Banana peel have been determined. Many kinetic models like intra particle diffusion, pseudo first order and pseudo second order were applied to the experimental data (section 2.4 and 2.5) and error function is given in section 2.15.

### 5.1.6.1 Adsorption Kinetics of fluoride removal by GAC

Adsorption kinetics provides information on the mechanism of adsorption of fluoride on GAC. Adsorption kinetic models like intra-particle diffusion, pseudo first order and pseudo second order are studied in present study. Studies of these models explain the behaviour of fluoride removal on GAC adsorbents.

**Table 5.1.6.1 Various kinetic parameters for studied models for GAC**

Adsorbent	Kinetic models								
	Pseudo First order			Pseudo Second order			Intra-particle Diffusion		
	$K_1$ ( $\text{min}^{-1}$ )	$q_{e(\text{cal})}$ ( $\text{mg/g}$ )	$R^2$	$K_2$ ( $\text{g/mg}\cdot\text{min}$ )	$q_{e(\text{cal})}$ ( $\text{mg/g}$ )	$R^2$	$K_p$ ( $\text{mg/g}\cdot\text{min}^{1/2}$ )	$X_i$	$R^2$
<b>GAC</b>	0.0253	0.09	0.88	0.62	0.688	0.99	0.004	0.627	0.92

From the Table 5.1.6.1 and Fig.5.1.6.1 (a-c), we observed that pseudo second order kinetic fits best from all kinetic models studied for GAC on the basis of maximum correlation coefficient. This gives us the information on possible mechanism of removal of fluoride due to chemisorption (Lu and Gibb, 2008). The equilibrium up take of fluoride ( $q_{e(\text{cal})}$ ) (0.688 mg/g) obtained from pseudo second order kinetics shows maximum which explains best to the model fits with experimental data.

#### 5.1.6.1.1 Concluding Remarks

Pseudo second order kinetic fits best from all kinetic models studied for GAC on the basis of maximum correlation coefficient. This gives us the information on possible mechanism of removal of fluoride due to chemisorption.

### 5.1.6.2 Adsorption Kinetics of fluoride removal by *Citrus limetta peel*

The adsorption kinetics of the fluoride removal by *Citrus limetta peel* was explained by using various kinetics models such as pseudo first-order, pseudo second-order, and Weber and Morris intra-particle diffusion model. Adsorption kinetics gives information on the mechanism of bio sorption of fluoride on Citrus Limetta based biosorbents.

**Table 5.1.6.2 Various kinetic parameters for studied models for *Citrus limetta peel***

Adsorbent	Kinetic models								
	Pseudo First order			Pseudo Second order			Intra-particle Diffusion		
	$K_1$ ( $\text{min}^{-1}$ )	$q_{e(\text{cal})}$ ( $\text{mg/g}$ )	$R^2$	$K_2$ ( $\text{g/mg.min}$ )	$q_{e(\text{cal})}$ ( $\text{mg/g}$ )	$R^2$	$K_p$ ( $\text{mg/g min}^{1/2}$ )	$X_i$	$R^2$
<i>Citrus Limetta</i>	0.059	0.205	0.92	0.63	1.94	0.99	0.027	1.7 3	0.93

From the Table 5.1.6.2 and Fig. 5.1.6.2 (a-c) for *Citrus Limetta* best fitted model observed was pseudo second order kinetics on the basis of maximum correlation coefficient. This gives us information on possible mechanism of removal of fluoride due to chemisorption (Lu and Gibb, 2008). The equilibrium up take of fluoride ( $q_{e(\text{cal})}$ ) (1.942 mg/g) obtained from pseudo second order kinetics shows maximum which best explains the model fits with experimental data.

#### 5.1.6.2.1 Concluding Remarks

Pseudo second order kinetic fits best from all kinetic models studied for *citrus limetta peel* on the basis of maximum correlation coefficient. This gives us information on possible mechanism of removal of fluoride due to chemisorption.

#### 5.1.6.3 Adsorption Kinetics of fluoride removal by Ground nut shell

Adsorption kinetics explains the change of concentration of fluoride with respect to time. Adsorption kinetics gives information on the mechanism of biosorption of fluoride on Groundnut shell bio sorbents. There are three models that are explained at optimum parameter values. The models are as follows: Pseudo first order Model, Pseudo second order Model and Intra-particle diffusion Model.

**Table 5.1.6.3 Various kinetic parameters for studied models for Ground nut shell**

Adsorbent	Kinetic models								
	Pseudo First order			Pseudo Second order			Intra-particle Diffusion		
	$K_1$ ( $\text{min}^{-1}$ )	$q_{e(\text{cal})}$ ( $\text{mg/g}$ )	$R^2$	$K_2$ ( $\text{g/mg.min}$ )	$q_{e(\text{cal})}$ ( $\text{mg/g}$ )	$R^2$	$K_p$ ( $\text{mg/gmin}^{1/2}$ )	$X_i$	$R^2$
<b>Ground nut shell</b>	0.042	0.274	0.99	0.333	1.18	0.99	0.026	0.92	0.92

From the Table 5.1.6.3 and Fig.5.1.6.3 (a-c), we observed that pseudo second order kinetic fits best from all kinetic models studied for Ground nut shell on the basis of maximum correlation coefficient. This gives us information on possible mechanism of removal of fluoride due to chemisorption (Lu and Gibb, 2008). The equilibrium up take of fluoride ( $q_{e(\text{cal})}$ ) (0.6877  $\text{mg/g}$ ) obtained from pseudo second order kinetics shows maximum which best explains the model fits with experimental data.

#### 5.1.6.3.1 Concluding Remarks

Pseudo second order kinetic fits best from all kinetic models studied for Ground nut shell on the basis of maximum correlation coefficient. This gives us information on possible mechanism of removal of fluoride due to chemisorption.

#### 5.1.6.4 Adsorption Kinetics of fluoride removal by Neem leaves

The adsorption kinetics of the fluoride removal by Neem leaves was explained by using various kinetic models such as pseudo first-order, pseudo second-order, and Weber and Morris intra-particle diffusion model. Adsorption kinetics gives information on the mechanism of bio sorption of fluoride on Neem leaves based bio sorbents.

**Table 5.1.6.4 Various kinetic parameters for studied models for Neem leaves**

Adsorbent	Kinetic models								
	Pseudo First order			Pseudo Second order			Intra-particle Diffusion		
	$K_1$ ( $\text{min}^{-1}$ )	$q_{e(\text{cal})}$ ( $\text{mg/g}$ )	$R^2$	$K_2$ ( $\text{g/mg.min}$ )	$q_{e(\text{cal})}$ ( $\text{mg/g}$ )	$R^2$	$K_p$ ( $\text{mg/g min}^{1/2}$ )	$X_i$	$R^2$
<b>Neem leaves</b>	0.0806	0.173	0.89	1.027	1.54	0.99	0.027	1.39	0.99



Table 5.1.6.4 and Fig.5.1.6.4 (a-c) shows the plots of linear form of pseudo first-order kinetic model for the three sorbents. The plots were found linear with good correlation coefficients (>0.9) indicating the applicability of pseudo first-order model in the present study. The pseudo first-order rate constant ( $k_1$ ) and  $q_{e(cal)}$  values were determined for adsorbent from the slope and the intercept of corresponding plot.

#### 5.1.6.4.1 Concluding Remarks

Pseudo second order kinetic fits best from all kinetic models studied for Neem leaves on the basis of maximum correlation coefficient. This gives us information on possible mechanism of removal of fluoride due to chemisorption.

#### 5.1.6.5 Adsorption Kinetics of fluoride removal by Virgin turmeric and MnO<sub>2</sub> coated turmeric

Adsorption kinetics gives information on the mechanism of bio sorption of fluoride on turmeric based bio sorbents. Biosorption kinetics models like intra-particle diffusion, pseudo first order and pseudo second order are studied in present study. Studies of these models explain the biosorption behaviour of fluoride removal on turmeric based bio adsorbents.

**Table 5.1.6.5 Various kinetic parameters for studied models for Virgin turmeric and MnO<sub>2</sub> coated turmeric**

Adsorbent	Kinetic models								
	Pseudo First order			Pseudo Second order			Intra-particle Diffusion		
	$K_1$ ( $\text{min}^{-1}$ )	$q_{e(cal)}$ ( $\text{mg/g}$ )	$R^2$	$K_2$ ( $\text{g/mg}\cdot\text{min}$ )	$q_{e(cal)}$ ( $\text{mg/g}$ )	$R^2$	$K_p$ ( $\text{mg/g}\cdot\text{min}^{1/2}$ )	$X_i$	$R^2$
MnO <sub>2</sub> coated turmeric	0.039	0.202	0.974	0.434	1.369	0.999	0.026	1.13 2	0.92
Turmeric based bio sorbent	0.053	0.0485	0.948	0.254	1.557	0.997	0.033	1.22 1	0.93

From the Table 5.1.6.5, we observed that pseudo second order kinetic fits best from all kinetic models studied for turmeric based and MnO<sub>2</sub> coated turmeric bio sorbent on the basis of maximum correlation coefficient. This gives us information on possible mechanism of turmeric biosorption of fluoride was chemisorption. Electron sharing/ exchange, coordination and/chelation and

complexation between flouride and turmeric based bio sorbents are rate limiting step in flouride bio sorption of turmeric (Lu and Gibb, 2008).The equilibrium up take of flouride ( $q_{e(cal)}$ ) (1.37 mg/g and 1.56 mg/g) obtained from pseudo second order kinetics shows maximum which best explains the model fits with experimental data.

#### 5.1.6.5.1 Concluding Remarks

Pseudo second order kinetic fits best from all kinetic models studied for Virgin turmeric and MnO<sub>2</sub> coated turmeric on the basis of maximum correlation coefficeint. This gives us information on possible mechanism of removal of fluoride due to chemisorption.

#### 5.1.6.6 Adsorption Kinetics of fluoride removal by *Java plum seed (Syzygiumcumini)*

The adsorption kinetics of the fluoride removal by *Java plum seed (Syzygiumcumini)* was explained by using various kinetics models such as pseudo first-order, pseudo second-order, intra-particle diffusion model. Adsorption kinetics gives information on the mechanism of biosorption of fluoride on *Java plum seed (Syzygiumcumini)* based adsorbents.

**Table 5.1.6.6 Various kinetic parameters for studied models for *Java plum seed (Syzygiumcumini)***

Adsorbent	Kinetic models								
	Pseudo First order			Pseudo Second order			Intra-particle Diffusion		
	$K_1$ (min <sup>-1</sup> )	$q_{e(cal)}$ (mg/g)	$R^2$	$K_2$ (g/mg.min)	$q_{e(cal)}$ (mg/g)	$R^2$	$K_p$ (mg/g min <sup>1/2</sup> )	$X_i$	$R^2$
<b>Java plum</b>	0.076	0.247	0.93	0.221	2.95	0.99	0.034	1.7	0.99

The studies showed that the pseudo-second order kinetic model gave the best fit, with  $R^2 = 0.99$ , for fluoride adsorption using *Java plums (Syzygium cumini)*, which suggested that the possible mechanism for the adsorption might be chemisorption based. The correlation coefficients as well as the various parameters for each model obtained were tabulated in Table 5.1.6.9

#### 5.1.6.6.1 Concluding Remarks

Pseudo second order kinetic fits best from all kinetic models studied for Java plum seed (*Syzygiumcumini*) on the basis of maximum correlation coefficeint. This gives us information on possible mechanism of removal of fluoride due to chemisorption.

### 5.1.6.7 Adsorption Kinetics of fluoride removal by Banana peel

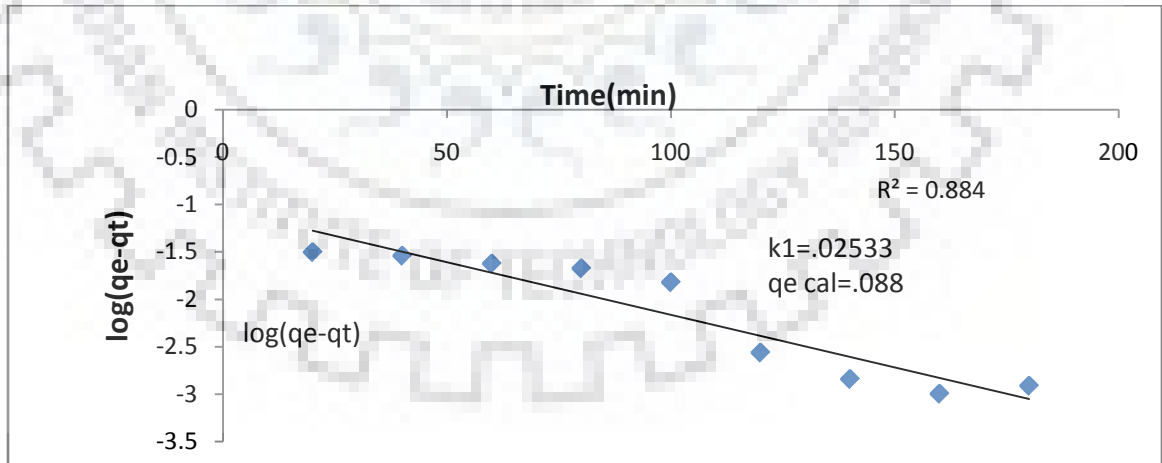
The adsorption kinetics of the fluoride removal by banana peel was explained by using various kinetics models such as pseudo first-order, pseudo second-order, and intra particle diffusion model. Adsorption kinetics gives information on the mechanism of adsorption of fluoride on banana peel based biosorbents.

**Table 5.1.6.7 Various kinetic parameters for studied models for Banana peel**

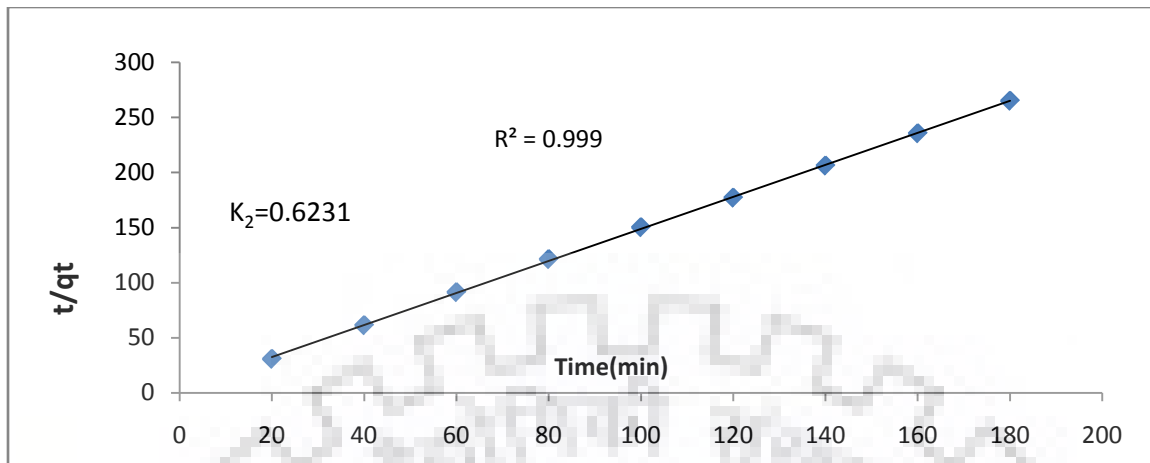
Adsorbent	Kinetic models								
	Pseudo First order			Pseudo Second order			Intra-particle Diffusion		
	$K_1$ ( $\text{min}^{-1}$ )	$q_{e(\text{cal})}$ ( $\text{mg/g}$ )	$R^2$	$K_2$ ( $\text{g/mg}\cdot\text{min}$ )	$q_{e(\text{cal})}$ ( $\text{mg/g}$ )	$R^2$	$K_p$ ( $\text{mg/g}\cdot\text{min}^{1/2}$ )	$X_i$	$R^2$
Banana peel	0.094	0.5199	0.911	0.486	1.206	1.000	0.02	1.01	0.885

#### 5.1.6.7.1 Concluding Remarks

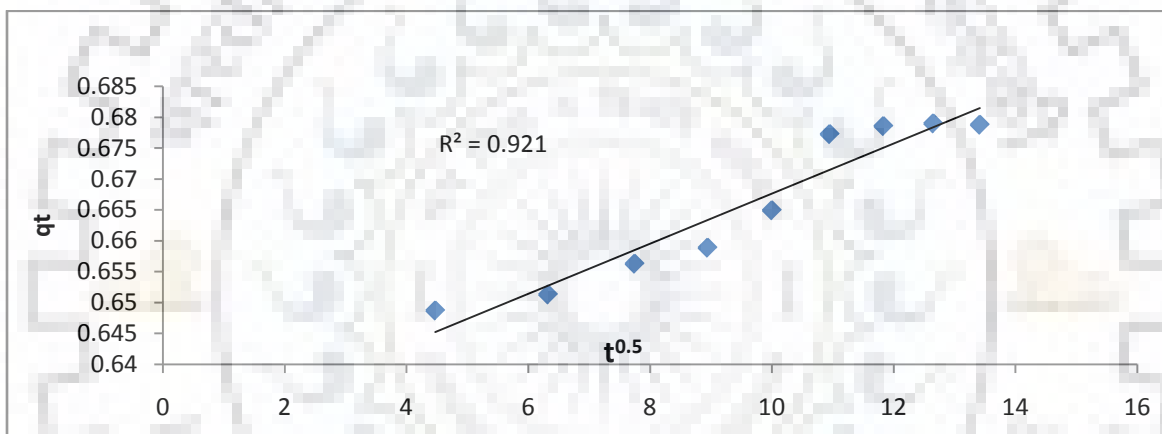
Pseudo second order kinetic fits best from all kinetic models studied for Banana peel on the basis of maximum correlation coefficient. This gives us information on possible mechanism of removal of fluoride due to chemisorption.



(a)

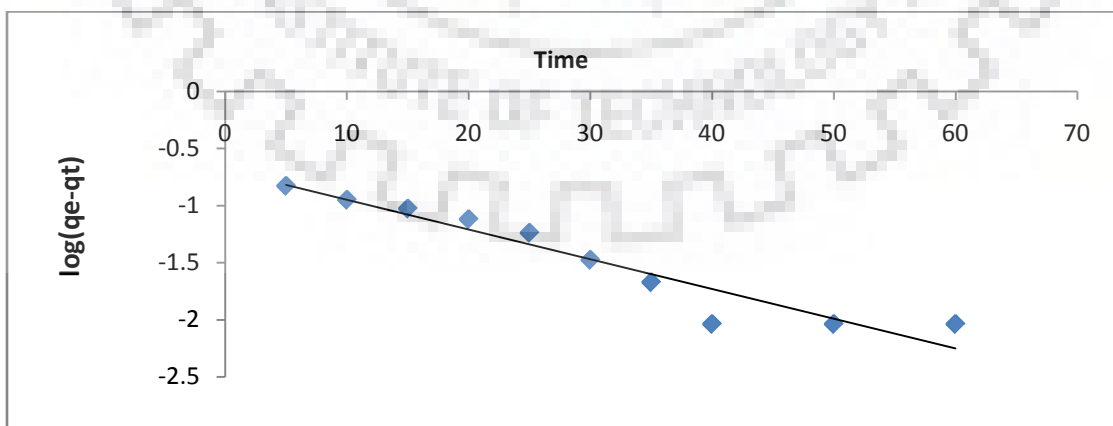


(b)

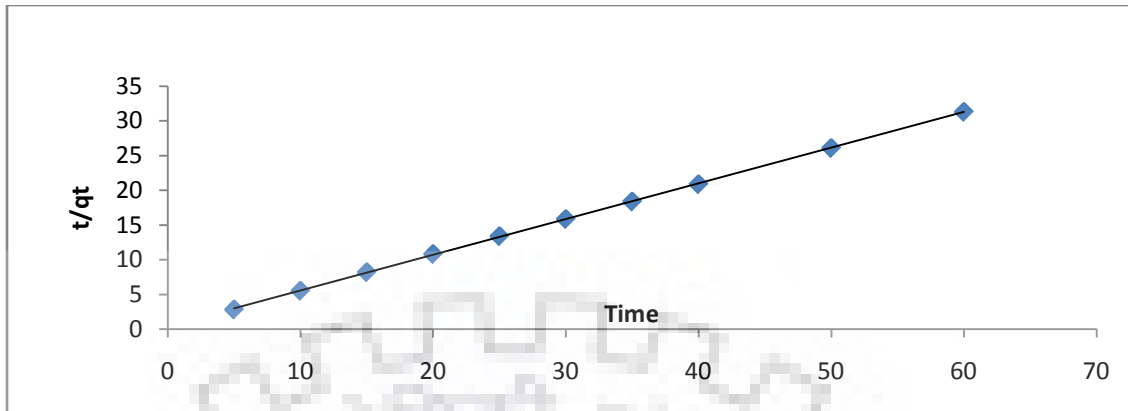


(c)

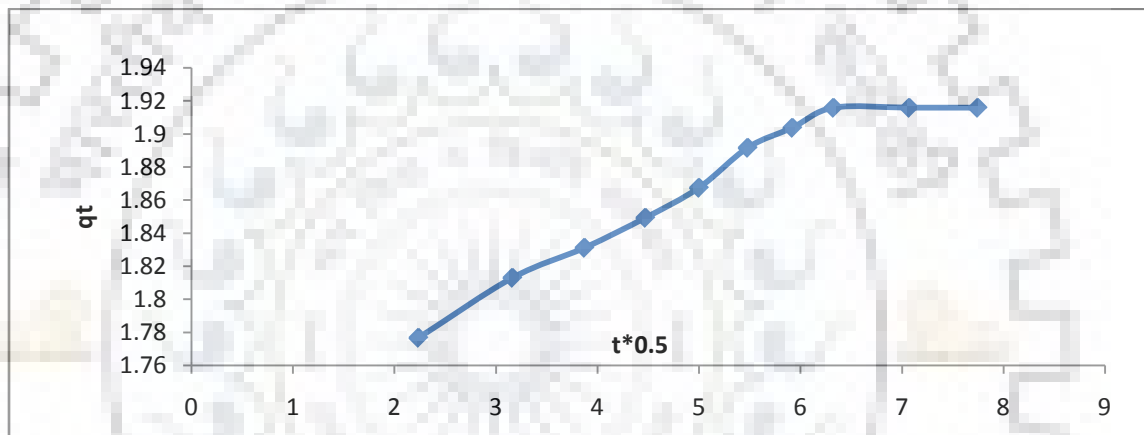
**Fig.5.1.6.1. Kinetic models for GAC (a) Pseudo-first order model (b) Pseudo-second order model and (c) Intra-particle Diffusion model**



(a)

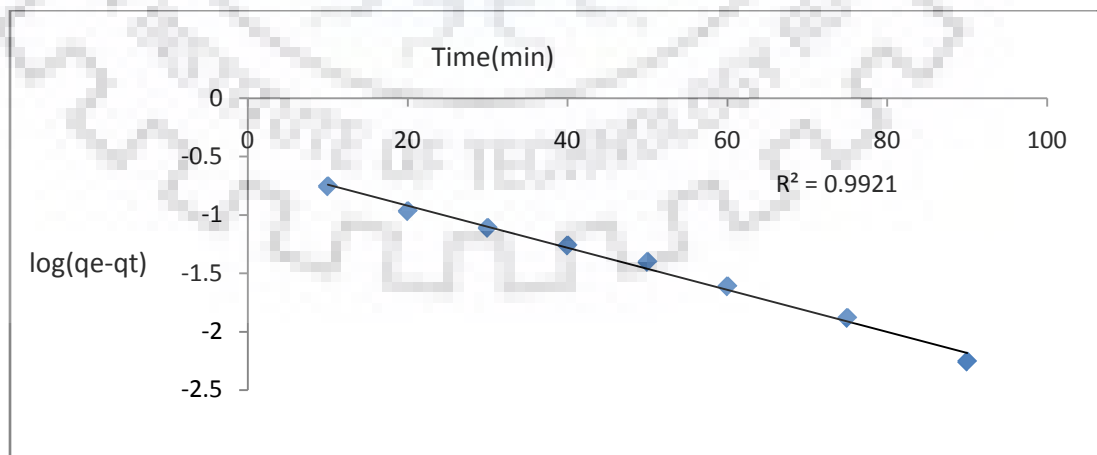


(b)

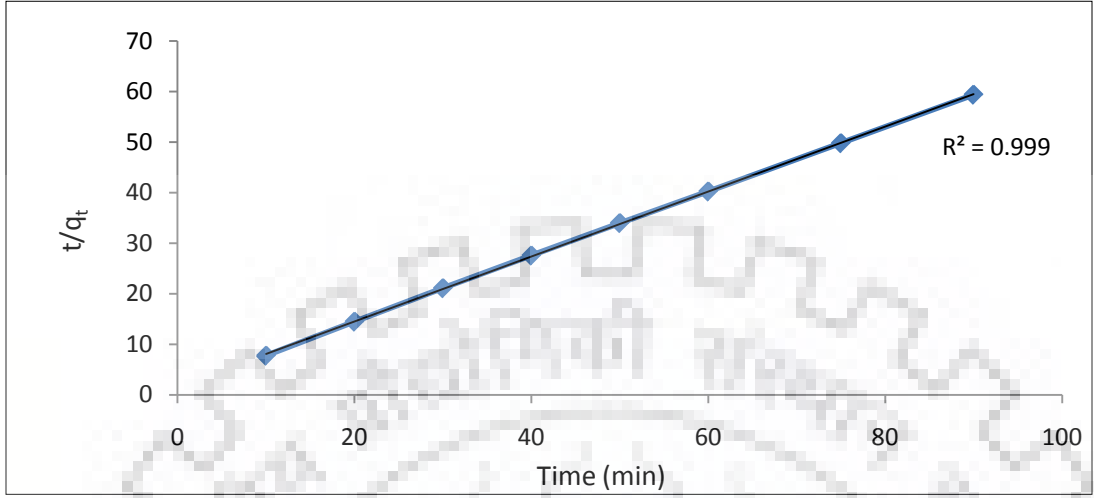


(c)

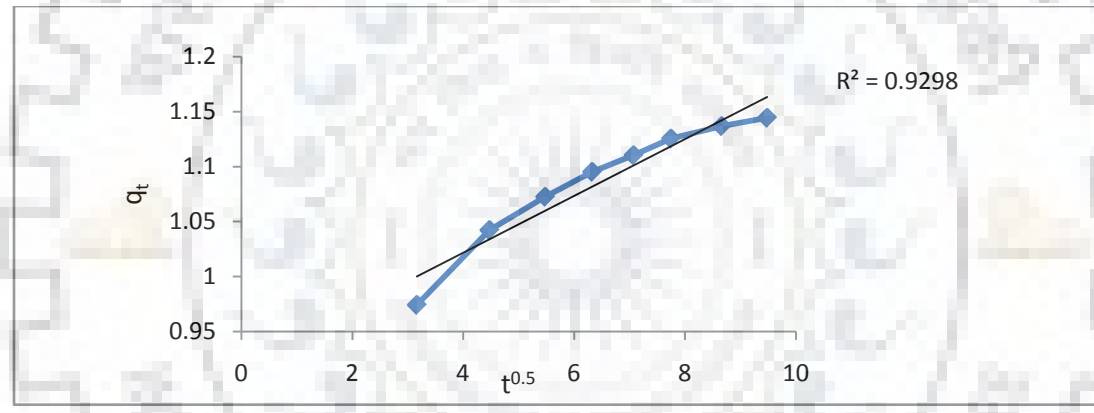
**Fig.5.1.6.2. Kinetic models for Citrus Limetta Peel (a) Pseudo-first order model (b) Pseudo-second order model and (c) Intra-particle Diffusion model**



(a)

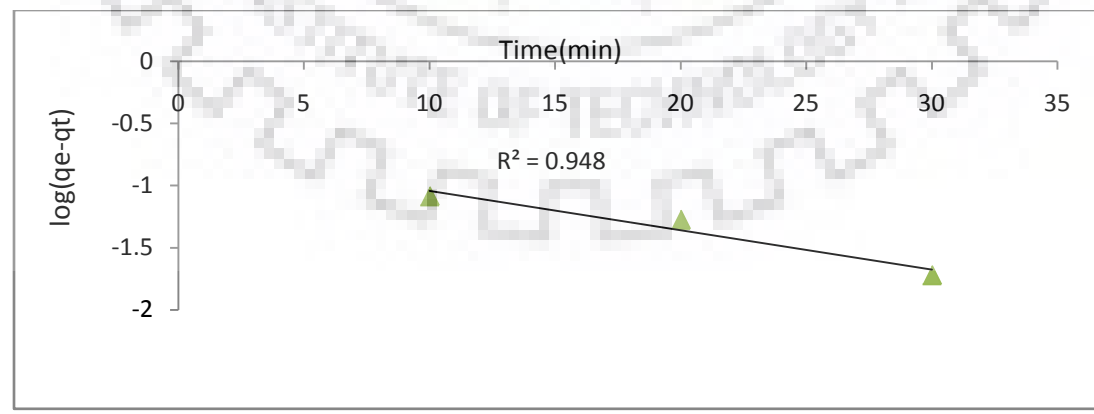


(b)

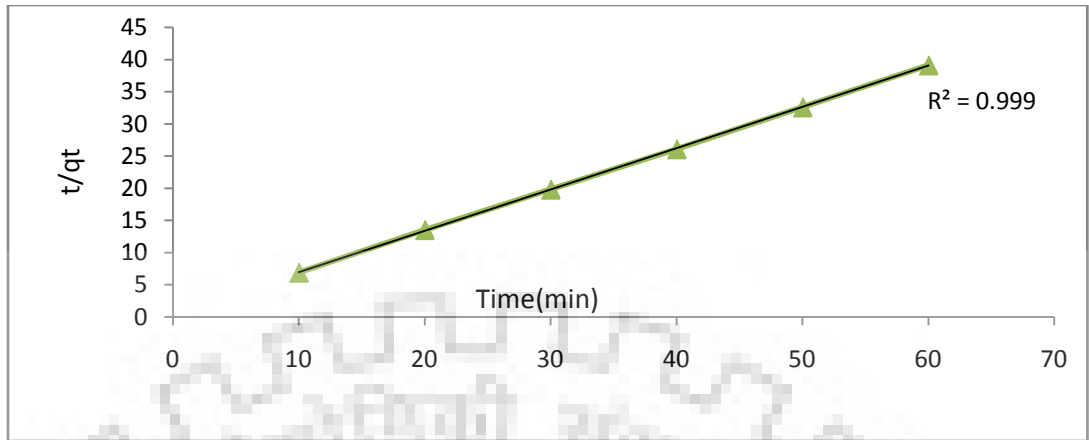


(c)

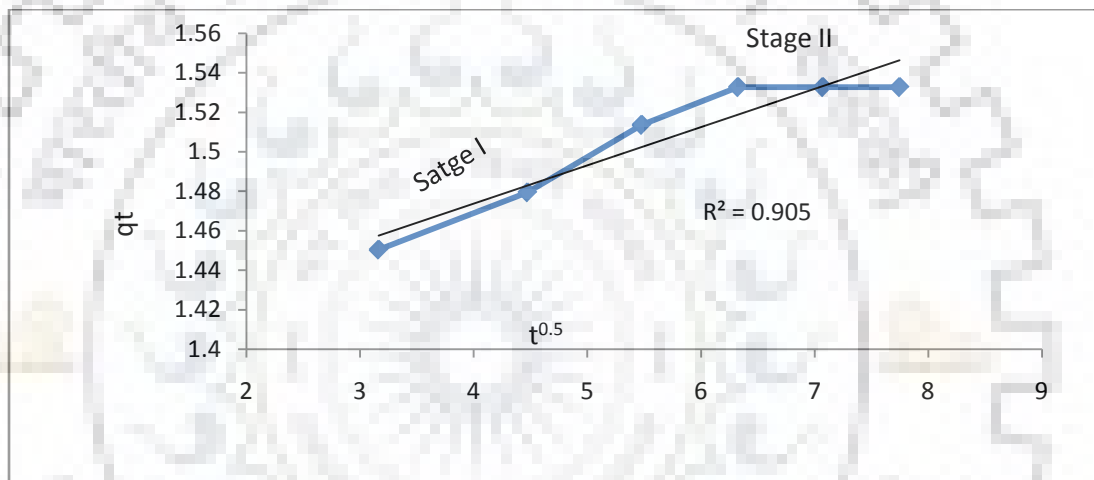
**Fig.5.1.6.3. Kinetic models for Ground nut shell (a) Pseudo-first order model (b) Pseudo-second order model and (c) Intra-particle Diffusion model**



(a)

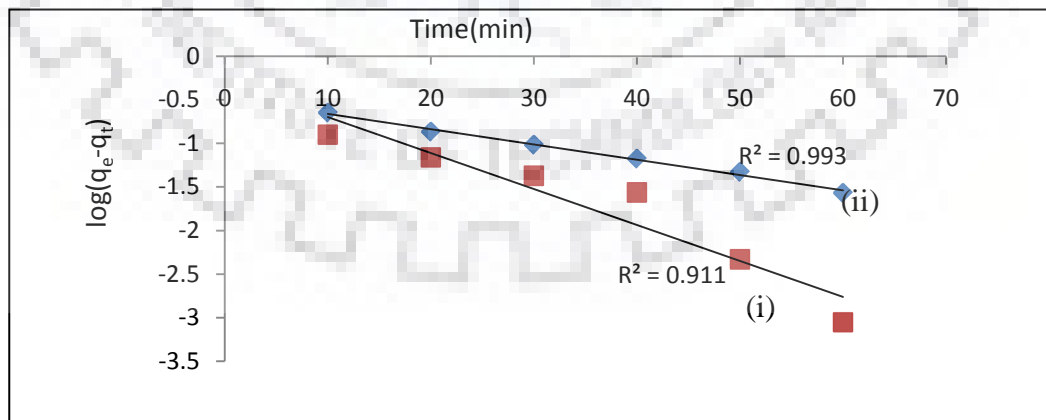


(b)

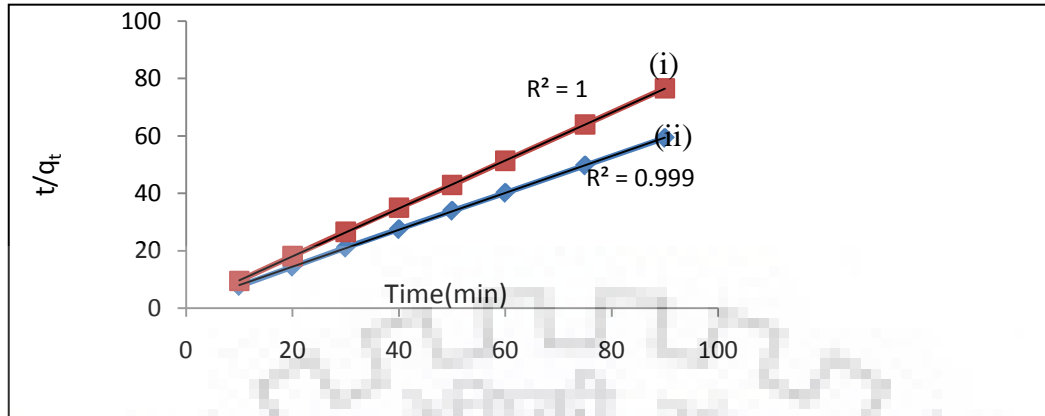


(c)

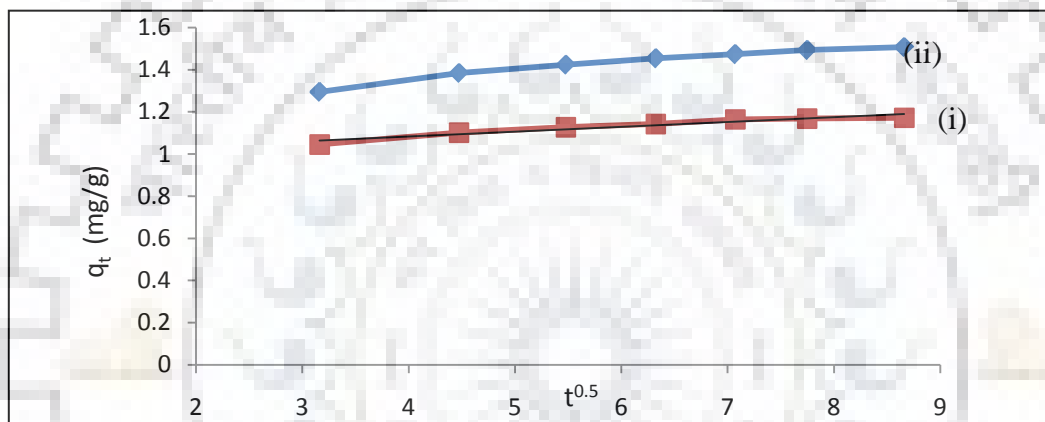
**Fig.5.1.6.4. Kinetic models for Neem leaves (a) Pseudo-first order model (b) Pseudo-second order model and (c) Intra-particle Diffusion model**



(a)

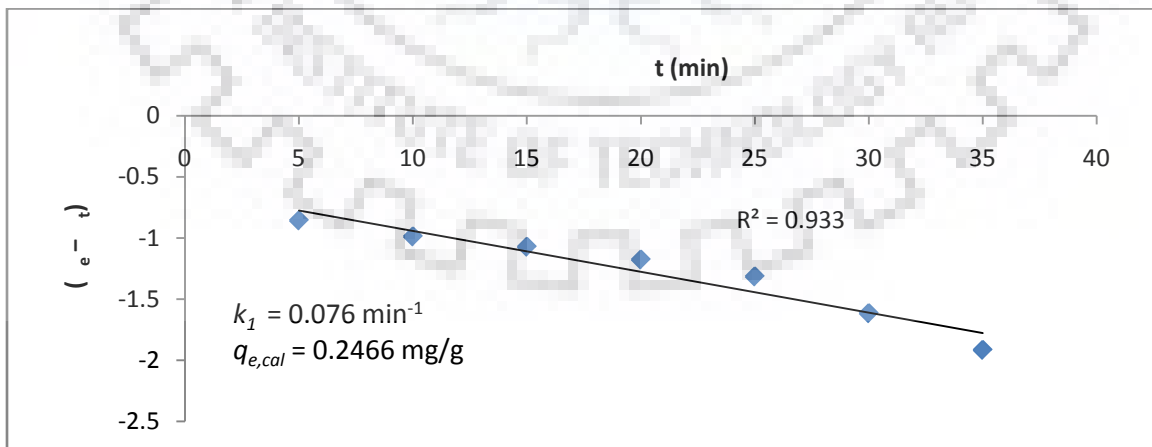


(b)



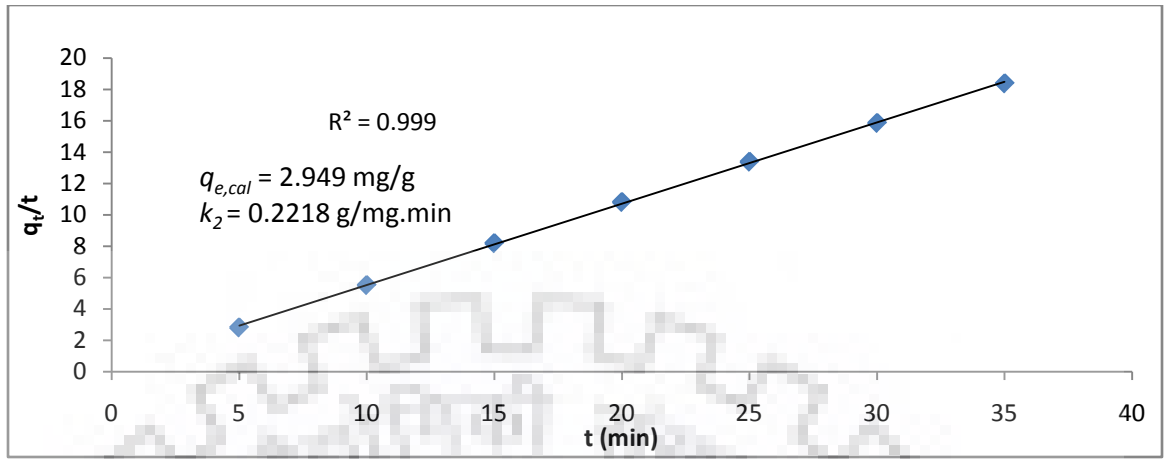
(c)

**Fig.5.1.6.5. Kinetic models for Virgin turmeric and (ii)  $MnO_2$  coated turmeric (a) Pseudo-first order model (b) Pseudo-second order model and (c) Intra-particle Diffusion model**

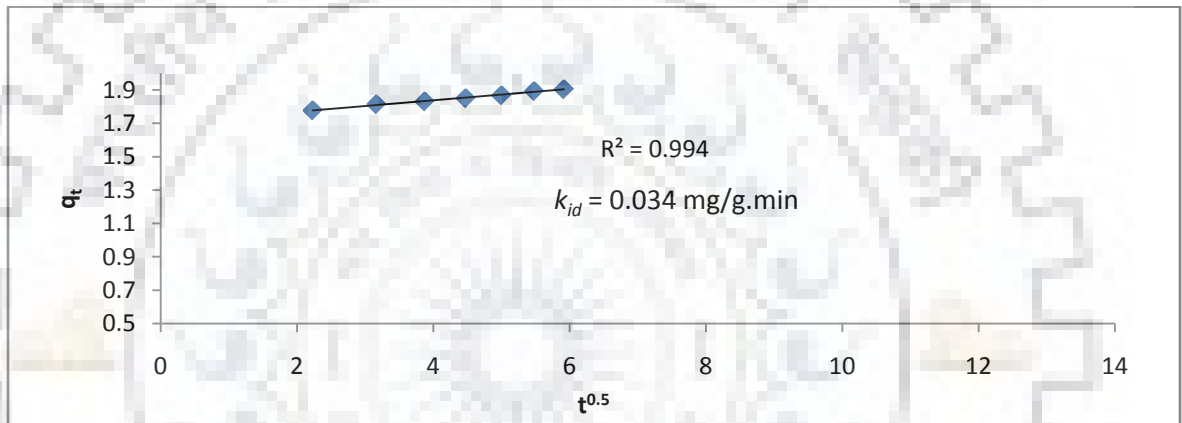


(a)



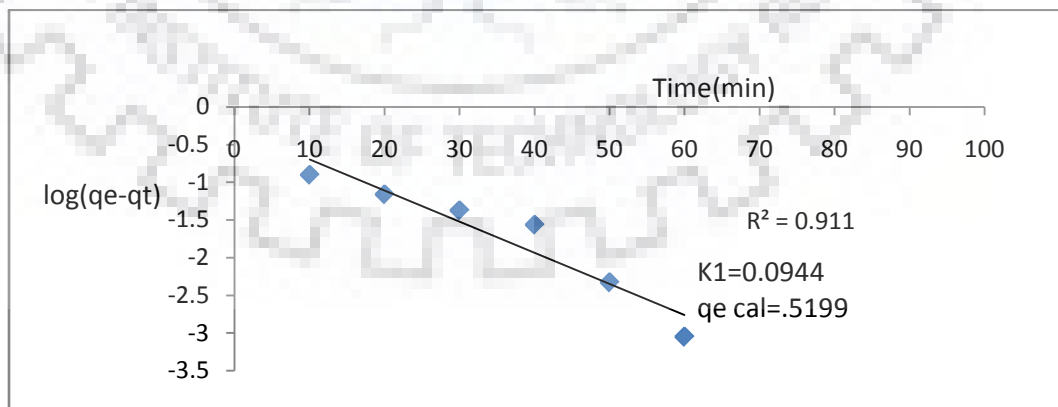


(b)

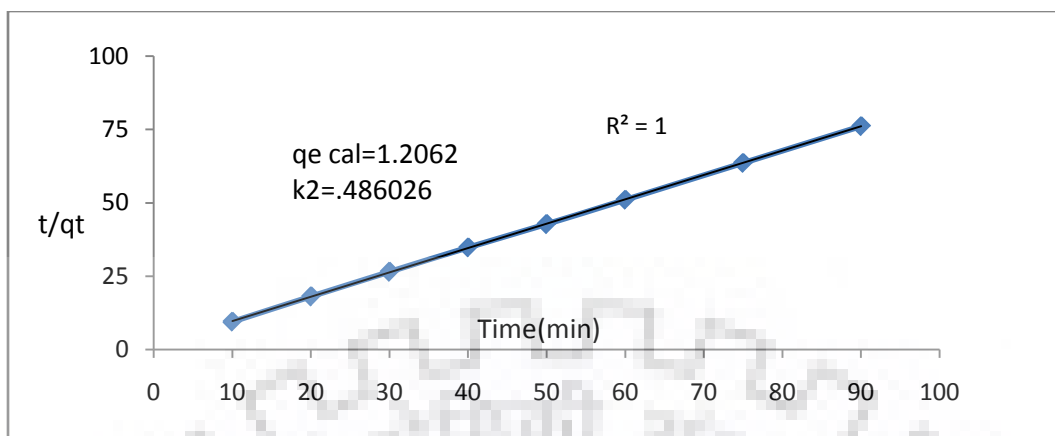


(c)

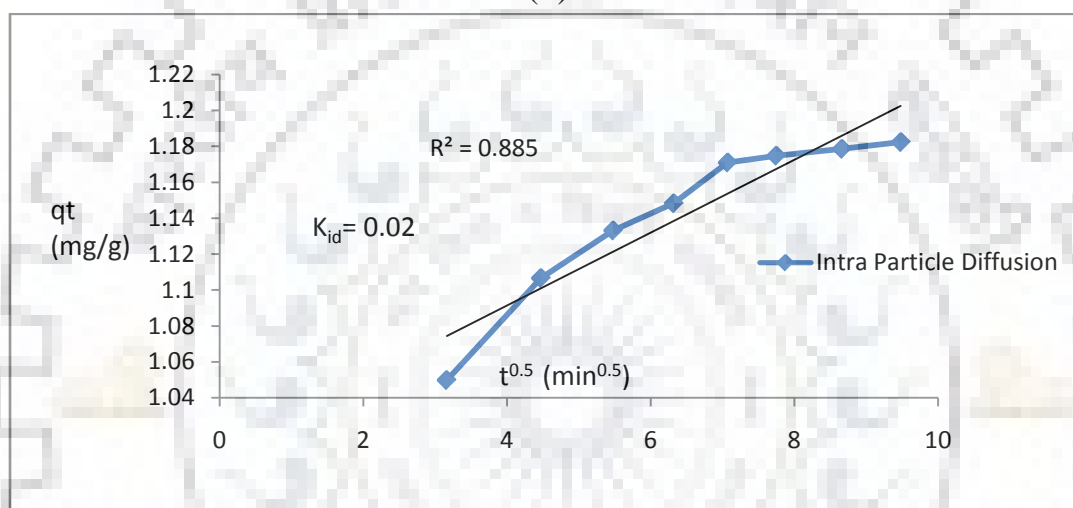
**Fig.5.1.6.6. Kinetic models for *Java plum seed (Syzgiumcumini)*(a) Pseudo-first order model (b) Pseudo-second order model and (c) Intra-particle Diffusion model**



(a)



(b)



(c)

**Fig.5.1.6.7. Kinetic models for Banana peel (a) Pseudo-first order model (b) Pseudo-second order model and (c) Intra-particle Diffusion model**

### 5.1.6.8 Concluding Remark

Pseudo second order kinetic fits best from all kinetic models studied for all adsorbents on the basis of maximum correlation coefficient.

**Table 5.1.6.8: Summary of Kinetics model parameters for removal of Fluoride from Simulated Synthetic Waste Water**

Type of adsorbent	Pseudo first order model			Pseudo second order model			Intra particle diffusion		Expt. $q_e$ (mg/g)
	Calculated $q_e$ (mg/g)	$K_1$ (min <sup>-1</sup> )	$R^2$	Calculated $q_e$ (mg/g)	$K_2$ (g/mg. min)	$R^2$	$K_{id}$ (g/mg. min <sup>1/2</sup> )	$R^2$	
GAC	0.088	0.253	0.884	0.688	0.623	0.99	0.004	0.92	0.68

Type of adsorbent	Pseudo first order model			Pseudo second order model			Intra particle diffusion		Expt. $q_e$ (mg/g)
	Calculated $q_e$ (mg/g)	$K_1$ ( $\text{min}^{-1}$ )	$R^2$	Calculated $q_e$ (mg/g)	$K_2$ (g/mg.min)	$R^2$	$K_{id}$ (g/mg.min <sup>1/2</sup> )	$R^2$	
SLP	0.205	0.059	0.918	1.9	0.678	0.99	0.027	0.94	1.9
<i>Java plum</i>	0.247	0.076	0.933	2.9	0.222	0.99	0.034	0.99	1.9
GNS	0.274	0.0415	0.992	1.2	0.333	0.99	0.004	0.92	1.1
Banana	0.519	0.0944	0.911	1.2	0.486	1	0.020	0.89	1.2
Neem Patti	0.173	0.0806	0.898	1.5	1.0	0.99	0.026	0.99	1.9
Turmeric	0.0485	0.053	0.948	1.6	0.254	1	0.033	0.93	1.2
MnO <sub>2</sub> Coated Turmeric	0.202	0.039	0.974	1.4	0.434	0.99	0.026	0.92	1.5

### 5.1.7 Isotherms study

In this study Langmuir, Freundlich and Temkin isotherm models were used to describe the equilibrium adsorption isotherms for the removal of fluoride from simulated synthetic waste water prepared in laboratory. In section 2.2.1, section 2.2.2 and in section 2.2.3 all the three models are mentioned (Gupta et al., 2005; Gupta et al., 2012; Ozkaya et al., 2006).

#### 5.1.7.1 Isotherms study of fluoride removal by GAC

An isotherm study describes the way by which adsorbate interact with adsorbent to attain equilibrium during adsorption process. In present study we used three equilibrium isotherm models (Langmuir, Freundlich and Temkin isotherm models) to understand the equilibrium isotherm for the present system. The fluoride adsorption isotherm of the GAC adsorbent at optimal pH 4.0 was investigated and the obtained results are shown in Fig.5.1.7.1 (a-c). The experimental data were analyzed by Langmuir, Freundlich and Temkin model equations and the constants are summarized in Table 5.1.7.1. According to correlation coefficient ( $R^2$ ), the Langmuir equation is more suitable to describe the adsorption behaviour than Freundlich model and Temkin model which indicates that the uptake may be due to a monolayer adsorption (Yu et al. 2015).

**Table 5.1.7.1 Isotherm parameters obtained by fitting experimental data for the studied models**

Adsorbent	Langmuir			Freundlich			Temkin		
	b (L/mg)	q <sub>m</sub> (mg/g)	R <sup>2</sup>	K <sub>F</sub> (mg/g). (L/mg) <sup>-1/n</sup>	n	R <sup>2</sup>	A <sub>T</sub> (L/mg)	B <sub>T</sub> (KJ/mol)	R <sup>2</sup>
GAC	2.4	1.6	0.88	0.771	2.9	0.863	49.2	12.2	0.813

#### 5.1.7.1.1 Concluding Remarks

In present study we were used three equilibrium isotherm models (Langmuir, Freundlich and Temkin isotherm models) to understand the equilibrium isotherm. The Langmuir equation is more suitable to describe the adsorption behaviour than Freundlich model and Temkin model which indicates that the uptake may be due to a monolayer adsorption.

#### 5.1.7.2 Isotherms study of fluoride removal by *Citrus limetta peel*

In biosorption process the behaviour of biosorbate interaction with bio sorbent to attain equilibrium is depicted by isotherm study. We studied three models for the adsorption characteristics namely, Freundlich, Langmuir, and Temkin. All the models are subsequently explained in their linear form.

Langmuir Adsorption Isotherm: In this isotherm it is seen that a formation of monolayer on the surface of bio sorbent and no further adsorption takes places. Freundlich isotherm validates the formation of two layers on the surface of citrus limetta peel. Temkin ignores the low and extreme values of concentration and assumes that with coverage of surface heat of absorption decreases linearly. Correlation coefficients and isotherm constants of studied isotherms models are given in Table.5.1.7.2.

**Table 5.1.7.2 Isotherm parameters obtained by fitting experimental data for the studied models**

Adsorbents	Langmuir			Freundlich			Temkin		
	b (L/mg)	q <sub>m</sub> (mg/g)	R <sup>2</sup>	K <sub>F</sub> (mg/g). (L/mg) <sup>-1/n</sup>	n	R <sup>2</sup>	A <sub>T</sub> (L/mg)	b <sub>T</sub> (KJ/mol)	R <sup>2</sup>
<i>Citrus Limetta Peel</i>	1.4	3.0	0.99	1.6	0.99	0.88	6.2	2.3	0.98

### 5.1.7.2.1 Concluding Remarks

Highest correlation coefficient was observed for Langmuir isotherm as compared to Freundlich and Temkin isotherm model which implies that Langmuir isotherm fits better for fluoride adsorption on Citrus Limetta.

### 5.1.7.3 Isotherms study of fluoride removal by Ground nut shell

The graphical representation of amount of fluoride adsorbed on surface of groundnut shells and the equilibrium fluoride concentration is shown in adsorption isotherm. The data is recorded at the optimum values of parameters. There are three isotherms models that are checked for the validity. The models are Langmuir isotherm model, Freundlich isotherm model and Temkin isotherm models which are shown in Fig. 5.1.7.3 (a-c).

**Table 5.1.7.3 Isotherm parameters obtained by fitting experimental data for the studied models**

Adsorbent	Langmuir			Freundlich			Temkin		
	b (L/mg)	q <sub>m</sub> (mg/g)	R <sup>2</sup>	K <sub>F</sub> (mg/g). (L/mg) <sup>-1/n</sup>	n	R <sup>2</sup>	A <sub>T</sub> (L/mg)	b <sub>T</sub> (KJ/mol)	R <sup>2</sup>
Groundnut shell	0.448	2.3	0.989	3.5	1.8	0.966	3.8	4.5	0.994

### 5.1.7.3.1 Concluding Remarks

In present study we were used three equilibrium isotherm models (Langmuir, Freundlich and Temkin isotherm models) to understand the equilibrium isotherm. The Langmuir equation is more suitable to describe the adsorption behaviour than Freundlich model and Temkin model which indicates that the uptake may be due to a monolayer adsorption.

### 5.1.7.4 Isotherms study of fluoride removal by Neem leaves

In present study, three equilibrium isotherm models (Langmuir, Freundlich and Temkin isotherm models) were used to understand the equilibrium isotherm. The fluoride adsorption isotherm of the GAC adsorbent at optimal pH 4.0 was investigated and the obtained results are shown in Fig. 5.1.7.3 (a-c). The experimental data were analyzed by Langmuir, Freundlich and Temkin model equations.

**Table 5.1.7.4 Isotherm parameters obtained by fitting experimental data for the studied models**

Adsorbents	Langmuir			Freundlich			Temkin		
	b (L/mg)	q <sub>m</sub> (mg/g)	R <sup>2</sup>	K <sub>F</sub> (mg/g). (L/mg) <sup>-1/n</sup>	n	R <sup>2</sup>	A <sub>T</sub> (L/mg)	b <sub>T</sub> (KJ/mo)	R <sup>2</sup>
Neem leaves	0.225	3.6	0.92	0.65	1.3	0.99	3.6	4.2	0.96

#### 5.1.7.4.1 Concluding Remarks

The experimental data were analyzed by Langmuir, Freundlich and Temkin model equations. According to correlation coefficient (R<sup>2</sup>), the Langmuir equation is more suitable to describe the adsorption behaviour than Freundlich model and Temkin model which indicates that the uptake may be due to a monolayer adsorption (Yu et al. 2015).

#### 5.1.7.5 Isotherms study of fluoride removal by Virgin turmeric and MnO<sub>2</sub> coated turmeric

An isotherm study describes the way by which bio sorbates interact with bio sorbents to attain equilibrium during biosorption process. In present study three equilibrium isotherm models (Langmuir, Freundlich and Temkin isotherm models) which are given in Fig. 5.1.7.5 (a-c) for MnO<sub>2</sub> coated turmeric and Fig. 5.1.7.5 (d-f) for Virgin turmeric, to understand the equilibrium isotherm.

**Table 5.1.7.5 Isotherm parameters obtained by fitting experimental data for the studied models**

Biosorbent	Langmuir			Freundlich			Temkin		
	B (L/mg)	q <sub>m</sub> (mg/g)	R <sup>2</sup>	K <sub>F</sub> (mg/g). (L/mg) <sup>-1/n</sup>	n	R <sup>2</sup>	A <sub>T</sub> (L/mg)	B <sub>T</sub> KJ/mol	R <sup>2</sup>
MnO <sub>2</sub> Coated Turmeric	0.99	2.3	0.989	1.0	2.3	0.914	9.0	4.9	0.967
Turmeric	0.359	3.3	0.98	0.893	1.7	0.96	3.1	3.2	0.99

### 5.1.7.5.1 Concluding Remarks

Form Table 5.19. It can be observed that Langmuir Isotherm model displays high correlation coefficient ( $R^2$ ) than Freundlich and Temkin isotherm models, which implies Langmuir isotherm model fits better than both isotherm models for  $MnO_2$  coated turmeric bio sorbent.

Temkin isotherm model best fits for turmeric based bio sorbent. We also see that, biosorption capacity was high in Temkin isotherm which favours experimental data of biosorption best fits to Temkin isotherm model for maximum fluoride removal in case of  $MnO_2$  coated turmeric bio sorbent. Langmuir isotherm best fits for turmeric based bio sorbents for fluoride removal since it shows maximum removal capacity relative to other studied model.

### 5.1.7.6 Isotherms study of fluoride removal by *Java plum seed (Syzgiumcumini)*

In biosorption process the behaviour of biosorbate interaction with bio sorbent to attain equilibrium is depicted by isotherm study. We studied three models for the adsorption characteristics namely, Freundlich, Langmuir, and Temkin. All the models are subsequently explained in their linear form from Fig. 5.1.7.6 (a-c).

Langmuir Adsorption Isotherm: In this isotherm it is seen that a formation of monolayer on the surface of bio sorbent and no further adsorption takes places. Freundlich isotherm validates the formation of two layers on the surface of *Java plum seed (Syzgiumcumini)*. Temkin ignores the low and extreme values of concentration and assumes that with coverage of surface heat of absorption decreases linearly. Correlation coefficients and isotherm constants of studied isotherms models are given in Table.5.1.7.6.

**Table 5.1.7.6 Isotherm parameters obtained by fitting experimental data for the studied models**

Model	Parameters	Correlation coefficient
Langmuir	$q_{max} = 3.0 \text{ mg/g}$ $b = 1.4 \text{ l/mg}$	$R^2 = 0.99$
Temkin	$A=13.8$ $B=3799.95 \text{ (l/g)}$	$R^2 = 0.97$
Freundlich	$n = 2.6$ $K_f = 1.6 \text{ mg/g}$	$R^2 = 0.93$

### 5.1.7.6.1 Concluding Remarks

For the isotherm modelling of adsorption of fluoride ions by Java plums seed from synthetic simulated waste-water, the Langmuir isotherm model gave the best fit for a linear regression model, with a correlation coefficient of  $R^2 = 0.99$ . This signifies that the adsorption mechanism follows the Langmuir mechanism closely. This indicated that the adsorption is a monolayer process.

### 5.1.7.7 Isotherms study of fluoride removal by Banana peel

An isotherm study describes the way by which bio sorbates interact with bio sorbents to attain equilibrium during bio sorption process. In present study three equilibrium isotherm models (Langmuir, Freundlich and Temkin isotherm models) which are given in Fig. 5.1.7.7 (a-c) to understand the equilibrium isotherm.

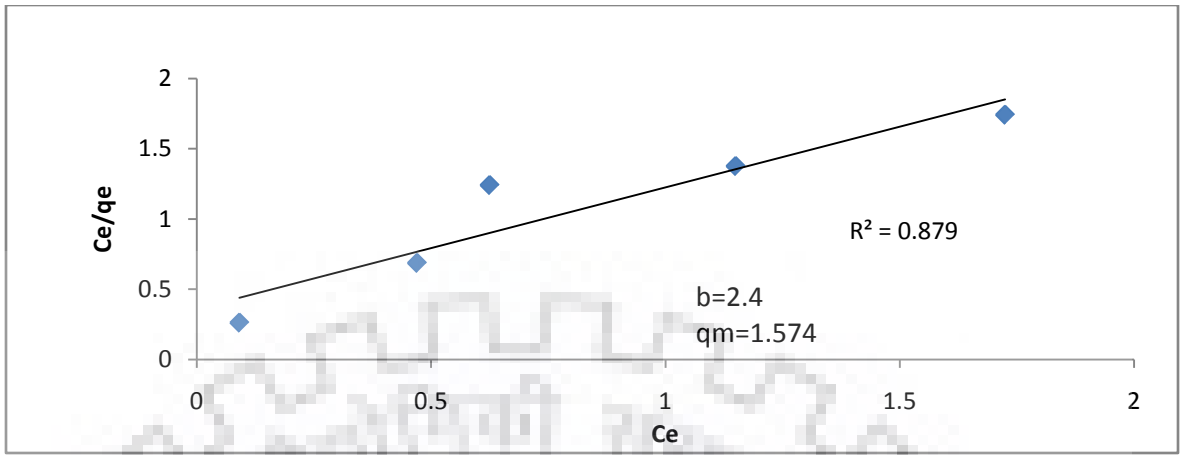
**Table 5.1.7.7 Isotherm parameters obtained by fitting experimental data for the studied models**

Adsorbents	Langmuir			Freundlich			Temkin		
	b (L/mg)	$q_m$ (mg/g)	$R^2$	$K_F$ (mg/g). (L/mg) <sup>-1/n</sup>	n	$R^2$	$A_T$ (L/mg)	$b_T$ KJ/mol	$R^2$
Banana peel	0.359	3.3	0.98	0.893	1.7	0.95	3.1	3.207	0.99

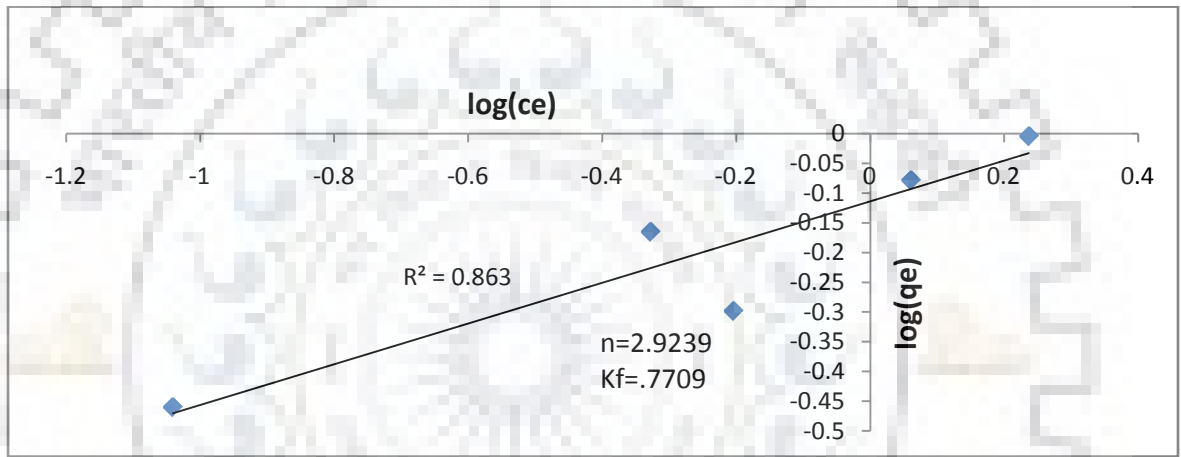
### 5.1.7.7.1 Concluding Remarks

The experimental data were analyzed by Langmuir, Freundlich and Temkin model equations. According to correlation coefficient ( $R^2$ ), the Langmuir equation is more suitable to describe the adsorption behaviour than Freundlich model and Temkin model which indicates that the uptake may be due to a monolayer adsorption (Yu et al. 2015).

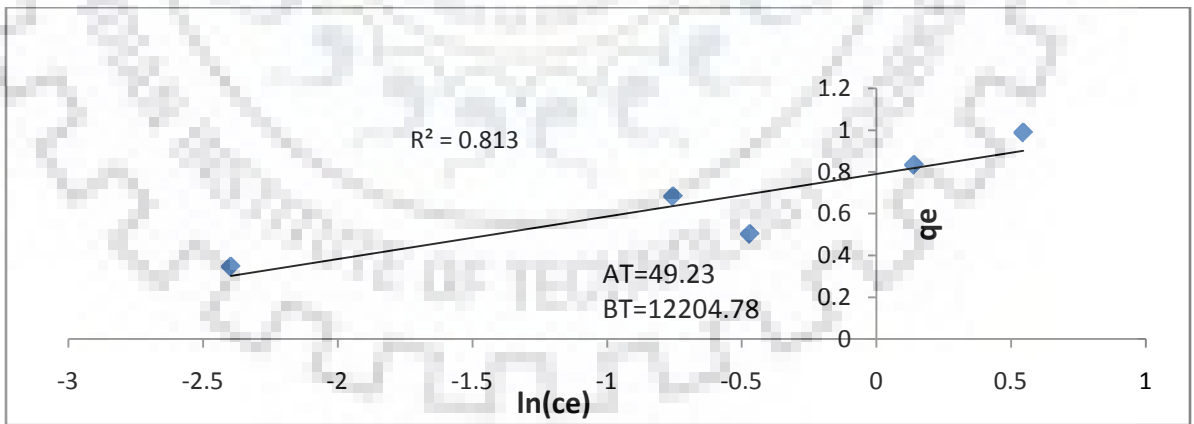




(a)

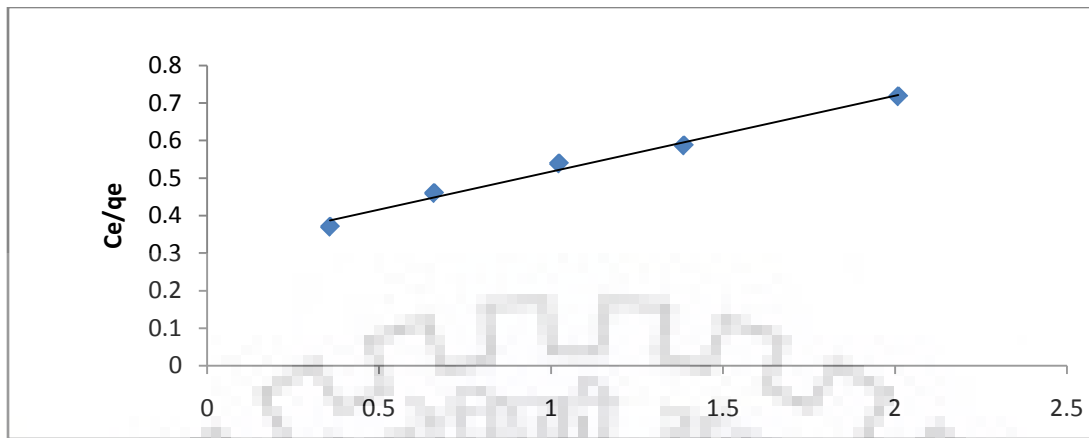


(b)

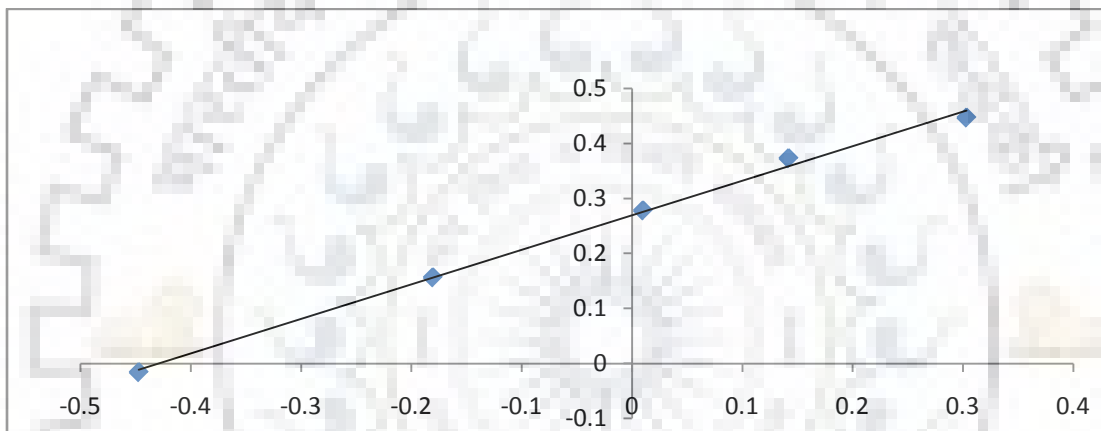


(c)

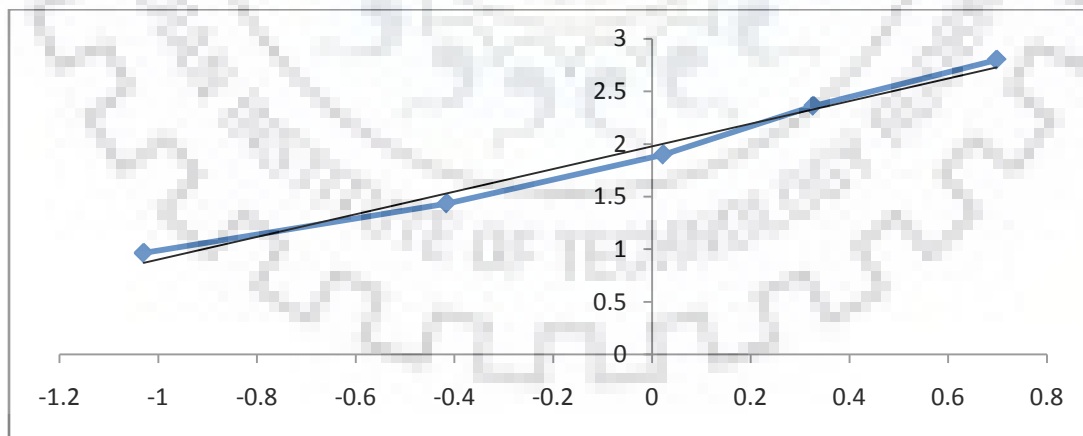
**Fig.5.1.7.1. Isotherm models for GAC (a) Langmuir isotherm model (b) Freundlich isotherm model and (c) Temkin isotherm model**



(a)

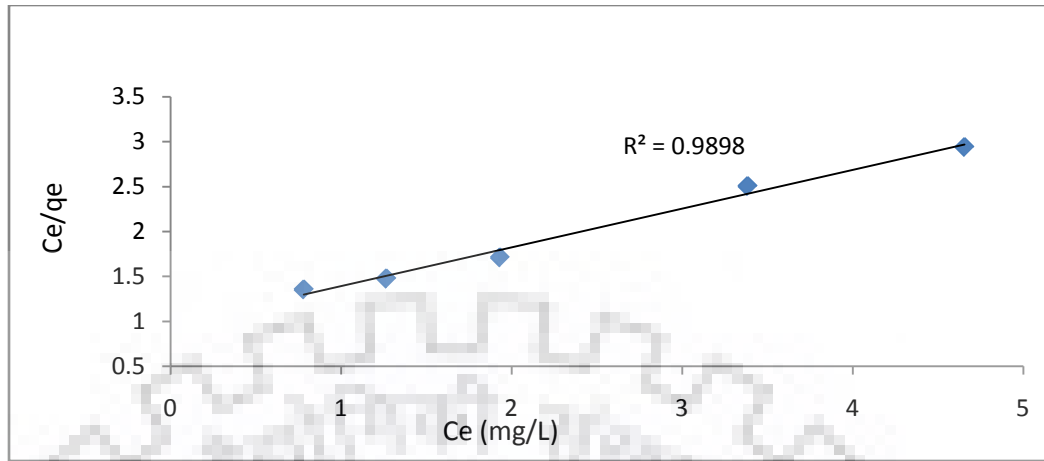


(b)

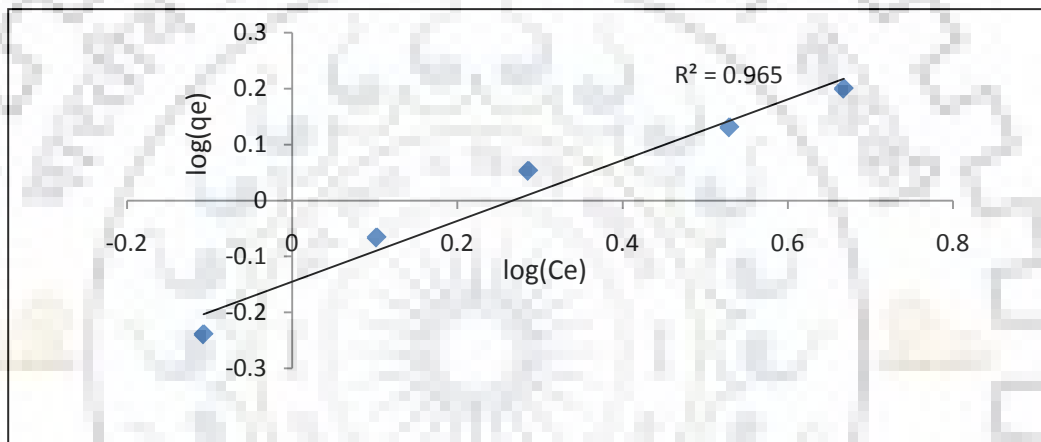


(c)

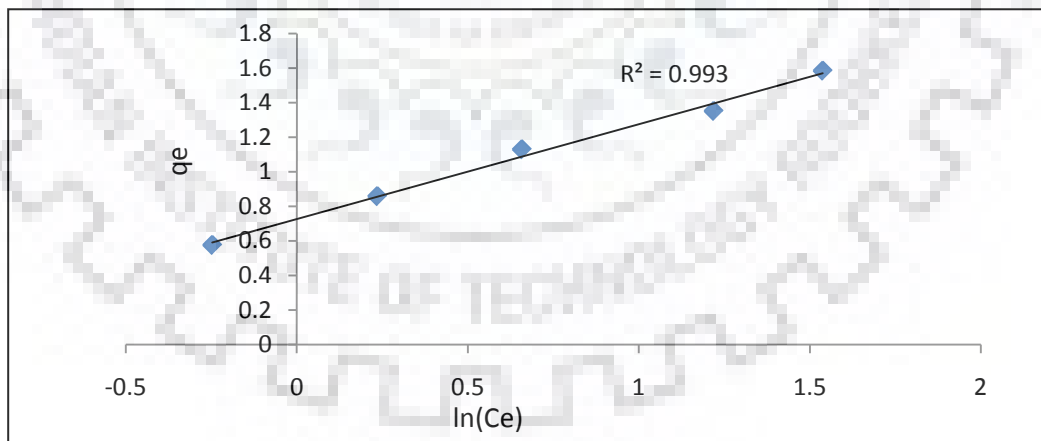
**Fig.5.1.7.2. Isotherm models for *Citrus Limetta Peel* (a) Langmuir isotherm model (b) Freundlich isotherm model and (c) Temkin isotherm model**



(a)

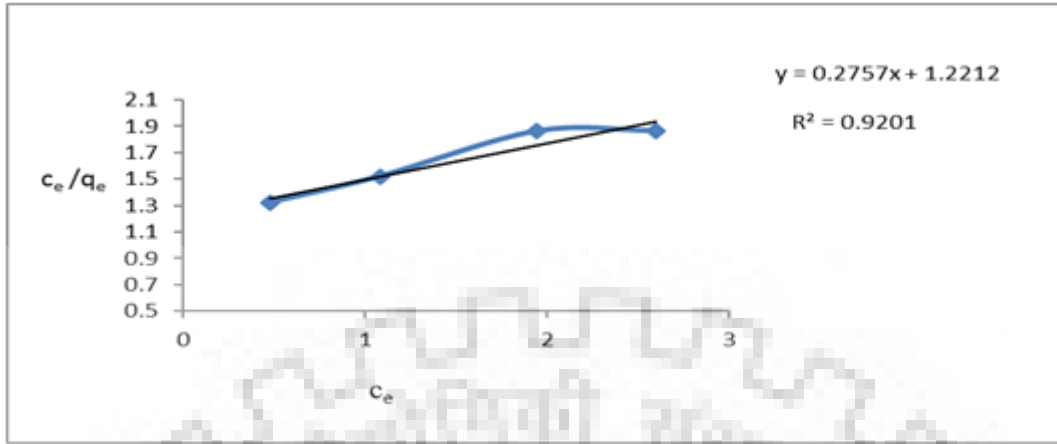


(b)

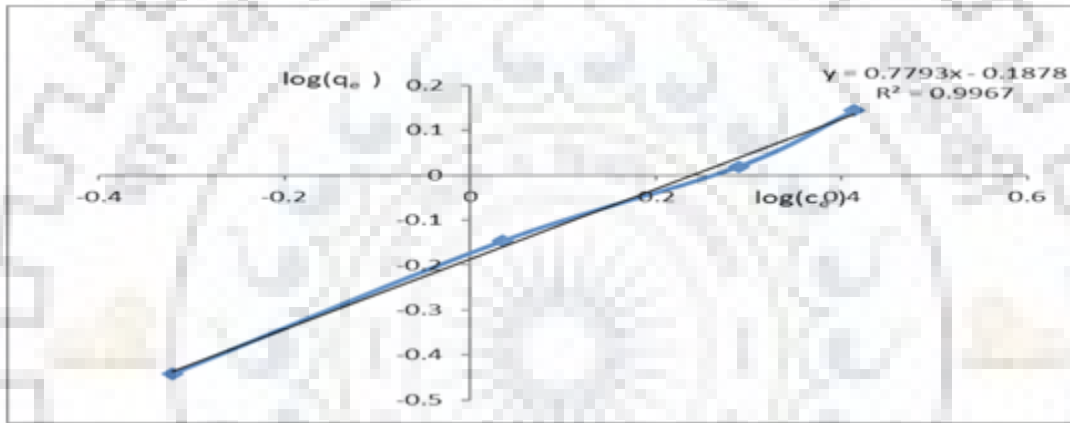


(c)

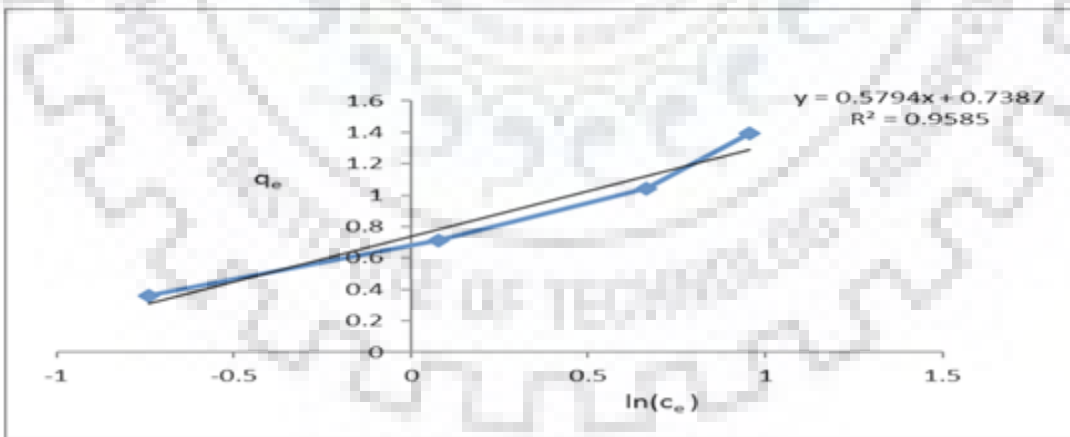
**Fig.5.1.7.3. Isotherm models for Ground nut shell (a) Langmuir isotherm model (b) Freundlich isotherm model and (c) Temkin isotherm model**



(a)

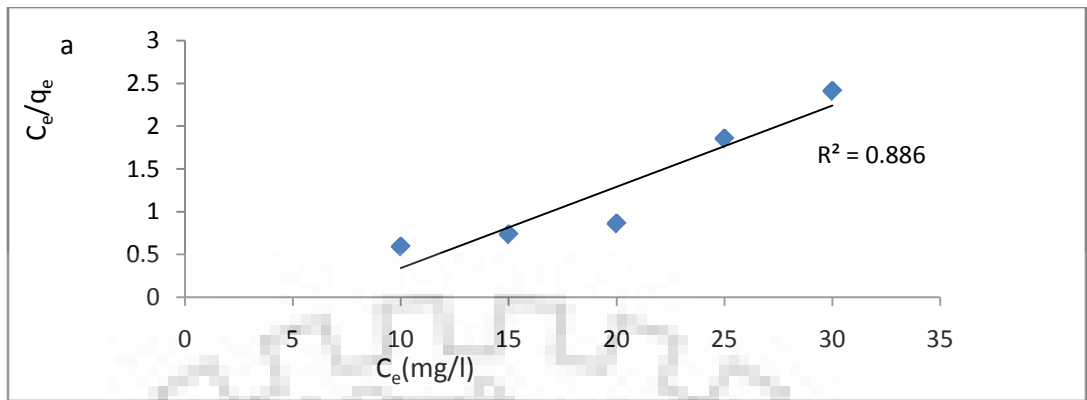


(b)

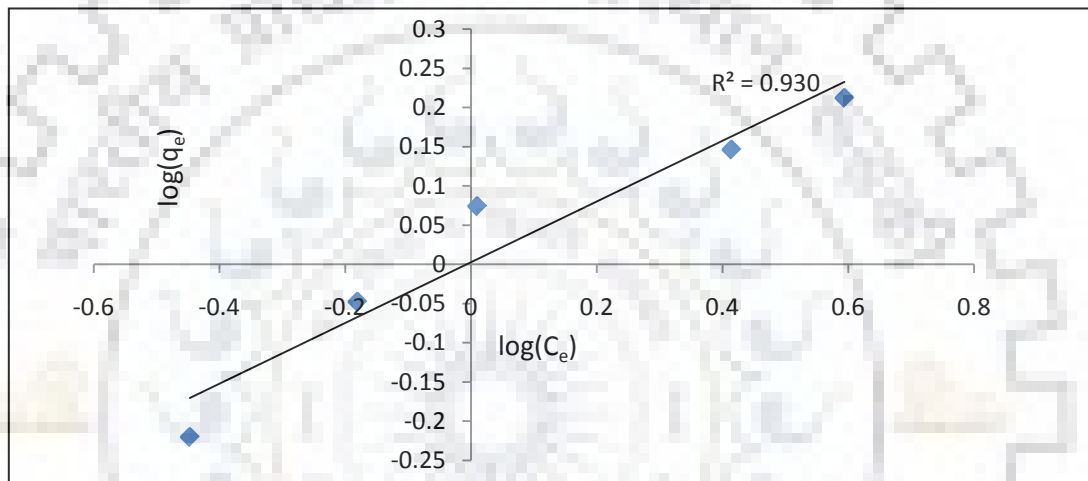


(c)

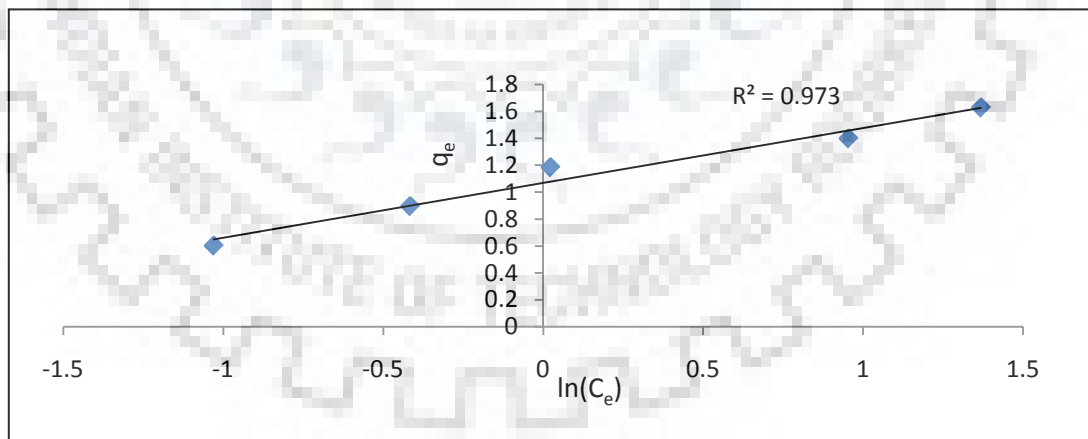
**Fig.5.1.7.4. Isotherm models for Neem leaves (a) Langmuir isotherm model (b) Freundlich isotherm model and (c) Temkin isotherm model**



(a)

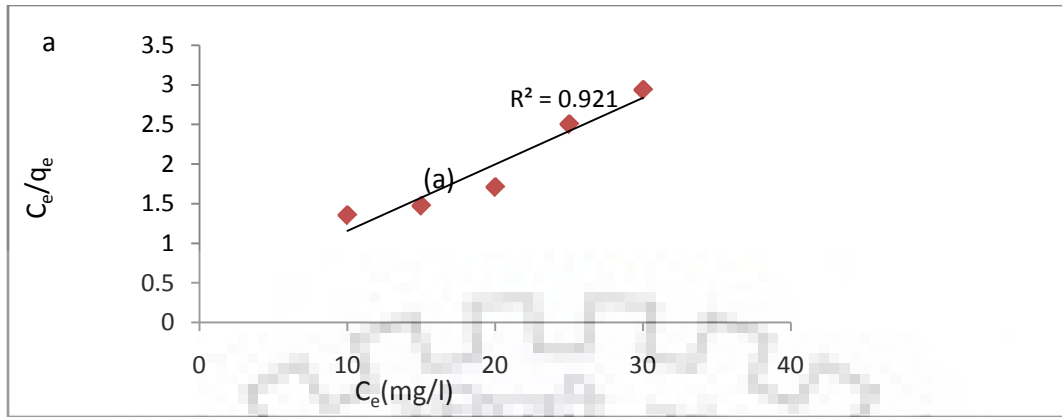


(b)

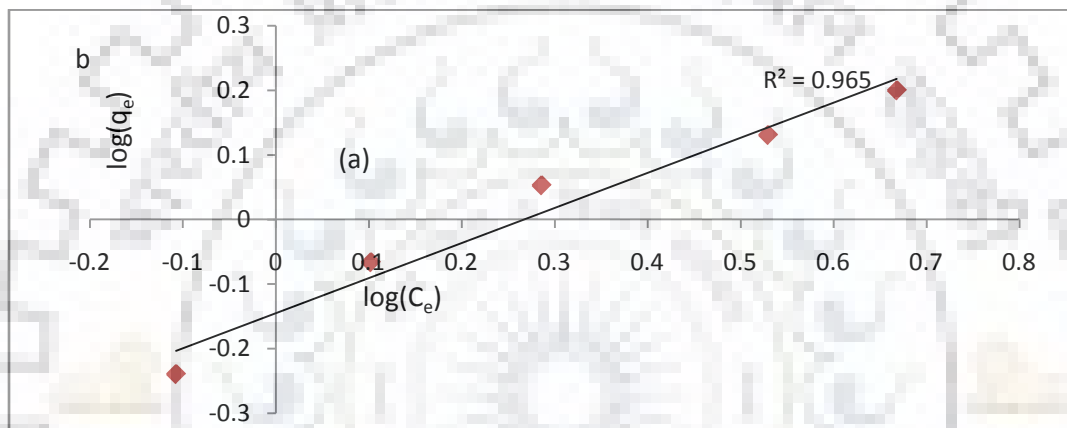


(c)

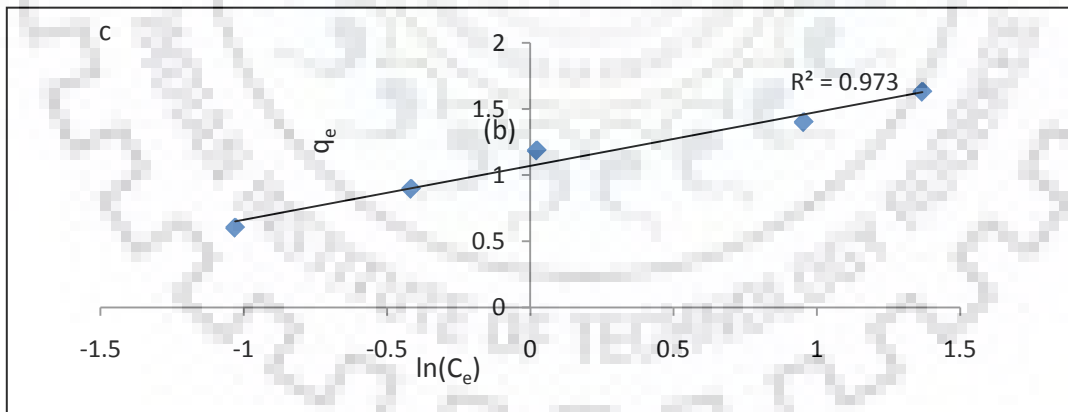
**Fig.5.1.7.5. Isotherm models for  $\text{MnO}_2$  coated turmeric (a) Langmuir isotherm model (b) Freundlich isotherm model and (c) Temkin isotherm model**



(d)

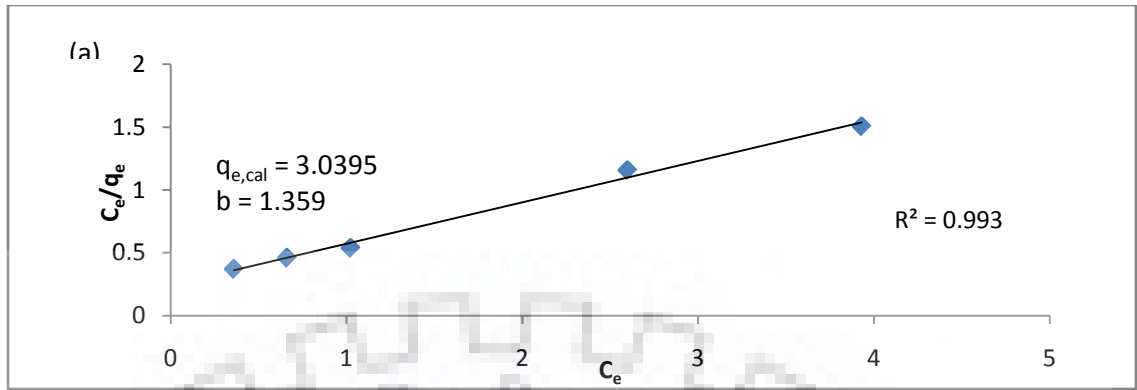


(e)

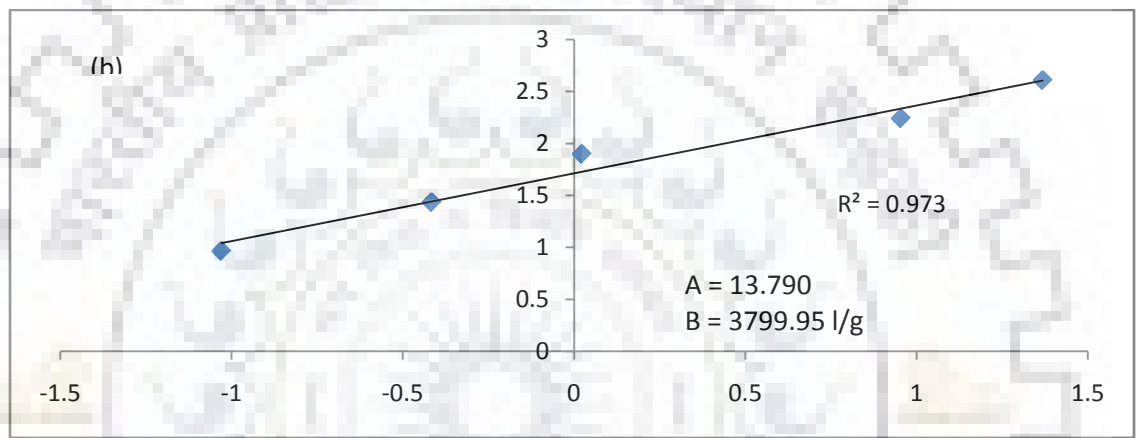


(f)

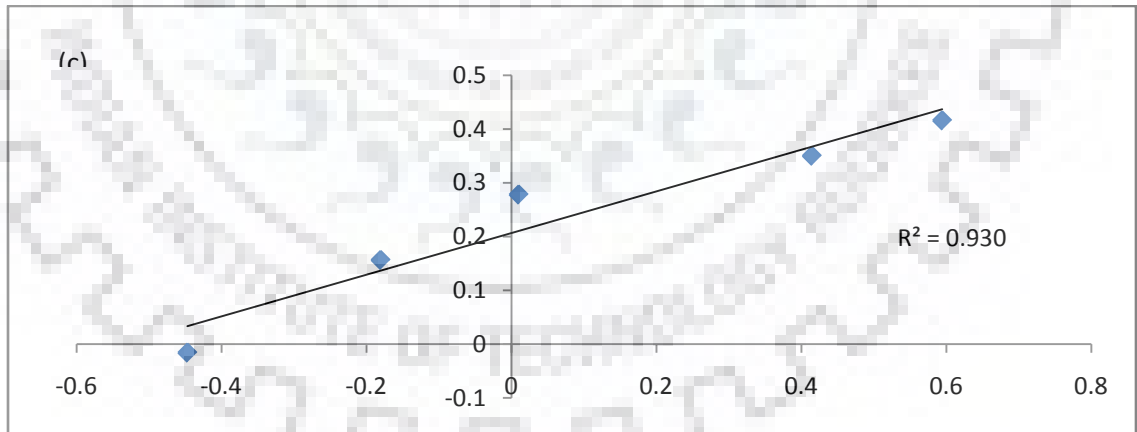
**Fig.5.1.7.5. Isotherm models for Turmeric (d) Langmuir isotherm model (e) Freundlich isotherm model and (f) Temkin isotherm model**



(a)

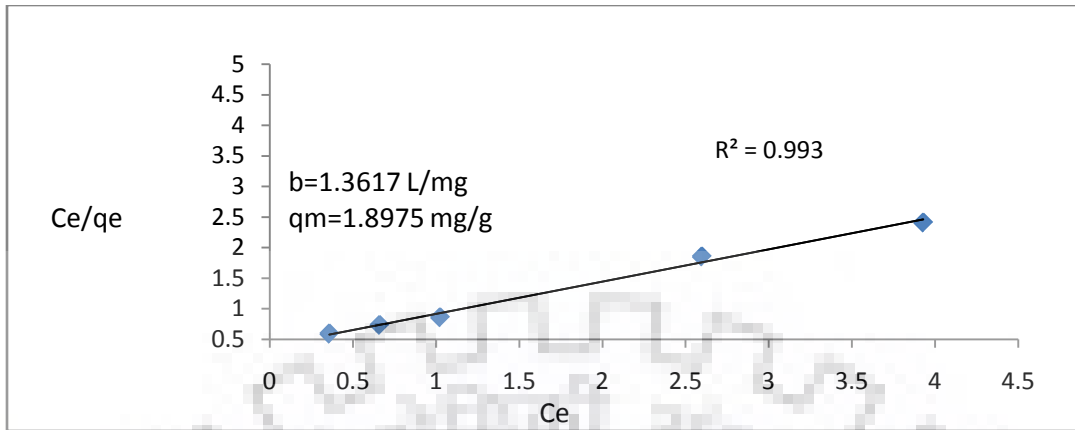


(b)

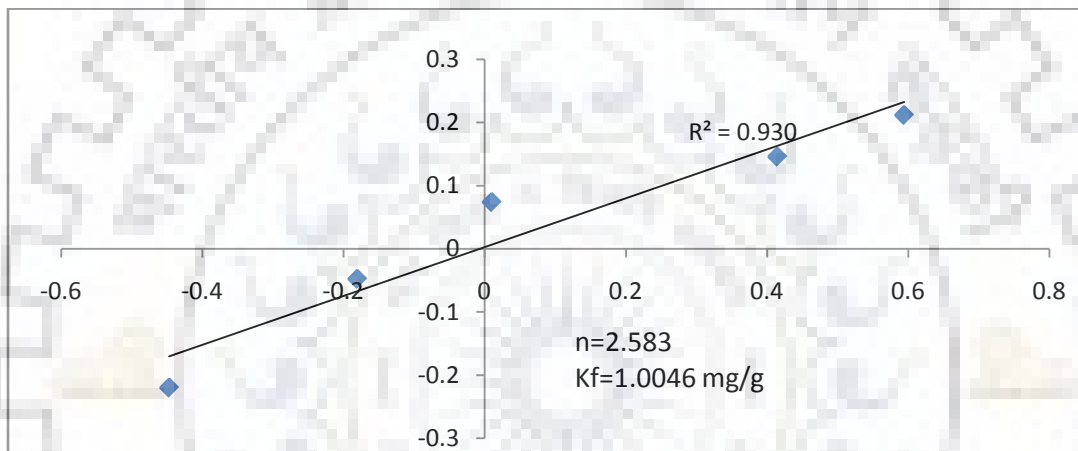


(c)

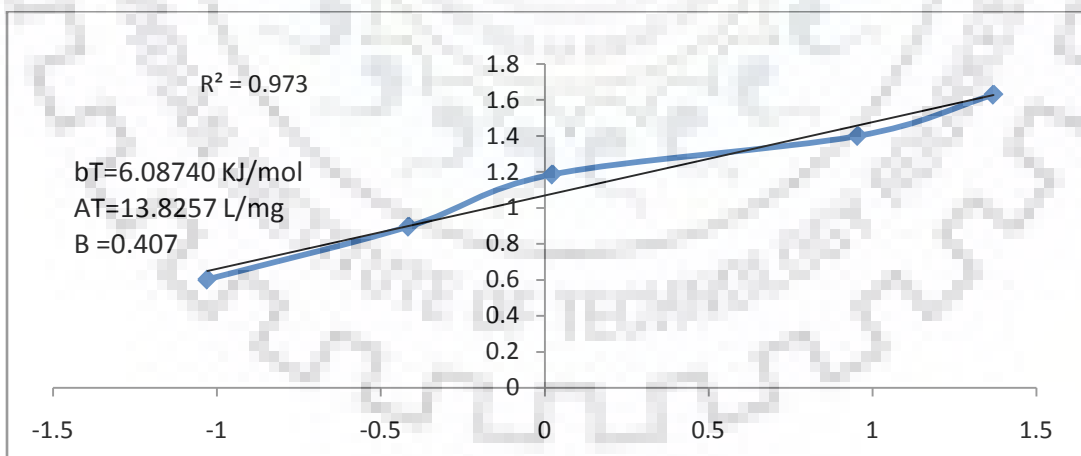
**Fig.5.1.7.6. Isotherm models for Java plum seed (*Syzygiumcumini*)(a) Langmuir isotherm model (b) Freundlich isotherm model and (c) Temkin isotherm model**



(a)



(b)



(c)

**Fig.5.1.7.7. Isotherm models for Banana peel (a) Langmuir isotherm model (b) Freundlich isotherm model and (c) Temkin isotherm model**



### 5.1.7.8 Concluding remark

In present study we were used three equilibrium isotherm models (Langmuir, Freundlich and Temkin isotherm models) to understand the equilibrium isotherm. The Langmuir equation is more suitable to describe the adsorption behaviour than Freundlich model and Temkin model which indicates that the uptake may be due to a monolayer adsorption.

**Table 5.1.7.8: Summary of isotherm model parameters for removal of Fluoride from Simulated Synthetic Waste Water**

Type of adsorbent	Freundlich isotherm model			Langmuir isotherm model			Temkin isotherm model		
	$K_f$ (mg/g). (l/mg) <sup>-1/n</sup>	n	R <sup>2</sup>	$K_L$ (L/mg)	$Q_0$ (mg/g)	R <sup>2</sup>	$b_T$ KJ/mol	$A_T$ (L/mg)	R <sup>2</sup>
GAC	0.771	2.9	0.863	2.4	1.6	0.88	12.204	49.2	0.81
Citrus lemitt peel	1.6	2.6	0.997	1.4	3.3	0.98	2.304	6.2	0.98
<i>Java plum seed</i>	1.6	2.6	0.930	1.4	3.0	0.99	3.799	13.8	0.97
GNS	3.5	1.8	0.965	0.449	2.3	0.99	4.521	3.8	0.99
BANANA	1.0	2.6	0.930	1.4	1.9	0.99	2.356	1.5	0.97
NEEM PATTI	0.650	1.3	0.996	0.225	3.6	0.92	4.189	3.6	0.96
TURMUR IC	0.893	1.7	0.959	0.359	3.3	0.98	3.207	3.1	0.99
MnO <sub>2</sub> Coated Turmeric	1.0	2.3	0.914	0.993	2.3	0.99	4.860	9.0	0.97

### 5.1.8 Comparative Study of Batch and Column Performance of Fluoride Adsorption by *Java Plum Seed (Syzygiumcumini)*

#### 5.1.8.1 The Column Adsorption Experiment

This test was conducted in a Reactor Column of SS pipe. The diagram of the test- setup is presented in Illustration 3.3.2 (a) and (b) in section 3.3.2. SS pipe columns of different lengths ( $Z_1 = 20$ ,  $Z_2 = 40$ ,  $Z_3 = 60$ ,  $Z_4 = 80$  and  $Z_5 = 100$  cm) and 9 cm inside diameter had been brought in use for the top of the reactor is at 100 cm with net volume 6.36 liter. Four equidistant ports of diameter 1.25 cm were introduced in the reactor for the collection of samples along the height of reactor (excluding

inlet and outlet). The upper and lower parts of the reactor had been joined to the main column with the help of two joints, based on SS screen (mesh no: 16 BSS, breadth aperture: 1.00). Reactor had been filled with a certain amount of *Java plum seed (Syzgiumcumini)* with a particle size of 2-4 mm as a fixed-bed absorber.

Bed had been sealed with the help of rubber gasket and cotton pads to prevent the leakage of effluent and loss of adsorbent. Afterwards, the bed had been made wet with pure water and left for the night to form a compact arrangement of particle with no voids or channels. Fluoride solution of the concentration (20 mg/l) had been put through this bed of *Java plum seed (Syzgiumcumini)* in upper-flow manner. This was done in order to avert the moving of fluid because of the gravitation force effect. It also ensures an equal spread of the effluent throughout the column. The tests had been conducted with room temperature. A peristaltic pump had been brought in use to regulate and maintain constant flow rates (12, 23 and 40 ml/min) in each experiment. The rate of flow of the peristaltic pump was checked regularly by collecting sample of the effluent at intermediate times and calculated by making use of a measuring cylinder. Samples of effluent were taken with an intermission of 1 h and were studied by spectrophotometric (SPADNS) process for residual fluoride ion concentration by using UV Spectrophotometer (Hach, DR 5000). Desired breakthrough concentration ( $C_b$ ) was taken as 7.5 %, which is  $0.075 C_i/C_o$  or 1.5 mg/L fluoride concentration.

Prior to column study, (as mentioned in section 5.1.8.2), batch adsorption experiments were carried out (as mentioned in section 5.1.8.3) and the data obtained from modelling of these batch experiments, column study was carried out.

#### **5.1.8.2 Batch Adsorption Experiment**

A stock solution (concentration of 100 mg F/L) was prepared by dissolving 0.221 g anhydrous sodium fluoride in 1L of Millipore water. This solution was diluted to obtain the required concentration for further use. All batch studies were performed using a round bottom flask with a working volume of 50 ml. After adding a known weight of the adsorbent, the flask was shaken (120rpm) on a horizontal rotary shaker (Ramie). When the equilibrium time was reached, the liquid sample was filtered through a 0.45 $\mu$ m filter paper and the filtrate was analyzed for residual fluoride. The following equation was used to calculate the amount of fluoride absorbed:

$$q_e = \frac{(C_0 - C_e)V}{m}$$

Where:

- $q_e$  Fluoride absorbed ( $\text{mg g}^{-1}$ )
- $C_0$  Initial fluoride concentration ( $\text{mg L}^{-1}$ )
- $C_e$  Concentration of fluoride in solution at equilibrium time ( $\text{mg L}^{-1}$ )
- $V$  Volume (L)
- $m$  Mass of adsorbent (g).

The effect of the initial fluoride concentration absorption capacity was studied using  $20 \text{ mg L}^{-1}$  at a pH  $6.9 \pm 0.1$ . The effect of pH was measured over the pH range of 2 to 12 and adjusted using 0.1 M NaOH and 0.1M HCl solutions with an initial fluoride concentration of  $20 \text{ mg L}^{-1}$ . The effect of contact time (0 - 60min) was determined at different time intervals with an initial fluoride concentration of  $20 \text{ mg L}^{-1}$ .

### 5.1.8.3 Mathematical Modeling

#### 5.1.8.3.1 Thomas Model

Thomas model is useful for the evaluation of column performance. It helps in the prediction of breakthrough curves for the effluent and maximum adsorption capacity of an adsorbent. It can be written as (Fengshen et al., 2003), (Oliverj et al., 1986):

$$\frac{C_t}{C_0} = \frac{1}{\left(1 + \exp \left[ k_T \frac{q_0 m - C_0 V}{Q_v} \right] \right)}$$

The linearized form of the above equation can be written as:

$$\ln \left( \frac{C_0}{C_t} - 1 \right) = k_T q_0 \frac{m}{Q_v} - k_T C_0 \frac{V}{Q_v}$$

Where,

- $C_0$  Initial fluoride concentration (mg/L)
- $C_t$  Concentration of fluoride at time, t, (mg/L)
- $Q_v$  Volumetric flow rate of fluoride solution (mL/min)
- $q_0$  Maximum solid phase concentration of fluoride (maximum column adsorption capacity) (mg/g)
- $k_T$  Thomas rate constant (L min mg);
- $V$  Throughput volume (L)
- $m$  mass of adsorbent (g).

Here,  $k_T$  and  $q_0$  can be determined from the slope and the intercept of the linear plot of  $\ln[(C_0/C_t)-1]$  versus  $V$  respectively.

Thomas model is based on following assumptions:

- (i) Langmuir kinetics for adsorption and desorption.
- (ii) Axial dispersion of the adsorbate is neglected.

A constant separation factor; separation factor ( $R_L$ ) is defined by Webber and Chakkravorti can be represented as: –

$$R_L = 1/(1+C_0K_L)$$

Where,

$K_L$  = Langmuir constant (L/mg)

$C_0$  = Adsorbate initial concentration (mg/L)

It is applicable to either favourable or unfavourable isotherms. In this circumstance, lower  $R_L$  value reflects that surface assimilation is more favourable. In a deeper justification,  $R_L$  value shows the surface assimilation character to be either unfavourable ( $R_L > 1$ ), linear ( $R_L = 1$ ), favourable ( $0 < R_L < 1$ ) or irreversible ( $R_L = 0$ ).

The main drawback of the Thomas model is that it is based on second order reaction kinetics, whereas, adsorption is usually not limited by chemical reaction kinetics but in fact it is controlled by inter-phase mass transfer (Aksu and Gönen, 2004, Mathialagan and Viraraghavan, 2002).

#### **5.1.8.3.2 The Empty Bed Residence Time Model (EBRT)**

The Empty Bed Residence Time (EBRT) is a design producer for the design of an adsorber. The major design parameters are:

- (i) Empty Bed Residence Time (EBRT) or Empty Bed Contact Time (EBCT)
- (ii) Adsorbent exhaustion rate

These parameters can be correlated for a fixed bed column to determine the operating and capital costs of the adsorption system (Perrich, 1981, Mckay and Bino, 1990). (Negrea et al., 2011, Guo et al., 2008), has been reported that empty bed contact time is a critical parameter in the adsorption processes especially if the adsorption mainly depends on the contact time between the adsorbent and adsorbate.

The Empty Bed Residence Time (EBRT) is defined as the time taken by the liquid to completely fill the empty column and it determines the residence time during which the solution treated becomes constant with the adsorbent.

$$EBRT \text{ (min)} = \frac{\text{Bed volume}}{\text{Volumetric flow rate of the liquid}} \quad (3)$$

The adsorbent exhaustion rate is the mass of the adsorbent used per volume of liquid treated at the breakthrough, and is given as:

$$\text{Adsorbent exhaustion rate (g/L)} = \frac{\text{Mass of adsorbent used}}{\text{Volume of liquid treated at break through}} \quad (4)$$

The adsorbent exhaustion rates are plotted against the EBRT values, and a single operating line can be constructed to correlate these two variables. Thus, to select the optimum combination of adsorbent exhaustion rate and the liquid retention time, the operating line should first be established.

The equation (3,4) reveal that with the lower adsorbent exhaustion rate, the volume treated at the breakthrough point becomes larger and hence longer EBRT and smaller amount of adsorbent is needed per unit volume of feed treated which implies a lower operating cost; however, larger column will have to be used. On the other hand, the higher the adsorbent exhaustion rate, the smaller the EBRT, the higher the operating cost and smaller column is needed which will reduce the construction cost.

#### 5.1.8.3.4 Continuous Column Study Using *Java Plum Seeds (Syzygiumcumini)*

##### 5.1.8.3.4.1 Fixed-Bed Design Models

The Bed Depth Service Time model (BDST), the Empty Bed Residence Time model (EBRT) and the Thomas Model are selected for this study which are used to predict, optimize and describe the fixed-bed column operation, respectively.

##### 5.1.8.3.4.2 Bed Depth Service Time Model

Fig 5.1.8.3.4.2 shows the BDST plots ( $T_b$  versus  $D$ ), which is constructed from the Table. 5.1.8.3.4.2 (a) and (b) for the influent fluoride concentration of 20 mg/l and flow rates of 12, 23 and 40 ml/min at 7.5% breakthrough time for 20, 40, 60 and 100 cm bed heights. The coefficients  $N_0$  and  $K$  for the three flow rates are calculated based on equation:

$$T_b = \frac{N_0 D}{C_0 V} - \frac{1}{K C_0 \ln\left(\frac{C_0}{C_b} - 1\right)}$$

Where

$T_b$  service at breakthrough point (h),

$N_0$  bed capacity ( $\text{mg cm}^3$ ),

$D$  packed-bed column depth (cm),

$V$  linear flow rate through the bed ( $\text{cm h}^{-1}$ ),

$C_0$  and  $C_b$  are, respectively, the influent and the breakthrough fluoride concentration ( $\text{mg/L}$ )

$K$  is the adsorption rate constant ( $\text{L mg}^{-1} \text{h}^{-1}$ ).

The equation of a straight line on BDST curve can be expressed as  $y = ax + b$ ,

Where

$y$  service time,

$x$  bed depth,

$a$  slope,

$b$  ordinate intercept.

The numerical value of the slope ( $a$ ) =  $N_0/C_0V$  and the intercept ( $b$ ) =  $-\frac{1}{K C_0 \ln\left(\frac{C_0}{C_b} - 1\right)}$ , the adsorptive capacity of the system,  $N_0$  and the rate constant  $K$ , can be evaluated from the slope and intercept of a straight line plotted as the service time against the bed depth from experimental data respectively. The minimum bed depth ( $D_{\min}$ ) which represents the theoretical depth of adsorbent able to prevent the adsorbent concentration from exceeding  $C_b$  is obtained when  $T_b = 0$ , according to the following equation:

$$D_{\min} = \frac{v \ln\left(\frac{C_0}{C_b} - 1\right)}{K N_0}$$

The slope of the line presented by  $y = ax + b$  can be used to predict the performance of the bed, if there is change in the initial solute concentration  $C_{01}$  to a new  $C_{02}$ . Hutchins (Hutchins, (1973)) proposed that the new slope  $a_2$  and new intercept  $b_2$  can be estimated by Equations:

$$a_2 = \frac{a_1 C_{01}}{C_{02}}$$

$$b_2 = \frac{b_1 C_{01}}{C_{02}} \frac{\ln\left(\frac{C_{02}}{C_b} - 1\right)}{\ln\left(\frac{C_{01}}{C_b} - 1\right)}$$

McKay et al. (Mckay et al., 1984) stated that if design data is required for a change in volumetric flow rate of solute to the same adsorption system, the new slope with the intercept remaining unchanged can be written as:

$$a_2 = \frac{a_1 Q_1}{Q_2} = \frac{a_1 v_1}{v_2}$$

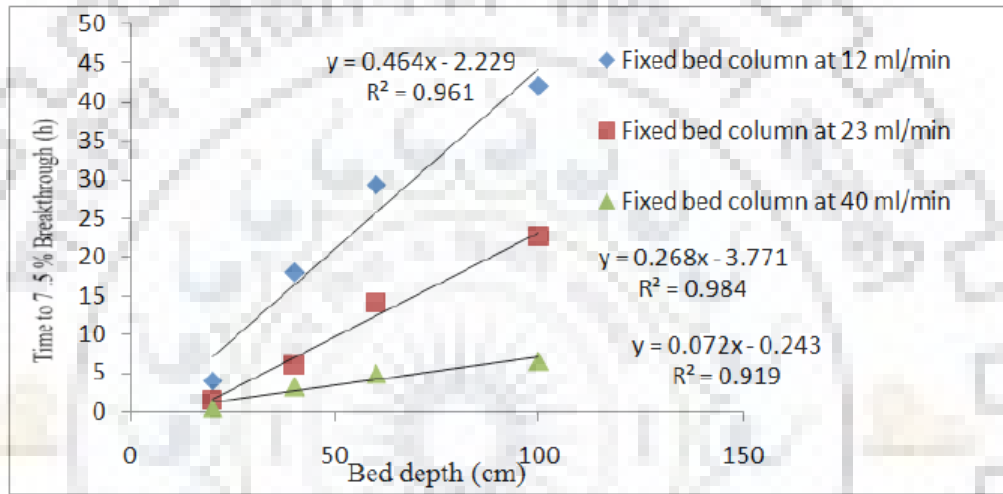


**Fig. 5.1.8.3.4.2** BDST Plot at 7.5% Breakthrough in a Fixed-bed Column at Different Flow Rates

**Table.5.1.8.3.4.2 (a)** Data of Variable Bed Depth at a Fixed Flow Rate in a Fixed-bed Column for the Removal of 20mg/L of Fluoride by *Java plum seed (Syzygiumcumini)*

Q flow rate (ml/min cm <sup>2</sup> )	Bed height (cm)	Bed volume (cm <sup>3</sup> )	Weight of adsorbent m (g)	EBRT (min)	V <sub>b</sub> (L)	T <sub>b</sub> (hr)	Adsorbent exhaustion rate (g/l)
12 ml/min 0.1886 (ml/min cm <sup>2</sup> )	20	1272.34	300	106.03	2.947	4	101.79
	40	2544.68	600	212.01	13.465	18	44.55
	60	3817.02	900	318.0	20.818	29.33	43.23
	100	6361.7	1500	530.14	29.042	42	51.64
23ml/min 0.3615 (ml/min cm <sup>2</sup> )	20	1272.34	300	55.319	2.031	1.5	147.71
	40	2544.68	600	110.639	7.988	6	75.11
	60	3817.02	900	165.957	19.264	14	46.79

Q flow rate (ml/min cm <sup>2</sup> )	Bed height (cm)	Bed volume (cm <sup>3</sup> )	Weight of adsorbent m (g)	EBRT (min)	V <sub>b</sub> (L)	T <sub>b</sub> (hr)	Adsorbent exhaustion rate (g/l)
	100	6361.7	1500	276.595	30.998	22.5	48.39
40 ml/min 0.6287 (ml/min cm <sup>2</sup> )	20	1272.34	300	31.808	1.074	0.45	279.329
	40	2544.68	600	63.617	7.574	3.17	79.39
	60	3817.02	900	152.68	11.676	4.83	77.07
	100	6361.7	1500	159.04	15.644	6.5	95.588

**Table.5.1.8.3.4.2 (b) Constant of BDST Curve**

Q flow rate (ml/min cm <sup>2</sup> )	V(cm/hr)	Slope	Intercept	Depth D (cm)	N <sub>0</sub> (mg/cm <sup>3</sup> )	K (L mg <sup>-1</sup> hr <sup>-1</sup> ) ×10 <sup>-3</sup>	X (mg/g)
0.1886	11.316	0.464	-2.29	4.963	0.105012	54.8479	0.358
0.3615	21.69	0.268	-3.771	14.071	0.11625	33.307	0.382
0.6287	37.722	0.072	-0.248	3.445	0.0543	506.45	0.1929

The data in the Table.5.1.8.3.4.2 (a) and (b) shows that EBRT (Empty Bed Residence Time), V<sub>b</sub> and T<sub>b</sub> increase with decreasing flow rate or increasing bed depth. The equations of linear relationship were obtained with correlation coefficients of 0.961, 0.984 and 0.92 for 12, 23 and 40 ml/min respectively. The adsorption capacity (X) was calculated to be 0.358, 0.382 and 0.1929 mg/g for 12, 23 and 40 ml/min flow rate respectively. This shows that as the flow rate increases, the adsorption capacity decreases. This may be due to decrease in contact time.

### 5.1.8.3.5 Effect of Bed Depth

The adsorption of fluoride on *java plum seed (Syzgiumcumini)* is presented in the form of breakthrough curves where the concentration ratio C<sub>t</sub>/C<sub>0</sub> is plotted versus time (hr). Fig 5.1.8.3.5 (a-c) shows the breakthrough curves of fluoride adsorption on *Java plum seed (Syzgiumcumini)*s at different bed depths (20, 40, 60, and 100 cm) and at a constant flow rates of 12, 23 and 40ml/min. Results indicate that breakthrough volume V<sub>b</sub> and breakthrough time T<sub>b</sub> increases with increasing bed depth .The breakthrough time T<sub>b</sub> is directly related with D according to the equation  $T_b = \frac{N_0 D}{C_0 V} - \frac{1}{K C_0 \ln\left(\frac{C_0}{C_b} - 1\right)}$ , thus as bed depth increases the breakthrough time also increases and which in



turn leads to an increase in treated volume ( $V_b$ ). When the bed depth increases, the adsorption performance increases due to increase in adsorption mass which provide greater adsorption site.

The breakthrough curve indicated in Figure 5.1.8.3.5 (a) shows that at lower bed depths, the shape of the curve does not show the characteristic S shape profile produced in ideal adsorption systems, but exclusively for the 100 cm column, the shape is approaching S shape curve. Increasing bed depth increase the EBRT from 106.03 to 530.04 for  $12 \text{ mL min}^{-1}$  flow rate and similar trends were also followed with other flow rates.

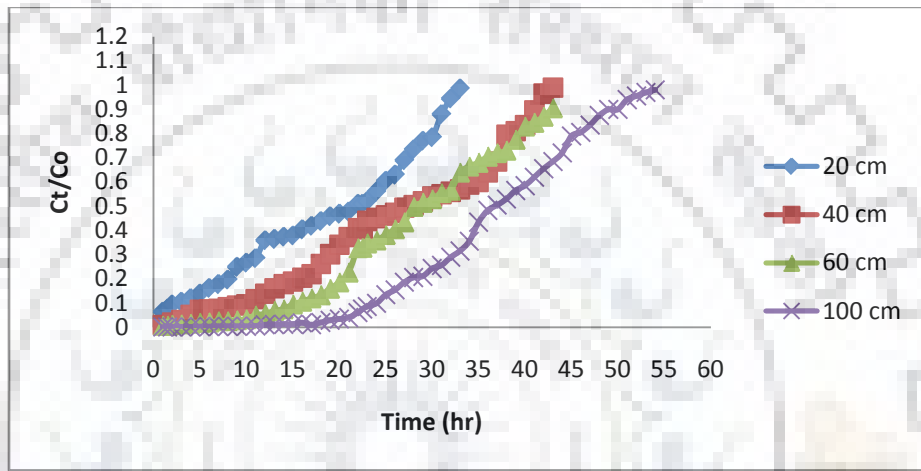


**Fig. 5.1.8.3.5 (a) Effect of Bed Depth on Breakthrough Time at a Constant Flow Rate of  $23 \text{ mL min}^{-1}$  ( $C_0=20 \text{ mg L}^{-1}$ )**

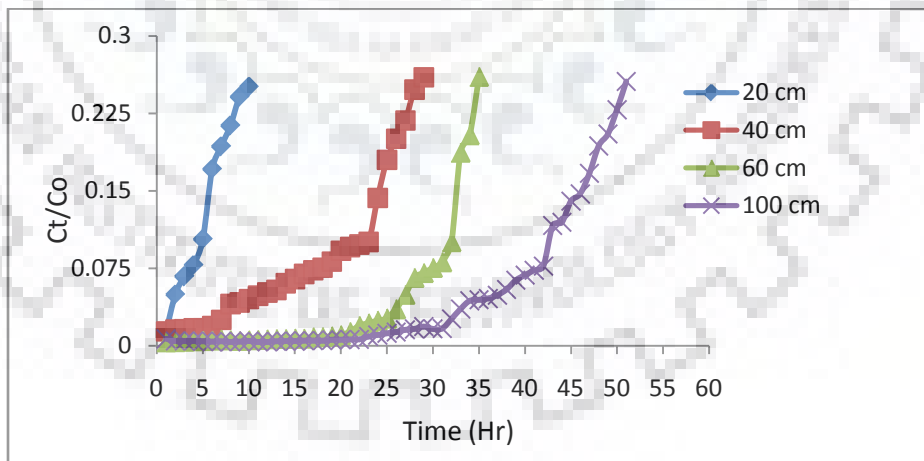


**Fig. 5.1.8.3.5 (b) Effect of Bed Depth on Breakthrough Time at a Constant Flow Rate of  $12 \text{ mL min}^{-1}$  ( $C_0=20 \text{ mg L}^{-1}$ )**

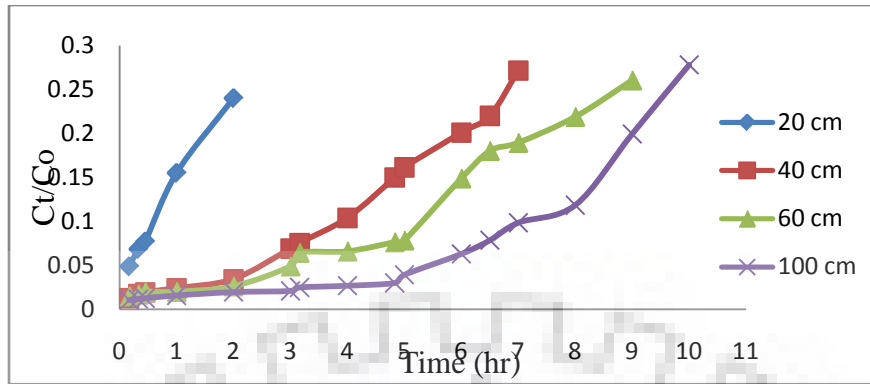


Fig. 5.1.8.3.5 (c) Effect of Bed Depth on Breakthrough Time at a Constant Flow Rate of 40 mL min<sup>-1</sup> (C<sub>0</sub>=20 mg L<sup>-1</sup>)

### 5.1.8.3.6 Effect of Flow Rate

Figure 5.1.8.3.6. Shows that the effect of rate on the breakthrough time at fixed-bed depth of 100 cm. A rise in flow rate from 23 to 40 mL min<sup>-1</sup> decreases the volume of the processed water at the breakthrough and thus decreases the service time of the bed. It can be seen from Table 5.1.8.3.4.2, 30.9 L of water had been processed at a flow rate of 23 mL min<sup>-1</sup> while 15.6 L was processed at a flow rate of 40 mL min<sup>-1</sup> and the breakthrough time also decreased from 22.5 to 6.5 h for 23 and 40 mL min<sup>-1</sup> flow rates, respectively. It is because of the reduction in contact time of the fluoride and adsorbent at higher flow rate. When the rate of absorption is regulated by intra-particle diffusion, a quick breakthrough occurred resulting in a low bed adsorption capacity (Christian et al., 2005). While the flow rate decreases, the contact time in the column is higher and intra-particle diffusion after that becomes stronger. In this way, the adsorbate will get more time to diffuse into the particles of the adsorbent with a greater adsorption capacity is achieved. The slope of the BDST plot will be higher for smaller flow rates.

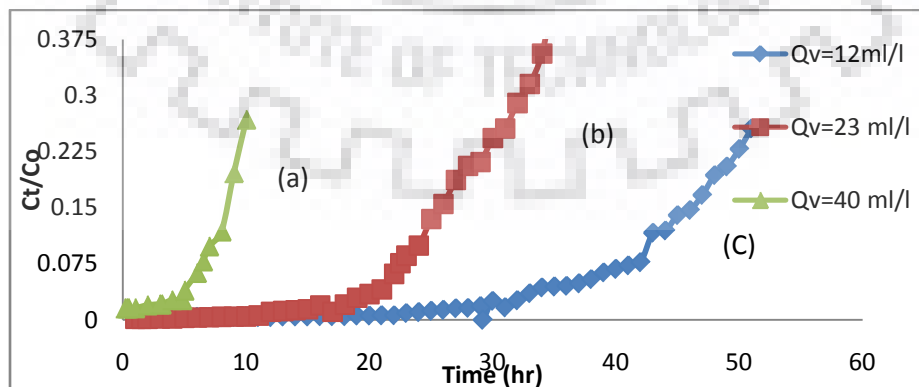


Fig.5.1.8.3.6 Effect of Flow Rate on Breakthrough Time in a 100 cm Fixed Bed Column; (a) 40, (b) 23, (c) 12 mL min<sup>-1</sup> (C<sub>0</sub> = 20 mg L<sup>-1</sup>)

### 5.1.8.3.7 Effect of Empty Bed Contact Time

Fig 5.1.8.3.7 is a plot of the adsorbent exhaustion rate against EBRT at various adsorbent bed heights like 20, 40, 60 and 100 cm. It can be seen from the figure that adsorbent exhaustion rate decreases with increasing EBRT. Shown in Table 5.1.8.3.4.2, the data of variable bed depth (20, 40, 60 and 100cm) at different flow rates (12, 23 and 40ml/min) in a column reactor for the removal of fluoride. The data in Table 5.1.8.3.4.2 shows that EBRT,  $V_b$  and  $T_b$  increased with increasing bed depth. It is clear that when the EBRT increases with flow rate, the bed volume will have to be longer, thus allowing more solution to be treated but resulting in a lower adsorbent exhaustion rate.

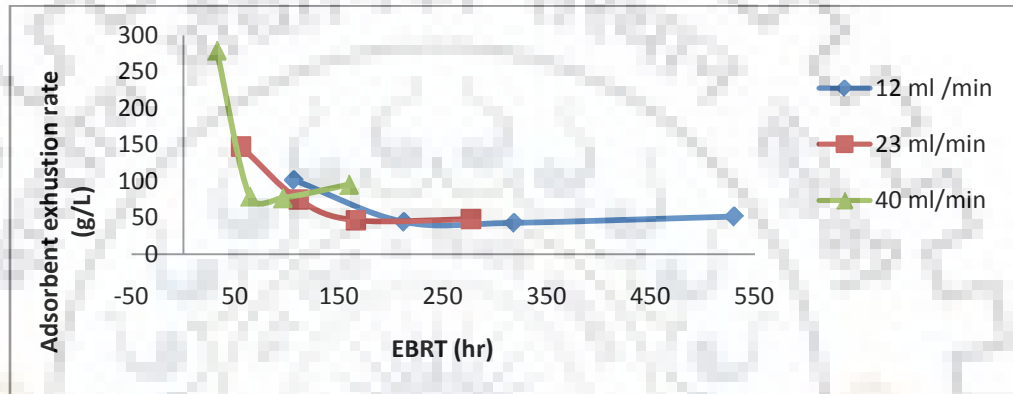
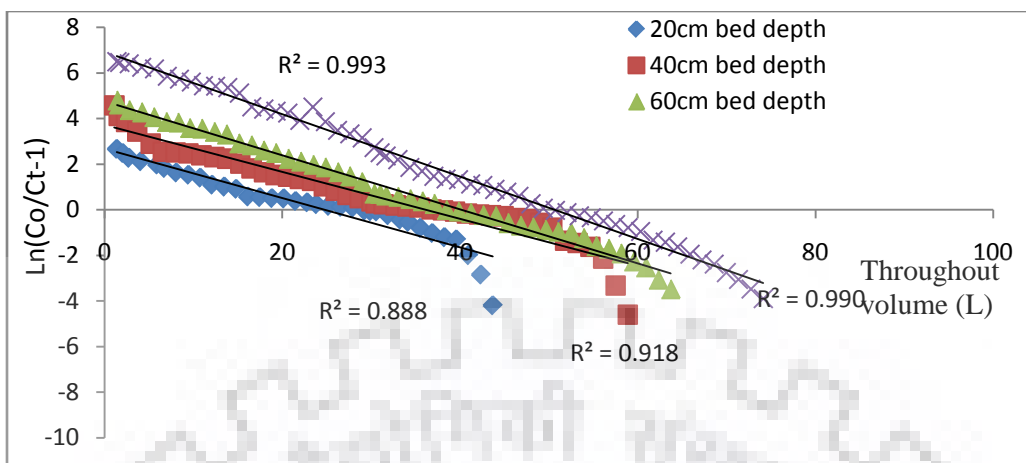


Fig. 5.1.8.3.7 Adsorbent Exhaustion Rate versus EBRT

### 5.1.8.3.8 Thomas Model

The data obtained through continual flow mode studies had been applied to work out the kinetic parameters by making use of the Thomas model which is very much used for column studies. The Thomas model had been used in explaining the absorption kinetics and evaluating the maximum solid phase concentration ( $q_0$ ) and the rate constant ( $k_T$ ). The linearized Thomas model plot is shown in figure.5.1.8.3.8. From the plot, the rate constant  $k_T$  and the maximum solid phase concentration of the solute  $q_0$  was collected. The Table 5.1.8.3.8 shows summary of the linearized Thomas model parameters.



**Fig. 5.1.8.3.8 Liberalized Thomas Model plot at 7.5% Breakthrough for Adsorption of 20 mg L<sup>-1</sup> Fluoride Solution with 23 mL min<sup>-1</sup> Flow Rate at Different Bed Depths**

**Table 5.1.8.3.8 Liberalized Thomas Model Parameter at 7.5% Breakthrough**

D (cm) C <sub>o</sub> (mg/l) Q(ml/min)	K <sub>T</sub> (L mg <sup>-1</sup> min <sup>-1</sup> )×10 <sup>-3</sup>	q <sub>o</sub> (mg g <sup>-1</sup> )	R <sup>2</sup>	Equation of line
20,20,23	0.124	1.654	0.888	Y= -0.108x +2.68
40,20,23	0.117	1.214	0.918	Y= -0.102x+3.72
60,20,23	0.136	0.893	0.990	Y= -0.118x+4.75
100,20,23	0.156	0.678	0.993	Y= -0.136x+6.92

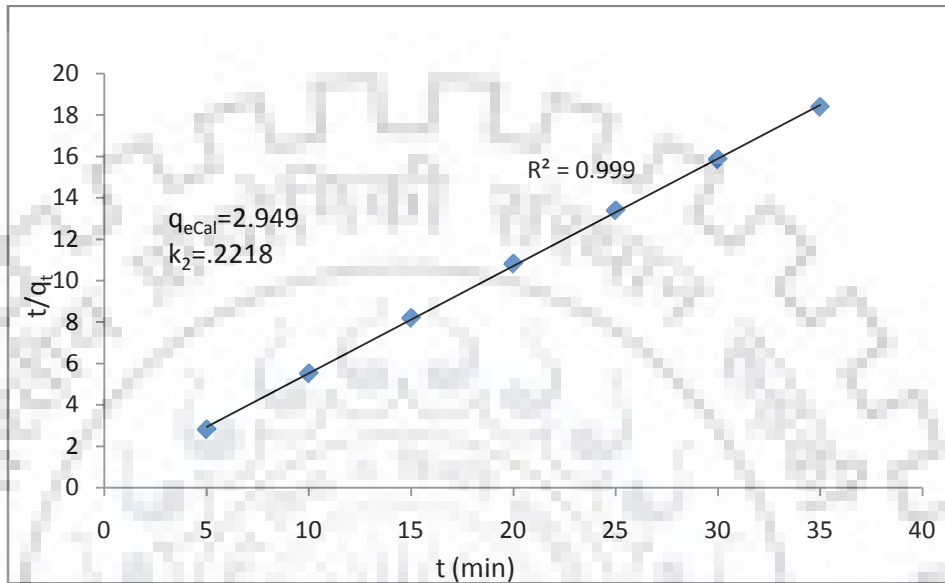
#### 5.1.8.4 Batch Study

##### 5.1.8.4.1 Effect of Adsorption Kinetics and Contact Time

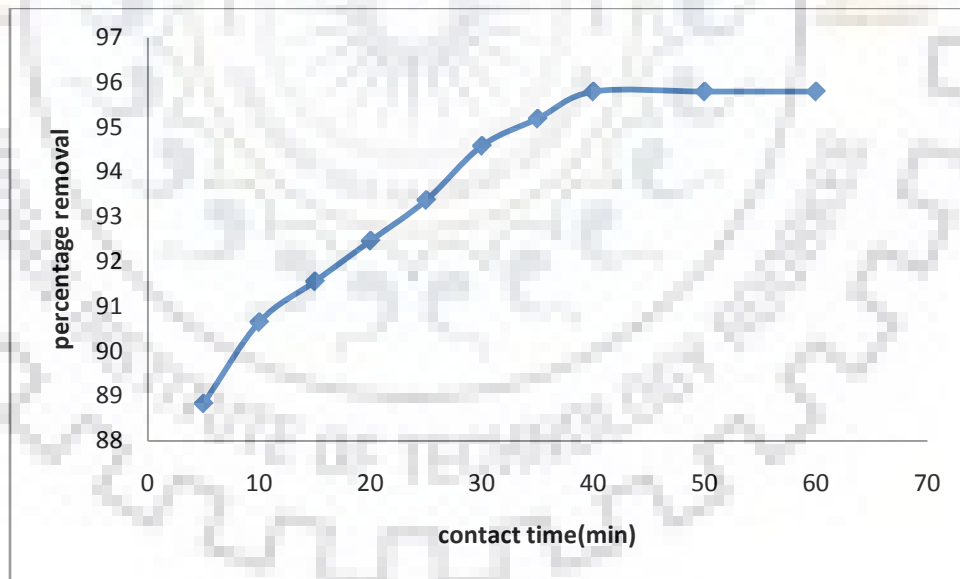
As can be seen from Fig (5.1.8.4.1(a) and (b)), the fluoride adsorption process occurred in two stages. The first rapid stage was where 70-80 percent adsorption was achieved in 20 min, and a slower second stage, with equilibrium attained in 60 min. The first stage was due to the rapid initial accumulation of fluoride in the *Java plum* seed (*Syzygiumcumini*) surface, when the relatively large surface area was utilized. With the surface binding sites being increasingly occupied, the adsorption process slowed. The second stage was due to the penetration of fluoride ions to the inner active sites of the adsorbent. This matches with the observations in similar studies (Sangi et al., 2008, Qaiser et al., 2009). The experimental data obtained was analyzed using a pseudo-second-order Lagergren equation.

$$\frac{t}{q_t} = \frac{1}{K_2 q_e^2} + \frac{t}{q_e}$$

Where  $q_t$  and  $q_e$  represent the amounts of fluoride adsorbed (mg F/g) at a given time  $t$  (min) and at equilibrium time respectively.  $K_2$  is the second-order rate constant for this adsorption. A linear relationship with a correlation coefficient of 0.9994 was found between  $t/q_t$  and  $t$  that indicated fluoride adsorption on the *Java plum seed (Syzgiumcumini)* is a chemisorption process.



**Fig. 5.1.8.4.1 (a) Pseudo-Second Order Model**



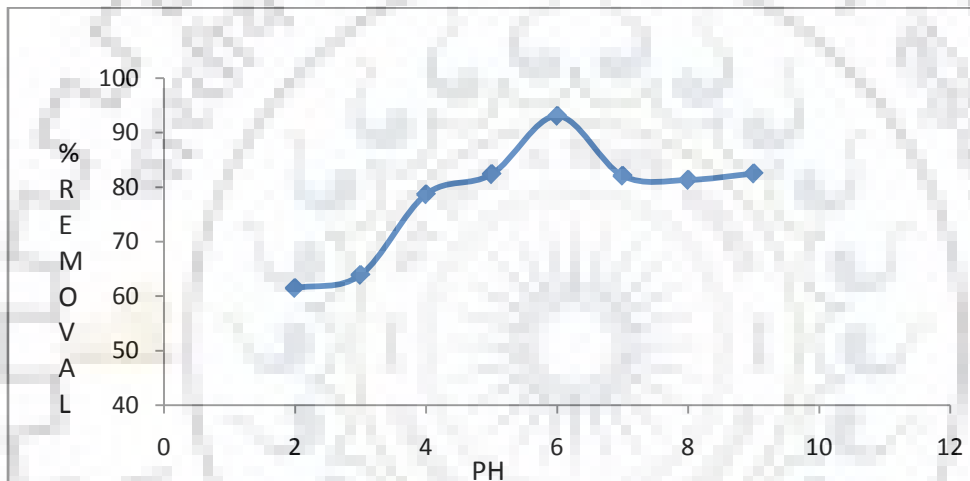
**Fig. 5.1.8.4.1 (b) Percentage Removal versus Time**

Fig.5.1.8.4.1(a) and Fig.5.1.8.4.1(b) indicates the effect of contact time on fluoride adsorption on *Java plum seed (Syzgiumcumini)* (adsorption kinetics) (initial fluoride concentration 20 mg/ L,

initial pH  $6.9 \pm 0.1$ , equilibrium contact time up to maximum 1 hour, adsorbent dosage 20 g/L, shaken speed 120 rpm and temperature  $30 \pm 1^\circ\text{C}$ ).

#### 5.1.8.4.2 Effect of pH

Solution pH plays an important role during the adsorption process. The numbers of chemically active sites are influenced by varying the solution pH. To determine the optimum pH value, the pH of the solution was varied from 2.0 to 10. As shown in Fig 5.1.8.4.2, the maximum adsorption of fluoride occurs over the pH range 5-6.5. Fluoride removal was not favoured at pH below 5.0. This can be attributed to the distribution of fluoride and  $\text{HF}^-$  in solution that is controlled by pH. When the pH of solution exceeded 7.0, fluoride adsorption decreased.



**Fig. 5.1.8.4.2 Effect of pH on Fluoride Adsorption on *Java plum seed (Syzgiumcumini)* (Initial Fluoride Concentration 20 mg/L Equilibrium Contact Time 1 hr, Adsorbent Dose 20g/L, Shaken Speed 120 rpm and Temp  $30 \pm 1^\circ\text{C}$ )**

#### 5.1.8.4.3 Adsorption Isotherm Models

Equilibrium during a adsorption process is achieved when the concentration of adsorbate in bulk solution is in dynamic balance with that on the liquid-solid interface. Therefore, the Langmuir and Freundlich model were utilized to describe the equilibrium data. The Langmuir model is based on the hypothesis that uptake of the adsorbed molecules occurs on a homogenous surface by monolayer sorption without interaction between the adsorbed molecules, and is expressed as follows (Langmuir, 1916).

$$q_e = q_{max} b C_e \frac{1}{1 + bC_e}$$

Eq. can be written in a linear form as:

$$\frac{C_e}{q_e} = \frac{C_e}{q_{max}} + \frac{1}{q_{max} b}$$

Where  $q_{max}$  represents the maximum adsorption capacity and  $b$  is a constant related to affinity and energy of binding sites.

The Freundlich model proposed a multilayer sorption with a heterogeneous energetic distribution of active sites and with interaction of adsorbed molecules. It is expressed mathematically as follows (Freundlich, 1906):

$$q_e = K_F C_e^{1/n}$$

In logarithmic, one can write as;

$$\ln(q_e) = \frac{1}{n} \ln(C_e) + \ln(K_F)$$

Where  $K_F$  and  $n$  are Freundlich coefficients,  $K_F$  provides an indication of the adsorption capacity and  $n$  is related to the intensity of adsorption.

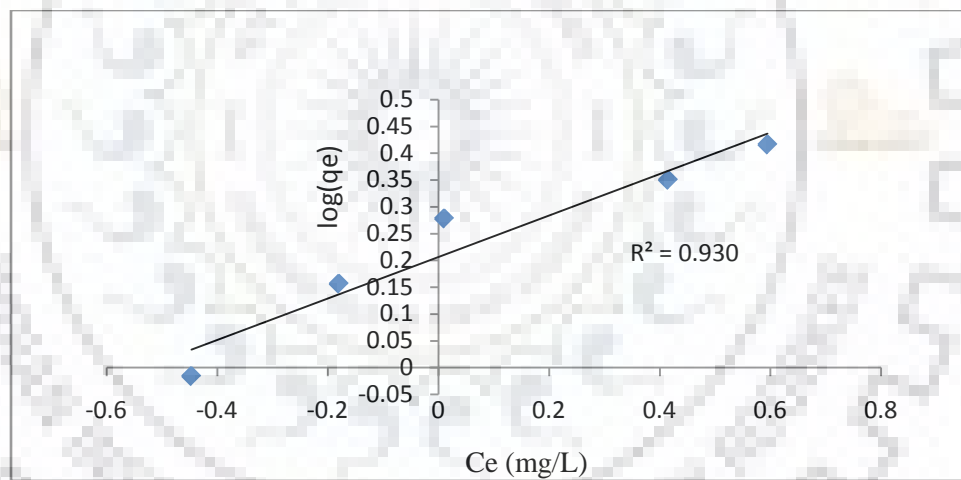


**Fig. 5.1.8.4.3 (a) Freundlich Isotherm Plot for Fluoride Adsorption on *Java plum seed* (*Syzgiumcumini*) (Initial Fluoride Concentration  $20 \text{ mg L}^{-1}$ , Initial pH  $6.9 \pm 0.1$ , Equilibrium Contact Time 1 hour, Adsorbent Dosage  $20 \text{ g/L}$ , Shaken Speed 120 rpm and Temperature  $30 \pm 1^\circ \text{C}$ ).**

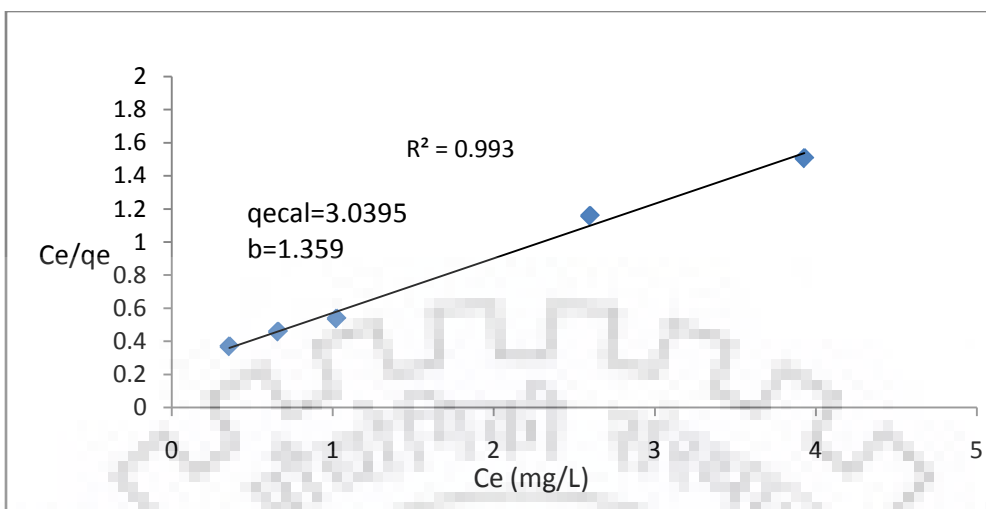


**Fig. 5.1.8.4.3 (b) Langmuir Isotherm Plot for Fluoride Adsorption on *Java plum seed* (*Syzgiumcumini*) (Initial Fluoride Concentration 20 mg L<sup>-1</sup>, Initial pH 6.9±0.1, Equilibrium Contact Time 1 hour, Adsorbent Dosage 20 g/L, Shaken Speed 120 rpm and Temperature 30±1°C).**

**Table 5.1.8.4.3: Langmuir and Freundlich Isotherm Parameters for the Adsorption of Fluoride on *Java plum seed* (*Syzgiumcumini*)**

Langmuir isotherms		Freundlich isotherms	
q <sub>max</sub> (mg/g)	3.0	n	2.6
b(L/mg)	1.4	K <sub>f</sub> (mg/g)	1.6
R <sup>2</sup>	0.993	R <sup>2</sup>	0.930

Fig.5.1.8.4.3 (a) and Fig.5.1.8.4.3 (b) shows the Freundlich and Langmuir isotherms along with the experimental data. From the isotherm constant and correlation coefficient values, it can be concluded that the obtained adsorption data can be better described by the Freundlich isotherm model. This result suggests that various active sites on, or alternatively a heterogeneous of several minerals in *Java plum seed* (*Syzgiumcumini*), have different affinities for fluoride ions (Fuhrman et al., 2004).

### 5.1.8.5 Characterization of the *Java plum seed* (*Syzgiumcumini*)

#### 5.1.8.5.1 SEM

The surface morphology of the *Java plum* examined by SEM in Fig 5.1.8.5 shows the scanning electron micrograph (SEM) of *Java plum* adsorbent used for adsorption studies. It was revealed from Fig 5.1.8.5.1 (a) and Fig 5.1.8.5.1 (b) that these adsorbents had irregular and porous surface.



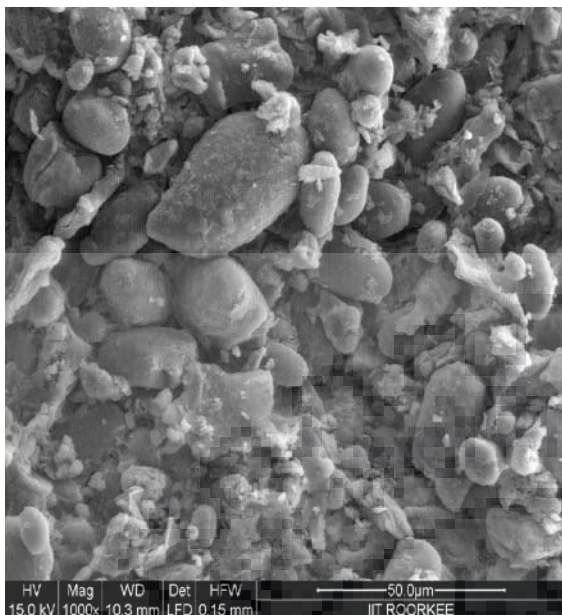
Difference in the adsorbent capacity of adsorbent *Java plum seed (Syzgiumcumini)* of different sizes) was mainly due to difference in their surface porosity.

#### 5.1.8.5.2 EDX

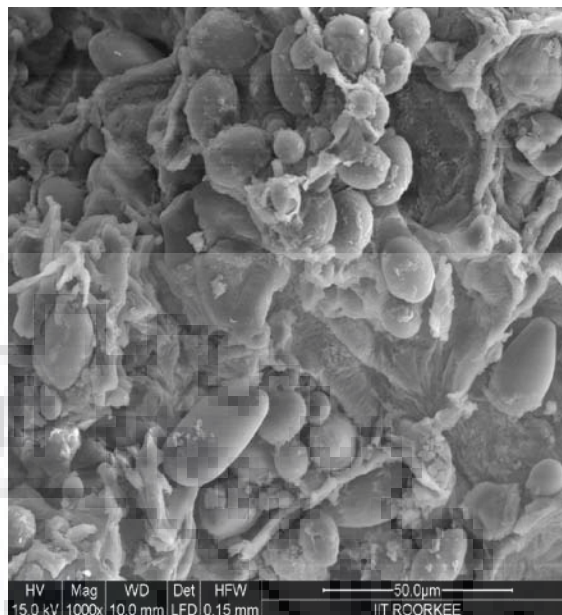
EDX of *Java plum seed (Syzgiumcumini)* before and after adsorption of fluoride ions are shown in Fig 5.1.8.5.2, it is clear that various elements such as carbon, oxygen and very small amount of calcium etc. were present in virgin adsorbent but fluoride was not present there. When the EDX of the adsorbent was carried out after the adsorption of fluoride ion, fluoride was present on the surface of adsorbent about 0.59 wt % which confirmed the adsorption of fluoride by these adsorbent (Singh, T. P., Majumder, C. B. 2016).

**Table 5.1.8.5.2 EDX analysis of *Java plum seed (Syzgiumcumini)* before and after adsorption of fluoride in tabular form**

Element	Weight % before Biosorption	Weight % after Biosorption
C K	48.9	49.5
O K	48.3	47.1
AlK	0.61	0.63
SiK	2.1	0.69
FK	–	0.59
MgK	–	0.23
CaK	–	1.3

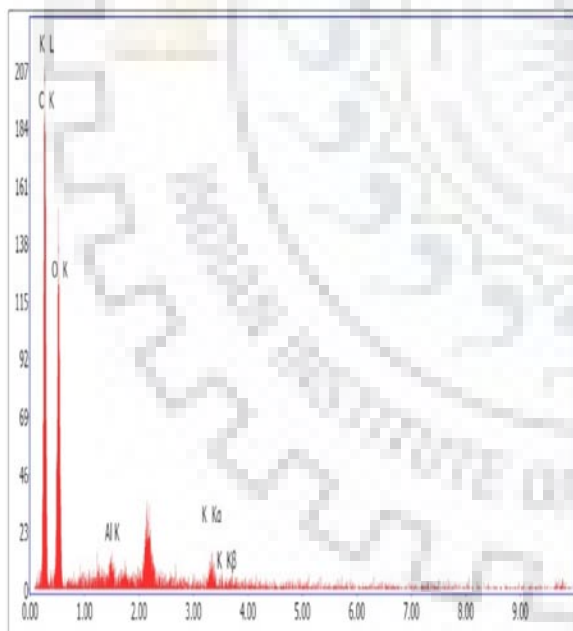


**(a) Java plum seed (*Syzygiumcumini*) before adsorption**

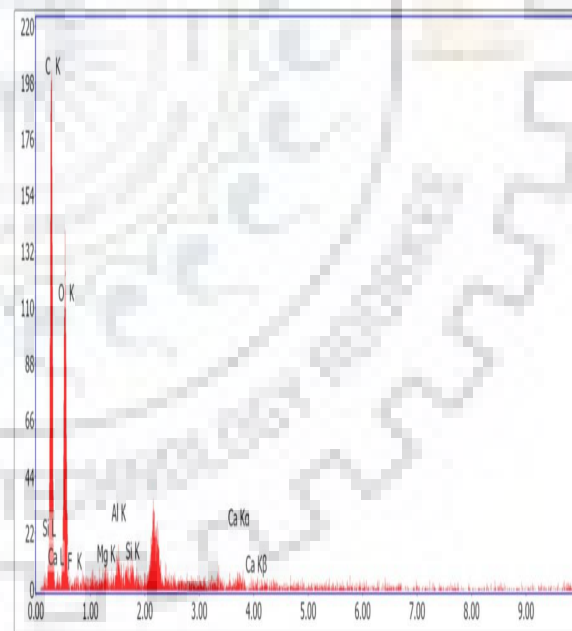


**(b) Java plum seed (*Syzygiumcumini*) after adsorption**

**Fig.5.1.8.5.1 SEM image of *Java plum seed (Syzygiumcumini)* before adsorption and after adsorption**



**(a) Java plum seed (*Syzygiumcumini*) before Adsorption**



**(b) Java plum seed (*Syzygiumcumini*) after Adsorption**

**Fig 5.1.8.5.2 EDX of *Java plum seed (Syzygiumcumini)* before and after adsorption**

### **5.1.8.5.3 Concluding Remarks on Continuous Adsorption Column Study Using *Java Plum Seed (Syzgiumcumini)***

In current study, the fluoride adsorption of *Java plum seed (Syzgiumcumini)* was studied for batch and fixed-bed column adsorption systems. Batch experiment indicates that the time to attain equilibrium was 1hr and adsorption followed the pseudo-second order kinetic model. Maximum adsorption of fluoride was achieved within the pH range 5.0-7.0. The adsorption of fluoride on java plum in batch system can be best described by Freundlich and Langmuir Isotherm. The adsorption capacity was shown in Table 5.1.8.3.4.2 (a) and (b). The bed column breakthrough curves were analyzed at different flow rates, bed depth and initial fluoride concentration. Thomas and BDST models were successfully used for predicting breakthrough curves for fluoride removal by affixed bed *Java Plum Seed (Syzgiumcumini)* using different flow rates and depth. Therefore, the use of *Java Plum Seed (Syzgiumcumini)* as an adsorbent for fluoride removal is potentially cost effective and may provide an alternative method for fluoride removal from contaminated water.

### **5.1.9 Continuous Study on *Citrus Limetta Peel (Bioremoval Process)***

#### **5.1.9.1 General**

Biological processes are a common phenomenon in our natural ecosystem. In the present work, organic pollutants are generally removal by simultaneous adsorption and bioaccumulation (SAB). Fluoride waste water industries are glass, electroplating, aluminium, steel, chemical industries, and oil Refinery. Concentration of fluoride in industrial waste water varies from 15 mg/L to 20 mg/L after coagulation process. Fluoride is essential but toxic when in excess for human health. In drinking water fluoride concentration should not be less than 0.5 mg/L and not to be exceeded than 1.5 mg/L.

#### **5.1.9.2 Optimization of Parameter**

##### **5.1.9.2.1 pH Optimization**

Optimization of pH is one of the important parameters. It affects the simultaneous adsorptive bioaccumulation of the pollutants. During SAB, optimum removal of pollutants occurred mostly in pH range of 6 to 7. In our case, maximum fluoride removal (93.14%) occurred at pH 5. From this study it has been observed that there is no significant difference in fluoride removal during pH range of 4-8. At pH 8, fluoride removal was 92.3%. So we can perform the next optimization parameters like time, initial concentration and dose of adsorbents at the neutral pH range. We are not performing

the experiment at pH 4 to avoid water become acidic and to avoid the consumption of acid. Fig. 5.1.9.2.1 shows graph between pH and Percentage removal. From graph we can easily see that maximum removal occurs in acidic region.

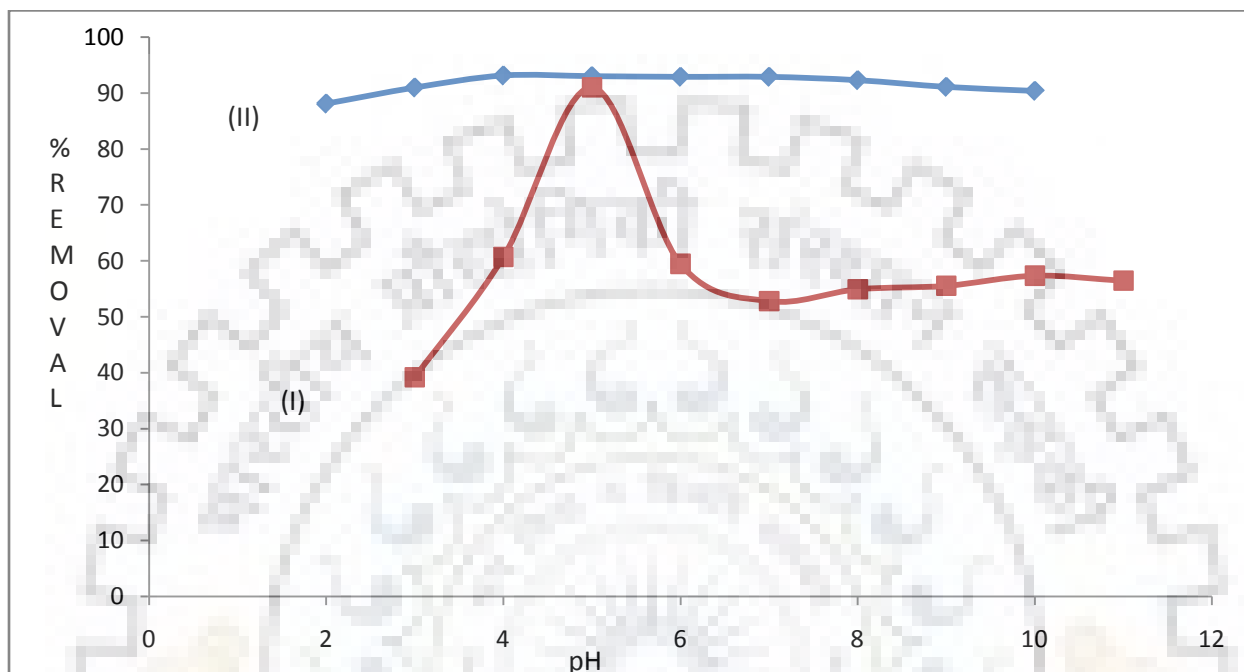


**Fig. 5.1.9.2.1** Graph Plotted between the Percentage Removal of Fluoride and pH (i) *Citrus Limetta peel alone* (ii) *SAB (CLP and bacteria)*

### 5.1.9.2.2 Dose Optimization

Adsorbent dose effect was studied on fluoride removal between the range of 4-20 mg/L at 20 mg/l of fluoride. Micro-organism takes the time 2h to grow. Adsorbent is added to immobilize the microorganism on adsorbent surface for 12h and then pollutant was added. The experiment was carried out at 30 °C and at 120 rpm for 70h after the addition of pollutant. Figure No. 5.1.9.2.2 shows that percentage Removal of fluoride increases up to 14 mg/L, after that percentage removal efficiency (92.99 - 93.2 %) is almost same for all rest dose of adsorbent i.e. in between 14-20 mg/l. Because of this reason the optimum adsorbent dose is 14 mg/L.

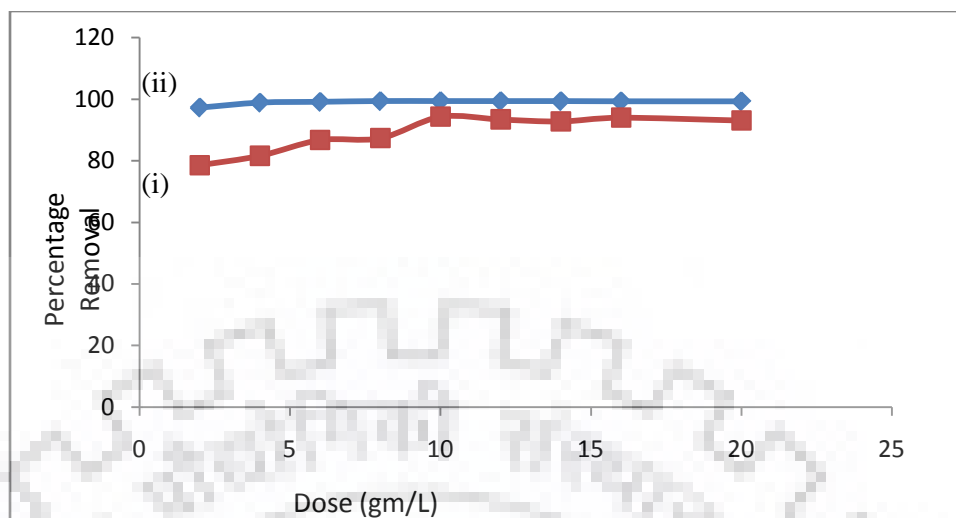


**Fig.5.1.9.2.2 Graph Plotted Between the Percentage Removal of Fluoride and Dose and Effect of Adsorbent Dose on the (ii) Bio Removal of Fluoride and (i) Citrus Limetta peel**

### 5.1.9.2.3 Initial Concentration

From the graph give the number the percentage removal of fluoride decreases as on increasing the initial fluoride concentration in case of bio removal (bio accumulation) like adsorption and adsorption capacity increases as on increasing the concentration of fluoride until the equilibrium was reached for a definite time (87h). It has been found that from the comparison between adsorption and bio accumulation processes, adsorption capacity as well as percentage removal both are high. Percentage removal of fluoride at equilibrium was obtained 93.0 % at 20 ppm concentration after 87 hours.

**Table 5.1.9.2.3: Cooperative Data for Different Optimization Parameters for Bioremoval and Adsorption**

Process	Initial Conc. (mg/L)	Contact Time	Optimum Dose (g/L)	Optimum pH	Adsorption Capacity $q_e$ (mg/g)	Percentage Removal
Adsorption	20	60 (min)	16	5	0.752	91.00
SAB	20	87 (h)	14	5	1.35	93.1

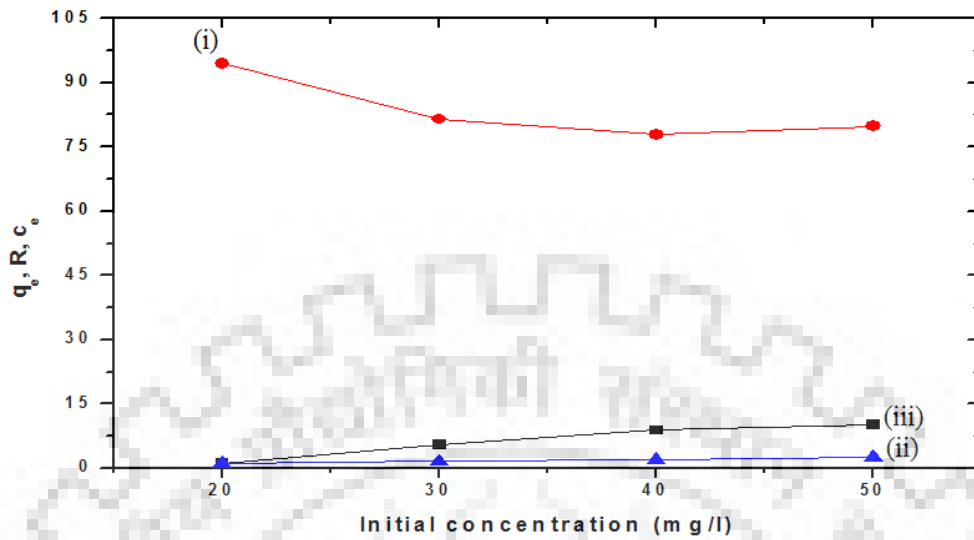


**Fig.5.1.9.2.3 Graph Plotted Between (i) Percentage Removal versus Initial Concentration (mg/l), (ii) Adsorption Capacity  $q_e$ (mg/g) and (iii) Residual Concentration  $c_e$ (mg/l).**

From the comparison between the adsorption and simultaneous adsorption and bioaccumulation, removal of fluoride increased at optimum pH, contact time, dose and same initial concentration. Adsorption capacity is also increased for simultaneous adsorption and bioaccumulation process. Contact time for SAB process is very high as compare to adsorption.

#### 5.1.9.2.4 Contact Time

Contact time was optimized in this study initially removal of fluoride increases on increasing the contact time for both the processes. Optimum time for biological process is high as compare to the value in case of adsorption only for sweet lemon adsorbent as shown in Fig. 5.1.9.2.4.

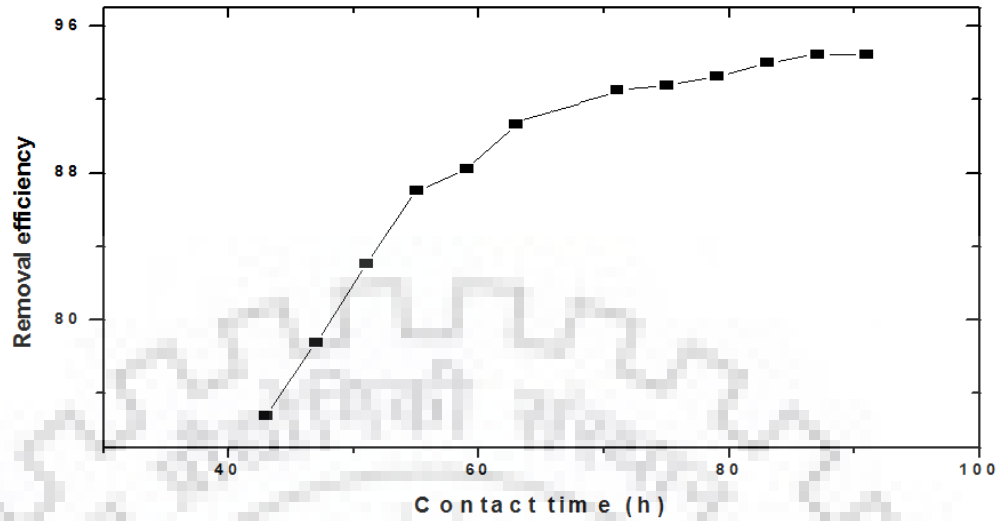


**Fig. 5.1.9.2.4 Graph Plotted Between the Percentage Removal of Fluoride and Contact Time (h) on the Bio Removal of Fluoride**

### 5.2.0 SAB Adsorption Kinetics

#### 5.2.0.1 Pseudo-first Order Model (Liljana et al., (2001))

$$\log(q_e - q_t) = \log(q_e) - \frac{k_1}{2.303} t$$

Where,

$q_t$  Adsorption after time  $t$  (mg/g)

$q_e$  Adsorption at equilibrium (mg/g)

$k_1$  Rate constant for the first order model ( $\text{h}^{-1}$ )

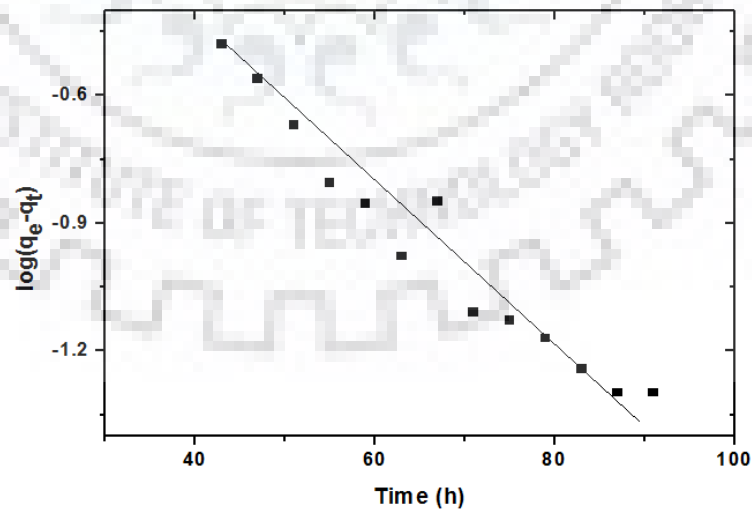


**Fig. 5.2.0.1 Pseudo First Order Kinetics Plotted between Log ( $q_e - q_t$ ) versus Time (h)**

### 5.2.0.2 Pseudo-Second-Order Model (Christian et al., 2005)

$$\frac{t}{q_t} = \frac{t}{q_e} + \frac{1}{K_2 q_e^2}$$

Where,

$q_t$  Adsorption after time  $t$  (mg/g)

$q_e$  Adsorption at equilibrium (mg/g)

$K_2$  Rate constant for second order model ( $\text{g mg}^{-1} \text{h}^{-1}$ )

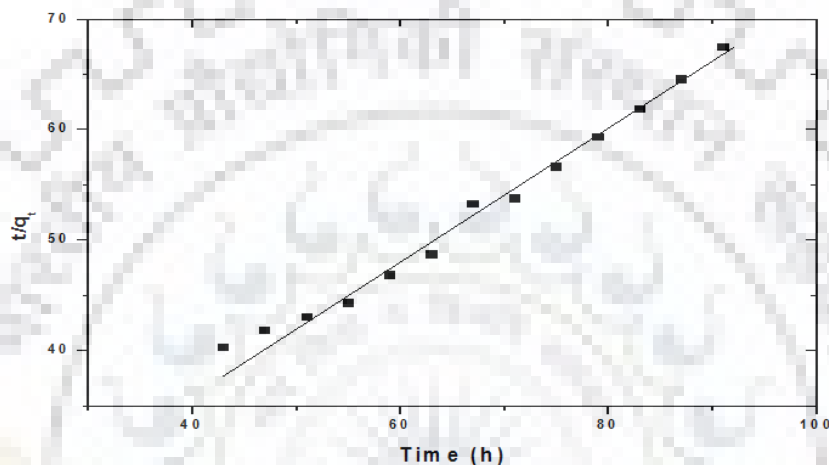


Fig. 5.2.0.2 Pseudo Second Order Kinetics Plotted between  $t/q_t$  versus Time (h)

Table 5.2.0.2: Comparison Table for Kinetic Study in Bio-Removal and Adsorption Process.

Adsorbent	Pseudo-first order			Pseudo-second-order		
	$K_1$	$q_{ecal}(\text{mg/g})$	$R^2$	$K_2$	$q_{ecal}(\text{mg/g})$	$R^2$
SAB	$0.042(\text{h}^{-1})$	8.1	0.95	$0.0245(\text{h}^{-1})$	1.7	0.99
<i>Citrus Limetta Peels</i>	$0.086(\text{min}^{-1})$	0.509	0.96	$0.295(\text{min}^{-1})$	0.795	0.99

### 5.2.0.3 Concluding Remarks

From the comparison table adsorption capacity of bio removal process is greater than adsorptive process. In both process, pseudo-second-order kinetic model favours because of its greater regression coefficient value. Calculated adsorption capacity  $q_{ecal}$  (1.7 mg/g) for bio removal adsorption is too close to experimental value ( $q_e = 1.4$ ) for second order kinetic. Similarly, for



adsorptive process experimental value (0.752 mg/g) is near to the calculated value (0.795 mg/g). So both processes follow the pseudo-second-order kinetic model.

### 5.2.1 SAB Adsorption Isotherms

Since SAB and adsorption are isothermal processes; adsorption isotherms are used to explain these processes. The fundamental importance of the equilibrium adsorption isotherms is to design of adsorption system. Parameters of bioaccumulation equilibrium and adsorption are easily characterized by adsorption isotherms. These parameters are helpful in determining the adsorption capacity of adsorbent materials. In order to evaluate an adsorption isotherm, it is fundamental to develop an equation which precisely represents the results and which may be used for design purpose. Conventional adsorption models are used to describe the equilibrium established between adsorbed component on the adsorbent and unadsorbed component in solution (represented by adsorption isotherms). To analyze the equilibrium data for adsorption and bioaccumulation of fluoride by *citrus limetta peel*-immobilized *Actinobacter baumannii*, Langmuir, Freundlich, Temkin and Linear Adsorption models were used.

#### 5.2.1.1 Langmuir Model

Langmuir model is as given in equation (Ghorai and Pant, 2005)

$$q_e = \frac{KaC_e}{1 + aC_e}$$

Where K and a are isotherm constants.

Langmuir constant (K) is fluoride adsorbed per unit weight of adsorbent, at equilibrium time. Langmuir constant (a), energy related to adsorption (i.e. affinity of the binding sites). Langmuir equation is valid for monolayer sorption unto a surface with a finite number of identical sites. The basic assumption of Langmuir model is that sorption takes place at specific sites within the adsorbent. Separation factor is the essential characteristics of Langmuir isotherms can be described in equation below (Bohart and Adams, 1920)

$$R_L = \frac{1}{1 + aC_e}$$

The separation factor (R) indicates the isotherm shape as follows:  $R < 1$  unfavourable,  $R > 1$  unfavourable,  $R = 1$  linear,  $0 < R < 1$  favourable and  $R = 0$  irreversible.

The plot for Langmuir isotherm for bioremoval and adsorption is shown in fig. 5.2.1.1 (a) and (b).

### 5.2.1.2 Freundlich Isotherm

Freundlich isotherm model is given in equation

$$q_e = K_f C_e^{\frac{1}{n}}$$

Where,

$K_f$  and  $n$  are Freundlich constants.

$K_f$  is roughly an indicator of the adsorption capacity and  $n$  is the adsorption intensity.

The Freundlich isotherm is used for heterogeneous surface energy systems.

The plot for Freundlich isotherm for bioremoval and adsorption is shown in fig. 5.2.1.2 (a) and (b).

### 5.2.1.3 Temkin Model

Temkin Model Equation given as (Hutchins, 1973)

$$q_e = \frac{RT}{b_T} \ln(A_T) + \frac{RT}{b_T} \ln(C_e)$$

Where,

R Universal gas Constant

T Temperature (K)

$q_e$  Adsorption capacity (mg/g)

$c_e$  Equilibrium concentration (mg/l)

$A_T$  Adsorption constants

$b_T$  Adsorption constants.

The plot for Temkin model for bioremoval and adsorption is shown in fig. 5.2.1.3 (a) and (b).

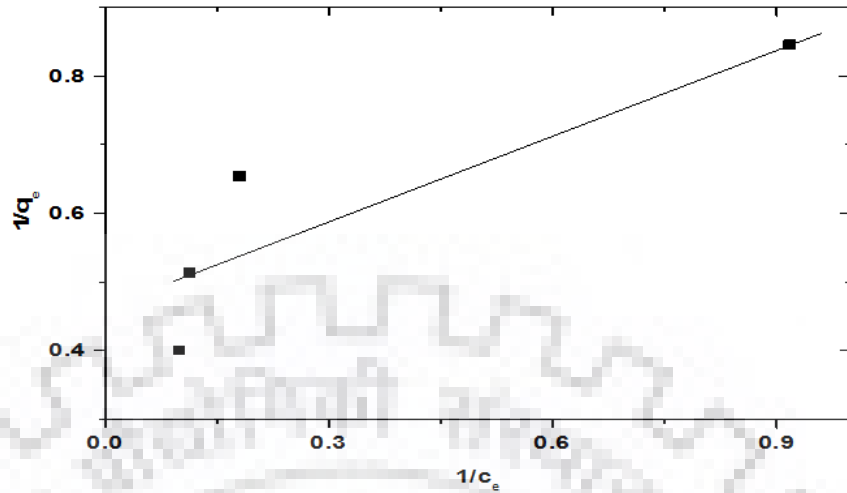


**Fig.5.2.1.1 (a) Graph for Langmuir Isotherm Model Plotted between  $1/q_e$  vs.  $1/c_e$  for Bio Removal**

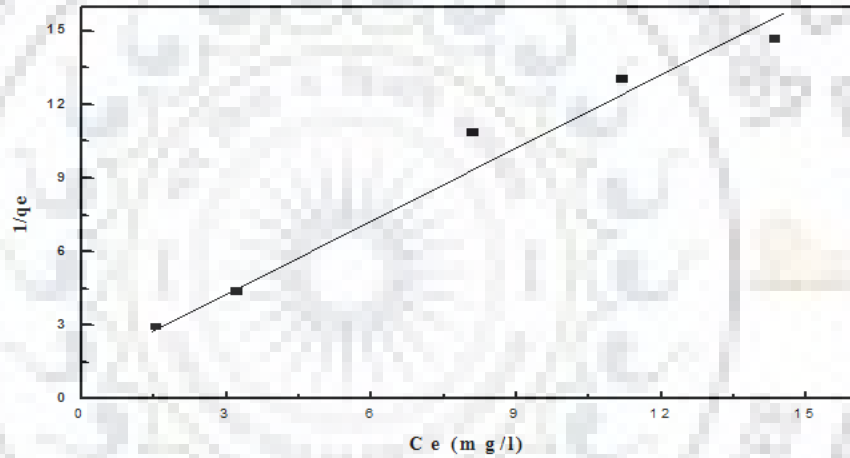


**Fig. 5.2.1.1 (b) Graph for Langmuir Isotherm Model Plotted between  $1/q_e$  vs.  $1/c_e$  for Adsorption**

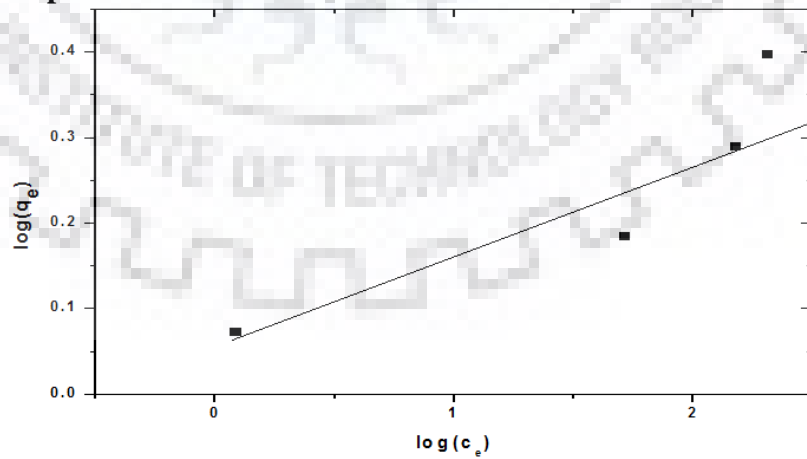


**Fig. 5.2.1.2 (a) Graph for Freundlich Isotherm Model Plotted between  $\log(q_e)$  vs.  $\log(c_e)$  for Bio Removal**

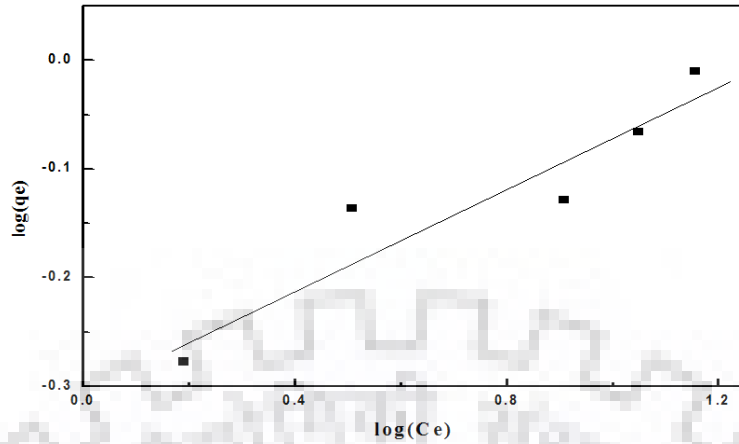


**Fig. 5.2.1.2 (b) Graph for Freundlich Isotherm Model Plotted between Log ( $q_e$ ) vs.  $\log(c_e)$  for Adsorption**

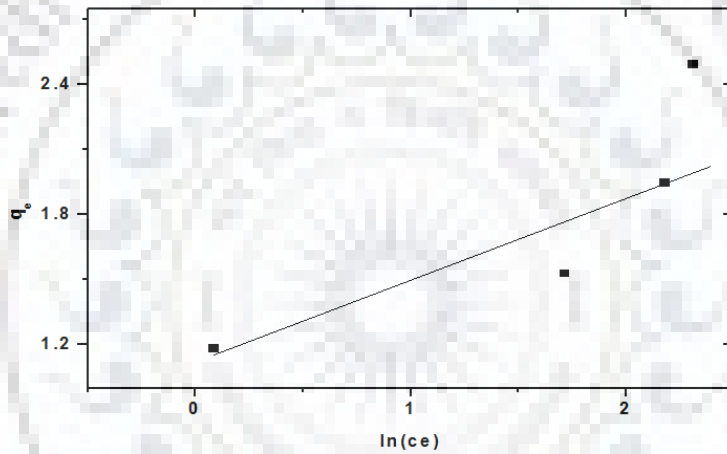


**Fig. 5.2.1.3 (a) Graph for Temkin Isotherm Model Plotted between  $q_e$  vs.  $\ln(c_e)$  for Bio Removal**

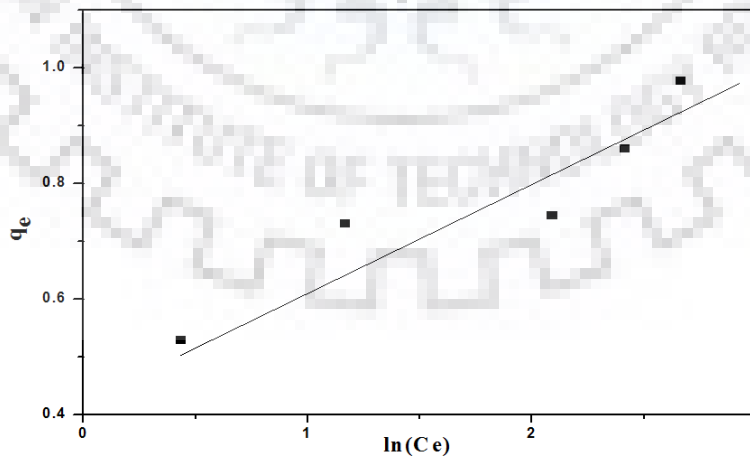


**Fig. 5.2.1.3 (b) Graph for Temkin Isotherm Model Plotted Between  $q_e$  vs.  $\ln(c_e)$  for Adsorption**

**Table 5.2.1 Comparative Data for Adsorption Isotherm for Adsorptive and Bio Removal**

Process	Adsorbent	Langmuir			Freundlich			Temkin		
		K (mg/g)	b (L/mg)	R <sup>2</sup>	K <sub>f</sub> (mg/g)	n	R <sup>2</sup>	A <sub>T</sub> L/mg	b <sub>T</sub> KJ/mol	R <sup>2</sup>
Adsorption	<i>Citrus Limetta Peels</i>	0.554	1.037	0.97	0.500	4.22	0.88	16.69	14.9	0.87
SAB	<i>Citrus Limetta Peels Actinobacter micro- organism</i>	12.6	4.1	0.85	4.1	0.292	0.88	106.2	2.5	0.79

From the study of isotherm models for both processes, it has been found that the values of isotherms parameters for all models have been increased by using bioaccumulation processes as shown in Table .5.2.1.

## 5.2.2 SAB Continuous Reactor Study Treatment of Fluoride Bearing Contaminated Water Using SAB in a Laboratory Scaled up – Flow Bio – Column Reactor by *Java plum seed (Syzygiumcumini)*

### 5.2.2.1 Materials and Methods

#### 5.2.2.1.1 Chemicals

All the chemicals used in this study were of analytical reagent grade and were purchased from Himedia Laboratories Pvt. Ltd. Mumbai India. All the solutions were prepared in milli-Q water (Q-H<sub>2</sub>O, Millipore corp. with resistivity of 18.2 MΩ- cm). Fluoride solution of 2000 mg/L was prepared by dissolving 4.42 gm of sodium fluoride (NaF) in 1L of millipore water.

#### 5.2.2.1.2 Strains and Medium

*Acinetobacter baumannii* MTCC 11451 was used in the present study. This bacterium was supplied by Microbial type culture collection, Chandigarh, India. The strains were revived according to the instructions given by MTCC (MTCC guidelines). Cultures were stored on agar plates till further use and were sub cultured after every 15-30 days. All inoculations were performed in aseptic conditions in laminar air flow unit (rescholar equipment, India). The composition of growth media specific to above mentioned strain is given in Table 5.2.2.1.2

**Table 5.2.2.1.2: Composition of Media for Microorganisms**

Micro-organisms	Media compositions	(g/l)
<i>Acinetobacter baumannii</i> (MTCC 11451)	Sodium Chloride, NaCl	(10)
	Tryptone	(10)
	Yeast Extract	(5)

### 5.2.2.1.3 Acclimatization

The acclimatization of all four strains in fluoride environment was performed as follows:

The culture was sub-cultured from agar plate in 100 ml of steam sterilized prescribed media (Table.5.2.2.1.2) in 250 ml round bottom flask. The media was supplemented with 20mg/l of fluoride. The conical flask were agitated/incubated in an incubator shaker (Metrex MO-250, India) at room temperature (30°C) with agitation speed of 120 rpm for 24 hours. After 24 hours the synthetic medium in flask turned turbid indicating significant bacterial growth in the flasks.

### 5.2.2.1.4 Batch Bioaccumulation Experiments

Batch experiments were carried out in 250 ml round bottom flask with working volume of sample 100 ml at 30°C and 120rpm in an incubator cum-orbital shaker (Metrex, MO-250, India). The flask were covered with both cotton plug and aluminium crimp cap. All the flasks containing growth medium were steam sterilized in an autoclave at 121±1°C for 45 min at 15psi pressure. All the batch experiments were conducted for the optimization of parameters like contact time, initial concentration, pH and dose of adsorbents. Microbial culture grows in 21 hour and dead phase started after 71h from the study of growth curve of microbial culture. A preliminary test showed that the equilibrium adsorption and bio-accumulation contact time was obtained after 86 hour. At the end of this period, the solutions were centrifuged and residual concentrations of fluoride at the equilibrium were determined.

### 5.2.2.1.5 Experimental Setup

The experimental setup to remove fluoride from industrial waste water is carried in a bio reactor column of SS pipe was shown in Fig.3.3.2 (a) and (b) in section 3.3.2. The length of SS pipe column varied by 20 cm each starting from  $Z_1 = 20$  to  $Z_5 = 100$  cm, internal diameter of 9 cm, height 100 cm and net volume 6.4 lit. It was equipped with a total of four equidistant ports (excluding inlet and outlet) of 1.3 cm diameter for collecting liquid sample along the height of reactor. The top portion

and the bottom portion were connected with the main column using two flange joints, supported on SS screen (mesh no: 16 BSS, width aperture: 1.00 mm). The reactor was filled with weighted amount of *Java plum seed (Syzgiumcumini)* having a particle size of 2-4 mm as a fixed-bed adsorber. The bed was supported and closed using cotton pad and rubber, respectively, to prevent the flow of adsorbent along with the effluent. Then, the bed was rinsed with distilled water and left over night to ensure a closely packed arrangement of particle without voids, channels, or cracks. Synthetic fluoride solution of known concentration (20 mg/L) was fed through a bed of *Java plum seed (Syzgiumcumini)* in up-flow mode to avoid channelling due to gravity and to ensure a uniform distribution of the effluent throughout the column. The experiments were carried out at room temperature. A peristaltic pump was used to control the flow rates (12, 23 and 40 ml/min) and the flow rates were maintained constant during each experiment. Periodic flow rate check carried out by collecting sample at the effluent for a given time and measured using measuring cylinder. Samples of effluent were collected at 1h intervals and analyzed using Spectrophotometric (SPADNS) method for fluoride ion concentration using UV spectrophotometer (Hach, DR 5000). The volume of treated water was measured at 1h interval and the average flow rate was calculated based on these values, because the flow rate becomes unstable due to various bed depth conversion varied flow resistance. The desired breakthrough concentration ( $C_b$ ) was determined at 7.5 % of the initial concentrations (20 mg/L).

#### **5.2.2.1.5.1 The Empty Bed Residence Time Model (EBRT)**

The Empty Bed Residence Time (EBRT) is a design parameter for the design of an adsorber. Major design parameters are:

- (i) Empty Bed Residence Time (EBRT) or Empty Bed Contact Time (EBCT).
- (ii) Adsorbent exhaustion rate.

These parameters can be correlated for a fixed bed column to determine the operating and capital costs of adsorption system (Perrich, 1981, Mckay and Bino, 1990. Negrea et al. 2011, Guo et al. 2008) and has been reported that empty bed contact time is a critical parameter in the adsorption processes especially if the adsorption mainly depends on the contact time between the adsorbent and adsorbate.

The empty bed residence time EBRT is defined as the time required for the liquid to fill the empty column and it determine the residence time during which the solution treated is become constant with the adsorbent:

$$EBRT (min) = \frac{Bed\ volume}{Volumetric\ flow\ rate\ of\ the\ liquid} \quad (3)$$

The adsorbent exhaustion rate is the mass of the adsorbent used per volume of liquid treated at the breakthrough:

$$Adsorbent\ exhaustion\ rate\ (g/L) = \frac{Mass\ of\ adsorbent\ used}{Volume\ of\ liquid\ treated\ at\ breakthrough} \quad (4)$$

The adsorbent exhaustion rates are plotted against the EBRT values, and a single operating line can be constructed to correlate these two variables. Thus, to select the optimum combination of adsorbent exhaustion rate and the liquid retention time, the operating line should first be established.

The equation (3, 4) reveals that with the lower adsorbent exhaustion rate ,volume treated at the breakthrough point become larger and hence longer EBRT and smaller amount of adsorbent is needed per unit volume of feed treated which implies a lower operating cost; however, larger column will have to used. On the other hand, the higher the adsorbent exhaustion rate, the smaller the EBRT, the higher the operating cost and smaller column is needed which will reduce the construction cost.

#### 5.2.2.1.5.2 Fixed-Bed Design Models

The Bed Depth Service Time model (BDST), the Empty Bed Residence Time model (EBRT) and the Thomas model are selected for this study, which are used to predict, optimize and describe the fixed-bed column operation, respectively.

#### 5.2.2.1.5.3 Bed Depth Service Time Model

Fig.5.2.2.1.5.3 shows the BDST plots ( $T_b$  versus  $D$ ), which is constructed from the Table 5.58 for the influent fluoride concentration of 20mg/l and flow rates of 12, 23 and 40ml/min at 7.5 % breakthrough time for 20, 40, 60 and 100 cm bed heights. The coefficients  $N_0$  and  $K$  for the three flow rates are calculated based of equation.



$$T_b = \frac{N_0 D}{C_0 v} - \frac{1}{K C_0 \ln\left(\frac{C_0}{C_b} - 1\right)}$$

Where,

- $T_b$  Service at breakthrough point (h),
- $N_0$  Bed capacity ( $\text{mg cm}^3$ ),
- $D$  Packed-bed column depth (cm),
- $v$  Linear flow rate through the bed ( $\text{cm h}^{-1}$ ),
- $C_0$  Influent fluoride concentration (mg/L)
- $C_b$  Breakthrough fluoride concentration (mg/L)
- $K$  Adsorption rate constant ( $\text{L mg}^{-1} \text{h}^{-1}$ ),

The equation of a straight line on BDST curve can be expressed as  $y = ax + b$ ;

Where,

- $y$  Service time,
- $x$  Bed depth,
- $a$  Slope,
- $b$  Ordinate intercept.

The numerical value of the slope ( $a$ ) =  $N_0/C_0 v$  and the intercept ( $b$ ) =  $-\frac{1}{K C_0 \ln\left(\frac{C_0}{C_b} - 1\right)}$ , the adsorptive capacity of the system,  $N_0$  and the rate constant,  $K$ , can be evaluated from the slope and intercept of a straight line plotted as the service time against the bed depth from experimental data, respectively. The minimum bed depth ( $D_{\min}$ ) which represents the theoretical depth of adsorbent able to prevent the adsorbent concentration from exceeding  $C_b$  is obtained when  $T_b = 0$ , according to the following equation:

$$D_{\min} = \frac{v \ln\left(\frac{C_0}{C_b} - 1\right)}{K N_0}$$

The slope of the line presented by  $y = ax + b$  can be used to predict the performance of the bed, if there is change in the initial solute concentration  $C_{01}$  to a new  $C_{02}$ . Hutchins (Hutchins, 1973) proposed that the new slope  $a_2$  and new intercept  $b_2$  can be estimated by Eq.

$$a_2 = \frac{a_1 C_{01}}{C_{02}}$$

$$b_2 = \frac{b_1 C_{01}}{C_{02}} \frac{\ln\left(\frac{C_{02}}{C_b} - 1\right)}{\ln\left(\frac{C_{01}}{C_b} - 1\right)}$$

(Mckay et al., 1984) stated that if design data are required for a change in volumetric flow rate of solute to the some adsorption system, the new slope with the intercept remaining unchanged can be written as:

$$a_2 = \frac{a_1 Q_1}{Q_2} = \frac{a_1 v_1}{v_2}$$

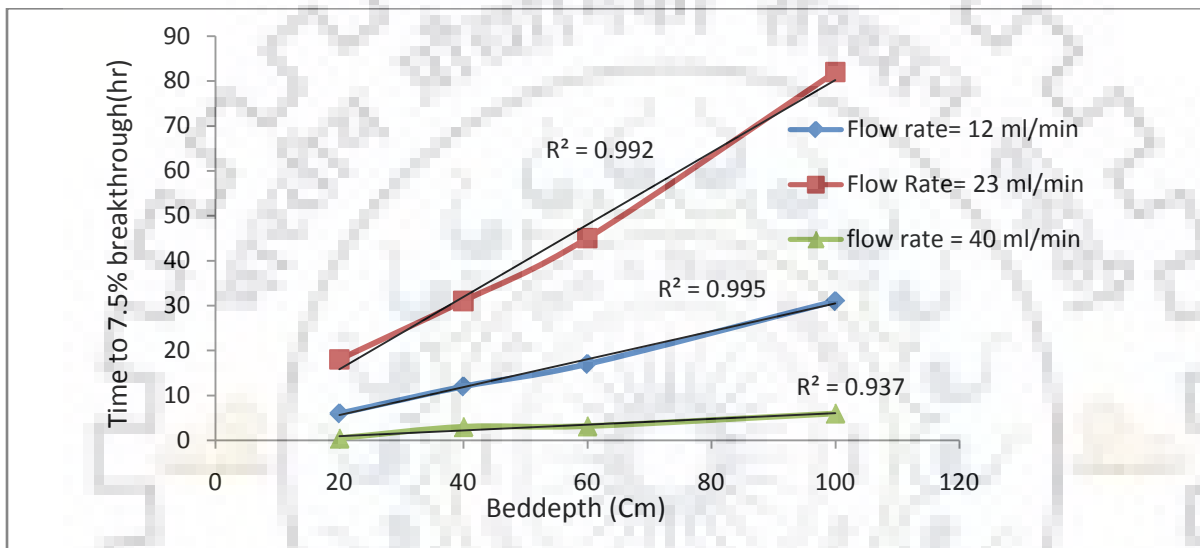


**Fig.5.2.2.1.5.3 BDST Plot at 7.5% Breakthrough in a Fixed-Bed Column at Different Flow Rates**

**Table 5.2.2.1.5 (a) Data of Variable Bed Depth at a Fixed Flow Rate in a Fixed-bed Bio Column Reactor for the Removal of 20mg/l of Fluoride by *Java plum seed (Syzygiumcumini)***

Q flow rate (ml/min cm <sup>2</sup> )	Bed height (cm)	Bed volume (cm <sup>3</sup> )	Weight of adsorbent m (g)	EBRT (min)	V <sub>b</sub> (L)	T <sub>b</sub> (hrs)	Adsorbent exhaustion rate (g/L)
12 ml/min 0.1886 (ml/min cm <sup>2</sup> )	20	1272.3	483.4	106.0	4.4	6	109.8
	40	2544.7	969.1	212.0	9.0	12	107.4
	60	3817.0	1451.9	318.0	12.1	17	119.9
	100	6361.7	2419.9	530.1	21.3	31	113.4
23ml/min 0.3615 (ml/min cm <sup>2</sup> )	20	1272.3	483.4	55.3	22.8	18	21.2
	40	2544.7	969.1	110.6	43.5	31	22.3
	60	3817.0	1451.9	165.9	63.7	45	22.8
	100	6361.7	2419.9	276.6	74.1	82	32.6
40ml/min	20	1272.3	483.4	31.8	1.1	0.45	450.1

Q flow rate (ml/min cm <sup>2</sup> )	Bed height (cm)	Bed volume (cm <sup>3</sup> )	Weight of adsorbent m (g)	EBRT (min)	V <sub>b</sub> (L)	T <sub>b</sub> (hrs)	Adsorbent exhaustion rate (g/L)
0.6287 (ml/min cm <sup>2</sup> )	40	2544.7	969.1	63.6	7.6	3	127.9
	60	3817.0	1451.9	152.7	12.1	3.2	120.1
	100	6361.7	2419.9	159.0	19.3	6	125.5

**Table 5.2.2.1.5 (b) Constant of BDST curve**

Q flow rate (ml/min cm <sup>2</sup> )	V (cm/hr)	Slope (hr/cm)	Intercept (hr)	Depth D (cm)	N <sub>0</sub> (mg/L)	K (L mg <sup>-1</sup> hr <sup>-1</sup> )	X (mg/g)	R <sup>2</sup>
0.1886	11.3	0.311	-0.628	2.0	70.7	0.2	0.171	0.99
0.3615	21.7	0.805	-0.314	0.744	182.9	0.4	0.865	0.99
0.6287	37.7	0.064	-0.384	166.5	1.7	0.327	0.110	0.94

#### 5.2.2.1.5.4 Effect of Flow Rate

The performance of a bio-column reactor is highly determined by its flow rate. Contact time is directly proportional to flow rate thus increasing the flow rate will increase in contact time which will eventually result in less concentration of pollutants in the output. But we must consider the fact that with the increase in flow rate treatment capacity of the reactor decreases. In literature a wide range of flow rate values have been used.

Generally, for laboratory purposes flow rate with low value is used to treat industrial water by indigenous microbes. In the said process, tap water (without inoculated media) is passed for 2-3 days in order to get a biolayer of microbes. However, longer the flow rate is normally used for the treatment of industrial effluents, where microbe inoculated media is used to develop the bio-layer on the adsorbent bed. In the present study, we choose three flow rate (12, 23 and 40 ml/min) and study the effect of flow rate on the fluoride concentration in the treated water. Fig.5.2.2.1.5.4 depicts data collected from top of the reactor. From Fig.5.2.2.1.5.4 it is evident that for all the flow rate values the fluoride concentration in the treated water increases initially and after ~4-5 hours, it starts to decrease.

After 30 hours the fluoride concentration in the treated water reduces to ~1.5 ppm, which is below the minimum concentration layer (MCL) of fluoride in industrial wastewater. Maximum

concentration of fluoride in the treated water is found after ~3 hour of operation, which reduces gradually with operation time. This indicates that the microbes need some time to adjust in the continuous operation of the reactor.

Similar observation has been reported recently during the fluoride removal in a bio-column reactor using SRB (Jong and Parry, 2003). With the increase in flow rate value, the contact time of the water sample with the bio-layer increases. Due to this reason fluoride concentration in the treated water using a flow rate value of 18 h is less than those obtained by flow rate values of 12 and 6 h. For higher flow rate values, the water sample gets lower contact time with adsorbent and at the initial stage of operation; it leaves the reactor before the microbes of the bio-film cope up with the continuous operation. Hence, at the initial stage of operation the fluoride removal is less. With the increase in time bacterial mass accommodate them in the continuous mode of operation. Effect of flow rate on the fluoride removal becomes negligible after ~30 hours at high flow rate. Hence, flow rate of 23ml/min is optimum for the bio-treatment process.

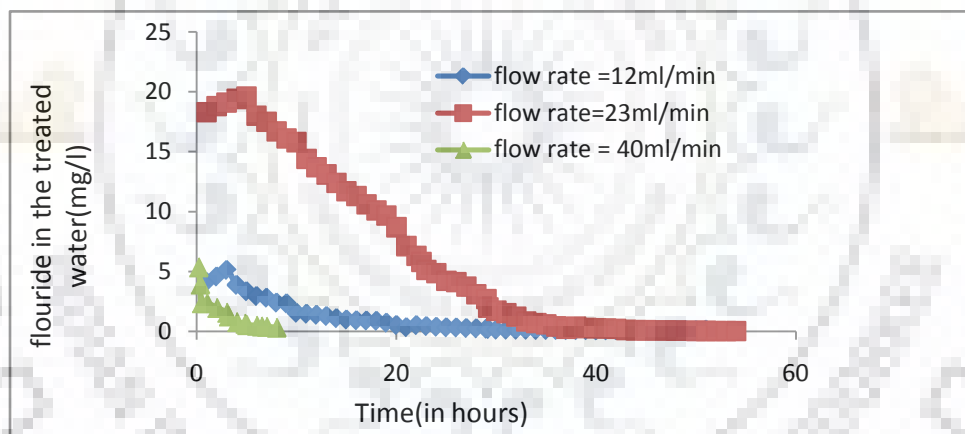
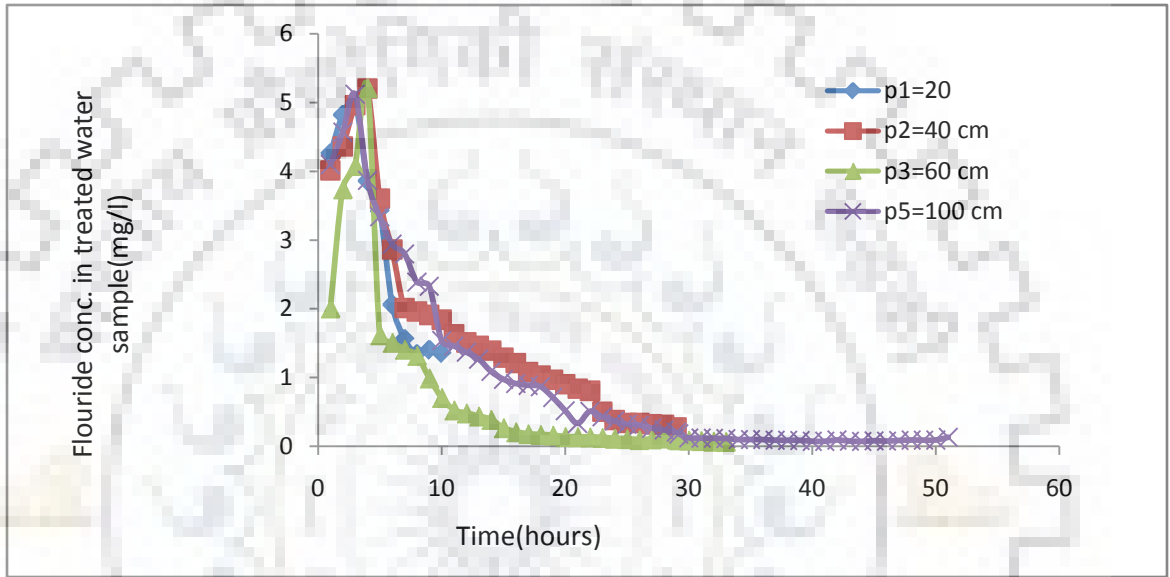


**Fig.5.2.2.1.5.4 Effect of Flow Rate on the Fluoride Removal in the Biocolumn Reactor (Height=100cm, Initial Fluoride Concentration= 20mg/L)**

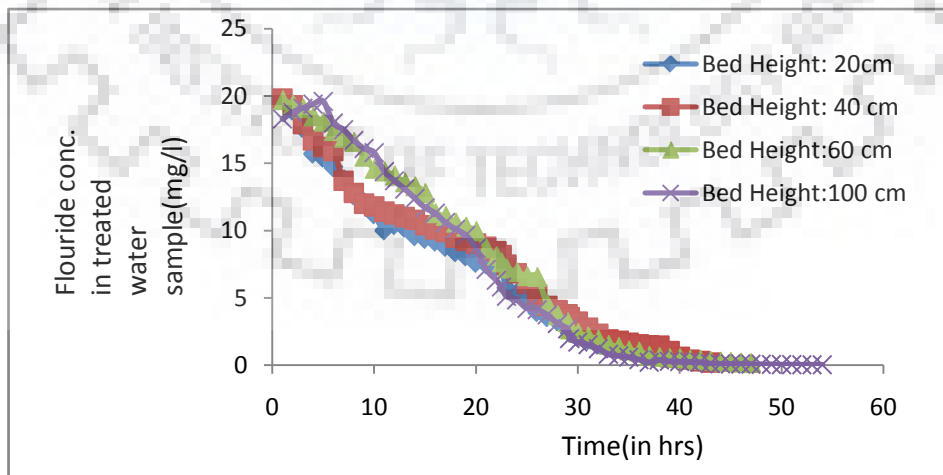
#### 5.2.2.1.5.5 Effect of Bed Height

When we vary bed height keeping flow rate constant we observe a change in contact time of the sample. Fig.5.2.2.1.5.5 (a-c) and Fig.5.2.2.1.5.6 shows the effect of changing bed height on the fluoride concentration in treated water at flow rate of 12, 23 and 40 ml/min. Figures were in good agreement with the trend as mentioned in literature (Mondal and Majumder, 2007). From Fig.5.2.2.1.5.6 and Fig.5.2.2.1.5.7 (a), (b), it is clear that fluoride concentration decreases to ~1.5 ppm which is MCP of fluoride in waste water after 7,12,6 and 10 hours after starting reactor from

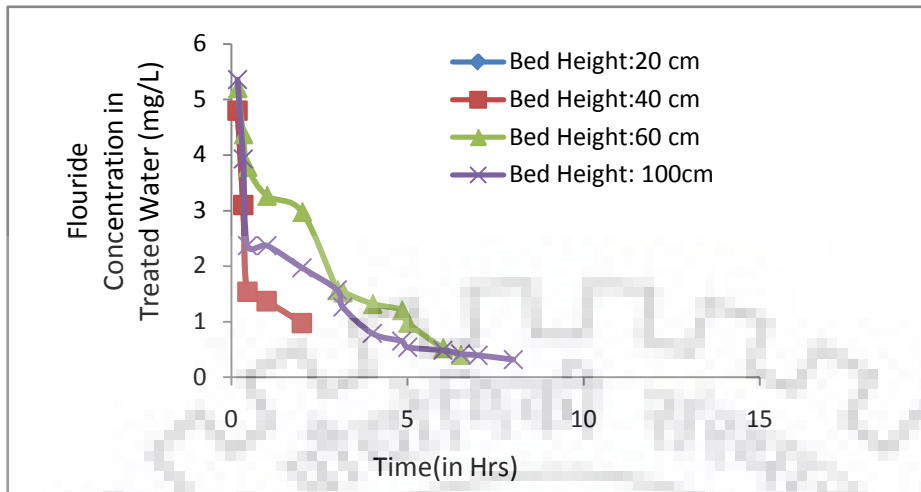
point P<sub>1</sub>, P<sub>2</sub>, P<sub>3</sub> and P<sub>5</sub> respectively when flow rate was 12ml/min. All of the data were recorded in Table.5.2.2.1.5 (a) and (b). Initially bacteria took some time to settle them in the continuous flow of operation of the reactor. From Fig.5.2.2.1.5.4, Fig.5.2.2.1.5.5 (a) and (b), we can observe that when we decrease the bed height, decrease in contact time is noted which results into lower fluoride removal from waste water. After some time when bacteria are adjusted in the reactor, the effect of bed height tends to diminish.



**Fig.5.2.2.1.5.5 (a) Effect of Bed Height on Fluoride Removal in the Bio-Column Reactor (Flow rate: 12 ml/min, Initial Fluoride Concentration= 20mg/L)**



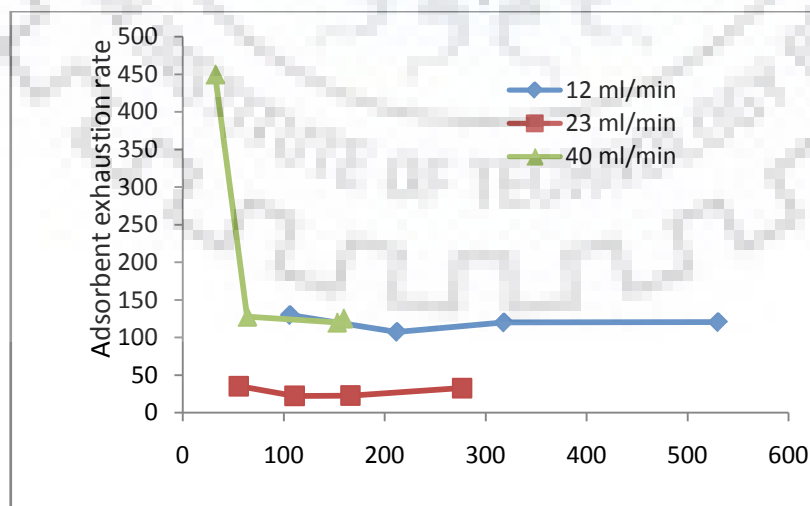
**Fig.5.2.2.1.5.5 (b) Effect of Bed Height on Fluoride Removal in the Bio-Column Reactor (Flow Rate: 23 ml/min, Initial Fluoride Concentration = 20mg/L)**



**Fig.5.2.2.1.5.5 (c) Effect of Bed Height on Fluoride Removal in the Bio-Column Reactor (Flow Rate: 40 ml/min, Initial Fluoride Concentration= 20mg/L)**

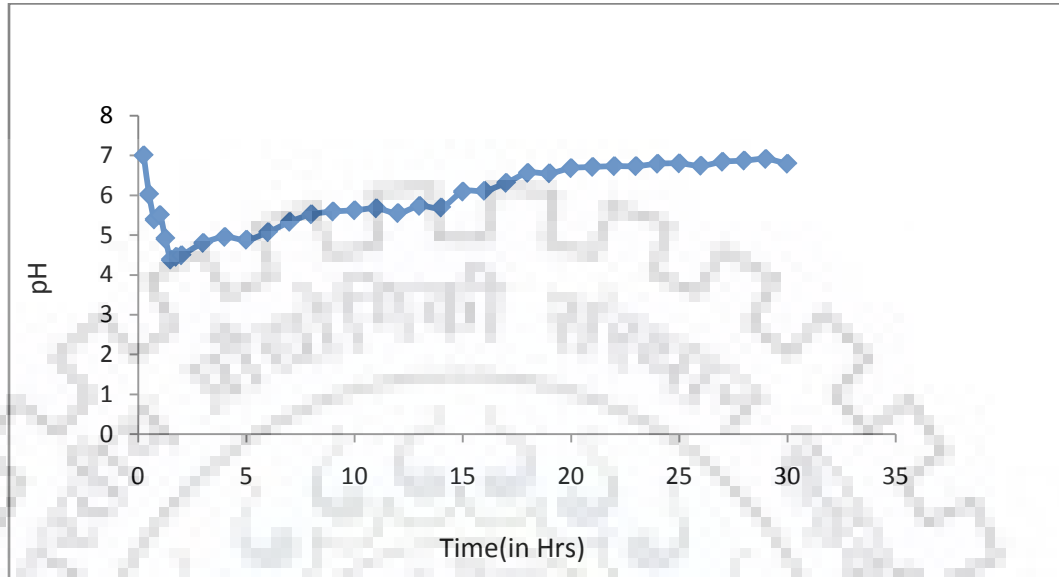
#### 5.2.2.1.5.6 Effect of Empty Bed Contact Time

Fig.5.2.2.1.5.6 shows the plot in which adsorbent exhaustion rate is represented on Y-axis and X-axis is denoted by EBRT. This graph is plotted at various adsorbent bed heights (20, 40, 60, 100 cm) from the Fig.5.2.2.1.5.6. It can be clearly depicted that for flow rate 40 ml/min the value of adsorbent exhaustion rate decreases gradually with increase in EBRT. In Table.5.2.2.1.5 (a), we have recorded various data which validated that with the increase in bed depth we can observe an increase in  $V_b$ ,  $T_b$  and EBRT of the bio-column reactor. It is evident that with increase in EBRT at a constant flow rate, we will get higher value of bed volume, which gives access to treat more solution but results in lower adsorbent exhaust rate.



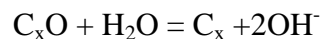
**Fig.5.2.2.1.5.6 Adsorbent Exhaustion Rate versus EBRT**

### 5.2.2.1.5.7 Variation of pH and DO (Dissolved Oxygen) of Treated Waste Water with Time



**Fig. 5.2.2.1.5.7 (a) Change of pH with Time of Operation in Bio-Column Reactor**

Another important point which is noted during the experiment is the slight change in the pH with the time as shown in Fig. 5.2.2.1.5.7 (a). The graph plotted in Fig. 5.2.2.1.5.7 (b) is for the waste water collected from top of bioreactor (height=100cm) when flow rate of pollutant is 23ml/min. From figure 5.2.2.1.5.7, it is evident that initially the pH decreases slightly and starts to increase after 2 hours of operation of the reactor, which signifies that the bacteria is adapted in the new environment. After around 25 hours of operation the pH reaches 7.5. Similar change in pH was reported recently on the arsenic removal by using SRB in bio-column reactor (Mondal and Majumder, 2007), Bhatt et al., 1983). The procedure and reason for such slight increase in pH is not well understood. However, some time back it has been reported that the reactions of molecular oxygen at the surface of the carbon results complex  $C_xO$  or  $C_xO_2$ . This adsorbed oxygen complex, in neutral solution, is sufficiently active to cause an oxidation of water as per the following reaction (Mckay et al., 1984, Mckay and Bino, 1990).



The hydroxyl ion may combine with  $H_2O$  resulting in a net increase in the pH of the solution (Jadia and Fulekar, 2009).

It is also observed that dissolved oxygen in treated waste water is around  $\sim 3.9$  mg/L at starting but after 15-16 hours of operation it falls down to 0.19 mg/L as shown in Fig.5.2.2.1.5.7 (b). After that, till the end of operation DO remain more or less constant. The probable reason for sudden decrease in dissolved oxygen could be settlement of bacteria. Once the microbes is settled DO also reaches a constant value.

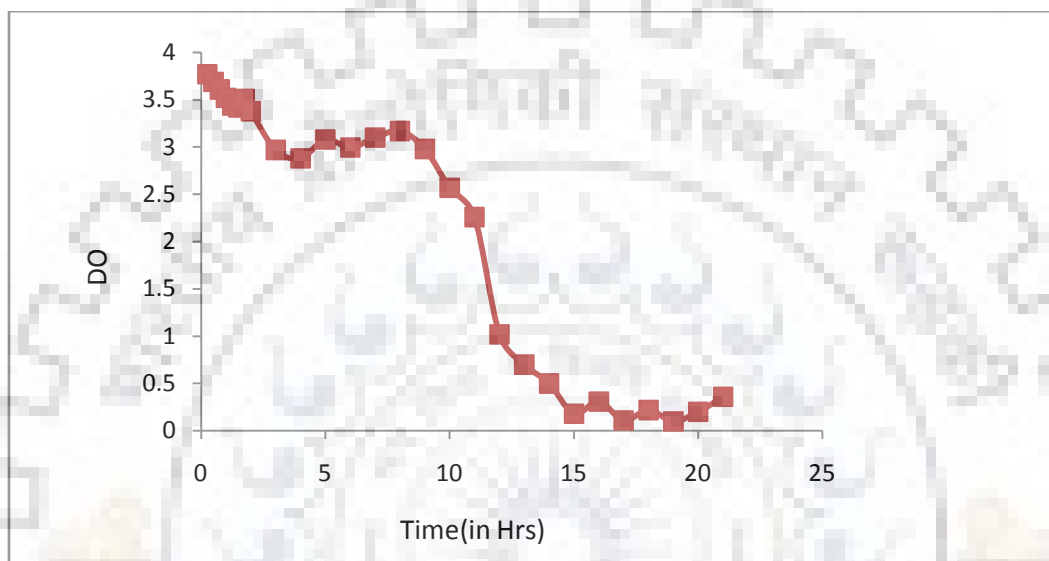


**Fig.5.2.2.1.5.7 (b) Variation of DO with Time**

#### **5.2.2.1.5.8 Concluding Remarks**

From the above discussions the following concluding remarks are drawn:

- The bio-column reactor is capable to reduce the concentration of the pollutants in the effluent water below their permissible limit.
- Bio-column reactor must be backwashed for effective continuous operation.
- At the initial stage, the flow rate and bed height have significant influence on the removal of fluoride from the contaminated water. However, after some time of operation (approximately 24-25 hours) such influence is negligible under the experimental conditions.
- Fluoride is removed after  $\sim 24$  hours of operation.
- DO reduce along the bed height of the reactor, which supports the aerobic nature of the bacteria.
- pH of the solution slightly decreases initially for the first hours and increases within small range (6.5–7.5).



- The BDST model was successfully applied to analyze column performance and evaluate the model parameter. The BDST equations of linear relationship between the bed depth and the service time were obtained with correlation coefficients of 0.99, 0.99 and 0.94 for 12, 23 and 40 ml/min flow rate respectively.
- The Empty Bed Residence Time (EBRT) model which optimizes the empty bed residence time and the sorbent utilization rate was successfully applied with optimum contact time greater than about 159.0, 276.6 and 530.1 min for 40, 23 and 12 ml/min flow rates, respectively, with the corresponding usage rate of 125.5, 32.6 and 113.4 g/L.

### 5.2.3 Distribution of Residence Time for Packed Bed Column Reactor Using a Packing of Bio-Adsorbent (*Java plum seed (Syzgiumcumini)*)

#### 5.2.3.1 Experimental Setup

In a packed bed bioreactor response of RTD experiments were carried out. The schematic diagram of experimental setup, which consists of packed bed bioreactor, injection point, mixing tank fitted with stirrer (feed chamber), peristaltic pump, filter unit for water, pressure gauge, level indicator, and sampling port is shown in figure Fig.3.3.2 (a) and (b) in section 3.3.2. The reactor was made up of SS 316 (Stainless Steel 316) with an inner diameter 9 cm, height 100 cm and working volume of 6.4 L. The reactor was filled with *Java plum seed (Syzgiumcumini)* of particle size of 2-6 mm and bulk density of 71.66 g/100ml. The reactor assembly was a close circuit unit. Five equidistant ports (P<sub>1</sub>, P<sub>2</sub>, P<sub>3</sub>, P<sub>4</sub> and P<sub>5</sub>) of 1.25 cm diameter were used to collect liquid samples along the height of the reactor. The final pore volume (void space) of the reactor with *Java plum seed (Syzgiumcumini)* packed bed reactor was between 1300-1400 ml.

#### 5.2.3.2 Materials

All the experiments were performed at room temperature (298K).

- Tracer solution of conc. Hydrochloric acid (HCl)
- Phenolphthalein
- Millipore water (R=18.2M  $\Omega$ -cm)
- conductivity meter (HACH)
- N/10 NaOH

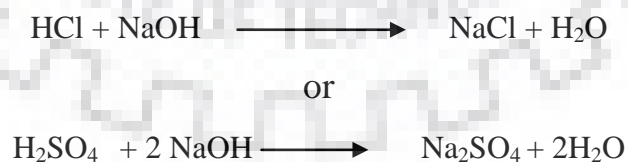
**Table 5.2.3.1: Feature of Bio-column Reactor**

Sr No	Description	Value
1	Diameter of reactor (cm)	9.0
2	Total height of reactor (cm)	100
3	Volume of reactor (liters)	6.4
4	Number of sampling point (cm)	5.0
5	Height of sampling point (cm)	20,40,60,80, and 100 cm
6	Diameter of sampling point (cm)	1.3
7	Total Weight of Absorbent (gm)	2420
8	Density of Bed (gm/mL)	0.717
9	Actual Volume of Reactor (Liters)	2.9

### 5.2.3.3 Procedures

In this experiment, we first close the drain valve provided at the bottom of the feed tank to fill it with water. When the feed tank is filled with water, an injection containing 20 ml conc. HCl is placed at the tracer injecting point after opening the dead end. Once it is ensured that knob provided on the pumps is at zero position, rotation selection switch is set towards clockwise rotation arrow while setting other switch provided on the pump towards manual option. When the flow rate gets stabilized, inject quickly the pulse tracer from the syringe. Start the stop watch simultaneously. Collect 10 ml of exit stream sample from the top at 0.5min interval. Take the sample and titrate with N/10 NaOH using phenolphthalein as the indicator.

### 5.2.3.4 Reactions Involved



### 5.2.3.5 Results and Discussion

We dedicated this section to discuss results obtained after performing above said experiments of those of measurement by RTD.

### 5.2.3.5.1 Calculation of Dispersion Number

Elements of fluid taking different routes through the reactor may take different lengths of time to pass through the reactor. The distribution of these times for the stream of fluid leaving the vessel is called the exit age distribution “E”, or the residence time distribution RTD of fluid. The RTD is represented in such a way that the area under the curve is unity (SinghTP et al., 2015),

$$\int_0^{\infty} E dt = 1$$

The mean residence time is

$$T = \int_0^{\infty} t E dt = 1 = \sum t E \Delta t$$

When a tracer is injected into a packed bed at a location more than two or three particle diameters downstream from the entrance and measured some distance upstream from the exit, the system is analogous to an open vessel system. For such a system there is no discontinuity in the flow at the point of tracer injection or at the point of tracer measurement, the variance for open system is-

$$\sigma_{\theta}^2 = \frac{\sigma_t^2}{\tau^2} = \frac{2}{P_e} + \frac{8}{P_e^2}$$

Where,

$$P_e = \frac{DL}{UL}$$

L Characteristic Length (m)

DL Effective Dispersion Coefficient (m<sup>2</sup>/s)

U Superficial Velocity (m/s) based on empty cross- section

The vessel dispersion number is given as inverse of the Peclet number.

The mean residence time,  $\theta = \frac{t}{\tau}$

$$E_{\theta} = \tau E$$

$$C_{\theta} = \tau C$$

Theoretical corresponding mean residence time

$$\tau_{th} = \left(1 + \frac{2}{P_e}\right) \tau$$

The variance of a continuous distribution measured at a finite number of equidistant locations is given by-

$$\sigma_t^2 = \frac{\sum(t_i^2 C_i)}{\sum C_i} - \left[\frac{\sum t_i C_i}{\sum C_i}\right]^2$$

$$\tau = \frac{\sum t_i C_i}{\sum C_i}$$

The Dispersion number can be written as:

$$\frac{D_l}{UL} = \frac{-1 + \sqrt{1 + 8\sigma_\theta^2}}{8}$$

Where

$$\sigma_\theta^2 = \frac{\sigma_t^2}{\tau^2}$$

### 5.2.3.5.2 Calculation of Peclet Number

Peclet number is reciprocal of dispersion number and can be calculated easily once we know the dispersion number.

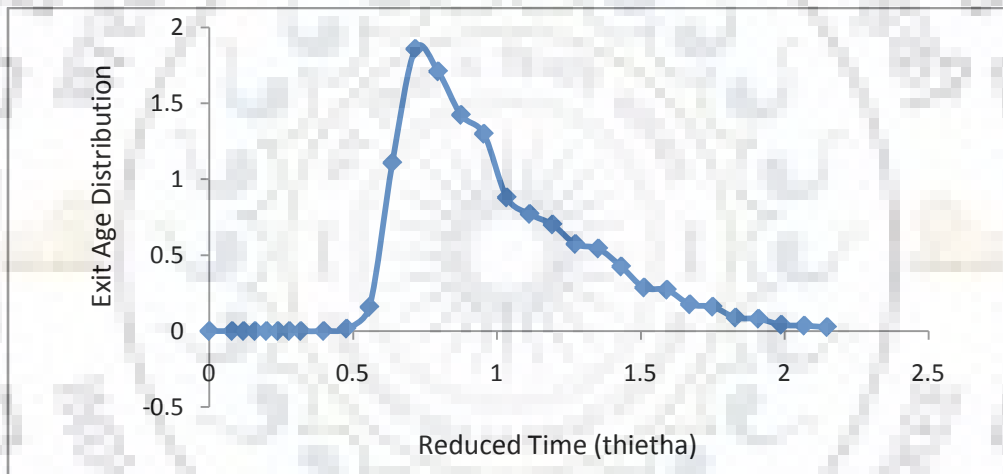


**Fig.5.2.3.5 Graph Showing Variation of Exit Age Distribution with Reduced Time for Packed Bed Reactor**

### 5.2.3.5.3 Concluding Remarks

In present study, Residence Time Distribution for packed bed reactor for step input change was investigated experimentally. Residence Time Distribution method provide a useful tool for efficient operation design and system improvement. The variance ( $\sigma^2$ ), Mean residence time ( $\tau_m$ ) and Dispersion number of experimental Residence Time Distribution provide a good prediction of the model.

**Table 5.2.3.5. Experimental Residence Time Distributions for Packed Bed Reactor**

Residence Time Distribution measure	$\sigma^2$	$P_e$	$\sigma^2_{\square}$	$\tau_m$	$\frac{D_t}{UL}$
Experimental Residence Time Distribution for step change	242.1	22.2	0.1065	12.6	0.0451

#### 5.2.4 Implementation of the present work for treatment of fluoride contaminated AIS auto glass effluent

In the present study anion analysis of waste water from AIS auto glass industry (Mangalore, Near Roorkee) was done in IA Lab, Chemical Engineering Department, IIT Roorkee, India. The concentration of fluoride was found to be approx. 13mg/L. The consortium culture of *Acinetobacter baumannii* (MTCC NO.-11451) was immobilized onto the surface of jamun seeds in packed bed column being operated at an EBCT of 12h and bed height of 93 cm. Table represents the characteristics of waste water obtained from AIS glass industry. Result of the above experiment is also represented in Fig. 5.2.4.

**Table 5.2.4(a) Characteristics of AIS auto glass industrial waste water (Mangalore, Near Roorkee, India).**

Peak Number	Retention time min.	Area ( $\mu\text{S/cm}$ ) min	Height $\mu\text{S/cm}$	Concentration ppm	Component name
1	4.8	0.0012	0.009	Invalid	
2	5.6	0.0301	0.211	13.5	Fluoride
3	5.9	0.0546	0.294	Invalid	
4	5.6	0.2399	0.726	Invalid	
5	8.5	1.0	5.2	10.4	Chloride
6	10.1	0.0494	0.216	-3.9	Nitrite
7	11.8	0.0458	0.070	Invalid	
8	12.7	0.0016	0.007	Invalid	
9	14.5	0.2185	0.673	10.3	Bromide
10	25.6	18.3	38.9	21.8	Sulfate
11	29.4	0.0087	0.016	Invalid	

**Table 5.2.4 (b) Removal of fluoride from AIS glass industry effluent in the column reactor by *Acinetobacter baumannii* with time (h)**

Sr. No.	Time (h)	Left fluoride concentration (mg/L)
1	0	20.0
2	12	18.8
3	24	17.2
4	36	15.3
5	48	14.2
6	60	13.1
7	72	12.2
8	84	11.1
9	96	10.2
10	108	9.3
11	120	8.6
12	132	7.8
13	144	6.7
14	156	6.1
15	168	5.1
16	180	3.8
17	192	2.3
18	204	2.2
19	216	1.9
20	228	1.7
21	240	1.0
22	252	0.865

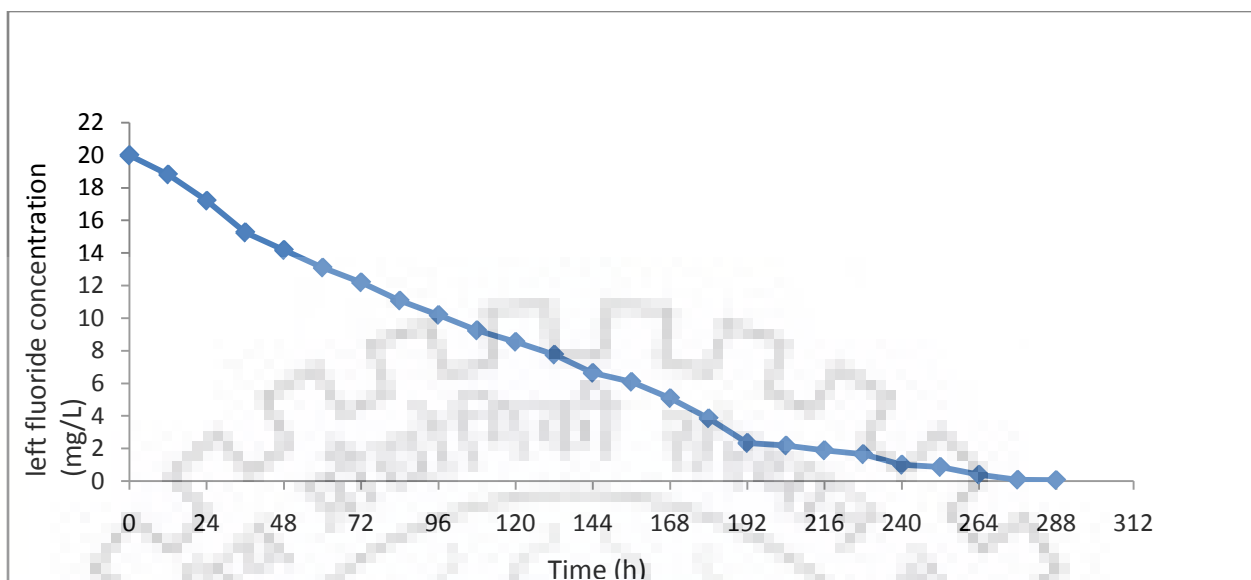


**Fig. 5.2.4 Removal of fluoride from AIS glass industry effluent in the column reactor by *Acinetobacter baumannii***

#### 5.2.4.1 Concluding remarks

- Removal of fluoride was achieved in continuous bio column reactor packed with consortium culture of *Acinetobacter baumannii* in jamun seeds immobilized waste biomass.
- For removal of fluoride from synthetic waste water an EBCT of 4 h was found to be sufficient to bring down the effluent concentration down the prescribed regularity level of fluoride.
- Effect of bed height onto the removal of fluoride was investigated which shows that percentage removal fluoride was increased with the increase in bed height.
- Do (Dissolved oxygen) was found to decreased with the time, while pH was decreased initially and then becomes constant.
- The time required for the industrial waste water to reach the regulatory level of pollution control board limit for the discharge by industries (1.5 mg/L for Fluoride) was more than that of single component simulated synthetic waste water of fluoride, prepared in the laboratory.
- Various kinetic models were applied to the experimental data.

# DEFLUORIDATION OF INDUSTRIAL WASTEWATER USING *Eichhornia crassipes* (Phytoremediation)

## 5.2.5 Experimental Setup

Experiments for the study of phytoremediation under synthetic conditions were carried out in the fluid particle research lab of Indian Institute of Technology, Roorkee. Batch system was used to perform the above said experiments. For plants feed of different concentration of fluoride at different pH were provided for 10 continuous days. In the chamber CO<sub>2</sub> & O<sub>2</sub> exchange was observed which was controlled by the controller attached to the system. Fig.3.6 (a) in section 3.6 shows the Plant growth chamber used for the experiment. Synthetic conditions created to perform experiments are shown in Table.5.2.5.

**Table 5.2.5: Atmospheric Conditions for Plant Growth Chamber**

Parameter	Value
Running Time	10 days
Day and Night Time	16 hours day and 8 hours night
Temperature	27-30°C
Humidity	60% - 65%

## 5.2.6 Prepreation of Hoagland's Solution

D.R. Hoagland and D.R. Arnon in 1938 first developed the nutrient solution in which plant can grow without soil, which was later revised by D.R. Arnon in 1950. This solution is named as Hoagland Solution on the name of inventor D.R. Hoagland. For plant growth, hydroponic water culture was used. The solution consists of three major constituents as follow:

- Macronutrients
- Micronutrients
- Phosphates

For the preparation of Hoagland's solution the compounds were weighed by using weighing machine and stock solution was prepared in different bottles. To those bottles, 800 ml of millipore water was added to make it a litre. The contents were shaken well and mixed.



Hoagland Solution emerges as a useful component to grow plants which require fewer amounts of nutrients. Generally for aquatic plants (10-20) % of this solution is used. 10% of this solution was used for our investigations. Table.5.2.6 shows various constituents and their concentrations in the Hoagland's solution.

**Table 5.2.6 Constituents of Hoagland Solution**

Component	Stock Solution	MI Stock Solution/ L
<b>Macronutrients</b>		
2M KNO <sub>3</sub>	202 g/L	2.5
1M Ca[NO <sub>3</sub> ] <sub>2</sub> •4H <sub>2</sub> O	236 g/0.5L	2.5
Iron [Sprint 138 iron chelate]	15 g/L	1.5
2M MgSO <sub>4</sub> •7H <sub>2</sub> O	493 g/L	1
1M NH <sub>4</sub> NO <sub>3</sub>	80 g/L	1
<b>Micronutrients</b>		
H <sub>3</sub> BO <sub>3</sub>	2.86 g/L	1
MnCl <sub>2</sub> •4H <sub>2</sub> O	1.81 g/L	1
ZnSO <sub>4</sub> •7H <sub>2</sub> O	0.22 g/L	1
CuSO <sub>4</sub> •5H <sub>2</sub> O	0.051 g/L	1
H <sub>3</sub> MoO <sub>4</sub> •H <sub>2</sub> O	0.09 g/L	1
Na <sub>2</sub> MoO <sub>4</sub> •2H <sub>2</sub> O	0.12 g/L	1
<b>Phosphate</b>		
1M KH <sub>2</sub> PO <sub>4</sub>	136 g/L	0.5

### 5.2.7 Result and Discussion

**Table 5.2.7 Variation of Contact Time on Removal of Fluoride**

Contact time(Days)	Initial concentraton of(mg/L)	Amount adsorbed by (mg/L)	Final concentration of (mg/L)	%Removal
0	20	0	20	0
1	20	1	19	5.0
2	20	2.5	17.5	12.5
3	20	4.2	15.8	21.0

Contact time(Days)	Initial concentraton of(mg/L)	Amount adsorbed by (mg/L)	Final concentration of (mg/L)	%Removal
4	20	4.5	15.5	22.5
5	20	5	15	25.0
6	20	5.4	14.6	27.0
7	20	5.8	14.2	29.0
8	20	6.2	13.8	31.0
9	20	6.6	13.4	33.0
10	20	6.9	13.0	34.9

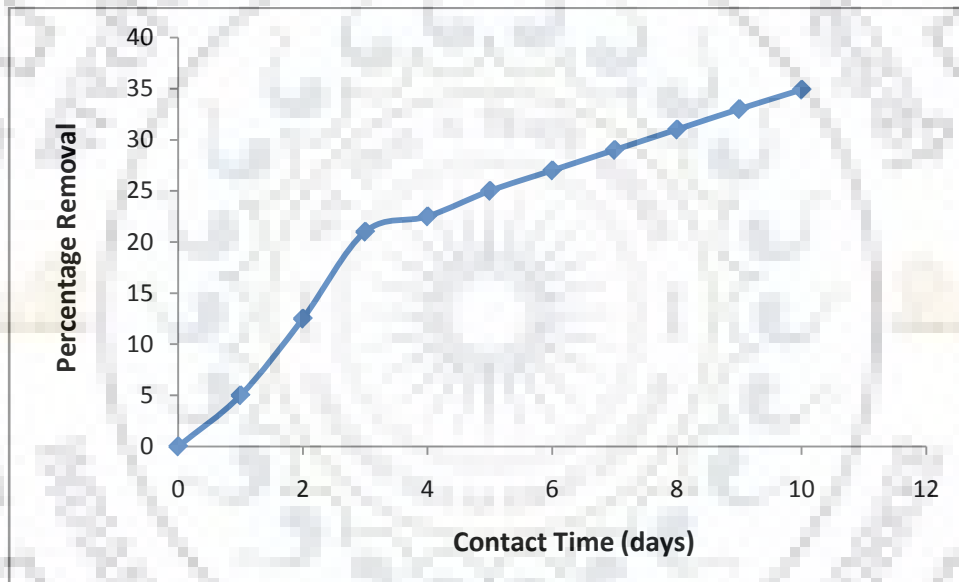


**Fig. 5.2.7 Effect of Contact Time on Percentage Removal**

### 5.2.8 Effect of Initial Fluoride Concentration

In this part of experiment, concentration of the solution as varied while keeping pH of the solution constant (pH=7). From the results a graph was obtained which has been plotted in Fig. 5.2.8. From the figure it it can be seen that concentration of fluoride decreases with time. Thus this plant is an effective adsorbent for defluoridation. A drastic fall in concentration after day 2 was observed while it remains more or less same after day 5.

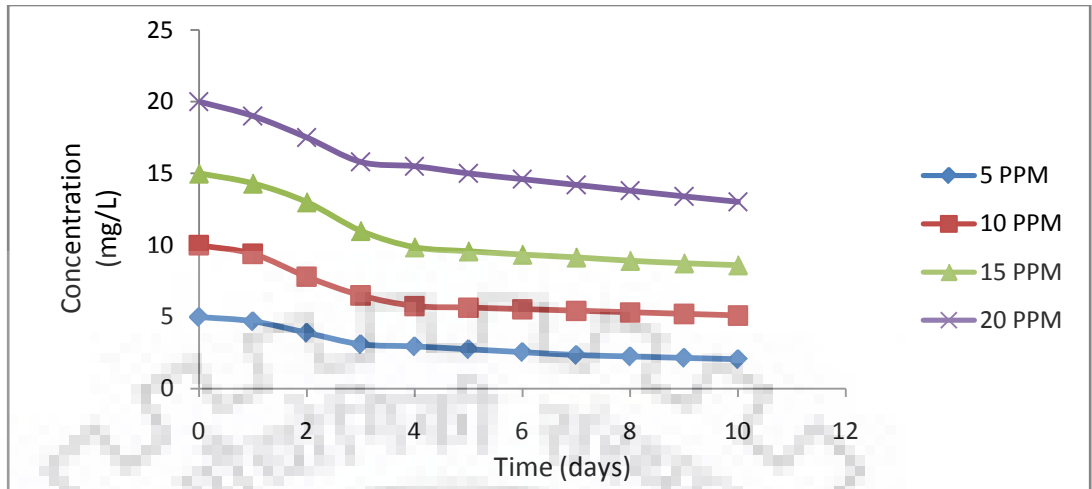


**Fig.5.2.8. Concentration versus Time for Fluoride Having Constant pH for *Water Hyacinth***

### 5.2.9 Effect of pH

Here, in this section the concentration of solution was kept constant at 10 mg/L while pH of the solution was changed using 69% concentrated Nitric acid [HNO<sub>3</sub>] and sodium hydroxide [NaOH]. An interesting phenomenon was observed which proved that maximum removal is obtained at pH of 7.

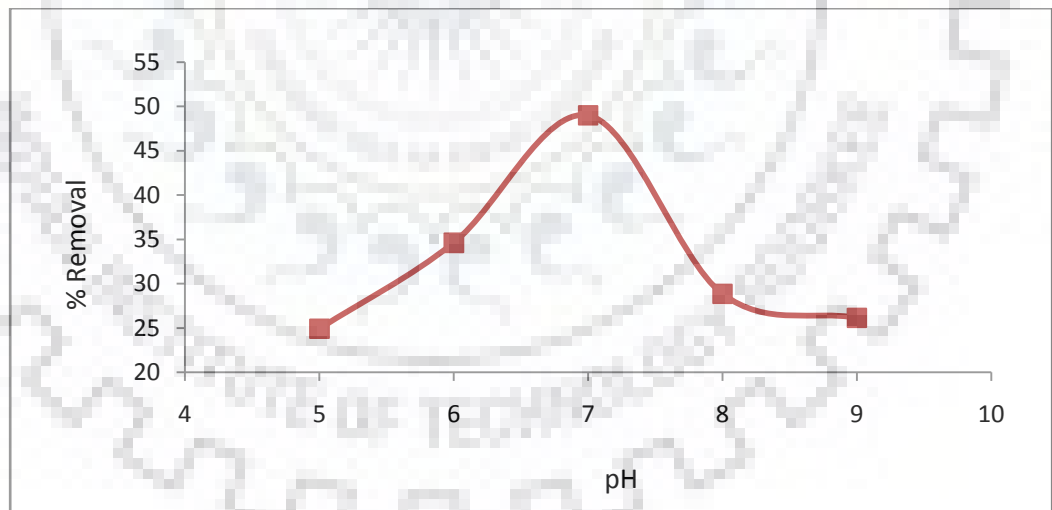


**Fig.5.2.9 Percentage Removal versus Concentration Study with varying pH for *Water Hyacinth***

### 5.2.10 Effect of Initial Concentration on Percentage Removal

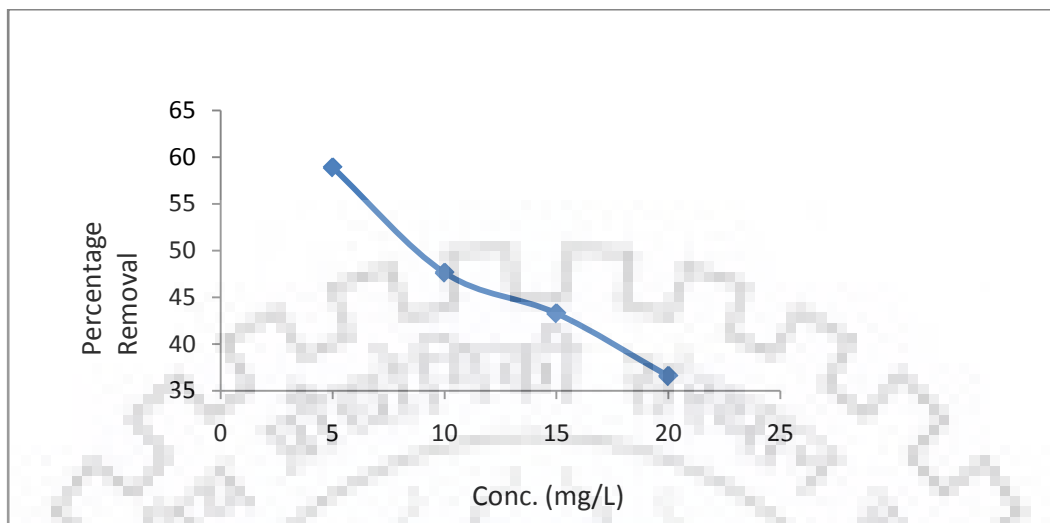


**Fig 5.3.10 Percentage Removal Vs Time for *Water Hyacinth***

From Fig.5.3.10 it could be easily deciphered that with increase in initial concentration negative change in Percentage Removal was seen. It is shown in figure that when we increased initial concentration from 5 to 20 mg/L percentage removal decreases from ~58% to ~36%.

### 5.2.11 Accumulation of Fluoride

Fluoride gets accumulated in the different parts of the plant. Data showing accumulation of fluoride among various parts of the plants is shown in Table 5.2.11 and Fig 5.2.11. It can be easily seen that for plant, maximum accumulation is observed in roots than stems and leaves.

**Table 5.2.11 Accumulation of Fluoride in Root, Stem and Leaves for *Eichhornia crassipes***

Fluoride concentration (mg/L)	Root [ $\mu\text{gm}/\text{gram Dw}$ ]	Stem [ $\mu\text{gm}/\text{gram Dw}$ ]	Leaves [ $\mu\text{gm}/\text{gram Dw}$ ]	Total accumulation
5	501.0	145.5	70.4	716.9
10	746.8	162.0	116.9	1025.7
15	972.0	292.8	194.0	1458.8
20	1148.5	408.9	342.0	1899.4

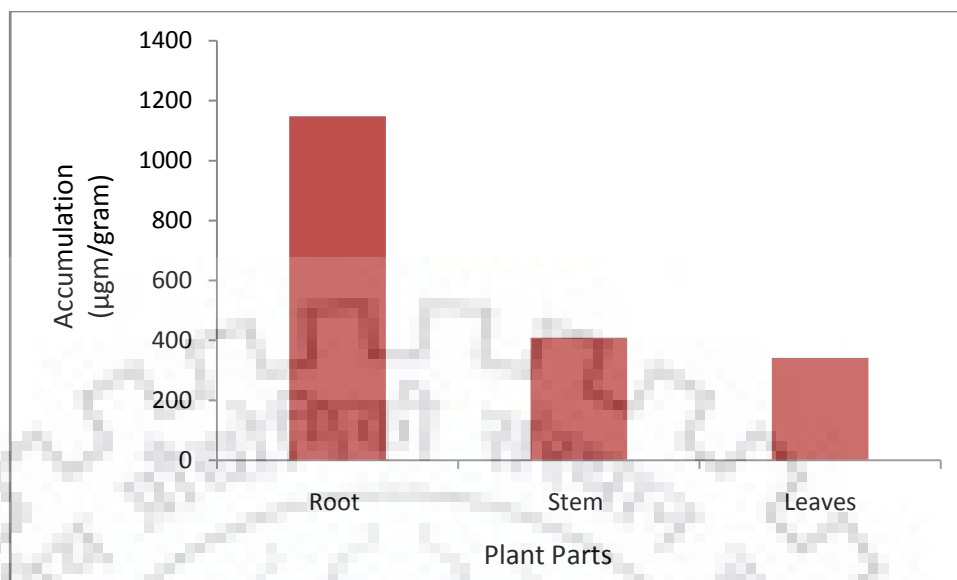


**Fig. 5.2.11 Accumulation for 20 ppm for *Water Hyacinth***

#### 5.2.11.1 Concluding Remarks

From the above said performed experiments we can conclude that

- Fluoride accumulates maximum in roots followed by stem and leaves respectively in *Eichhornia crassipes*.
- With increase in initial concentration, there is a decrease in defluoridation process for *Eichhornia crassipes*.
- At constant pH there is a decrease in concentration of fluoride with time which means *Eichhornia crassipes* can be used as a good adsorbent for fluoride using phytoremediation.
- If pH is diverted from neutral point, there is a decrease in Percentage Removal of fluoride for *Eichhornia crassipes*.

### 5.3 Comparative Study of *Ipomoea aquatica* and *Eichhornia Crassipes*

#### 5.3.1 Results and Discussions

##### 5.3.1.1 Removal of Fluoride with Time

The effect of time on fluoride concentration was calculated. A sample of 20 mg/L fluoride solution was taken and exposed to plant. It was noticed that there is decrease in fluoride concentration with passage of time.

**Table 5.3.1.1 (a) Data Showing Effect of Contact Time on Fluoride Concentration**

<b>Plant Name</b>	<b>Contact time(Days)</b>	<b>Initial concentration (mg/L)</b>	<b>Amount adsorbed by(mg/L)</b>	<b>Final concentration (mg/L)</b>
<i>Ipomoea aquatica</i>	0	20	0	20
	1	20	0.2586	19.7
	2	20	4.7	15.3
	3	20	5.2	14.8
	4	20	5.5	14.5
	5	20	5.5	14.5
	6	20	5.5	14.5
	7	20	5.3	14.7
	8	20	5.2	14.8
	9	20	5.4	14.6
	10	20	5.1	14.9
<i>Eichhornia crassipes</i>	0	20	0	20
	1	20	1	19
	2	20	2.5	17.5
	3	20	4.2	15.8
	4	20	4.5	15.5
	5	20	5	15
	6	20	5.4	14.6
	7	20	5.8	14.2
	8	20	6.2	13.8
	9	20	6.6	13.4
	10	20	6.9	13.0

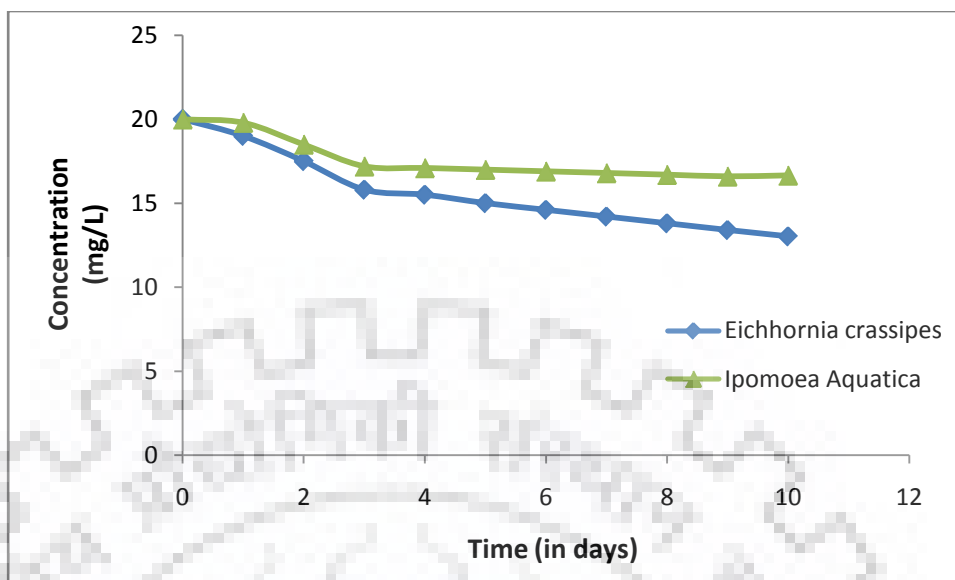
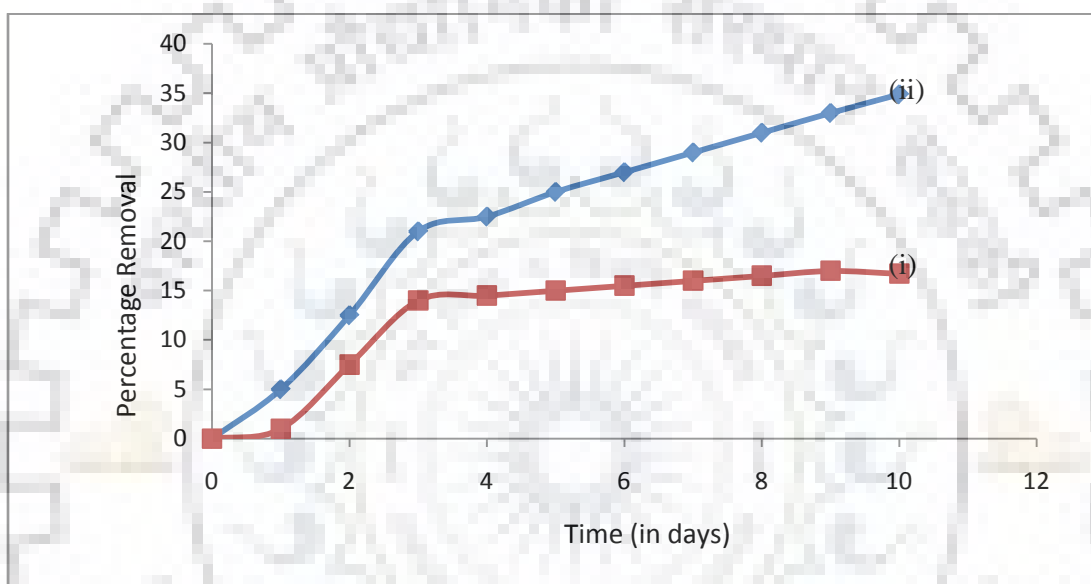


Fig. 5.3.1.1 (a) Effect of Time on Concentration of Fluoride

Table 5.3.1.1 (b) Percentage Removal of Fluoride

Plant Name	Contact time(Days)	Initial concentration (mg/l)	Amount adsorbed by(mg/l)	Percentage Removal
<i>Ipomoea aquatica</i>	0	20	0	0
	1	20	0.259	1.3
	2	20	4.7	23.3
	3	20	5.2	26.2
	4	20	5.5	27.4
	5	20	5.5	27.5
	6	20	5.5	27.3
	7	20	5.3	26.4
	8	20	5.2	26.2
	9	20	5.4	27.0
	10	20	5.1	25.3
	0	20	0	0
	1	20	1	5.0
	2	20	2.5	12.5
	3	20	4.2	21.0
	4	20	4.5	22.5
	5	20	5	25.0

Plant Name	Contact time(Days)	Initial concentration (mg/l)	Amount adsorbed by(mg/l)	Percentage Removal
<i>Eichhornia crassipes</i>	6	20	5.4	27.0
	7	20	5.8	29.0
	8	20	6.2	31.0
	9	20	6.6	33.0
	10	20	6.9	34.9



**Fig.5.3.1.1 (b) Shows Percentage Removal of Fluoride from Water in Touch with Plants (ii) *Eichhornia crassipes* and (i) *Ipomoea aquatica* for Concentration of 20 mg/L**

### 5.3.2 Chlorophyll Study for *Ipomoea aquatica* and *Eichhornia crassipes*

Chlorophyll was determined before and after the fluoride exposure to the plant. Chlorophyll was measured by the method defined in the previous chapter, using the formulas given below. The Notations used in the formula were described in the chapter four. (Singh T P., Majumder, C.B. 2017).

$$C_a = \frac{(12.3D663-0.86D645)V}{d*w*1000}$$

$$C_b = \frac{(19.3D645-3.60D663)V}{d*w*1000}$$



Where,

$C_a$  Chlorophyll concentration a [mg/gram of FW]

$C_b$  Chlorophyll concentration b [mg/gram of FW]

D Absorbance or Optical density [at wavelength 663 & 645]

D Distance of light path

V Final volume [mL]



**Fig 5.3.2 (a) Chlorophyll Study for *Ipomoea aquatic***



**Fig.5.3.2 (b) Chlorophyll Study for *Eichhornia crassipes***

**Table 5.3.2 (a) Chlorophyll Results of *Ipomoea aquatica* before and after Exposure to 20 ppm Fluoride Solution for 10 Days**

Chlorophyll Content	Before Exposure [mg/gram Fresh Weight]	After Exposure to 20ppm Fluoride for 10 days[mg/gram Fresh Weight]
Chlorophyll A	1.7	0.83
Chlorophyll B	0.90	0.49

**Table 5.3.2 (b) Chlorophyll Results for *Eichhornia crassipes* before and after Exposure to 20 ppm Fluoride Solution for 10 Days**

Chlorophyll content	Before Exposure[mg/gram fresh weight]	After exposure to 20 mg/L Fluoride for 10 days[mg/gram fresh weight]
Chlorophyll a	0.698	0.058
Chlorophyll b	0.092	0.028

$C_a$  and  $C_b$  are in mg/gram fresh weight of plant. The results show that the chlorophyll content of plant was considerably affected by the fluoride exposure. It was decreased due to the effect of fluoride on the plant.

### 5.3.3 Accumulation of Fluoride in Different Parts of Plants

Accumulation of fluoride was estimated after the completion of the experiment [10 days]. The whole process has been described in the previous chapter. Ultraviolet Spectrophotometer was used to determine the accumulation of fluoride in different parts of plants. The results obtained are summarized in the Table 5.3.3 (a) and Table 5.3.3 (b). Results show that as the concentration of fluoride increases, the accumulation increases. Fluoride was mostly accumulated in roots followed by leaves and stem.

**Table 5.3.3 (a) Accumulation of fluoride in Root, Stem and Leaves for *Ipomoea aquatica***

Fluoride concentration (mg/L)	Root [µgm/gram Dw]	Stem [µgm/gram Dw]	Leaves [µgm/gram Dw]	Total Accumulation
5	199.5	54.1	85.5	338.9
10	387.5	99.9	181.7	669.1
15	683.2	183.4	253.5	1120.2
20	870.2	209.9	330.3	1410.5

**Table 5.3.3 (b) Accumulation of fluoride in Root, Stem and Leaves for *Eichhornia crassipes***

Fluoride concentration (mg/L)	Root [ $\mu\text{gm}/\text{gram Dw}$ ]	Stem [ $\mu\text{gm}/\text{gram Dw}$ ]	Leaves [ $\mu\text{gm}/\text{gram Dw}$ ]	Total accumulation
5	501.0	145.5	70.4	716.9
10	746.8	162.0	116.9	1025.8
15	972.0	292.8	194.0	1458.8
20	1148.5	408.9	342.0	1899.4

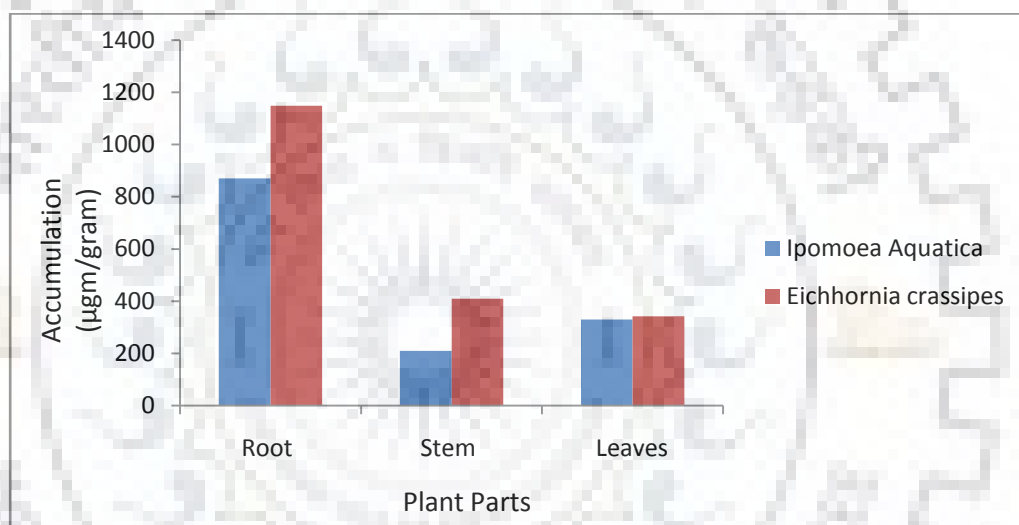


**Fig. 5.3.3 Pictorial Representation of Fluoride Accumulated by Different Parts of Plant**

### 5.3.4 Bio Mass Degradation

It was found that the biomass degradation of the plant was due to fluoride exposure. As the concentration of the fluoride was increased degradation also increased. Maximum degradation was found for the 20 ppm solution from 1.9 grams to 0.429 grams. In case of pH study when the pH was basic in nature the degradation was highest from 2.4 to 1.0. The summary of biomass degradation for both the study is shown in Table 5.3.4 (a) and 5.3.4 (b).

**Table 5.3.4 (a) Summary of Bio Mass Degradation for *Ipomoea aquatica***

Concentration (In mg/L)	Weight Before [grams]	Weight After [grams]	pH	Weight Before [grams]	Weight After [grams]
5	3.2	2.8	5	2.6	0.429
10	1.8	1.0	6	1.5	1.1
15	1.7	0.816	8	3.0	2.8
20	1.9	0.429	9	2.4	1.0

**Table 5.3.4 (b) Summary of Bio mass Degradation for *Eichhornia crassipes***

Concentration	Weight Before[grams]	Weight After [grams]	pH	Weight Before[grams]	Weight After [grams]
5	32	29.2	5	28	12.1
10	26	23	6	32.6	26.2
15	24.5	19.7	8	42	36.1
20	19.7	12.9	9	26.8	24.2

### 5.3.5 Effect of Contact Time on Concentration

To study the effect of contact time on concentration pH was kept constant at  $7.3 \pm 0.1$  while, the concentration of fluoride was changed from 5 to 10, 15 and 20 mg/L. This concentration was prepared by dissolving Sodium Fluoride (NaF) in 10% of the Hoagland solution. Results were obtained for removal of fluoride from both plants and results were incorporated in Table 5.3.5. This follows the trend that has been reported by Maine et al. (2004).

**Table 5.3.5 Initial and Final concentration of Fluoride**

Name of Plant	Initial Concentration	Final Concentration
<i>Ipomoea Aquatica</i> [Water spinach]	5	2.9
	10	6.4
	15	11.1
	20	16.7
<i>Eichhornia crassipes</i> [Water Hyacinth]	5	2.1
	10	5.1
	15	8.6
	20	13.0

Major Change in fluoride concentration is noted after completion of 24 hours to 72 hours of process in which there was a major decrease after which concentration remains more or less same for rest days out of 10 days of operation. Fig.5.3.6 (a) shows Change in concentration of fluoride for *Ipomoea aquatica* with increase in time while Fig.5.3.6 (b) indicates for *Eichhornia crassipes*.

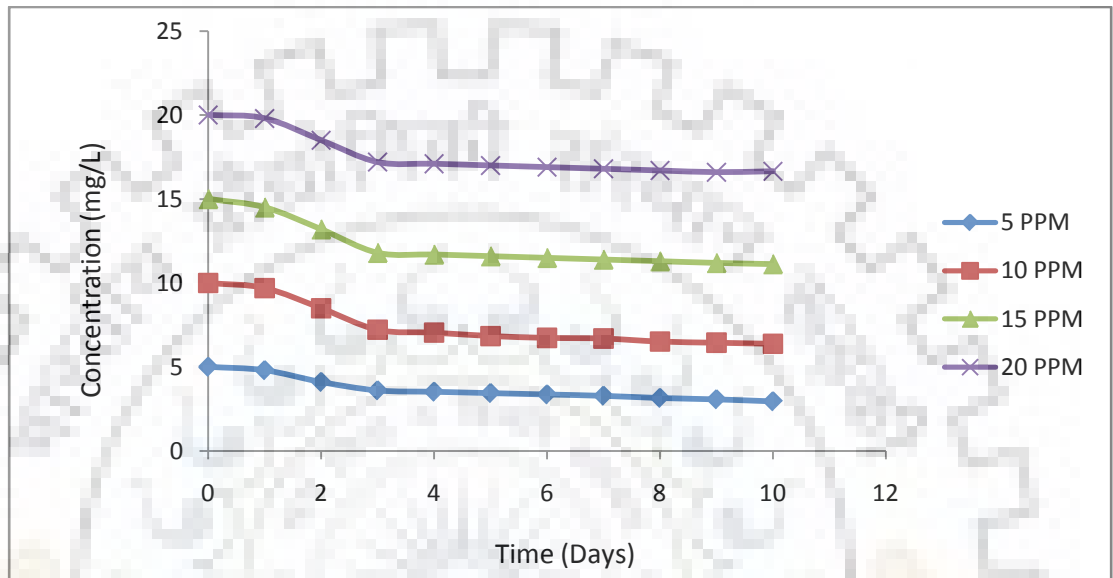


**Fig.5.3.6 (a) Effect of Contact Time on Concentration of Fluoride for *Ipomoea aquatica***

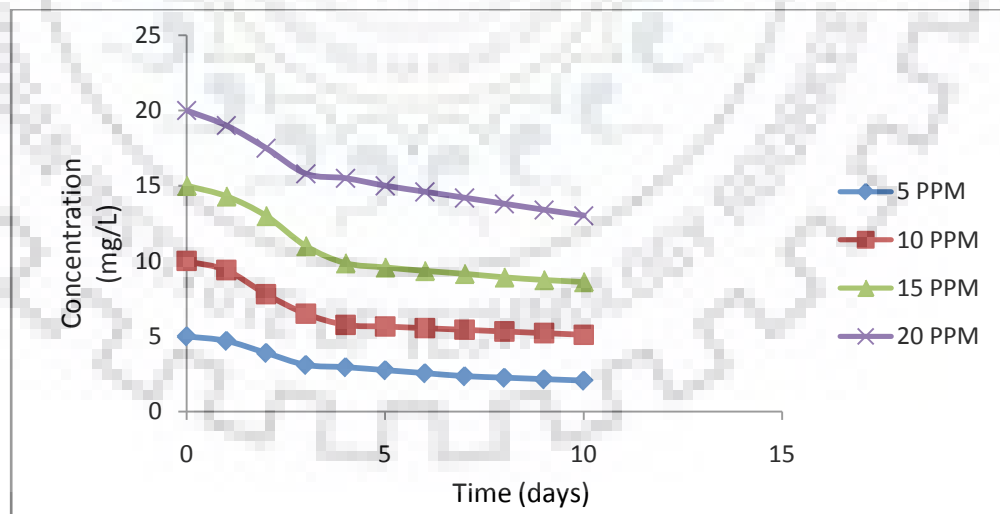


**Fig.5.3.6 (b) Effect of Contact Time on Concentration of Fluoride for *Eichhornia crassipes***

### 5.3.7 Effect of Contact Time on Percentage Removal

Investigations were done in order to find out percentage removal of fluoride at different concentration through plants of *Eichhornia crassipes* and *Ipomoea aquatica*. It was found that major part is removed within 24 to 72 hours of operation after which there is very less change in removal of fluoride. Table 5.3.7 shows the data obtained during the investigation in tabular form while Fig.5.3.7 (a) and 5.3.7 (b) represents it in pictorial form.

**Table 5.3.8 Percentage Removal of Fluoride**

Name of Plant	Concentration of Fluoride	Percentage Removal
<i>Ipomoea aquatica</i> [Water spinach]	5	40.9
	10	36.2
	15	25.8
	20	16.7
<i>Eichhornia crassipes</i> [Water Hyacinth]	5	58.9
	10	49.0
	15	42.6
	20	34.9

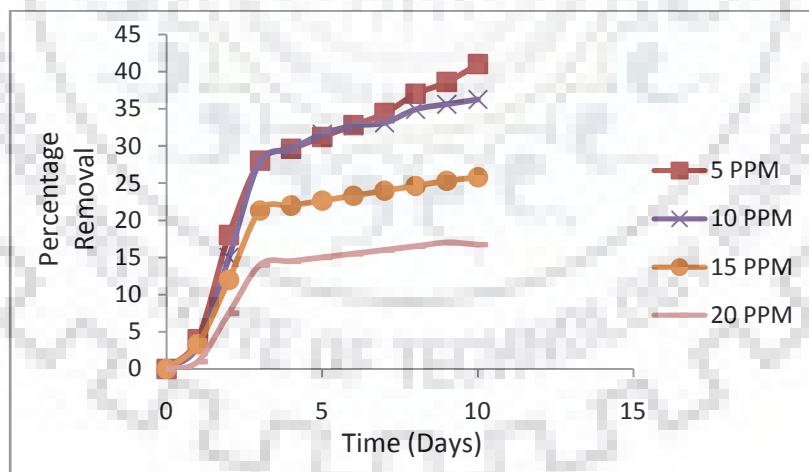


**Fig.5.3.7 (a) Percentage Removal versus Time for Fluoride Having Constant pH for *Ipomoea aquatica***

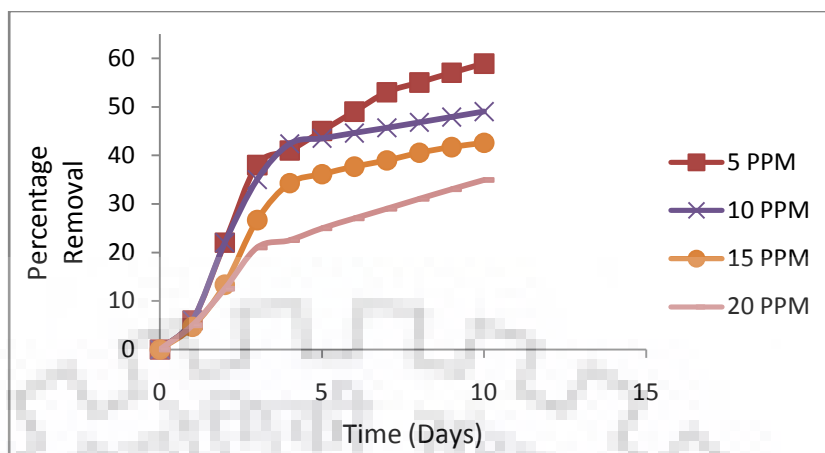


**Fig.5.3.7 (b) Percentage Removal versus Time for Fluoride Having Constant pH for *Eichhornia crassipes***

### 5.3.8 Effect of pH

In second set, we kept concentration of fluoride was kept constant at 10 mg/L and was changed pH from 5 to 9. We used 69% concentrated Nitric acid [HNO<sub>3</sub>] and sodium hydroxide [NaOH] in order to maintain pH. Results show that with change in pH, there is a negative effect on percentage removal of fluoride. Neither increase nor decrease in pH favours reaction through which fluoride is accumulated in plant. Thus, it was concluded that neutral pH is best for fluoride removal from these plants. Table.5.3.8 compares Percentage Removal of fluoride at various pH for both plants used while Fig.5.3.8 depicts it in the pictorial form.

**Table 5.3.8: Summary of Percentage Removal with pH Variation**

Name of Plant	pH	Percentage Removal
<i>Ipomoea aquatica</i> [Water spinach]	5	16.8
	6	24.0
	7	36.2
	8	28.9
	9	20.4
<i>Eichhornia crassipes</i> [Water Hyacinth]	5	24.9
	6	34.6
	7	49.0
	8	28.9
	9	26.2

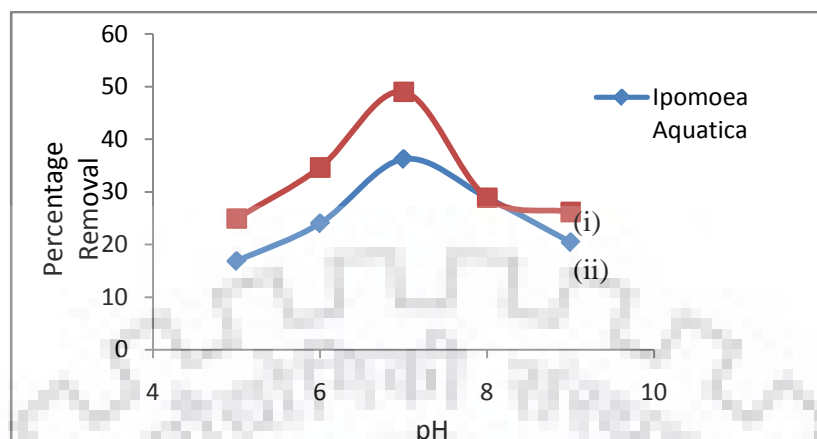


**Fig.5.3.8 Variation of Fluoride Removal Percentage with pH (i) Ipomoea Aquatica (ii) Eichhornia crassipes**

### 5.3.8 .1 Concluding Remarks

In Present study we had taken two aquatic plant species have been taken which viz. *Ipomoea aquatica* [Water spinach] and *Eichhornia crassipes* [Water Hyacinth]. They were grown in plant growth chamber and studied for 10 days exposure period to fluoride of different concentrations and pH. The removal efficiency of *Ipomoea aquatica* [Water spinach] was found to be 40.9 % and for *Eichhornia crassipes* [Water Hyacinth] it was found to be 58.9 %. Results show that *water hyacinth* had better removal efficiency to remediate fluoride. In pH study for both the plants shows negative results, as we increase or decrease the pH of the solution the removal efficiency was decreased for both the plants. Accumulation of fluoride was found mainly in the roots of both plants, it was found 872.9  $\mu\text{g}/\text{gram}$  DW for *Ipomoea Aquatica* and 1148.5  $\mu\text{g}/\text{gram}$  Dw for *Eichhornia crassipes*. Both the plants show the biomass degradation due to the fluoride exposure.

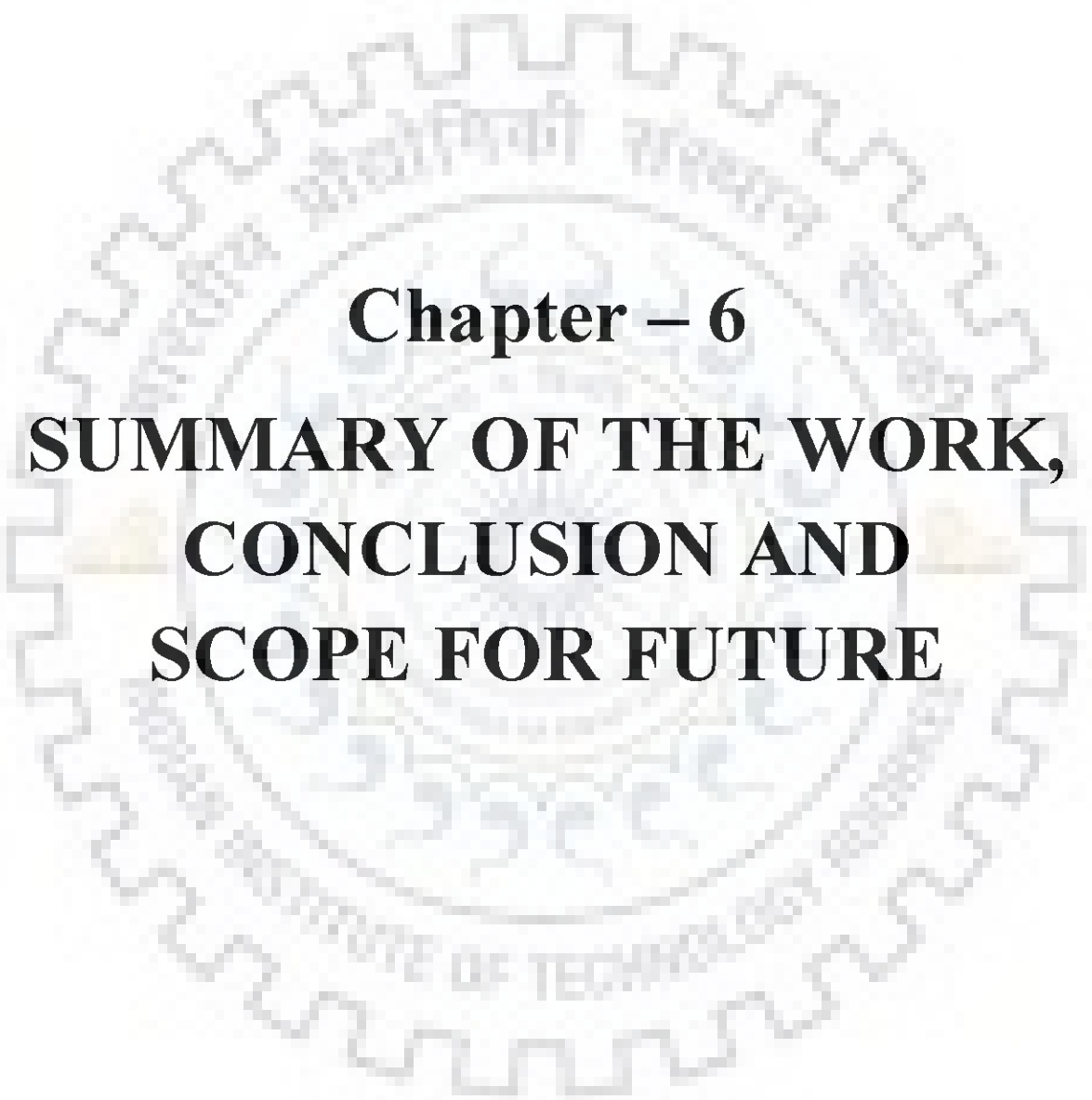
On the basis of experiments done we can conclude following points:

- *Water Hyacinth* has better removal efficiency for fluoride than *Ipomoea aquatica*.
- *Water Hyacinth* shows more potential to sustain the fluoride exposure as compared to *Ipomoea Aquatica*. As we see that the *Ipomoea aquatica* plant which was exposed to 20 ppm solution had almost died at the end of the experiment.
- Variation in pH shows undesirable results for both the plants. As we see that the maximum removal was found when the pH was nearby neutral.



- Due to the effect of fluoride biomass degradation takes place in both the plants.
- Both the plants also show the decreases in chlorophyll content after exposure.
- In *Ipomoea Aquatica* the accumulation of fluoride was found in order Roots > Leaves > stem.
- In *Water Hyacinth* the accumulation of fluoride was found in order: Roots > stem > Leaves.
- *Water Hyacinth* has better remediating properties than *Ipomoea Aquatica*.





**Chapter – 6**  
**SUMMARY OF THE WORK,**  
**CONCLUSION AND**  
**SCOPE FOR FUTURE**



# SUMMARY OF THE WORK, CONCLUSION AND SCOPE FOR FUTURE

---

### 6.1 Introduction

Present investigation was carried for the fluoride remediation from industrial waste water e.g glass industry, electroplating industry, Automobile Industry, plastic industry and so on. Various physical and chemical methods have been reported in the literature as its possible treatment technology, with several merits and demerits. The present fluoride speciation analytical technique has also number of limitations. With this point of view, an elaborate and detailed work has been carried out and summarized below under the heading of conclusions of the present work.

### 6.2 Summary of the Present Work

#### 6.2.1 Adsorptive

Adsorptive studies using various selected adsorbents have optimized and given in table 6.2.1.

- Mechanism of adsorption kinetics was found to follow pseudo-second order reaction, and the mechanism of fluoride removal on adsorbents was found to be complex. Both the surface adsorption and intra-particle diffusion contributes to the rate-determining step.
- High removal efficiency of adsorbent banana peel, groundnut shell and presence of others ions in groundwater did not significantly affect the defluoridation process.
- Adsorption isotherm models: Langmuir, Freundlich and Temkin were studied. Out of these the best plots for Adsorption Isotherm was Langmuir model.
- SEM, FTIR, and EDX are characterized before and after adsorption for its morphology, functional groups and constituent composition.

**Table 6.2.1 Summary of optimized parameters and results obtained of various selected adsorbents for Fluoride removal**

Sr. No.	Parameters		pH	Removal percentage	Dose (g/L)	Removal percentage	Time (min)	Removal percentage	Initial concentration (mg/L)	Removal Percentage
	⇔ Adsorbents ↓									
1	GAC		4	97.9	32	97.4	140	95.0	20	97.7
2	Citrus limetta Peel		5	91.0	10	94.3	40	95.8	20	95.8
3	Ground Nut Shell		7	88.5	16	89.9	75	90.5	20	90.3
4	Banana Peel		6	93.1	20	94.9	90	90.0	20	94.3
5	Neem Leaves		4	83.6	16	85.5	40	95.8	20	87.0
6	Virgin Turmeric		6	92.5	20	93.9	60	93.9	20	94.3
	MnO <sub>2</sub> Coated Turmeric		7	87.5	18	88.9	75	90.0	20	89.0
7	Java plum seed		6	93.2	10	99.4	40	95.9	20	94.9

### 6.2.2 Adsorptive and Bio removal (batch)

From the comparative study results have been summarized as below:

- Removal efficiency of bio removal (SAB) is very high (93.1 %) as compare to *citrus limetta* peel alone (91.0 %).
- From the bioadsorption kinetics results show that bio removal process is very slow process. It follows the pseudo second order kinetics. Rate constant for bio removal is less than the adsorptive process.
- Removal process occurred due to the bio-accumulation of fluoride by the microbes because adsorbent active sites are covered with the microbial layer.
- Bio removal process is a time consuming process as compare to the adsorptive process.
- Bio removal process follows the Freundlich isotherm model whereas adsorptive process is well suited to Langmuir isotherm model.

### 6.2.3 Bio Column Reactor

Following conclusions have been summarized from the study of Bio Column Reactor:

- The bio-column reactor is capable to reduce the concentration of the pollutants in the effluent water below their permissible limit.
- Bio-column reactor needs to be backwashed to regenerate it for its effective continuous operation.
- At the initial stage, the flow rate and bed height have significant influence on the removal of fluoride from the contaminated water. However, after some time of operation (approximately 24-25 hours) such influence is negligible under the experimental conditions.
- Fluoride is removed almost completely after ~24 hours of operation.
- Dissolved Oxygen decreases along the bed height of the reactor, which supports the aerobic nature of the microbes.
- pH of the solution slightly decreases initially for the first hours and increases within the small range (6.5–7.5).
- The BDST model was successfully applied to analyze the column performance and to evaluate the model parameters. The BDST equations of linear relationship between the bed

depth and the service time were obtained with correlation coefficient values of 0.995, 0.992 and 0.937 for 12, 23 and 40 ml/min flow rate of Peristaltic Pump respectively.

- The Empty Bed Residence Time (EBRT) model which optimizes the empty bed residence time and the sorbent utilization rate was successfully applied with optimum contact time greater than about 159.0, 276.6 and 530.1 min for 40, 23 and 12 ml/min flow rates, respectively with the corresponding usage rate of 125.5, 32.6 and 113.4 g/L. The optimum dose of adsorbent for batch system was 3 g/100 mL.

#### 6.2.4 Fixed Bed Column Reactor

- The adsorption of fluoride on to *Java plum* seed (*Syzygiumcumini*) in a packed bed column was studied. The experimental results showed that it is feasible to use *Java plum* seed (*Syzygiumcumini*) as a bio-adsorbent for fluoride removal in a fixed-bed adsorption process.
- The impact of changing the column operating variables, such as bed depth, flow rate and initial concentration were investigated, and it is found that lower bed depth, higher influent concentration and flow rate could result in lower treated volumes ( $V_b$ ) and therefore decreases the service time( $T_b$ ) of the bed.
- The capacity of column system estimated from BDST model, in the flow rates of 12 and 23 and 40 mL min<sup>-1</sup> were 0.358, 0.382 and 0.193 mg g<sup>-1</sup> respectively.
- The BDST model was successfully applied to analyze column performance and evaluate the model parameters. The BDST equations of linear relationship between the bed depth and the service time were obtained with correlation coefficients of 0.961, 0.984 and 0.919 for 12, 23 and 40 mL min<sup>-1</sup> flow rates, respectively. The BDST model gave a good prediction for the change of system parameters, such as flow rate and the initial concentration (Table 5.1.8.3.4.2(a) & (b)).
- The Empty Bed Residence Time (EBRT) model which optimizes the Empty Bed Residence Time and the sorbent utilization rate was applied successfully with optimum contact time greater than about 159.0, 276.6 and 530.1 min for 40, 23 and 12 mL min<sup>-1</sup> flow rates, respectively, with the corresponding usage rate of 154.7, 78.1 and 83.3 g L<sup>-1</sup>. The optimum dose for batch system was found to be 3.1 g / 100 mL and it is close to the adsorbent exhaustion rate of 12 mL min<sup>-1</sup>.

- The application of Thomas model has showed that the adsorption capacity of bio-adsorbent is highly dependent on the flow rate, initial fluoride concentration, and bed depth and has a greater numerical value provided lower concentration of fluoride, lower flow rate and higher bed depth. And the Thomas rate constant decreases with increasing bed depth, decreasing initial concentration, and flow rate.

### 6.2.5 Phytoremediation

Phytoremediation is one of the latest methods for remediation of pollutants from soil, water land, water reservoir etc. with the point of view; experiments were conducted and have been summarized here below

- Among *Water Hyacinth* and *Ipomoea aquatica*, former is a better defluoridation agent than the latter.
- We got amazing unexpected results when we changed pH of the system. It was observed that fluoride removal efficiency decreases irrespective of increase or decrease in pH. It is also noted that maximum removal of fluoride was obtained when pH was almost neutral.
- To sustain fluoride, water hyacinth is way better than *Ipomoea Aquatica*. The *Ipomoea aquatica* plant which was used to study the effect of 20 mg/L solution of fluoride on plant almost died at the end of the experiment.
- After exposure both the plants show the decrease in content of chlorophyll.
- Both the plants show a degradation of biomass due to exposure of fluoride.
- Accumulation of fluoride is found in the following order stems < leaves < roots for *Ipomoea aquatica* plants.
- In case of *Water Hyacinth* accumulation of fluoride was found in order roots > stems > leaves.

### 6.2.6 Conclusion of the Present Work

The fluoride remediation of industrial waste water has been carried out and the present work has been summarized below

- The GAC, *citrus limetta* peel, groundnut shell, banana peel, neem leaves, virgin turmeric & MnO<sub>2</sub> coated and *java plum seed (Syzygiumcumini)* removed 97.7%, 95.8 %, 90.3%, 94.3%,



87.0%, 94.3% ,89.0 % and 94.9 % respectively from an aqueous solution of  $20 \text{ mgL}^{-1}$  fluoride.

- Mechanism of adsorption kinetics was found to follow pseudo-second order reaction, and the mechanism of fluoride removal on adsorbents was found to be complex.
- Best plots for Adsorption Isotherm was Langmuir model after studying Langmuir, Freundlich and Temkin adsorption isotherm models.
- Removal efficiency of bio removal is very high (93.1 %) as compare to *citrus limetta* peel (91.00 %).
- Removal process occurred due to the bio-accumulation of fluoride by the bacteria because adsorbent active sites are covered by the micro-organism.
- The bio-column reactor is capable to reduce the concentration of the pollutants in the effluent water below their permissible limit.
- At the initial stage, the flow rate and bed height have significant influence on the removal of fluoride from the contaminated water. However, after some time of operation (approximately 24-25 hours) such influence is negligible under the experimental conditions.
- DO reduce along the bed height of the reactor, which supports the aerobic nature of the bacteria.
- The Empty Bed Residence Time (EBRT) model which optimizes the empty bed residence time and the sorbent utilization rate was successfully applied with optimum contact time greater than about 159.0, 276.6 and 530.1 min for 40, 23 and 12 ml/min flow rates, respectively, with the corresponding usage rate of 125.5, 32.6 and 113.4 g/L. The optimum dose for batch system was 3 g/100 mL.
- Among Water Hyacinth and *Ipomoea aquatica*, former is a better defluoridation agent than the latter.
- It was observed that fluoride removal efficiency decreases irrespective of increase or decrease in pH. It is also noted that maximum removal of fluoride was obtained when pH was almost neutral.
- Accumulation of fluoride is found in order stems<leaves<roots for *Ipomoea aquatica* plants.
- In case of *Water Hyacinth* accumulation of fluoride was found in order roots> stems> leaves

### 6.3 Scope of Future Investigation

Since it is not possible to come to all aspects in the concerned areas, there are possibilities of doing the work left to give the completeness of research present work can be extended further, which are listed below

- Bio column reactor should be modeled so that scale up of the reactor can be done for the industrial installation.
- Investigation should be carried out with the modeling of phytoremediation technology of fluoride removal.
- Application of adsorbent for fluoride removal in large scale units from ground water samples should be verified by pilot studies by using BDST model.
- Investigation on bio-column reactor with higher flow rate (lower EBCT) should be done following the modeling of bio-column reactor.





## **List of Publications**

### **Published in International journal**

1. Defluoridation of Industrial Wastewater using Eichhornia Crassipes, *International Journal of Science, Engineering and Technology*, Volume 3 ISSUE 3 MAY-JUNE 2015,p.753-756.
2. Distribution of Residence Time for Packed Bed Column Reactor using a Packing of Bio-adsorbent (Java plum seed (Syzgiumcumini)), *International Journal of Science, Engineering and Technology*, Volume 3 ISSUE 3 MAY-JUNE 2015, p.757-760.
3. Kinetics for removal of fluoride from aqueous solution through adsorption from Mousambi Peel, Ground Nut Shell and Neem Leaves, *International Journal of Science, Engineering and Technology*, Volume 3 ISSUE 4 JULY-AUGUST 2015,p.879-883.
4. Removal of Fluoride from Industrial Waste Water by using living plant (IPOMOEA AQUATICA), *World Journal of Pharmacy and Pharmaceutical Sciences*, Volume 4 ISSUE 07, 2015.p.1276-1284.
5. Validation of CFD Model and Deciphering the Behaviour of Packed Bed Reactor by Comparative Technique of RTD and CFD, *World Journal of Pharmacy and Pharmaceutical Sciences*, Volume 4 ISSUE 07, 2015.p.1195-1202.
6. Removal of Fluoride using Groundnut Shell in Batch Reactor: Kinetics and Equilibrium Studies, *World Journal of Pharmacy and Pharmaceutical Sciences*, Volume 4 ISSUE 09, 2015.p.603-613.
6. Removal of Fluoride using treated Banana Peel in Batch Reactor: Kinetics and Equilibrium Studies, *World Journal of Pharmacy and Pharmaceutical Sciences*, Volume 4 ISSUE 09, 2015.p.693-704.
8. Removal of Fluoride using Sweet Lemon Peel in Batch Reactor: Kinetics and Equilibrium Studies, *World Journal of Pharmacy and Pharmaceutical Sciences*, Volume 4 ISSUE 11, 2015.p.775-787.
9. Fluoride Removal From Sewage Water Using Sweet Lemon peel As Biosorbents, *International Journal of Pharmacy and Pharmaceutical sciences*, Volume 8 Issue 7,2016,p.85-92

10. Comparing Fluoride Removal Kinetics of Adsorption Process From Aqueous Solution by Biosorbents, *Asian Journal of Pharmaceutical and Research Volume 9 Issue 4 July, 2016.p.1-5.*
11. Exploring Defluoridation Capacity of Turmeric on Industrial Sewage, *Asian Journal of Pharmaceutical and Research Volume 9 Issue 4 July, 2016.p.243-252.*
12. Effect of Co-existing Ions Defluoridation Capacity of Java plum seed (*Syzygiumcumini*), *World Journal of Pharmacy and Pharmaceutical Sciences, Volume 5 Issue 6 2016.p.730-737. DOI: 10.20959/wjpps20166-6516*
13. Adsorption of Fluoride from Industrial Waste Water in Fixed Bed Column using Java Plum, *Asian Journal of Pharmaceutical and Research, Vol 9 Suppl December 3 2016*
14. Treatment of Fluoride bearing contaminated water using SAB in a laboratory scale up-flow bio-column reactor by Java plum seed (*Syzygiumcumini*), *Asian Journal of Pharmaceutical and Research, Vol 9 Suppl December 3 2016*
15. Removal of Fluoride using Neem Leaves Batch Reactor: Kinetics and Equilibrium Studies, *Asian Journal of Pharmaceutical and Research (Accepted at 18 July, 2016)*
16. Singh TP, Majumder CB. Comparison of Properties of Defluoridation of *Ipomoea aquatica* and *Eichhornia crassipes* by the means of Phytoremediation, *Journal of Hazardous, toxic & radioactivity* .March,2017(DOI 10.106/ (ASCE) HZ 2153-5515.0000371)

#### **Conference Paper Presentations:**

1. Removal of Fluoride using treated Neem Leaves Batch Reactor: Kinetics and Equilibrium Studies, *International Conference of Biomedical Engineering and Supportive Technologies at Bundelkhand Institute of Engineering and Technology, 2-3 September, 2016*

#### **Under Review Journals:**

1. Comparative Study of Batch and Column Performance of Fluoride Adsorption by Java Plum Core/Seeds, *Journal of Hazardous, toxic & radioactivity* (Under Review with comment since 22-09-2015).

## **REFERENCES**

- Aharoni C, Sideman S, Hoffer E. Adsorption of phosphate ions by collodion-coated alumina. *Journal of Chemical Technology and Biotechnology*. 1979 Jan 1;29(7):404-12.
- Aharoni C, Ungarish M. Kinetics of activated chemisorption. Part 2.-Theoretical models. *Journal of the Chemical Society, Faraday Transactions 1: Physical Chemistry in Condensed Phases*. 1977;73:456-64.
- Aksu Z, Gönen F. Biosorption of phenol by immobilized activated sludge in a continuous packed bed: prediction of breakthrough curves. *Process biochemistry*. 2004 Jan 30;39(5):599-613.
- Amor Z, Bariou B, Mameri N, Taky M, Nicolas S, Elmidaoui A. Fluoride removal from brackish water by electrodialysis. *Desalination*. 2001 Apr 1;133(3):215-23.
- Anasuya A, Bapurao S, Paranjape PK. Fluoride and silicon intake in normal and endemic fluorotic areas. *Journal of trace elements in medicine and biology*. 1996 Dec 31;10(3):149-55.
- Annadurai G, Babu SR, Mahesh KP, Murugesan T. Adsorption and bio-degradation of phenol by chitosan-immobilized *Pseudomonas putida* (NICM 2174). *Bioprocess Engineering*. 2000 Jun 1;22(6):493-501.
- Basha S, Khambhaty Y, Mody K, Jha B. Kinetics, equilibrium and thermodynamic studies on biosorption of hexavalent chromium by dead fungal biomass of marine *Aspergillus niger*. *Chemical Engineering Journal*. 2009 Jan 1;145(3):489-95.
- Bayari CS, Kazanci N, Koyuncu H, Çinar SS, Gökçe D. Determination of the origin of the waters of Köyceğiz Lake, Turkey. *Journal of Hydrology*. 1995 Mar 31;166(1):171 -91.
- Bhatt DJ, Bhargava DS, Panesar PS. Effect of pH on phenol removal in moving media reactors. *Indian Journal of Environmental Health*. 1983;25(4):261-7.
- Bhatnagar A, Ji M, Choi YH, Jung W, Lee SH, Kim SJ, Lee G, Suk H, Kim HS, Min B, Kim SH. Removal of nitrate from water by adsorption onto zinc chloride treated activated carbon. *Separation Science and Technology*. 2008 Feb 25;43(4):886-907.

- Bohart GS, Adams EQ. Some aspects of the behavior of charcoal with respect to chlorine. 1. Journal of the American Chemical Society. 1920 Mar;42(3):523-44.
- Bulusu KR, Sundaresan BB, Pathak BN, Nawlakhe WG, Kulkarni DN, Thergaonkar VP. Fluorides in water. Defluoridation Methods and their Limitations".(60). 1979:1-25.
- Castel C, Schweizer M, Simonnot MO, Sardin M. Selective removal of fluoride ions by a two-way ion-exchange cyclic process. Chemical Engineering Science. 2000 Sep 30;55(17):3341-52.
- Chakrabarty S, Sarma HP. Defluoridation of contaminated drinking water using neem charcoal adsorbent: kinetics and equilibrium studies. Int J ChemTech Res. 2012;4(2):511-6.
- Craveiro F, Malina J. Anaerobic degradation of phenol and bioregeneration of granular activated carbon. Journal of Hazardous Materials. 1991 Sep 30;28(1):189-90.
- Cunningham SD, Shann JR, Crowley DE, Anderson TA. Phytoremediation of contaminated water and soil. 1997
- Deng Y., Nordstrom D.K., Blaine McCleskey R. 2011. Fluoride geochemistry of thermal waters in Yellowstone National Park: I. Aqueous fluoride speciation, Geochim. Cosmochim. Acta 75, 4476–4489
- Dushenkov V, Kumar PN, Motto H, Raskin I. Rhizofiltration: the use of plants to remove heavy metals from aqueous streams. Environmental science & technology. 1995 May;29(5):1239-45..
- Eaton AD, Clesceri LS, Franson MA, Greenberg AE. Standard methods for the examination of water and wastewater . Section 2540 Solids.1995.
- Eaton AD, Clesceri LS, Franson MA, Greenberg AE. Standard methods for the examination of water and wastewater . Section 2540 Solids. 1995.
- Eckenfelder WW. Industrial water pollution control. McGraw-Hill; 1989.
- Ehrhardt HM, Rehm HJ. Phenol degradation by microorganisms adsorbed on activated carbon. Applied Microbiology and Biotechnology. 1985 Jan 1;21(1-2):32-6.
- Fan X, Parker DJ, Smith MD. Adsorption kinetics of fluoride on low cost materials. Water Research. 2003 Dec 31;37(20):4929-37.

- Freundlich U. Die adsorption in lusungen. 1906:385-470.
- Genç-Fuhrman H, Tjell JC, McConchie D. Adsorption of arsenic from water using activated neutralized red mud. *Environmental science & technology*. 2004 Apr 15;38(8):2428-34.
- Ghorai S, Pant KK. Equilibrium, kinetics and breakthrough studies for adsorption of fluoride on activated alumina. *Separation and purification technology*. 2005 Apr 30;42(3):265-71.
- Gulay M, Kurutepe S, Surucuoglu S, Sezgin C, Gazi H, Ozbakkaloglu B. Increasing antimicrobial resistance in *Escherichia coli* isolates from community-acquired urinary tract infections during 1998-2003 in Manisa, Turkey. *Japanese journal of infectious diseases*. 2005 Jun 1;58(3):159.
- Guo H, Stüben D, Berner Z, Kramar U. Adsorption of arsenic species from water using activated siderite–hematite column filters. *Journal of hazardous materials*. 2008 Mar 1;151(2):628-35.
- Gupta VK, Ali I, Saini VK. Defluoridation of wastewaters using waste carbon slurry. *Water Research*. 2007 Aug 31;41(15):3307-16.
- Hao OJ, Huang CP. Adsorption characteristics of fluoride onto hydrous alumina. *Journal of environmental engineering*. 1986 Dec;112(6):1054-69.
- Ho YS, McKay G. The kinetics of sorption of divalent metal ions onto sphagnum moss peat. *Water research*. 2000 Feb 15;34(3):735-42.
- Hu CY, Lo SL, Kuan WH, Lee YD. Removal of fluoride from semiconductor wastewater by electrocoagulation–flotation. *Water research*. 2005 Mar 31;39(5):895-901.
- Hutchins RA. New method simplifies design of activated-carbon systems. *Chemical Engineering*. 1973 Jan 1;80(19):133-8.
- Jadia CD, Fulekar MH. Phytoremediation of heavy metals: Recent techniques. *African journal of biotechnology*. 2009 Mar 20;8(6).
- Jong T, Parry DL. Removal of sulfate and heavy metals by sulfate reducing bacteria in short-term bench scale upflow anaerobic packed bed reactor runs. *Water Research*. 2003 Aug 31;37(14):3379-89.



Kalinske AA. Enhancement of biological oxidation of organic wastes using activated carbon in microbial suspensions. *Water and Sewage Works*. 1972 Jun;119(6):62-4.

Killedar DJ, Bhargava DS. Effects of stirring rate and temperature on fluoride removal by fishbone charcoal. *Indian Journal of Environmental Health*. 1993;35(2):81-7.

Kumar E, Bhatnagar A, Ji M, Jung W, Lee SH, Kim SJ, Lee G, Song H, Choi JY, Yang JS, Jeon BH. Defluoridation from aqueous solutions by granular ferric hydroxide (GFH). *Water Research*. 2009 Feb 28;43(2):490-8.

Kumar KV, Subanandam K, Ramamurthi V, Sivanesan S. Solid liquid adsorption for wastewater treatment: Principle design and operation. Anna University College of Technology, India. 2004.

Kumar PN, Dushenkov V, Motto H, Raskin I. Phytoextraction: the use of plants to remove heavy metals from soils. *Environmental science & technology*. 1995 May;29(5):1232-8.

Lagergren S. About the theory of so-called adsorption of soluble substances. 1898.

Langmuir I. The Constitution and Fundamental Properties of Solids and Liquids. PART I. SOLIDS. *Journal of the American Chemical Society*. 1916 Nov;38(11):2221-95.

Liao XP, Shi BI. Adsorption of fluoride on zirconium (IV)-impregnated collagen fiber. *Environmental science & technology*. 2005 Jun 15;39 (12):4628-32.

Liao XP, Shi B. Selective removal of tannins from medicinal plant extracts using a collagen fiber adsorbent. *Journal of the Science of Food and Agriculture*. 2005 Jun 1;85(8):1285-91.

Lu, S., Gibb, S. W. (2008). Copper removal from waste water using spent grain as biosorbent. *Bioresource Technology*, 99(6), 1509-1517.

Lv L. Defluoridation of drinking water by calcined MgAl-CO<sub>3</sub> layered double hydroxides. *Desalination*. 2007 Apr 5;208(1):125-33.

Maheshwari RC. Fluoride in drinking water and its removal. *Journal of Hazardous Materials*. 2006 Sep 1;137(1):456-63.

Malay DK, Salim AJ. Comparative study of batch adsorption of fluoride using commercial and natural adsorbent. *Research Journal of Chemical Sciences*. 2011 Oct;1(7):68-75.

Markovska L, Meshko V, Noveski V. Adsorption of basic dyes in a fixed bed column. *Korean Journal of Chemical Engineering*. 2001 Mar 1;18(2):190-5.

Mathialagan T, Viraraghavan T. Adsorption of cadmium from aqueous solutions by perlite. *Journal of Hazardous Materials*. 2002 Oct 14;94(3):291-303.

McKay G, Bino MJ. Simplified optimisation procedure for fixed bed adsorption systems. *Water, Air, and Soil Pollution*. 1990 May 1;51(1-2):33-41.

Mckay G, Blair HS, Gardner JR. The adsorption of dyes onto chitin in fixed bed columns and batch adsorbers. *Journal of Applied Polymer Science*. 1984 May 1;29(5):1499-514.

Mckay G, Otterburn MS, Sweeney AG. The removal of colour from effluent using various adsorbents—III. Silica: rate processes. *Water Research*. 1980 Dec 31;14(1):15-20.

Meenakshi S, Viswanathan N. Identification of selective ion-exchange resin for fluoride sorption. *Journal of Colloid and Interface Science*. 2007 Apr 15;308(2):438-50.

Mohammad A., Majumder C.B. 2014. Removal of fluoride from synthetic waste water by using ‘bio-adsorbents, *International Journal of Research in Engineering and Technology*, 03,776-785.

Mohan SV, Bhaskar YV, Karthikeyan J. Biological decolourisation of simulated azo dye in aqueous phase by algae *Spirogyra* species. *International journal of environment and pollution*. 2004 Jan 1;21(3):211-22.

Mohan SV, Karthikeyan J. Removal of lignin and tannin colour from aqueous solution by adsorption onto activated charcoal. *Environmental Pollution*. 1997 Dec 31;97(1):183-7.

Mohapatra D, Mishra D, Mishra SP, Chaudhury GR, Das RP. Use of oxide minerals to abate fluoride from water. *Journal of colloid and interface science*. 2004 Jul 15;275(2):355-9.

Mondal P, Balomajumder C. Treatment of resorcinol and phenol bearing waste water by simultaneous adsorption biodegradation (SAB): optimization of process parameters. *International Journal of Chemical Reactor Engineering*. 2007 Jan 1;5(1).

Mondal P, Majumder CB, Mohanty B. Treatment of arsenic contaminated water in a laboratory scale up-flow bio-column reactor. *Journal of hazardous materials*. 2008 May 1;153(1):136-45.

Muhammad F, Ramli A, Subbarao D. Some Studies on the Synthesis and Surface Properties of Mixed Oxides of Alumina and Magnesia. *Research Journal of Chemistry and Environment*. 2011;15(2):715-20.

Nagendran R, Selvam A, Joseph K, Chiemchaisri C. Phytoremediation and rehabilitation of municipal solid waste landfills and dumpsites: A brief review. *Waste Management*. 2006 Dec 31;26(12):1357-69.

Ndiaye PI, Moulin P, Dominguez L, Millet JC, Charbit F. Removal of fluoride from electronic industrial effluent by RO membrane separation. *Desalination*. 2005 Mar 1;173(1):25-32.

Negrea A, Lupa L, Ciopec M, Negrea P. Experimental and modelling studies on As (III) removal from aqueous medium on fixed bed column. *Chemical Bulletin of "Politehnica" University of Timisoara, ROMANIA Series of Chemistry and Environmental Engineering*. 2011;56(70):2.

Onyango MS, Kojima Y, Aoyi O, Bernardo EC, Matsuda H. Adsorption equilibrium modeling and solution chemistry dependence of fluoride removal from water by trivalent-cation-exchanged zeolite F-9. *Journal of Colloid and Interface Science*. 2004 Nov 15;279(2):341-50.

Onyango MS, Kojima Y, Kumar A, Kuchar D, Kubota M, Matsuda H. Uptake of fluoride by Al<sup>3+</sup> pretreated low-silica synthetic zeolites: adsorption equilibrium and rate studies. *Separation Science and Technology*. 2006 Apr 1;41(4):683-704.

Ortiz-Pérez D, Rodríguez-Martínez M, Martínez F, Borja-Aburto VH, Castelo J, Grimaldo JI, de la Cruz E, Carrizales L, Díaz-Barriga F. Fluoride-induced disruption of reproductive hormones in men. *Environmental Research*. 2003 Sep 30;93(1):20-30.

Panday KK, Prasad G, Singh VN. Mixed adsorbents for Cu (II) removal from aqueous solutions. *Environmental Technology*. 1986 Jan 1;7(1-12):547-54.

Parthasarathy N, Buffle J, Haerdi W. Study of interaction of polymeric aluminium hydroxide with fluoride. *Canadian journal of chemistry*. 1986 Jan 1;64(1):24-9.

Pavlatou A, Polyzopoulos NA. The role of diffusion in the kinetics of phosphate desorption: the relevance of the Elovich equation. *Journal of Soil Science*. 1988 Sep 1;39(3):425-36.

Perrich JR. Activated carbon adsorption for wastewater treatment. CRC PRESS INC., BOCA RATON, FL. 1981.

Perrotti AE, Rodman CA. Factors involved with biological regeneration of activated carbon. InAIChE Symp. Ser 1974 (Vol. 70, No. 144, pp. 317-325).

Phantumvanit P, Songpaisan Y, Moller IJ. A defluoridator for individual households. InWorld Health Forum (WHO) 1988 (Vol. 9, No. 4, pp. 555-58). World Health Organization.

Pommerenk P, Schafran GC. Adsorption of inorganic and organic ligands onto hydrous aluminum oxide: evaluation of surface charge and the impacts on particle and NOM removal during water treatment. Environmental science & technology. 2005 Sep 1;39(17):6429-34.

Prakasam, R.S., Chandra Reddy, P.L., Manisha, A., Ramakrishna, S.V., Defluoridation of drinking water using Eichhornia sp.. IJEP 19 (2), 119–124. 1998.

Qaiser S, Saleemi AR, Umar M. Biosorption of lead from aqueous solution by Ficus religiosa leaves: batch and column study. Journal of Hazardous Materials. 2009 Jul 30;166(2):998-1005.

Ramanaiah SV, Mohan SV, Sarma PN. Adsorptive removal of fluoride from aqueous phase using waste fungus (Pleurotus ostreatus 1804) biosorbent: Kinetics evaluation. ecological engineering. 2007 Sep 3;31(1):47-56.

Rao NM, Bhaskaran CS. Studies on defluoridation of water. Journal of fluorine chemistry. 1988 Oct 31;41(1):17-24.

Reardon EJ, Wang Y. A limestone reactor for fluoride removal from wastewaters. Environmental science & technology. 2000 Aug 1;34(15):3247-53.

Rudzinski W, Panczyk P, Schwarz JA, Contescu CI. Surfaces of nanoparticles and porous materials. 1998; 355

Ruixia L, Jinlong G, Hongxiao T. Adsorption of fluoride, phosphate, and arsenate ions on a new type of ion exchange fiber. Journal of colloid and interface science. 2002 Apr 15;248(2):268-74.

Salt DE, Blaylock M, Kumar NP, Dushenkov V, Ensley BD, Chet I, Raskin I. Phytoremediation: a novel strategy for the removal of toxic metals from the environment using plants. *Nature biotechnology*. 1995 May 1;13(5):468-74.

Sangi MR, Shahmoradi A, Zolgharnein J, Azimi GH, Ghorbandoost M. Removal and recovery of heavy metals from aqueous solution using *Ulmuscarpinifolia* and *Fraxinus excelsior* tree leaves. *Journal of hazardous materials*. 2008 Jul 15;155(3):513-22.

Seader JD, Henley EJ. *Separation process principles*.

Shen F, Chen X, Gao P, Chen G. Electrochemical removal of fluoride ions from industrial wastewater. *Chemical Engineering Science*. 2003 Mar 31;58(3):987-93.

Simons R. Trace element removal from ash dam waters by nanofiltration and diffusion dialysis. *Desalination*. 1993 Jan 1;89(3):325-41.

Singh TP, Majumder CB. Removal of fluoride using *Citrus limetta* peel in batch reactor: kinetics and equilibrium studies. *World J Pharm Pharm Sci*. 2015 Aug 27;4:775-87.

Singh TP, Majumder CB. Removal of Fluoride from Industrial Waste Water by using living plant (*IPOMOEA AQUATICA*), *World Journal of Pharmacy and Pharmaceutical Sciences*, Volume 4 ISSUE 07, 2015.p.1276-1284.

Singh TP, Bhatnagar J, Majumder C. Distribution of Residence Time for Packed Bed Column Reactor using a Packing of Bio-adsorbent (*Java plum seed (Syzygiumcumini)*), *International Journal of Science, Engineering and Technology*, Volume 3 ISSUE 3 MAY-JUNE 2015, p.757-760.

Singh TP, Majumder CB. Kinetics for removal of fluoride from aqueous solution through adsorption from mousambi peel, groundnut shell and neem leaves. *Int J Sci Eng Technol*. 2015;3:879-3.

Singh TP, Majumder CB. Comparison of Properties of Defluoridation of *Ipomoea aquatica* and *Eichhornia crassipes* by the means of Phytoremediation, *Journal of Hazardous, toxic & radioactivity* .March,2017(DOI 10.106/ (ASCE) HZ 2153-5515.0000371)

Singha B, Das SK. Biosorption of Cr (VI) ions from aqueous solutions: kinetics, equilibrium, thermodynamics and desorption studies. *Colloids and surfaces B: Biointerfaces*. 2011 May 1;84(1):221-32.

Sivasamy A, Singh KP, Mohan D, Maruthamuthu M. Studies on defluoridation of water by coal-based sorbents. *Journal of Chemical Technology and Biotechnology*. 2001 Jul 1;76(7):717-22.

Standard I (2005) Drinking water-specification. Second Revision, IS, 10500

Taty-Costodes VC, Fauduet H, Porte C, Ho YS. Removal of lead (II) ions from synthetic and real effluents using immobilized *Pinussylvestris* sawdust: adsorption on a fixed-bed column. *Journal of hazardous materials*. 2005 Aug 31;123(1):135-44.

Thakre D., Jagtap S., Sakhare N., Labhsetwar N., Meshram S., Rayalu S. 2010. Chitosan based mesoporous Ti–Al binary metal oxide supported beads for defluoridation of water, *Chem. Eng. J.* 158, 315–324.

Thomas, H.C., Heterogeneous ion exchange in a flowing system, *Journal of the American Chemical Society*, 66, 1664–1666, 1944.

Tüzün I, Bayramoğlu G, Yalçın E, Başaran G, Celik G, Arica MY. Equilibrium and kinetic studies on biosorption of Hg (II), Cd (II) and Pb (II) ions onto microalgae *Chlamydomonas reinhardtii*. *Journal of Environmental Management*. 2005 Oct 31;77(2):85-92.

Vara Prasad MN, de Oliveira Freitas HM. Metal hyperaccumulation in plants: biodiversity prospecting for phytoremediation technology. *Electronic Journal of Biotechnology*. 2003 Dec;6(3):285-321.

Viswanathan N, Sundaram CS, Meenakshi S. Removal of fluoride from aqueous solution using protonated chitosan beads. *Journal of Hazardous Materials*. 2009 Jan 15;161(1):423-30.

Wasewar K.L., Prasad B., Gulipalli S., 2009. Removal of selenium by adsorption onto granular activated carbon (GAC) and powdered activated carbon (PAC), *Clean Soil Air Water* 37, 872–883.

Water S, World Health Organization. Guidelines for drinking-water quality [electronic resource]: incorporating first addendum. Vol. 1, Recommendations. 2006.

Weber WJ, Morris JC. Preliminary appraisal of advanced waste treatment processes. InProc. Int. Conf. Advances in Water Poll. Res 1963 (Vol. 2, pp. 231-241).

Weber WJ, Morris JC. Kinetics of adsorption on carbon from solution. Journal of the Sanitary Engineering Division. 1963 Mar;89(2):31-60.

World Health Organization. Fluorine and fluorides. World Health Organization; 1984.

Xiaojian Z, Zhansheng W, Xiasheng G. Simple combination of biodegradation and carbon adsorption—the mechanism of the biological activated carbon process. Water research. 1991 Feb 1;25(2):165-72.

YuY., YuL., Chen J. P, 2015. Adsorption of fluoride by Fe–Mg–La triple-metal composite: Adsorbent preparation, illustration of performance and study of mechanisms, Chem. Eng. J. 262, 839–846.

Zewge F. Investigation leading to the Defluoridation of water in Ethiopia. A report submitted to the Ethiopian Science and Technology Commission, Addis Ababa, Ethiopia. 2001.

### Derivation of BDST Equation

For modeling the breakthrough data, we used the BDST model which was originally proposed by Bohart and Adams in 1920 for the adsorption of chlorine and hydrogen chloride on carbon. Considering a given portion of adsorbing material, its adsorption capacity diminishes at a rate given by:

$$\frac{\partial N}{\partial t} = -KNC \quad (1)$$

Considering the liquid phase, the solute concentration is diminishing at the rate given by:

$$\frac{\partial C}{\partial D} = -\frac{k}{v}NC \quad (2)$$

Where:

N = Adsorption capacity per volume of bed (mg cm<sup>-3</sup>)

C = Solute concentration in solution (mg L<sup>-1</sup>)

K = Adsorption rate constants (L mg<sup>-1</sup>h<sup>-1</sup>)

v = Linear flow rate through the bed (cm h<sup>-1</sup>)

D = bed depth (cm)

If N<sub>0</sub> is the average adsorption capacity per volume of the bed and C<sub>0</sub> is the initial solute concentration in solution then the non-dimensional parameters can be defined as:

$$N' = \frac{N}{N_0}; C' = \frac{C}{C_0}; D' = \frac{KN_0}{v}D; \text{ and } t' = KC_0t$$

Their derivatives being as follows:

$$\partial N' = \frac{\partial N}{N_0}; \partial C' = \frac{\partial C}{C_0}; \partial D' = \frac{KN_0}{v} \partial D; \text{ and } \partial t' = KC_0 \partial t$$

Introducing these new parameters into equation (1) and (2):

$$\frac{\partial N'}{\partial t} = -N'C' \quad (3)$$

$$\frac{\partial C'}{\partial D'} = -N'C' \quad (4)$$

On the following initial conditions:

$$\text{Where } t' = 0 \Rightarrow C' = 1 \quad (5)$$

$$D' = 0 \Rightarrow C' = 1 \quad (6)$$

Integrating equation (3) with the initial condition (5), we will have:

$$N' = e^{-t'} \quad (7)$$



Integrating equation (4) with the initial condition (6), we will have:

$$C' = e^{-D'} \quad (8)$$

If equation (4) is divided by  $(C')^2$  :

$$\frac{\partial N' / C'^2}{\partial t} = \frac{N'}{C'} \quad (9)$$

Introducing Eq. (7) and Eq. (8) in to Eq. (9):

$$-\frac{\partial C' / C'^2}{\partial D'} = e^{(D'-t')} \quad (10)$$

Integrating Eq. (10):

$$\frac{1}{C'} = e^{(D'-t')} - f(t') \quad (11)$$

Introducing the initial condition Eq. (6) in to Eq. (11):

$$f(t') = e^{-t'} - 1 \quad (12)$$

Then, introducing Eq. (12) in to Eq. (11):

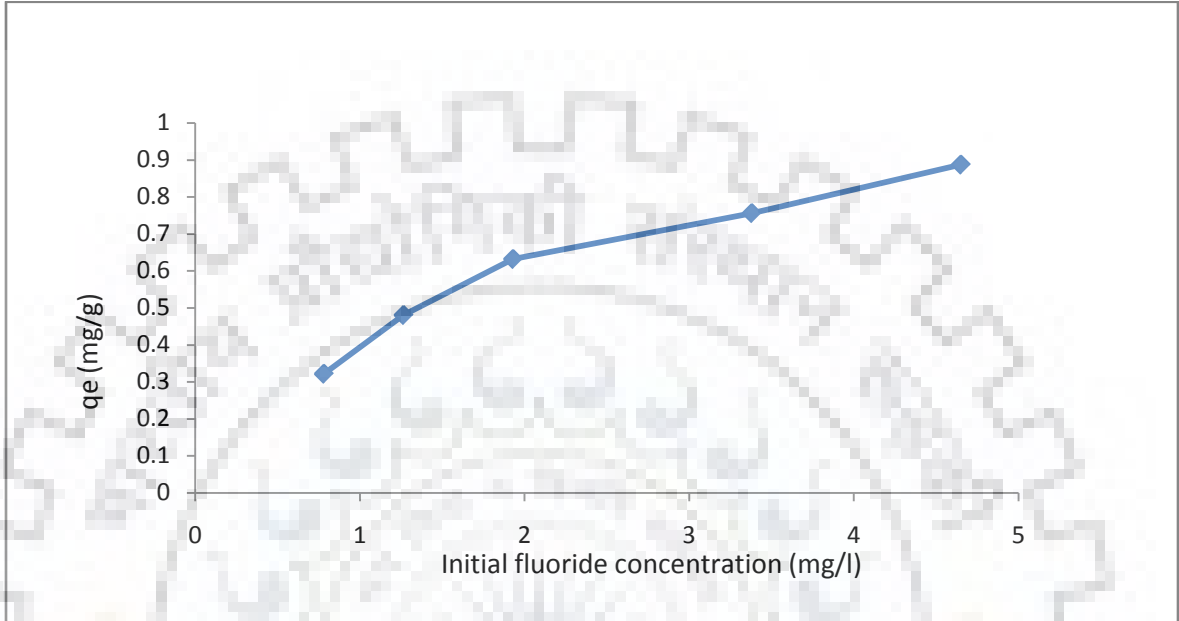
$$\begin{aligned} \frac{1}{C'} &= e^{(D'-t')} - e^{-t'} + 1 \\ \frac{1}{C'} - 1 &= (e^{-D'} - 1)e^{-t'} \\ \ln\left(\frac{1}{C'} - 1\right) &= \ln[(e^{-D'} - 1)e^{-t'}] \\ \ln\left(\frac{1}{C'} - 1\right) &= \ln(e^{-D'} - 1) - t' \quad (13) \end{aligned}$$

By substituting the non-dimensional parameters by the initial variables ( $C_0$  and  $N_0$ ) Eq. (13) becomes:

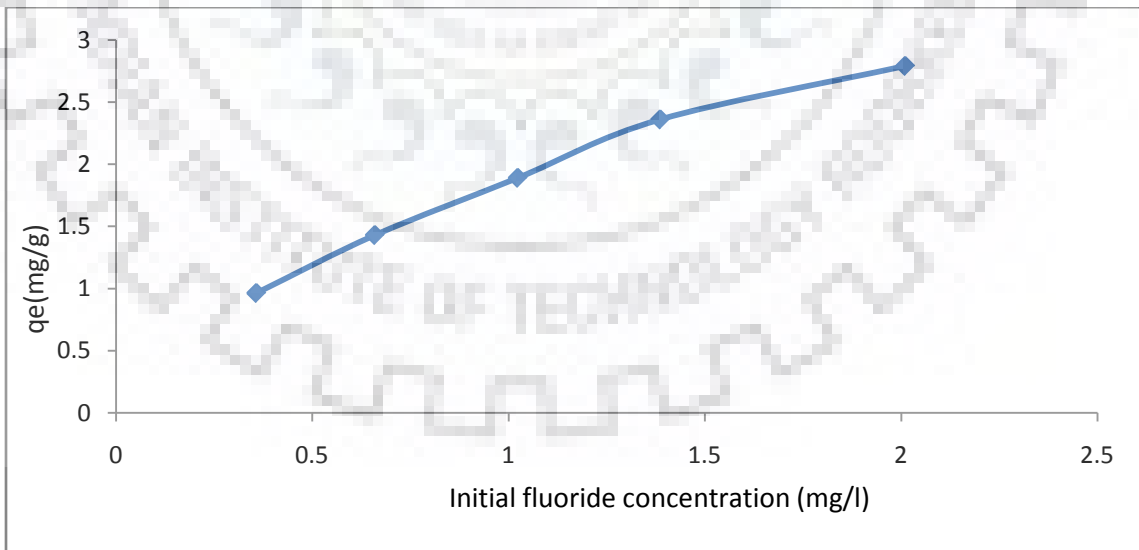
$$\ln\left(\frac{C_0}{C} - 1\right) = \ln\left(e^{\frac{KN_0 D}{v}} - 1\right) - KC_0 t \quad (14)$$

Because  $e^{\frac{KN_0 D}{v}} \gg 1$  then the unit term on the right hand side of Eq. (32) is often neglected, thus  $\ln\left(e^{\frac{KN_0 D}{v}} - 1\right) \cong \frac{KN_0 D}{v}$ , So the linear relationship between the service time and bed depth can be written as:

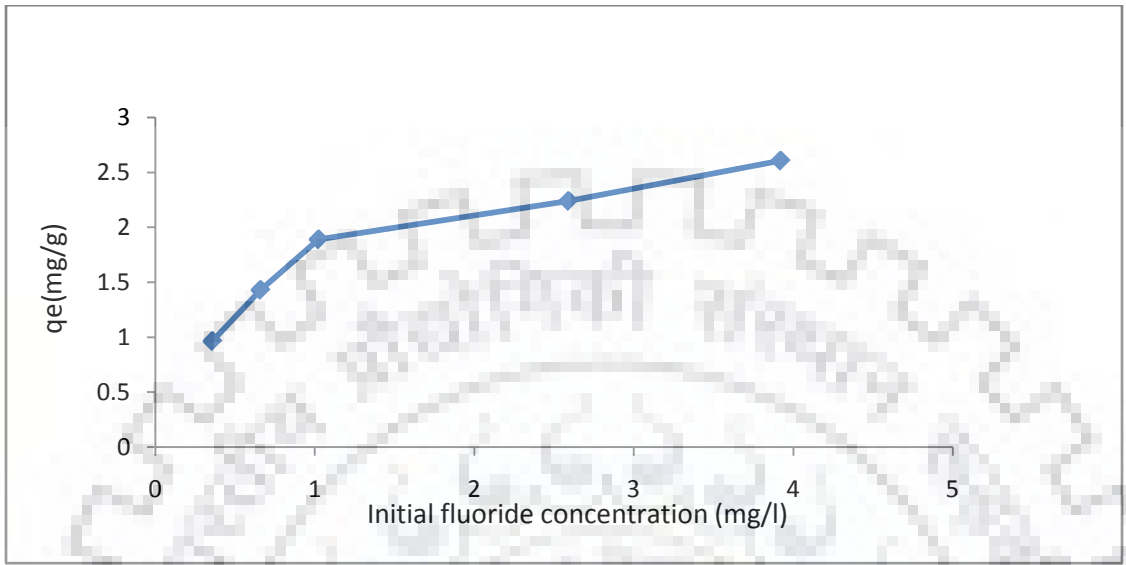
$$t = \frac{N_0}{C_0 v} D - \frac{1}{KC_0} \ln\left[\frac{C_0}{C} - 1\right] \quad (15)$$



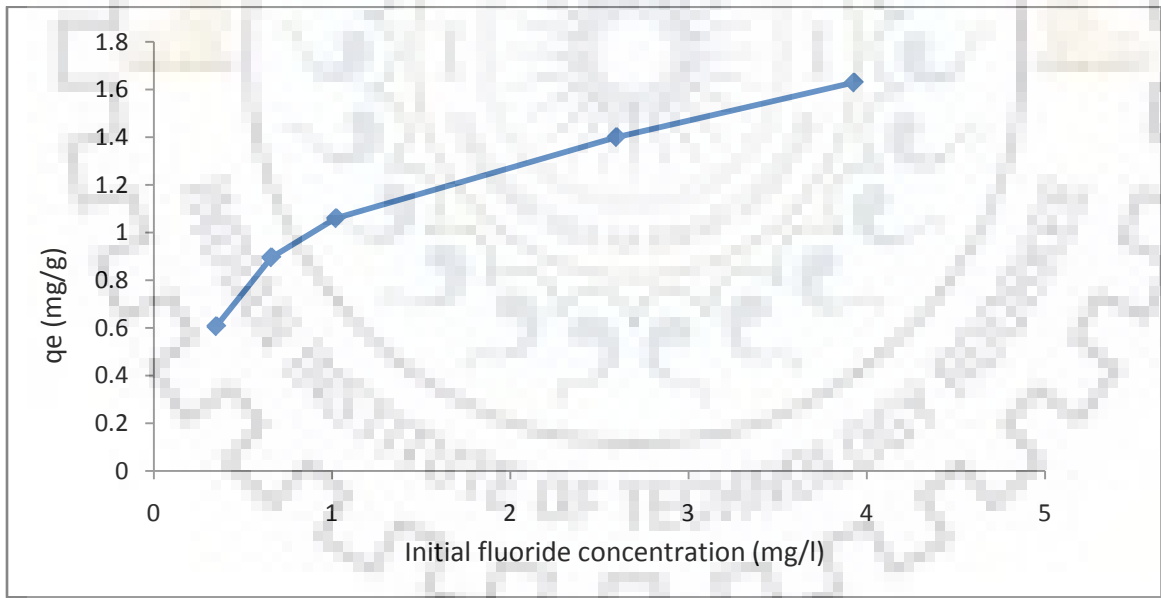
Effect of initial concentration for removal of fluoride by GAC.



Effect of initial concentration for removal of fluoride by Citrus Limetta Peel.



Effect of initial concentration for removal of fluoride by Java Plum Seed.



Effect of initial concentration for removal of fluoride by Banana Peel.

## Effect of Initial Fluoride Concentration

The effect of initial concentration on percentage removal was investigated at their optimum dose, pH and contact time on adsorbents onto different concentration of fluoride solutions (10, 15, 20, 25,30 mg L<sup>-1</sup>). Fig (5.1.4.4.1, 5.1.4.4.2.,5.1.4.4.6 etc.) GAC, Citrus Limetta Peel Java Plum Seed, Banana Peel etc, describes the effect of initial fluoride concentration on the fluoride removal efficiency. The results illustrated that fluoride removal efficiency decreased by increasing the initial fluoride concentration because of the fixed dose of adsorbent capacity adsorbents gets saturated at high concentration. The Pore volume and active sites of the adsorbents are filled by the fluoride finally and its removal is decreased. Similar trend has been reported for fluoride removal by using Neem charcoal (Chakrabarty and Sharma, 2012)

The adsorption capacity of fluoride adsorbed per unit adsorbent ( $q_e$ ) (mg g<sup>-1</sup>) was calculated according to following Equation [23].

$$q_e = \frac{(C_i - C_e)}{m} V \text{mg/g}$$

Where

C <sub>i</sub>	Initial fluoride concentration.
C <sub>e</sub>	Final fluoride concentrations.
V	Volume of the solution (L).
m	Mass of the adsorbent (g).

The results of Fig. GAC. Citrus Limetta Peel .Java Plumb Seed, Banana Peel etc shows in appendix B which demonstrates that the amount of adsorbed fluoride increased with the increase in fluoride initial concentrations. This increase in fluoride concentration gradient was the driving force behind overcoming all mass transfer resistances of the fluoride, between the aqueous and solid phases. It also led to an increase the equilibrium sorption, unit sorbent saturation was achieved. Similar trend has been reported for adsorption capacity tea ash, applied for fluoride removal (Mondal et al; 2012).



**Table A.1 Input and output parameters for the adsorption of fluoride onto the surface of GAC using synthetic simulated single component solution.**

Exp. Set No.	Run No.	pH	Temp (°C)	Adsorbent dose (g/50 mL)	Initial concentration of fluoride (mg/L)	Contact time (minute)	Final concentration of fluoride (mg/L)	Output Parameters % Removal of fluoride
			<b>Input Parameter (pH Optimization)</b>					
1	1	2	30	0.5	20	30	1.2	93.8
1	2	3	30	0.5	20	30	0.962	95.2
1	3	4	30	0.5	20	30	0.44	97.9
1	4	5	30	0.5	20	30	0.818	95.9
1	5	6	30	0.5	20	30	1.8	91.2
1	6	7.5	30	0.5	20	30	1.7	91.7
1	7	8	30	0.5	20	30	1.7	91.7
1	8	9	30	0.5	20	30	1.7	91.7
1	9	10	30	0.5	20	30	1.6	91.9
1	10	11	30	0.5	20	30	1.5	92.5
			<b>Input Parameter (Temperature)</b>					
1	11	4	20	0.5	20	30	13.3	33.7
1	12	4	25	0.5	20	30	11.5	42.7
1	13	4	30	0.5	20	30	0.28	98.6
1	14	4	35	0.5	20	30	1.9	90.3

1	15	4	40	0.5	20	30	3.5	82.7		
			<b>Input Parameter (dose)</b>							
1	16	4	30	0.2	20	30	2.6	86.9		
1	17	4	30	0.4	20	30	1.8	91.0		
1	18	4	30	0.6	20	30	1.4	92.3		
1	19	4	30	0.8	20	30	1.2	93.8		
1	20	4	30	1	20	30	1.1	94.7		
1	21	4	30	1.2	20	30	0.98	95.1		
1	22	4	30	1.4	20	30	0.74	96.0		
1	23	4	30	1.6	20	30	0.52	97.4		
1	24	4	30	1.8	20	30	0.64	96.8		
1	25	4	30	2.0	20	30	0.66	96.7		
<b>Exp. Set No.</b>	<b>Run No.</b>	<b>pH</b>	<b>Temp (°C)</b>	<b>Adsorbent dose (g/50 mL)</b>	<b>Initial concentration of fluoride (mg/L)</b>	<b>Contact time (minute)</b>		<b>Ads. Cap. <math>q_e</math></b>	<b>% Removal</b>	
<b>Input Parameter (Fluoride Concentration)</b>										
1	26	4	30	1.6	10	30	0.09	0.3096	99.1	
1	27	4	30	1.6	15	30	0.255	0.4607	98.3	
1	28	4	30	1.6	20	30	0.46	0.6835	97.7	
1	29	4	30	1.6	25	30	1.2	0.5875	95.4	
1	30	4	30	1.6	30	30	1.7	0.8884	94.3	

Input Parameter (Contact Time)								Ads. Cap. $q_t$	% Removal
1	31	4	30	1.6	20	20	1.8	0.5687	90.9
1	32	4	30	1.6	20	40	1.8	0.5687	91.2
1	33	4	30	1.6	20	60	1.8	0.5687	91.9
1	34	4	30	1.6	20	80	1.5	0.5781	92.3
1	35	4	30	1.6	20	100	1.4	0.5812	93.1
1	35	4	30	1.6	20	120	1.0	0.950	94.9
1	36	4	30	1.6	20	140	0.994	0.5939	95.0
1	37	4	30	1.6	20	160	0.98	0.5943	95.1
1	38	4	30	1.6	20	180	0.988	0.5943	95.1
			Run No. 26-30, 31-38 were used for Equilibrium and Kinetic modelling respectively						



**Table A.2 Input and output parameters for the adsorption of fluoride onto the surface of Citrus limetta peel using synthetic simulated single component solution.**

Exp. Set No.	Run No.	pH	Temp (°C)	Adsorbent dose (g/50 mL)	Initial concentration of fluoride (mg/L)	Contact time (minute)	Final concentration of fluoride (mg/L)	Output Parameters % Removal of fluoride
<b>Input Parameter (pH Optimization)</b>								
1	39	3	30	0.5	4	30	12.2	39.2
1	40	4	30	0.5	20	30	7.9	60.7
1	41	5	30	0.5	20	30	1.8	91.0
1	42	6	30	0.5	20	30	8.1	59.5
1	43	7	30	0.5	20	30	9.4	52.8
1	44	8	30	0.5	20	30	9.0	54.9
1	45	9	30	0.5	20	30	8.9	55.5
1	46	10	30	0.5	20	30	8.5	57.4
1	47	11	30	0.5	20	30	8.7	56.5
<b>Input Parameter (Temperature)</b>								
1	48	5	20	0.5	20	30	13.3	33.7
1	49	5	25	0.5	20	30	11.5	42.7
1	50	5	30	0.5	20	30	0.28	98.6
1	51	5	35	0.5	20	30	2.0	90.3
1	52	5	40	0.5	20	30	3.5	82.7

Exp. Set No.	Run No.	pH	Temp (°C)	Adsorbent dose (g/50 mL)	Initial concentration of fluoride (mg/L)	Contact time (minute)	Final concentration of fluoride (mg/L)	Output Parameters % Removal of fluoride	
<b>Input Parameter (dose)</b>									
1	53	5	30	0.1	20	30	4.3	78.6	
1	54	5	30	0.2	20	30	3.7	81.6	
1	55	5	30	0.3	20	30	2.6	86.7	
1	56	5	30	0.4	20	30	2.5	87.3	
1	57	5	30	0.5	20	30	1.1	94.3	
1	58	5	30	0.6	20	30	1.3	93.4	
1	59	5	30	0.7	20	30	1.4	92.8	
1	60	5	30	0.8	20	30	1.2	93.9	
1	61	5	30	1.0	20	30	1.4	93.1	
<b>Input Parameter (Fluoride Concentration)</b>								<b>Ads. Cap. q<sub>e</sub></b>	<b>% Removal</b>
1	62	5	30	0.5	10	30	0.357	0.9643	96.4
1	63	5	30	0.5	15	30	0.66	1.434	95.6
1	64	5	30	0.5	20	30	1.8	1.82	90.9
1	65	5	30	0.5	25	30	2.4	2.76	90.5
1	66	5	30	0.5	30	30	2.0	2.8	93.3
<b>Input Parameter (Contact Time)</b>								<b>Ads. Cap. q<sub>t</sub></b>	<b>% Removal</b>
1	67	5	30	0.5	20	5	2.2	1.77	88.9

Exp. Set No.	Run No.	pH	Temp (°C)	Adsorbent dose (g/50 mL)	Initial concentration of fluoride (mg/L)	Contact time (minute)	Final concentration of fluoride (mg/L)	Output Parameters	
								% Removal of fluoride	
1	68	5	30	0.5	20	10	1.9	1.81	90.7
1	69	5	30	0.5	20	15	1.7	1.83	91.6
1	70	5	30	0.5	20	20	1.5	1.84	92.5
1	71	5	30	0.5	20	25	1.3	1.67	93.4
1	72	5	30	0.5	20	30	1.1	1.89	94.6
1	73	5	30	0.5	20	35	0.9	1.90	95.2
1	74	5	30	0.5	20	40	0.854	1.91	95.8
1	75	5	30	0.5	20	50	0.854	1.91	95.8
1	76	5	30	0.5	20	60	0.854	1.91	95.8
Run No. 62-66, 67-76 were used for Equilibrium and Kinetic modeling respectively									

**Table A.3 Input and output parameters for the adsorption of fluoride onto the surface of Ground Nut Shell using synthetic simulated single component solution.**

Exp. Set No.	Run No.	pH	Temp (°C)	Adsorbent dose (g/50 mL)	Initial concentration of fluoride (mg/L)	Contact time (minute)	Final concentration of fluoride (mg/L)	Output Parameters % Removal of fluoride
<b>Input Parameter (pH Optimization)</b>								
3	77	2	30	0.5	20	30	5.2	73.9
3	78	3	30	0.5	20	30	4.6	76.9
3	79	4	30	0.5	20	30	3.9	80.2
3	80	5	30	0.5	20	30	3.2	84.1
3	81	6	30	0.5	20	30	2.5	87.7
3	82	7	30	0.5	20	30	2.3	88.5
3	83	8	30	0.5	20	30	3.3	83.5
3	84	9	30	0.5	20	30	3.8	80.8
3	85	10	30	0.5	20	30	4.4	78.1
3	86	11	30	0.5	20	30	4.7	76.3
3	87	12	30	0.5	20	30	4.9	75.5
<b>Input Parameter (Temperature)</b>								
3	88	7	20	0.5	20	30	13.2	33.7
3	89	7	25	0.5	20	30	11.5	42.7
3	90	7	30	0.5	20	30	0.284	98.6
3	91	7	35	0.5	20	30	1.9	90.3

Exp. Set No.	Run No.	pH	Temp (°C)	Adsorbent dose (g/50 mL)	Initial concentration of fluoride (mg/L)	Contact time (minute)	Final concentration of fluoride (mg/L)	Output Parameters % Removal of fluoride
3	92	7	40	0.5	20	30	3.5	82.7
<b>Input Parameter (dose)</b>								
3	93	7	30	0.2	20	30	4.6	76.8
3	94	7	30	0.3	20	30	4.3	78.6
3	95	7	30	0.4	20	30	3.5	82.6
3	96	7	30	0.5	20	30	2.9	85.7
3	97	7	30	0.6	20	30	2.3	88.4
3	98	7	30	0.7	20	30	2.2	89.0
3	99	7	30	0.8	20	30	2.0	89.9
3	100	7	30	0.9	20	30	2.0	89.9
3	101	7	30	1.0	20	30	2.0	89.9
<b>Input Parameter (Fluoride Concentration)</b>								<b>Ads. Cap. <math>q_e</math></b>
3	102	7	30	0.8	10	30	0.781	0.576
3	103	7	30	0.8	15	30	1.3	0.856
3	104	7	30	0.8	20	30	1.9	1.13
3	105	7	30	0.8	25	30	3.4	1.35
3	106	7	30	0.8	30	30	4.7	1.58
<b>Input Parameter (Contact Time)</b>								<b>Ads. Cap. <math>q_t</math></b>

<b>Exp. Set No.</b>	<b>Run No.</b>	<b>pH</b>	<b>Temp (°C)</b>	<b>Adsorbent dose (g/50 mL)</b>	<b>Initial concentration of fluoride (mg/L)</b>	<b>Contact time (minute)</b>	<b>Final concentration of fluoride (mg/L)</b>	<b>Output Parameters % Removal of fluoride</b>
3	107	7	30	0.8	20	10	5.1	1.29
3	108	7	30	0.8	20	20	3.4	1.38
3	109	7	30	0.8	20	30	2.9	1.42
3	110	7	30	0.8	20	40	2.6	1.453
3	111	7	30	0.8	20	50	2.3	1.473
3	112	7	30	0.8	20	60	2.1	1.493
3	113	7	30	0.8	20	75	1.9	1.507
3	114	7	30	0.8	20	90	1.8	1.517
Run No. 102-106, 107-114 were used for Equilibrium and Kinetic modeling respectively								

**Table A.4 Input and output parameters for the adsorption of fluoride onto the surface of Neem leaves using synthetic simulated single component solution.**

Exp. Set No.	Run No.	pH	Temp (°C)	Adsorbent dose (g/50 mL)	Initial concentration of fluoride (mg/L)	Contact time (minute)	Final concentration of fluoride (mg/L)	Output Parameters % Removal of fluoride
<b>Input Parameter (pH Optimization)</b>								
4	115	2	30	0.5	20	30	12.6	36.8
4	116	3	30	0.5	20	30	6.8	66.0
4	117	4	30	0.5	20	30	3.3	83.6
4	118	5	30	0.5	20	30	5.8	71.2
4	119	6	30	0.5	20	30	8.3	58.4
4	120	8	30	0.5	20	30	9.2	53.9
4	121	9	30	0.5	20	30	9.4	53.3
4	122	10	30	0.5	20	30	9.1	54.4
<b>Input Parameter (Temperature)</b>								
4	123	4	20	0.5	20	30	13.3	33.7
4	124	4	25	0.5	20	30	11.5	42.7
4	125	4	30	0.5	20	30	0.3	98.6
4	126	4	35	0.5	20	30	1.9	90.3
4	127	4	40	0.5	20	30	3.5	82.7
<b>Input Parameter (dose)</b>								
4	128	4	30	0.1	20	30	4.3	78.6
4	129	4	30	0.2	20	30	3.7	81.6

Exp. Set No.	Run No.	pH	Temp (°C)	Adsorbent dose (g/50 mL)	Initial concentration of fluoride (mg/L)	Contact time (minute)	Final concentration of fluoride (mg/L)	Output Parameters % Removal of fluoride	
4	130	4	30	0.3	20	30	2.7	86.7	
4	131	4	30	0.4	20	30	4.3	78.3	
4	132	4	30	0.5	20	30	3.2	84.0	
4	133	4	30	0.6	20	30	2.9	85.3	
4	134	4	30	0.7	20	30	2.9	85.3	
4	135	4	30	0.8	20	30	2.9	85.5	
4	136	4	30	1.0	20	30	2.9	85.5	
<b>Input Parameter (Fluoride Concentration)</b>								<b>Ads. Cap. <math>q_e</math></b>	<b>% Removal</b>
4	137	4	30	0.6	10	30	0.5	0.792	95.2
4	138	4	30	0.6	15	30	1.1	1.2	92.8
4	139	4	30	0.6	20	30	1.9	1.51	90.3
4	140	4	30	0.6	25	30	2.6	1.87	89.6
<b>Input Parameter (Contact Time)</b>								<b>Ads. Cap. <math>q_t</math></b>	<b>% Removal</b>
4	141	4	30	0.6	20	5	2.2	1.48	88.9
4	142	4	30	0.6	20	10	1.9	1.45	90.7
4	143	4	30	0.6	20	15	1.7	1.46	91.6
4	144	4	30	0.6	20	20	1.5	1.47	92.5
4	145	4	30	0.6	20	25	1.3	1.49	93.4
4	146	4	30	0.6	20	30	1.1	1.51	94.6



Exp. Set No.	Run No.	pH	Temp (°C)	Adsorbent dose (g/50 mL)	Initial concentration of fluoride (mg/L)	Contact time (minute)	Final concentration of fluoride (mg/L)	Output Parameters	
								% Removal of fluoride	
4	147	4	30	0.6	20	35	0.962	1.52	95.2
4	148	4	30	0.6	20	40	0.842	1.53	95.8
4	149	4	30	0.6	20	50	0.842	1.53	95.8
4	150	4	30	0.6	20	60	0.842	1.53	95.8
Run No. 137-140, 141-150 were used for Equilibrium and Kinetic modeling respectively									



**Table A.5 Input and output parameters for the adsorption of fluoride onto the surface of Turmeric using synthetic simulated single component solution.**

<b>Exp. Set No.</b>	<b>Run No.</b>	<b>pH</b>	<b>Temp (°C)</b>	<b>Adsorbent dose (g/50 mL)</b>	<b>Initial concentration of fluoride (mg/L)</b>	<b>Contact time (minute)</b>	<b>Final concentration of fluoride (mg/L)</b>	<b>Output Parameters % Removal of fluoride</b>
<b>Input Parameter (pH Optimization)</b>								
1	151	2	30	0.5	20	60	4.1	79.7
1	152	3	30	0.5	20	60	3.6	81.8
1	153	3.5	30	0.5	20	60	3.5	82.7
1	154	4	30	0.5	20	60	3.2	84.2
1	155	5	30	0.5	20	60	2.5	87.5
1	156	6	30	0.5	20	60	1.5	92.5
1	157	7	30	0.5	20	60	2.1	89.8
1	158	8	30	0.5	20	60	2.9	85.4
1	159	9	30	0.5	20	60	3.9	80.6
1	160	10	30	0.5	20	60	4.5	77.3
1	161	11	30	0.5	20	60	4.7	76.8
1	162	12	30	0.5	20	60	5.2	73.8
<b>Input Parameter (Temperature)</b>								
1	163	6	20	0.5	20	30	13.3	33.7
1	164	6	25	0.5	20	30	11.5	42.7
1	165	6	30	0.5	20	30	0.284	98.6
1	166	6	35	0.5	20	30	1.9	90.3

Exp. Set No.	Run No.	pH	Temp (°C)	Adsorbent dose (g/50 mL)	Initial concentration of fluoride (mg/L)	Contact time (minute)	Final concentration of fluoride (mg/L)	Output Parameters % Removal of fluoride	
1	167	6	40	0.5	20	30	3.5	82.7	
<b>Input Parameter (dose)</b>									
1	168	6	30	0.2	20	60	3.4	83.2	
1	169	6	30	0.3	20	60	2.7	86.5	
1	170	6	30	0.4	20	60	2.5	87.7	
1	171	6	30	0.5	20	60	2.1	89.5	
1	172	6	30	0.6	20	60	1.9	90.7	
1	173	6	30	0.7	20	60	1.7	91.7	
1	174	6	30	0.8	20	60	1.5	92.5	
1	175	6	30	0.9	20	60	1.4	93.1	
1	176	6	30	1.0	20	60	1.2	93.9	
<b>Input Parameter (Fluoride Concentration)</b>								<b>Ads. Cap. q<sub>e</sub></b>	<b>% Removal</b>
1	177	6	30	0.8	10	60	0.476	0.595	95.2
1	178	6	30	0.8	15	60	0.774	0.88	94.8
1	179	6	30	0.8	20	60	1.1	1.17	94.3
1	180	6	30	0.8	25	60	2.7	1.39	89.3
1	181	6	30	0.8	30	60	3.9	1.62	86.7
<b>Input Parameter (Contact Time)</b>								<b>Ads. Cap. q<sub>t</sub></b>	<b>% Removal</b>

Exp. Set No.	Run No.	pH	Temp (°C)	Adsorbent dose (g/50 mL)	Initial concentration of fluoride (mg/L)	Contact time (minute)	Final concentration of fluoride (mg/L)	Output Parameters	
								% Removal of fluoride	
1	182	6	30	0.5	20	10	3.3	1.04	83.6
1	183	6	30	0.5	20	20	2.4	1.10	88.1
1	184	6	30	0.5	20	30	1.9	1.12	90.2
1	185	6	30	0.5	20	40	1.7	1.14	91.4
1	186	6	30	0.5	20	50	1.4	1.16	93.2
1	187	6	30	0.5	20	60	1.3	1.16	93.5
1	188	6	30	0.5	20	75	1.3	1.17	93.8
1	189	6	30	0.5	20	90	1.2	1.17	94.0
Run No. 177-181, 182-189 were used for Equilibrium and Kinetic modeling respectively									

**Table A.6 Input and output parameters for the adsorption of fluoride onto the surface of MnO<sub>2</sub> coated Turmeric using synthetic simulated single component solution.**

Exp. Set No.	Run No.	pH	Temp (°C)	Adsorbent dose (g/50 mL)	Initial concentration of fluoride (mg/L)	Contact time (minute)	Final concentration of fluoride (mg/L)	Output Parameters % Removal of fluoride
<b>Input Parameter (pH Optimization)</b>								
3	190	2	30	0.5	20	30	5.4	72.9
3	191	3	30	0.5	20	30	4.8	75.9
3	192	4	30	0.5	20	30	4.2	79.2
3	193	5	30	0.5	20	30	3.4	83.1
3	194	6	30	0.5	20	30	2.7	86.7
3	195	7	30	0.5	20	30	2.5	87.5
3	196	8	30	0.5	20	30	3.5	82.5
3	197	9	30	0.5	20	30	4.0	79.8
3	198	10	30	0.5	20	30	4.6	77.1
3	199	11	30	0.5	20	30	4.3	75.3
3	200	12	30	0.5	20	30	5.1	74.5
<b>Input Parameter (Temperature)</b>								
3	201	7	20	0.5	20	30	13.3	33.7
3	202	7	25	0.5	20	30	11.5	42.7
3	203	7	30	0.5	20	30	0.284	98.6
3	204	7	35	0.5	20	30	1.9	90.3
3	205	7	40	0.5	20	30	3.5	82.7

Exp. Set No.	Run No.	pH	Temp (°C)	Adsorbent dose (g/50 mL)	Initial concentration of fluoride (mg/L)	Contact time (minute)	Final concentration of fluoride (mg/L)	Output Parameters % Removal of fluoride
<b>Input Parameter (dose)</b>								
3	206	7	30	0.2	20	30	4.8	75.8
3	207	7	30	0.3	20	30	4.5	77.6
3	208	7	30	0.4	20	30	3.7	81.6
3	209	7	30	0.5	20	30	3.1	84.7
3	210	7	30	0.6	20	30	2.5	87.4
3	211	7	30	0.7	20	30	2.4	88.0
3	212	7	30	0.8	20	30	2.3	88.6
3	213	7	30	0.9	20	30	2.2	88.9
3	214	7	30	1.0	20	30	2.2	88.9
<b>Input Parameter (Fluoride Concentration)</b>								<b>Ads. Cap. q<sub>e</sub></b>
3	215	7	30	0.8	10	30	0.9	0.568
3	216	7	30	0.8	15	30	1.4	0.866
3	217	7	30	0.8	20	30	2.0	1.125
3	218	7	30	0.8	25	30	3.3	1.35
3	219	7	30	0.8	30	30	4.7	1.5
<b>Input Parameter (Contact Time)</b>								<b>Ads. Cap. q<sub>t</sub></b>
3	220	7	30	0.8	20	10	4.5	1.29

<b>Exp. Set No.</b>	<b>Run No.</b>	<b>pH</b>	<b>Temp (°C)</b>	<b>Adsorbent dose (g/50 mL)</b>	<b>Initial concentration of fluoride (mg/L)</b>	<b>Contact time (minute)</b>	<b>Final concentration of fluoride (mg/L)</b>	<b>Output Parameters % Removal of fluoride</b>
3	221	7	30	0.8	20	20	3.4	1.38
3	222	7	30	0.8	20	30	2.9	1.42
3	223	7	30	0.8	20	40	2.6	1.453
3	224	7	30	0.8	20	50	2.3	1.473
3	225	7	30	0.8	20	60	2.1	1.493
3	226	7	30	0.8	20	75	1.9	1.507
3	227	7	30	0.8	20	90	1.8	1.517
Run No. 215-219, 220-227 were used for Equilibrium and Kinetic modeling respectively								

**Table A.7 Input and output parameters for the adsorption of fluoride onto the surface of Java plum seed using synthetic simulated single component solution.**

Exp. Set No.	Run No.	pH	Temp (°C)	Adsorbent dose (g/50 mL)	Initial concentration of fluoride (mg/L)	Contact time (minute)	Final concentration of fluoride(mg/L)	Output Parameters % Removal of fluoride
<b>Input Parameter (pH Optimization)</b>								
5	228	2	30	0.5	20	30	7.7	61.5
5	229	3	30	0.5	20	30	7.2	63.8
5	230	4	30	0.5	20	30	3.4	82.9
5	231	5	30	0.5	20	30	3.5	82.4
5	232	6	30	0.5	20	30	1.4	93.2
5	233	7	30	0.5	20	30	3.6	82.1
5	234	8	30	0.5	20	30	3.3	83.3
5	235	9	30	0.5	20	30	3.3	83.6
<b>Input Parameter (Temperature)</b>								
5	236	6	20	0.5	20	30	13.3	33.7
5	237	6	25	0.5	20	30	9.5	52.7
5	238	6	30	0.5	20	30	0.3	98.6
5	239	6	35	0.5	20	30	1.9	90.3
5	240	6	50	0.5	20	30	3.5	82.7
<b>Input Parameter (dose)</b>								
5	241	6	30	0.1	20	30	4.3	78.6



Exp. Set No.	Run No.	pH	Temp (°C)	Adsorbent dose (g/50 mL)	Initial concentration of fluoride (mg/L)	Contact time (minute)	Final concentration of fluoride(mg/L)	Output Parameters % Removal of fluoride
5	242	6	30	0.2	20	30	4.0	79.9
5	243	6	30	0.4	20	30	3.2	83.8
5	244	6	30	0.5	20	30	0.118	99.4
5	245	6	30	0.6	20	30	0.412	97.9
5	246	6	30	0.8	20	30	2.624	86.9
5	247	6	30	1.0	20	30	1.0	95.0
<b>Input Parameter (Fluoride Concentration)</b>								<b>Ads. Cap. <math>q_e</math></b>
5	248	6	30	0.5	10	30	0.356	0.964
5	249	6	30	0.5	15	30	0.725	1.43
5	250	6	30	0.5	20	30	1.0	1.90
5	251	6	30	0.5	30	30	3.9	2.61
<b>Input Parameter (Contact Time)</b>								<b>Ads. Cap. <math>q_t</math></b>
5	252	6	30	0.5	20	5	2.2	1.77
5	253	6	30	0.5	20	10	1.9	1.81
5	254	6	30	0.5	20	15	1.7	1.83
5	255	6	30	0.5	20	20	1.5	1.84
5	256	6	30	0.5	20	25	1.3	1.86
5	257	6	30	0.5	20	30	1.1	1.89
5	258	6	30	0.5	20	35	0.942	1.90

<b>Exp. Set No.</b>	<b>Run No.</b>	<b>pH</b>	<b>Temp (°C)</b>	<b>Adsorbent dose (g/50 mL)</b>	<b>Initial concentration of fluoride (mg/L)</b>	<b>Contact time (minute)</b>	<b>Final concentration of fluoride(mg/L)</b>	<b>Output Parameters % Removal of fluoride</b>
5	259	6	30	0.5	20	40	0.822	1.91
5	260	6	30	0.5	20	50	0.822	1.91
5	261	6	30	0.5	20	60	0.822	1.91
Run No. 248-251, 252-261 were used for Equilibrium and Kinetic modeling respectively								

**Table A.8 Input and output parameters for the adsorption of fluoride onto the surface of Banana Peel using synthetic simulated single component solution.**

Exp. Set No.	Run No.	pH	Temp (°C)	Adsorbent dose (g/50 mL)	Initial concentration of fluoride (mg/L)	Contact time (minute)	Final concentration of fluoride(mg/L)	Output Parameters % Removal of fluoride
<b>Input Parameter (pH Optimization)</b>								
2	262	2	30	0.5	20	60	5.7	71.7
2	263	3	30	0.5	20	60	5.2	73.8
2	264	3.5	30	0.5	20	60	5.1	74.7
2	265	4	30	0.5	20	60	4.8	76.2
2	266	5	30	0.5	20	60	4.1	79.5
2	267	6	30	0.5	20	60	1.4	93.1
2	268	7	30	0.5	20	60	3.6	81.8
2	269	8	30	0.5	20	60	4.5	77.4
2	270	9	30	0.5	20	60	5.5	72.6
2	271	10	30	0.5	20	60	6.1	69.3
2	272	11	30	0.5	20	60	6.3	68.8
2	273	12	30	0.5	20	60	6.8	65.8
<b>Input Parameter (Temperature)</b>								
2	274	6	20	0.5	20	30	13.3	33.7
2	275	6	25	0.5	20	30	11.5	42.7
2	276	6	30	0.5	20	30	0.284	98.6
2	277	6	35	0.5	20	30	1.9	90.3

Exp. Set No.	Run No.	pH	Temp (°C)	Adsorbent dose (g/50 mL)	Initial concentration of fluoride (mg/L)	Contact time (minute)	Final concentration of fluoride(mg/L)	Output Parameters % Removal of fluoride	
2	278	6	40	0.5	20	30	3.5	82.7	
<b>Input Parameter (dose)</b>									
2	279	6	30	0.2	20	60	3.2	84.2	
2	280	6	30	0.3	20	60	2.5	87.5	
2	281	6	30	0.4	20	60	2.3	88.7	
2	282	6	30	0.5	20	60	1.9	90.5	
2	283	6	30	0.6	20	60	1.7	91.7	
2	284	6	30	0.7	20	60	1.5	92.7	
2	285	6	30	0.8	20	60	1.3	93.5	
2	286	6	30	0.9	20	60	1.2	94.1	
2	287	6	30	1.0	20	60	1.0	94.9	
<b>Input Parameter (Fluoride Concentration)</b>								<b>Ads. Cap. q<sub>e</sub></b>	<b>% Removal</b>
2	288	6	30	0.8	10	60	0.952	0.566	95.2
2	289	6	30	0.8	15	60	0.88	0.88	95.6
2	290	6	30	0.8	20	60	1.3	1.17	93.6
2	291	6	30	0.8	25	60	2.1	1.39	89.6
2	292	6	30	0.8	30	60	2.6	1.62	86.9
<b>Input Parameter (Contact Time)</b>								<b>Ads. Cap. q<sub>t</sub></b>	<b>% Removal</b>

Exp. Set No.	Run No.	pH	Temp (°C)	Adsorbent dose (g/50 mL)	Initial concentration of fluoride (mg/L)	Contact time (minute)	Final concentration of fluoride(mg/L)	Output Parameters	
								% Removal of fluoride	
2	293	6	30	0.8	20	10	3.3	1.04	83.6
2	294	6	30	0.8	20	20	2.4	1.10	88.1
2	295	6	30	0.8	20	30	1.9	1.12	90.2
2	296	6	30	0.8	20	40	1.1	1.14	91.4
2	297	6	30	0.8	20	50	1.4	1.16	93.2
2	298	6	30	0.8	20	60	1.3	1.16	93.5
2	299	6	30	0.8	20	75	1.3	1.17	93.8
2	300	6	30	0.8	20	90	1.2	1.17	94.0
Run No. 288-292, 293-300 were used for Equilibrium and Kinetic modeling respectively									

**Table A.9 Growth Studies of Acinetobacter baumannii MTCC No. 11451**

Exp. Set No.	Run No.	pH	Temp (°C)	Time (hr)	OD (Optical Density)
6	301	7	30	0	0.00
6	302	7	30	3	0.09
6	303	7	30	6	1.2
6	304	7	30	9	1.7
6	305	7	30	12	1.9
6	306	7	30	15	1.9
6	307	7	30	18	1.9
6	308	7	30	21	2.1
6	309	7	30	24	2.2
6	310	7	30	27	2.2
6	311	7	30	30	2.2
6	312	7	30	33	2.2
6	313	7	30	36	2.2
6	314	7	30	39	2.2
6	315	7	30	42	2.2
6	316	7	30	45	2.2
6	317	7	30	48	2.2
6	318	7	30	51	2.2
6	319	7	30	54	2.2
6	320	7	30	57	2.2

6	321	7	30	60	2.1
6	322	7	30	63	2.1
6	323	7	30	66	2.0
6	324	7	30	69	2.0
6	325	7	30	72	2.0
6	326	7	30	75	2.0
6	327	7	30	78	2.0
6	328	7	30	81	2.0
6	329	7	30	84	1.9
6	330	7	30	87	1.9
6	331	7	30	90	1.9
6	332	7	30	91	1.9
6	333	7	30	94	1.8
6	334	7	30	97	1.8
6	335	7	30	90	1.7

**Table A.10 Input and output parameters for the simultaneous adsorption and bioaccumulation of fluoride using *Acinetobacter baumannii* MTCC No. 11451 immobilized *citrus limetta* Peel for synthetic simulated single component solution.**

Exp. Set No.	Run No.	pH	Temp (°C)	Adsorbent dose (g/100 mL)	Initial concentration of fluoride (mg/L)	Contact time (minute)	Final concentration of fluoride(mg/L)	Output Parameters % Removal of fluoride
<b>Input Parameter (pH Optimization)</b>								
7	336	2	30	1	20	3600	2.4	88.1
7	337	3	30	1	20	3600	1.8	90.9
7	338	4	30	1	20	3600	1.4	93.1
7	339	5	30	1	20	3600	1.4	93.0
7	340	6	30	1	20	3600	1.4	92.9
7	341	7	30	1	20	3600	1.4	92.9
7	342	8	30	1	20	3600	1.5	92.3
7	343	9	30	1	20	3600	1.8	91.1
7	344	10	30	1	20	3600	1.9	90.4
<b>Input Parameter (Temperature)</b>								
7		7	20	1	20	3600	13.3	33.7
7	345	7	25	1	20	3600	9.5	52.7
7	346	7	30	1	20	3600	0.284	98.6
7	347	7	35	1	20	3600	1.9	90.3
7	348	7	50	1	20	3600	3.5	82.7
<b>Input Parameter (dose)</b>								



Exp. Set No.	Run No.	pH	Temp (°C)	Adsorbent dose (g/100 mL)	Initial concentration of fluoride (mg/L)	Contact time (minute)	Final concentration of fluoride(mg/L)	Output Parameters % Removal of fluoride
7	349	7	30	0.4	20	3600	0.24	98.8
7	350	7	30	0.6	20	3600	0.188	99.1
7	351	7	30	0.8	20	3600	0.14	99.3
7	352	7	30	1.0	20	3600	0.14	99.3
7	353	7	30	1.2	20	3600	0.142	99.3
7	354	7	30	1.4	20	3600	0.142	99.3
7	355	7	30	1.6	20	3600	0.154	99.2
7	356	7	30	1.8	20	3600	0.154	99.2
<b>Input Parameter (Fluoride Concentration)</b>								<b>Ads. Cap. q<sub>e</sub></b>
7	357	7	30	1	20	3600	0.074	1.9
7	358	7	30	1	30	3600	0.386	2.9
7	359	7	30	1	40	3600	0.434	3.9
7	360	7	30	1	50	3600	0.444	4.9
<b>Input Parameter (Contact Time)</b>								<b>Ads. Cap. q<sub>t</sub></b>
7	361	7	30	1	20	300	8.1	0.84
7	362	7	30	1	20	600	6.1	0.99
7	363	7	30	1	20	900	4.5	1.1
7	364	7	30	1	20	1200	4.6	1.2
7	365	7	30	1	20	1500	2.4	1.3

<b>Exp. Set No.</b>	<b>Run No.</b>	<b>pH</b>	<b>Temp (°C)</b>	<b>Adsorbent dose (g/100 mL)</b>	<b>Initial concentration of fluoride (mg/L)</b>	<b>Contact time (minute)</b>	<b>Final concentration of fluoride(mg/L)</b>	<b>Output Parameters % Removal of fluoride</b>
7	366	7	30	1	20	1800	2.1	1.3
7	367	7	30	1	20	2100	1.9	1.3
7	368	7	30	1	20	2400	1.7	1.3
7	369	7	30	1	20	2700	1.6	1.3
7	370	7	30	1	20	3000	1.5	1.3
7	371	7	30	1	20	3300	1.4	1.3
7	372	7	30	1	20	3600	1.4	1.3
7	373	7	30	1	20	3900	1.4	1.3
7	374	7	30	1	20	4200	1.3	1.3
7	375	7	30	1	20	4500	1.3	1.3
7	376	7	30	1	20	4800	1.1	1.3
7	377	7	30	1	20	5100	1.3	1.3
7	378	7	30	1	20	5400	1.1	1.3

Run No. 242-245, 246-263 were used for Equilibrium and Kinetic modeling respectively

**Table A.11 Input and output parameters for the simultaneous adsorption and bioaccumulation of fluoride using *Acinetobacter baumannii* MTCC No. 11451 immobilized Jamun Guthali for synthetic simulated single component solution.**

Exp. Set No.	Run No.	pH	Temp (°C)	Adsorbent dose (g/100 mL)	Initial concentration of fluoride (mg/L)	Contact time (minute)	Final concentration of fluoride (mg/L)	Output Parameters % Removal of fluoride
<b>Input Parameter (pH Optimization)</b>								
8	379	2	30	1	20	2400	2.4	88.1
8	380	3	30	1	20	2400	1.8	90.9
8	381	4	30	1	20	2400	1.4	93.1
8	382	5	30	1	20	2400	1.4	93.0
8	383	6	30	1	20	2400	1.4	92.9
8	384	7	30	1	20	2400	1.4	92.9
8	385	8	30	1	20	2400	1.5	92.3
8	386	9	30	1	20	2400	1.8	91.1
8	387	10	30	1	20	2400	1.9	90.4
<b>Input Parameter (Temperature)</b>								
8	388	7	20	1	20	2400	13.3	33.7
8	389	7	25	1	20	2400	9.5	52.7
8	390	7	30	1	20	2400	0.284	98.6
8	391	7	35	1	20	2400	1.9	90.3
8	392	7	50	1	20	2400	3.5	82.7
<b>Input Parameter (dose)</b>								

Exp. Set No.	Run No.	pH	Temp (°C)	Adsorbent dose (g/100 mL)	Initial concentration of fluoride (mg/L)	Contact time (minute)	Final concentration of fluoride (mg/L)	Output Parameters % Removal of fluoride	
8	393	7	30	0.4	20	2400	2.6	86.9	
8	394	7	30	0.6	20	2400	2.4	87.9	
8	395	7	30	0.8	20	2400	2.3	88.5	
8	396	7	30	1.0	20	2400	2.2	89.0	
8	397	7	30	1.2	20	2400	2.1	89.3	
8	398	7	30	1.4	20	2400	2.1	89.7	
8	399	7	30	1.6	20	2400	2.0	89.9	
8	400	7	30	1.8	20	2400	2.0	89.9	
8	401	7	30	2.0	20	2400	2.0	89.9	
<b>Input Parameter (Fluoride Concentration)</b>								<b>Ads. Cap. <math>q_e</math></b>	<b>% Removal</b>
8	402	7	30	1.8	20	2400	2.8	0.95	85.9
8	403	7	30	1.8	30	2400	3.2	1.4	83.8
8	404	7	30	1.8	40	2400	3.6	1.8	82.2
8	405	7	30	1.8	50	2400	4.2	2.2	79.0
<b>Input Parameter (Contact Time)</b>								<b>Ads. Cap. <math>q_t</math></b>	<b>% Removal</b>
8	405	7	30	1.8	20	300	3.9	0.894	80.6
8	406	7	30	1.8	20	600	3.6	1.059	82.2
8	407	7	30	1.8	20	900	3.4	0.92	82.9

Exp. Set No.	Run No.	pH	Temp (°C)	Adsorbent dose (g/100 mL)	Initial concentration of fluoride (mg/L)	Contact time (minute)	Final concentration of fluoride (mg/L)	Output Parameters	
								% Removal of fluoride	
8	408	7	30	1.8	20	1200	3.4	0.92	82.9
8	409	7	30	1.8	20	1500	3.4	0.92	82.8
8	410	7	30	1.8	20	1800	3.4	0.92	82.9
8	411	7	30	1.8	20	2100	3.4	0.95	83.2
8	412	7	30	1.8	20	2400	3.3	0.95	83.6
Run No. 288-291, 289-299 were used for Equilibrium and Kinetic modeling respectively									

**Table A.12: Summary of Kinetics model parameters for removal of Fluoride from Simulated Synthetic Waste Water**

Type of adsorbent	Pseudo first order model			Pseudo second order model			Intra particle diffusion		Experimental $q_e$ (mg/g)
	Calculated $q_e$ (mg/g)	$K_1$ ( $\text{min}^{-1}$ )	$R^2$	Calculated $q_e$ (mg/g)	$K_2$ (g/mg.min)	$R^2$	$K_{id}$ ( $\text{mg/g min}^{1/2}$ )	$R^2$	
GAC	0.088	.02533	0.884	0.6877	0.6231	0.999	0.004	0.921	0.68
SLP	0.205	0.0599	0.918	1.942	0.6783	0.999	0.027	0.936	0.89
JAMUN	0.2466	0.076	0.933	2.949	0.2218	0.999	0.034	0.994	1.30
GNS	0.2742	0.0415	0.992	1.1750	0.3325	0.999	0.004	0.921	1.49
BANANA	0.5199	0.0944	0.911	1.206	0.486	1	0.020	0.885	1.17
NEEM PATTI	0.1729	0.0806	0.898	1.5432	1.0266	0.999	0.026	0.993	1.04
TURMURIC	0.0485	0.053	0.948	1.557	0.254	1	0.033	0.929	1.17
MnO <sub>2</sub> Coated Turmeric	0.202	0.039	0.974	1.369	0.434	0.999	0.026	0.921	1.49

**Table A.13 : Summary of isotherm model parameters for removal of Fluoride from Simulated Synthetic Waste Water**

Type of adsorbent	Freundlich isotherm model			Langmuir isotherm model			Temkin isotherm model		
	$K_f$ (mg/g).(l/mg) <sup>-1/n</sup>	n	R <sup>2</sup>	$K_L$ (L/mg)	Q <sub>0</sub> (mg/g)	R <sup>2</sup>	b <sub>T</sub>	A <sub>T</sub> (L/mg)	R <sup>2</sup>
GAC	0.771	2.924	0.863	2.4	1.574	0.879	12204.78	49.23	0.813
SLP	1.607	2.584	0.997	1.359	3.309	0.988	2304.72	6.24	0.983
JAMUN	1.607	2.584	0.930	1.359	3.039	0.993	3799.95	13.790	0.973
GNS	3.490	1.840	0.965	0.449	2.320	0.989	4521.11	3.761	0.993
BANANA	1.005	2.583	0.930	1.362	1.898	0.993	2356.54	1.463	0.973
NEEM PATTI	0.6501	1.284	0.996	0.225	3.636	0.920	4189.49	3.577	0.958
TURMURIC	0.893	1.709	0.959	0.359	3.344	0.979	3207.55	3.060	0.992
MnO <sub>2</sub> Coated Turmeric	1.037	2.314	0.914	0.993	2.283	0.989	4860.86	9.032	0.967

**Table A.14: Comparison of the Defluoridation Efficiency of Different Biomass Based Sorbents**

<b>Adsorbent</b>	<b>pH</b>	<b>Adsorption capacity (mg g<sup>-1</sup>)</b>	<b>References</b>
MnO <sub>2</sub> Coated Tamarind Fruit Shell	6.5	1.9	Sivasankar et al (2010)
peepal	2	1.5	Dr A.R.Tembhurkar et al.(2009)
Moringaindica based activated carbon	2.0	0.2	Karthikeyan and Llango(2007)
Powdered biomass (Azadirachta indica + Ficus religiosa + Acacia catechu wild)	2.0	0.04	Jamode et al., 2004a and Jamode et al., 2004b
Neem	8	-	Dr A.R.Tembhurkar et al.(2009)
zirconium (iv)-impregnated groundnut (Arachis hypogea) shell carbon	-	2.32	Alagumuthu and Rajan (2010a)
Zirconium impregnated cashew nut (Anacardium occidentale) shell carbon	7.0	1.83	Alagumuthu and Rajan (2010b)
Sawdust raw	6.0	1.73	A. K. Yadav et.al
Wheat straw raw	6.0	1.93	A. K. Yadav et.al
Activated bagasse carbon	6.0	1.15	A. K. Yadav et.al
Groundnut shell	7.0	1.13	<b>Current study<sup>1</sup></b>
Banana peel	6.0	1.17	<b>Current study<sup>1</sup></b>



<b>Adsorbent</b>	<b>pH</b>	<b>Adsorption capacity (mg g<sup>-1</sup>)</b>	<b>References</b>
Sweet lemon peel	5.0	1.82	<b>Current study<sup>1</sup></b>
Java plum Seed	6.0	1.90	<b>Current study<sup>1</sup></b>
GAC	4.0	0.6835	<b>Current study<sup>1</sup></b>
Neem Leaves	4.0	1.51	<b>Current study<sup>1</sup></b>